AMAP 2021 Update Assessment of Mercury in the Arctic

National Data Check

The following pages comprise the v0 (15 March 2021) compiled draft of substantive chapters of the AMAP 2021 Update Assessment of Mercury in the Arctic. It does not include the Introduction (Chapter 1) or the Conclusions (Chapter 11).

The purpose of the national data check is to ensure completeness and correctness of included national data and information, and to identify any relevant missing data/information or studies so that these can be introduced before the peer review stage. As far as possible, the check should also ensure that national data and studies presented in the current draft have been correctly interpreted.

The materials are still under development and will be subjected to a comprehensive peer review at a later stage. As such the drafts have not yet been through any linguistic editing; cited references may still be incomplete; graphics are very preliminary, and include notes describing suggestions for eventual graphics; the drafts contain some preliminary content and/or notes about work still to be undertaken (these notes are included as they may indicate information that authors are aware of, but that is not yet introduced, and therefore assist the completeness checking process). It is not the intention that the current round of checking addresses e.g. linguistic/technical editing issues.

The goal of the assessment is to produce a 'scientifically independent' assessment, so any comments should be with respect this objective, i.e., comments should be scientific and not attempt to insert or reflect national political views, etc.

Note that these draft chapters are confidential and should not be cited, copied or circulated outside the context of this review.

* This is Chapter 2 of the AMAP Mercury Assessment*

Chapter 2: Temporal trends of mercury in arctic media and biota

Chapter Leads: Adam Morris, Frank Rigét, Philippe J. Thomas, Simon Wilson

Contributing Authors: Sandy Steffen, Geoff Stupple, Bryan Adlard, Kristin Eccles

Contributors:

Abiotic time-series data: Kaare Kemp, Katriina Kyllönen, Katrine Aspmo Pfaffhuber, Henrik Skov, Alexandra Steffen, Geoff Stupple, others?

Biota time-series data: Birgitta Andreasen, Claus Bech, Pierre Blévin, Birgit Braune, Paco Bustamante, Jan Ove Bustnes, Paloma Carvalho, Oliver Chastel, Sara Danielsson, Marlene Evans, Anita Evenset, Suzanne Faxneld, Jerome Fort, Geir Gabrielsen, Mary Gamberg, David Gremillet, Magali Houde, Karista Hudelson, Jane Kirk, Robert Letcher, Lisa Loseto, Melissa McKinney, Derek Muir, Sara Pedro, Marianna Pinzone, Amanda Poste, Frank Rigét, Heli Routti, Gary Stern, Philippe J. Thomas, Cortney Watt, Øystein Wiig

Human time-series data: Khaled Abass, Caty Blanchette, Alexey Dudarev, Eva Cecilie Bonefeld-Jorgensen, Brian Laird, Melanie Lemire, Manhai Long, Karin Nordstrom, Kristin Olafsdottir, Mylene Ratelle, Arja Rautio, Maria Wennberg

Statistical Methods: Rob Fryer

Table of Contents

2.1 Introduction

The previous AMAP assessment of mercury in the Arctic (AMAP, 2011) included a comprehensive review of time-series of mercury in abiotic and biotic media available at that time. It addressed both long-term datasets (i.e., comparing modern with historical or pre-industrial Hg concentrations) to estimate the relative importance of natural and anthropogenic Hg inputs in modern biota and the environment, and short-term datasets (i.e., covering the past one to three decades) to illustrate how Hg concentrations have changed in recent times and suggest likely trends in the near-term future.

Regarding long-term (pre-industrial to present day) trends, the 2011 assessment (AMAP, 2011) documented an approximate ten-fold increase in Hg concentration in upper trophic level marine biota over the past few centuries, much greater than the increase in ambient environmental Hg levels. It also described steep increase in biotic Hg levels during the late 19th to 20th century compared to relatively constant values over the previous four to six centuries, with an average rate of Hg increase over the past 150 years typically within the range of 1% to 4% per year. No new information has been obtained that would alter these conclusions and the current assessment provides a further example based on analysis of long-term temporal trends in tree rings (see section 2.5.4).

In relation to trends in recent decades, the 2011 assessment (AMAP, 2011) evaluated available time-series data for mercury in air, from four locations in Canada, Iceland, Sweden and Russia. It further reviewed results from a number of biota temporal trend monitoring studies using a consistent statistical analytical methodology. Of the ca. 80 biota time-series considered, 16% showed a statistically significant increasing trend, 5% a statistically significant downward trend, and 25% showed a statistically significant non-linear trend, with the rest showing no statistically significant trend. Most of the time series showing significantly increasing trends involved marine species. A greater number of significantly increasing trends occurred in Canada and Greenland compared with northern Europe. In 2011, the statistical power of available time-series to detect trends was evaluated; with a recommendation that monitoring be continued to increase the power and adequacy of time-series to meet temporal trend detection objectives. A lack of appropriate monitoring data from the Alaskan, Russian or Finnish areas of the Arctic was noted.

Continued monitoring efforts under national programs have generated time-series for mercury in an array of matrices and locations in the circumpolar Arctic. Air monitoring data are available from additional stations, and a number of biota time-series have been extended. In addition to providing information on trends at individual sites, the available data allow spatial patterns in trends to be considered. Temporal analyses are essential for the assessment of the effectiveness of international regulatory efforts aiming to reduce mercury emissions and their effects, such as the global Minamata Convention on Mercury and Heavy Metals Protocol to the UN ECE Convention on Long-range Transbounday Air Pollution (CLRTAP).

For the first time, the current assessment also includes a chapter on (Arctic) human health impacts associated with mercury exposure (see Chapter 7). This work is coordinated with an ongoing update AMAP Assessment of Human Health in the Arctic (REF). Time-series of mercury in human populations of adequate length to assess temporal trends are available from only a few Arctic sites, and may be influenced by interventions such as food advisories; they are therefore addressed separately from other biotic temporal trends, and also referenced under Chapter 7.

The current assessment also includes for the first time a spatial assessment of Hg temporal trends using geographically weighted regression model (GWR) methods. As Hg temporal trends have been shown to vary in space, and across matrix, GWR methods for the analysis of spatial data may be a useful analysis tool and a method to address spatial non-stationarity issues inherent with these Hg temporal trend datasets.

The temporal trends assessment presented in this chapter therefore focusses on recent trends (time-series covering the past few decades) of mercury in air and biota, with a particular emphasis on trends since ca. 2000. The temporal trends are evaluated using consistent, robust statistical approaches, with the objective of producing results that can be compared in a 'meta analysis'. One objective of this chapter is to provide basic information on temporal trends and spatial patterns in the trends that will be considered in more detail in subsequent chapters.

The chapter is structured around a set of policy-relevant science questions; as follows:

i) Are concentrations of total and speciated mercury changing significantly in Arctic air over time? (see section 2.4)

ii) Are concentrations of total mercury changing significantly in Arctic biota over time? (see section 2.5)

iii) Are concentrations of mercury changing significantly in Northern humans over time? (see section 2.x) and

iv) How does geographically-based weighting affect the spatial and temporal trends of mercury in biota? (see section 2.x)

2.2 Time-Series Available for the Current Assessment

Time-series made available for updated trend analysis are shown in Table 2.1 (air), Table 2.2 (biota), and Table 2.3 (humans). From these, datasets were filtered to focus on those that met selection criteria as described in Section 2.3.

Time series datasets were provided by all Arctic countries with the exception of the USA; Alaskan seabird time-series datasets were reported in the 2011 AMAP mercury assessment but these time-

2110 series had not been updated with additional mercury analyses since that time. Russia also continues to
2111 be a significant gap in relation to available time-series, represented in this assessment only by a single
2112 air monitoring stations.

2113 *TO BE INSERTED: Figure 2.1. Map of sampling locations for time-series included in the current*
2114 *assessment.*

Table 2.1. Time-series available for temporal analysis of mercury concentrations in air.

Country	Location	Matrix	Form	*n*	First year	Last year
Canada	Alert	Air	GEM	11	1995	2017
Canada	Alert	Air	Speciated	16	2002	2017
Canada	Little Fox Lake	Air	GEM	11	2007	2017
Finland	Virolahti	Air	GEM	11	2008	2018
Finland	Hyytiala	Air	GEM	11	2008	2018
Finland	Pallas	Air	GEM	11	2008	2018
NE Greenland	StationNord	Air	GEM	11	2008	2018
Norway	Andoya	Air	GEM	9	2010	2018
Norway	NyAlesund (Svalbard)	Air	GEM	18	2001	2018
Russia	Amderma	Air	GEM	9	2001	2009
United States	Anchorage	Air	GEM	5	2014	2018

Table 2.2. Time-series available for temporal analysis of mercury concentrations in biota.

Country	Location/Station (Latitude, Longitude)	Species	Tissue[a]	Basis[b]	Sub-Division	*n*[c]	Years[d]
		Terrestrial Mammals					
CA	Old Crow (67.57°, -139.83°)	*Rangifer tarandus*	KI	D		26 (26)	1991 (1991 - 2017)
CA	Western Hudson Bay (61.11°, -94.06°)	*Rangifer tarandus*	KI	D		13 (13)	2006 (2006 - 2018)
NO	Svalbard (77.88°, 20.98°)	*Vulpes lagopus*	LI	W		11 (11)	1998 (1998 - 2014)
		Freshwater Fish					
CA	GSL-West Basin (60.82°, -115.79°)	*Esox lucius*	MU	W		23 (20)	1976 (1989 - 2018)
SE	Storvindeln (65.7°, 17.13°)	*Esox lucius*	MU	W		46 (46)	1968 (1968 - 2018)
CA	Fort Good Hope (61.34°, -135.65°)	*Lota lota*	LI	W		20 (20)	1988 (1988 - 2018)

Country	Location/Station (Latitude, Longitude)	Species	Tissue[a]	Basis[b]	Sub-Division	*n*[c]	Years[d]
CA	Fort Good Hope (61.34°, -135.65°)	*Lota lota*	MU	W		19 (19)	1995 (1995 - 2018)
CA	GSL-East Arm (62.41°, -110.74°)	*Lota lota*	MU	W		17 (17)	1993 (1993 - 2018)
CA	GSL-West Basin (60.82°, -115.79°)	*Lota lota*	MU	W		26 (24)	1975 (1992 - 2018)
~~FO~~	~~Leitisvatn (62.05°, -7.23°)~~	~~*Salmo trutta*~~	~~MU~~	~~W~~	~~Undefined~~	~~1 (1)~~	~~2017 (2017 - 2017)~~
~~FO~~	~~Mjáuvøtn (62.13°, -7°)~~	~~*Salmo trutta*~~	~~MU~~	~~W~~	~~Undefined~~	~~1 (1)~~	~~2017 (2017 - 2017)~~
CA	GSL-East Arm (62.41°, -110.74°)	*Salvelinus namaycush*	MU	W		21 (21)	1993 (1993 - 2018)
CA	GSL-West Basin (60.82°, -115.79°)	*Salvelinus namaycush*	MU	W		25 (25)	1979 (1979 - 2018)
CA	Lake Kusawa (60.41°, -136.26°)	*Salvelinus namaycush*	MU	W		20 (20)	1993 (1993 - 2018)
CA	Lake Laberge (61.06°, -135.11°)	*Salvelinus namaycush*	MU	W		23 (23)	1993 (1993 - 2018)
CA	Amituk Lake (75.05°, -93.75°)	*Salvelinus alpinus*	MU	W		18 (16)	1989 (2001 - 2018)
CA	Char Lake (74.71°, -94.9°)	*Salvelinus alpinus*	MU	W		13 (13)	1993 (1993 - 2018)
CA	Lake Hazen (81.8°, -71°)	*Salvelinus alpinus*	MU	W		18 (18)	1990 (1990 - 2018)
CA	North Lake (74.78°, -95.09°)	*Salvelinus alpinus*	MU	W		14 (14)	2000 (2000 - 2018)
CA	Resolute Lake (74.69°, -94.94°)	*Salvelinus alpinus*	MU	W		22 (22)	1993 (1993 - 2018)
DK/GL	Isortoq (60.54°, -47.33°)	*Salvelinus alpinus*	MU	W		11 (11)	1994 (1994 - 2018)
FO	Á Mýrunum (62.17°, -7.09°)	*Salvelinus alpinus*	MU	W	Undefined	10 (10)	2000 (2000 - 2014)
NO	Bjørnøya (74.45°, 19.12°)	*Salvelinus alpinus*	MU	D		12 (12)	1998 (1998 - 2015)
SE	Abiskojaure (68.29°, 18.59°)	*Salvelinus alpinus*	MU	W		37 (37)	1981 (1981 - 2018)
		Marine Invertebrates (mussels)					
~~IS~~	~~Bolaklettur (64.34°, -21.69°)~~	~~*Mytilus edulis*~~	~~SB~~	~~D~~		~~2 (2)~~	~~2012 (2012 - 2013)~~
IS	Grímsey (66.55°, -18.02°)	*Mytilus edulis*	SB	D		16 (16)	1993 (1993 - 2013)
~~IS~~	~~Hvalskurðara (65.9°, -22.83°)~~	~~*Mytilus edulis*~~	~~SB~~	~~D~~		~~3 (3)~~	~~2016 (2016 - 2018)~~
IS	Hvalstod Hvalfjordur (64.4°, -21.45°)	*Mytilus edulis*	SB	D		19 (19)	1993 (1993 - 2013)
IS	Hvassahraun (64.05°, -22.29°)	*Mytilus edulis*	SB	D		21 (21)	1993 (1993 - 2018)
IS	Hvitanes Hvalfjordur (64.36°, -21.5°)	*Mytilus edulis*	SB	D		22 (22)	1993 (1993 - 2018)

Country	Location/Station (Latitude, Longitude)	Species	Tissue[a]	Basis[b]	Sub-Division	*n*[c]	Years[d]
IS	Mjoifjordur (Dalatangi°) (65.27°, -13.58°)	*Mytilus edulis*	SB	D		13 (13)	1997 (1997 - 2018)
IS	Mjoifjordur (head°) (65.19°, -14.01°)	*Mytilus edulis*	SB	D		15 (15)	1996 (1996 - 2018)
IS	Mjoifjordur (Hofsa°) (65.2°, -13.82°)	*Mytilus edulis*	SB	D		15 (15)	1995 (1995 - 2018)
~~IS~~	~~North-Northwest off Iceland (66.92°, -22.89°)~~	~~*Mytilus edulis*~~	~~SB~~	~~D~~		~~3 (1)~~	~~1996 (2016 - 2016)~~
IS	Straumur Straumsvik (64.18°, -22.24°)	*Mytilus edulis*	SB	D		21 (21)	1993 (1993 - 2018)
IS	Ulfsa Skutulsfjordur (66.06°, -23.17°)	*Mytilus edulis*	SB	D		17 (17)	1997 (1997 - 2018)
NO	Skallneset (70.14°, 30.34°)	*Mytilus edulis*	SB	W		22 (22)	1994 (1994 - 2017)
NO	Brashavn (69.9°, 29.74°)	*Mytilus edulis*	SB	W		19 (19)	1997 (1997 - 2017)
NO	Husvaagen area (68.25°, 14.66°)	*Mytilus edulis*	SB	W		19 (19)	1997 (1997 - 2017)
~~NO~~	~~Moholmen (B5°) (66.31°, 14.13°)~~	~~*Mytilus edulis*~~	~~SB~~	~~W~~		~~1 (1)~~	~~2017 (2017 - 2017)~~
~~NO~~	~~Bjørnbærviken (B9°) (66.28°, 14.05°)~~	~~*Mytilus edulis*~~	~~SB~~	~~W~~	-	~~1 (1)~~	~~2017 (2017 - 2017)~~
		Marine Fish					
CA	Queen Maud Gulf (69.12°, -105.06°)	*Salvelinus alpinus*	MU	W		17 (13)	1977 (2004 - 2018)
DK/GL	Avanersuaq (77.28°, -69.14°)	*Myoxocephalus scorpius*	LI	W		9 (8)	1987 (1995 - 2018)
DK/GL	Ittoqqortoormiit (70.29°, -21.58°)	*Myoxocephalus scorpius*	LI	W		12 (11)	1985 (1995 - 2018)
DK/GL	Qeqertarsuaq (69.15°, -53.32°)	*Myoxocephalus scorpius*	LI	W		14 (14)	1994 (1994 - 2018)
FO	Mýlingsgrunnur (62.38°, -7.42°)	*Gadus morhua*	MU	W	Undefined	27 (27)	1979 (1979 - 2016)
FO	Mýlingsgrunnur (62.38°, -7.42°)	*Gadus morhua*	MU	W	Medium (size)	29 (29)	1979 (1979 - 2017)
IS	North-Northwest off Iceland (66.92°, -22.89°)	*Gadus morhua*	MU	W		24 (24)	1990 (1990 - 2018)
IS	Northeast off Iceland (65.24°, -12.13°)	*Gadus morhua*	MU	W		23 (23)	1990 (1990 - 2018)
NO	Varangerfjorden (69.82°, 29.76°)	*Gadus morhua*	MU	W		21 (21)	1994 (1994 - 2017)
NO	Tromsø harbour (69.65°, 18.97°)	*Gadus morhua*	MU	W		7 (7)	2009 (2009 - 2017)
NO	Bjørnerøya (east°) (68.19°, 14.71°)	*Gadus morhua*	MU	W		21 (21)	1992 (1992 - 2017)
		Seabirds					
CA	Prince Leopold Island (74.04°, -90.03°)	*Fulmarus glacialis*	EH	D		19 (19)	1975 (1975 - 2017)

Country	Location/Station (Latitude, Longitude)	Species	Tissue[a]	Basis[b]	Sub-Division	*n*[c]	Years[d]
CA	Coats Island (62.47°, -83.1°)	*Uria lomvia*	EH	D		15 (15)	1993 (1993 - 2017)
CA	Prince Leopold Island (74.04°, -90.03°)	*Uria lomvia*	EH	D		19 (19)	1975 (1975 - 2017)
DK/GL	Ittoqqortoormiit Ukaleqarteq (70.72°, -21.55°)	*Alle alle*	BL	D		10 (10)	2005 (2005 - 2015)
DK/GL	Ittoqqortoormiit Ukaleqarteq (70.72°, -21.55°)	*Alle alle*	FE	D		10 (10)	2007 (2007 - 2016)
FO	Koltur (61.99°, -6.99°)	*Cepphus grylle*	EH	W	Undefined	11 (11)	1999 (1999 - 2016)
FO	Skúvoy (61.77°, -6.8°)	*Cepphus grylle*	EH	W	Undefined	10 (10)	1999 (1999 - 2014)
FO	Sveipur (61.95°, -6.72°)	*Cepphus grylle*	LI	W	Juvenile	9 (9)	1995 (1995 - 2015)
FO	Sveipur (61.95°, -6.72°)	*Cepphus grylle*	FE	W	Juvenile	8 (8)	1996 (1996 - 2015)
FO	Tindhólmur (62.08°, -7.43°)	*Cepphus grylle*	FE	W	Juvenile	6 (6)	2005 (2005 - 2015)
FO	Tindhólmur (62.08°, -7.43°)	*Cepphus grylle*	LI	W	Juvenile	6 (6)	2005 (2005 - 2015)
~~FO~~	~~Vestmanna (62.15°, -7.16°)~~	~~*Fulmarus glacialis*~~	~~MU~~	~~W~~	~~Undefined~~	~~1 (1)~~	~~2017 (2017 - 2017)~~
~~FO~~	~~Vestmanna (62.15°, -7.16°)~~	~~*Fulmarus glacialis*~~	~~MU~~	~~W~~	~~Pullus~~	~~3 (3)~~	~~2008 (2008 - 2017)~~
~~FO~~	~~Vestmanna (62.15°, -7.16°)~~	~~*Fulmarus glacialis*~~	~~FE~~	~~W~~	~~Undefined~~	~~1 (1)~~	~~2017 (2017 - 2017)~~
~~FO~~	~~Vestmanna (62.15°, -7.16°)~~	~~*Fulmarus glacialis*~~	~~FE~~	~~W~~	~~Pullus~~	~~2 (2)~~	~~2016 (2016 - 2017)~~
~~FO~~	~~Vestmanna (62.15°, -7.16°)~~	~~*Fulmarus glacialis*~~	~~LI~~	~~W~~	~~Undefined~~	~~1 (1)~~	~~2017 (2017 - 2017)~~
~~FO~~	~~Vestmanna (62.15°, -7.16°)~~	~~*Fulmarus glacialis*~~	~~LI~~	~~W~~	~~Pullus~~	~~2 (2)~~	~~2016 (2016 - 2017)~~
NO	Svalbard-Kongsfjorden area (79°, 11.67°)	*Rissa tridactyla*	ER	D		15 (15)	2000 (2000 - 2016)
		Marine Mammals					
CA	Southern Beaufort (69.5°, -133.58°)	*Delphinapterus leucas*	LI	W	Small	23 (23)	1981 (1981 - 2017)
CA	Southern Beaufort (69.5°, -133.58°)	*Delphinapterus leucas*	LI	W	Large	23 (23)	1981 (1981 - 2017)
CA	Southern Beaufort (69.5°, -133.58°)	*Delphinapterus leucas*	MU	W	Small	23 (23)	1981 (1981 - 2017)
CA	Southern Beaufort (69.5°, -133.58°)	*Delphinapterus leucas*	MU	W	Large	22 (21)	1981 (1993 - 2017)
CA	Southern Beaufort (69.5°, -133.58°)	*Delphinapterus leucas*	EP	W	Small	20 (20)	1993 (1993 - 2017)
CA	Southern Beaufort (69.5°, -133.58°)	*Delphinapterus leucas*	EP	W	Large	20 (20)	1993 (1993 - 2017)
CA	Southern Hudson Bay (56.54°, -79.22°)	*Delphinapterus leucas*	LI	W	Small	15 (15)	1994 (1994 - 2016)

Country	Location/Station (Latitude, Longitude)	Species	Tissue[a]	Basis[b]	Sub-Division	*n*[c]	Years[d]
CA	Southern Hudson Bay (56.54°, -79.22°)	*Delphinapterus leucas*	LI	W	Large	17 (17)	1994 (1994 - 2016)
CA	Southern Hudson Bay (56.54°, -79.22°)	*Delphinapterus leucas*	MU	W	Small	15 (15)	1994 (1994 - 2016)
CA	Southern Hudson Bay (56.54°, -79.22°)	*Delphinapterus leucas*	MU	W	Large	17 (17)	1994 (1994 - 2016)
FO	Føroyskar Hvalvágir (62.00°, -7.00°)	*Globicephala melas*	MU	W	Undefined	20 (17)	1979 (1997 - 2017)
FO	Føroyskar Hvalvágir (62.00°, -7.00°)	*Globicephala melas*	MU	W	Adult	15 (12)	1979 (1997 - 2015)
FO	Føroyskar Hvalvágir (62.00°, -7.00°)	*Globicephala melas*	MU	W	Juvenile male	18 (16)	1986 (1997 - 2017)
FO	Føroyskar Hvalvágir (62.00°, -7.00°)	*Globicephala melas*	LI	W	Adult	12 (12)	2001 (2001 - 2017)
FO	Føroyskar Hvalvágir (62.00°, -7.00°)	*Globicephala melas*	LI	W	Juvenile male	6 (6)	2001 (2001 - 2015)
CA	Eastern Beaufort Sea (71.99°, -125.25°)	*Phoca hispida*	LI	W	Adult	14 (12)	1987 (2001 - 2017)
CA	Eastern Beaufort Sea (71.99°, -125.25°)	*Phoca hispida*	LI	W	Juvenile	13 (11)	1987 (2001 - 2017)
CA	Eastern Beaufort Sea (71.99°, -125.25°)	*Phoca hispida*	MU	W	Adult	14 (12)	1987 (2001 - 2017)
CA	Eastern Beaufort Sea (71.99°, -125.25°)	*Phoca hispida*	MU	W	Juvenile	14 (12)	1987 (2001 - 2017)
CA	Resolute Passage (74.7°, -94.83°)	*Phoca hispida*	LI	W	Adult	16 (16)	1993 (1993 - 2017)
CA	Resolute Passage (74.7°, -94.83°)	*Phoca hispida*	LI	W	Juvenile	15 (15)	1993 (1993 - 2017)
CA	Resolute Passage (74.7°, -94.83°)	*Phoca hispida*	MU	W	Adult	15 (14)	1993 (2004 - 2017)
CA	Resolute Passage (74.7°, -94.83°)	*Phoca hispida*	MU	W	Juvenile	15 (14)	1993 (2004 - 2017)
CA	Southern Labrador Sea (56.54°, -61.7°)	*Phoca hispida*	LI	W	Adult	9 (9)	1997 (1997 - 2017)
CA	Southern Labrador Sea (56.54°, -61.7°)	*Phoca hispida*	LI	W	Juvenile	8 (8)	1998 (1998 - 2017)
CA	Southern Labrador Sea (56.54°, -61.7°)	*Phoca hispida*	MU	W	Adult	10 (10)	1997 (1997 - 2017)
CA	Southern Labrador Sea (56.54°, -61.7°)	*Phoca hispida*	MU	W	Juvenile	9 (9)	1998 (1998 - 2017)
CA	Western Hudson Bay (61.11°, -94.06°)	*Phoca hispida*	LI	W	Adult	15 (15)	1992 (1992 - 2017)
CA	Western Hudson Bay (61.11°, -94.06°)	*Phoca hispida*	LI	W	Juvenile	14 (13)	1992 (2003 - 2017)
CA	Western Hudson Bay (61.11°, -94.06°)	*Phoca hispida*	MU	W	Adult	14 (13)	1992 (2003 - 2017)
CA	Western Hudson Bay (61.11°, -94.06°)	*Phoca hispida*	MU	W	Juvenile	14 (13)	1992 (2003 - 2017)
DK/GL	Ittoqqortoormiit (70.29°, -21.58°)	*Phoca hispida*	LI	W	Undefined	6 (6)	1999 (1999 - 2016)
DK/GL	Avanersuaq (77.28°, -69.14°)	*Phoca hispida*	LI	W	Adult	10 (10)	1994 (1994 - 2018)

Country	Location/Station (Latitude, Longitude)	Species	Tissue[a]	Basis[b]	Sub-Division	*n*[c]	Years[d]
DK/GL	Avanersuaq (77.28°, -69.14°)	*Phoca hispida*	LI	W	Juvenile	12 (12)	1984 (1984 - 2018)
DK/GL	Ittoqqortoormiit (70.29°, -21.58°)	*Phoca hispida*	LI	W	Adult	14 (14)	1986 (1986 - 2018)
DK/GL	Ittoqqortoormiit (70.29°, -21.58°)	*Phoca hispida*	LI	W	Juvenile	14 (14)	1986 (1986 - 2018)
DK/GL	Qeqertarsuaq (69.15°, -53.32°)	*Phoca hispida*	LI	W	Undefined	6 (1)	1994 (2018 - 2018)
DK/GL	Qeqertarsuaq (69.15°, -53.32°)	*Phoca hispida*	LI	W	Juvenile	14 (14)	1994 (1994 - 2018)
CA	Southern Hudson Bay (56.54°, -79.22°)	*Ursus maritimus*	LI	D	Adult female	10 (10)	2006 (2006 - 2017)
CA	Southern Hudson Bay (56.54°, -79.22°)	*Ursus maritimus*	LI	D	Adult male	10 (10)	2006 (2006 - 2017)
CA	Southern Hudson Bay (56.54°, -79.22°)	*Ursus maritimus*	LI	D	Juvenile	7 (7)	2007 (2007 - 2015)
CA	Western Hudson Bay (61.11°, -94.06°)	*Ursus maritimus*	LI	D	Adult female	6 (6)	2007 (2007 - 2017)
CA	Western Hudson Bay (61.11°, -94.06°)	*Ursus maritimus*	LI	D	Adult male	10 (10)	2007 (2007 - 2017)
CA	Western Hudson Bay (61.11°, -94.06°)	*Ursus maritimus*	LI	D	Juvenile	8 (8)	2007 (2007 - 2015)
DK/GL	Ittoqqortoormiit (70.29°, -21.58°)	*Ursus maritimus*	LI	W	Undefined	14 (14)	1986 (1986 - 2018)
DK/GL	Ittoqqortoormiit (70.29°, -21.58°)	*Ursus maritimus*	LI	W	Adult female	22 (22)	1984 (1984 - 2018)
DK/GL	Ittoqqortoormiit (70.29°, -21.58°)	*Ursus maritimus*	LI	W	Adult male	24 (24)	1984 (1984 - 2018)
DK/GL	Ittoqqortoormiit (70.29°, -21.58°)	*Ursus maritimus*	LI	W	Juvenile	28 (28)	1983 (1983 - 2018)
DK/GL	Ittoqqortoormiit (70.29°, -21.58°)	*Ursus maritimus*	HA	D	Undefined	12 (11)	1987 (2000 - 2018)
DK/GL	Ittoqqortoormiit (70.29°, -21.58°)	*Ursus maritimus*	HA	D	Adult female	16 (14)	1984 (1999 - 2018)
DK/GL	Ittoqqortoormiit (70.29°, -21.58°)	*Ursus maritimus*	HA	D	Adult male	17 (16)	1984 (1999 - 2018)
DK/GL	Ittoqqortoormiit (70.29°, -21.58°)	*Ursus maritimus*	HA	D	Juvenile	21 (21)	1984 (1984 - 2018)
NO	Svalbard (77.88°, 20.98°)	*Ursus maritimus*	HA	D	Adult female	25 (25)	1990 (1990 - 2016)
NO	Svalbard (77.88°, 20.98°)	*Ursus maritimus*	HA	D	Juvenile	10 (10)	1998 (1998 - 2014)

[a] BL = whole blood, EH = egg homogenate, EP = epidermis, ER = erythrocytes, FE = feathers, HA = hair, LI = liver, MU = muscle, SB = soft body (whole),

[b] Wet (W) or dry (D) weight concentrations

[c] Both the total available years and the years used in the trend analysis (in parentheses) are shown

[d] The earliest available year in the time-series is shown along with the beginning and endpoints for the best-fit trend (in parentheses)

Table 2.3. Time-trends selected for temporal analysis of mercury concentrations in human blood.

Country	Location/Station	n	Years
Denmark/Greenland	Disko Bay	7	1994 - 2013
Denmark/Greenland	Nuuk	8	1999 - 2013
Canada	Kuujjuaq	12	1992 - 2016

2.3 Selection of Data for Trend Analysis and Statistical Methods

Detailed descriptions of the statistical calculations and R-coding are provided in Appendix 2.

2.3.1 Selection Criteria and Regression Analysis for Air Time Series

Temporal trend analysis of GEM concentrations was performed using a seasonal Mann-Kendall test on data from 10 sites located around the Arctic, subarctic and beyond. This trend analysis method is recommended for use on data is not normally distributed and which may have data gaps. The Mann-Kendall test compares month to month, every possible combination of data points for a trend (where data completeness exceeds 75%). The combinations are looked at to add robustness, while the monthly bins account for seasonal variability.

2.3.2 Selection Criteria and Regression Analysis for Biota Time Series

In wildlife, mercury was assessed as THg rather than as MeHg alone as in the last AMAP mercury assessment (AMAP, 2011). This helps to mediate any effects of demethylation (MeHg → tiemanite) observed in the liver of some seabirds and marine mammals (AMAP 2011, Dietz et al. 1990, Wagemann et al. 1998). Where possible the same tissues were modeled for a given species, and in most cases, comparable datasets were generated for the different locations though in some cases differences in national monitoring plans and sampling prevented congruent tissue-specific comparisons. For example, because Norwegian polar bears are not hunted for subsistence, only hair was available for analysis from this subpopulation. If more than one tissue was available, these were also modeled for intraspecies comparisons of trends in the different tissue compartments which can be an important consideration for monitoring and modeling efforts.

Of the 110 biota time-series that were appropriate for trend assessment the temporal range of the data varied from 6 to 46 years, with a mean range of ~16 years. The bulk of the wildlife data were for marine mammals (53 time-series), > freshwater fish (20) > seabirds (12) ≥ marine invertebrates (mussels) (12) > marine fish (10) > terrestrial mammals (3). Where appropriate, the marine mammals were sub-divided by age and sex (some seabirds, ringed seals, polar bears) or size (cetaceans).

Log-linear trends were calculated from regressions of annual medians of individual log concentration values against year for each time-series 1) over the full range of years provided (if gaps in the data

were < 5 years), and 2) trends over the last 20 years (1999–2019). Non-linear trends were also tested for significance and were ranked with the significant linear models using the Akaike Information Criteria for Small Sample Sizes (AIC_C) which was used to find the best-fit models for each dataset.

2.3.3 Biota Time Series Power Analysis

To be added after the final analyses are completed (and potentially with an adjustment to a 5 % annual change in the power calculations rather than 10 % annual change)

2.3.4 Geographically Weighted Regression Analysis

Spatial models to examine trends in Hg across biota time-series datasets were generated from land cover data [source?], The land cover data and Hg time-series datasets were imported and analysed in ArcDesktop (ArcGIS © v.10.3.1 and 10.4, Environmental Systems Research Institute, Redlands, CA, USA).

The dependent variable (or Hg time trends) was tested for global and local clustering using the global Moran's I and local Getis and Ord's G* statistics. The tests were specified using inversely weighted spatial relationships. A general linear model was used to determine which landscape variables and matrix-specific specifc variable (including sex, species, matrix type - independent variables), could explain the greatest amount of variance in Hg temporal trends at each site (dependent variable). The independent landscape and matrix variables included a set of XX variables as presented in Table X.

2.4 Are concentrations of total and speciated mercury changing significantly in Arctic air over time?

The results of trend analysis in air are summarized in Table 2.4.

Table 2.4. Results of temporal analysis of total and speciated mercury concentrations in air (pg m^{-3}).

TO BE COMPILED/INSERTED

TO BE INSERTED

Figure 2.2. Trends of gaseous elemental mercury (GEM) concentrations in air (pg m^{-3}) at circumpolar locations.

TO BE INSERTED

Figure 2.3. Trends of mercury species concentrations (pg m^{-3}) in air from Alert, Nunavut.

Of the 10 stations measuring concentrations of GEM in air, 8 exhibited decreasing trends of mercury over their assessment periods including Alert (Canada), Anchorage (USA) and the European and Asian sites at Station Nord (Greenland), Amderma (Russia), Pallas (Findland), Hyytiala (Finland), and Andoya (Norway), however the third Finnish site Virolahti had no significant trend. Mercury concentrations at Little Fox Lake (Canada), the most westerly sampling location, had the only significantly increasing trend. The increase at this site has been attributed to increased mercury emissions from Asia based on global modeling efforts and back trajectory calculations (reference).

Alert and Station Nord are the most northern sites and show similar AMDE-driven seasonal trends, as well as similar annual changes. Seasonal trends of concentrations at these sites decreased through late winter with the largest decrease occurring during the springtime AMDEs. Within European sites there was a discernible latitudinal trend in the sites; the most northern locations showed the largest decreases (e.g., Andoya), while those further south had reduced or insignificant trends (e.g., Virolahti).

Text to be further developed

2.5 Are concentrations of total mercury changing significantly in Arctic biota over time?

2.5.1 Trends in biota species groups

The results of trend analysis in circumpolar wildlife and fish are summarized in Table 2.5.

Table 2.5. Results of temporal analysis of total mercury concentrations (µg kg^{-1}) in (A) terrestrial mammals, fish and invertebrates, and (B) seabirds and marine mammals. The number of years included in the fitted/tested linear trends are shown in parentheses and significant log-linear regressions ($p < 0.05$) are represented by (↑) or (↓). If a significant non-linear trend was detected, those are also indicated. Seabirds and marine mammals were tested in sub-divided datasets as indicated in Table 2.2 and in (B).

(A)	Country	Location/Station	Species	Tissue[a]	Non-linear Trend	Linear Trend
Terrestrial Mammals						
CA		Old Crow	*Rangifer tarandus*	KI		(26)
CA		Western Hudson Bay	*Rangifer tarandus*	KI		(13)
NO		Svalbard	*Vulpes lagopus*	LI		(11)
Freshwater Fish						
CA		Amituk Lake	*Salvelinus alpinus*	MU	Y	**(16)** ↓
CA		Char Lake	*Salvelinus alpinus*	MU		(13)
CA		Lake Hazen	*Salvelinus alpinus*	MU		**(18)** ↓
CA		North Lake	*Salvelinus alpinus*	MU		(14)
CA		Resolute Lake	*Salvelinus alpinus*	MU	Y	(22)
DK/GL		Isortoq	*Salvelinus alpinus*	MU		(11)
FO		Á Mýrunum	*Salvelinus alpinus*	MU		(10)
NO		Bjørnøya	*Salvelinus alpinus*	MU		**(12)** ↑
SE		Abiskojaure	*Salvelinus alpinus*	MU		**(37)** ↓
CA		GSL-East Arm	*Salvelinus namaycush*	MU		(21)
CA		GSL-West Basin	*Salvelinus namaycush*	MU		**(25)** ↑
CA		Lake Kusawa	*Salvelinus namaycush*	MU		**(20)** ↓
CA		Lake Laberge	*Salvelinus namaycush*	MU	Y	**(23)** ↓
CA		Fort Good Hope	*Lota lota*	MU		**(19)** ↑
			Lota lota	LI		**(20)** ↑

(A)	Country	Location/Station	Species	Tissue[a]	Non-linear Trend	Linear Trend
CA		GSL-East Arm	*Lota lota*	MU	Y	**(17)** ↑
CA		GSL-West Basin	*Lota lota*	MU		**(24)** ↑
CA		GSL-West Basin	*Esox lucius*	MU		(20)
SE		Storvindeln	*Esox lucius*	MU	Y	**(46)** ↓
			Marine Invertebrates (mussels)			
NO		Skallneset	*Mytilus edulis*	SB	Y	**(22)** ↓
NO		Brashavn	*Mytilus edulis*	SB		(19)
NO		Husvaagen area	*Mytilus edulis*	SB	Y	(19)
IS		Grímsey	*Mytilus edulis*	SB		(16)
IS		Hvalstod Hvalfjordur	*Mytilus edulis*	SB		(19)
IS		Hvassahraun	*Mytilus edulis*	SB		(21)
IS		Hvitanes Hvalfjordur	*Mytilus edulis*	SB		(22)
IS		Mjoifjordur	*Mytilus edulis*	SB		**(13)** ↑
IS		Mjoifjordur	*Mytilus edulis*	SB		**(15)** ↑
IS		Mjoifjordur	*Mytilus edulis*	SB		(15)
IS		Straumur Straumsvik	*Mytilus edulis*	SB		(21)
IS		Ulfsa Skutulsfjordur	*Mytilus edulis*	SB		(17)
			Marine Fish			
CA		Queen Maud Gulf	*Salvelinus alpinus*	MU		(13)
DK/GL		Avanersuaq	*Myoxocephalus scorpius*	LI		(8)
DK/GL		Ittoqqortoormiit	*Myoxocephalus scorpius*	LI		**(11)** ↑
DK/GL		Qeqertarsuaq	*Myoxocephalus scorpius*	LI		**(14)** ↑
FO		Mýlingsgrunnur	*Gadus morhua*	MU	Y	**(27)** ↑

(A)	Country	Location/Station	Species	Tissue[a]	Non-linear Trend	Linear Trend
IS		North-Northwest off Iceland	*Gadus morhua*	MU		(24)
IS		Northeast off Iceland	*Gadus morhua*	MU		(23)
NO		Varangerfjorden	*Gadus morhua*	MU	Y	(21)
NO		Tromsø harbour	*Gadus morhua*	MU		**(7)** ↑
NO		Bjørnerøya	*Gadus morhua*	MU		(21)

2210

(B) Country	Location	Species	Tissue[a]	THg Trends								
				Non-Linear Trend	Linear (No Sub-Divisions)	Adult			Juvenile		Size	
						Mixed	M	F	Mixed	M	Large	Small
Seabirds												
CA	Coats Island	*Uria lomvia*	EH		(15)							
CA	Prince Leopold Island	*Uria lomvia*	EH	Y	(19)							
CA	Prince Leopold Island	*Fulmarus glacialis*	EH		**(19)** ↑							
DK/GL	Ittoqqortoormiit Ukaleqarteq	*Alle alle*	BL		(10)							
		Alle alle	FE		(10)							
FO	Sveipur	*Cepphus grylle*	LI						**(9)** ↑			
		Cepphus grylle	FE						(8)			
FO	Tindhólmur	*Cepphus grylle*	LI						(6)			
		Cepphus grylle	FE						(6)			
FO	Koltur	*Cepphus grylle*	EH		**(11)** ↑							
FO	Skúvoy	*Cepphus grylle*	EH		**(10)** ↑							
NO	Svalbard-Kongsfjorden	*Rissa tridactyla*	ER		**(15)** ↓							
Marine Mammals												
CA	Southern Beaufort Sea	*Delphinapterus leucas*	MU								(21)	(23)
		Delphinapterus leucas	LI	Y							**(23)** ↓	(23)

		Delphinapterus leucas	EP	Y							**(20)** ↓	**(20)** ↓
CA	Southern Hudson Bay	*Delphinapterus leucas*	MU								(17)	(15)
		Delphinapterus leucas	LI								(17)	(15)
FO	Føroyskar Hvalvágir	*Globicephala melas*	MU	Y	(17)	(12)				**(16)** ↑		
FO	Føroyskar Hvalvágir	*Globicephala melas*	LI			(12)				(6)		
CA	Eastern Beaufort Sea	*Phoca hispida*	MU	Y		**(12)** ↓			**(12)** ↓			
		Phoca hispida	LI			(12)			(11)			
CA	Resolute Passage	*Phoca hispida*	MU			(14)			**(14)** ↓			
		Phoca hispida	LI			(16)			(15)			
CA	Southern Labrador Sea	*Phoca hispida*	MU			(10)			**(9)** ↓			
		Phoca hispida	LI			**(9)** ↑			(8)			
CA	Western Hudson Bay	*Phoca hispida*	MU	Y		**(13)** ↓			**(13)** ↓			
		Phoca hispida	LI			(15)			(13)			
DK/GL	Avanersuaq	*Phoca hispida*	LI			(10)			(12)			
DK/GL	Ittoqqortoormiit	*Phoca hispida*	LI			(14)			(14)			
DK/GL	Qeqertarsuaq	*Phoca hispida*	LI		(14)							
CA	Southern Hudson Bay	*Ursus maritimus*	LI				(10)	(10)	(7)			
CA	Western Hudson Bay	*Ursus maritimus*	LI				**(10)** ↑	(6)	(8)			
DK/GL	Ittoqqortoormiit	*Ursus maritimus*	LI	Y			(24)	(22)	(28)			
		Ursus maritimus	HA				**(16)** ↑		**(21)** ↑			
NO	Svalbard	*Ursus maritimus*	HA					**(25)** ↑	(10)			

[a] BL = whole blood, EH = egg homogenate, EP = epidermis, ER = erythrocytes, FE = feathers, HA = hair, LI = liver, MU = muscle, SB = soft body (whole)

a. Terrestrial mammals

Of the three available datasets for terrestrial mammals, none resulted in significant linear or non-linear trends (Table 2.5-A). The power statistics for these data indicate that the data were adequate to detect up to 10 % annual changes with power ≥ 80 % so the lack of significant trends are not due to mathematical limitations of the data.

b. Freshwater fish

Freshwater populations of landlocked Arctic char provided nine datasets for comparison throughout Northern Canada (Ellesmere and Cornwallis Islands), SE Greenland, the Faroe Islands, Norway (Bear Island) and Sweden (Figure 2.1). Of these, two time-series generated strong, significant decreasing linear trends in the Canadian high Arctic, and in northern Sweden. In contrast the trend in Bear Island char was temporally shorter, but did indicate that THg was increasing in these fish. Of interest is that significant non-linear trends were also observed in Amituk Lake as well as Resolute Lake char, and in the most recent time-frames of those models (2013 or 2014 to 2018) concentrations do appear to have increased as they have in Norway.

Trends of THg were also generated for lake trout, which were only available for Canadian locations in the Northwest Territories and the Yukon. The lake trout in two Yukon lakes (Kusawa and Laberge) exhibited decreasing trends over the assessment period, while those in trout from the West Basin of Great Slave Lake increased over time (Table 2.5A). A species-specific comparison of burbot between populations in the Northwest Territories on the Mackenzie River (Fort Good Hope) and Great Slave Lake showed similar increasing trends at all three locations, and that the trends were similar in liver and muscle agreed in the Fort Good Hope fish, though the trends in liver were increasing slightly more rapidly.

Lastly, northern pike only generated significant decreasing linear trend as well as a non-linear trend in the Swedish population, but neither was significant in the West Basin of Great Slave Lake. The non-linear trend for the Swedish pike indicate an inflection point and reversal of the trend from increasing to decreasing in the early 1990s (insert year from regression formula/inflection point), which agrees reasonably well with the decreasing trend observed in the Swedish Char.

In freshwater systems, characteristics of the lakes and the structure of the local food web can substantially impact the bioavailability, bioaccumulation and trends of Hg in resident fish ( ).

TO BE INSERTED Figure 2.4. Selected trends of total mercury in tissues of freshwater fish (μg kg^{-1}).

c. Marine invertebrates (mussels)

Mussel time-series were available for a number of European locations as part of the AMAP monitoring programme; these data are archived at the AMAP thematic data centre at ICES. As sessile, filter-feeding organisms, mussels can provide valuable temporospatial information on contaminant

distributions and trends, however there were no comparative data available in northern North America or Asia.

d. Marine fish

Text to be developed

TO BE INSERTED Figure 2.5. Selected trends of total mercury in tissues of marine fish (µg kg^{-1}).

e. Seabirds

f. Marine mammals

Text to be developed

TO BE INSERTED Figure 2.6. Selected trends of total mercury in tissues of marine mammals (µg kg^{-1}).

2.5.2 Geographical Patterns in Biota Trends (Latitude and Longitude)

Few trends with latitude were evident when plotting all of the trend data together or when separated by ecological group (e.g., freshwater fish, marine fish, marine mammals, seabirds). Only seabirds exhibited a significant correlation with latitude, with more rapidly decreasing trends observed at higher latitudes ($r^2 = 0.37$, $p = 0.035$). This regression was heavily weighted to lower latitudes with few high latitude trends available to plot, so this may be a misleading relationship (Figure 2.7).

Only non-linear relationships were significant between the calculated trends of THg with longitude (Figure 2.8), and unlike latitude, seabirds were the only group of wildlife without any trend with longitude. For marine mammals, the trends were smallest at the most western longitudes in the Canadian Arctic (~-125°) before increasing from west to east through Greenland before then leveling off and remaining relatively consistent from Greenland to the remaining European locations (maximum ~21°). The overall trend of all time-series also follows this pattern, but has a more subtle increase before the trends level off throughout Greenland and Europe.

TO BE INSERTED

Figure 2.7. Trends of mercury in select species as a function of latitude (°).

TO BE INSERTED

Figure 2.8. Trends of mercury in select species as a function of longitude (°).

2.5.3 Geographically Weighted Regression

Still in progress, but we have added a few figures that will be included in the analysis. We are still working on modeling the effects of matrix type (incl- species, sex, tissue type, etc)

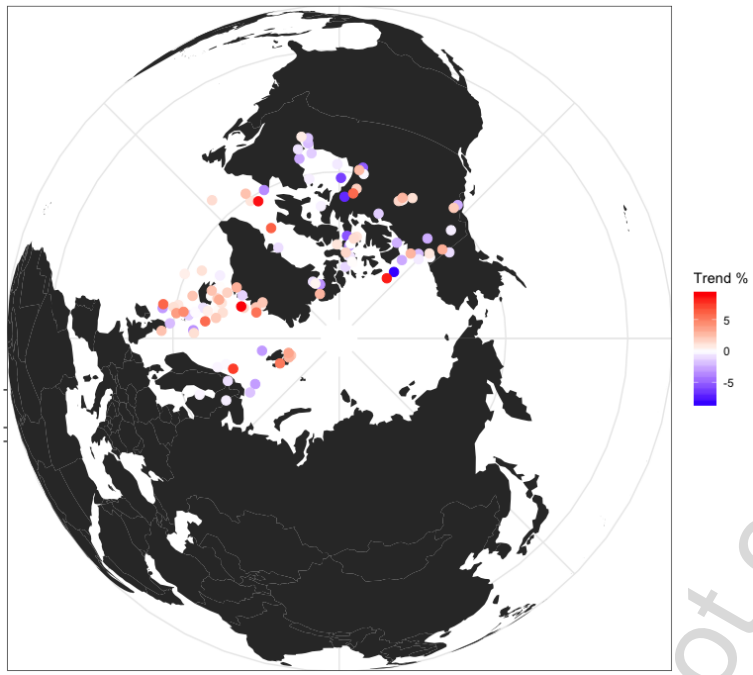

Figure 2.x. Distribution of linear trends in wildlife across all species and life stages. Red indicates locations where mercury is increasing over time. Blue indicates location where mercury is decreasing over time. White indicates no trend in mercury over time.

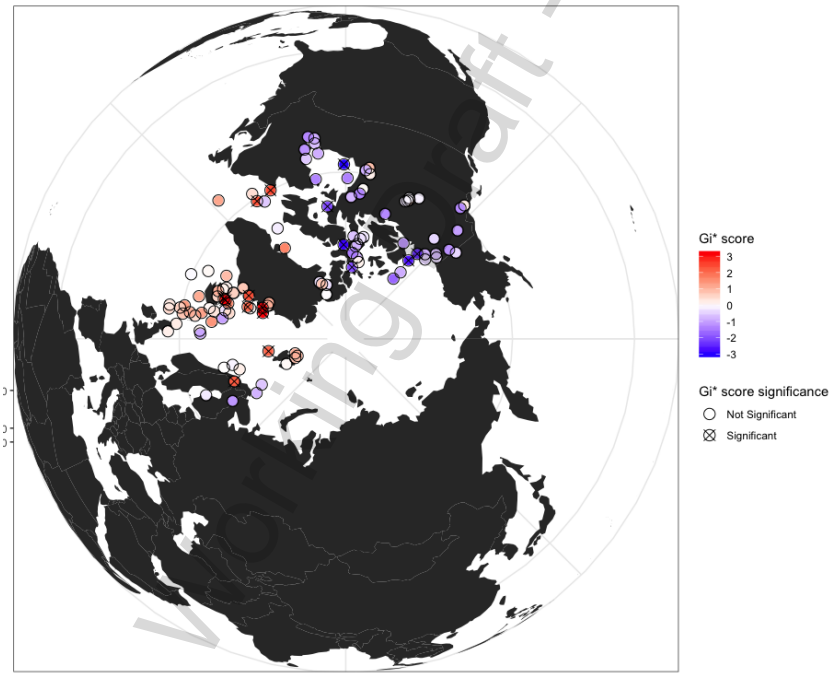

Figure 2.y. Getis and Ord's Gi inverse distance clustering, indicating how similar linear trends are to the surrounding points. Blue indicates clusters of negative trends and red indicates clusters of*

increasing mercury trends. Clusters that are statistically significant at an alpha=0.05 are marked with an X.

2.5.4 Temporal Analysis of Mercury Concentrations in Tree Rings

Text to be developed

Table 2.a. Time-series available.

Country	Location	Species	n trees	Interval	First year	Last year
Canada	Mackenzie Delta (68.40N, 133.80W)	White spruce (*Picea glauca (Moench) Voss.*)	21	Average of 5- and 25-year segments	1550	2014
Canada	Old Crow (67.5696N, 139.8288W)	White spruce (*Picea glauca (Moench) Voss.*)	12	5-year Segments	1698	2017
Canada	Scree Hill (65.07N, 138.157W)	White spruce (*Picea glauca (Moench) Voss.*)	20	5-year segments	1738	2005

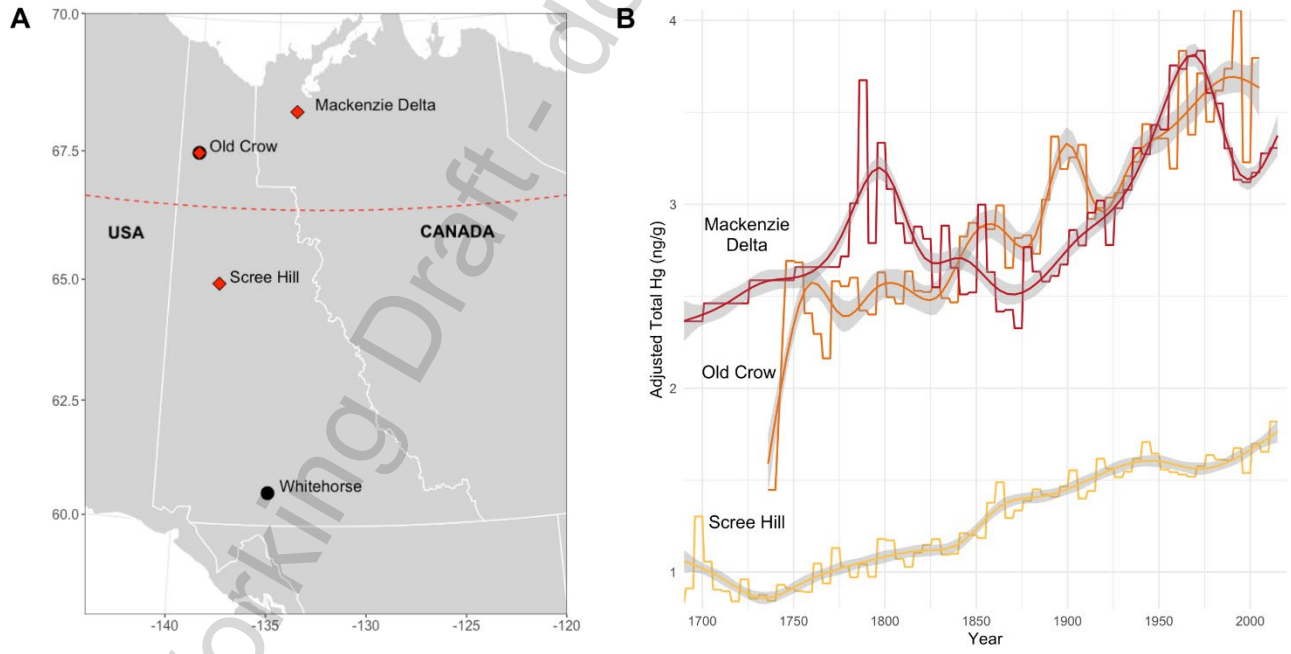

Figure 2.9. Results of temporal analysis of mercury concentrations in tree rings. (A) is an overview of time series locations. The red dashed line indicates the 60°N. The black circles are communities in the Yukon and the red diamonds represent the sample locations for the temporal mercury series. (B) A comparison between tree ring mercury temporal trends from Mackenzie Delta, Northwest Territories

(red), Old Crow, Yukon (orange), and Scree Hill, Yukon (yellow). Site average records are represented by the ridged line and the smooth line represented a 15-knot cubic spline with a 95% confidence interval. Site averages are only calculated for time periods that have at least three trees.

2.5.5 Power Analysis for Wildlife Time-Series

Text to be developed: Power and adequacy of the datasets to successfully detect significant changes are important considerations for temporal assessments, and for statistical comparisons in general.

2.6 Are concentrations of mercury changing significantly in Northern humans over time?

The results of trend analysis in human biomedia are summarized in Table 2.6.

Table 2.6. Results of temporal analysis of mercury concentrations (µg L^{-1}) in human blood.

TO BE COMPILED/INSERTED

Text to be developed

TO BE INSERTED Figure 2.6. Selected trends of total mercury in blood of northern humans (µg L-1).

2.7 Key Conclusions

Text to be developed

References

3000

* This is Chapter 3 of the AMAP Mercury Assessment*

3001
3002
3003

Chapter 3: Changes in Arctic mercury levels: emissions sources, pathways and accumulation

Addresses the policy question: Where does mercury in the Arctic environment come from, and how does it get there?

Coordinating lead author: Ashu Dastoor (ashu.dastoor@canada.ca)

Authors/Co-authors:

Section 3.2: **Simon Wilson**, Johannes Bieser, Marilena Muntean, Frits Steenhuisen

Section 3.3: **Ashu Dastoor, Theodore Dibble**; **Huiting Mao**; Kenjiro Toyota; **Leiming Zhang, Colin Thackray**, Yanxu Zhang, Anne Soerensen, **Hélène Angot**, Oleg Travnikov Tom Douglas, Sandy Steffen, **Daniel Obrist**, Martin Jiskra, **Rob Mason**, Brian DiMento, Yanxu Zhang

Section 3.4: **Erin Trochim, Martin Jiskra**, **Daniel Obrist**, Kyra St. Pierre, **Tom Douglas, Jane Kirk**, Derek Muir, Sarah Roberts, **Peter Outridge**, Jeroen Sonke, Cuicui Mu, Tingjun Zhang, **Kyra St. Pierre**, Christian Zdanowicz

Section 3.5: **Peter Outridge,** Lars-Eric Heimbuerger, **Rob Mason**, Brian DiMento, Jane Kirk, Carl Lamborg, Anne Soerensen, Yanxu Zhang

Section 3.6: **Christian Zdanowicz**

Section 3.7: **Ashu Dastoor**, Oleg Travnikov and modeling team

Section 3.8: **Ashu Dastoor**, Oleg Travnikov and modeling team

Data Contributors: Kyllönen Katriina, Michelle Nerentrop, Katarine Gårdfeldt, Sofi Jonsoon

3024
3025
3026
3027

3028 **Table of Contents**

3.1 Where does mercury in the Arctic environment come from, and how does it get there?

[Introduction] Author: Ashu Dastoor

Evidence of notable increase in mercury (Hg) concentrations in present-day Arctic environments compared to preindustrial levels while anthropogenic sources of Hg within the region are scant led to considerable scientific investigation in past few decades revealing that most Hg in the region is sourced from outside the Arctic (AMAP, 2011). Mercury is released into the air from both anthropogenic and natural sources in inorganic form, which then circulates and accumulates in global environments through a series of complex physicochemical processes involving advection, diffusion, chemical and phase transformations and exchanges between air, land and water. Mercury enters the Arctic via a number of pathways, including the atmosphere, river exports and ocean currents. Arctic being a large and remote region, there is still paucity of measurements of Hg in Arctic physical environments, especially the Arctic Ocean. However, major ongoing measurements efforts (e.g.,GEOTRACES; REF) and new techniques such as mercury stable isotopic signatures (REF) have elucidated Hg pathways with greater clarity since the last AMAP Hg assessment (REF). Strides have also been made in understanding of mercury chemistry and development of atmospheric Hg models for the Arctic (REFS). The aim of this chapter is to assess the impact of global sources of mercury emission on the present-day mercury levels in the Arctic ecosystems based on progress made in measurements and process-based model simulations in the past decade. The chapter provides a quantitative synthesis of recent advances in knowledge of the global sources of mercury emissions, and spatial distributions and total mercury budgets of both inorganic and organic mercury in Arctic atmospheric, terrestrial and marine environments.

The main species of Hg emitted to the atmosphere, gaseous elemental mercury (Hg(0)), has a long residence time in air (months; REF); thus, Hg(0) undergoes long-range transport (REF). Direct uptake of ambient Hg(0) by vegetation is a major pathway for its removal from the atmosphere. In air, Hg(0) reacts with strong oxidants, such as halogens, to form oxidized mercury species (Hg(II)), which have relatively short atmospheric residence times and therefore are rapidly deposited to underlying surfaces, such as landscapes and water bodies (REF). In polar regions, the oxidation of Hg(0) and subsequent deposition as Hg(II) is enhanced during polar spring due to dramatic increase in photochemical production of bromine species from snowpacks over sea ice, a phenomena called Atmospheric Mercury Depletion Events (AMDEs). Arctic Ocean during springtime provides the physical and chemical conditions required for atmospheric transformation and deposition of Hg (Moore et al.REF). In contrast, Hg inputs via oceans, rivers, and coastal erosion already comprise mainly inorganic Hg(II), as well as small amounts of methylated Hg(II) and dissolved gaseous Hg(0), because of transformations that occurs in these reservoirs before Hg reaches the Arctic environment. Only a very small fraction of Hg present in the environment is in the organic form (referred to as methylmercury (MeHg)). MeHg is produced from inorganic Hg species mainly in aquatic ecosystems

through biochemical processes mediated by naturally-occurring microorganisms. Since MeHg is the mercury species that biomagnifies in food chains, it is important to know where and how much of the MeHg is present in Arctic environments.

The chapter begins by describing the global sources of emissions that contribute to mercury contamination in the Arctic (Section 3.2). Mercury emissions sources are followed by up-to-date understanding of processes involved in Hg transport to and accumulation in the Arctic, and levels of Hg in Arctic atmosphere, terrestrial and marine environments (Sections 3.3-3.5). Hg exchange fluxes between air, and soils, vegetation, cryosphere and water are also reported in Section 3.3-3.5. Removal of mercury from the biologically-active Arctic environments occurs through burial of Hg in long-term storage archives such as lake sediments, ocean sediments, subsurface soils, and glacial ice; these estimates are presented in the above sections. In addition, the chapter also discusses potential contributions of melting permafrost (Sections 3.4.5), and ice sheets, ice caps and glaciers (Sections 3.6) to downstream Arctic environments. Source apportionment of Hg in the Arctic with respect to emission sources is presented in Section 3.7-3.8. Section 3.9 provides a comprehensive picture of the mass balance of mercury circulating in Arctic environments. Key results and knowledge gaps are summarized in Section 3.10. Processes leading to or affecting mercury uptake by biota are described in the next chapter.

3.2 What (and how much) are the sources of mercury emissions to air contributing to mercury in Arctic environments?

[provide estimates of Hg emissions from natural and anthropogenic sources to air]

Authors: **Simon Wilson**, Johannes Bieser, Marilena Muntean, Frits Steenhuisen

3.2.1 Global estimates of natural and anthropogenic mercury emissions to air

The *Global Mercury Assessment 2018* (AMAP/UN Environment, 2019) presents an updated global mercury budget that estimates present day, total global emissions of mercury to air at approximately 8000 t per year; 4600 t per year from terrestrial sources and 3400 t from marine sources. These emissions comprise ca. 500 t from natural (geogenic) sources; ca. 1600 t from re-emissions from soil, vegetation and open biomass burning and 3400 t evasion from surface ocean waters; and ca. 2500 t from anthropogenic sources. The atmosphere is estimated to hold ca. 4400 t of mercury, representing a percentage increase due to human activities of ca. 450%, see Figure X1.

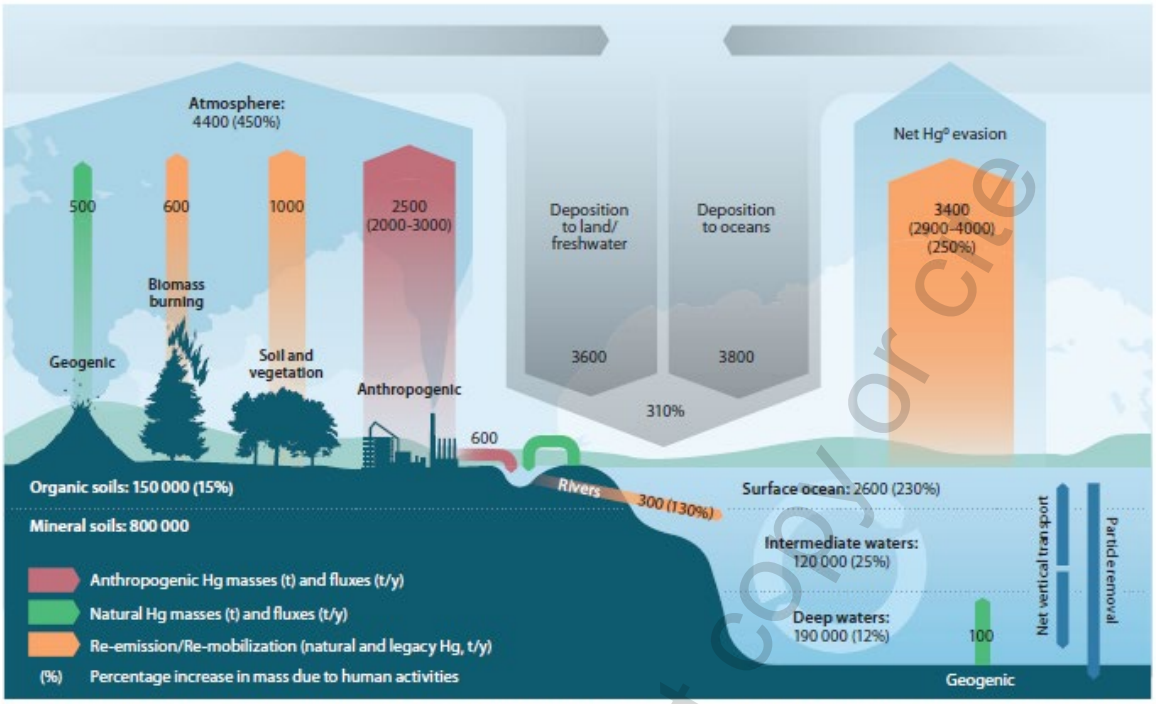

Figure 2.3 Updated global Hg budget showing the anthropogenic impact on the Hg cycle since the pre-anthropogenic period (prior to 1450 AD) (see text for explanation of its derivation). Ranges are given in brackets after the best estimate values; percentages in brackets represent the estimated increase in mass or flux due to human activities since the pre-anthropogenic period (i.e., pre-1450 AD).

Figure X1 …[= GMA 2018 Figure 2.3]

Although current annual emissions to air from anthropogenic sources (contributing ca. 30%) and natural sources (contributing <10%) are substantially lower than re-emissions/evasion from soils/vegetation and surface ocean waters, which contribute ca. 60%, it should be recognized that the latter – essentially a result of natural processes – are themselves partly (largely?) a consequence of the build-up of mercury in the environment following historical anthropogenic emissions and releases. Action to reduce present day anthropogenic mercury emissions and releases, through for example the global Minamata Convention on mercury, is therefore the key to reducing further accumulation of mercury in environmental media and future re-emissions of mercury.

The global budget further includes an estimate of ca. 600 t of mercury released to aquatic environments in 2015 from anthropogenic sources; an amount that does not include releases associated with artisanal and small-scale gold mining (ASGM) activities, which are estimated to contribute ca. 1200 t of mercury in combined releases to land and water in 2015 (AMAP/UN Environment, 2019). These releases are additional to the significant contribution that ASGM makes to emissions to air.

3.2.2 Anthropogenic emissions

3.2.2.1 Global anthropogenic emissions in 2015

As part of the work to produce the *Global Mercury Assessment 2018* (UN Environment 2019), a joint AMAP/UN-Environment expert group was established to prepare a global inventory of mercury

3147 emissions to air from anthropogenic sources in 2015. This work built on earlier AMAP global
3148 anthropogenic emissions inventory work reported in AMAP metals/mercury assessments (AMAP
3149 1998, 2005, 2011) and applied a revised methodological approach that was introduced in preparing
3150 the global inventory for 2010 (AMAP/UNEP, 2013).

3151 Results of this 2015 anthropogenic emissions inventory are presented in detail in the *Technical*
3152 *Background report to the Global Mercury Assessment 2018* (AMAP/UN Environment, 2019). The
3153 inventory estimates national emissions for ca. 220 countries in 11 (sub-continental) regions for each
3154 of 17 main emission sectors. Tables Y1 and Y2 and Figures X2 summaries the resulting 2015
3155 emission estimates, which total ca. 2220 t (2000-2820 t), by region and sector.

3156

▼ Quantities of mercury emitted to air from anthropogenic sources in 2015, by different sectors in different regions.

	Sector group (emissions, tonnes)				Regional total (range), tonnes	% of global total
	Fuel combustion	Industry sectors	Intentional-use (including product waste)	Artisanal and small-scale gold mining		
Australia, New Zealand & Oceania	3.57	4.07	1.15	0.0	8.79 (6.93-13.7)	0.4
Central America and the Caribbean	5.69	19.1	6.71	14.3	45.8 (37.2-61.4)	2.1
CIS & other European countries	26.4	64.7	20.7	12.7	124 (105-170)	5.6
East and Southeast Asia	229	307	109	214	859 (685-1430)	38.6
EU28	46.5	22.0	8.64	0.0	77.2 (67.2-107)	3.5
Middle Eastern States	11.4	29.0	12.1	0.225	52.8 (40.7-93.8)	2.4
North Africa	1.36	12.6	6.89	0.0	20.9 (13.5-45.8)	0.9
North America	27.0	7.63	5.77	0.0	40.4 (33.8-59.6)	1.8
South America	8.25	47.3	13.5	340	409 (308-522)	18.4
South Asia	125	59.1	37.2	4.50	225 (190-296)	10.1
Sub-Saharan Africa	48.9	41.9	17.1	252	360 (276-445)	16.2
Global inventory	533	614	239	838	2220 (2000-2820)	100.0

12

3157

3158 *Table Y1 ...*

▼ Quantities of mercury emitted to air from anthropogenic sources in 2015, by different sectors.

Sector	Mercury emission (range), tonnes	Sector % of total
Artisanal and small-scale gold mining (ASGM)	838 (675-1000)	37.7
Biomass burning (domestic, industrial and power plant) *	51.9 (44.3-62.1)	2.33
Cement production (raw materials and fuel, excluding coal)	233 (117-782)	10.5
Cremation emissions	3.77 (3.51-4.02)	0.17
Chlor-alkali production (mercury process)	15.1 (12.2-18.3)	0.68
Non-ferrous metal production (primary Al, Cu, Pb, Zn)	228 (154-338)	10.3
Large-scale gold production	84.5 (72.3-97.4)	3.8
Mercury production	13.8 (7.9-19.7)	0.62
Oil refining	14.4 (11.5-17.2)	0.65
Pig iron and steel production (primary)	29.8 (19.1-76.0)	1.34
Stationary combustion of coal (domestic/residential, transportation)	55.8 (36.7-69.4)	2.51
Stationary combustion of gas (domestic/residential, transportation)	0.165 (0.13-0.22)	0.01
Stationary combustion of oil (domestic/residential, transportation)	2.70 (2.33-3.21)	0.12
Stationary combustion of coal (industrial)	126 (106-146)	5.67
Stationary combustion of gas (industrial)	0.123 (0.10-0.15)	0.01
Stationary combustion of oil (industrial)	1.40 (1.18-1.69)	0.06
Stationary combustion of coal (power plants)	292 (255-346)	13.1
Stationary combustion of gas (power plants)	0.349 (0.285-0.435)	0.02
Stationary combustion of oil (power plants)	2.45 (2.17-2.84)	0.11
Secondary steel production *	10.1 (7.65-18.1)	0.46
Vinyl-chloride monomer (mercury catalyst) *	58.2 (28.0-88.8)	2.6
Waste (other waste)	147 (120-223)	6.6
Waste incineration (controlled burning)	15.0 (8.9-32.3)	0.67
Total	*2220 (2000-2820)*	*100*

Colour coding indicates main sector groups
(**Stationary combustion**, dark blue; **Industry**, light blue; Sectors associated with **Intentional use**, dark orange; **ASGM**, light orange).

* Sectors included for the first time in the 2015 inventory.

Table Y2 ...

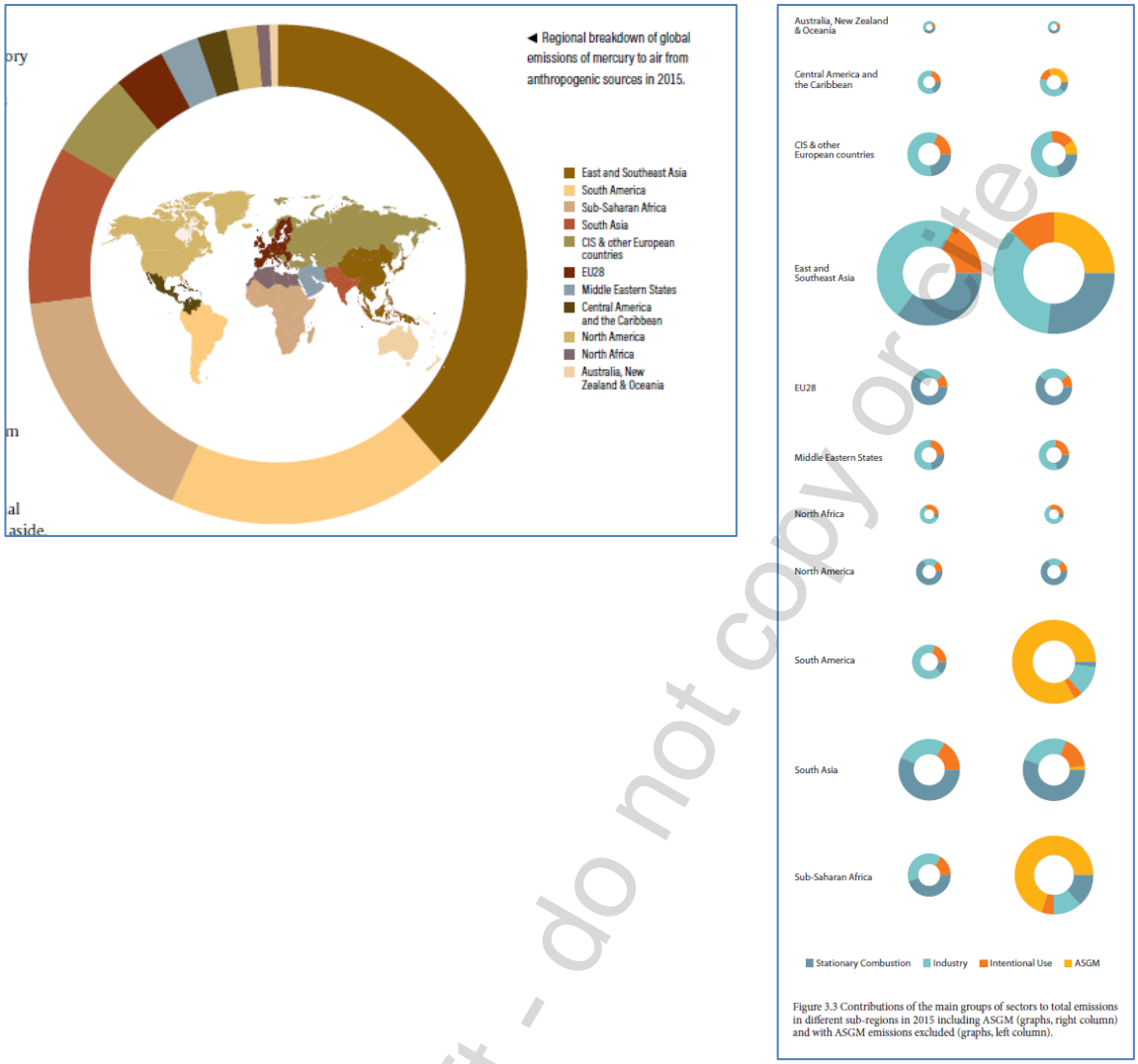

Figure X2 SELECT FROM ABOVE FIGURES AND/OR CROSS REF TO FIGURE IN 3.2.3.3

The 2015 inventory (AMAP/UN Environment, 2019) estimates identify sources in Asia as responsible for about 50% of global mercury emissions in 2015, with East and Southeast Asia contributing ca. 40% and South Asia 10% (see Figure X2). This reflects the growth in industrial development in these regions in recent decades and, in particular, the use of coal as a primary source of energy. Stationary combustion of fossil fuels and biomass burning is responsible for some 24% of global estimated emissions (21% from coal burning). Industrial activities involving high temperature processes, such as metal smelting and cement production are responsible for a further 28% of global emissions.

The other main sources of mercury emissions are associated with intentional use of mercury. These include use in mercury–added products such as lamps, batteries, and instruments, etc., as well as in dental amalgam, all of which generate wastes that are sources of emissions, especially where wastes are subject to uncontrolled burning. They also include mercury use in industrial processes, such as manufacture of vinyl chloride and chlor-alkali production using the mercury process. However, by far

the largest source of mercury emissions from intentional mercury use is that associated with ASGM, which globally is estimated to contribute ca. 38% of the total anthropogenic emissions inventory. ASGM contributes ca. 70% and up to 80% of emissions in South America and Sub-Saharan Africa, respectively, as well as contributing a significant part of the emissions in East and Southeast Asia. As a result, South America and Sub-Saharan Africa are responsible for ca. 18% and 16% of the global emissions, respectively. However, if ASGM emissions are excluded, the pattern of regional contributions changes and South America, in particular, is far lower in the ranking. Overall, the patterns of both regional and sectoral contributions to global emissions in 2015 were similar to those in 2010.

The inventory methodology also recognizes that there may be additional emissions from sectors that it is not possible to quantify using the current methodology and available data, and that these could contribute an additional few tens to hundreds of tonnes of mercury emissions per year. These include anthropogenic emissions associated with incineration of industrial and sewage sludge and some hazardous wastes, oil and gas extraction (upstream of refineries) and agricultural burning. Some of these sources may be significant in a local and/or Arctic context.

Global mercury emissions inventories prepared by EDGAR (see section XXX) do include estimates of emissions from agricultural burning, totaling ca. 90 tonnes in 2012. Mercury emissions from field burning of agricultural residues are estimated for individual countries in EDGARv4.tox2. The EDGAR agricultural emissions estimates over the period 1970-2012 show a consistent increasing trend, almost doubling since 1970. In 2012, their share in total (EDGAR) global mercury emissions was about 5%, with greatest contributions from Brazil (17%), India (15%) and Indonesia (11%).

Comparing the 2015 global inventory results with other national and regional emissions estimates is not straight-forward. No comparable global inventories exist for 2015.

Muntean et al (2018) compared global emissions estimates from the Emission Database for Global Atmospheric Research (EDGAR) database for 2010 (totaling ca. 1770 t) with 2010 GMA inventory estimates reported in AMAP/UNEP (2013) (which after update in 2018 total ca. 1810 t).

Comparisons of the 2015 GMA inventory estimates with preliminary national estimates prepared as Minamata Initial Assessments (MIAs) for a number of mainly developing countries lacking routine emissions reporting mechanisms (ADD REF) revealed inconsistencies (AMAP/UN Environment, 2019). In some cases these could be explained by the fact that MIA estimates applied activity data for recent years rather than a specific target year (as for the 2015 global inventory. Together with emissions factors, activity data – data on production of industrial materials and mercury-added products, and consumption of raw materials including fossil fuels – form the basis for most national/regional emissions estimates. Both emissions factors and activity data have associated uncertainties that were considered in the inventory work. Measurement-based emissions are still only

available for a relatively few, generally large, point sources of emissions, and these have other sources of uncertainties when used to calculate annual emissions totals. Comparisons with other national estimates from countries that maintain emissions inventory systems and with regional estimates for 2015 reported under the UN ECE Convention on Long-range transboundary air pollution (LRTAP) indicated a generally reasonable level of consistency with respect to national total emissions, considering the associated uncertainties (AMAP/UN Environment, 2019). However, estimates for particular emissions sectors were more variable; reflecting to a large degree differences in the way emissions are classified or categorized under different mercury emissions reporting systems, many of which have been adapted from systems developed for reporting emissions of other pollutants. These are major considerations that would need to be addressed in any regulatory emissions reporting context. [POLICY-RELEVANT CONCLUSION]

3.2.2.2 Geospatial distribution

An important additional component of the work on the 2015 inventory was its geospatial distribution, to generate datasets that could be used by modelers investigating, for example, long-range atmospheric transport of mercury (see section ZZZ). This work comprised allocation of national mercury emissions totals to specific point sources or their area-wide distribution (within 0.25 degree grid cells), based on expected emissions distributions for the sectors concerned. The methods applied, and results of this work are detailed in Steenhuisen and Wilson (2019); Figure X3 presents the geospatially distributed inventory (for total mercury emissions) viewed from an Arctic perspective.

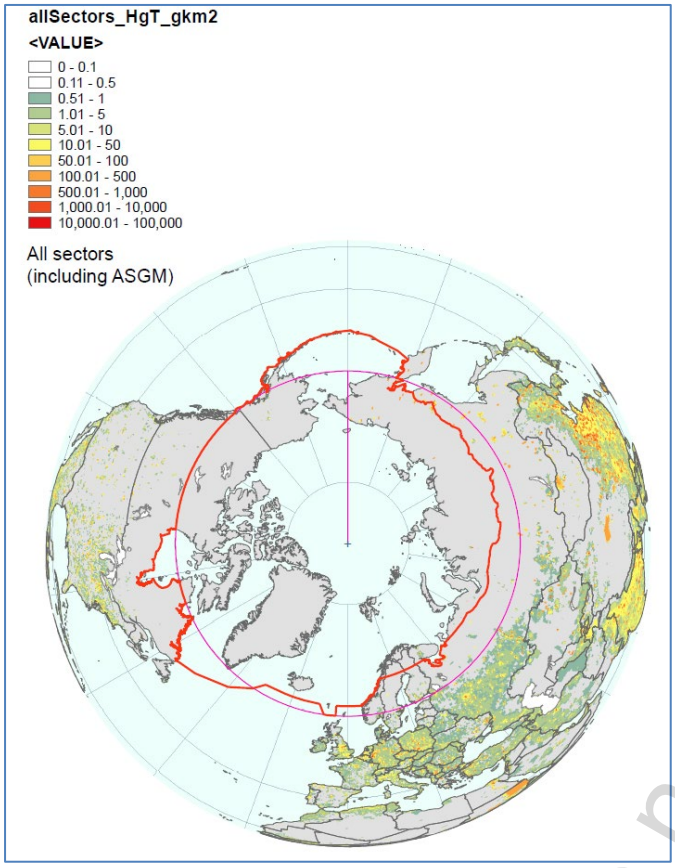

Figure X3 …[g/km2 or tonnes per cell?]

3.2.2.3 Trends in anthropogenic emissions

Mercury emissions to air have changed over time. Historically gold and silver mining have been major sources of mercury emissions and releases. With the advent of the industrial revolution (ca. 1850s) and the subsequent rise of fossil fuel economies, mercury emissions increased (AMAP 2011; AMAP/UN Environment, 2019). Emissions during the first part of the 21st century are estimated at around 2000-2500 tonnes per year, increasing in some geographical regions and decreasing in others.

Comparisons between global anthropogenic emission inventories produced at different times since the 1990s (Pacyna and AMAP REFS) is complicated by the fact that over time additional sectors have been added to the inventories, as well as changes in applied methods for calculating emissions.

In the GMA 2018 work (AMAP/UN Environment, 2019) it was only considered appropriate to compare the 2015 inventory results with results for the 2010 inventory (AMAP/UNEP 2013), which was prepared using a similar methodology, and then only after the latter had been updated to introduce new sectors considered in 2015 (e.g. biomass burning in power generation, industry and domestic), newly available 2010 activity data, and some changes in methods for calculating emissions from ASGM and disposal of mercury-added product wastes). The results (Figure X4) indicate that

estimated global anthropogenic emissions of mercury to the atmosphere for 2015 are approximately 20% higher than in 2010. Within this trend, modest decreases in emissions in North America and the European Union (associated with continuing action to reduce emissions and shifts in fuels used for energy – away from coal) are more than offset by increased emissions in other regions, Asia in particular. The overall trend appears to reflect a continuation of an upturn in global emissions, following decreasing emissions during the last decade(s) of the 20th century as described in previous AMAP work (AMAP, 2011).

This contrasts somewhat with results of global emissions estimates from EDGAR (Muntean et al 2014, 2018) which show an increasing rather than decreasing trend in global emissions in the last decades of the 20th century. Muntean et al. (2018) report global anthropogenic mercury emission trends over the period 1970-2012 based on analysis of data compiled in the Emission Database for Global Atmospheric Research (EDGAR) (see Figure X4). The EDGAR dataset applies a consistent methodology across all years. They show global emissions (excluding ASGM) increasing by 45% over the period 1970-2012 (Muntean, pers.comm.).

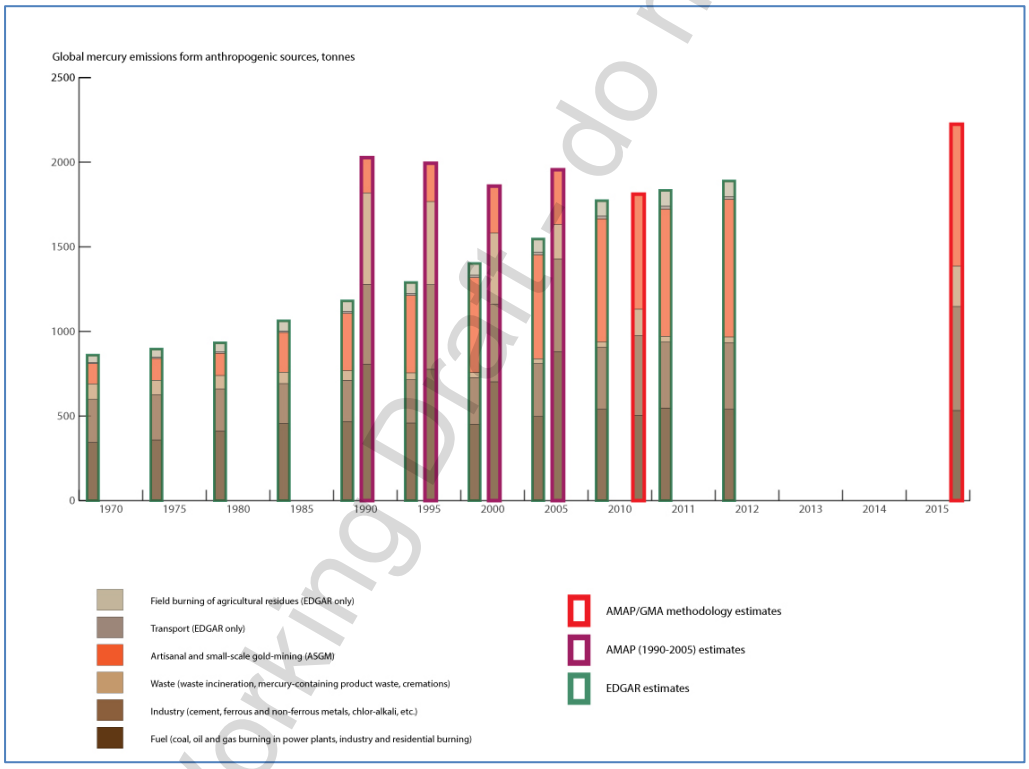

Figure X4 …. [THIS IS A NEW COMBINED FIGURE SHOWING EDGAR TRENDS FOR 1970-2012, AMAP PUBLISHED (CA. PACYNA ET AL) ESTIMATES FOR, 1990/1995/2000/2005 AND AMAP-GMA ESTIMATES FOR 2010 AND 2015 …. NEED TO MAKE CLEAR THAT ESTIMATES PRODUCED USING DIFFERENT METHODS WONT BE DIRECTLY COMPARABLE]

Analysis of the magnitude of changes in estimated emissions between 2010 and 2015 by region and sector reveals that emissions in North America and the EU28 decreased across most sectors, resulting in modest decreases (ca. 11 tonnes) in total estimated emissions in each of these two regions Table Y3]. In all other regions, total regional emissions increased between 2010 and 2015. In some regions, notably South America, increased ASGM activity contributed significantly to the increased emission both in percentage and absolute terms; in others, such as East and Southeast Asia, increased emissions are associated with industrial development and therefore reflected in industry and energy sectors, in particular non-ferrous metal production (NFMP). On a percentage basis, the greatest increase (ZZ%) was associated with mercury production in Central America and the Caribbean, due to new mercury production from mines in Mexico, and also industrial coal combustion in the same region (ZZZ%), but this corresponds to only a few tonnes of emitted mercury. In absolute terms, the sectors showing the largest increases in estimated emissions were ASGM, NFMP, cement production, mercury-product waste disposal, and coal combustion in power plants, contributing respectively, 159, 79, 47, 32 and 24 tonnes in a total increase for all sectors of 413 tonnes. Sectors with decreasing estimated emissions included (mercury process) chlor-alkali production, which is being phased-out globally, and oil combustion in industry; however, the associated reductions were relatively small in absolute terms (6 and 2 tonnes, respectively). In general, apart from ASGM-related emissions, mercury emissions are strongly related to 'industrial activity' that in most regions reflects consumption of fuels and raw materials to produce energy, cement, and ferrous and non-ferrous metals, etc. and increased industrial activity in many regions more than offsets emissions reductions achieved through, for example, greater application of air pollution control devices.

Absolute change by sector group (kg)					
	Fuel	Industry	Waste	ASGM	Total
Australia, New Zealand & Oceania	-355	62	314	0	21
Central America and the Caribbean	-66	4125	885	2220	7165
CIS & other European countries	-2203	8419	4587	675	11479
East and Southeast Asia	16270	114400	62318	-30244	162745
EU28	-1822	-2593	-6599	0	-11015
Middle Eastern States	-514	3625	3358	225	6694
North Africa	289	340	2217	0	2846
North America	-7123	860	-4966	0	-11229
South America	1407	946	76	162699	165128
South Asia	25601	10257	9992	3375	49224
Sub-Saharan Africa	-2101	1620	10566	19850	29935
Grand Total	29384	142060	82748	158800	412992

Percentage change by sector group					
	Fuel	Industry	Waste	ASGM	Total
Australia, New Zealand & Oceania	-9.0	-9.0	-9.0	-9.0	-9.0
Central America and the Caribbean	-1.1	27.6	15.2	18.4	18.6
CIS & other European countries	-7.7	15.0	28.4	5.6	10.2
East and Southeast Asia	7.6	59.5	132.5	-12.4	23.4
EU28	-3.8	-10.5	-43.3		-12.5
Middle Eastern States	-4.3	14.3	38.5		14.5
North Africa	27.1	2.8	47.5		15.8
North America	-20.9	12.7	-46.2		-21.8
South America	20.6	2.0	0.6	91.6	67.6
South Asia	25.9	21.0	36.8	300.0	28.0
Sub-Saharan Africa	-4.1	4.0	161.0	8.6	9.1
Grand Total	5.8	30.1	52.9	23.4	22.8

Table Y3

In addition to the challenges in comparing national/sector estimates over time, there are similar challenges with respect to comparing geospatially distributed emissions for different years/periods, which have the added complexity of documenting changes in locations of emissions in terms of, in particular at major point sources. Information concerning new power plants and industrial facilities, closure of plants and changes in fuels and technology applied at energy production and industrial facilities to, e.g., control emissions is generally lacking and unavailable in the public domain. This is a particular problem in areas with rapidly developing economies and in countries lacking consistent long-term tracking of mercury emissions. [POLICY-RELEVANT CONCLUSION]

The trends in increasing anthropogenic emissions in recent years are poorly?? Reflected in current atmospheric trends in air concentrations observed at Arctic background air monitoring sites, most of which show decreasing trends. Trends in air concentrations are discussed in detail in section XXX, This inconsistency between emissions estimates and air concentration trends may be related to proximity of monitoring sites to regions where emissions have declined significantly in recent decades (North America and Europe) or to effects of changes in speciation of emitted mercury (see section 3.2.2.4) but is a subject requiring further investigation. [FUTURE WORK]

3.2.2.4 Mercury emissions speciation

An acknowledged deficiency in the GMA inventory work and its associated geospatial distribution concerns the approach currently employed to define the mercury species that are emitted to the atmosphere. The GMA work applied an outdated and simplistic generic speciation scheme to classify total (HgT) mercury emissions between gaseous elemental mercury (GEM, Hg^0), divalent/reactive

mercury (Hg^{2+}) and particulate mercury according to the source sector concerned. [NB: NEED TO STANDARDIZE ON NOTATION FOR SPECIES THROUGHOUT REPORT] Mercury species emitted depend on a number of factors, including the air pollution control devices (APCDs) that are applied at emission point sources. Application of APCDs has changed considerably over recent decades, with developments taking place in different countries at different times. The applied GMA inventory methodology attempts to reflect this in terms of quantifying emission totals, but this has not been reflected in GMA inventory geospatial distribution work to date – although the most recent inventory tools allow for this to be done, it has been outside the scope of the work.

A large number of recent publications have documented specification aspects of emissions, generally at large point sources such as power plants, smelters and other industrial facilities, in particular in Asia (add REFs). This represents a considerably body of new information available to improve speciation schemes.

Muntean et al. (2018) performed a comprehensive literature review on mercury speciation for different sectors and developed three retrospective emissions scenarios based on different hypotheses related to the proportion of mercury species in the total mercury emissions. The reference scenarios the split factors provided in AMAP/UNEP (2008). This scheme has been applied to all global anthropogenic emissions inventories reported in AMAP and UN-Environment GMA work (inventories for the years 1990-2015), as well as in EDGARv4.tox2. The other two scenarios apply split factors derived primarily from field measurements; from EPA's ICR (Bullock and Johnson, 2011) and from recent scientific literature (AMAP/UNEP, 2008; Chen et al., 2013; Friedli et al., 2001; Friedli et al., 2003a; Friedli et al., 2003b; Giang et al., 2015; Park et al., 2008; UNEP, 20 14; Wu et al., 2012; Zhang et al., 2015), respectively. The variation between the proportion of elemental mercury (Hg^0) and reactive mercury (Hg-P and Hg^{2+}) in the scenarios corresponding to the speciation scheme applied to the AMAP/GMA inventories and the scheme based on recent scientific literature for different sectors is presented in Figure (X6). The share of the total global mercury emissions that comprise reactive/particulate mercury emissions was 25.3% for the reference scenario, and 22.9% and 21.4% for the other two emissions scenarios. However, regional mercury speciation footprints may differ considerably depending on the characteristics of mercury emitting sources located in different regions (see details in Muntean et al., 2018). Much of the recent literature on emissions speciation at industrial facilities concerns plants in East Asia (China, Japan and Republic of Korea). An evaluation of the three scenarios using the GEOSChem global 3-D mercury model showed a variation in deposition estimates of approximately ±10%. A comparison with measurements within a nested grid in sensitivity simulations for the United States indicated that speciated emissions estimated based on field measurements can improve wet deposition estimates near sources.

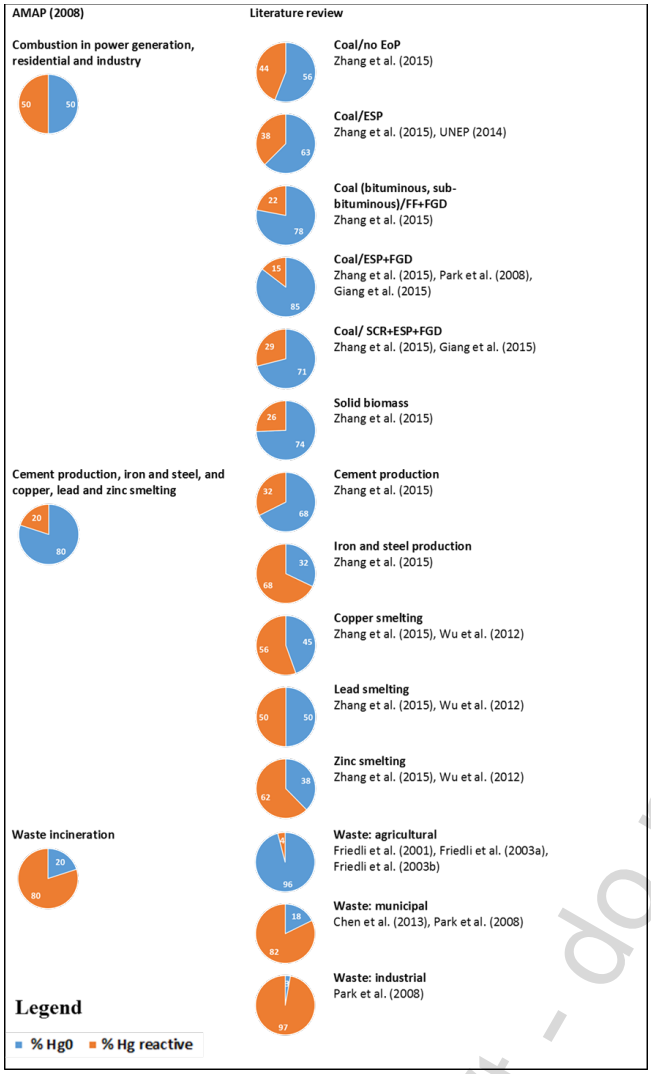

Figure X6 …

Changes in speciation from GEM/Hg^0 to particulate or reactive mercury species would imply that mercury may be captured or deposited closer to its source regions and therefore have less potential for transport to the Arctic.

Appropriate speciation of (geospatially distributed) mercury emissions datasets is important to modelling atmospheric transport from source to receptor regions including the Arctic (see section xxx). Newly available information on speciation of emissions at major point sources presents the possibility for better addressing this aspect in future work; however, a significant gap in knowledge still concerns the fate of mercury emitted from ASGM activities. Mercury used to amalgamate/concentrate gold is evaporated to recover the gold and is therefore by definition emitted as GEM/Hg^0. ASGM emissions occur close to the ground and thus the emitted mercury may be subject to chemical transformations through interaction with surfaces that alter speciation more

rapidly than might be the case for GEM emitted for example from power plant stacks.

[KNOWLEDGE GAPS AND FUTURE WORK]

3.2.2.5 Anthropogenic emissions and releases in an Arctic context

In the GMA work (AMAP/UN Environment, 2019) an updated mercury budget for the Arctic Ocean was prepared [ADD CROSS-REF TO SECTION IN ASSESSMENT WHERE THIS IS DISCUSSED], and the Arctic region was also evaluated in atmospheric transport source-receptor modelling work [ADD CROSS-REF TO SECTION IN ASSESSMENT WHERE THIS IS DISCUSSED].

Sources within the Arctic region (north of 60 degrees N) contribute only a small part of the global anthropogenic mercury emissions, ca. 14 tonnes (<1%) of the total estimated inventory of 2220 tonnes in 2015. The respective contributions from different countries are shown in Table Y4.

Country	Estimated anthropogenic emissions (N of 60 degree N) in 2015, kg
Canada	354
Kingdom of Denmark – Faroe Islands	0.86
Kingdom of Denmark -Greenland	0.54
Finland	910
Iceland	21
Norway (mainland)	237
Norway (Svalbard, Jan Mayen)	6.1
Russia	12100
Sweden	106
United Kingdom (Shetland Islands)	0.47
United States (Alaska)	124
Total	**13860**

Table Y4 – Emissions in the Arctic region (N of 60 degrees) sources

The majority of the anthropogenic emissions in the Arctic region occurs in Russia, and is associated with relatively few point sources, including the non-ferrous metal smelters at Norilsk and on the Kola Penninsula (see Figure X7). The Arctic also hosts coal-fired power plants, with other industrial facilities (including cement and ferrous metals production, mining and oil refining operations) in or in close proximity to the Arctic. In North America, small point source emissions are associated with diesel generators and waste dumps in a number of communities; similar emission occur in other parts of the Arctic but locations of these sources are not defined in the available datasets.

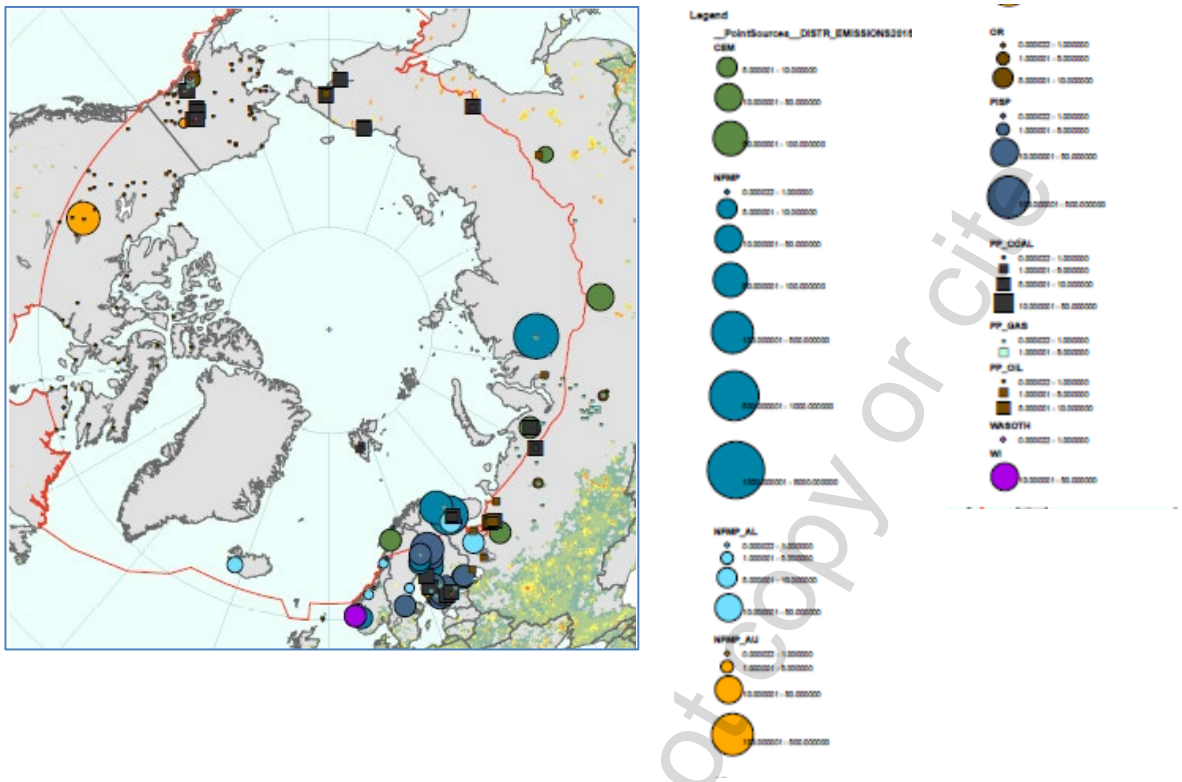

Figure X7 … Locations of point source mercury emissions in the Arctic

3380

3381 Although the anthropogenic emissions within the Arctic region are small, it should be recognized that
3382 the Arctic Council countries contribute significantly to global emissions, and together with Arctic
3383 Council Observer countries were responsible for ca. 44% of the estimated global anthropogenic
3384 emissions in 2015 (see Table Y5).

3385

Country	Total estimated emissions 2015, tonnes (AMAP/UN-Environment, 2019)	% Global total	Change in estimated emissions 2010-2015 (+ increase; - decrease)
Austria	0.92		-8.3
Belgium	1.18		-17.1
Bulgaria	9.62		11.9
Canada	4.02		-14.3
Denmark	0.43		-35.9
Faroe Islands	0.00		42.7
Greenland	0.00		-43.5
Finland	1.21		-13.7
Iceland	0.03		-11.9
Norway	0.55		15.2

Russia	60.95		13.1
Sweden	0.86		-13.6
United States	36.33		-22.5
Arctic Council Members	116.1	5.2	-3.3
China	563.78		12.6
China – Hong Kong	1.46		12.5
France	3.79		-25.7
Germany	16.28		-1.4
India	205.86		28.1
Italy	4.09		-26.4
Japan	15.01		16.1
Republic of Korea	6.95		0.8
Netherlands	1.55		8.9
Poland	11.38		-8.4
Singapore	1.62		3.0
Spain	3.99		-29.0
Switzerland	0.58		20.0
United Kingdom	4.27		-18.4
Arctic Council Observers	840.6	37.8	14.2
Other EU	17.6	0.8	-20.8
Arctic Council members, observers and rest of EU	974.4	43.8	10.9

Table Y5 – Contributions of Arctic Council members and observers to global emissions in 2015, and changes in emissions between 2010 and 2015

3.2.3 Natural emissions and emissions as a result of natural processes with emphasis on sources relevant to the Arctic

(need to add a section on re-emission estimates)

Due to sparse population and limited human activities in the arctic, natural emissions play an important. Anthropogenic emissions are also an important input into the region, but need to be transported there via atmosphere or ocean. Moreover, a large fraction of mercury from atmospheric long range transport is deposited over land and ice and thus is subject to natural processes that can lead to storage or release of both natural and anthropogenic legacy pollution. Here, we do not explicitly distinguish between natural and anthropogenic legacy pollution and focus on the mass budget of mercury fluxes into the arctic atmosphere and ocean through natural processes such as

wildfires, thawing permafrost, and melting ice. Typically, emission inventories focus on mass input into a certain compartment. The arctic is a complex region comprised of various compartments (atmosphere, ocean, lithosphere, biosphere, cryosphere). Thus, here we focus on mercury fluxes from long term storages into the arctic atmosphere and ocean where it is readily transformed and transported.

3.2.3.1 Biomass burning

The term 'biomass burning' can refer to a range of different processes both anthropogenic and natural. Anthropogenic biomass burning typically means the intentional combustion of plant material in agriculture as means of waste incineration. More broadly it can also include energy production from biomass combustion. Here, we refer solely to natural emissions which are usually distinguished by using the term wild fires.

Wild fires include forest fires which make up the majority of the global emissions from this sector. However, they include a range of other sources such as grassland fires and smoldering natural fires (e.g. peat, bog, or subsurface coal-bed fires). Especially in the arctic region, in recent years, smoldering fires have been observed ever more frequent. Due to satellite observations, today it is possible to detect even small fires with remote sensing techniques using temperature anomalies. Based on calculations of total carbon emissions in the Global Fire Emission Database v4.1 (GFED4) we estimate the total Hg emission flux from wild fires within the arctic circle (Randerson et al., 2018). The emission factors for mercury from wild fires in the literature cover a large range from 18-34 µg/kg fuel for small scale fires and 58-640 µg/kg fuel for large scale fires (Battye and Battye, 2002; Urbanski, 2014; Webster et al., 2016). The discrepancy is partly due to the additional release of mercury from soils in large scale burns. Based on this, we estimate for the annual Hg flux from wild fires in the arctic over the last 20 years to be in the range of 3 000 – 14 000 kg Hg p.a.. However, the inter annual variability of wild fire emissions is large ranging from 500 kg in 2011 to 50 000 kg in 2001.

Moreover, to determine the impact of wild fires on the arctic mercury budget it is necessary to determine the long range transport of mercury from these sources. Numerical dispersion studies on the impact of wild fires on black carbon deposition in the arctic region can be used to estimate the mercury flux from these sources (Evangeliou et al., 2016). Mercury emitted from wild fires is either in the form of GEM that is readily transported via the atmosphere or in the form of oxidized mercury that will stick to the abundant carbon particles in the plume. Based on dispersion studies we estimate an additional 1 700 to 6 500 kg of mercury from wild fires outside the arctic circle to be transported to the arctic region per year. Finally, it has been shown that gaseous Hg forms effectively accumulate in tundra plants (Obrist et al., 2017)

3.2.3.2 Permafrost

Permafrost has been identified as a major global Hg storage. With 793±461 Gg Hg it contains more Hg than atmosphere, ocean, and all other soils together (Schuster et al., 2018). Through precipitation and seasonal thawing, mercury stored in the frozen soil is released and transported into the arctic ocean via rivers and rivulets. Moreover, the fraction of wildfire emissions deposited over the permafrost region and plant uptake of GEM by tundra biomass and subsequent release into the rivers is an additional pathway of mercury into the arctic hydrological cycle (Jiskra et al., 2018). The annual inflow of mercury through rivers has been a controversial subject to a range of studies including measurement campaigns and modeling. The annual riverine Hg inflow is estimated to be in the range of 45 000 – 62 000 kg p.a. (Dastoor and Dunford, 2014; Zhang et al., 2015). Based on model studies it is estimated that the ocean is a net source for atmospheric mercury. Current estimates are an average annual net release of 59 000 kg p.a. (Soerensen et al., 2016). This flux is in the same order of magnitude as the riverine inflow allowing the conclusion that Hg from permafrost is ultimately emitted into the atmosphere where it can be dispersed on a global scale.

The riverine outflow exhibits a large inter and intra annual variability. It has been shown, that thawing and associated flooding contribute disproportionately to mercury outflow in rivers. Sondergaard et al. (2015) showed for one basin that 10% of the water outflow was during flooding events, but 30% of the annual mercury load was associated to them. This implicates that rising temperatures will have a non linear effect on the release and subsequent transport of mercury to the arctic ocean. Finally, a major question is the fraction of mercury that is transported into the arctic ocean in the form of MeHg. It was found that about 1.7% of the mercury in rivers is in the form of MeHg (Sonke et al. 2018). This amounts to an annual inflow of 780 – 1050 kg of MeHg into the Arctic Ocean per year.

3.2.3.3 Glaciers and ice sheets

Greenland contains the second largest ice cap on Earth, containing about 2.5x106 km³ of ice, which is 10% of the global ice mass. The annual amount of melt water has been estimated based on remote sensing gravity data to be 239±23 km³ p.a. (Chen et al., 2016). The largest fraction of melt water runoff is found in east Greenland with 90 km³ p.a. in the south east and 74 km³ p.a. in the north east. This leaves 75 km³ p.a. of melt water from west Greenland. Additionally, to the Greenland melt water, there is currently an annual mass loss of 25-75 km³ observed in Svalbard.

There is a comparably rich data set of Greenland ice cores analyzed for mercury (Appelquist et al., 1978; Boutron et al., 1998; Zheng, 2015). The measured total mercury concentrations in ice cores are in the range of 1.0 – 3.2 p/g ice with highest levels were found between 1991 and 2000 which is in line with the European anthropogenic Hg emission development. Generally, the mercury content in the ice has been steadily increasing with peaks in the past probably caused by volcanic activity. On average THg concentrations increased over time with 1.0 pg/g in 1748-1850, 1.6 pg/g in 1851-1970, and 2.2 pg/g in 1971-2010. In total the Greenland ice sheet contains 2 500 to 5 500 tons of mercury.

To estimate the current inflow of mercury from Greenland melt water we use the most recent measurements of 1.7 pg/g THg in 2001-2010. Based on this we estimate an annual Hg inflow of 406±120 kg from Greenland and 126±37 kg from Svalbard.

Due to climate change the melting rate of the arctic ice sheets has been increasing in recent years (Zheng et al., 2015). This means, that in the next decade the ice with the highest mercury (3.2 pg/g) content due to high emissions in Europe and Russia in the 90ties will melt which will lead to an increased total water flux combined with increased mercury per km³. However, on the long term the amount of melt water will have to double in order to compensate for the lower THg concentrations (1.0 – 1.6 pg/g) in older ice layers.

Finally, we assess the fate of mercury from melting ice sheets in the arctic ocean. Due to the prevailing ocean currents, melt water from Svalbard will be transported northwards, while melt water from Greenland will be transported southwards with the east and west Greenland current. This means that the majority of melt water released from Greenland ice sheets will at first be transported away from the arctic region towards the Labrador Current. A fraction will eventually be transported to the Arctic Ocean with a significant lag time in the range of decades. In conclusion, the amount of mercury released from ice sheets makes up only a fraction of the annual inflow from arctic rivers and is mostly not directly transported into the arctic.

3.2.3.4 Climate change influences

The observed warming of the atmosphere has been especially pronounced in the arctic. With increasing temperatures all natural emission fluxes described above will increase over time. We already observe more forest fires and ground vegetation smoldering in the arctic tundra. Also forest fires outside the arctic will increase as well as a long range transport source of Hg to the area. The ice sheets in Greenland and Svalbard will melt with increasing velocity, however, the released amount of mercury will in time be compensated by lower concentrations in older ice layers. The thawing of permafrost, that is already the major source for mercury in the Arctic Ocean, will increase and potentially release vast amounts of the mercury stored therein. Permafrost, which is already a major flux of mercury into the arctic will become an even more important source. Finally, a major question for the net Hg budget in the arctic is the influence of reduced ice pack coverage of the arctic ocean. It is to be expected, that after centuries of being a sink, the arctic will become a major source for mercury in the global cycle due to increased air-sea exchange.

3.3 How much mercury does atmospheric circulation transport to Arctic environments?

[provides estimates of total and methyl Hg concentrations in the Arctic atmosphere and Hg exchange rates between air and Arctic ecosystems]

3.3.1 How does atmospheric Hg enter Arctic environments?

a. Atmospheric circulation Authors: **Ashu Dastoor**

In-situ measurements and modelling provide evidence for pollution transport to the Arctic from southern latitudes that is dominated by northern Eurasian sources in the lower troposphere in winter (e.g., winter and early spring haze) and by mid-latitude North American and Asian sources in mid troposphere to lower stratosphere (Fisher et al., 2010; Hirdman et al., 2010; Hecobian et al., 2011; Brock et al., 2011; Schmale et al., 2011; Sodemann et al., 2011; Stohl et al., 2006 & 2013; Law et al., 2014; Monks et al., 2015; Sharma et al., 2013; Arnold et al., 2016; Willis et al., 2018). In winter and spring, transport of anthropogenic mercury emissions from Eurasia led to the highest observed elemental mercury concentrations at Ny-Ålesund (Stohl et al., 2007, Hirdman et al., 2009). Fuelberg et al. (2010) noted that mid-latitude cyclones were more frequent and followed a more northerly course over eastern Asia and the northern Pacific, but were less common over the North Atlantic during spring. Evidence for springtime episodic transport of mercury from Asian sources to western North America is well documented (Jaffe et al., 2005; Weiss-Penzias et al., 2007, Obrist et al., 2008; Faïn et al., 2009b); these air plumes were shown to penetrate into the Arctic in a modeling study (Dastoor et al. ??). Add Hg transport event results from Durnford et al. 2011. Add any information available from vertical profile measurements (Slemr et al ??).

The thermal stratification of the lower atmosphere at high-latitudes, particularly during the winter months, causes an isolation of the high Arctic lower troposphere from lower latitudes creating a transport barrier referred to as the polar dome (coincident with Arctic front) (Klonecki, 2003). The polar dome exhibits a strong influence on the transport of air masses from mid-latitudes, enhancing it during winter and inhibiting it during summer. The spatial extent of the polar dome strongly varies seasonally, from about 40^0 N polewards in the winter (especially over Eurasia), enveloping the snow covered North American and Eurasia, to roughly north of the 70^0 N in the summer (Klonecki, 2003; Jiao and Flanner 2016). Synoptic-scale weather systems frequently disturb this transport barrier and foster exchange between air masses from mid-latitudes and the Arctic region.

Atmospheric transport into the Arctic lower troposphere requires a diabatic cooling of air masses to facilitate penetration into the polar dome either from above, or sideways. In a modeling study, Stohl (2006) identified three main pollution transport mechanisms from major anthropogenic emission regions to the Arctic lower troposphere, confirmed by the POLARCAT and NETCARE measurement campaigns (REFS). These are: 1) wintertime low-level transport over snow-covered regions at time scales of 10-15 days into the polar dome mainly from northern Eurasia; 2) low-level fast transport (i.e., taking 4 days or less) from mid-latitude emission regions located within polar front (mainly Europe) followed by uplift at the Arctic front and slow decent; and 3) lifting of pollutants mainly due

to convection in southern mid-latitudes followed by upper tropospheric transport in warm conveyor belts associated with frontal systems and eventual slow descent due to radiative cooling into the polar dome at time scales of ~2 weeks. Only the last pathway is frequent for pollution originating from North America and Asia. In contrast to the first two low level transport pathways, oxidation and wet scavenging processes in lifted air can lead to a significant removal of mercury outside the Arctic in the third transport pathway. Arctic lower troposphere is thermally very stably stratified during the winter months accompanied by surface inversions persisting for several days; this leads to reduced dry deposition during the transport process. Furthermore, the lower troposphere is extremely dry in winter, which prevents scavenging by precipitation. The age of the surface air in the high Arctic is about 1 week in winter and 2 weeks in summer, and rapidly decreases with altitude to about 3 days in the upper troposphere (Stohl 2006). In addition to the above pathways, mercury emitted from strong boreal fire events can be lofted by pyroconvection and entrained into the polar dome (Fromm et al. ??). The transport of smoke from wildfires in Siberia has been reported in literature (e.g., POLARCAT summer campaigns; Harrigan et al. 2011).

Lower tropospheric transport in and around the Arctic region has a distinct pattern marked by pronounced continental flow in winter and marine air transport in summer. In wintertime, synoptic-scale atmospheric circulation in the Arctic is mainly influenced by three major semi-permanent pressure systems: 1) low-pressure center located in sub-polar North Pacific Ocean, just south of the Bering Sea area (the Aleutian Low); 2) low-pressure system southeast of Greenland near Iceland in the North Atlantic Ocean (the Icelandic Low); and 3) a high pressure center situated over eastern Siberia (the Siberian High) (REF). Less intense highs are located over western North America and the mid North Atlantic Ocean (the Subtropical High). The cyclonic circulation around the Icelandic Low in combination with the Siberian High transports pollution from source regions in northern Europe and Siberia into the Arctic. Also, North American pollutants flow along the southern portion of the Icelandic low to northern Europe. The Aleutian low induces eastward transport of air from East Asia to North America along its southern portion over mid to subtropical latitudes, and then along western Canada and Alaska into the western Arctic. The same circulation also transports chemical species from western North America into the Arctic. The seasonal change in transport patterns are caused by the weakening of the Icelandic and Aleutian lows in summer, and the replacement of wintertime continental highs by low-pressure systems caused by seasonally changing land-sea contrasts in surface heating.

Mid-latitude atmospheric blocking events, quasi-stationary features characterized by high-pressure cell centered around 60^0 N with a low-pressure cell to the south of it lasting up to 15 days, are known to significantly increase the transport of air pollution to the Arctic (Raatz ??). More frequent in winter/spring, blocking events are predominantly observed in the NE Atlantic and the NE Pacific with approximately 2.5 times more events in the Atlantic (Iversen ??). From monthly to decadal timescales,

two major low-frequency variability modes influence atmospheric transport to the Arctic, i.e., the Pacific-North America pattern (PNA) and the North Atlantic Oscillation (NAO) (REF). During the positive phase of the NAO, associated with strengthening of Icelandic Low, transport from all three Northern Hemisphere continents (Europe, North America and Asia in order of significance) into the Arctic is enhanced, resulting in higher Arctic pollution levels (Eckhardt et al., 2003; Duncan and Bey, 2004). On the other hand, during the negative phase of the NAO (or positive phase of the PNA), the weaker Icelandic Low results in a decrease of air transport from Europe and Siberia and increased transport from North America to the Arctic (Christensen et al. ??).

Above atmospheric pathways can directly transport Hg-rich air masses from global anthropogenic Hg source regions to the Arctic. Atmospheric life time of the most dominant species of Hg in air, Hg(0), is over several months (REF); this allow a global-scale (or hemispheric scale) transport and mixing of mercury in troposphere and develop a well-mixed tropospheric background Hg pool. Atmospheric transport of background air masses is an important contributor of mercury influx into the Arctic. In addition to direct atmospheric transport, atmospheric Hg, like other semi-volatile compounds, is also transported to the Arctic via a global distillation phenomenon. Emitted Hg is successively deposited to terrestrial and aquatic surfaces and re-emitted back to the atmosphere, and continues over time to hop through the environment in the direction of the prevailing winds favoring accumulation in the colder regions such as the Arctic.

Need to add microclimate in the Arctic and its impact on concentrations, deposition and AMDEs.

Unusual warm sea surface temperatures and low sea ice concentrations in the Arctic are reported to cause atmospheric circulation anomalies in winter (Lee et al., 2015; Francis and Vavrus, 2012; Francis et al., 2017). Compared to other regions of the Northern Hemisphere, nearly twice the rate of rise in surface and lower tropospheric temperatures in the Arctic (the Arctic amplification) can cause important changes in the mid-latitude circulation patterns, thereby changing pollution transport pathways into the Arctic (Holland and Bitz, 2003; Screen and Simmonds, 2010; Cohen et al., 2014; Pithan et al., 2018).

b. Atmospheric chemical and phase transformations

Authors: **Theodore Dibble**; Huiting Mao; Kenjiro Toyota

- Add aqueous and particle phase transitions
- Describe AMDEs related oxidation here and remove from other sections

The oxidation of gaseous elemental mercury (GEM) to Hg(II) strongly influences the residence time of mercury in the atmosphere. This influence arises from the high deposition velocities of oxidized mercury, relative to GEM, for both gaseous oxidized mercury (GOM) and particulate-bound mercury (PBM). Faster oxidation of GEM leads to a shorter residence time for mercury in the atmosphere.

Conversely, reduction of Hg(II) to GEM extends the lifetime of mercury. Both oxidation and reduction can occur homogeneously and heterogeneously, but the uncertainties in these processes are enormous. Laboratory experiments and investigations using theoretical chemistry have suggested rate constants for many homogeneous processes. Theoretical work carried out in the last several years has reported rate constants for many gas-phase reactions in the Br- and OH-initiated oxidation of GEM, but rate constants derived from theory are not as reliable as those that can be obtained from laboratory experiments under favorable conditions. Unfortunately, reported reaction rate constants often disagree by orders of magnitude (Subir et al., 2012).

Gas-phase oxidation of mercury occurs in two steps (Dibble et al., 2020; Dibble et al., 2012; Goodsite et al., 2004):

$$X + Hg + M \leftrightarrows XHg\bullet + M \quad (X = OH, Cl, Br) \qquad (1, -1)$$

$$XHg\bullet + \bullet Y + M \rightarrow XhgY + M \qquad (2)$$

where M is any gas-phase molecule and •Y = NO_2, HOO, ROO•, and halogen oxides (but not NO). Decomposition of XHg• (reaction -1) competes with reaction (2) to a modest extent for X=Br, but severely limits the effectiveness of oxidation by OH. Table 1 lists recommended rate constants for use in modeling GEM oxidation initiated by Br, Cl, and OH. Recently (Saiz-Lopez et al., 2019) suggested that photolysis of BrHg• would be non-negligibly fast in the atmosphere. Unfortunately, almost all our chemical and kinetic knowledge relies on computational chemistry with inherently high uncertainties.

Table 1. Recommended rate constants for GEM oxidation initiated by X = Br, Cl, and OH derived from (Horowitz et al. 2017) and (Dibble et al. 2020).

Reaction	**Rate Constant**[a, b]	**Uncertainty**[c]
$Br + Hg + M \rightarrow BrHg\bullet + M$	$k_{1a}(T) = 1.4 \times 10^{-32}\ (T/298)^{-1.9}$	50%
$BrHg\bullet + M \rightarrow Br + Hg + M$	$k_{-1a}(T) = 1.6\times 10^{-9}\ (T/298)^{-1.9}\ e^{-7800/T}$	200%
$Cl + Hg + M \rightarrow ClHg\bullet + M$	$k_{1b}(T) = 2.2 \times 10^{-32}\ e^{(680(1/T-1/298))}$	50%
$OH + Hg + M \rightarrow HOHg\bullet + M$	$k_{1c}(T) = 3.34 \times 10^{-33}\ e^{+43/T}$	20%
$HOHg\bullet + M \rightarrow OH + Hg + M$	$k_{-1c}(T) = 1.22 \times 10^{-9}\ e^{-5720/T}$	15%[d]
$XHg\bullet + NO_2 + M \rightarrow$ *syn*-XHgONO	$k_0(T) = 7.1 \times 10^{-29}\ (T/300)^{-4.5}$ $k_\infty(T) = 1.2 \times 10^{-10}\ (T/300)^{-1.9}$	300%
$XHg\bullet + \bullet Y \rightarrow XhgY$ •Y = (HOO, ROO, ClO, BrO, IO)	$k_0(T) = 2.3 \times 10^{-29}\ (T/300)^{-4.4}$ $k_\infty(T) = 6.9 \times 10^{-11}\ (T/300)^{-2.4}$	300%

a) Values of k_1 and k_0 possess units of cm^6 $molecule^{-2}$ sec^{-1}. Values of k_{-1} and k_∞ are in cm^3 $molecule^{-1}$ sec^{-1}.

b) $k_0(T)$ and $k_\infty(T)$ are used in the Troe expression (Eqns. 16 and 17 in the text) to get $k([M],T)$

c) Estimated values at 298 K.

d) Uncertainty estimate only valid at 1 atm.

Computations further indicate that most BrHgY compounds and BrHgOH will readily undergo photo-reduction to BrHg• + •Y or even GEM (Saiz-Lopez et al., 2018) (Francés-Monerris et al. 2020). By contrast, BrHgONO photolysis generates mostly BrHgO• + NO. (Lam et al., 2019a,b), mapped out the chemistry of BrHgO•, finding that it largely abstracted hydrogen atoms to make BrHgOH, as shown in Scheme 1.

While the mechanism of Br-initiated oxidation of GEM is more advanced than for initiation by other radicals, there exists huge uncertainty in the concentration field of Br. Recent advances in instrumentation may change this situation (Wang et al., 2019), at least in atmospheric mercury depletion events (AMDEs).

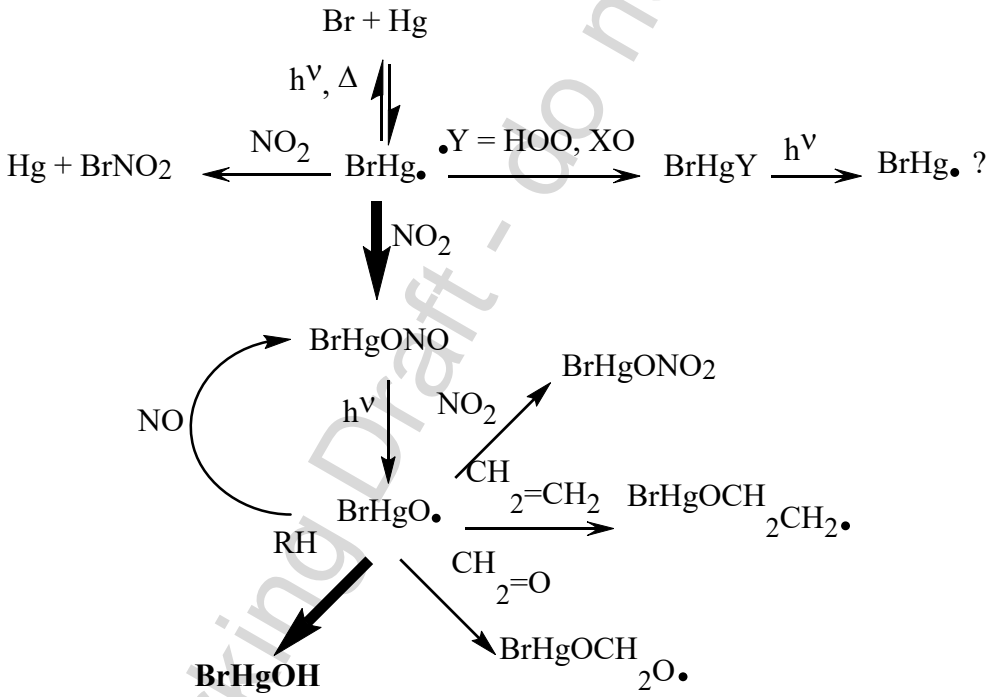

Scheme 1. Gas-phase reduction and oxidation reactions in the Br-initiated oxidation of Hg(0).

Most models of the oxidation of mercury use OH and ozone as the primary oxidants. The reaction of OH with Hg(0) proceeds via:

$$OH + Hg\ (+M) \leftrightarrows HOHg\bullet\ (+M) \qquad (1c, -1c)$$

The reversibility of this reaction was highlighted by (Calvert Lindberg, 2005) and was conclusively demonstrated in (Dibble et al., 2020). While it has been suggested that HOHg• would react with O_2:

$$HOHg\bullet + O_2 \leftrightarrows HgO + HOO \quad (3)$$

to make Hg(II), reaction (3) is so endothermic due to the instability of gaseous HgO (Cremer et al., 2008; Peterson et al., 2007; Shepler and Peterson, 2003). This makes reaction (3) irrelevant in the atmosphere.

The reaction of Hg(0) with ozone has been studied several times (Pal Ariya, 2004; Rutter et al., 2012; Spicer et al., 2005). The rate constant is so low, and the propensity of Hg(0) to be oxidized at surfaces is so high (Hynes et al. 2009), that one must exercise extreme caution in interpreting these experiments. The reaction had initially been proposed to proceed via:

$$Hg + O_3 \rightarrow HgO + O_2 \quad (4)$$

but gaseous HgO would immediately fall apart to regenerate GEM, which is inconsistent with the observed loss of GEM in the experiments.

Sommar et al. (1997) reported the reaction Hg + NO_3 to possess a rate constant of 4×10^{-15} cm^3 $molecule^{-1}$ sec^{-1}, but with enormous uncertainty. One computational study suggested that the Hg-NO_3 bond energy in •$HgNO_3$ was only 5 kcal/mole, which would render •$HgNO_3$ so unstable that it would fall apart before it could react with another radical to make GOM in the experiment, let alone in the atmosphere.

GEM oxidation has been proposed to be initiated by Cl_2, Br_2, HOOH, BrO, ClO (Subir et al., 2012). Rate constants for these reactions have been measured in environmental chambers. These reactions are proposed to occur by insertion of the mercury atom into the middle of the oxidant to produce, e.g., $HgBr_2$ or $Hg(OH)_2$. GEM is rather unreactive, so it seems unlikely that these reactions would proceed without very high activation energies. In fact, high-level calculations (Balabanov and Peterson, 2004) find a rate constants below 10^{-30} cm^3 $molecule^{-1}$ sec^{-1} for Hg + Br_2 and Hg + BrO.

Numerous investigators reported on the oxidation and reduction of aqueous mercury compounds in the dark and under illumination (Fitzgerald et al., 2007). Major oxidants include OH, O_3, and HOCl. Reduction of Hg(II) by HOO/O_2^- has been proposed but appears to be sufficiently endothermic that it can be ignored (Gårdfeldt and Jonsson, 2003). Phot-reduction of mercury species in the aqueous phase may be occurring by interaction of mercury compounds with organic matter and/or metals. Recently, (Saiz-Lopez et al., 2018) reported photo-reduction rate constants from rainwater samples for use in modeling DOM effects on Hg(II) photo-reduction. Curiously, they noted that in almost half their experiments, [Hg(II)] initially increased or stayed constant before decreasing. It seems that our understanding of photo-reduction is far from complete.

Regional and global chemical transport models (CTMs) have been applied to simulate spatiotemporal distributions of atmospheric mercury concentrations with the ultimate goal of accurately quantifying atmospheric Hg deposition, which is essential to developing mercury emission reduction policies and assessing the efficacy of the Minamata Convention. To accurately simulate Hg deposition, it is foremost important for models to reproduce the observed atmospheric concentrations of GEM, GOM, and PBM. Currently, annual mean GEM concentrations can be simulated reasonably well with model bias of 5% - 62%, but diurnal to seasonal cycles of GEM were not well captured (Baker and Bash, 2012; Bieser et al., 2014). Simulated concentrations on regional scales were predominantly determined by GEM boundary conditions (BCs) (Pongprueksa et al., 2008; Baker and Bash, 2012; Ye et al., 2018). Modeled reactive mercury (GOM+PBM) concentrations showed large overprediction compared with observations over a wide range from ~10% to a factor of 10 (Seigneur et al., 2004; Selin et al., 2007; Ryaboshapko et al., 2007; Baker and Bash, 2012; Bieser et al., 2014; Ye et al., 2018). Such overprediction appear to stem from at least three sources, 1) underbiased GOM concentrations in measurements (Gustin et al., 2015); 2) overestimated gas-phase GEM oxidation kinetics in models (Zhang et al., 2012; Kos et al., 2013; Bieser et al., 2014); and 3) neglect of gas-phase photo-reduction (Saiz-Lopez et al., 2018). Despite great uncertainties in simulated GOM and PBM, modeled Hg wet deposition has shown surprisingly good agreement with measurements (e.g. 21% fractional bias) (Holloway et al., 2012). Since GOM and PBM dominate Hg wet deposition, this reasonable agreement is due likely to compensating errors in multiple simulated parameters determining wet deposition (Baker and Bash, 2012; Bieser et al., 2014; Ye et al., 2018).

As reviewed above, major progress has been made in understanding complex GEM oxidation mechanisms using computational approaches in recent years. Incorporating the new findings in a few models has shown significant improvement in simulation of Hg wet deposition. Including the second stage oxidation of HgBr by HO_2, NO_2, and BrO as well as new kinetics for HgBr dissociation in the global CTM GEOS-Chem, Horowitz et al. (2017) reduced the overestimation of Hg wet deposition to 0 – 30% globally compared to previous studies. Ye et al. (2018) implemented detailed Hg and Br chemical mechanisms, including new kinetic data from Dibble et al. (2012), in CMAQ-Hg, and captured observed spatiotemporal variations in GOM concentrations and Hg wet deposition with a few percentage of fractional bias and normalized mean bias over the Northeast U.S. domain.

Atmospheric Hg chemistry is apparently key, among a multitude of factors, to accurate simulation of Hg deposition, during Arctic AMDEs. Modeling studies have estimated contributions of 10% - 55% of total annual atmospheric Hg deposition to the Arctic (Skov et al., 2004; Outridge et al., 2008). Considering re-emission of Hg and snow redox chemistry, Dastoor et al. (2008) suggested a much smaller but still significant net deposition flux without providing an estimate of contribution from AMDEs. On the contrary, the soil, snow, and atmospheric measurement data from Obrist et al. (2017)

suggested a negligible contribution from AMDEs. Much work remains needed to quantify atmospheric Hg deposition to Arctic ecosystems.

Here we present a brief summary and perspective. Our understanding of the mechanisms of gas-phase mercury redox chemistry has been worked out to a large degree, but major gaps remain. These mechanisms are mostly known from computational studies, so the associated rate constants are highly uncertain. There is a clear need for laboratory experiments to determine reaction kinetics. This may be particularly difficult for OH-initiated oxidation, as the gaseous HOHg• radical has never been detected in the laboratory. Moreover, the lack of measurement data on atmospheric concentrations of atomic bromine creates large uncertainties in model predictions of the extent of Br-initiated oxidation. Because the oxidation of GEM is so slow compared to transport (except during AMDEs), it is difficult for regional and global measurements of GEM/GOM/PBM to diagnose specific problems in chemical mechanisms. This problem is exacerbated by the uncertainties in measurements of PBM and GOM. We suggest that AMDEs provide the most fruitful area for model-measurement intercomparisons, because the rapid concentration changes are largely controlled by chemical processes rather than transport. Another factor is that Br concentrations are much higher than in the rest of the atmosphere, making it feasible to carry out point measurements of the concentrations of Br and other radicals that drive the chemistry. Last, but not least, the ability to determine the molecular composition of GOM in the field would enable more specific diagnoses of the limitations of our current mechanisms and rate constants.

Add the new paper "**Is oxidation of atmospheric mercury controlled by different mechanisms in the** 1 **polluted continental boundary layer vs. remote marine boundary layer?"** Maor Gabay, Shira Raveh-Rubin, Mordechai Peleg, Erick Fredj, Eran Tas Maor Gabay *et al* 2020 *Environ. Res. Lett.* In press

c. Mercury exchange between air and Arctic surfaces

Introduction

- Define Hg removal and revolatilization processes in the Arctic for all surfaces in different seasons

High latitude locations, particularly in the northern Arctic, experience two markedly different seasons, each with their own unique Hg deposition mechanisms. As in lower latitudes, Hg can be deposited directly to vegetation surfaces (Demers, Blum, and Zak 2013; Jiskra et al. 2017; Obrist et al. 2017) and organic matter (Bartels-Rausch et al. 2011) during the summer. However, there are also unique wintertime and springtime mechanisms that lead to the deposition of Hg to the Arctic. In earth's high latitudes winter lasts for up to nine months, wintertime deposition of Hg to snow and ice surfaces can be significant. In the springtime, high reactive Hg species produced during AMDEs are persistently scavenged from the air by snow and ice crystals as well as dry deposited to snowpacks leading to

anomalously elevated Hg deposition to snow and ice surfaces along the coast (Durnford and Dastoor 2011; Thomas A. Douglas et al. 2012; T. A. Douglas et al. 2008; Thomas A. Douglas and Blum 2019)). Once deposited to the snow pack some mercury is re-emitted to the atmosphere by photo-reduction (Ferrari et al. 2005; Johnson et al. 2008; St. Louis et al. 2005), but 25 to 50% of AMDE Hg is believed to be retained and available as a component in snow melt (Thomas A. Douglas et al. 2012; Thomas A. Douglas and Blum 2019).

Mercury uptake by precipitation Authors: **Huiting Mao**

Clouds provide medium for aqueous or heterogeneous reactions via gas-particle partitioning, adsorption, photoredox, and methylation (Ariya et al., 2015; Subir et al., 2012; Andersson et al., 2008; Wang et al., 2015; Seigneur et al., 1998; Amirbahman et al., 2013; Berguist et al., 2007; Gu et al., 2011; Gårdfeldt et al., 2003; Siciliano et al., 2005; Hammerschmidt et al., 2007; Li et al., 2018), and precipitation clouds, or precipitation in general, remove reactive mercury (=GOM+PBM) from the atmosphere, the latter termed as wet deposition. Wet deposition has been suggested to contribute 50-90% of total Hg deposition to surface waters, especially in precipitation-abundant regions (Sorensen et al., 1990; Lamborg et al., 1995; Mason and Sullivan, 1997; Scherbatskoy et al., 1998; Landis and Keeler, 2002). In the Arctic smaller mercury wet deposition flux has been observed and estimated than in lower latitudes due to less rain amounts, shorter seasons favoring GEM oxidation, and less anthropogenic influence (Sanei et al., 2010; Obrist et al., 2017).

Measurement-based mercury wet deposition flux is determined from Hg concentrations in precipitation and rates of precipitation. GOM and PBM comprise the majority of mercury wet deposition due to their high solubility (Guentzel et al., 2001; Sakata and Asakura, 2007; Schroeder and Munthe, 1998). In addition to anthropogenic emissions, reactive mercury is produced from photochemical oxidation of GEM, and hence emissions and meteorological factors can affect Hg wet deposition and precipitation Hg concentrations. Over the past decades anthropogenic emissions of mercury have been decreasing over North America and Europe while increasing in East Asia (UNEP, 2013). However, studies have not shown a strong consistent relation between changes in anthropogenic Hg emissions and wet Hg deposition (Risch et al., 2008; Prestbo and Gay, 2009; Weiss-Penzias et al., 2016), indicating complex mechanisms driving large variabilities in Hg wet deposition over different regions and time periods.

Wet deposition flux of mercury in three-dimensional chemical transport models is estimated using the precipitation rate and in some models the cloud water (ice) concentration (Byun and Ching, 1999) while in others in- and below-cloud scavenging ratios (Berge and Jakobsen, 1998; Jacob et al., 2000; ENVIRON, 2011). The transfer of gas-phase compounds to the surface of an ice particle is not well represented or not represented at all. For example, it was not accounted for in the community multiscale air quality modeling system (CMAQ), and in GEOS-Chem the ratio of sticking coefficients

of trace gases on the ice surface was assumed (Jacob et al., 2000). All approaches ultimately depend in large part on simulated precipitation rates and vertical distributions of atmospheric reactive mercury concentrations, and yet the latter is limited by significant uncertainty in our current understanding of atmospheric chemistry of Hg as reviewed in Section 3.3.1b.

Arctic warming can potentially influence Hg wet deposition at least by increasing reactive mercury through increasing GEM emissions from permafrost thaw (Hindzman et al., 2005, and references therein; Rowland et al., 2010) and altering kinetics of Hg oxidation reactions (Goodsite et al., 2004; Dibble et al., 2012). Therefore, accurate estimates of Hg wet deposition in the Arctic are becoming increasingly critical to Arctic mercury budgets and developing mercury pollution mitigation strategies to protect human and ecosystem health.

d. Air-surface exchange of mercury Authors: **Leiming Zhang**

Any gaseous or particulate pollutants in the atmosphere can be transported to Earth's surfaces where they are adsorbed and removed from the atmosphere. This process is referred to as dry deposition and is quantified using flux (e.g., kg ha^{-1} yr^{-1}, μg m^{-2} yr^{-1}) representing pollutant mass removed from the atmosphere by per unit surface area in unit time. On the other hand, the Earth's surfaces can also be a source of certain chemical species by releasing them into the atmosphere, a process that is referred to as emission. For such chemical species, dry deposition and emission happen simultaneously and constantly, resulting in bi-directional air-surface flux exchange. One process can dominate over the other, resulting in net dry deposition or emission flux, depending on the chemical species physical and chemical properties as well as meteorological and biological conditions. In the case of speciated atmospheric mercury, dry deposition process dominates for GOM and PBM over nearly any natural surfaces while bi-directional flux exchange have been frequently observed for GEM (Zhang et al., 2009, Wright et al., 2016).

Most existing measurement methods for quantifying dry deposition and air-surface exchange fluxes of speciated atmospheric mercury can be grouped into three major categories, including micrometeorological approaches, dynamic gas flux chambers, and surrogate surface approaches (Wright et al., 2016, Zhu et al., 2016). Flux measurements using any of these approaches are subject to large uncertainties. For example, concentrations at different heights need to be measured using the micrometeorological approaches, but measuring mercury at very low concentrations is very challenging due to technological limitations of the available instruments (Jaffe et al., 2014). Dynamic gas flux chambers can be deployed over soil, water, low canopy, or tree branches; however, the measured fluxes may not be representative of an entire area due to heterogeneity in land use cover. In addition, different designs inside the dynamic gas flux chambers can cause the measured fluxes to differ by up to one order of magnitude (Eckley et al., 2010). Surrogate surfaces may not perform the same way as natural surfaces in collecting mercury, and uncertainties in the measured GOM and PBM

dry deposition are larger than a factor of two depending on the selected surrogate surfaces and instrument setup (as detailed in Wright et al., 2016). A new surrogate surface sampler was recently developed utilizing a three-dimensional deposition surface, which is expected to mimic the physical structure of many natural surfaces more closely than the traditional flat surrogate surface designs (Hall et al., 2017). Collocated measurements using different techniques should be performed to constrain the measurements uncertainties (Fritsche et al., 2008; Zhu et al., 2015; Osterwalder et al., 2018). Standardized protocols should be developed for commonly used measurement techniques.

Measurements of mercury in litterfall and throughfall can also provide some knowledge of mercury deposition over forest canopies. Mercury in litterfall is considered to be mostly from atmospheric dry deposition of GEM, and can be used as a rough and conservative estimation of atmospheric mercury dry deposition (the portion that is retained in leaves). Mercury in throughfall also includes a portion of previously dry deposited mercury (the portion that is washed off from the canopy). Concurrent measurements of litterfall, throughfall, and open-space wet deposition measurements can be used to estimate dry deposition on seasonal or longer time scales, whereby dry deposition is approximated as litterfall plus throughfall minus open-space wet deposition (Wright et al., 2016).

Modeling methods for estimating mercury dry deposition either use the inferential approach, which calculates flux as a product of surface air concentration and modeled dry deposition velocity of speciated mercury, or use the bi-directional air-surface exchange model, which simulates emission from and deposition to land surfaces simultaneously (see a detailed review in Wright et al., 2016). Briefly, early modeling studies mostly only considered dry deposition of GOM and PBM using the inferential approach, while later studies have also included GEM in the dry deposition budget using either inferential approach (dry deposition only) (De Simone et al., 2014 ; Dastoor et al., 2015; Song et al., 2015) or bidirectional air-surface exchange approach (Bash, 2014; Wang et al., 2014). Note that flux uncertainties from using these modeling approaches are expected to be on a similar order of magnitude to those of field flux measurements because models were initially developed and validated using the limited flux measurements.

Dry and wet deposition are the only removal mechanisms depleting pollutants from the atmosphere because all the other processes either produce additional pollutants mass (emission), convert pollutants from one chemical form to another (chemical transformation), or move pollutants from one place to another (transport and diffusion). Thus, the rates of dry and wet deposition control the overall lifetimes of pollutants or groups of pollutants in the atmosphere. Note that while wet deposition process is episodic, dry deposition process happens all the time even during precipitation, and over any surface. On regional to global scales, dry and wet deposition are equally important for the majority of atmospheric pollutants, including mercury (Wright et al., 2016, Zhang et al., 2016). Dry deposition velocity varies by up to two orders of magnitude between GOM, PBM and GEM or between different surface types (Zhang et al., 2009). The lifetime in air due to dry deposition removal

is best estimated to be hours to days for GOM, days to weeks for PBM, and months to years for GEM, depending on surface type among other conditions. For example, GEM can be effectively removed by canopies with large leaf area if soil emission is limited (resulting in its lifetime of a few months), while its dry removal can be very limited over bare soil and water surfaces (resulting in its lifetime of years) (Cohen et al., 2016).

Text Box 1: Models

Authors: **Colin Thackray**, Yanxu Zhang, Kenjiro Toyota, Anne Soerensen, Ashu Dastoor

Four global atmospheric mercury models have been applied to study mercury cycling in polar regions – GLEMOS (Travnikov and Ilyin 2009), GEOS-Chem (Fisher et al. 2012; Holmes et al., 2010), GEM-MACH-Hg (Dastoor et al., 2008; Durnford et al., 2012; Kos et al., 2013); and the Danish Eulerian Hemispheric Model (Christensen et al., 2004). These atmospheric models simulate Hg(0) and Hg(II) concentrations and deposition resulting from redox chemistry based on oxidant concentrations and reaction rates, and physics and transport based on meteorological variables. The largest differences among models in the polar-regions are related to the representation of Hg(0)-Br oxidation mechanism and reaction rates (see section 3.3.1), concentrations of Br species, photo-reduction and re-emission parameterization of mercury from snowpack, and mercury evasion fluxes from the Arctic Ocean (Angot et al. 2016a). Durnford et al (2012) developed and implemented a dynamic multi-layer snowpack-meltwater parameterization in GEM-MACH-Hg. Fisher et al. (2012) and Durnford et al. (2012) introduced evasion of mercury from the Arctic Ocean during summer to explain the observed summertime maximum in Hg(0) concentrations (Steffen et al. 2005; Berg et al. 2013). Toyota et al. (2014) developed a detailed one-dimensional air–snowpack model for interactions of bromine, ozone, and mercury in the springtime Arctic which provided a physicochemical mechanism for AMDEs and concurrently occurring ozone depletion events (ODEs). The authors also developed a temperature dependent GOM-PBM partitioning mechanism explaining its observed seasonal transition (Steffen et al. 2014).

Ocean models have been developed for ocean Hg cycles (MITgcm, Zhang et al. 2014; Zhang et al. 2015; Zhang et al. 2019; Zhang et al. in press; Wu et al., in revision; NEMO, Semeniuk and Dastoor 2017; HAMOCC, Archer and Blum 2018; FATE-Hg, Kawai et al. 2020). These models simulate the photochemical/abiotic and biological transformations between Hg(0) and inorganic Hg(II) and methylmercury (MeHg; both MMHg and DMHg), the partitioning of Hg(II) and MMHg onto particulate organic carbon (POC) to form particle-bound Hg^P and $MMHg^P$, and the sinking of Hg^P and $MMHg^P$ to deeper waters. This POC pool includes both detritus and living plankton. These models also simulate exchange of Hg(0) and DMHg with the atmosphere and are forced by atmospheric

Hg(II) deposition and Hg(0) concentrations in the marine boundary layer from an atmospheric Hg simulation.

The uptake of seawater MeHg by plankton and transfer to higher trophic levels is included in some studies (e.g. Schartup et al. 2018; Zhang et al. 2020). The uptake of MeHg by phytoplankton is modeled as an instantaneous equilibrium process with the ratio of MeHg concentration in phytoplankton over the seawater concentration as a function of the cell diameter and dissolved organic carbon concentrations. Trophic transfer of MeHg from phytoplankton to zooplankton is calculated after phytoplankton uptake based on the biomass of phytoplankton grazed by zooplankton, the biomass concentration of phytoplankton, and the assimilation efficiency of zooplankton. Unassimilated MeHg grazed by zooplankton returns to the seawater in the form of $MMHg^P$. Losses from plankton reflect MMHg elimination through fecal excretion and mortality. Isotope fractions are also included in Archer and Blum (2018) by slightly perturbing the rates of chemical transformations between the isotopes. Reaction rates for the transformation between species in the ocean are based on experimentally measured values, but are sometimes adjusted to match available observations, or scaled based on environmental parameters (e.g. organic carbon reaction rate, solar radiation intensity, and temperature).

Calculation of a balanced Arctic Ocean mercury budget has been performed using a multi-compartment box model (Soerensen et al., 2016). Hg species (Hg(0), Hg(II) and MeHg) in the polar mixed layer, subsurface ocean, deep ocean, shelf sediments, and Central Basin sediments were modeled using boundary inputs dictated by coastal erosion, river inputs, atmospheric deposition, snow and ice melt, and advective transport, with removal controlled by evasion, diffusion, particle settling, and advective transport. These calculations show that high total mercury (Hg) in Arctic seawater relative to other basins reflects large freshwater inputs and sea ice cover that inhibits losses through evasion. Sources of uncertainty include the magnitude of the benthic sediment resuspension source for coastal regions, the magnitude of terrestrial influence on river discharges to the Arctic, and how these and internal rates vary over time. As a trade-off for lack of spatial resolution, this type of model can be applied over longer timescales (e.g. 1850-2010) than spatially resolved models (Soerensen et al., 2016).

Despite significant advances in model representations of Hg cycling in the Arctic atmosphere and ocean, important gaps remain. Two major uncertainties for atmospheric models are reduction processes and oxidant concentrations. Atmospheric reduction of Hg(II) has been represented as a heterogeneous process, but recent work has shown that photo-reduction of oxidized mercury species should be significant in the gas phase (Saiz-Lopez et al., 2018; Saiz-Lopez et al., 2019). Calculated photolysis cross sections for the Hg(II) species formed during oxidation of Hg(0) indicate that gaseous oxidized Hg could be short-lived in the presence of sunlight. This process is unrepresented in existing Arctic studies, and challenges elements of the current model of atmospheric redox.

Reduction in the atmosphere acts in opposition to oxidation, which also carries significant uncertainty in the models. While recent advances in computational chemistry studies have narrowed down some of the major gaps in the kinetics and mechanisms of gas-phase Hg oxidation, leading to increased confidence in the primary role of Br-initiated oxidation in the global troposphere (see section 3.3.1), concentrations of Br are uncertain. Along with their role in oxidizing Hg(0), bromine radicals also participate in other photochemistry (e.g. the catalytic destruction of O_3). The modeling of bromine chemistry is challenging in general, and is especially complicated in polar environments. The photochemical production of gaseous inorganic bromine occurs from saline surface snowpack on sea ice, wind-blown snow particles and sea-salt aerosol, when these salt-containing substrates mix with acid compounds ubiquitous in the atmosphere, are exposed to gaseous oxidants, or are illuminated by sunlight (Abbatt et al., 2012; Pratt et al., 2013; Wren et al., 2013; Custard et al., 2017). Knowledge gaps exist in the quantification of all of the processes controlling bromine chemistry, and model studies have simulated springtime bromine chemistry in the polar boundary layer with various levels of complexity.

For simulating the Br-initiated Hg oxidation in atmospheric models, concentrations from other models of tropospheric chemistry and transport are used for Br-radical and other reactive chemical compounds such as NO_2, HO_2, BrO and OH (reacting with HgBr to form Hg(II) products) (e.g. Horowitz et al., 2017). However, given the currently limited capabilities of models to compute bromine chemistry in the polar boundary layer over sea ice, atmospheric Hg models employ indirect approaches to derive Br-radical concentrations (e.g. assuming BrO concentrations in the boundary layer over sunlit sea ice (Holmes et al., 2010; Angot et al., 2016; Fisher et al., 2012), or using the monthly satellite climatology of BrO over sea ice (Dastoor et al., 2008). Toyota et al. (2014) proposed that multiphase bromine chemistry could also play a role in gaseous Hg(II)-PBM (particulate-bound mercury) partitioning. This model simulated the formation of PBM occurring as Hg(II)-bromide complexes after ozone depletion, when the concentrations of particulate Br^- are relatively high. The model also predicted the formation of PBM to occur more favorably at lower temperatures, in accordance with observed seasonal trends of the Hg(II)-PBM partitioning at Alert in the Canadian Arctic (Cobbett et al., 2007; Steffen et al., 2014). This partitioning is a factor in determining the atmospheric lifetime of mercury against dry and wet depositions (Amos et al., 2012; Steffen et al., 2014), and highlights the deep connection between the dually uncertain Hg and Br cycles.

Terrestrial inputs of Hg to the Arctic ocean via rivers have been shown to contribute to the seasonality and magnitude of atmospheric and ocean concentrations (Fisher et al., 2012; Soerensen et al., 2016; Sonke et al., 2018). The Arctic terrestrial loading of Hg is connected to the atmosphere through deposition and evasion, and to the Arctic Ocean via river outflow. Changes in atmospheric Hg deposition to – and retention in – Arctic soils, permafrost, and watersheds through time make this a dynamic contributor to Arctic Hg fate. Currently, models of terrestrial Hg loading, transformation and

export are not used in conjunction with models of the coupled atmosphere-ocean system to build a consistent estimate of these connected fluxes. Future coupling of terrestrial models to existing atmosphere and ocean simulations would fill an important gap in simulating the Arctic Hg cycle.

3.3.2 How much Hg is present in Arctic surface air?

Authors: **Hélène Angot**, Ashu Dastoor, Robert Mason, Oleg Travnikov (Kyllönen Katriina, Michelle Nerentrop, Katarine Gårdfeldt, Sofi Jonsoon – data contribution)

- Add model estimates of surface air concentrations using EDGAR 2010 and AMAP 2010 anthropogenic emissions
- Discuss comparison of modeled concentrations using above two anthropogenic emissions inventories.
- Discuss changes in Hg concentrations (and causes) between 2010 and 2015
- Add results from the model DEHM (Jesper Chritensen, Aarhus University, Denmark) to multi-model ensemble (if available).

For this AMAP assessment, Hg concentrations in Arctic surface air were investigated by an ensemble of chemical transport models using the new inventory of Hg anthropogenic emissions developed for the Global Mercury Assessment 2018 (AMAP/ UN Environnement 2019). Three global chemical transport models for Hg (GEM-MACH-Hg, GEOS-Chem, GLEMOS) – with parameterization of Arctic specific processes (e.g., AMDEs) – were applied in the study.

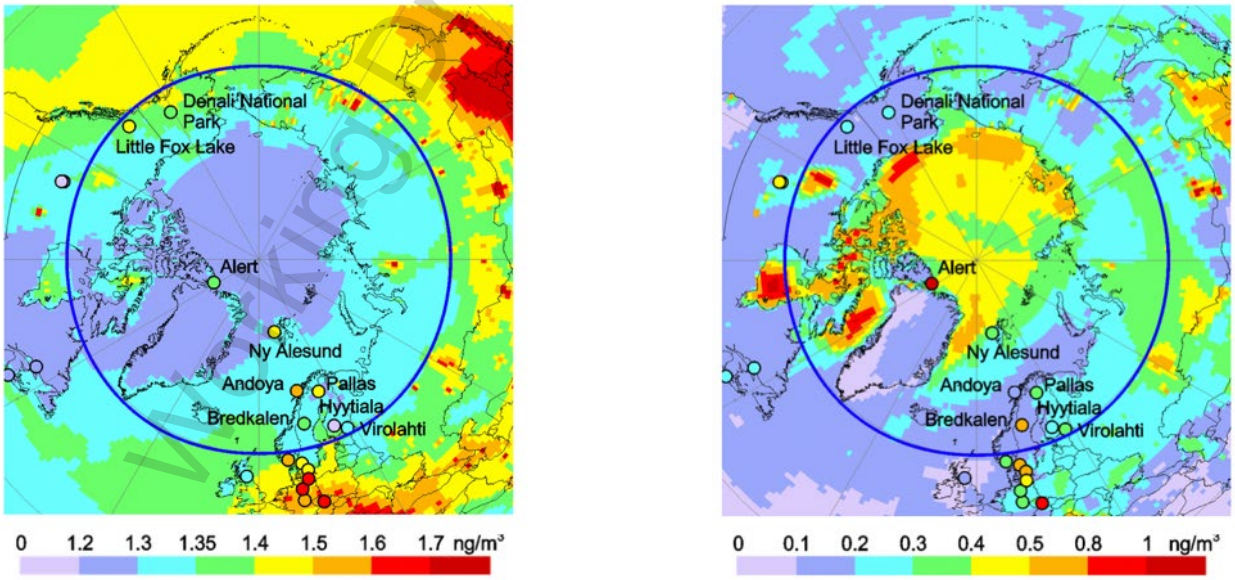

Figure 1: (left) Model ensemble mean Hg(0) concentration in Arctic surface air in 2015. (right) Seasonal amplitude of Hg(0) concentration in 2015 (i.e., difference between the highest and lowest monthly values). Circles show observations in the same color scale. The blue line delimits the Arctic domain (> 60°N).

The mean distribution of Hg(0) concentrations in Arctic surface air in 2015 as simulated by the model ensemble is shown in Figure 1. The annual mean Hg(0) concentration at Arctic monitoring stations is 1.38 ± 0.11 ng/m^3 for observations and 1.33 ± 0.03 ng/m^3 with the model ensemble. With a relative bias[1] of -3.8%, the model ensemble slightly underestimates Hg(0) concentrations. Figure 2 gives an easier comparison of modeled and observed Hg(0) surface air concentrations at Arctic monitoring sites in 2015. Considering a 10% uncertainty for observations, model results are overall within the range of expected values.

[1] $RBIAS = \frac{\overline{M} - \overline{O}}{\overline{O}} 100\%$

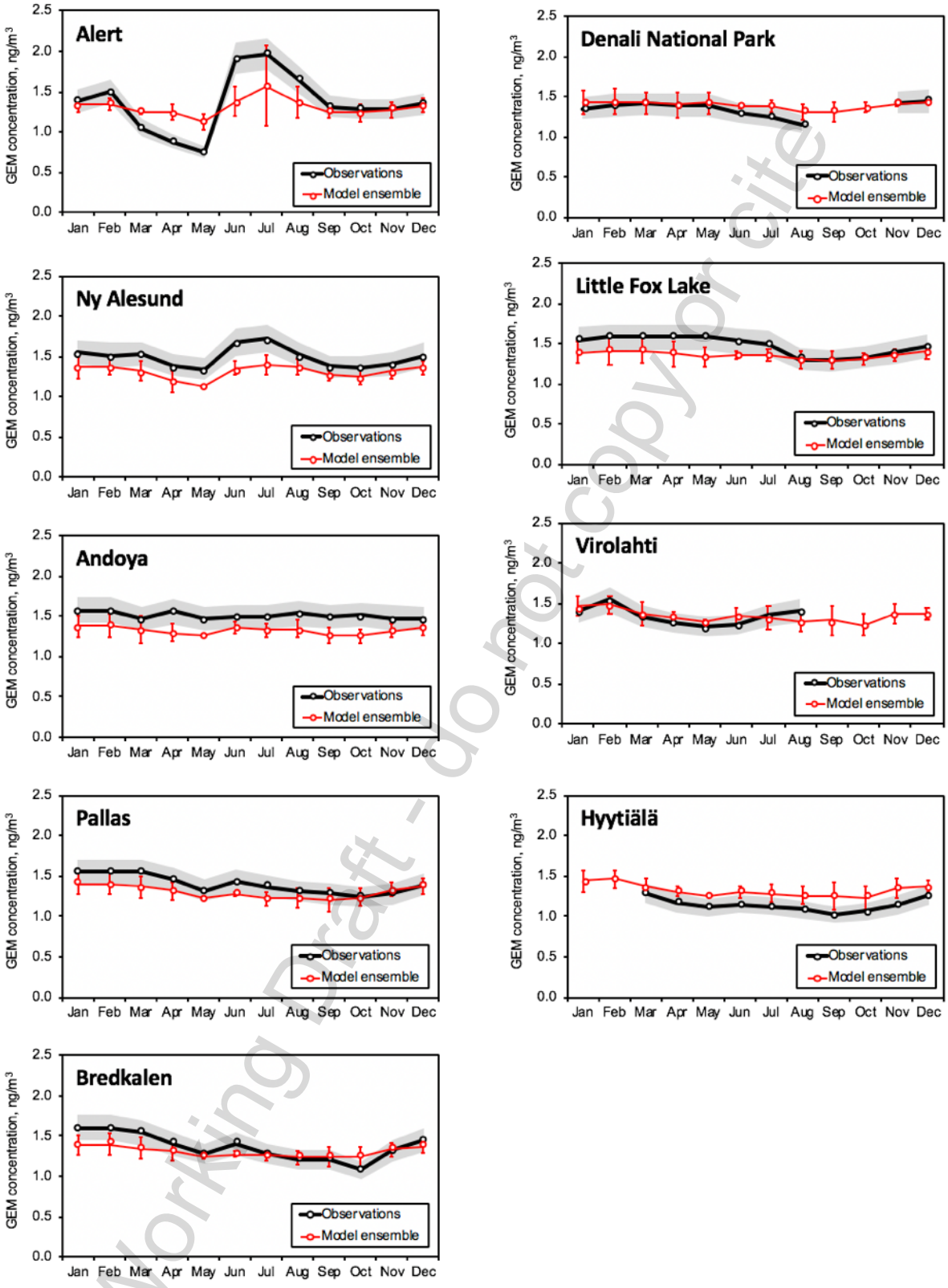

Figure 2: Modeled and observed Hg(0) surface air concentrations at Arctic monitoring sites in 2015. Black lines denote observations; red lines show arithmetic mean of the model ensemble. Shaded areas show a ±10% uncertainty for observations while whiskers present the standard deviation of simulated values among the models.

Dastoor and Durnford (2014) conducted a comprehensive evaluation of GEM-MACH-Hg simulated concentrations of Hg(0) and Hg(II) in air with measurements at Alert (Canada), Ny-Ålesund (Norway), Amderma (Russia), and Utqiagvik (Barrow, USA) from 2005-2009 while Angot et al. (2016) evaluated the three above-mentioned global models using atmospheric monitoring data of mercury concentrations for 2011-2015 at 4 Arctic sites (Alert, Station Nord (Greenland), Ny-Ålesund and Andøya). The model median concentrations of Hg(0) were found within the range of observed medians at all locations. DiMento et al. (2019) recently reported Hg(0) concentrations over the western Arctic Ocean during the 2015 U.S. Arctic GEOTRACES cruise (August to October; from Dutch Harbor, AK to the North Pole and back). Observed Hg(0) concentrations, averaging 1.2 ± 0.1 ng/m^3, are in the range of values simulated by the model ensemble in fall (Figure 3d). Additionally, a summer cruise was performed from Longyearbyen (Svalbard) to the Arctic Ocean onboard IB Oden in August-September 2016 (Nerentorp 2016). Mean Hg(0) concentrations of 1.4 ± 0.2 ng/m^3 are also in the range of values simulated by the model ensemble in summer (Figure 3c). A more thorough evaluation of model outputs is however hampered by the limited number of ground-based monitoring sites and by the absence of year-round measurements over the Arctic Ocean. Measurements carried out onboard RV *Polarstern* under the umbrella of the Multidisciplinary drifting Observatory for the Study of Arctic Climate (MOSAiC) expedition (https://mosaic-expedition.org) from October 2019 to October 2020 will partly fill this gap.

According to Figure 1, the distribution of Hg(0) concentrations is characterized by a latitudinal gradient with elevated concentrations (above 1.4 ng/m^3) in the temperate latitudes and the lowest concentrations (below 1.4 ng/m^3) above 60°N, suggesting transport of anthropogenic mercury from lower latitudes to the Arctic. The seasonal amplitude of Hg(0) concentrations as simulated by the model ensemble is shown in Figure 1 (left panel). The model ensemble reproduces the characteristic seasonality in the western Arctic, with low Hg(0) concentrations in spring driven by AMDEs (Figure 3b) and high Hg(0) concentrations in summer attributed to oceanic re-emission of mercury (Figure 3c). The more pronounced seasonal cycle observed at Alert than at other Arctic sites (Figure 2) is also well captured by the model ensemble. The temporal correlation[2] between the model ensemble results and observations at Arctic sites is 0.77. It should however be noted that the model ensemble underestimates the seasonal amplitude at Alert (Figure 1b) due to the underestimation of the amplitude of both the spring minimum and summer maximum (Figure 2). As noted by Angot et al. (2016), the models correctly reproduce enhanced total oxidized mercury concentrations (i.e., oxidized gaseous and particulate mercury) at Alert and Ny-Ålesund during the AMDEs season but underestimate the values compared to measurements. Angot et al. (2016) evaluated modelled interannual variability in Hg(0) concentrations using GEOS-Chem and GEM-MACH-Hg simulations from 2011-2014. Interannual variability in the frequency of AMDEs was fairly well reproduced by

[2] Temporal correlation coefficient of monthly mean values averaged over the measurement sites.

GEM-MACH-Hg but real-time modeling of the distribution of bromine concentrations and sea-ice dynamics is needed to improve the models (Moore et al. 2014). Simulated Hg(0) interannual variability in GEOS-Chem and GEM-MACH-Hg in winter was lower than measured which suggests an impact of interannual variability in anthropogenic emissions; the models used 2010 global anthropogenic Hg emissions (AMAP/UNEP 2013) for simulations from 2011-2014.

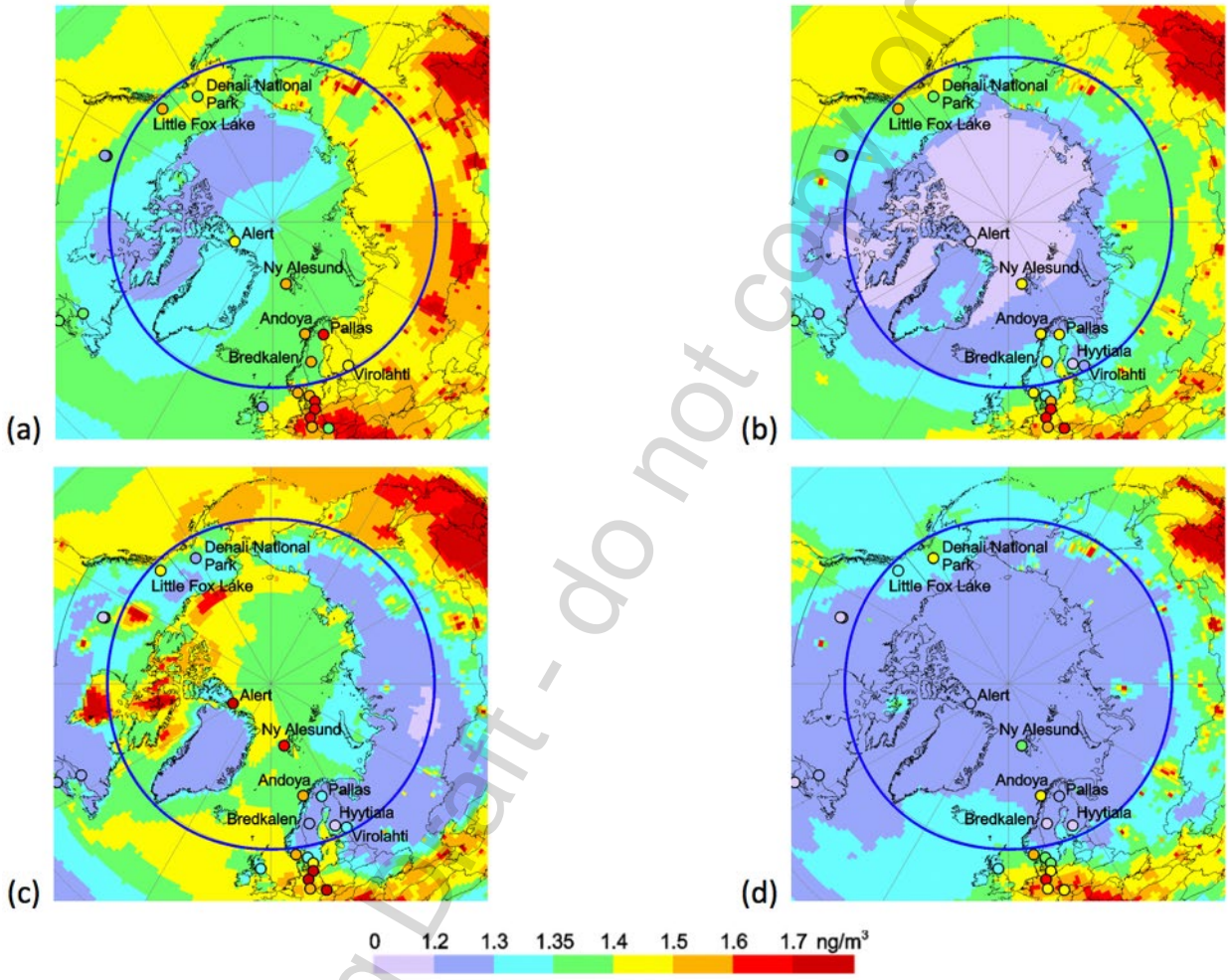

Figure 3: Year 2015 model ensemble mean Hg(0) concentration in surface air in (a) winter, (b) spring, (c) summer, and (d) fall. Circles show observations in the same color scale. The blue line delimits the Arctic domain (> 60°N).

3.3.3 How much Hg is exchanged between atmosphere and Arctic surfaces?

[provide estimates of spatial distribution Hg exchange rates (fluxes) between air, and terrestrial and marine surfaces – vegetation, soils, snow on land, snow over sea-ice, sea-ice, open ocean]

a. Hg deposition by precipitation

Authors: **Hélène Angot, Tom Douglas, Huiting Mao, Robert** Mason, Daniel Obrist, Sandy Steffen, Oleg Travnikov

- Add model estimates of wet deposition using EDGAR 2010 and AMAP 2010 anthropogenic emissions; discuss comparison of model estimates using two above anthropogenic emissions inventories.
- Discuss changes in wet deposition (and causes) between 2010 and 2015
- Add results from the model DEHM (Jesper Christensen, Aarhus University, Denmark) to multi-model ensemble (if available).

The median distribution of Hg wet deposition fluxes in 2015 as simulated by the model ensemble is shown in Figure 1. According to the model ensemble, the Arctic is characterized by relatively low wet deposition fluxes over continental areas (below 13 ng/m^2/day on average, i.e. below 5 µg/m^2/year), especially in arid areas of Greenland, northern Canada, and Siberia, but higher wet deposition fluxes above the Arctic Ocean (see below). Global measurement data have shown annual wet deposition fluxes varying from a couple of µg/m^2 to ~30 µg/m^2 (Sprovieri et al. 2017; Mao, Ye, and Driscoll 2017; Zhou et al. 2018; Qin et al. 2016). Smaller Hg wet deposition fluxes have been observed in the Arctic due to less rain amounts, shorter seasons favoring GEM oxidation, and less anthropogenic influence. Obrist et al. (2017) estimated that 71% of total Hg deposition in the Arctic resulted from dry deposition of GEM and the remaining from that of reactive Hg, indicative of a small contribution from wet deposition. Sanei et al. (2010) reported wet deposition fluxes of 0.5-2.0 µg/m^2/year at two Canadian sub-Arctic sites. A multi-year (2008-2015) wet deposition record from an arctic tundra site reported by Pearson et al. (2019) at Gates of the Arctic National Park in Alaska showed a mean annual wet deposition flux of 2.1±0.7 µg/m^2/year, with an inter-annual range of 1.2 to 3.0 µg/m^2/year. Annual Hg wet deposition at this site was the lowest annual flux measured across any of the NADP network stations in the U.S. and Canada, accounting only for about 20% of mean Hg wet deposition measured across 99 lower latitude stations (mean of 9.7±3.9 g/km^2/year). Comparison to four other Alaska subarctic and boreal sites showed consistently low Hg wet deposition across all northern stations (annual fluxes of 2.3 µg/m^2/year at Nome; 3.0 µg/m^2/year at Glacier Bay; 4.8 µg/m^2/year in Kodiak, and 4.5 µg/m^2/year at Dutch Harbor). These low Hg wet deposition fluxes were attributed to a combination of low annual precipitation (363 mm/year on average at Gates of the Arctic) and low Hg concentrations in precipitation (median: 3.6 ng/L), and are consistent with low snow Hg concentrations (0.5-1.7 ng/L; Agnan et al. 2018; Thomas A Douglas and Sturm 2004). DiMento et al. (2019) recently reported data over the western Arctic Ocean during the 2015 U.S. Arctic GEOTRACES cruise (August to October; from Dutch Harbor, AK to the North Pole and back). Precipitation Hg concentrations were similar to those found in surface snow (~ 1 ng/L) and markedly lower than reported in lower regions of the Arctic. Assuming an annual precipitation of 340 mm/year

over the Arctic Ocean (Serreze et al. 2006), these results suggest a wet deposition flux < 0.5 µg/m^2/year, i.e., an order of magnitude lower than the flux suggested by the model ensemble (~ 6 µg/m^2/year). However, available measurement data cover limited regions of the Arctic and cannot provide complete evaluation of the regional spatial pattern. Additional year-round data are especially needed over the Arctic Ocean itself.

Add model-measurement comparison for Alaska sites. Add cruise data to the maps

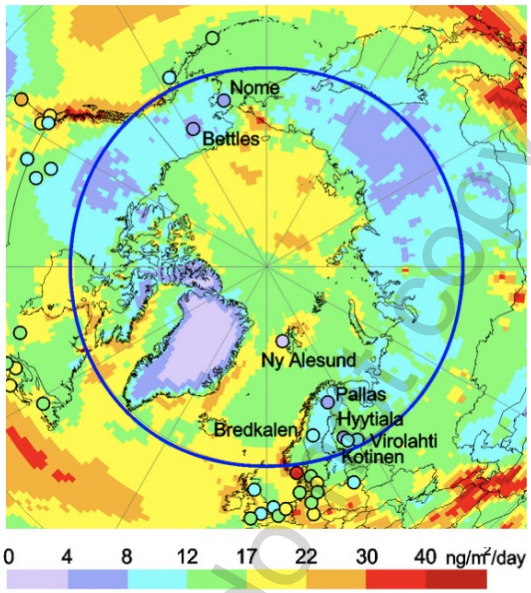

Figure 1: Model ensemble mean Hg wet deposition flux in 2015 (background contour) and observations (circles). The blue line delimits the Arctic domain (> 60°N).

An evaluation of the performance of the model ensemble at reproducing the observed seasonal cycle at Arctic sites is given by Figures 2 and 3. Overall, the model ensemble accurately reproduces the seasonal pattern – with higher wet deposition of Hg in summertime,but fluxes are overestimated by a factor of 2 on average at the 8 sites above 60^0 N (6.5±2.4 *vs.* 11.7±2.6 ng/m^2/day) mainly during summertime. The models also overestimated precipitation amount by a factor of 2-5, which can explain the discrepancy between modeled and measured wet deposition fluxes. A comprehensive evaluation of the three participating models against 2011-2014 arctic measurements was recently performed by Angot et al. (2016). The authors suggested that a lower collection efficiency of precipitation in polar regions due to frequent strong winds and blowing snow condition can lead to underestimated measured precipitation amounts. At the high Arctic site, Ny-Ålesund, the three models overestimated wet deposition fluxes from February-June by a factor of ??. Ny-Ålesund is an elevated site (474 m above sea level) in proximity to open ocean, geographically distinct from two other high Arctic sites, Alert and Barrow. It is likely that spatial resolution of models is insufficient to represent the topological effects on meteorology. Reactive bromine concentrations utilized in the

models are empirically derived, which is another source of uncertainty in simulating oxidized Hg concentrations in models impacting wet deposition. During springtime precipitation events, mercury concentrations in snow collected on tables have been measured at Alert and Barrow, sites shown to be impacted by AMDEs. At both sites, median snow mercury concentrations were reported to be high with significantly higher values at Barrow (ref needed); these were well simulated by GEM-MACH-Hg (Alert: 8.4 ngL-1 modeled and 7.5 ngL^{-1} measured; Barrow: 37 ngL^{-1} modeled and 47 ngL^{-1} measured in 2005). Modeled median Hg concentrations in seasonal snowpack were also within the measured range in GEM-MACH-Hg (6.0 ng/L modeled, 4.9-6.0 ng/L measured at Alert in spring 2005).

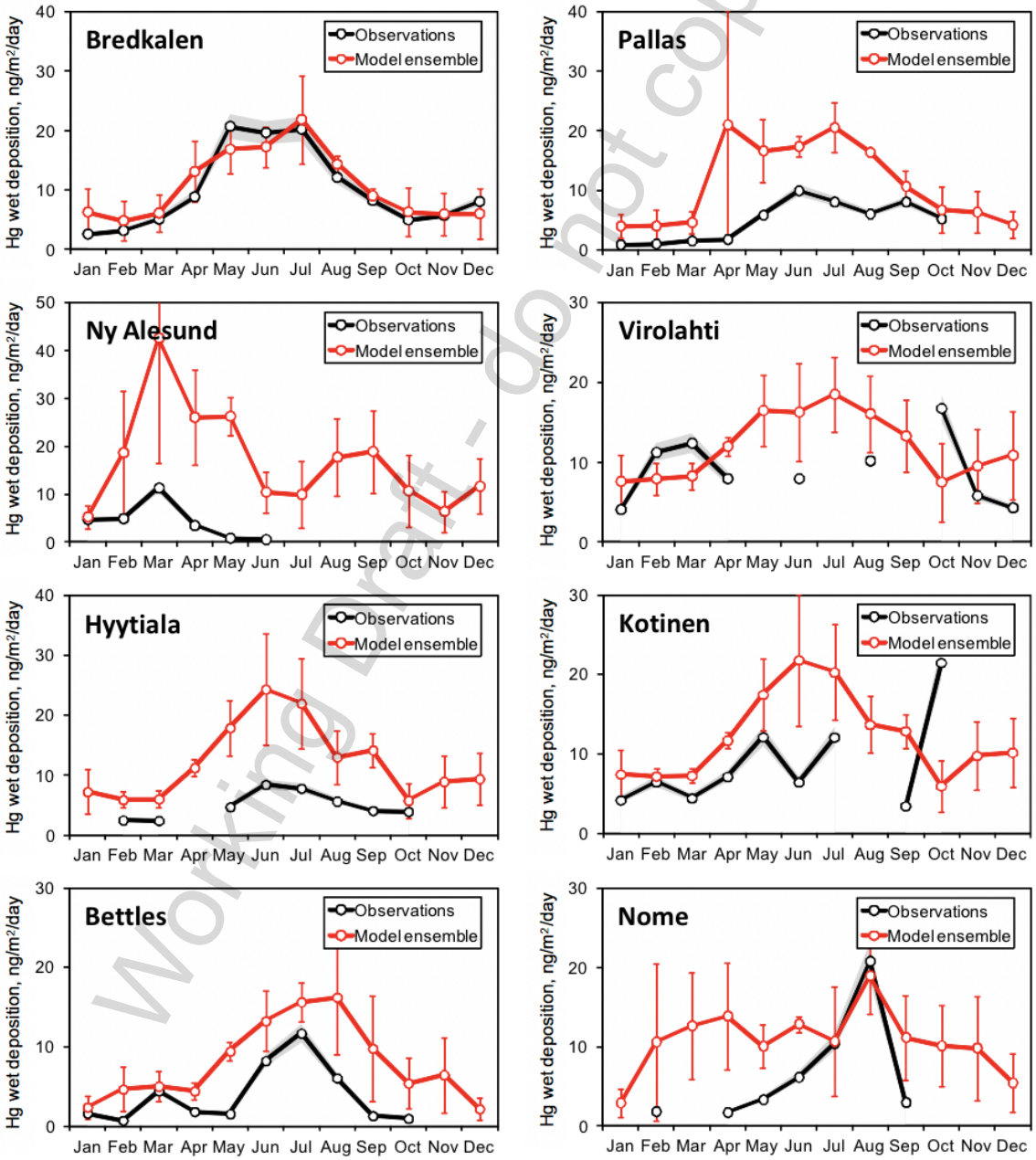

Figure 2: Year 2015 modeled and observed Hg wet deposition at the Arctic measurement sites. Black lines denote observations; red lines show arithmetic mean of the model ensemble. Shaded areas show ±10% uncertainty for observations while whiskers present the standard deviation of simulated values among the models.

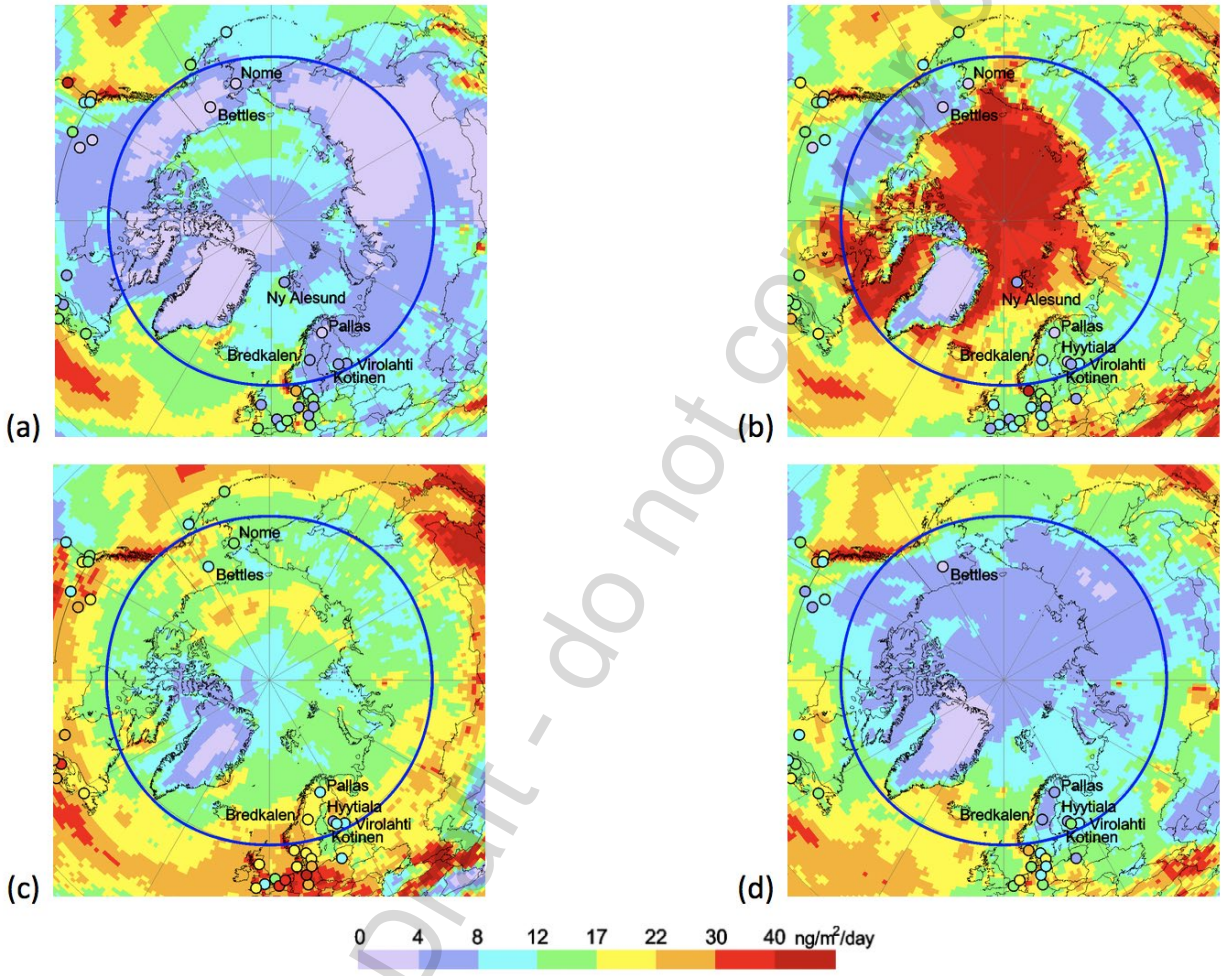

Figure 3: Year 2015 model ensemble mean Hg wet deposition in (a) winter, (b) spring, (c) summer, and (d) fall. Circles show observations in the same color scale. The blue line delimits the Arctic domain (> 60°N).

b. Interfacial exchange of Hg between air and terrestrial surfaces

Authors: **Daniel Obrist**, Tom Douglas, Martin Jiskra,

Add estimates from multi-model ensemble and comparison with measurements

Deposition to the arctic tundra and plant-driven Hg deposition:

Lower-latitude studies show that atmospheric Hg deposition to terrestrial environments is dominated (btw. 50% to 90%) by plant uptake of gaseous atmospheric Hg(0) via stomatal and cuticular uptake pathways, which is transferred to soils when plants die off or shed leaves (termed litterfall) or when plant surfaces are washed off by rain (termed throughfall). Plant-driven deposition dominates over wet deposition in all regions of the world (Fu, Yang et al. 2016, Wang, Bao et al. 2016, Wright, Zhang et al. 2016, Zhang, Wu et al. 2016)). Stable Hg isotopes analyses confirm that plant-derived gaseous Hg(0) deposition is the dominant source in most upland soils (accounting for 54-94% of Hg (Demers, Blum et al. 2013, Jiskra, Wiederhold et al. 2015, Enrico, Roux et al. 2016, Zheng, Obrist et al. 2016, Obrist, Agnan et al. 2017, Wang, Luo et al. 2017)).

Plant-driven Hg deposition is likely the dominant source of Hg in the tundra as well. A recent mass balance deposition study in the tundra at Toolik Field Station, Alaska measured dry deposition of gaseous elemental Hg(0) by a micrometeorology flux-gradient approach (Obrist et al., 2017). The study reported that gaseous Hg(0) dry deposition accounted for 71% of total atmospheric Hg deposition, dominating annual total net Hg deposition of 6.5 ± 0.7 μg m^{-2} yr^{-1}. Wet deposition was negligible (0.2 ± 0.1 μg m^{-2} yr^{-1}) and atmospheric Hg(II) dry deposition accounted for 2.5 μg m^{-2} yr^{-1} (range 0.8–2.8 μg m^{-2} yr^{-1}). Much of the Hg(0) deposition occurred via plant Hg uptake and subsequent transfer to tundra soils (Olson et al., 2018, Jiskra et al., 2019). These studies show that tundra ecosystems contain aboveground Hg biomass pools of up to 28.8 μg m^{-2} (Obrist et al., 2017, Olson et al., 2019) which is similar in magnitude as foliar Hg biomass residing in forests (15 to 45 μg m^{-2}). Due to annual plant turnover, much of this biomass is conveyed to soils via plant senescence and litterfall each year. An earlier study estimated a Hg deposition mass balance in northern Alaska based on sediment records, and reported total lake mercury deposition between 4.2 and 8.9 μg m^{-2} yr^{-1} (Fitzgerald et al. 2005). That study estimated wet deposition of 1.5±0.6 μg m^{-2} yr^{-1}, dry particulate Hg deposition of 0.1 μg m^{-2} yr^{-1}, and possible contribution via AMDEs of 2.1 ±1.3 μg m^{-2} yr^{-1}. However, terrestrial contribution from soils dominated as a source to lake sediments via surface runoff (1.4+0.6 μg m^{-2} yr^{-1}) and soil erosion (2.6+1.8 μg m^{-2} yr^{-1}), providing evidence that upland Hg sources dominate as Hg sources to arctic lakes. In addition to summertime Hg(0) deposition via plants, Hg(0) deposition also is observed during winter under the snowpack which may be attributable to sorption to soils, litter, or lichen under the snowpack (Obrist et al., 2017, Agnan et al. 2018, Jiskra at al. 2019), although the importance of this process for deposition loads is unknown. In barren tundra areas of the Arctic that lack significant vegetation cover (e.g., the Canadian Arctic Archipelago, northern Greenland, Svalbard, etc), wet and dry deposition processes directly to snow and soil surfaces probably dominate because the plant-uptake pathway is unavailable.

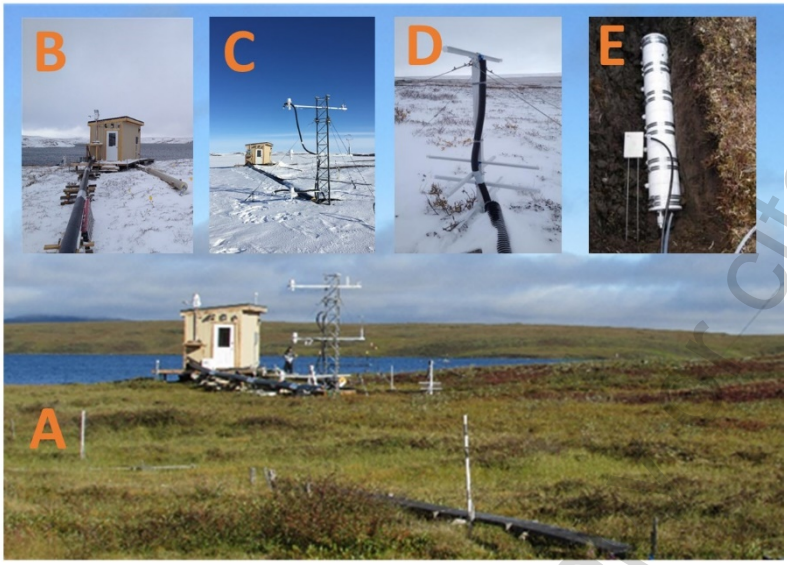

Figure 1. Mass balance deposition study in the tundra of northern Alaska (Toolik Field station). Instrumentation to measure gaseous Hg(0) deposition includes a tower system to measure ecosystem-level atmosphere-surface Hg(0) exchanges). From Obrist et al., 2017.

c. Interfacial exchange of Hg between air and marine surfaces

Authors: **Rob Mason**, Ashu Dastoor, Brian DiMento, Yanxu Zhang (Michelle Nerentrop, Katarine Gårdfeldt, Sofi Jonsoon – data contribution)

Add estimates from multi-model ensemble and comparison with measurements

Inputs of Hg to the surface waters of the Arctic from the atmosphere have been estimated from measurements made at coastal locations, studies in the Canadian Arctic Archipelago (CAA), and from limited measurements from vessels in the Arctic (see Sections 3.3.2 & 3.3.3a). Estimates of wet and dry deposition of inorganic Hg from cruise data, which are from the fall, are lower than those likely found during polar sunrise where AMDEs and Hg deposition are heightened. Monthly estimates, made by DiMento et al. (2019) based on their cruise measurements from the collection of wet deposition and surface snow samples, were lower than measured by others in the CAA and elsewhere in the Arctic (Soerensen et al., 2016 and references therein). The overall low precipitation (340 mm yr^{-1}; Serreze et al., 2006) at high latitudes results in relatively low wet deposition of Hg to the Arctic. Monthly wet deposition for the fall, calculated from the measured concentrations, Arctic Ocean surface area, and yearly precipitation, is estimated to be 0.2 Mg of total Hg. Based on the measurements in aerosols and an estimated dry deposition velocity of 0.5 cm s^{-1} (Holmes et al., 2009), given that there appeared to be mainly fine particulate aerosols over the open Arctic, 0.05 Mg of Hg were deposited per month via dry aerosol deposition (DiMento et al., 2019). Similarly, RGHg was deposited at a rate of 0.3 Mg mth^{-1}, based on the measured ionic Hg concentrations over open water, which were all near the Tekran instrument detection limit. The total atmospheric deposition to the

surface Arctic Ocean was thus estimated as 0.54 Mg mth^{-1} Hg, or 6.5 Mg yr^{-1}, with this estimate excluding any additional inputs from enhanced deposition during AMDE's in spring. Wet deposition represented 38% of the Hg flux, with dry deposition making up the remainder.

These atmospheric input estimates of Hg are lower than those of Soerensen et al. (2016), whose estimate covers the entire year, of 2.5 Mg mth^{-1} Hg on average (30 Mg yr^{-1}; Table x1). The estimate of Soerensen et al. is lower than other estimates for atmospheric input (Sonke et al., 2018; Outridge et al., 2008; Dastoor and Dunford, 2014; Zhang et al., 2020), which all appear high compared with the actual measurements over the offshore waters of the Arctic. Overall the measured concentrations by DiMento et al. (2019) are much lower than other measurements in the Arctic region, which are mostly measured at coastal land locations or in the CAA (Sections 3.3.2 & 3.3.3a).

In terms of evasion to the atmosphere, while various studies have measured water column Hg^0 concentrations and estimated evasion fluxes within the CAA (Table 2), there are only two studies that have made high resolution measurements of Hg^0 within the central Arctic Ocean (Andersson et al., 2008; DiMento et al., 2018; Fig. x1). These studies found different concentrations in the Arctic open waters although both studies showed the buildup of Hg^0 in the surface waters under the ice, suggesting the potential for a large release of Hg^0 from the underlying water during ice melt in spring/summer, in agreement with atmospheric observations and modeling. Significantly, this suggests that the seasonal gas exchange dynamics of Hg^0 could change substantially with the rapidly decreasing ice cover of the warming Arctic Ocean.

Table x1: Model Hg flux estimates (Mg yr^{-1}) for the Arctic Ocean for both the external inputs and the gas evasion flux to the atmosphere. For the air-sea exchange fluxes, their percentage contribution to the total input or export from the mixed layer is also given

Model estimates. All values in Mg yr^{-1}	**Atmos. Input**	**Rivers**	**Other Inputs**	**Total Inputs**	**Gas Evasion**
Outridge et al. (2008)	97 (47%)	13	96	206	10 (5%)
Dastoor & Dunford (2014)	58 (37%)	50	50	158	33 (21%)
Soerensen et al. (2016)	30 (42%)	50	71	151	85 (56%)
Sonke et al. (2019)	76 (51%)	44	30	150	99 (66%)
Zhang et al. (2020)*	168(100%)	N/A	N/A	168	98 (58%)

*Assuming all the atmospheric deposition enters the ocean even if sea-ice exists.

Figure 1: Dissolved elemental Hg (fM) in Arctic Ocean surface waters. Figures from : a) Andersson et al. (2008) & b) DiMento et al. (2019).

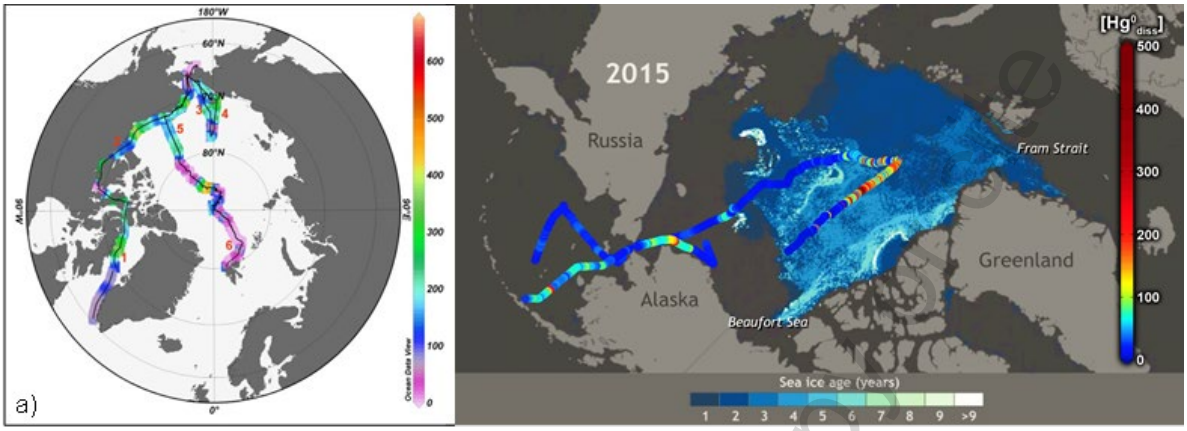

Overall, the model estimates for Arctic Ocean Hg^0 evasion in Table 1 reflect the results of earlier studies in the CAA, and the Andersson et al. (2008a) work (Table 2). These studies report higher concentrations overall than measured by DiMento et al., (2019) during the 2015 Arctic GEOTRACES cruise and result in much higher evasion estimates that would be predicted based on the cruise data (Table 2). To support the high evasion values in the models requires substantial inputs of Hg from the terrestrial environment (rivers, ice melt, glacial inputs), which are not consistent with other measurements (Table 1). The lower values for Hg^0 evasion, measured on the 2015 cruise, are more consistent with estimates of lower inputs of Hg to the Arctic from terrestrial sources (Sonke et al., 2019; Outridge et al., 2008; Table 1).

*Table 2: Dissolved elemental Hg (Hg^0) (fM) in the Arctic Ocean mixed layer, and estimated fluxes (Mg mth^{-1}). Data from the literature as noted. Note: * this is the maximum summer value.*

Study/location	**Hg0 (fM)**	**Flux (Mg mth^{-1})**
GEOTRACES 2015 open water	32 ± 30	1.0
GEOTRACES 2015 continuous ice	101 ± 98	<0.2
Kirk et al (2008) CAA	130 ± 50	-
Andersson et al (2008a)	220 ± 110	19
Fisher et al (2013) model average	210*	7.5
Dastoor & Dunford (2014) model	-	2.8
Soerensen et al (2016) model average	180	7.1
Zhang et al (2020) model average	37	8.2

Higher Hg^0 under ice (as opposed to open water) during the 2015 GEOTRACES cruise (DiMento et al., 2019; Fig. 2) is consistent with results from Antarctica (Nerentorp Mastromonaco et al. 2017a; 2017b). The timescale for surface water Hg^0 concentrations to return to open water values after ice removal, assuming the only sink to be gas evasion, and with no additional formation, is on the order of several weeks (DiMento, 2019). The radon data collected by Rutgers van der Loeff et al. (2014) in the Arctic concur with this estimate for the rate of change in concentration for an unreactive gaseous tracer. Net formation of Hg^0 would however impact this rate of change in the Arctic mixed layer as it could influence the overall concentration and degree of saturation. Both photochemical oxidation and reduction will be 50tmospher and the redox reactions are enhanced by UV radiation (Ci et al., 2016; Jeremiason et al., 2015; O'Driscoll et al., 2007; Whalin and Mason, 2006), which does not penetrate through the ice to any significant degree (Perovich, 2006). The rates of these reactions (10^{-4} – 10^{-6} s^{-1} depending on light levels and light penetration) indicate that the mixed layer open waters should come to steady state in terms of photochemical transformations within days (Whalin and Mason, 2007).

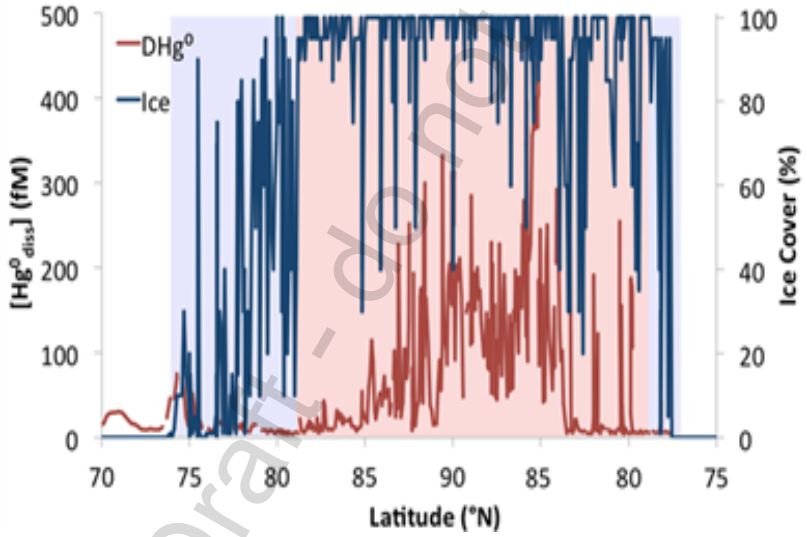

Figure 3: The dissolved Hg^0 (Hg^0_{diss}) concentration (DHg^0; fM; red line) and the ice cover (%, dark blue line) along the U.S. Arctic GEOTRACES cruise track within the marginal ice (light blue shading; 73.5-81 °N, 79-77.5 °N) and contiguous ice (light red shading; 81-90-79 °N) zones (DiMento et al., 2019).

Therefore, there should be a rapid response in terms of the relative Hg^0 concentration with the decrease in ice cover. Under the opposite scenario, the buildup of Hg^0 under ice after its formation is likely a slower biologically-mediated process. Biotic reduction rates have been related to primary productivity and range from 10^{-2} d^{-1} (~10^{-7} s^{-1}), with dark (non-photochemical) oxidation rates of the same order (Fantozzi et al., 2009; Hu et al., 2013; Kim et al., 2016; Moolash et al., 2014; Soerensen et

al., 2010; Whalin et al., 2007; Mason, 2016; Wang et al., 2016). Overall, the characteristic time to steady state would be several months, if no other losses occurred.

For gas exchange, applying the overall average calculated Hg^0 evasion rate to the entire Arctic (39 ng m^{-2} d^{-1}) is unreasonable because evasion does not occur under ice where predicted fluxes are greatest. Applying the average Hg^0 flux in open waters (10 ng m^{-2} d^{-1}; DiMento and Mason, 2019) to the average area of open water (40.3 % open water; 11.1 x 10^6 km^2 total area with 6.65 x 10^6 km^2 ice coverage; NSIDC, 2016; Soerensen et al., 2016), we calculate an evasion of 1.4 Mg mth^{-1}. This flux is about five times lower than the average monthly flux reported by Soerensen et al. (2016). Although deposition and evasion were similar in magnitude in our study, our estimate does not account for evasion of Hg deposited on snow and ice cover. Soerensen et al. (2016) estimated that atmospheric deposition and snow and ice melt inputs were similar in magnitude. Accounting for this melt term, we would expect to find greater evasion than atmospheric input indicating the need for coastal and riverine inputs, as well as water transport from the Atlantic and Pacific, to make up the difference between atmospheric inputs of Hg to the Arctic Ocean surface waters and the loss by gas evasion. The conclusion that there is net evasion at the Arctic Ocean surface to the atmosphere has been predicted in previous studies (Sonke et al., 2018; Fisher and other papers).

d. Total Hg exchange between air and Arctic surfaces

Authors: **Ashu Dastoor**, Hélène Angot, Daniel Obrist and Oleg Travnikov

- Add multi-model ensemble estimates of net deposition fluxes of Hg for each month showing contributions from wet and dry deposition separately to land and ocean.
- Add multi-model ensemble estimates of total Hg deposition to the largest river watersheds in the Arctic for each month
- Add estimates of total Hg deposition from the model DEHM (Jesper Christensen, Aarhus University, Denmark).

Based on Obrist et al's (2018) study from the Alaska tundra, Sonke et al. (2018) scaled up measured deposition from Toolik Field station to the entire permafrost soil area (22.79 million square kilometers) estimating a total atmospheric Hg deposition of 210 Mg y^{-1} to the global permafrost zone. Add comparison of net deposition flux observations at Toolik with modeling estimates, and provide model estimate for entire permafrost soil area.

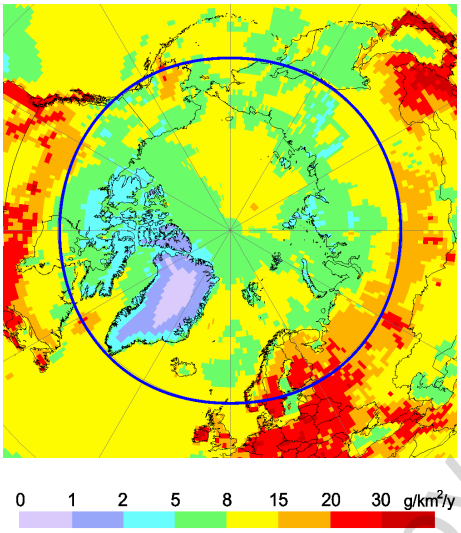

Fig. 1. Simulated (model ensemble mean) annual Hg deposition in the Arctic. The blue line delimits the Arctic domain (north of 60°N) [Preliminary results] Add boundaries of river catchments.

Add maps of seasonal Hg deposition

3.4 How much mercury do terrestrial systems transport to downstream environments in the Arctic?

[provide estimates of total and methyl Hg concentrations in the terrestrial environments, riverine and erosion total and methyl Hg export rates to the Arctic Ocean, and contribution of permafrost total and methyl Hg to downstream environments]

3.4.1 How does the terrestrial Hg enter downstream environments?

a. Watersheds and riverine systems

Author: **Erin Trochim**

Water travels in Arctic watersheds through a variety of paths (Bring et al. 2016). In conventional basins, water exists in the two primary forms of groundwater and surface water. Groundwater includes subsurface water like large aquifers. Surface water includes streams, rivers and lakes. Arctic basins often differ in critical ways. First, water can be stored as ice in the ground due to the presence of permafrost, or ground that remains frozen for two or more years. If this ice thaws, either seasonally or permanently, or grows, it can either contribute or store water. As water enters the watershed as either rain or snow, it begins the second unique process. Due to limited infiltration because of the ice in permafrost, water primarily remains in the active layer or soil that seasonally thaws, although variability occurs depending on the ice content of the soil (Walvoord and Kurylyk 2016).

Typically, water is then transported down hillslopes in preferential pathways. These include in between microtopography in terms of mounds like tussocks and hummocks and distinctive ribbons known as water tracks. In continuous permafrost water tracks can move water off of hillslopes depending on the amount of rainfall and antecedent water storage conditions (Rushlow and Godsey 2017) and have been shown to enhance flow (Evans et al. 2020). Water tracks take on a variety of forms, cannot be defined by incision alone and appear to be primarily controlled by surficial geology (Trochim et al. 2016). Lake distribution in permafrost regions is also highly affected by surficial geology where the highest densities are found in glaciated areas and the lowest in areas free from permafrost (Smith et al. 2007). Even though overall precipitation rates are low, lakes are more common here globally than anywhere else (Charles et al. 2014). Permafrost distribution alters the hydraulic connectivity to create distinctive water patterns and lake dynamics (Rey et al. 2019). These effects are also found around rivers, which often have taliks or unfrozen areas underneath them. Rivers with higher amounts of permafrost had larger amounts of annual total and baseflow change (Song et al. 2019). All these landforms and processes combine with climate to create unique watersheds and riverine systems.

Additional complexity can occur in watersheds due in variations in permafrost extent and its effects on lateral flow, evapotranspiration and the degree to which thermokarst or thawing of ice-rich permafrost is affecting water transportation. In boreal regions with discontinuous permafrost areas, lateral perennial thaw zones (PTZs) can provide complex, alternate pathways for water to flow (Walvoord et al. 2019). Lateral inflows in rivers in continuous permafrost shows variation between years and sub catchments (King et al. 2020). These lateral flows are also present the boreal lowlands varied over time, where lakes went from being relative similar in the spatiotemporal patterns to being heterogeneous in areas with less permafrost (Rey et al. 2019). In contrast, evapotranspiration and the partitioning between evaporation and transpiration can vary, and depend on climatic factors and microtopographic features (Young-Robertson et al. 2018). As permafrost loss from a basin is factored in, it is expected that more shifts will occur wetland and lakes with peat due to higher ice contents (Selroos et al. 2019). Detailed investigations have indicated the key role that microtopography also plays as permafrost degrades (Langford et al. 2019). Over time as permafrost thaw progresses, we may see a decrease in the runoff ratio and changes in preferential flow paths (Stone et al. 2019). These complexities are a key area of consideration for understanding watershed basins and routing in Arctic regions.

A paragraph is needed to explain, the riverine water export (why, how much and when) to the Arctic Ocean

b. Arctic soils and permafrost Author: **Chien-Lu Ping (needs to be condensed)**

3.4.2 How much Hg is present in Arctic terrestrial environments?

[Big picture on spatial distribution of Hg in terrestrial environments; note that observed temporal trends are covered in chapter 2]

Box 2. Mercury Stable Isotopes: Identification of mercury sources in Arctic terrestrial ecosystems

Authors: **Martin Jiskra**, Douglas, Thomas, Daniel Obrist

Hg has seven stable isotopes that can undergo both mass dependent fractionation (MDF, reported as δ^{202}Hg) and mass-independent fractionation of odd mass number (odd-MIF, reported as Δ^{199}Hg and Δ^{201}Hg) and even mass number (even-MIF, reported as$\Delta\Delta^{200}$Hg and Δ^{204}Hg) isotopes (Blum et al., 2014;Obrist et al., 2018). Atmospheric Hg sources and emission processes in arctic tundra ecosystems are associated with characteristic MDF and MIF (Figure XYZ).

Uptake of atmospheric Hg(0) by vegetation is associated with mass-dependent fractionation and discriminates heavy isotopes, resulting in an enrichment of lighter Hg in vegetation (negative δ^{202}Hg values, arrow 1 in Figure XYZ) and consequently a depletion of light isotopes in atmospheric Hg(0) (positive δ^{202}Hg values)(Obrist et al., 2017;Olson et al., 2019;Jiskra et al., 2019). Absence of mass-independent fractionation (Δ^{199}Hg and Δ^{200}Hg) has been observed during foliar uptake of Hg(0) in temperate regions (Yuan et al., 2018) and is not expected to occur in the Arctic either. Using a chamber experiment Sherman et al. (2010) showed that following Hg(II) deposited during AMDEs there was a strong re-emission of Hg(0) driven by photo-induced reduction processes. The photoreduction of Hg(II) in snow was associated with a strong fractionation of odd-mass Hg stable isotopes (Arrow 2 in Figure XYZ) and Δ^{199}Hg values of -5.5‰ were observed, some of the most negative Δ^{199}Hg values reported globally (Sherman et al., 2010). The two characteristic Hg stable isotope fractionation processes, uptake of Hg(0) by vegetation and snow and photo-reduction of AMDE-derived Hg(II) in snow, make Hg stable isotopes a potent tracer for sources and processes in the Arctic.

Obrist et al. (2017) measured the Hg stable isotope signature of atmospheric Hg deposition (Hg(0), Hg(II) in snow) and different ecosystem sinks (bulk vegetation, organic and mineral soils) at Toolik field station, on the Arctic Coastal Plain in northern Alaska 200km from the Arctic Ocean. Using a multi-isotope mixing model they concluded that the uptake of Hg(0) by vegetation was the dominant source of atmospheric Hg deposition, representing 90% of the total Hg in vegetation (interquartile range (IQR): 86% to 94%), 71% in organic soils (IQR: 56% to 81%), and between 25 and 54 % in mineral soils. The absence of large negative Δ^{199}Hg values in ecosystem sinks, suggests a large part of Hg deposited during AMDEs is emitted back to the atmosphere. For Utqiaġvik on the coast of the Arctic Ocean a re-emission between 76 to 91 % was estimated based on Hg stable isotopes (Douglas

and Blum, 2019). Other studies focused on identifying the fraction of AMDE-derived Hg that remains in the snowpack report roughly 75% of the AMDE Hg is re-emitted within a week (Douglas et al., 2012;Douglas et al., 2017). At inland sites, such as the Toolik Field station 200km from the Alaskan coast, a re-emission of >95% has been estimated (Obrist et al., 2017). As a consequence, AMDE derived Hg(II) deposition appears to have only a minor contribution to total Hg in Arctic ecosystems.

Douglas and Blum (2019) observed that Hg(0) dry deposition to the snowpack represented a significant contribution of total deposition to snow close to the Arctic Coast. They suggested high concentrations of reactive halogens promoted the oxidation of atmospheric Hg(0) within the snowpack and contributed significantly to Hg(0) dry deposition to the ecosystem. A similar process has been observed in frost flowers, ice crystals forming over sea ice containing high halogen concentrations, which were characterized by positive Δ^{199}Hg (max = 0.9 ‰) resulting from re-emission of Hg(0) after AMDE's (Sherman et al., 2012). On the Arctic coastal plain, 200km from the coast where halogen concentrations in snow are substantially lower, no significant deposition of Hg(0) to the snowpack was observed and net Hg(0) deposition fluxes during winter were consistent with uptake of Hg(0) by surface vegetation including lichen (Jiskra et al., 2019). Olson et al. (2019) measured Hg stable isotope signatures in different plant species and suggested that the uptake of atmospheric Hg(0) was the major source of Hg in all plant species. Different Δ^{199}Hg values in plant species, however, suggested different extent of photo-reductive Hg loss inducing Δ^{199}Hg anomalies, with lichen showing significant Hg loss through photo-reduction whereas no indication for photoreductive loss was observed for vascular plants.

The isotopic fingerprint of tundra soil Hg, characterized by vegetation and ecosystem Hg(0) uptake, has been identified in the Arctic Ocean, adding further constraint on the importance of tundra soils and river runoff as important Hg source. For Hg stable isotopes measured in coastal seawater a river source of terrestrial Hg of 50 to 80 % was suggested (Štrok et al., 2015). In a paleo reconstruction of Hg sources to deep Arctic ocean sediments, Gleason et al. (2017) concluded that tundra soil Hg represented the major source of Hg to ocean sediments. Hg stable isotope signatures have been reported for a number of different marine biota in the Arctic Ocean, i.e. murre eggs (Point et al., 2011;Day et al., 2012), ringed seals (Masbou et al., 2015;Masbou et al., 2018), polar bears and beluga whales (Masbou et al., 2018) and pilot whales (Li et al., 2014). Masbou et al. (2018) reviewed Hg stable isotope values in marine biota and concluded that terrestrial Hg represents the dominant source based on Δ^{200}Hg values, which are not affected by post deposition processes. Masbou et al. (2018) further suggested that the terrestrial Hg is exported from the Arctic Ocean to the North Atlantic where it represents a significant source of Hg in the food web.

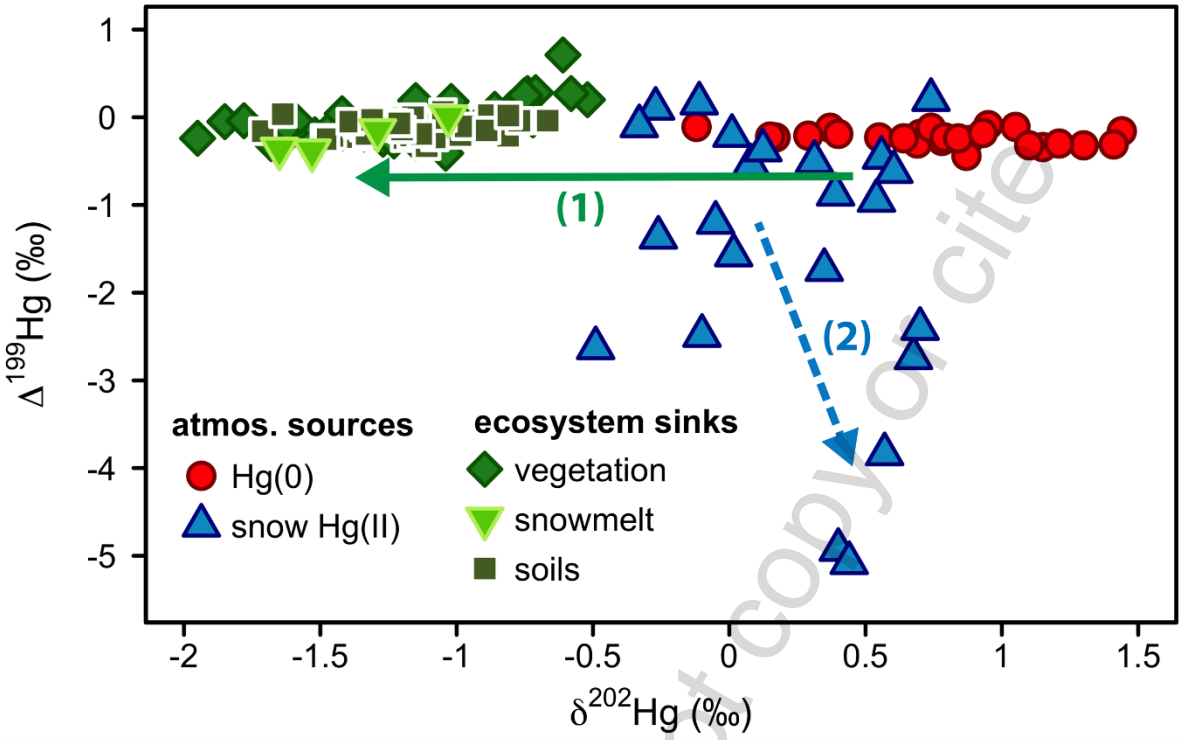

Figure XYZ: **Synthesis of Hg stable isotope fingerprints in terrestrial arctic Hg cycling.** Mass independent (Δ^{199}Hg) vs. mass dependent (δ^{202}Hg) of atmospheric sources (Hg(0) and Hg(II) in snow)(Sherman et al., 2010;Obrist et al., 2017;Jiskra et al., 2019) and ecosystem sinks (vegetation, snowmelt and soils)(Biswas et al., 2008;Obrist et al., 2017;Olson et al., 2019;Douglas and Blum, 2019). Two processes drive Hg stable isotope fractionation in the terrestrial arctic, (1) uptake of atmospheric Hg(0) by vegetation and snow (Demers et al., 2013;Jiskra et al., 2019;Douglas and Blum, 2019) and (2) photochemical reduction of Hg(II) in snow (Sherman et al., 2010).

a. Vegetation

Authors : **Daniel Obrist et al.**

Olson et al., 2019 summarized vegetation Hg concentration across multiple studies with a total of 150 arctic vegetation samples and showed substantial variability among different functional groups. Hg concentrations averaged 64 ± 6 µg kg^{-1} in lichen (46 samples; 23 to 186 µg kg^{-1}); 59 ± 6 µg kg^{-1} in mosses (n = 40; 19 to 195 µg kg^{-1}), and 9 ± 1 and 11 ± 2 µg kg^{-1} in vascular plants (grasses and herbaceous). Pronounced concentration differences between vascular plant and lichen and mosses have been reported before across temperate sites as well as in the Arctic, including by Wojtun et al. (2013) in Greenland (lichen: 30 to 100 µg kg^{-1}; mosses: 20 to 100 µg kg^{-1}; vascular plants: 10-30 µg kg^{-1}). Hg concentrations from Arctic vascular plants are generally below concentrations from temperate plants; for example, Wang et al., 2016 summarized vegetation Hg concentrations across 168 lower latitude sites globally and estimated mean vegetation Hg concentrations of 54±22 µg kg^{-1}. On the other hand, bulk vegetation Hg concentrations in the Arctic can be high due to a high

representation of non-vascular vegetation (i.e., mosses and lichen, Olson et al., 2018) which has implications for plant-derived Hg deposition as discussed in section 3.3.3.

St. Pierre et al. (2018) provide a detailed analysis of Hg concentrations in arctic lichen, which are critically important forage substrates for caribou, showing median total Hg concentrations on Bathurst and Devon Islands in northern Canada of 66.8 μg kg^{-1} (range from 36 to 361 μg kg^{-1}). Lichen Hg concentrations were two orders of magnitude higher than underlying soils suggesting atmospheric deposition as a dominant source of Hg, with sources likely including Hg^0 uptake, dust, and wet Hg deposition. Total and methyl-Hg enrichment in lichen were greater at coastal sites than inland sites suggesting proximity to polynyas leading to enhanced Hg deposition, possibly via AMDEs, halogens, ocean evasion and/or boundary layer mixing. Summarizing Hg levels in lichen from other arctic studies, St. Pierre et al., (2018) shows substantial variability in lichen Hg concentrations (10−270 μg kg^{-1}). Lichen concentrations were 48±5 to 107±123 μg kg^{-1} (Gamberg 2009) and 43 to 255 μg kg^{-1} (Chiarrenzelli et al., 2001) in the Northwest territories in Canada; 10 to 270 μg kg^{-1} in northern Quebec in Canada (Crête et al. 1992); 43 to 56 μg kg^{-1} (Landers et al., 1995) and 32 to 47 μg kg^{-1} (Lokken et al. 2009) in Alaska; and 13 to 98 μg kg^{-1} in White Sea, Russia (Shevenchki et al., (2013). Earlier studies also reported moss Hg data, including 55 μg kg^{-1} in feathermoss across northern Alaska (Landers et al. 1995) and 113 μg kg^{-1} in fringe mosses and lichen from Svalbard (Drbal et al. (1992).

The potential use of lichen and mosses as monitors for atmospheric Hg exposure and/or deposition in the Arctic has shown limited success. Nickel et al. (2015) correlated concentrations of heavy metals in atmospheric deposition with Hg accumulation in moss and soils across large south-to-north gradients in Norway, including Arctic location, and showed that correlations were weak for Hg. Harmens et al., (2010) previously showed a lack of correlations between modelled atmospheric Hg deposition and moss concentrations across a large network of sites in Europe and report that moss collected in Norway showed no distinct north-to-south patterns in spite of expected gradients in atmospheric Hg pollution.

b. Soils

Authors: **Daniel Obrist**, Peter Outridge, Kyra St. Pierre

Hg concentrations and Hg/C ratios in active-layer and permafrost soils

Substantial progress has been made to understand Hg levels in arctic soils and in the Arctic and boreal permafrost zone. We summarized data from five publications with available arctic soil data with a total sample size of 1294 data points (Lim et al 2020, in press; Leitch 2006; Olson et al., 2018; Outridge and Sanei, 2010; Schuster et al.,) to provide the following summary statistics of Arctic soil concentrations:

4483

Soil type	Mean	Median	IQR	Min	Max	Data points
Soil samples – all	68 (1740)	55 (813)	37 – 95 (196 – 1855)	3	303	1294
Active layer – all	81 (582)	65 (270)	45 – 103 (86 – 487)	4	303	380
Active layer – Surface (top 30 cm + peat + organic soils)	87 (191)	70 (148)	45 – 121 (61 – 318)	7	303	277
Active layer – Below-surface (>30 cm and mineral soils)	66 (1510)	60 (927)	45 – 87 (548 – 2058)	4	149	103
Permafrost – all	63 (2042)	48 (1225)	36 – 91 (261 – 2087)	3	284	912

4484 Concentrations of Hg in active layer soils and permafrost layers reported from the Arctic. All
4485 concentrations are reported in μg kg^{-1}. Parenthesis are concentration ratios of Hg to carbon in μg kg^{-1}
4486 C.

4487 Schuster et al. (2018) measured Hg concentrations across 13 northern permafrost cores (0-300 cm)
4488 along a ~500 km transect in northern Alaska. They reported total Hg concentrations in permafrost
4489 ranging from 17 to 207 μg kg^{-1} (mean of 64 μg kg^{-1}), and across all soil samples (including active-
4490 layer), they report median Hg concentrations of 43 ± 30 ng μg kg^{-1} and a Hg-to-carbon ratios (Hg/C)
4491 of 1,600 ± 900 μg Hg kg^{-1} C. Olson previously summarized Hg concentrations of arctic soils (478 data
4492 points) of 40 μg kg^{-1} in both organic and mineral soils with and Hg/C ratios (295 sample points) of
4493 174 μg kg^{-1} C in upper (0-30 cm, organic) soils and 621 μg kg^{-1} C in deeper (30-100 cm) mineral
4494 soils. Lim et al. (2020) reported Hg concentrations and Hg/C ratios for six peat cores along a
4495 latitudinal transect (56°N to 67°N) in the western Siberian lowlands, an area for which few Hg
4496 observations exist, despite the fact that Eurasian permafrost contains 54% of the C inventory in
4497 northern soils. Hg concentrations in peat cores ranged from 7 to 284 μg kg^{-1} with a median (±IQR) of
4498 67±57 μg kg^{-1}. The Hg/C ratio ranged from 50 to 2,000 μg kg^{-1} C with a median of 133 μg kg^{-1} C Hg
4499 soil pool (0 to 100 cm) increased with latitude from 0.8 mg Hg m^{-2} at 56°N to 13.7 mg Hg m^{-2} at
4500 67°N.

4501 Several studies have evaluated depth distributions in active layer soils. Olson et al., 2018 reported
4502 report highest Hg concentrations in organic surface layers at Toolik field station (151 ± 7 μg kg^{-1}),
4503 followed by A-horizons (108 ± 10 μg kg^{-1}), B-horizons (mean of 87 ± 5 μg kg^{-1}), and lowest in the
4504 frozen horizon at the bottom of the pits (transient permafrost layer; 56 ± 2 μg kg^{-1}). Although soil Hg

concentrations declined in concentrations with depth as observed previously in temperate soil studies (e.g., Obrist et al., 2011), Olson et al. suggested that depth declines in Hg were not as pronounced in Arctic soils compared to temperate studies possibly due to enhanced soil mixing via cryoturbation processes. The data summary on arctic soil Hg concentrations in Table 1 shows a 14% decline in Hg concentrations between the surface organic soils and deeper mineral soil layer. Similar depth distributions were observed across other Alaska sites such as in Halbach et al. (2017) also reported higher ranges, medians, and means in organic surface soils compared to minerals soils in Svalbard.

Other recent arctic soil Hg studies include: Hao et al. (2013) with a baseline of 270 μg kg^{-1} (range of 210 to 380 μg kg^{-1}) in surface soils at Ny Alesund; Loseto et al., (2004) with a range of 10 to 250 μg kg^{-1} in the humus layer of wetland soils; St. Pierre et al. (2015) with a range of <1 to 86 μg kg^{-1} in surface soils of the High Canadian Arctic; Riget et al. (2000) with geometric means of <10 to 30 μg kg^{-1} in mineral and 20 to 117 μg kg^{-1} in organic soils of Greenland; the previous AMAP assessment with a range of 40 and 150 μg kg^{-1} in soils from the Russian Arctic; St. Pierre et al., (2018) with a median of 0.18 μg kg^{-1} and a range of 0.98 to 86.4 μg kg^{-1} in soils of Bathurst and Devon Island in the Canadian Arctic Archipelago; and Douglas and Blum 2019) with Hg concentrations of 320 μg kg^{-1} in surface organics, 63 to 80 μg kg^{-1} in active layer soils, and 66 to 83 μg kg^{-1} in permafrost soil sof northern Alaska. Peat deposits from drained thaw lake basins near Utqiaġvik, Alaska have yielded elevated total Hg concentrations in surface layers (<100 years old) (Biswas et al., 2008), and peat core cross sections showed elevated Hg concentrations in surface vegetation and the upper soil horizon compared to lower (older and more decomposed) permafrost peats (Douglas et al. 2019).

It is now widely understood that sources of Hg in active layer soils are largely driven by atmospheric Hg deposition. Source attribution based on elemental ratios and Hg stable isotopes showed that for a Toolik Field station in Alaska about 70 % (56 % to 81 %, IQR) of Hg in surface O-horizons were derived from atmospheric Hg(0), 54 % (43 % to 62 %, IQR) in A mineral horizons, and 24 % (14 % to 34 %, IQR) in B horizons (Obrist et al., 2017). Based on limited samples, geogenic bedrock concentrations along the Dalton Highway in Alaska where most Arctic samples were taken (Schuster et al., 2018, Olson et al., 2018) were estimated at 32 μg kg^{-1} (Obrist et al., 2017, Olson et al., 2018). Geogenic fractions in mineral soils of Alaska were estimated between 20% in A horizons to 40% in B horizons (Obrist et al. 2017, Olson et al. (2018), with the rest originating from external sources such as atmospheric deposition. Halbach et al., 2017 similarly reported that surface soil Hg in Svalbard was not associated with typical geogenic elements (e.g., Al, As, Cr, Cu, Fe, Ni) indicating soil Hg to be largely derived from atmospheric deposition accumulating in organic-rich surface soils.

Mass estimates of soil Hg in arctic active-layer and permafrost soil

Schuster et al. 2018 estimated Hg pools contained in Northern Hemisphere permafrost regions extrapolating measured Hg/C ratios along the Alaska transect using soil carbon maps from the

Northern Circumpolar Soil Carbon Database (NCSCD) (Hugelius, Tarnocai, et al., 2013; Hugelius et al., 2014). They estimate that permafrost soils (0-3 m) contain 1,656 ± 962 Gg Hg of which 793 ± 461 Gg Hg is frozen in permafrost layers and 863 ± 501 Gg are stored in the active layer. In regards to spatial distribution, they predicted that soils with high carbon content and high sedimentation show highest Hg mass, as for example across the North Slope of Alaska and the Mackenzie River basin in Canada. Using a similar scaling approach, Olson et al., 2018 summarized Hg/C ratios derived from 15 published studies on arctic soils reporting a median Hg/C ratio of 274 μg kg^{-1} (range 25-833 μg kg^{-1}) for organic soils and 621 μg kg^{-1} (range 450 to 911 μg kg^{-1}) for mineral soils. Using the same soil carbon inventory of Hugelius et al. (2014), they estimated a lower median Arctic tundra active-layer soil Hg pool in the upper 0-30 cm of 26 Gg with a range of 21 to 42 Gg. For 30 to 100 cm depth, they estimated a Hg mass of 158 Gg (range of 115 to 232 Gg), for a total active-layer soil Hg pool size in the Arctic in the upper 100 cm of 184 Gg (range of 136 Gg to 274 Gg). Lim et al., (2020) reviewed pan-arctic Hg/C ratios including new data from western Siberian and estimated Hg/C ratios of 190 (IQR of 90 to 240) μg $kg^{-1}$for organic soils and 770 (IQR of 320 to 800) μg kg^{-1} in mineral soils. Using the pan-arctic carbon budget of Hugelius et al. (2014), they estimated a Hg pool of 67 (IQR of 37 to 88) Gg for 0 to 30 cm depth, 225 (IQR of 102 to 320) Gg for 0 to 100 cm, and 557 (371 to 699) Gg for 0 to 300 cm. In summary, both Olson et al. (2018) and Lim et al. (2020) suggest about three to four times lower soil Hg pools compared to Schuster et al. (2018). For example, they estimate 184 Gg (Olson et al.) and 225 Gg (Lim et al.) of Hg to reside in the top 1 m of soils (largely active layer), compared to Schuster's estimate of 863 Gg in active layer. Similarly, Lim et al. estimated 557 Gg of Hg in the top 3 m depth of permafrost compared to Schuster et al.'s 1,656 Gg. These lower estimates are in part due to new data from Western Siberia in Lim et al., who reported lower Hg/C ratios and possibly lower geogenic Hg concentrations in Siberian soils compared to northern Alaska soils. Another likely reason is that Hg/C ratios in Schuster et al. are based exclusively on permafrost data, leading to a bias towards higher Hg/C ratios. Our data summary in Table 1 shows that Hg/C ratios in surface soils and active layer soils to be much lower compared to permafrost soils, which is driven in large parts by lower carbon contents in deeper soil.

It has been proposed that Arctic active-layer and permafrost soils contain massive amounts of Hg and form the largest Hg pool size of Hg globally storing nearly twice as much Hg as in all other soils, the ocean, and the atmosphere combined (Schuster et al., 2018). A caveat to this statement, however, is that the Arctic pool sizes by Schuster et al. were estimated to a depth of 300 cm while global soil pool estimates are generally limited to surface soils only (i.e., upper 30 cm: ~240 Gg; Smith-Downey et al., 2010, ~300 Gg; Hararuk et al., 2013, 250 to 1,000 Gg with a best estimate of 500 Gg; Amos et al., 2015, 1078 Gg (842 – 1254 Gg, IQR; Lim et al. 2020). When comparing the same soil depths, Lim et al. (2020) estimates Arctic soil pools of the upper 30 cm to account for about 7% of the global soil pool.

c. Snow melt and ionic pulses as Hg sources

Authors: **Tom Douglas**

Hg concentrations – spatial distribution; *total mass estimates in snow and meltwater (also report comparison with Hg deposition estimates from models)*

Studies from coastal Utqiaġvik (formerly Barrow, Alaska) indicate that arctic inland and coastal deposition sources may differ substantially to those observed in the inland tundra and that along coastal sites, a critical source of Hg to soils and watersheds derives from snowmelt. One of the most unique aspects of the Arctic terrestrial system is the spring freshet: during spring melt, which can occur in as little as 10 days (Figure 2), up to 70% of the yearly surface water discharge runs from the land to the sea (McNamara et al., 1998). Riverine dissolved organic carbon (DOC) concentrations peak during melt and roughly 60% of the annual DOC export from major Arctic rivers occurs during breakup (Guo et al., 2011). Ultimately, Hg in the snow pack meets one of three simple fates during spring snow melt: 1) it is re-emitted during snow metamorphism and melt, 2) it ends up in the fresh water or marine system from runoff, or 3) it is are taken up by tundra and taiga ecosystems. The early pulse of melt water from this snow includes an "ionic" pulse of major elements and Hg, however, the majority of the Hg deposited during winter season is re-emitted prior to movement of melt water across the landscape (Dommergue et al., 2003; Douglas et al., 2017).

Douglas et al. (2017) reported a strong pulse of major ions and Hg in a small watershed during spring snowmelt, with dissolved Hg meltwater runoff of 8 and 14 ng L^{-1}, or up to 7 times greater than runoff reported from non-coastal Arctic locations. Douglas and Blum (2019) subsequently measured even higher snow Hg concentrations (69 to 416 ng L^{-1}), which was more than 30 times greater than the highest concentration reported from inland snow (e.g., Agnan et al., 2018). Based on stable Hg isotope signatures, they attribute atmospheric gaseous elemental mercury to compromise the majority of Hg in snow while AMDE comprised less (9 to 24% of total snow Hg). The suggested mechanism that dominates Hg deposition at the coastal site is Hg(0) deposition and oxidation of Hg(0) within the snowpack mediated by halogens which are enriched in coastal snowpack.

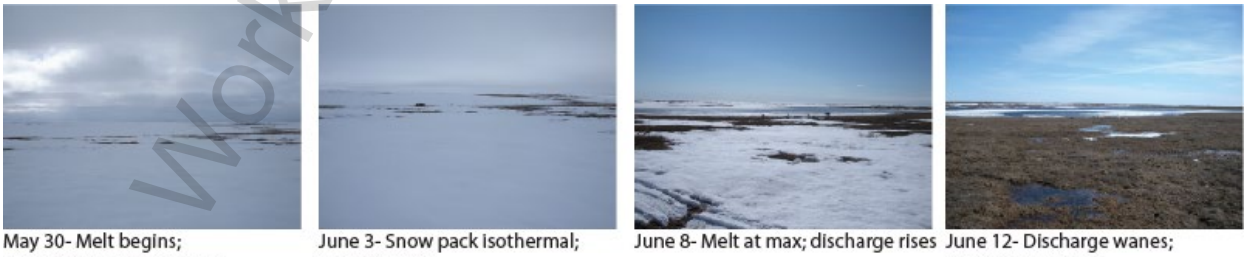

May 30- Melt begins; percolation columns form | June 3- Snow pack isothermal; runoff begins | June 8- Melt at max; discharge rises | June 12- Discharge wanes; most snow melted

Figure 2. Repeat images during spring melt in Utqiaġvik (formerly Barrow), Alaska during a typical spring melt. In a matter of a few weeks the tundra surface goes from completely snow covered to a wet vegetation and soil surface exposed to continuous sunlight.

d. Lakes sediments

Authors: **Jane Kirk**, Derek Muir, Sarah Roberts

Hg concentrations and fluxes in Arctic lake sediments; (also report comparison with Hg deposition estimates from models)

Box 3. Lake sediments as archives for Hg profiles

Authors: **Jane Kirk,** Derek Muir, Sarah Roberts

Reconstructing trends in anthropogenic Hg deposition using lake sediment cores

Hg sedimentary records are produced by the annual sinking of particulate-bound Hg to lake bottoms (Figure X). In southern temperate regions, sediment derived Hg deposition values have been shown to compare well to those obtained from wet precipitation instruments for modern times (Wiklund et al. 2017, Roberts et al. 2018) as well as to reliably track changes in reported Hg emissions from various industrial operations, such as smelters, Hg and gold mines, and chlor-alkali plants (Lockhart et al. 2000, Wiklund et al., 2017, Roberts et al. 2019). In the absence of long-term monitoring of wet and dry Hg deposition in Arctic regions, lake sediment cores provide a valuable tool to reconstruct current and past atmospheric Hg deposition (Chételat et al. 2015, Kirk et al. 2015). The ^{210}Pb method is often used to date intact lake sediments and derive sediment accumulation rates (g m^{-2} year^{-1}) for the past 100-150 years, with ^{137}Cs used as an independent tracer to validate the ^{210}Pb chronology (Oldfield and Appleby 1984, Blais et al. 1995). Cores which span the pre- and post-industrial periods (pre- and post-1850 CE) enable levels of anthropogenic Hg enrichment (or Enrichment Factors) to be calculated by comparing total Hg (all forms of Hg in a sample and herein referred to as Hg) concentrations recorded in the post-industrial sediments to a baseline level prior to industrialization. Hg enrichment factors and sediment accumulation rates (g m^{-2} year^{-1}) can then be used to calculate anthropogenic Hg fluxes (µg m^{-2} yr^{-1}) which reflect Hg deposition over time. To enable the comparison of sediment derived Hg fluxes from multiple lakes/locations, it is now common to apply a sediment focusing factor, which is based on a comparison of ^{210}Pb fluxes in lake sediment and catchment soils, and accounts for in-lake sedimentation processes (Blais et al. 1995, Perry et al. 2005, Muir et al. 2009). However, Hg fluxes recorded in lake sediments reflect Hg that has entered lakes both directly via atmospheric deposition as well as from catchment contributions (Figure X). To distinguish between Hg of anthropogenic versus geogenic origin, geochemical normalization can be applied to Hg concentration data given a

4639 strong correlation between Hg and lithogenic elements, such as aluminium (Al), titanium (Ti) and
4640 lithium (Li) (Loring 1991; Kersten and Smedes 2002; Wiklund et al. 2017; Roberts et al. 2019). Hg
4641 delivered to lakes via catchment runoff can also be accounted for in the sedimentary record using a
4642 "catchment effect" correction when sedimentary Hg accumulation is linearly correlated with the
4643 catchment area to lake area ratio, leaving a reconstruction of atmospheric deposition (Drevnick et al.
4644 2012, Wiklund et al. 2017, Roberts et al. 2019). Arctic lakes are currently experiencing stressors from
4645 climate warming, including increased lake primary production and catchment erosion. Thus,
4646 numerous recent studies (last ~10 year) have utilized the analyses of numerous novel proxies within
4647 the same or duplicate sediment cores to simultaneously examine changes to lake sedimentation rates,
4648 lake primary productivity, algal communities assemblages, and anthropogenic Hg deposition as well a
4649 the potential impact of these climate-driven processes on Hg deposition records (Stern et al., 2009;
4650 Jiang et al., 2011; Kirk et al., 2011; Burke et al., 2018; Korosi et al., 2018; Lehnherr et al., 2018,
4651 Outridge et al. 2018; Figure X). These studies represent the focus of the discussion below.

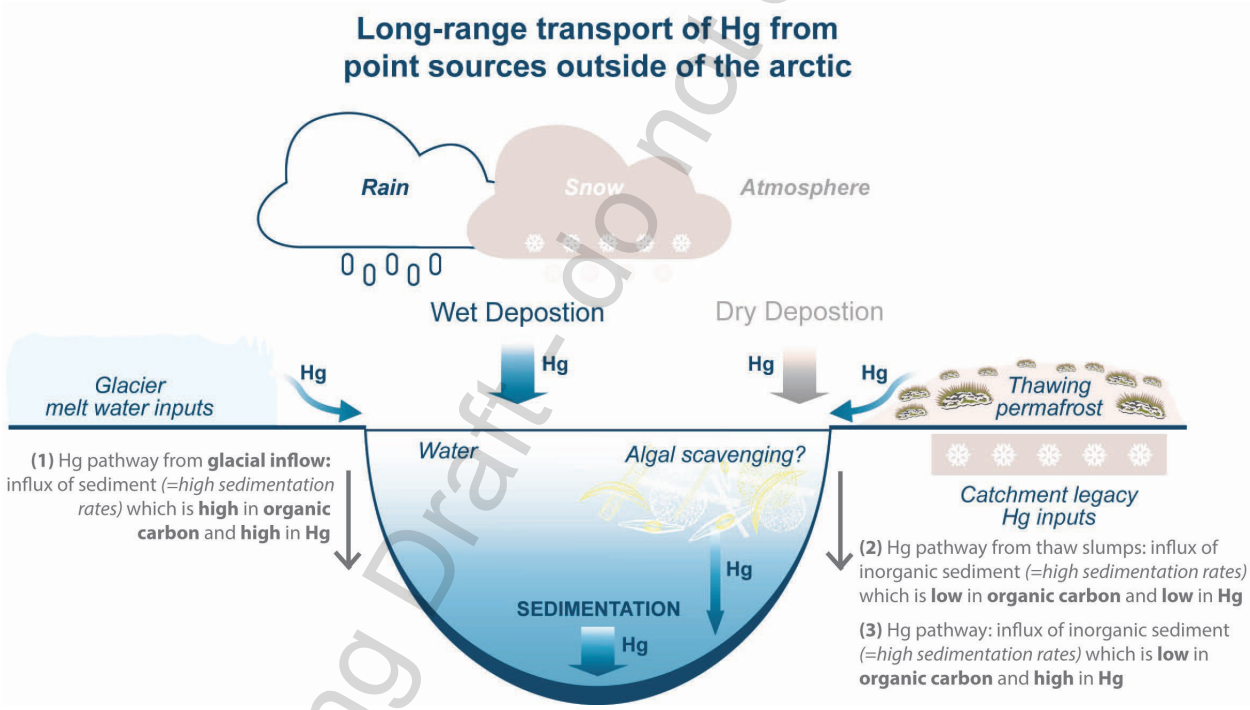

4652

4653

4654 ***Impacts of climate-induced changes to sediment delivery and sedimentation rates on Hg***
4655 ***accumulation in Arctic lakes***

4656 In the circumpolar arctic, climate warming is altering hydrological pathways in a number of different
4657 ways, including enhancing erosion, glacial melt and permafrost degradation, each which may alter the
4658 delivery of sediment, organic carbon, and hence Hg, to freshwater lakes. Numerous studies have
4659 noted widespread increases in sedimentation rates, particularly in the more recent sediment horizons
4660 and suggested that they are due to increased catchment erosion (Cooke et al. 2010, Muir et al. 2009,

Kirk et al. 2011, Fitzgerald et al. 2005). Thus, geological tracer/crustal elements or changes in sedimentation rates have been applied to Hg flux data to tease apart catchment and atmospheric Hg inputs so that these sedimentary records could be used to examine changes in atmospheric Hg deposition.

More recent studies have focused on examining the climate-induced mechanisms driving potential changes in Hg deposition at specific sites in the Arctic. For example, the impact of climate change on Lake Hazen (Figure X), which is the largest lake (by volume) within the high arctic circle (Lehnherr et al. 2018, St. Pierre et al. 2019, St. Pierre et al. 2019) has been examined in detail. Results show that Lake Hazen has been responding strongly to a climate warming of ~1°C in summer air temperatures, including deepening of the soil active layer, large mass losses from the watershed's glaciers resulting in a ~10 times increase in delivery of glacial meltwaters, a >70% decrease in lake water residence time, and an almost certainty of summer ice-free conditions in the near future (Lehnherr et al. 2018). A number of Lake Hazen sediment cores have been analysed for Hg, OC, carbon and nitrogen (C:N) ratios, stable N and C isotopes ($\delta^{15}N$ and $\delta^{13}C$), and algal (diatom) assemblages (Kirk et al. 2011, Lehnherr et al. 2018, St. Pierre et al. 2019). Results show that sedimentation rates (8X increase from 0.5 to 4.2 kg m^{-2} $year^{-1}$ between baseline pre-1948 and 2007) and OC accumulation rates (1000X increase from – to 14-71 g m^{-2} $year^{-1}$ 2007–2012) have dramatically increased in recent years (Lehnherr et al. 2018). Profiles of $\delta^{13}C$, $\delta^{15}N$ and C:N ratios show that the source of organic matter (OM) in Lake Hazen sediments is, and historically has been, primarily of terrestrial origin, likely from vegetation and soils destabilized by increased flow in the glacial rivers. The increased glacial flow and resulting sediment influx has driven enhanced Hg deposition (20 µg m^{-2} yr^{-1} during the baseline period versus 180 µg m^{-2} yr^{-1} post-2000; Table X), as well as legacy organochlorine pesticides (OCPs) previously stored in the glacier. These results demonstrate that climate-induced glacial melt and subsequent increased river flow have increased the loading of terrestrial Hg to Lake Hazen, which is being recorded in the lake sediments.

Two recent studies examined the impacts of climate-induced permafrost degradation on Hg, sediment, and OC delivery to Canadian sub-Arctic lakes by assessing a series of "thermokarst" lakes, or lakes created and/or expanded as ice-rich permafrost soils degrades causing land subsidence and water impoundment (Deison et al., 2012; Burke et al., 2018). Deison et al. (2012) analyzed dated sediment cores from 14 thermokarst affected lakes in the Mackenzie Delta uplands, Northwest Territories, using a case-control analysis of lakes where retrogressive thaw slumps were present and absent. They found that focus corrected sedimentation rates were ~2X higher in lakes with retrogressive thaw slump development on their shorelines (slump-affected lakes) (269 ± 66 SD g m^{-2} yr^{-1}) compared to lakes where thaw slumps were absent (reference lakes) (120 ± 37 g m^{-2} yr^{-1}) due to higher influx of new material into slump-affected lakes. They also saw higher OC concentrations in sediment profiles from reference lakes than in slump lakes and a strong inverse relationship between mercury

concentrations and sedimentation rate in the 14 study lakes ($R^2 = 0.68$, $P<0.01$), which explained 68% of the variation in surface Hg concentrations. The authors concluded that retrogressive thaw slump development decreased concentrations of OC and Hg in the lake sediments due to dilution by rapid inorganic sedimentation in the slump-affected lakes.

Burke et al. (2018) recently analysed Hg in sediment cores from three thermokarst lakes on the Arctic Coastal Plain of Alaska (Figure X). The authors found that Hg fluxes in two of the three lakes were variable and high over the past century (92.0 and 78.6 µg m^{-2} yr^{-1}; Table X), and were closely related to sedimentation rate (97 and 99% of variation explained by sedimentation rate), demonstrating that Hg deposition to the lake bottoms was largely controlled by influx of sediment. Interestingly, in one of these two lakes, Hg concentrations were significantly related to OM of both allochthonous and/or autochthonous origin while in the other, Hg was negatively related to OM and positively related to % mineral matter. In the third lake, however, Hg fluxes were lower (14.2 µg m^{-2} yr^{-1} ; Table X), more temporally uniform, and were more strongly related to sediment Hg concentration than sedimentation rate. Burke et al. (2018) also carried out a meta-analyses, which included 37 previously published Arctic and Alaskan lakes (Muir et al. 2009, Fitzgerald et al. 2005, Drevnick et al. 2012, Landers et al. 2008, Deison et al. 2012, Bindler et al. 2001, Engstrom et al. 1997), and compared Hg accumulation, available sediment proxy data, and landscape type. Results indicate that thermokarst lakes have significantly higher and more variable Hg accumulation rates than non-thermokarst lakes, suggesting that properties such as thermal erosion, thaw slumping, and low hydraulic conductivity makes these lakes prone to high and variable Hg accumulation rates.

Impacts of Changing Lake Primary Productivity on Lake Sediment Hg Records

For climate sensitive regions, such as the circumpolar arctic and sub-arctic, lake sediment cores are natural archives of both climate-driven processes, such as increased primary productivity and changes in algal communities, as well as anthropogenic contaminant deposition both of which are ongoing and have occurred largely simultaneously since the mid-20th century. Numerous studies have simultaneously reconstructed Hg deposition and climate-induced changes to primary productivity and algal community assemblages using a multi-proxy approach, including analyses of Hg, total organic carbon (TOC), C:N ratios, and $\delta^{15}N$, $\delta^{13}C$ and microfossil diatom abundance, as well as the novel application of visual reflectance spectroscopy (VRS) to measure chlorophyll *a* (chl-*a*) and Rock-Eval to measure S2 carbon (Kirk et al. 2011, Outridge et al., 2007, Stern et al., 2009; Rydberg et al 2010; Jiang et al., 2011; Sanei et al 2012; Outridge et al., 2019, Korosi et al. 2018, Cooke et al. 2012, Lehnherr et al. 2018, Deison et al. 2012, Burke et al. 2018). VRS-chl-*a* provides a good indicator of trends in primary productivity as it measures both chlorophyll *a* and it degradation products (Michelutti et al. 2005) while S2 carbon is a high molecular weight, kerogen derived aliphatic hydrocarbon fraction of OC which is thought to correspond to the biomacromolecular structure of algal cell walls (Carrie et al. 2010; Stern et al. 2009; Outridge et al. 2007). Some studies have found

strong positive correlations between Hg accumulation in sediments and proxies of lake primary production, such as TOC and S2 carbon, and suggested that this relationship was due to "algal scavenging" of Hg or the absorption/adsorption of available Hg in the water column by algal biomass followed by its sinking and sedimentation (Sanei et al. 2012; Grasby et al. 2013). It has further been estimated that 70-96% of Hg deposition recorded in sediments over the post-industrial period in Canadian and Norwegian Arctic lakes can be attributed to algal scavenging (Outridge et al., 2007, Stern et al., 2009; Rydberg et al 2010; Jiang et al., 2011; Sanei et al 2012; Outridge et al., 2019), which has implications for the use of sedimentary records to reconstruct anthropogenic Hg deposition. However, other studies have found strong relationships between proxies of primary productivity, such as S2 carbon and VRS chl a, in only a subset of lakes and concluded that the effect of algal scavenging on the sedimentary Hg record was not a wide-spread phenomenon across the circumpolar arctic (Cooke et al., 2012; Korosi et al., 2018, Kirk et al. 2011, Lehnherr et al. 2018, Deison et al. 2012). Kirk et al. (2011) examined algal assemblages, S2 carbon, and VRS-chl *a* in 14 lake spanning latitudinal and longitudinal gradients across the Canadian high and sub Arctic. They found that although increases in anthropogenic Hg deposition (anthropogenic Hg fluxes corrected for catchment contributions in 14 lakes: 0.3-16 $\mu g\ m^{-2}\ y^{-1}$) and inferred lake primary productivity were observed in all or most lakes, a significant positive relationship between Hg and S2 carbon was only observed in a subset of study lakes. Deison et al. (2012) analysed Hg, S2 carbon, and VRS-chl *a* in 14 dated lake sediment cores from reference and slump-affected lakes in the Mackenzie Delta and found significant relations between S2 carbon and Hg in surface sediments of all lakes; however throughout the entire sediment profile, they found significant relationships between Hg and S2 carbon and Hg and VRS-chl *a* in 5 of the 8 lakes factors and suggested that factors besides algal scavenging affect Hg delivery to sediments. Similarly, Burke et al. (2018) analysed Hg, OM, and VRS-chl a in three thermokarst lakes from the Arctic Coastal Plain in Alaska and found significant relationships between concentrations of Hg and VRS-Chl *a* and %OM in 2 of the 3 lakes. Korosi et al. (2018) examined diatom fossil remains, VRS chl *a*, and Hg profiles from 8 lakes on Cape Herschel, Ellesmere Island spanning four different microclimates, which established based on 30 years of lake ice-cover observations and diatom-based reconstructions of ice cover and primary productivity. For example, "warm" lakes experienced early (~1850) and marked limnological responses to climate warming while "cool" lakes show a later response (~1950) due to a longer ice-covered season. The authors found that in some lakes, there was a strong association between Hg and VRS-chl *a* concentrations. However, measures of Hg enrichment (Efs comparing post-1990s to pre-industrial 1850 Hg concentrations) were comparable across lakes in all four climatic zones, despite marked differences in the magnitude of increased primary productivity. For example, West, a "cold" lake which has not yet experienced increases in primary productivity or alterations to the diatom assemblage, showed a 4.4 in recent Hg enrichment. The authors concluded that although climate warming, and associated increased primary productively, have the potential to increase Hg sequestration to lake sediments, algal scavenging may

not be widespread across the Arctic and correlations between proxies of primary productivity and Hg may be spurious.

As described above, Lehnherr et al. (2018) examined the impact of climate-induced changes to the sedimentary Hg record at Lake Hazen, an ultra-oligotrophic lake. The authors analysed $\delta^{13}C$ and $\delta^{15}N$ in the sediments and lake water column and found that autochthonous OC is rapidly decomposed at the sediment–water interface, rather than accumulated in the sediments. The authors thus concluded that the sediment archive is not sensitive to changes in algal productivity, which may be increasing in Lake Hazen due to decreased ice cover and increased nitrogen and phosphorus inputs from glacial rivers.

A recent study examined THg, C/N, S2 carbon, diatom abundance as well as the fraction of Hg in Arctic sediment bound to OM (Hg-OM) using a sequential extraction method (Bloom et al. 2003; Kim et al. 2003) in three lakes spanning different vegetation ecozones (grassy tundra, barren tundra, and boreal forest region) (Outridge et al. 2019). To overcome possible effects of anthropogenic contamination on natural algal processes, only pre-industrial sediment horizons (ca A.D. 600-1800) were examined. Outridge et al. (2019) found that concentrations of S2 carbon and organic matter (OM) bound Hg (OM-Hg) were significantly related in two of the lakes, but not in the boreal lake. Outridge et al. (2019) suggests that the absence of relationships between sediment OM and THg in some lakes may be due a limitation of forms of Hg and/or labile OM suitable for binding eachother, such as complexation of Hg by humic acids (Le Faucheur et al. 2014; Schartup et al. 2015). They suggest that the importance of algal scavenging may vary over time as the lake's climate and environmental settings change and that algal scavenging may partially explain the discrepancy between recent Hg flux increases observed in many Arctic lake sediments and decreasing or stable atmospheric Hg concentrations (Goodsite et al. 2013).

Comparison of sediment and model derived Hg deposition fluxes:

A few studies have compared 67tmospheric depositional Hg fluxes ($\mu g\ m^{-2}\ yr^{-1}$) obtained from dated lake sediment cores to those from atmospheric deposition models. Fluxes obtained from the Global and Regional Atmospheric Heavy Metals (GRAHM) model (Dastoor et al., 2015) for the Canadian arctic (~ 4.5 $\mu g\ m^{-2}\ yr^{-1}$ in the high Arctic north of 66.5°), ~ 7 $\mu g\ m^{-2}\ year^{-1}$ in Yukon sub-Arctic, ~ 7.5 $\mu g\ m^{-2}\ year^{-1}$ in North West Territories sub-Arctic and ~ 6.5 $\mu g\ m^{-2}\ year^{-1}$ in Nunavut sub-Arctic) showed good agreement with sediment derived values corrected for particle focussing, changing sedimentation rates, and/or erosional inputs and for the Canadian high (2.8 $\mu g\ m^{-2}\ year^{-1}$) and sub Arctic (7.5 $\mu g\ m^{-2}\ yr^{-1}$) (Muir et al. 2009). In addition, both the GRAHM model and Muir et al. (2009) report a significant decrease in Hg fluxes with increasing latitude. However, a comparison of Canadian arctic-Greenland fluxes derived from three different models (Danish Eulerian Hemispheric Model (DEHN; Christenson et al. 2004, Global EMEP Multi-Media Modeling System

(GLEMEP; Travnikov et al. 2009), and GRAHM) found discrepancies largely from the 1990s to present day between modelled Hg fluxes and sedimentary Hg fluxes from arctic lakes (Goodsite et al. 2013). These recent discrepancies may be a reflection of 1. Difficulties in establishing ^{210}Pb chronologies in Arctic sediment cores (Goodsite et al. 2013, Cooke et al. 2010, Wolfe et al. 2004), 2. A paucity of measurements of Hg in air resulting in uncertainty in Hg deposition estimates (Chételat et al. 2015), or 3. Anthropogenic climate warming, such as increased primary productivity, driving increased Hg delivery to lakes and lake sediments (Goodsite et al., 2013, Korosi et al. 2018, Outridge et al. 2019) and demonstrate the need for more work on this front. *New info to be added from Jane and Ashu*

As Arctic lakes experience a combination of climate-induced changes to catchment runoff, sedimentation rates, lake ice-cover and lake primary productivity, as well as changing atmospheric contaminant deposition sourced from urban and industrial regions across the globe, recent studies demonstrate that careful analyses of multiple proxies are needed to improve our understanding of Hg sedimentary records and sediment-based reconstructions of anthropogenic Hg deposition (e.g., Korosi et al. 2018, Kirk et al. 2011, Outridge et al. 2019). Hg stable isotope analyses of dated lake sediment cores from temperate zones has been utilized to examine changing Hg sources and may be of values in Arctic lakes. For example, in remote Canadian lakes, down core Hg stable isotope analyses demonstrated that 42 ± 26% of inorganic Hg was deposited directly from the atmosphere (Chen et al., 2016; Obrist et al., 2018). In a boreal forested region in Sweden, Hg stable isotope analyses showed that inorganic Hg in forest runoff originated from the deposition of Hg through foliar uptake rather than from precipitation (Jiskra et al., 2017; Obrist et al., 2018).

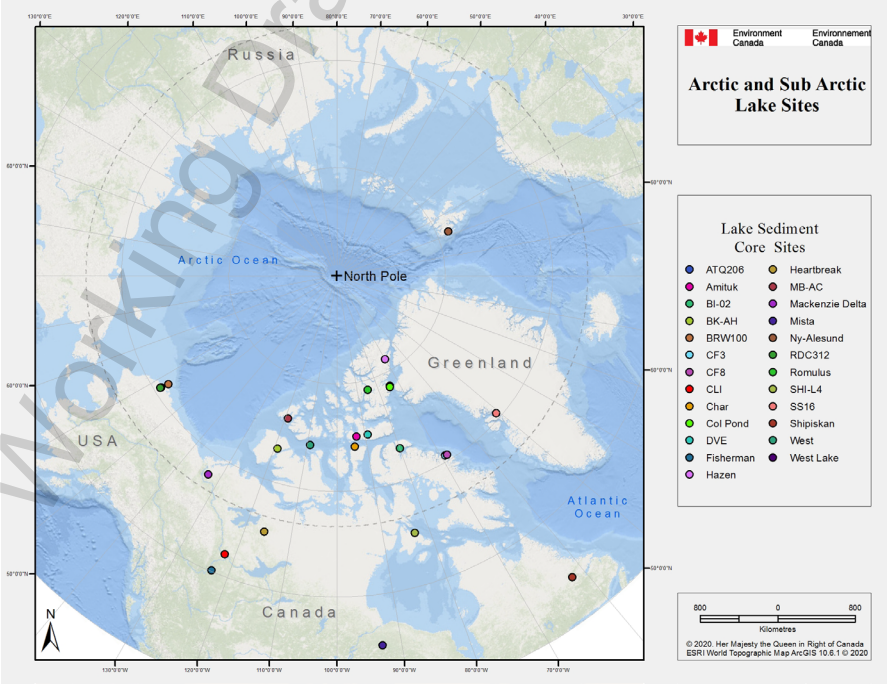

3.4.3 How much mercury do rivers transport to the Arctic Ocean?

Authors: **Peter Outridge**, Jeroen E. Sonke, Cuicui Mu & Tingjun Zhang

Rivers are an important transport pathway between the atmospheric Hg accumulated in terrestrial watersheds, natural Hg eroded from catchment geology, and the Arctic Ocean. There have been no published studies on groundwater transport of Hg into the Arctic Ocean, and so this potential source will not be considered further in detail. Early work on groundwater flows directly into the Arctic Ocean from coastlines suggested that they are <10% of the total river flows (Stein and Macdonald 2004). However, groundwater is an important and increasing component of total river discharge (e.g., for the Yukon River; Walvoord and Striegl, 2007). It is also noteworthy that, in other parts of the world, subsurface groundwater discharge may directly contribute as much Hg to coastal marine environments as atmospheric deposition (Outridge et al., 2018).

Earlier sections of this Chapter (3.3.3 and 3.4.2) summarized the current state of knowledge of present-day rates of atmospheric Hg wet and dry deposition onto Arctic catchment areas, uptake of GEM by Arctic vegetation, and soil Hg concentrations and mass. The permafrost regions which underlie much of the total Arctic Ocean river catchment area have accumulated a large mass of Hg – 225 $x10^3$ t in the upper 1m (range of 102-320 $x10^3$ t) – through 10 millenia of the Holocene and previous inter-glacial stages (Schuster et al., 2018; Olson et al., 2018; Lim et al., 2020).

The hydrological and geomorphological processes and influential factors responsible for mobilizing the soil Hg and transporting it downslope and downstream to freshwater environments are as yet poorly understood. Lim et al. (2020) found that maximum riverine particulate Hg concentrations and fluxes occurred in areas of sporadic/discontinuous permafrost in western Siberia, and were due to the release of large amounts of particulate Hg from thawing permafrost. Rivers draining southern, permafrost-free or northern, continuous permafrost regions exhibited lower Hg concentrations and fluxes than the intermediate regions of discontinuous permafrost. Small catchments with large areas of organic matter-rich permafrost were especially important sources of suspended Hg load. At the thawing permafrost boundary, where the active layer was deepest, deep and intermediate peat horizons were dominant contributors to the riverine Hg loading rather than soil mineral layers, surface peat and plant litter (Lim et al., 2020).

It is clear that Arctic catchment soils act as a buffer between atmospherically-sourced Hg and the Hg in river and lake waters. The soil buffer acts to temporally and quantitatively "dislocate" deposited Hg from riverine Hg by slowing the transfer of atmospheric Hg into freshwater environments. This dislocation accounts for the finding that much of the Hg in tundra soil active layers was deposited prior to the Industrial Period (Olson et al., 2018), the implication being that it has been stored in soils for millennia. Soil retention of Hg also partly explains the lack of a significant relationship between the rates of current atmospheric Hg deposition and river Hg fluxes in the Arctic and elsewhere

(Brigham et al., 2009; Domagalski et al., 2016). Many environmental factors that vary between Arctic river catchments, including precipitation, river discharge rates, topography, land use, proportion of permafrost area, active layer thickness, vegetation cover and hydrogeological features, also influence river Hg flux (Domagalski et al., 2016; Sonke et al., 2018; Mu et al., 2019; Lim et al., 2020). Furthermore, pore-waters in active layers during thaw periods contain elevated levels of methyl Hg compared to nearby river and lake waters (Schuster et al., 2011; Gordon et al., 2016; Olson et al., 2018), showing that soils are sites of net Hg methylation and may be concentrated sources of MeHg to adjacent rivers and subsequently to the ocean.

The river catchments that drain into the Arctic Ocean (as defined by AMAP, 2011; see Fig 3.4.3) yield an annual freshwater runoff of about 3300 km^3, with the Russian rivers the Yenisey (620 km^3), Lena (523 km^3), and Ob (404 km^3), and the Mackenzie River (330 km^3) in Canada, contributing the highest flows and the Mackenzie the largest sediment load (Stein and Macdonald 2004). The earliest oceanic Hg mass balance (Outridge et al., 2008; see also AMAP, 2011) estimated a total riverine Hg outflow to the ocean of about 13 t/yr total Hg based on sparse riverwater Hg concentration data only for the Mackenzie River. Since then, expanded sampling campaigns and the use of different upscaling or modeling approaches have yielded a variety of estimated river Hg outflows of between 16 and 108 t/yr (Fisher et al., 2012; Kirk et al., 2012; Durnford et al., 2012; Amos et al., 2014; Dastoor and Durnford 2014; Zhang et al., 2015; Soerensen et al., 2016; Sonke et al., 2018; Mu et al., 2019).

The latter two studies are notable additions to the Arctic river Hg estimates because they are based on recent analyses of river water Hg concentrations in seven of the largest rivers, including for the first time seasonal data from the Russian sector of the Arctic. Based on the multiyear data sets from the Arctic Great Rivers Observatory (Holmes et al., 2018; www.arcticgreatrivers.org/data) for 2003-2017, Mu et al. (2019) calculated the export of total Hg from the six largest rivers (Yenisey, Lena, Ob, Mackenzie, Yukon and Kolyma) to be 20.1 t/yr (interquartile 14.8 to 28.8 t/yr). Approximately 53% of Hg exports occurred during spring, 43% in summer and 5% in winter, a pattern also observed in small Siberian rivers (Lim et al., 2020). However, these estimates were not scaled up to incorporate all rivers draining into the Arctic. Sonke et al (2018) made multi-year observations of dissolved and particulate Hg in the S. Dvina and Yenisey, confirming strong Hg export during the spring freshet in May-June, but also during the Fall wet season. Previous studies were reviewed, and two contrasting methodologies used to estimate pan-Arctic river Hg flows to derive similar results from both: total Hg:DOC relationships for rivers upscaled to the whole Arctic using riverine DOC flux data; and total Hg yield:run-off relationships for multiple Arctic watersheds upscaled to include all Arctic rivers. Annual total Hg outflows calculated by these methods were 43 t/yr, and 44±4 (1σ) t/yr, respectively, consisting of equal parts dissolved (22 t/yr) and particulate Hg (22 t/yr). These estimates include the relatively small rivers draining into Hudson Bay and Baffin Bay, however, with those excluded the Arctic Ocean river flux was 43±4 t/yr. The pan-Arctic MeHg flux (total of dimethyl- and

monomethyl-Hg), based on all available published data, was 0.8 t/yr (Sonke et al., 2018). The total Hg estimates by both methods agree closely with the most recent modeling-based values of 46 t/yr by Zhang et al. (2015), and 50 t/yr by Dastoor and Durnford (2014). For the oceanic mass balance presented later in this chapter, the riverine flux will be taken to be 43±4 t/yr. This is of similar magnitude, within uncertainty, to the coastal erosion Hg flux of 39 t/yr derived in section 3.4.4.

The importance of the contribution of terrestrial Hg sources to the Arctic Ocean Hg cycle is supported by stable Hg isotope data on Arctic marine sediments and biota. Paleo-sediment Hg isotope patterns clearly indicate terrestrial soil Hg sources were dominant prior to the industrial period (Gleason et al., 2017). A recent re-evaluation of published marine biota Hg isotope data also suggests that soil-derived Hg dominates the MeHg present in many top predators in the Arctic Ocean today (Masbou et al., 2018). The isotope data cannot at present distinguish between riverine and erosion Hg sources, since both represent a terrestrial soil isotope signal. Nonetheless, the importance of riverine and coastal erosion sources of Hg to the Arctic Ocean contrasts with other world oceans in which direct atmospheric Hg deposition generally dominates (Soerensen et al., 2016; Outridge et al., 2018). The finding of Hg- and organic carbon-enrichment in Labrador Current waters exiting from the Canadian Arctic Archipelago also suggests a significant terrestrial contribution to the overall Arctic Ocean Hg budget (Cossa et al., 2019).

Rivers may become more important Arctic Ocean Hg sources in future. An increase over recent decades in the discharge of major Arctic rivers is well established (e.g. Serreze et al 2006), with Eurasian rivers showing the greatest increase. Box et al. (2019) assessed the temporal trends in discharge for six of the largest Eurasian rivers (Ob, Pechora, Severnaya Dvina, Yenisei, Lena, and Kolyma), and for the two major North American Arctic rivers (Mackenzie and Yukon). By volume, the combined Eurasian river discharge is 1.8 times that of the two North American rivers. For the composite Eurasian river dataset, river flows increased on average by 18.7 km^3 per decade between 1981 and 2011, whereas the two North American rivers exhibited an increase of 5.9 km^3 per decade between 1975 and 2015. These volume increases correspond to 12% and 9% increases, respectively, for the two regions over approximately the past three decades. In parallel, permafrost thaw leads to deepening of active layer thickness, providing erodible organic matter to enhanced run-off. St Pierre et al. (2018) and Lim et al. (2018) illustrated how permafrost thaw and thaw slumping leads to enhanced riverine particulate Hg loads. The impact of these changes on the Arctic Hg cycle will be discussed in greater detail in the climate change chapter of this Report.

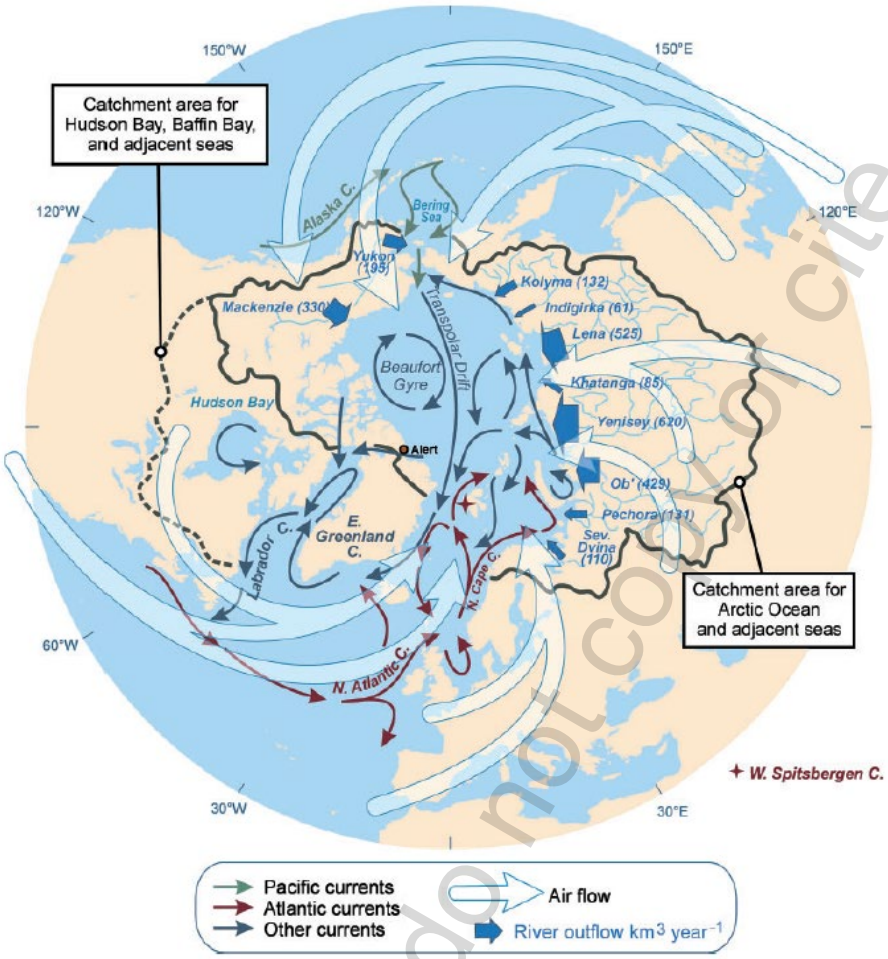

Figure 3.4.3 Map of Arctic river catchments as employed by AMAP (2011), showing annual freshwater discharges into the Arctic Ocean (km^3/yr). Note that the rivers draining into Hudson Bay, Hudson Strait and Baffin Bay are not included in this definition, but are encompassed by some of the river Hg mass balance studies discussed here. (Source: Outridge et al., 2008). NB Need to be redrawn removing the atmospheric and ocean current pathways, leaving only the river catchment boundaries and the blue arrows with discharge numbers

3.4.4 How much mercury does coastal erosion contribute to the Arctic Ocean?

Authors: **Peter Outridge** and Daniel Obrist

Coastal erosion rates along some parts of the Arctic Ocean coastline are among the highest in the world owing to the occurrence of long reaches of unlithified glacial till sediments occurring in elevated bluffs, comparatively rapid changes in relative sea-level, and the widespread presence of exposed ground ice that is susceptible to the eroding action of wind and water (Overduin et al., 2014; Gibbs et al., 2015). The overall long-term erosion rates in different sectors of the Arctic coastline, expressed in spatial terms, are typically 0.5-1.5 m/yr, with high local and regional variability (Lantuit

et al., 2012; Overduin et al., 2014; Couture et al., 2018). Susceptible sections of the Laptev, East Siberian and Beaufort sea coasts commonly exhibit losses of 3-10 m/yr with localized sites exceeding 20 m/yr (Jones et al., 2009; Lantuit et al., 2012; Günther et al., 2013).

Previous estimates of the Hg mass input to the Arctic Ocean from coastal erosion vary within a factor of three, between 15 and 47 t/yr, and were based either on scaled-up regional tundra soil Hg measurements or inferences from atmospheric-ocean models (Outridge et al., 2008; Fisher et al., 2012; Zhang et al., 2015; Soerenson et al., 2016). Based on soil/permafrost cores from eroding coastal bluffs along the Beaufort Sea (Leitch, 2006), Outridge et al. (2008) used a median soil Hg value of 110 ng/g DW to develop an oceanic erosion Hg mass estimate (see AMAP, 2011), whereas Soerensen et al. (2016) used a value of 81 ng/g. All of the above studies suggested that erosion contributed a significant fraction of the total inputs to the oceanic Hg mass balance. However, the paucity of data on permafrost and tundra soil Hg concentrations, and uncertainties around the erosion mass flux, were acknowledged weaknesses.

Recently, Olson et al. (2018), Schuster et al. (2018), and Lim et al (2020) provided new permafrost and tundra soil Hg concentration data for different areas of the Arctic. Olson et al. (2018) synthesized most of the available Arctic tundra soil Hg data (see Olson et al. for references), to which we have added data from Leitch (2006; N=262) and Lim et al. (2020; N=207, excluding data from a non-permafrost site in central Russia). Schuster et al.'s (2018) data were omitted from this calculation because their sampling excluded active layer soils, which would be eroded into the ocean along with permafrost. The exclusion of the active layer data could have significantly biased the results lower, because the active layer often contains substantially higher Hg concentrations than the underlying permafrost (e.g., Leitch, 2006; Outridge and Sanei, 2010; Olson et al., 2018). The combined data summary (N=985) indicates a mean (±S.D.) soil Hg concentration of 66.1±52.3 ng/g DW (median of 54.8 ng/g). The 25% and 75% interquartile values were 30.0 and 88.8 ng/g, respectively. These concentrations are used below to derive a new coastal erosion Hg flux estimate with uncertainties.

Published estimates of soil erosion mass loss into the Arctic Ocean as a whole remain rare since Rachold et al.'s (2004) calculation of 430 Mt/yr. However, based on the Arctic Coastal Dynamics Database, Lantuit et al. (2012) reported mean volumetric erosion losses for different sectors of the Arctic Ocean coastline, which are used here to calculate a soil erosion mass for the ocean (Table 3.4.4). There are two key assumptions in the calculation of eroded mass from eroded volume. The first is the use of a common bulk density of 1.2 g/cm^3 for the eroding material, which was derived from a significant inverse relationship between bulk density and soil organic carbon content in Canadian Arctic and sub-Arctic soils (Hossain et al., 2015). The second assumption is that the average soil organic carbon content in eroding coastal bluffs in the Yukon (4.5% TOC, used in this calculation; Couture et al., 2018) is applicable to the whole Arctic Ocean coastline. Couture et al.

(2018) represents the most comprehensive survey published to date of organic carbon in eroding Arctic coastal soils, although it is restricted to the Beaufort Sea coast of the Yukon.

By combining the resulting total coastal erosion rate (582 Mt/yr) with the mean and 25-75% interquartile soil Hg concentrations described above, erosion is estimated to contribute 38.5 t/yr total Hg to the ocean, with an interquartile range of 17.5 to 51.5 t/yr (see Table 3.4.4). This mean value falls within the range of previous estimates (see above) but is better constrained by data. Using the median soil Hg concentration of 54.8 ng/g gives an erosion flux of 32 t/yr. The Eurasian Arctic coastline, where erosion rates are highest, contributes the overwhelming majority (89%) of the total Hg influx; the Svalbard and Greenland Sea / Canadian Archipelago sectors contribute negligible amounts because their average erosion rates are very low (≤0.01 m/yr). This Hg flux calculation assumes that tundra soil Hg concentrations in the Eurasian sector of the Arctic, from which there are relatively few data (see Schuster et al., 2018; and Lim et al. 2020), are similar to the Alaskan – Canadian sectors.

The majority of the Hg contained in eroding coastal soils is likely to be natural in origin, deposited from the atmosphere during millenia of peat growth and soil formation after the end of the last global glaciation and before the industrial era. Olson et al. (2018) estimated that ~90% of the Hg in tundra soil profiles is natural, but pointed out that this estimate is affected by uncertainties such as the degree of thermokarst mixing of surface and mineral soils in active layers, and the timing and size of the anthropogenic atmospheric influx during the 20th century.

Methylmercury (MeHg) concentrations in soil and permafrost have not been reported from near the Arctic Ocean coastline, and are rare across the Arctic as a whole. St. Pierre et al. (2015) reported that soil MeHg concentrations varied by two orders of magnitude (0.02 – 2.11 ng/g DW) across several sites in the Canadian Arctic Archipelago, with a median of 0.12 ng/g. Independently, Soerensen et al. (2016) assumed a median of 0.8 ng/g DW (1% of total Hg) for their estimate of coastal erosion MeHg inputs into the Arctic Ocean. Based on the eroded soil mass calculated here, these concentrations would be equivalent to a MeHg flux ranging from 0.07 to 0.46 t/yr.

The speciation and fate of the total Hg and MeHg once in the ocean has not been studied. Like Hg in other soils world-wide (O'Connor et al., 2019), total Hg in the eroding material may be predominantly in particulate form bound to organic matter and minerals, with a minor fraction dissolved and bound to dissolved organic matter in soil porewater. Initially, eroded material was thought to predominantly settle out in coastal sediments (Hill et al., 1991), suggesting that this may also be the fate of much of the associated Hg and MeHg. However, Couture et al. (2018) calculated that only a minor fraction (~13%) of the eroded soil organic carbon was actually present in near-shore sediments, indicating that most of the carbon was either rapidly metabolized in the near-shore environment or was exported off the continental shelf by waves or sea ice. Because of the often strong association of Hg and organic

matter in tundra soils and permafrost (e.g., Schuster et al., 2018; Lim et al., 2020), Couture et al.'s findings suggest the possibility that the Hg from coastal erosion may also be remobilized during organic matter mineralization, and transported from coastal sediments to elsewhere in the oceanic environment. The finding, based on stable Hg isotopes, that top marine predators in the Arctic Ocean contain a predominance of Hg from terrestrial sources (Masbou et al., 2018) supports this suggestion, although Hg isotope analysis cannot distinguish between riverine and coastal erosion sources of terrestrial Hg in the ocean.

There is substantial evidence that average erosion rates are significantly increasing across many Arctic regions, and are now higher than at any time since observations began 50-60 years ago (Overduin et al., 2014; Irrgang et al., 2018). For example, erosion rates in rapidly eroding sections of the Laptev and Beaufort seas have doubled over the past 50 years (Jones et al., 2009; Günther et al., 2013). A number of interacting climatic, oceanographic and on-shore geomorphological processes have been suggested as contributing to this trend. These include: on-going warming and destabilization of coastal ground ice, a declining sea ice extent, increasing summertime sea-surface temperatures and wind speeds, and rising sea-levels; the changing ocean conditions promote increases in storm frequency and intensity, and thus in the effects of wave action upon thawing, exposed shoreline permafrost (Jones et al., 2009; Overduin et al., 2014).

Table 3.4.4 Calculation of coastal erosion total Hg flux into the Arctic Ocean.

Sector Name[A]	Length (km)[B]	Percent total length (%)	Mean cliff height (m a.s.l.)	Mean erosion rate (m/yr)	Mean vol. ground ice (vol. %)	Total vol. eroded (km^3/yr)	Vol. corrected for ice (km^3/yr)	Soil mass eroded (Mt/yr)[C]	Hg flux (t/yr)[D]
Russian Chuckchi Sea	2736	2.7	14.5	0.27	13.9	0.011	0.009	11.1	0.73
American Chuckchi Sea	4662	4.6	5.0	0.49	24.0	0.011	0.009	10.4	0.69
American Beaufort Sea	3376	3.3	1.5	1.15	26.9	0.006	0.004	5.2	0.35
Canadian Beaufort Sea	5672	5.6	6.7	1.12	29.4	0.043	0.030	36.3	2.40
Greenland Sea / Cdn. Archipelago	4656	4.6	No data	0.01	14.2	--	--	--	--
Svalbard	8782	8.7	14.0	0	0.0	0.000	--	--	--
Barents Sea	17965	17.7	10.5	0.42	16.2	0.079	0.067	79.8	5.27
Kara Sea	25959	25.6	14.0	0.68	23.7	0.248	0.189	227.1	15.01
Laptev Sea	16927	16.7	11.9	0.73	17.1	0.147	0.122	146.4	9.67
East Siberian Sea	8942	8.8	8.8	0.87	19.6	0.068	0.055	66.0	4.36
Total or Mean	**101447**	**100.0**	**9.7**	**0.57**	**18.5**	**0.614**	**0.485**	**582**	**38.5**

A: Arctic Ocean boundaries and area conforms to AMAP (2011).

B: Data on coastal geomorphology and erosion rates from the Arctic Coastal Dynamics Database (Lantuit et al., 2012). Erosion data are weighted with the length of the coastline in each sector to accurately represent the input of each sector in the whole ocean calculation.

C: Eroded volume corrected for ground ice volume, and converted to mass assuming a mean bulk density of 1.2 g/cm3 (derived from a strong inverse relationship between bulk density and soil organic carbon (SOC) in Arctic soils (Hossain et al., 2015) and the mean SOC of eroding Yukon coastal soils of 4.5% (Couture et al., 2018)).

D: Hg flux calculated from soil mass eroded assuming a mean Hg concentration of 66.1 ng/g DW in Arctic tundra and coastal soils (N=985; see text).

3.4.5 How and how much mercury do permafrost contribute to downstream environments in the Arctic?

[provide estimates of Hg contribution from permafrost to Arctic environments]

Authors: **Kyra St. Pierre**, Tom Douglas, Daniel Obrist, Christian Zdanowicz

Note: This section needs to be cross-referenced in Section 3.4.2b.

Permafrost within Arctic soils store an estimated 793 ± 461 Gg Hg, or 48% of the total Arctic soil pool (Schuster et al. 2018). As permafrost thaw is already widespread across the Arctic, these stores are thus a potentially important source of Hg to downstream environments. Ultimately the contribution of permafrost thaw to Hg mobilization depends on local conditions affecting Hg storage and permafrost properties (e.g., ice and carbon content; Vonk et al. 2015). In regions underlain by ice-rich permafrost, other landscape and climatic characteristics (e.g., topography, precipitation regimes) determine landscape susceptibility to different modes of thermokarst formation (Olefeldt et al. 2016).

Permafrost thaw in ice-rich, low relief regions may result in the formation of thermokarst wetlands, ponds and lakes (Vonk et al. 2015; Olefeldt et al. 2016). These systems have been repeatedly identified as Hg methylation hotspots across the Arctic due to the concurrent mobilization of carbon and nutrients, creating conditions suitable for methylation (Gordon et al. 2016, MacMillan et al. 2015). Gordon et al. (2016) observed MeHg concentrations up to an order of magnitude higher (0.43 ng L^{-1}) in the poor fens associated with recent permafrost thaw than in the hydrologically isolated bogs in the Scotty Creek catchment of the discontinuous permafrost zone. As thaw proceeds, hydrological connectivity between these previously isolated systems increases, potentially enhancing Hg exports across the landscape and into larger river systems (Godin et al. 2014; Jorgenson and Shur 2007). In some cases, these systems may drain, resulting in a momentary pulse of both organic and inorganic Hg into downstream systems (MacMillan et al. 2015).

St. Pierre et al. (2018) estimate that ~5% of the Hg in permafrost soils (88 Gg) of the circumarctic may occur in regions susceptible to the development of hillslope thermokarst features, such as retrogressive thaw slumps. These large features (up to 40 ha) can quickly mobilize vast amounts of previously stored, mostly particulate-bound Hg directly into streams, rivers or lakes and through to downstream ecosystems. On the Peel Plateau in the western Canadian Arctic, concentrations of total Hg and MeHg in streams were up to 2 orders of magnitude higher downstream of slumps than upstream, reaching concentrations of up to 1270 ng L^{-1} (mean: 448 ± 87 ng L^{-1}) and 7 ng L^{-1} (mean: 1.68 ± 0.64 ng L^{-1}), respectively, some of the highest Hg concentrations ever recorded. While concentrations were only measured up to 2 km downstream of the slumps in St. Pierre et al. (2018), Emmerton et al. (2013) reported total Hg concentrations in the mainstem Peel River (18 ng L^{-1}) higher than elsewhere in the Canadian Arctic (Northern Contaminants Program 2012), suggesting that these elevated concentrations could be at least partially attributed to permafrost thaw across the watershed.

Permafrost thaw has also been invoked to explain increases in Hg exports in the Yukon River (Schuster et al. 2011). Conversely, Hg mobilized by thaw slumps along lake shorelines is rapidly deposited to the bottom of the lakes. Deison et al. (2012) reported no difference in Hg deposition rates between slump-affected (26.61 ± 6.92 μg m^{-2} yr^{-1}) and reference lakes (25.35 ± 3.01 μg m^{-2} yr^{-1}) of the Mackenzie Uplands, an observation driven by lower total Hg concentrations, but higher sedimentation rates in the slump-affected lakes. The impact of slumps on lake shorelines may, however, differ depending on the lake and region.

With sampling sites spanning a 1700 km transect in the western Siberian Arctic, Lim et al. (2019) quantified particulate Hg yields from sites across a permafrost gradient: from where permafrost was absent (0.189 ± 0.048 g km^{-2} 6 $mnths^{-1}$), through to the isolated (0.205 ± 0.056 g km^{-2} 6 $mnths^{-1}$), sporadic (0.379 ± 0.096 g km^{-2} 6 $mnths^{-1}$), discontinuous (0.350 ± 0.225 g km^{-2} 6 $mnths^{-1}$), and continuous (0.170 ± 0.042 g km^{-2} 6 $mnths^{-1}$) permafrost zones. Maximal particulate Hg yields from areas underlain by sporadic and discontinuous permafrost zones suggest that particulate Hg fluxes to the Arctic Ocean may increase as warming continues and the permafrost zone boundaries shift northwards.

Much of the cited work, though, is biased to regions underlain by ice-rich permafrost, which favours the dramatic landscape destabilization and rapid (years to decades) pulses of materials to downstream ecosystems ('pulse disturbances'; Vonk et al. 2015). So called, 'press disturbances' from thawing permafrost (i.e., active layer deepening) occur more widely across northern landscapes, but is much more subtle and therefore the consequences are much more difficult to detect without longer term monitoring (multiple decades). Given the spatial and temporal variability in thaw processes, it is difficult (if not impossible) at present to quantify how much permafrost thaw contributes to Hg exports from Arctic watersheds. More work is needed to better constrain the permafrost thaw contribution to downstream ecosystems across the circumpolar region. Permafrost thaw is highly irregular across the landscape and may result in vastly different trends in Hg mobilization and accumulation rates, even within a single geographic region (Burke et al. 2018). There is potential in exploiting the well-documented relationships (e.g., Schuster et al. 2018; Sonke et al. 2018) between permafrost organic carbon and Hg exports to constrain the permafrost Hg contribution to downstream ecosystems.

3.5 How much mercury does ocean circulation transport to the Arctic Ocean? *[provide estimates of total and methyl Hg transport and concentrations in the Arctic Ocean]*

3.5.1 How and how much marine Hg enters the Arctic Ocean?

Authors: **Peter Outridge** and Lars-Eric Heimbuerger

The four main gateways for seawater Hg exchange between the Arctic Ocean and the Pacific and North Atlantic Oceans are the Bering Strait, the Canadian Arctic Archipelago and Davis Strait, Fram Strait, and the Barents Sea Opening (BSO; Fig. 3.5.1), with the latter two having the largest flow volumes. Seawater exchanges with the Pacific and Atlantic Ocean were estimated by Tsubouchi et al. (2018) to be: a northward inflow through the Bering Strait of 22.1 ± 22.1 km^3/yr; a northward net inflow through the BSO of 72.5 ± 37.8 x 10^4 km^3/yr; a southward net water outflow through Fram Strait of 34.7 ± 37.8 x 10^4 km^3/yr; and a southward net outflow of 66.2 ± 22.1 x 10^4 km^3/yr through Davis Strait. The inflow-outflow difference is made up by river inflows and precipitation (Haine et al., 2015).

North Pacific water flows unidirectionally into the Arctic Ocean through Bering Strait which has a broad, shallow (~50-m depth) sill that effectively restricts water inflow (Carmack et al 2016). From the Atlantic Ocean, surface, mid-depth and deep ocean waters enter the Arctic Ocean via Fram Strait and the Barents Sea; Arctic waters, representing a mixture of Pacific and internally-modified Atlantic waters, exit into the North Atlantic via Fram and Davis Straits (Haine et al 2015). Fram Strait is the only deep-water connection between the Arctic Ocean and the North Atlantic Ocean *via* the Nordic Seas. Relatively warm and saline North Atlantic water enters the Arctic Ocean here as the West Spitsbergen Current, while cold and less saline Arctic water masses exit the Arctic Ocean as the East Greenland Current. Because the salinity of Pacific water is less than that of the Atlantic water, Pacific waters overlie the Atlantic Layer over much of the western half of the Arctic Ocean (Carmack et al., 2016). The northward penetration and vertical mixing of Atlantic water with Pacific water is enhanced during periods of positive Arctic Oscillation Index which results in generally stronger southerly winds over the Barents and Greenland Seas. There is a net west-to-east movement of water, gases and other constituents via the Transpolar Drift from the Pacific to the Atlantic side, which is driven by the pressure gradient created in part by salinity and temperature differences between the two oceans (Carmack et al., 2016).

Two earlier studies estimated ocean current THg inputs to the Arctic Ocean, based on current volumes and reported THg concentrations in Pacific and Atlantic seawater, and found similar results: 48 t/yr THg (Outridge et al., 2008; see also AMAP 2011) and 53 t/yr (range of 40-62 t/yr; Soerensen et al., 2016). Most of this Hg comes from the North Atlantic (47 t/yr; Soerensen et al., 2016), particularly from deep and mid-depth waters, and is driven by the much greater Atlantic inflow volume and the similar range of THg concentrations for Atlantic and Pacific waters. Methylmercury (MeHg) inflow to the Arctic Ocean totalled 7 t/yr (range 3-13 t/yr), most of which again comes in Atlantic deep and mid-depth waters (6.8 t/yr; Soerensen et al., 2016). Support for the estimated low Bering Strait inflow of THg comes from seawater Hg measurements in the Bering Sea and Strait, conducted during a GEOTRACES 2015 cruise, which calculated a Hg inflow range of 1-14 t/yr (Agather et al., 2019).

The Hg mass calculations referred to above were based on average current volumes measured in the 1990s or 2000s. Evidence from a series of permanent *in situ* moorings indicates that the seawater volume flowing through Bering Strait has increased significantly over the last two decades at an average rate of 1.8%/yr (Østerhus et al., 2019). There is considerable inter-annual variability to the northward Bering flow, but the difference between the minimum in 2001 and maximum in 2014 represented an overall 70% increase (Woodgate, 2018). The most likely explanation for this trend is lower water pressure in the East Siberian Sea, caused by increasing westerly winds over the past two decades, that drives surface water from the shelf into the deeper ocean basin thereby creating a pressure differential between the Bering Sea and Arctic Ocean (Peralta-Ferriz and Woodgate, 2017). Inflow volumes from the North Atlantic side have remained relatively stable between the mid-1990s and mid-2010s, although there is a slight, non-significant, increasing trend (Østerhus et al., 2019). Because the Pacific supplies only about 10% of the total seawater inflow to the Arctic Ocean (Woodgate, 2018; Østerhus et al., 2019), the impact on Hg delivery to the Arctic Ocean as a whole from increasing Pacific inflows is likely to be minor. However, the Hg delivered could affect Hg budgets in the Chukchi and Beaufort Seas, where the effects of Pacific waters are noticeable on regional water chemistry, nutrient, and heat budgets (Woodgate et al., 2010; Torres-Valdez et al., 2013; Haine et al., 2015).

The Hg losses from the Arctic Ocean are due to outflowing ocean currents, evasion, and sedimentation on the continental shelves and deep basin. Evasion processes and flux estimates were reviewed in section 3.3.3 d. To provide perspective for the ocean losses discussion, it is reiterated that Hg evasion from ocean surface waters accounts for 12-99 t/y (Outridge et al., 2008; Soerensen et al., 2016), with a new best estimate of ???? (see section 3.3.3d). Losses in sedimentation will be covered in the following section 3.5.2. Previous estimates of the overall Hg loss rate in ocean outflows (excluding Hg entrained in sea-ice and snow) are reasonably similar to each other (68 t/yr - Outridge et al. (2008), and 79 t/yr - Soerensen et al., (2016)); for the purposes of the ocean mass balance budget (section 3.9), the latter value will be used. Compared to all other oceans, Arctic surface waters are enriched in Hg (Wang et al., 2012, Heimbürger et al., 2015; Agather et al., 2019), so that outflowing Arctic water entering the North Atlantic has a higher average THg concentration than Atlantic waters flowing into the Arctic (Cossa et al., 2018, 2019). Riverine THg inputs, together with sea ice restricting DGM evasion, have been cited as the explanation for higher seawater THg concentrations in Arctic surface water (Wang et al., 2012; Soerensen et al., 2016), although coastal erosion likely also plays an important role (see section 3.4.4). Similarly, more MeHg flows out of the Arctic Ocean into the North Atlantic (15 t/yr, range 8-27 t/yr; Soerensen et al., 2016) than flows in (7 t/yr; see above) because of terrestrial inputs and significant MeHg formation *in situ* (Lehnherr et al., 2011; Wang et al., 2012, 2018; Soerensen et al., 2016).

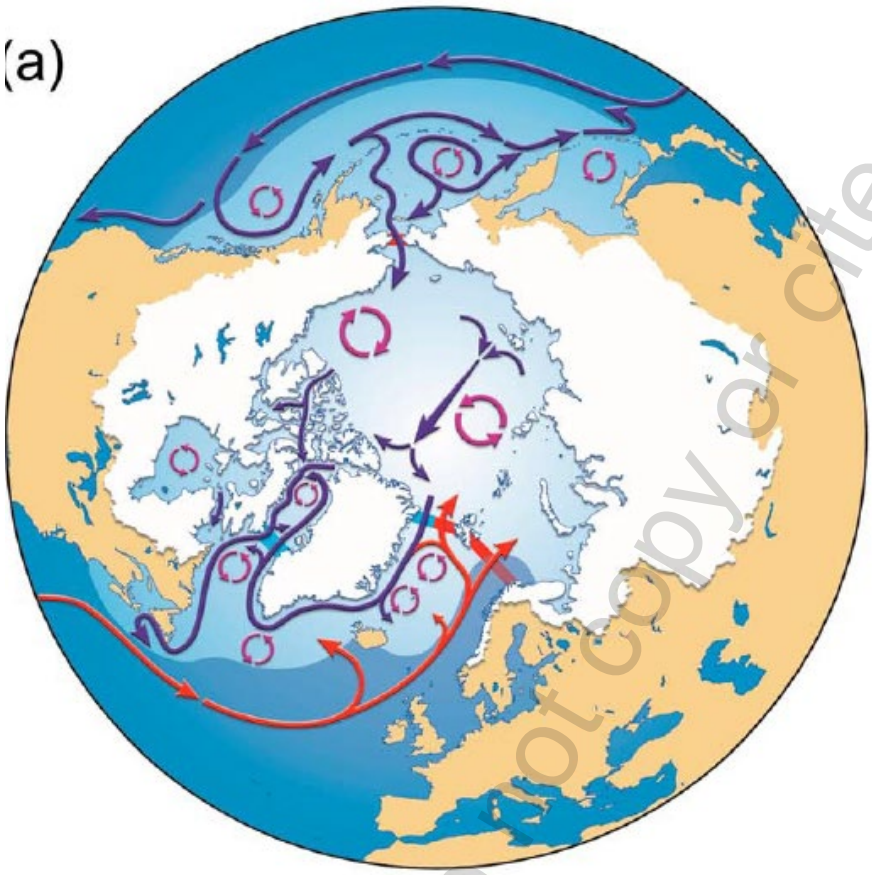

Figure 3.5.1 The Arctic Ocean and its seawater exchanges with the rest of the world oceans (source: Carmack et al 2016). The major ocean currents (long arrows), the four Arctic Ocean gateways in Fram Strait, the Barents Sea Opening, Davis Strait, and Bering Strait, and the gyral circulation patterns (circular arrows) are shown. Relatively warm, salty Atlantic waters (red arrows) enter the Arctic Ocean through Fram Strait and the Barents Sea, and are distributed within the Arctic Ocean in subsurface, topographically constrained boundary currents along the continental margin and undersea ridge system. Cooler and fresher Pacific origin waters (purple arrows) enter the Arctic Ocean through Bering Strait and, together with internally modified Atlantic origin waters, exit through the Canadian Arctic Archipelago, Davis Strait, and Fram Strait along eastern Greenland. The salt-stratified ocean domains are shown in light blue, and the terrestrial catchments contributing freshwater flows to the ocean are shown in white. Outside the Arctic Ocean, the thermally stratified subarctic oceans (darker blue) are distinguished from the salt-stratified northern ocean (lighter blue).

NB: Map to be redrawn during production if retained. Need to add labels for the various ocean gateways – Fram St, Davis St, etc. Or could use old "pathways" map from AMAP 2011 report.

3.5.2 How much Hg is present in the Arctic Ocean?

Authors: **Rob Mason**, Brian DiMento, Lars-Eric Heimbuerger, Jane Kirk, Carl Lamborg, Anne Soerensen, Yanxu Zhang

MeHg distribution in the Arctic Ocean to be added

There are few published data showing the vertical distributions of Hg in the open waters of the Arctic Ocean, with more data measured in coastal waters and within the Canadian Arctic Archipelago (Wang et al., 2018; Sorensen et al., 2016 and references therein). These data suggest that river discharge and other surface inputs, and sediment inputs are important sources of Hg to the coastal zone of the Arctic, but that much of this Hg is strongly removed on the shelf so that there is little transport to the central Arctic Ocean. Atmospheric inputs to the central basin are low given the low precipitation, except for periods when substantial MADE's are occurring (Soerensen et al., 2016). The two most recent published datasets for the open water are Heimburger et al. (2015) and Agather et al. (2019) (Fig. x). While both studies suggest the potential for higher concentrations in surface waters, especially on the shelf or closer to continents, the majority of the measurements of waters below 500 m are <0.2 ng/L (1 pM). The concentrations of Hg in Arctic waters are somewhat higher than those measured on recent cruises in the far North Atlantic Ocean (Cossa et al., 2018a; 2018b) but lower than those measured in the CAA (Wang et al., 2018).

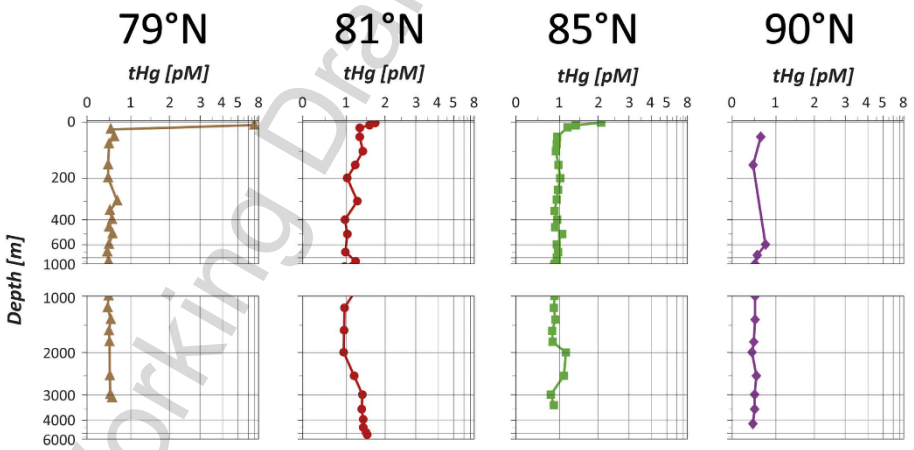

Figure x: Concentrations of total Hg measured vertically in the open waters of the Arctic Ocean. Data from a) Heimburger et al. (2015) and b) Agather et al. (2019).

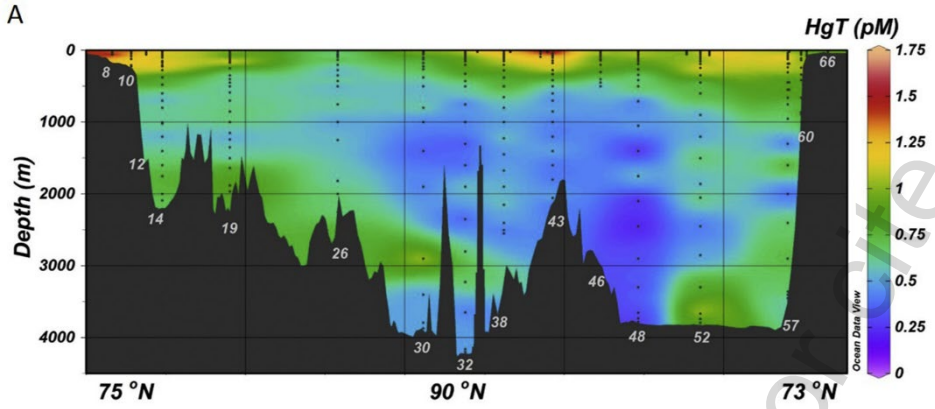

5222

5223 An estimate of the amount of Hg in the Arctic water column can be made based on these
5224 measurements and additional data. Soerensen et al. (2016) estimated that there was 2870 Mg of Hg in
5225 the Arctic Ocean (based on an average deep water concentration of 0.2 ng/L) with 80% being present
5226 in the waters below 200 m. The data of Agather et al. (2019) suggest a slightly lower value. Their
5227 average unfiltered Hg concentration was 0.17 ± 0.09 ng/L (0.86 ± 0.45pM) and the amount of Hg in
5228 the particulate was 0.02 ± 0.02 ng/L. Overall, these values translate into an inventory of 2400 Mg.
5229 The differences in these two estimates are small (<20%).

5230 The measured values from these two cruises are lower than the modeled values for surface water total
5231 Hg, such as those of Fisher et al., (2013), who predict a fall water concentration near 0.4 ng/L. The
5232 observations suggest that such estimates are too high, and this likely reflects the fact that such
5233 modeling was relying on the data from coastal waters and the CAA which are higher than found in the
5234 open waters of the Arctic Ocean, as noted above. The model of Sorensen et al. (2016) reflects the
5235 lower mode recent estimates of the concentration of Hg in offshore Arctic Ocean waters. Overall, the
5236 deep waters of the Arctic Ocean have a long residence time, 50-100 years based on the Sorensen et al.
5237 model, and the more recent data, and therefore suggest that the deep Arctic Ocean concentration will
5238 be changing slowly in response to anthropogenic and climate change.

5239

5240 **3.5.3 How much Hg exchanges between water and sediments in the Arctic Ocean?**

5241 Authors: **Peter Outridge** and Anne Soerensen

5242 Marine sediments exchange Hg with overlying seawater in two ways: sedimentation/resuspension of
5243 particulate Hg, and bi-directional diffusion of dissolved species. Only two studies have estimated
5244 some of these parameters on an Arctic-wide scale (Outridge et al., 2008; Soerensen et al., 2016).
5245 While their accuracy is limited by sparse sediment Hg concentration and speciation data, the
5246 sedimentation rates prevailing on the continental shelves and deep basin are relatively well
5247 constrained (Rachold et al., 2004). Rivers (especially the Yukon and Mackenzie Rivers), and coastal
5248 erosion, provide most of the organic and inorganic material accumulating in Arctic marine sediments

with the remainder from within-ocean primary production and wind-blown dust (Holmes et al., 2002; Rachold et al., 2004; Gamboa et al., 2017). Based on a balanced solids budget for the ocean developed largely from Rachold et al. (2004), sedimentation rates of solids on shelves and the deep basin amount to 490 Mt/yr and 134 Mt/yr, respectively (Soerensen et al., 2016).

Estimation of an average THg concentration in Arctic marine sediments is difficult because of the continuing paucity of measurements, especially in the deep basin. Outridge et al. (2008; used in AMAP, 2011) relied on an early report of an average THg concentration of 210 ng/g in shelf sediments (Macdonald and Thomas, 1991) to develop their shelf sedimentation Hg flux. But more recent studies (Canario et al., 2013; Fox et al., 2013) suggest the average THg concentration is in the 20-55 ng/g range. Gobeil et al. (1999) reported much higher THg in basin surface sediments (up to 116 ng/g), but attributed that to diagenetic redistribution of Hg within the sediment profile. Suspended sediment analyses from continental shelf waters show THg concentrations to be in the 30-70 ng/g range (Graydon et al., 2009; Pucko et al., 2014), although there are no data available from deep basin suspended sediments. For our purposes here, we rely on Soerensen et al.'s (2016) choice of 45 ng/g as the "best estimate" THg value for both shelf and basin sediments. Methyl Hg concentration measurements in marine sediments are even more sparse than those for THg. Based on a range of mean MeHg concentrations in Beaufort and Chukchi Sea shelf sediments of 0.15-0.37 ng/g (Fox et al., 2013), Soerensen et al. (2016) determined a best estimate for shelf and basin sediments of 0.2 ng/g and 0.05 ng/g, respectively.

Soerensen et al. (2016) combined the best estimates of THg and MeHg with the solids budget and arrived at a sedimentation load of 30 and 8 Mt/yr of THg, and 1.3 Mt /yr and 0.1 Mt /yr of MeHg, to the shelf and deep basin, respectively. Resuspension was not estimated due to an absence of data on solids resuspension. As no estimates on the partitioning of Hg^{II} and MeHg between the dissolved and solid phases are available from Arctic sediments, dissolved phases of Hg were calculated with data from North Atlantic estuarine and shelf regions (log K_d: Hg = 4.0, MeHg= 2.7; Hollweg et al., 2010; Schartup et al., 2015; Sunderland et al., 2006). The dissolved concentrations were used to calculate upper and lower bounds for diffusion flux of Hg species at the sediment-water interface. Diffusion to the overlaying water column was estimated at 5 t/y of THg from both shelf and deep basin sediments (total ocean: 10 t/yr), and 0.9 t/yr and 0.1 t/yr of MeHg from shelf and deep basin sediments, respectively (total ocean: 1.0 t/yr; Soerensen et al., 2016). Diffusion into the sediments from overlying waters was negligible.

3.6 How and how much mercury do ice sheets, ice caps and glaciers contribute to Arctic environments?

Authors: **Christian Zdanowicz**

This section needs to be cross-referenced in Section 3.2

Glaciers can export both inorganic and organic Hg to freshwater networks and the Ocean. The Hg is transported in meltwater streams produced by both seasonal thaw and long-term mass wastage (i.e., sustained negative mass balance), and the latter contribution is forecasted to increase in most glaciated areas of the Arctic and subarctic as high latitudes continue to warm in the 21st century (Milner *et al.*, 2017). The Hg exported from glacier-covered basins comes from atmospheric and geogenic sources. The former is Hg deposited to snow (primarily as Hg^0 or Hg^{2+}, but also as MeHg) and likely includes, in some basins, an unquantified fraction of Hg emitted from anthropogenic sources in the past two centuries. The geogenic Hg fraction is that derived from bedrock by glacial erosion and is bound or absorbed to suspended clay and silt mineral particles in turbid, glacier-fed streams.

The size of anthropogenic Hg pools in glaciers is largely unknown. Data from high-latitude (>50° N) glacier ice cores in Greenland, North America and central Asia show that some firn and ice strata that formed between the mid-19th and late 20th century are enriched in THg by factors of ~2 up to 15 relative to older, pre-industrial ice, the largest enrichments being reported in mountain ice caps of central Asia and the Yukon (Zdanowicz *et al.*, 2016; Eyrikh *et al.*, 2017, and references therein). However, to quantify the mass and release rate of legacy Hg in glaciers released requires site-specific knowledge of their internal structure, which is largely missing outside of Greenland, and of their mass turnover rates, which are likely to change in a warming climate. Some subarctic maritime glaciers with fast turnover rates (e.g., in Alaska) have had sustained negative mass balances for decades, and may have already released most of the legacy Hg that was stored in ice. Other small and ice caps glaciers have little or no net accumulation zones, and may only store a limited amount of legacy Hg. The largest potential glacial reservoir of anthropogenic Hg, the Greenland ice sheet, is experiencing accelerating mass wastage rates, but only ~35 % of mass losses in the past half-century occurred through surface melt, the remainder being due to dynamic discharge of tidewater glaciers, which mostly drain marginal areas of the ice sheet (Mouginot *et al.*, 2019). Furthermore, an unquantified, and possibly large, fraction of meltwater produced at the surface of Greenland is not immediately discharged, but accumulates instead within the firn, either by refreezing, or in liquid form within "firn aquifers", the extend, volume and water quality of which are largely unknown (e.g., Christianson *et al.*, 2015). Similar aquifers may exist on other Arctic ice caps (e.g., Svalbard). Mixing of meltwater issued from different parts of glaciers (or groundwater) within their drainage system further complicates matters, making accurate forecasts of Hg releases presently impossible.

Data on Hg and/or MeHg concentrations in glacier-fed streams of the Arctic and subarctic are available from sites in northeast Greenland (Rigét *et al.*, 2011; Søndergaard *et al.*, 2015), the

Canadian Arctic Archipelago (Baffin and Ellesmere Islands; St. Louis *et al.*, 2005; Zdanowicz *et al.*, 2013; St. Pierre *et al.*, 2019), the Yukon (Halm and Dornblaser, 2002; Zdanowicz *et al.*, 2018) and southeast Alaska (Nagorski *et al.*, 2014; Vermilyea *et al.*, 2017) (**Table X**). Most of these data come from measurements made during peak flow months (June-August). Together, they show that total Hg concentrations in filtered glacier meltwater (<45 □m; FTHg) are very low, typically <~2 ng L^{-1}, which compares well with the reported range of THg values in seasonal snow at non-coastal land sites or on glaciers of the Arctic and subarctic (cf section XX). The FTHg concentrations in glacier-fed rivers are also within the range of values found in the pre-industrial sections of Arctic glacier ice cores (Zdanowicz *et al.*, 2016), so there is presently no evidence of anthropogenically Hg-enriched meltwater being released from subarctic or Arctic glaciers. If such Hg is being released, it is too diluted to be distinguished from that naturally present in glacier ice. Reported concentrations of MeHg in filtered glacial meltwater (FMeHg) are <0.010 ng L^{-1} to 0.235 ng L^{-1}, and typically account for 1–25% of total Hg in water. These MeHg concentrations are also within the range found in pre-industrial Arctic ice cores. Unfiltered, total Hg concentrations (UTHg) in the turbid waters of subglacial or proglacial streams are commonly much higher than those of FTHg, ranging up to 28.4 ng L^{-1}, indicating that that the bulk of Hg in these streams is particle-bound (PHg). Estimates of the PHg fraction in glacier-fed streams range between 34─98%, and are typically >50 %. Where such measurements have been made, the mass fraction of MeHg that is particle-bound (i.e., PMeHg) is found to vary between 20 and 86 %.

The figures above make it clear that most riverine Hg export from glaciers is in particulate form, and is likely of geogenic, rather than atmospheric origin. The Hg content in stream sediments of upslope basins that are unimpacted by pollution point sources (e.g., mines) tends to reflect that of predominant bedrock lithologies (e.g., Nasr *et al.*, 2011; Nasr and Arp, 2018), and the same should be expected in suspended sediments of glacier-fed streams. Reported dry-weight concentrations of sediment-bound Hg (SHg) in these streams range between 5 and 250 ng g^{-1}, and are typically in the tens of ng g^{-1} (**Table X**). This is consistent with published data on SHg in streambed sediments of glacier-fed tributaries of the Yukon River (~6–80 ng g^{-1}; Friske *et al.*, 1994; Halm and Dornblaser, 2007), or seafloor sediments of inner fjords in Svalbard (~1–90 ng g^{-1}; Beldowski *et al.*, 2015; Liu *et al.*, 2015). Episodic, yet locally significant exports of riverine Hg can also occur during extreme flow outbursts accompanying Icelandic subglacial eruptions (jokülhlaups). In the 1996 jokülhlaup from Vatnajökull, a riverine THg concentration of 68 ng L^{-1} was recorded (Kristmannsdóttir *et al.,* 1999)

Published estimates of riverine Hg exports to subarctic or Arctic marine waters mostly concern the large rivers of Siberia and North America (cf section X). The Lena, Yukon, and Mackenzie Rivers are partially fed by meltwater from limited glacier-covered mountain areas (<6% ot total catchment area), but the magnitude of Hg contributions from glacial meltwater in these rivers is unknown. Likewise, melting glaciers could account for a substantial part of the Hg-enriched upper waters of the Labrador

Current issued from the eastern Canadian Arctic (Cossa *et al.*, 2018), but just how large this contribution may be is not known at present. Estimates of Hg fluxes based on direct or indirect measurements in glacier-fed streams of the Arctic and subarctic range between 0.14 and 16.40 kg y^{-1} for THg and between 0.03 and 50.3 g y^{-1} for MeHg (**Table Y**). When the fluxes are normalized by catchment area, they translate to annual yields ranging from 0.05 to 3.88 g km^{-2} y^{-1} for THg, and from 2.02 to 11.7 mg km^{-2} y^{-1} for MeHg, in basins with 21 to 82% glacier coverage. A published figure of 19.9 g THg km^{-2} y^{-1} from the Lemon Creek basin, Alaska (32 km^2; 55% glacier cover), estimated from fluorescing organic matter measurements, presently stands out as an outlier (Vermilyea *et al.*, 2017).

The majority of glaciated Arctic river basins have too limited ice coverage to strongly control their mean annual sediment yield (Overeem and Syvistki, 2008), although years of high summer melt rates may disproportionally impact sediment export in mountain catchments (Wada *et al.*, 2011). The data in **Tables X and Y** suggest that the same holds true of THg and MeHg yields from glaciated basins, which likely depend on additional factors such as climate, relief, stream length and drainage pattern. In the relatively near term (coming years to decades), the continued recession of mountain glaciers and small ice caps is expected to enhance sediment discharge into streams and lakes, followed by a longer-term decrease of the sediment flux as glaciers continue to shrink and thin, becoming less dynamic (Milner *et al.*, 2017). This is in fact observed in the Alps (Delaney *et al.*, 2018). In Greenland, sustained, larger sediment fluxes to surrounding marine waters are expected, particularly from fast-flowing tidewater glaciers, and a current estimate of the total suspended sediment output in meltwater is 1.294 Gt y^{-1} (Overeem *et al.*, 2017). Using a median SHg concentration of ~31 ng g^{-1} (after Søndergaard *et al.*, 2015), this translates to a sediment-bound export of ~40 t THg y^{-1}.

Given that most Hg presently released from glaciers is particle-bound and likely of geogenic origin (**Table X**), an increase in the glacial sediment flux does not necessarily lead to higher exposure risks to inorganic Hg or MeHg in downstream aquatic ecosystems, not unless other changes occur that enhance the bioavailability and/or methylation rates of the sediment-bound Hg pool. On land, such changes might occur with the development of seasonally wet areas in newly deglaciated forelands. In southeastern Alaska, for example, watersheds with greater wetland abundance have higher Hg concentrations, in both water and aquatic fauna, than glaciated basins (Nagorski *et al.*, 2014). Dissolved organic matter released from melting glaciers (Hood et al., 2009, 2015) could also promote Hg methylation in some aquatic environments, particularly in catchments where subglacial oxidation of sulfides also causes enhance sulfidization of ponds, wetlands and lakes Graham *et al.*, 2012). Cryoconite holes (dirt-filled melt cavities on glacier surfaces) are abundant over marginal or stagnant glacier ice, and can accumulate atmospherically-deposited impurities released by ice melt, as well as microbes (Cooke *et al.*, 2016). These micro-environments could potentially act as local hotspots of Hg

methylation in glacial environments, but direct supporting evidence for this is presently limited to a Tibetan glacier (Zhang *et al.*, 2020).

In the marine environment, meltwater plumes from tidewater glaciers carrying dissolved Hg may be injected into zones of locally high primary productivity in coastal surface waters, where subsequent methylation and biological uptake can occur (Schartup *et al.*, 2015). On the seafloor, however, rapid sedimentation of primarily inorganic matter released from glaciers can dilute the Hg content of surface sediments, as suggested by observations in fjords of Svalbard (Liu *et al.*, 2015). On the whole, therefore, the environmental impact of Hg releases from melting glaciers and ice caps is likely to be local, rather than widespread across the Arctic.

5400 Table X. Published data on Hg content in glacier-fed streams in the Arctic and subarctic.

River basin / Glacier			Sampling period		Hg concentrations in glacial streams								Data sources
	Basin area	Glacier cover	Month(s)	Year(s)	UTHg	PHg	FHg	SHg	TMeHg	PMeHg	FMeHg	SMeHg	
	km^2	%			(ng L^{-1})	(ng L^{-1})	(ng L^{-1})	(ng g^{-1})	(ng L^{-1})	(ng L^{-1})	(ng L^{-1})	(ng g^{-1})	
Greenland													
Zackenberg River	514	21	July-Aug	2009–13	4.5–7.5	4.1–7.2	0.25–0.53	25–42	⊢⊣	⊢⊣	⊢⊣	⊢⊣	1
Alaska													
Lemon Creek	32	55	May-Sept	2010	0.4⊢8.2	1–13	⊢⊣	37–259	⊢⊣	⊢⊣	⊢⊣	⊢⊣	2
Stonefly Creek	13	31	July	2007	1.44	0.97	0.47	33	0.030	0.010	0.020	⊢⊣	3
Gull Creek	6	2	July	2007	0.59	0.20	0.39	130	0.060	0.020	0.040	⊢⊣	3
Nunatak Creek	38	2	July	2007	0.27	0.19	0.08	⊢⊣	~0.010	<0.010	0.010	⊢⊣	3
Reid Creek	17	5	July	2007	4.62	3.73	0.89	90	0.050	0.010	0.040	⊢⊣	3
Taiya Creek	466	33	July	2007	0.88	0.53	0.35	15	~0.020	<0.010	0.020	⊢⊣	3
Skagway Creek	376	17	July	2007	⊢⊣	⊢⊣	0.37	⊢⊣	0.020	0.010	0.010	⊢⊣	3
Yukon													
Kusawa River	4 200	5	June	2013	⊢⊣	⊢⊣	⊢⊣	6–28	⊢⊣	⊢⊣	⊢⊣	⊢⊣	4
Atlin River	6 812	⊢⊣	June, Aug	2004	0.43–2.13	0.06–0.08	0.37–2.05	⊢⊣	<0.040	<0.010	<0.040	⊢⊣	5
Takhini River	7 050	2	June, Aug	2004	1.55–3.31	1.02–2.77	0.53–0.54	⊢⊣	<0.040	<0.040	<0.040	⊢⊣	5
White River	6 230	30	June, Sept	2004	22.7–28.24	22.0–26.3	0.70–1.94	80	<0.040	<0.060	<0.040	⊢⊣	5
Canadian Low Arctic													
Penny ice cap *(sub)**	⊢⊣	⊢⊣	June-July	2008-10	0.74–5.93	⊢⊣	⊢⊣	⊢⊣	⊢⊣	⊢⊣	⊢⊣	⊢⊣	6

Penny ice cap *(supra)**	⊷	⊷	June-July	2008-10	0.28–3.91	⊷	⊷	⊷	⊷	⊷	⊷	⊷	6
Weasel River	⊷	⊷	June	2008	1.52⊷2.04	⊷	⊷	⊷	≤0.020	⊷	⊷	⊷	6
Owl River	⊷	⊷	July	2008	1.13⊷1.53	⊷	⊷	⊷	≤0.020	⊷	⊷	⊷	6
Canadian High Arctic													
J. Evans Glacier *(sub)**	⊷	⊷	June-July	2001–02	1.52⊷4.06	1.22⊷3.68	0.17⊷0.57	⊷	0.050⊷0.127	<0.010⊷0.067	0.035⊷0.060	⊷	7
J. Evans Glacier *(supra)**	⊷	⊷	June-July	2001–02	0.17⊷0.93	0.03⊷0.53	0.14⊷0.60	⊷	0.080⊷0.235	0.011⊷0.193	0.020⊷0.075	⊷	7
Blister Creek	⊷	⊷	July-Aug	2015–16	⊷	⊷	⊷	14	⊷	⊷	⊷	⊷	
Snowgoose River	222	39	July-Aug	2015–16	⊷	⊷	⊷	26	⊷	⊷	⊷	0.042	8
Gilman River	992	71	July-Aug	2015–16	⊷	⊷	⊷	⊷	⊷	⊷	⊷	0.109	8
Turnabout River	678	38	July-Aug	2015–16	⊷	⊷	⊷	5	⊷	⊷	⊷	⊷	8
Very River	1035	26	July-Aug	2015–16	⊷	⊷	⊷	100	⊷	⊷	⊷	⊷	8
Ruggles River**	7 156	41	July-Aug	2015–16	0.17⊷1.20	0.31	0.26⊷0.32	⊷	<0.010–0.013	⊷	<0.010–0.013	⊷	8

UTHg: Total Hg in unfiltered water, UTHg = FHg + PHg; FHg: Total Hg in filtered water (0.45 mm), operationally equivalent to dissolved Hg (DHg); PHg: Total particulate-bound Hg retained after filtration (0.45 mm); SHg: Hg mass concentration (dry weight) in suspended or riverbed sediments; UMeHg, FMeHg and SMeHg are defined as for UTHg, FHg and PHg, but for MeHg values. *sub = subglacial or proglacial stream flow; supra = supraglacial stream flow. **Underlined figure is an average value. Data sources: 1 = Rigét et al. (2011) and Søndergaard et al. (2012); 2 = Vermilyea et al. (2017); 3 = Nagorski et al. (2014); 4 = Zdanowicz et al. (2018) and Friske et al. (1994); 5 = Halm and Dornblaser (2007) and Chesnokova et al. (2007); 6 = Zdanowicz et al. (2013); 7 = St. Louis et al. (2005); 8 = St. Pierre et al. (2019).

5411 Table Y. Published estimates of riverine Hg fluxes in glaciated basins of the Arctic and subarctic.

				Estimated annual Hg mass fluxes				Estimated annual Hg yield		Data
River basin / Glacier	Basin area	Glacier cover	Averaging period	UTHg	PHg	FHg	TMeHg	THg	MeHg	sources
	km^2	%		(kg y^{-1})	(kg y^{-1})	(kg y^{-1})	(g y^{-1})	(g km^{-2} y^{-1})	(mg km^{-2} y^{-1})	
Greenland										
Zackenberg River	514	21	2009–13	0.90–2.646	0.67–2.6	0.036–0.140	⊢⊣	1.4–3.1	⊢⊣	1
Alaska										
Lemon Creek*	32	55	2009	⊢⊣	⊢⊣	⊢⊣	⊢⊣	*19.9*	⊢⊣	2
Yukon										
Kusawa River**	4 200	5	2001-11	0.20–0.28	⊢⊣	⊢⊣	⊢⊣	0.05–0.07	⊢⊣	4
Canadian High Arctic										
Blister Creek	⊢⊣	⊢⊣	2015–16	0.01–0.03	⊢⊣	⊢⊣	0.03–0.11	0.61–1.96	⊢⊣	
Snowgoose River	222	39	2015–16	0.14–0.44	⊢⊣	⊢⊣	0.51–1.51	0.61–2.63	2.28–6.78	8
Abbé River	390	52	2015–16	0.24–1.03	⊢⊣	⊢⊣	0.87–3.38	0.72–3.30	2.23–8.68	8
Gilman River	992	71	2015–16	0.72–3.27	⊢⊣	⊢⊣	2.45–9.99	0.98–3.88	2.47–10.1	8
H. Nesmith River	1 274	82	2015–16	1.25–4.95	⊢⊣	⊢⊣	4.23–14.9	0.57–2.04	3.32–11.7	8
Turnabout River	678	38	2015–16	0.39–1.38	⊢⊣	⊢⊣	1.37–4.48	1.32–2.91	2.02–6.61	8
Very River	1035	26	2015–16	1.37–3.01	⊢⊣	⊢⊣	4.50–8.97	0.61–1.96	4.35–8.67	8
Ruggles River****	7 156	41	2015–16	8.35⊢16.40	⊢⊣	⊢⊣	16.2-50.3	⊢⊣	⊢⊣	8
			Overall range of values:	0.14–16.40	0.67–1.50	0.036–0.140	0.03–50.3	0.05–*19.9*	2.02–11.7	
			Excluding Lemon Creek:					0.05–3.88		

5412 *THg mass fluxes and basin yield estimated from fluorescent dissolved organic matter. The basin yield (italicized) is a possible outlier compared to all
5413 other reported values. **THg mass fluxes and basin yield are for glacier meltwater contribution only, not including subglacial flow. Data sources are as
5414 listed in Table X.

3.7 What are the relative contributions of geogenic, anthropogenic and remission sources of Hg to Arctic environments?

Authors: **Ashu Dastoor**, Oleg Travnikov and modeling team

- Provide source apportionment of Hg in Arctic ecosystems (terrestrial regions such as major watersheds, land within permafrost area, Arctic Ocean etc.) with respect to contributions from various air emissions sources, geogenic, contemporary anthropogenic, remissions of legacy Hg and biomass burning, to Hg concentrations in air, and to deposition fluxes to land and ocean in the Arctic using multi-model ensemble simulations.
- Check whether data (measurements/model) is available for source contributions to Arctic Ocean Hg concentrations via ocean circulation.

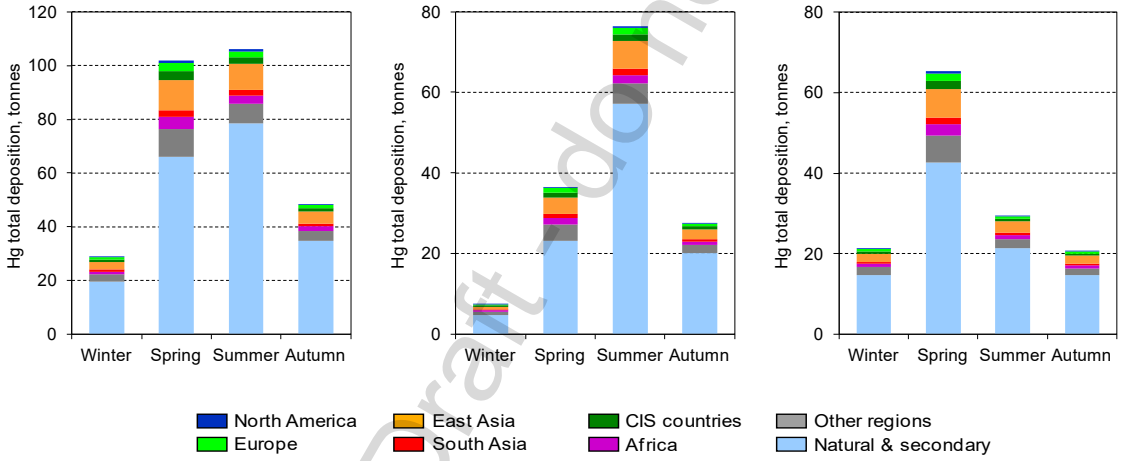

Color scale for anthropogenic source regions, and natural and secondary emissions (i.e., revolatilization of legacy emissions)

Fig. X Simulated (model ensemble mean) Hg deposition to the Arctic within 60°N (a), terrestrial Arctic (b), and aquatic Arctic (c) in 2015 and source contributions [Preliminary results]

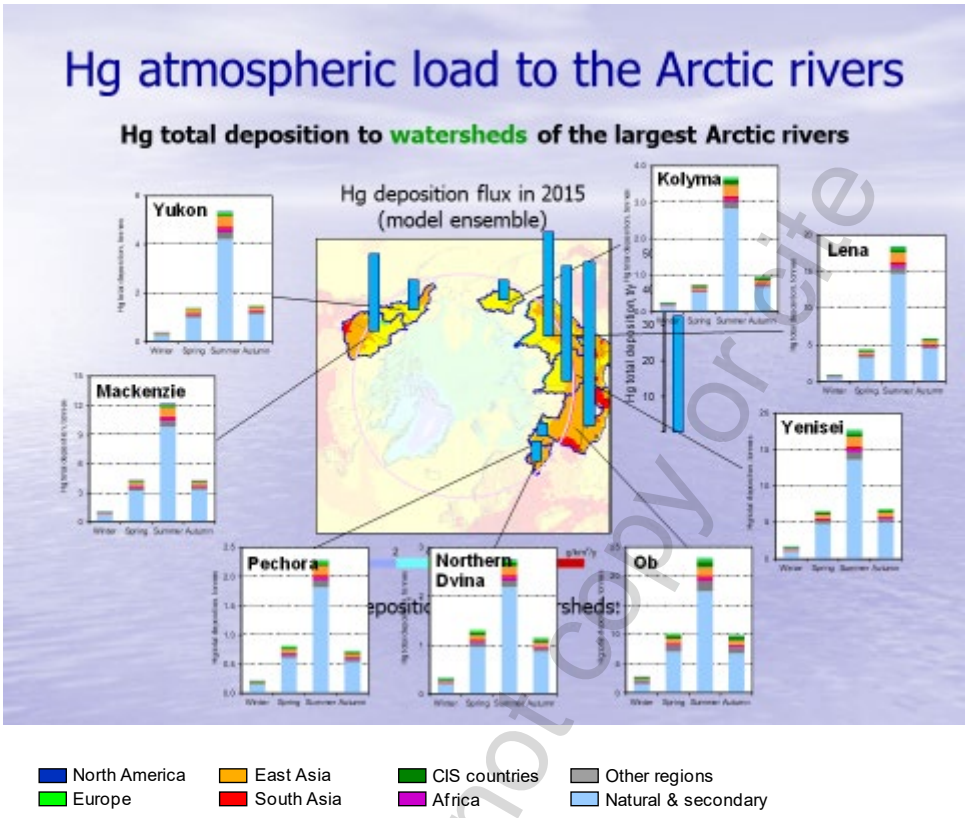

Fig. X Simulated (model ensemble mean) Hg deposition to watersheds of the largest Arctic rivers in 2015 shown as source contributions: Northern Dvina, Pechora, Ob, Yenisei, Lena, Kolyma, Mackenzie and Yukon [Preliminary results]

3.8 What is the relative contribution of local anthropogenic vs long-range anthropogenic sources of mercury to Arctic environments?

Authors: **Ashu Dastoor**, Oleg Travnikov and modeling team

- Provide spatial distribution and total anthropogenic emissions of Hg in the Arctic region and its comparison with global anthropogenic emissions (refer to Section 3.2)
- Describe source apportionment of Hg deposition in Arctic environments with respect to local vs long-range anthropogenic sources of mercury based on multi-model simulations (i.e., GEOS-Chem, GEM-MACH-Hg and GLEMOS) (see figure X below) [might add seasonal contributions in addition to annual].
- Add contribution of Arctic region anthropogenic emissions to deposition in circumpolar river catchments to illustrate the potential impact on river export of Hg to Arctic Ocean.

Anthropogenic emissions located north of 66° N were considered as anthropogenic emissions local to the Arctic region. Three global models were applied to estimate the relative contribution of Arctic region sources from human-activities to Hg deposition (GEOS-Chem, GEM-MACH-Hg and GLEMOS). Multi-model ensemble mean reveals that contribution of Arctic region anthropogenic emissions is small in general to the Arctic, especially over the Arctic Ocean (i.e., < 7 %). However, there are localized regions (mainly over land) of impact over 15 % (up to ??) to Hg deposition north of 60° N from anthropogenic sources over Eurasia which are located within the Arctic Ocean watersheds. Mercury export from circumpolar rivers is an important source of Hg to the Arctic Ocean (see Section 3.4.3). Obrist et al. (2017) observed an efficient uptake of atmospheric Hg(0), the dominant Hg species in emissions, by tundra vegetation and soils in the Arctic. In addition, local anthropogenic emissions also include significant primary emissions of oxidized Hg (??%) that is locally deposited via wet and dry deposition including to waterbodies, which can be directly delivered to the catchment streams. Recent studies have reported largest Hg river fluxes to the Arctic Ocean from Eurasia, representing 80% of Arctic river runoff, Yenisei, Lena and Ob being the (Sonke et al. 2018 and others) are the. The model ensemble mean estimated contributions of Arctic anthropogenic sources to total Hg deposition in the largest Eurasian river catchments, Yenisei, Lena, Ob …, are ??, ?? …… representing ?? % of all contemporary anthropogenic contribution to these watersheds (numbers to be filled in). It should be noted that the presented local source contributions depend on what is considered to be local sources in the Arctic. There are additional anthropogenic sources of Hg north of 60^0 N, particularly in Eurasia, that would enhance the contribution of local sources to the deposition and riverine Hg exports in the Arctic.

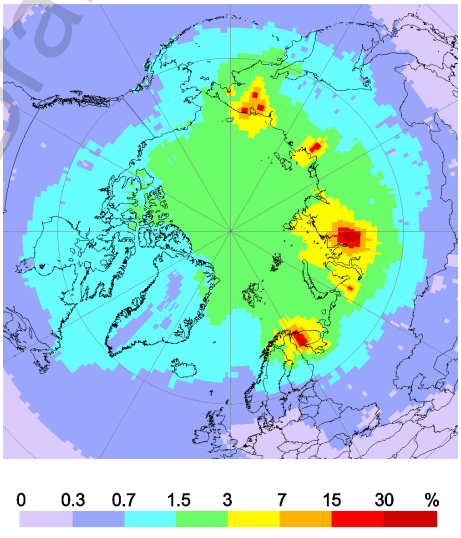

Fig. X. Relative contribution of the Arctic local emission sources (located north of 66°N) to annual Hg deposition from anthropogenic sources in 2015. Color scale needs to be revised to show the maximum impact, and draw major Arctic river catchment boundaries.

3.9 How much mercury is circulating in Arctic environments?

[provide mass balance estimates of total mass and exchange fluxes of total and methyl mercury in Arctic environments]

Authors: All

- Develop up-to-date diagram for mass balance of Hg in the Arctic showing total and methyl mercury in each compartment, Hg inputs/outputs and fluxes between compartments (air, soils, vegetation, cryosphere, ocean, sediments etc.) with uncertainty ranges from measurements and multi-model results. This section will combine estimates from all above sections to construct the mass balance picture.

Recent mass balance of mercury fluxes in the Arctic and Arctic Ocean (AO) were developed by Fisher et al. (2012), Durnford et al. (2012), Dastoor and Durnford (2014), Soerensen et al. (2016) and Sonke et al. (2018) based on measurement and modeling estimates. Using GEOS-Chem, Fisher et al. (2012) estimated mercury deposition to the Arctic ecosystems of 55 Mg y^{-1} (i.e., 25 Mg yr^{-1} directly to open ocean, 20 Mg yr^{-1} to ocean via snow melt on sea ice, and 10 Mg yr^{-1} to land via snow melt), evasion from ocean of 90 Mg yr^{-1} and a net Hg export to the Arctic atmosphere of 35 Mg y^{-1} north of 70°. In contrast, using GEM-MACH-Hg, Durnford et al. (2012) estimated mercury deposition of 153 Mg y^{-1} (i.e., 58 Mg yr^{-1} directly to open ocean, 50 Mg yr^{-1} to ocean via snow melt on sea ice, and 29 Mg yr^{-1} directly and 16 Mg yr^{-1} via snow melt to Arctic tundra), emission of 36 Mg yr^{-1} (i.e., 33 Mg yr^{-1} evasion from ocean and 3 Mg yr^{-1} from land) and a net surface gain of 117 Mg y^{-1} in the Arctic north of 66.5°. Fisher et al. (2012) concluded that AO is a net source of mercury to the atmosphere, i.e., 45 Mg yr^{-1}; whereas, Durnford et al. (2012) concluded that AO is a sink of atmospheric mercury, i.e., 75 Mgyr^{-1}. Two other global-scale mercury models, GLEMOS and DEHM, have estimated yearly net surface gain of mercury in the Arctic at 131 Mg y^{-1} and 110 Mg y^{-1}, respectively (Travnikov and Ilyin, 2009; Christensen et al. 2004) in close agreement with GEM-MACH-Hg (i.e., 117 Mg y^{-1}). Using an ocean circulation model, MITgcm, and GEOS-Chem, Zhang et al. (2015) revised Fisher et al. (2012) AO Hg evasion and estimated a net Hg export from AO to air of 23 Mg y^{-1}. Soerensen et al. (2016) also suggested a net emission of Hg to the atmosphere of 23 Mg y^{-1} from OA by combining direct deposition of Hg to ice-free AO from GEOS-Chem (Fisher et al. 2012, 2013) and average melt water (over sea-ice) contribution from GEOS-Chem (Fisher at al. 2012) and GEM-MACH-Hg (Dastoor and Durnford 2014) to come up with a total deposition of 76 Mg y^{-1}, and Hg evasion from AO of 99 Mg y^{-1} from Zhang et al. (2015). By upscaling deposition measurement at an Arctic tundra site from Obrist et al. (2017), Sonke et al. (2018) estimated a total deposition of 210 Mg yr^{-1} to Arctic permafrost; Hg fluxes between air and AO in Sonke et al. (2018) were adapted from Soerensen (2016). Durnford et al. (2012) modeled deposition of 170 Mg yr^{-1} to

terrestrial surfaces north of 60° with 77% (i.e., 131 Mg yr^{-1}) deposition directly to vegetation and soils and remaining to snowpack in good agreement with measured estimate by Sonke et al. (2018).

Fisher et al. (2012) inferred that a total of 95 Mg yr^{-1} input of mercury from circumpolar rivers and coastal erosion (80 Mg y^{-1} from rivers and 15 Mg y^{-1} from coastal erosion) and an evasion of 90 Mg yr^{-1} of Hg from AO was required to balance the observed summertime peak in surface air concentrations of Hg(0) at the Arctic sites. In contrast, Durnford et al. (2012) found that a 33 Mg yr^{-1} of mercury evasion from the AO was sufficient to reproduce the summertime peak Hg(0) concentrations in the Arctic. Dastoor and Durnford (2014) calculated springtime snowmelt contribution of riverine mercury to AO from North American, Russian and all Arctic watersheds in the range of 2.8-5.6, 12.7-25.4 and 15.5-31.0 Mg yr^{-1}, respectively, based on model simulated mercury in terrestrial meltwater and estimated a total export of 50 Mg yr^{-1} Hg from circumpolar rivers to AO based on measurements. Zhang et al. (2015) revised Fisher et al. (2012) estimates to infer a terrestrial Hg input of 62 Mg yr^{-1} to AO comprising 46 Mg yr^{-1} from rivers and 16 Mg yr^{-1} from coastal erosion. Soerensen et al. (2016) adopted the measurement based riverine Hg input to AO of 50 Mg yr^{-1} from Dastoor and Durnford (2014) and a coastal erosion of 34 Mg yr^{-1} (REF??) to suggest terrestrial input of 84 Mg yr^{-1} to AO. Using additional observations of mercury in Eurasian rivers, Sonke et al. (2018) estimated riverine Hg input to AO of 44 Mg yr^{-1} in agreement with the two latter estimates by Dastoor and Durnford (2014) and Zhang et al. (2015).

Fate of riverine Hg input to the oceans, including AO, is highly sensitive to the reactivity of Hg associated with particulate organic carbon, i.e., fraction of the HgP pool specified as refractory (Semeniuk and Dastoor 2014; Zhang et al. 2015). Zhang et al. (2015) assumed two extreme scenarios for riverine HgP reactivity in their ocean model simulations, i.e., all riverine HgP treated as refractory in global oceans and a completely reversible equilibrium of riverine HgP between solid and dissolved phases in AO. Reversible equilibrium partitioning of riverine HgP in AO was chosen based on the suggestions of low tributary particle loads and efficient degradation of particulate organic carbon by deltaic microbial communities in AO (Bouchez et al. 2010; Gordeev, 2006, Bianchi 2011; Macdonald et al. 2005; Rontani et al. 2014). The authors note that, in reality, the refractory portion of riverine HgP likely varies between watersheds (based on the nature of POC pool) and, therefore, the actual fate of Hg discharges from rivers in oceans including in AO lies between the two extreme cases assumed in Zhang et al. (2015). To account for a possible increase in rate of Hg evasion near river mouths in the Arctic in response to enhanced surface water turbulence due to rapid sea ice melt and ice rafting in estuaries driven by meltwater discharge, Zhang et al. (2015) doubled the piston velocity in their parameterization for air-sea exchange of Hg in these regions. Choice of above two conditions (i.e., equilibrium partitioning of riverine HgP and enhanced evasion rate in estuaries) resulted in evasion of most of the riverine Hg to the atmosphere in AO, mostly in the estuarine and shelf regions and remaining in open ocean rather than being buried in shelf sediments in Zhang et al. (2015)

simulations. Furthermore, in the absence of available measurements to constrain AO Hg evasion, Zhang et al. (2015) used observed atmospheric concentrations of Hg in the Arctic to constrain their riverine input and evasion flux in AO. Fisher et al. (2012) assumed Hg input from rivers to be uniformly distributed in the entire AO; whereas, both Durnford et al. (2012) and Zhang et al. (2015) suggest spatially varying evasion from AO, supported by observations (Andersson et al. 2008; Hirdman et al. 2009; Sommar et al, 2010). Zhang et al. (2015) evaluated their model simulated total concentrations of Hg in ocean surface water. Evaluation of speciated Hg and their fluxes between ocean layers and to air is required to fully constrain the model, currently hampered by a lack of observations.

Disagreements between modeling estimates of atmosphere-ocean-snowpack mercury fluxes in polar regions reflect both model and measurement uncertainties and gaps (Dastoor and Durnford 2014; Angot et al. 2016; Semeniuk and Dastoor et al. 2014; Zhang et al. 2015). In the absence of measured estimates of atmosphere-ocean Hg fluxes over AO, models have relied on observed surface air Hg concentrations of Hg(0) at Arctic sites to infer or constrain these fluxes (Fisher at al. 2012; Durnford et al. 2012; Zhang et al. 2015). The accuracy of model estimated fluxes depends on the level of sophistication in process parameterizations and evaluation with measurements. Dastoor and Durnford (2014) conducted a comprehensive evaluation of GEM-MACH-Hg simulated concentrations of speciated Hg in air, total mercury (THg) concentrations in precipitation and seasonal snowpack, and snow/air Hg fluxes at Arctic observation sites. Modeled median concentrations of Hg(0) and Hg(II) were within the observed range at all locations. Using a high spatiotemporally resolved model validation, Dastoor and Durnford (2014) found two summertime peaks in air concentrations, one in early summer supported primarily by re-emission of Hg from melting snowpack and meltwater and a second one in late summer supported by evasion of Hg from AO. Concentrations of Hg in freshly deposited snow in the springtime (i.e., AMDEs season) were observed to be significantly higher at Barrow than Alert (i.e., median concentration of 47 ng L^{-1} at Barrow, April-May, 2005, and 7.5 ng L^{-1} at Alert, March-May, 2005); these concentrations were also well matched by GEM-MACH-Hg (i.e., 37 ng L^{-1} at Barrow and 8.4 ng L^{-1} at Alert). The model simulated annual median mercury concentration in precipitation at Fort Vermillion (Canada) accurately (3.8 ng L^{-1} modeled; 3.9 ng L^{-1} measured in 2007) but over-estimated at Bettles (Alaska) (3.8 ng L^{-1} modeled; 2.1 ng L^{-1} measured in 2009). Modeled median mercury concentrations in seasonal snowpack were within the measured range (e.g. 6.0 ng L^{-1} modeled and 4.9-6.0 ng L^{-1} measured at Alert in spring 2005). Recently, Obrist et al. (2017) measured Hg fluxes at an Arctic tundra site (Toolik Field Station, Alaska, USA) and estimated a total Hg deposition of 9.2 μg m^{-2} y^{-1} at this site. Simulated Hg deposition in Durnford et al. (2012) and Dastoor et al. (2015) in this region were ~ 8 μg m^{-2} y^{-1} and 6-9 μg m^{-2} y^{-1}, respectively, in close agreement with Obrist et al. (2017).

Both modeling and measurement studies now provide a consistent picture for the riverine input of mercury to AO (i.e., 44-50 Mg yr-1) (Dastoor and Durnford 2014; Zhang et al. 2015; Sonke et al. 2018). One measurement-based total deposition of Hg to terrestrial surfaces in the Arctic (i.e., 210 Mg yr^{-1} to permafrost region; Sonke et al. 2018) is also consistent with modeled deposition by Durnford et al. (2012) (i.e., 170 Mg yr^{-1} north of 60°). As noted earlier, three of the four models applied to model Hg in the Arctic suggest a net deposition of Hg to the Arctic, i.e., 110-131 Mg yr^{-1} and 75 Mg yr^{-1} to AO (Travnikov and Ilyin, 2009; Christensen et al. 2004; Dastoor and Durnford 2014); whereas, GEOS-Chem results suggest a net export of mercury to the air from Arctic and AO, 35 Mg yr^{-1} and 23-45 Mg yr^{-1}, respectively (Fisher et al. 2012; Zhang et al. 2015). Air-ocean exchange of Hg fluxes currently lack adequate observational constraint. In addition, Hg biochemistry and physical processes in oceans are still poorly understood (Semeniuk and Dastoor 2014; Zhang et al. 2015). Improved understanding of Hg biogeochemistry and spatiotemporally distributed measurements of Hg concentrations and fluxes in all matrices of the Arctic, particularly AO, are needed to further develop and constrain model process representations. A critical gap in constraining mass balance of terrestrial Hg using models is the lack of ecohydrological models (i.e., biogeochemical-hydrology modeling) linking deposited mercury in terrestrial systems to mercury discharges from rivers to ocean margins, including AO.

3.10 Key Messages

[provide key messages from all sections]

Authors: all sections leads to provide key messages

3.11 References

Baker, K. R. and Bash, J. O.: Regional scale photochemical model evaluation of total mercury wet deposition and speciated ambient mercury, Atmospheric Environment, 49, 151–162, 2012.

Balabanov, N. B., Peterson, K. A. (2004). Accurate theoretical near-equilibrium potential energy and dipole moment surfaces of HgClO and HgBrO. *The Journal of Chemical Physics*, *120*(14), 6585–6592. https://doi.org/10.1063/1.1652435

Bieser, J., Matthias, V., Aulinger, A., Geyer, B., Hedgecock, I., DeSimone, F., Gencarelli, C. and Travnikov, O. (2014). Impact of Mercury Chemistry on Regional Concentration and Deposition Patterns, in *Air Pollution Modeling and its Application XXIII*, pp. 189–195, Springer, Cham.

Calvert, J. G., Lindberg, S. E. (2005). Mechanisms of mercury removal by O_3 and OH in the atmosphere. *Atmospheric Environment*, *39*(18), 3355–3367. https://doi.org/10.1016/j.atmosenv.2005.01.055

Cremer, D., Kraka, E., Filatov, M. (2008). Bonding in mercury molecules described by the normalized elimination of the small component and coupled cluster theory. *Chemphyschem : A*

European Journal of Chemical Physics and Physical Chemistry, *9*(17), 2510–2521. https://doi.org/10.1002/cphc.200800510

Dibble, T. S., Tetu, H. L., Jiao, Y., Thackray, C. P., Jacob, D. J. (2020). Modeling the OH-Initiated Oxidation of Mercury in the Global Atmosphere without Violating Physical Laws. *The Journal of Physical Chemistry A*, *124*(2), 444–453. https://doi.org/10.1021/acs.jpca.9b10121

Dibble, T. S., Zelie, M. J., Mao, H. (2012). Thermodynamics of reactions of ClHg and BrHg radicals with atmospherically abundant free radicals. *Atmospheric Chemistry and Physics*, *12*(21), 10271–10279. https://doi.org/10.5194/acp-12-10271-2012

Fitzgerald, W. F., Lamborg, C. H., Hammerschmidt, C. R. (2007). Marine Biogeochemical Cycling of Mercury. *Chemical Reviews*, *107*(2), 641–662. https://doi.org/10.1021/cr050353m

Francés-Monerris, A., Carmona-García, J., Acuña, A. U., Dávalos, J. Z., Cuevas, C. A., Kinnison, D. E., Francisco, J. S., Saiz-Lopez, A., Roca-Sanjuán, D. (2020). Photodissociation Mechanisms of Major Mercury(II) Species in the Atmospheric Chemical Cycle of Mercury. *Angewandte Chemie International Edition*. https://doi.org/10.1002/anie.201915656

Gårdfeldt, K., Jonsson, M. (2003). Is bimolecular reduction of Hg(II) complexes possible in aqueous systems of environmental importance. *Journal of Physical Chemistry A*, *107*(22), 4478–4482. https://doi.org/10.1021/jp0275342

Goodsite, M. E. Plane, J. M. C., Skov, H. (2004). A Theoretical Study of the Oxidation of Hg^0 to $HgBr_2$ in the Troposphere. *Environmental Science and Technology*, *38*(6), 1772–1776.

Gustin, M. S., Amos, H. M., Huang, J., Miller, M. B. and Heidecorn, K. (2015). Measuring and modeling mercury in the atmosphere: a critical review. *Atmospheric Chemistry and Physics, 15*(10), 5697–5713, doi:10.5194/acp-15-5697-2015.

Holloway, T., Voigt, C., Morton, J., Spak, S. N., Rutter, A. P. and Schauer, J. J. (2012). An assessment of atmospheric mercury in the Community Multiscale Air Quality (CMAQ) model at an urban site and a rural site in the Great Lakes Region of North America. *Atmospheric Chemistry and Physics, 12*(15), 7117–7133.

Horowitz, H. M., Jacob, D. J., Zhang, Y., Dibble, T. S., Slemr, F., Amos, H. M., Schmidt, J. A., Corbitt, E. S., Marais, E. A., Sunderland, E. M. (2017). A new mechanism for atmospheric mercury redox chemistry: implications for the global mercury budget. *Atmospheric Chemistry and Physics*, *17*, 6353–6371.

Hynes, A. J., Donohoue, D. L., Goodsite, M. E., Hedgecock, I. M. (2009). In *Mercury Fate and Transport in the Global Atmosphere*, Pirrone, N. and Mason, R., Eds. Springer, New York.

Kos, G., Ryzhkov, A., Dastoor, A., Narayan, J., Steffen, A., Ariya, P. A. and Zhang, L. (2013). Evaluation of discrepancy between measured and modelled oxidized mercury species, *Atmospheric Chemistry and Physics, 13*(9), 4839–4863, doi:10.5194/acp-13-4839-2013, 2013.

Lam, K. T., Wilhelmsen, C. J., Schwid, A. C., Jiao, Y., Dibble, T. S. (2019). Computational Study on the Photolysis of BrHgONO and the Reactions of BrHgO• with CH_4, C_2H_6, NO, and NO_2: Implications for Formation of Hg(II) Compounds in the Atmosphere. *The Journal of Physical Chemistry A*, *123*(8), 1637–1647. https://doi.org/10.1021/acs.jpca.8b11216

Lam, Khoa T., Wilhelmsen, C. J., Dibble, T. S. (2019). BrHgO• + C_2H_4 and BrHgO• + HCHO in Atmospheric Oxidation of Mercury: Determining Rate Constants of Reactions with Pre-Reactive Complexes and a Bifurcation. *The Journal of Physical Chemistry A*, *123*, 6045–6055. https://doi.org/10.1021/acs.jpca.9b05120

Obrist, D., Y. Agnan, M. Jiskra, C.L. Olson, D.P. Colegrove, J. Hueber, C.W. Moore, J.E. Sonke, et al. (2017). Tundra uptake of atmospheric elemental mercury drives Arctic mercury pollution. *Nature, 547*, 201–204.

Outridge PM, R. W. Macdonald, F. Wang, G. A. Stern, and A. P. Dastoor (2008). A mass balance inventory of mercury in the Arctic Ocean, *Environmental Chemistry, 5*, 89-111.

5672 Pal, B., Ariya, P. A. (2004). Studies of ozone initated reactions of gaseous mercury: kinetics, product
5673 stduies, and atmospehric implications. *Physical Chemistry Chemical Physics : PCCP*, *10*, 572–
5674 578. https://doi.org/10.1039/b801226a

5675 Peterson, K. A., Shepler, B. C., Singleton, J. M. (2007). The group 12 metal chalcogenides: an
5676 accurate multireference configuration interaction and coupled cluster study. *Molecular Physics*,
5677 *105*(9), 1139–1155. https://doi.org/10.1080/00268970701241664

5678 Pongprueksa, P., Lin, C. J., Lindberg, S. E., Jang, C., Braverman, T., Jr, O. R. B., Ho, T. C. and Chu,
5679 H. W. (2008). Scientific uncertainties in atmospheric mercury models III: Boundary and initial
5680 conditions, model grid resolution, and Hg(II) reduction mechanism. *Atmospheric Environment,*
5681 *42*(8), 1828–1845.

5682 Rutter, A. P., Shakya, K. M., Lehr, R., Schauer, J. J., Griffin, R. J. (2012). Oxidation of gaseous
5683 elemental mercury in the presence of secondary organic aerosols. *Atmospheric Environment*, *59*,
5684 86–92. https://doi.org/10.1016/j.atmosenv.2012.05.009

5685 Ryaboshapko, A., Jr, O. R. B., Christensen, J., Cohen, M., Dastoor, A., Ilyin, I., Petersen, G.,
5686 Syrakov, D., Artz, R. S., Davignon, D., Draxler, R. R. and Munthe, J. (2007). Intercomparison
5687 study of atmospheric mercury models: 1. Comparison of models with short-term measurements.
5688 *Science of the Total Environment, 376*(1–3), 228–240.

5689 Saiz-Lopez, A., Sitkiewicz, S. P., Roca-Sanjuán, D., Oliva-Enrich, J. M., Dávalos, J. Z., Notario, R.,
5690 Jiskra, M., Xu, Y, Wang, F., Thackray, C. P., Sunderland, E. M., Jacob, D. J., Travnikov, O.,
5691 Cuevas, C. A., Acuna, A. U., Rivero, D., Plane, J. M. C., Kinnison, D. E., Sonke, J. E. (2018).
5692 Photoreduction of gaseous oxidized mercury changes global atmospheric mercury speciation,
5693 transport and deposition. *Nature Communications*, *9*(1), 4796. https://doi.org/10.1038/s41467-
5694 018-07075-3

5695 Saiz-Lopez, A., Ulises Acuña, A., Trabelsi, T., Carmona-García, J., Z. Dávalos, J., Rivero, D.,
5696 Cuevas, C.A., Kinnison, D. E., Sitkiewicz, S. P., Roca-Sanjuan, D., Francisco, J. S. (2019). Gas-
5697 Phase Photolysis of Hg(I) Radical Species: A New Atmospheric Mercury Reduction Process.
5698 *Journal of the American Chemical Society*, *141*(22), 8698–8702.
5699 https://doi.org/10.1021/jacs.9b02890

5700 Seigneur, C., Vijayaraghavan, K., Lohman, K., Karamchandani, P. and Scott, C. (2004). Global
5701 Source Attribution for Mercury Deposition in the United States. *Environmental Science and*
5702 *Technology, 38*(2), 555–569.

5703 Selin, N. E., Javob, D. J., Park, R. J., Yantosca, R. M., Strode, S., Jaeglé, L. and Jaffe, D. (2007).
5704 Chemical cycling and deposition of atmospheric mercury: Global constraints from observations.
5705 *Journal of Geophysical Research D: Atmospheres, 112*(2).

5706 Shepler, B. C., Peterson, K. a. (2003). Mercury Monoxide: A Systematic Investigation of Its Ground
5707 Electronic State. *The Journal of Physical Chemistry A*, *107*(11), 1783–1787.
5708 https://doi.org/10.1021/jp027512f

5709 Skov, H., J. H. Christesen , M . E . Goodsite ,N. Z . Heidam , B. Jensen , P . Wåhlin, and G .
5710 Geernaert (2004). Fate of Elemental Mercury in the Arctic during Atmospheric Mercury
5711 Depletion Episodes and the Load of Atmospheric Mercury to the Arctic. *Environmental Science*
5712 *and Technology, 38*, 2373-2382.

5713 Sommar, J., Hallquist, M., Ljungström, E., Lindqvist, O. (1997). On the Gas Phase Reactions
5714 Between Volatile Biogenic Mercury Species and the Nitrate Radical. *Journal of Atmospheric*
5715 *Chemistry*, *27*(3), 233–247. https://doi.org/10.1023/A:1005873712847

5716 Spicer, C. W., Sumner, A. L., Satola, J., Mangaraj, R. (2005). Kinetics of mercury reactions in the
5717 atmosphere. *Report to the Florida Department of Environmental*.

5718 Subir, M., Ariya, P. A., Dastoor, A. P. (2012). A review of the sources of uncertainties in atmospheric
5719 mercury modeling II. Mercury surface and heterogeneous chemistry – A missing link.
5720 *Atmospheric Environment*, *46*, 1–10. https://doi.org/10.1016/j.atmosenv.2011.07.047

5721 Wang, S., McNamara, S. M., Moore, C. W., Obrist, D., Steffen, A., Shepson, P. B., Staebler, R. M.,
5722 Raso, A. R. W., Pratt, K. A. (2019). Direct detection of atmospheric atomic bromine leading to
5723 mercury and ozone depletion. *Proceedings of the National Academy of Sciences of the United*
5724 *States of America*, *116*(29), 14479–14484. https://doi.org/10.1073/pnas.1900613116

5725 Ye, Z., H. Mao, C. Driscoll, Y. Wang, C. Hogrefe, R. Volkmer, Y. Zhang, and L. Jaegle (2018).
5726 Evaluation of CMAQ Coupled with a State-of-the-Art Mercury Chemical Mechanism. *Journal of*
5727 *Advances in Modeling Earth Systems, 10*, 668–690. https://doi.org/10.1002/2017MS001161.

5728 Zhang, Y., Jaeglé, L., van Donkelaar, A., Martin, R. V., Holmes, C. D., Amos, H. M., Wang, Q.,
5729 Talbot, R., Artz, R., Brooks, S., Luke, W., Holsen, T. M., Felton, D., Miller, E. K., Perry, K. D.,
5730 Schmeltz, D., Steffen, A., Tordon, R., Weiss-Penzias, P. and Zsolway, R. (2012). Nested-grid
5731 simulation of mercury over North America. *Atmospheric Chemistry and Physics, 12*(14), 6095–
5732 6111, doi:10.5194/acp-12-6095-2012.

5733 Amirbahman, A.; Kent, D. B.; Curtis, G. P.; Marvin-Dipasquale, M. C. Kinetics of homogeneous and
5734 surface-catalyzed mercury(II) reduction by iron(II). Environ. Sci. Technol. 2013, 47 (13),
5735 7204−13.

5736 Andersson, M. E.; Sommar, J.; GÅrdfeldt, K.; Lindqvist, O. Enhanced concentrations of dissolved
5737 gaseous mercury in the surface waters of the Arctic Ocean. Mar. Chem. 2008, 110 (3−4),
5738 190−194.

5739 Ariya, P.A., Amyot, M., Dastoor, A., Deeds, D., Feinberg, A., Kos, G., Poulain, A., Ryjkov, A.,
5740 Semeniuk, K., Subir, M., Toyota, K., 2015. Mercury Physicochemical and Biogeochemical
5741 Transformation in the Atmosphere and at Atmospheric Interfaces: A Review and Future
5742 Directions. Chem. Rev. 115, 3760–3802. https://doi.org/10.1021/cr500667e.

5743 Berge, E. and Jakobsen, H. A.: A regional scale multi-layer model for the calculation of long-term
5744 transport and deposition of air pollution in Europe, Tellus, 50, 205–223, 1998.

5745 Bergquist, B. A.; Blum, J. D. Mass-Dependent and –Independent Fractionation of Hg Isotopes by
5746 Photoreduction in Aquatic Systems. Science 2007, 318 (5849), 417−420.

5747 Byun, D.W., Ching, J.K.S. (Eds.), 1999. Science Algorithms of the EPA Models-3

5748 Community Multiscale Air Quality (CMAQ) Modeling System (Rep. EPA-600/R-99/030). EPA,
5749 Washington, DC.

5750 D.J. Jacob, H. Liu, C.Mari, and R.M. Yantosca: Harvard wet deposition scheme for GMI, Harvard
5751 University Atmospheric Chemistry Modeling Group, February 2000.

5752 Dibble, T. S., M. J. Zelie, and H. Mao (2012), Thermodynamics of reactions of ClHg and BrHg
5753 radicals with atmospherically abundant free radicals, Atmos. Chem. Phys., 12, 10271–10279,
5754 2012.

5755 ENVIRON, 2011. User's Guide, Comprehensive Air Quality Model with Extensions (CAMx),
5756 Version 5.40. Environ International Corporation, California.

5757 GÅrdfeldt, K.; Munthe, J.; Strömberg, D.; Lindqvist, O. A kinetic study on the abiotic methylation of
5758 divalent mercury in the aqueous phase. Sci. Total Environ. 2003, 304 (1−3), 127−136.

5759 Goodsite, M.E., Plane, J.M.C., Skov, H., 2004. A Theoretical Study of the Oxidation of Hg0 to HgBr2
5760 in the Troposphere. Environ. Sci. Technol. 38, 1772–1776. https://doi.org/10.1021/es034680s

5761 Gu, B.; Bian, Y.; Miller, C. L.; Dong, W.; Jiang, X.; Liang, L. Mercury reduction and complexation
5762 by natural organic matter inanoxic environments. Proc. Natl. Acad. Sci. U. S. A. 2011, 108 (4),
5763 1479−1483.

5764 Guentzel J.L., Landing W.M., Gill G.A. and Pollman C.D., Processes influencing rainfall deposition
5765 of mercury in Florida, Environ. Sci. Technol. 3, 2001, 863–873.

5766 Hammerschmidt, C. R.; Lamborg, C. H.; Fitzgerald, W. F. Aqueous phase methylation as a potential
5767 source of methylmercury in wet deposition. Atmos. Environ. 2007, 41 (8), 1663−1668.

5768 Hinzman, L. D. et al., 2005: Evidence and implications of recent climate change in Northern Alaska
5769 and other Arctic regions. Climatic Change, 72, 251-298, doi:10.1007/s10584-005-5352-2.

5770 Lamborg, C. H., Fitzgerald, W. F., Vandal, G. M. and Rolfhus, K. R.: Atmospheric Mercury in
5771 Northern Wisconsin: Sources and Species, in Mercury as a Global Pollutant, pp. 189–198,
5772 Springer, Dordrecht, 1995.

5773 Landis, M.S. and Keeler, G.J., 2002. Atmospheric mercury deposition to Lake Michigan during the
5774 Lake Michigan mass balance study, Environ. Sci. Technol. 36, 4518–4524.

5775 Li, T. *, Y. Wang, H. Mao, S. Wang, R. Talbot, Y. Zhou*, Z. Wang, X. Nie*, and G. Qie* (2018),
5776 Insights on chemistry of mercury species in clouds over eastern China: Complexation and
5777 adsorption, Environ. Sci. Technol., 52, 5125−5134.

5778 Mason, R. P. and Sullivan, K. A. (1997). Mercury in Lake Michigan. Environ. Sci. Technol. 31,942 -
5779 947

5780 Obrist, D., Agnan, Y., Jiskra, M., Olson, C. L., Colegrove, D. P., Hueber, J.,...Helmig, D. (2017).
5781 Tundra uptake of atmospheric elemental mercurydrives Arctic mercury
5782 pollution.Nature,547(7662), 201–204. https://doi.org/10.1038/nature22997

5783 Prestbo, E.M., and Gay, D.A., 2009. Wet deposition of mercury in the U.S. and Canada, 1996–2005:
5784 Results and analysis of the NADP mercury deposition network (MDN), Atmos. Environ. 43,
5785 4223–4233.

5786 Risch, M.R., Fowler, K.K., 2008. Mercury in Precipitation in Indiana, January 2004 - December 2005
5787 U.S. Geological Survey Scientific Investigations Report 2008-5148.

5788 Rowland, J. C., C. E. Jones, G. Altmann et al. (2010), Arctic landscapes in transition: responses to
5789 thawing permafrost, Eos, *Transactions American Geophysical Union, 91*(26), 229–230.

5790 Sakata, M., Asakura, K., 2007. Estimating contribution of precipitation scavenging of atmospheric
5791 particulate mercury to mercury wet deposition in Japan. Atmos. Environ. 41, 1669–1680.

5792 Sanei, P.M. Outridge, F. Goodarzi, F. Wang, D. Armstrong, K. Warren, et al.Wet deposition mercury
5793 fluxes in the Canadian sub-Arctic and southern Alberta, measured using an automated
5794 precipitation collector adapted to cold regions, Atmos Environ, 44 (2010), pp. 1672-1681.

5795 Scherbatskoy, T., Shanley, J. B. and Keeler, G. J.: Factors controlling mercury transport in an upland
5796 forested catchment, Water Air Soil Pollut., 105(1–2), 427–438, 1998.

5797 Schroeder, W.H., Munthe, J., 1998. Atmospheric mercury - An overview. Atmos. Environ. 32, 809–
5798 822.

5799 Seigneur, C.; Abeck, H.; Chia, G.; Reinhard, M.; Bloom, N. S.; Prestbo, E.; Saxena, P. Mercury
5800 adsorption to elemental carbon (soot) particles and atmospheric particulate matter. Atmos.
5801 Environ. 1998, 32 (14−15), 2649−2657.

5802 Selin, N.E., Jacob, D.J., 2008. Seasonal and spatial patterns of mercury wet deposition in the United
5803 States: constraints on the contribution from North American anthropogenic sources. Atmos.
5804 Environ. 42(21), 5193–520.

5805 Siciliano, S. D.; O'Driscoll, N. J.; Tordon, R.; Hill, J.; Beauchamp, S.; Lean, D. R. S. Abiotic
5806 Production of Methylmercury by Solar Radiation. Environ. Sci. Technol. 2005, 39 (4), 1071.

5807 Sorensen, J. A., Glass, G. E., Schmidt, K. W., Huber, J. K. and Rapp, G. R.: Airborne mercury
5808 deposition and watershed characteristics in relation to mercury concentrations in water,
5809 sediments, plankton, and fish of eighty northern Minnesota lakes, Environ. Sci. Technol., 24(11),
5810 1716–1727, doi:10.1021/es00081a015, 1990.

5811 Subir, M., Ariya, P. A. and Dastoor, A. P.: A review of uncertainties in atmospheric modeling of
5812 mercury chemistry I. Uncertainties in existing kinetic parameters - Fundamental limitations and
5813 the importance of heterogeneous chemistry, Atmospheric Environment, 45(32), 5664–5676,
5814 2011.

5815 UNEP, 2013. Global Mercury Assessment 2013: Sources, Emissions, Releases and Environmental
5816 Transport. UNEP Chemicals Branch, Geneva, Switzerland.

5817 Wang, Y.; Li, Y.; Liu, G.; Wang, D.; Jiang, G.; Cai, Y. Elemental Mercury in Natural Waters:
5818 Occurrence and Determination of Particulate Hg(0). Environ. Sci. Technol. 2015, 49 (16),
5819 9742−9.

5820 Weiss-Penzias, P. S., Gay, D.A., Brigham, M.E., Parsons, M.T., Gustin, M.S., ter Schure, A., 2016.
5821 Trends in mercury wet deposition and mercury air concentrations across the U.S. and Canada.
5822 Sci. Total Environ. 568, 546–556.

5823 Abbatt, J. P. D., Thomas, J. L., Abrahamsson, K., Boxe, C., Granfors, A., Jones, A. E., King, M.D.,
5824 Saiz-Lopez, A., Shepson, P. B., Sodeau, J., Toohey, D. W., Toubin, C., von Glasow, R., Wren, S.
5825 N., and Yang, X.: Halogen activation via interactions with environmental ice and snow in the polar
5826 lower troposphere and other regions, *Atmos. Chem. Phys*., 12, 6237–6271, **2012**.

5827 Amos, H. M., Jacob, D. J., Holmes, C. D., Fisher, J. A., Wang, Q., Yantosca, R. M., Corbitt, E. S.,
5828 Galarneau, E., Rutter, A. P., Gustin, M. S., Steffen, A., Schauer, J. J., Graydon, J. A., Louis, V. L.
5829 St., Talbot, R. W., Edgerton, E. S., Zhang, Y., and Sunderland, E. M.: Gas-particle partitioning of
5830 atmospheric Hg(II) and its effect on global mercury deposition, *Atmos. Chem. Phys*., 12, 591–603,
5831 **2012**.

5832 Angot, H., Dastoor, A., De Simone, F., Gårdfeldt, K., Gencarelli, C. N., Hedgecock, I. M., Langer, S.,
5833 Magand, O., Mastromonaco, M. N., Nordstrøm, C., Pfaffhuber, K. A., Pirrone, N., Ryjkov, A.,
5834 Selin, N. E., Skov, H., Song, S., Sprovieri, F., Steffen, A., Toyota, K., Travnikov, O., Yang, X.,
5835 and Dommergue, A.: Chemical cycling and deposition of atmospheric mercury in polar regions:
5836 review of recent measurements and comparison with models, *Atmos. Chem. Phys*., 16, 10735–
5837 10763, **2016**.

5838 Archer, D. E.; Blum, J. D. A Model of Mercury Cycling and Isotopic Fractionation in the Ocean.
5839 *Biogeosciences* **2018**, *15* (20), 6297–6313. https://doi.org/10.5194/bg-15-6297-2018.

5840 Cobbett, F. D., Steffen, A., Lawson, G., and Heyst, B. J. V.: GEM fluxes and atmospheric mercury
5841 concentrations (GEM, RGM and Hg^p) in the Canadian Arctic at Alert, Nunavut, Canada
5842 (February–June 2005), *Atmos. Environ*., 41, 6527–6543, **2007**.

5843 Custard, K. D., Raso, A. R. W., Shepson, P. B., Staebler, R. M., and Pratt, K. A.: Production and Release
5844 of Molecular Bromine and Chlorine from the Arctic Coastal Snowpack, *ACS Earth and Space*
5845 *Chem*., 1, 142-151, **2017**.

5846 Christensen, J. H.; J. Brandt, L. M. Frohn, H. Skov. Modelling of Mercury in the Arctic with the Danish
5847 Eulerian Hemispheric Model. *Atmos. Chem. Phys.*, European Geosciences Union, **2004**, 4, 2251-
5848 2257

5849

5850 Horowitz, H. M., Jacob, D. J., Zhang, Y., Dibble, T. S., Slemr, F., Amos, H. M., Schmidt, J. A., Corbitt,
5851 E. S., Marais, E. A., and Sunderland, E. M.: A new mechanism for atmospheric mercury redox
5852 chemistry: implications for the global mercury budget, *Atmos. Chem. Phys*., 17, 6353–6371, **2017**.

5853 Kawai, T.; Sakurai, T.; Suzuki, N. Application of a New Dynamic 3-D Model to Investigate Human
5854 Impacts on the Fate of Mercury in the Global Ocean. *Environ. Model. Softw.* **2020**, *124*, 104599.

5855 Pratt, K. A., Custard, K. D., Shepson, P. B., Douglas, T. A., Pöhler, D., General, S., Zielcke, J., Simpson,
5856 W. R., Platt, U., Tanner, D. J., Huey, L. G., Carlsen, M., and Stirm, B. H.: Photochemical
5857 production of molecular bromine in Arctic surface snowpacks, *Nature Geosci.*, 6, 351–356, **2013**.

5858

5859 Saiz-Lopez, A.; S.P. Sitkiewicz, D. Roca-Sanjuán, J.M. Oliva-Enrich, J.Z Dávalos, R. Notario, M.
5860 Jiskra, Y. Xu, F. Wang, C.P. Thackray, E.M. Sunderland, D.J. Jacob, O. Travnikov, C.A. Cuevas,
5861 A.U. Acuña, D. Rivero, J. Plane, D.E. Kinnison, J.E. Sonke. **2018**. Photoreduction of gaseous

5862 oxidized mercury changes global atmospheric mercury speciation, transport and deposition. *Nature*
5863 *Comms*. 9, 4796

5864 Saiz-Lopez, A.; Acuña, A.U.; Trabelsi, T.; Carmona-García, J.; Dávalos, J.Z.; Rivero, D.; Cuevas, C.A.;
5865 Kinnison, D.E.; Sitkiewicz, S.P.; Roca-Sanjuán, D.; and Francisco J.S.: Gas-Phase Photolysis of
5866 Hg(I) Radical Species: A New Atmospheric Mercury Reduction Process, *Am. Chem. Soc.*,141, 22,
5867 8698-8702, **2019**.

5868 Schartup, A. T.; Qureshi, A.; Dassuncao, C.; Thackray, C. P.; Harding, G.; Sunderland, E. M. A Model
5869 for Methylmercury Uptake and Trophic Transfer by Marine Plankton. **2018**. *Environ. Sci. Technol.*
5870 52(2): 654-662

5871 Semeniuk, K.; Dastoor, A. Development of a Global Ocean Mercury Model with a Methylation Cycle:
5872 Outstanding Issues. *Global Biogeochem. Cycles* **2017**, *31* (2), 400–433.

5873 Soerensen, A.L.; D.J. Jacob, A.T. Schartup, J.A. Fisher, I Lehnherr, V.L. St. Louis, L.-E. Heimberger,
5874 J.E. Sonke, D.P. Krabbenhoft, E.M. Sunderland. **2016**. A mass budget for mercury and
5875 methylmercury in the Arctic Ocean. *Global Biogeochem. Cycles*

5876 Sonke, J.E.; Teisserenc, R.; Heimbürger-Boavida, L.-E.; Petrova, M.V.; Marusczak, N.; Le Dantec, T.;
5877 Chupakov, A.V.; Li, C.; Thackray, C.P.; Sunderland, E.M.; Tananaev, N.; and Pokrovsky, O.S.,
5878 *PNAS*, **2018**, 115 (50), E11586-E11594

5879

5880 Wren, S. N., Donaldson, D. J., and Abbatt, J. P. D.: Photochemical chlorine and bromine activation
5881 from artificial saline snow, Atmos. Chem. Phys., 13, 9789–9800, **2013**.Wu, P., E.J. Zakem, S.
5882 Dutkiewicz, and Y. Zhang. Biomagnification of methylmercury in marine plankton ecosystems,
5883 *Environ. Sci. Technol.*, in revision.

5884 Zhang, Y.; Jaegle, L.; Thompson, L. Natural Biogeochemical Cycle of Mercury in a Global Three-
5885 Dimensional Ocean Tracer Model. *Glob. Biogeochem. Cycles* **2014**, *28*.
5886 https://doi.org/10.1002/2014GB004814.

5887 Zhang, Y.; Jacob, D. J.; Dutkiewicz, S.; Amos, H. M.; Long, M. S.; Sunderland, E. M. Biogeochemical
5888 Drivers of the Fate of Riverine Mercury Discharged to the Global and Arctic Oceans. *Global*
5889 *Biogeochem. Cycles* **2015**, *29* (6), 854–864.

5890 Zhang, Y.; Soerensen, A. L.; Schartup, A. T.; Sunderland, E. M. A Global Model for Methylmercury
5891 Formation and Uptake at the Base of Marine Food Webs. *Global Biogeochem. Cycles*, *in Press*

5892 AMAP/ UN Environnement. 2019. "Technical Background Report for the Global Mercury
5893 Assessment 2018." Arctic Monitoring and Assessment Programme, Oslo, Norway/UN
5894 Environnement Programme, Chemicals and Health Branch, Geneva, Switzerland.
5895 https://www.amap.no/documents/doc/Technical-Background-Report-for-the-Global-Mercury-
5896 Assessment-2018/1815.

5897 AMAP/UNEP. 2013. "Technical Background Report for the Global Mercury Assessment 2013."
5898 Arctic Monitoring and Assessment Porgramme, Oslo, Norway. UNEP Chemicals Branch,
5899 Geneva, Switzerland. http://www.amap.no/documents/doc/technical-background-report-for-the-
5900 global-mercury-assessment-2013/848.

5901 Angot, H., A. Dastoor, F. De Simone, K. Gårdfeldt, C. N. Gencarelli, I. M. Hedgecock, S. Langer, et
5902 al. 2016. "Chemical Cycling and Deposition of Atmospheric Mercury in Polar Regions: Review
5903 of Recent Measurements and Comparison with Models." *Atmos. Chem. Phys.* 16 (16): 10735–63.
5904 https://doi.org/10.5194/acp-16-10735-2016.

5905 Dastoor, A. P., and D. A. Durnford. 2014. "Arctic Ocean: Is It a Sink or a Source of Atmospheric
5906 Mercury?" *Environmental Science and Technology* 48: 1707–17.

5907 DiMento, Brian P., Robert P. Mason, Steven Brooks, and Chris Moore. 2019. "The Impact of Sea Ice
5908 on the Air-Sea Exchange of Mercury in the Arctic Ocean." *Deep Sea Research Part I:*

Oceanographic Research Papers 144 (February): 28–38. https://doi.org/10.1016/j.dsr.2018.12.001.

Moore, Christopher W., Daniel Obrist, Alexandra Steffen, Ralf M. Staebler, Thomas A. Douglas, Andreas Richter, and Son V. Nghiem. 2014. "Convective Forcing of Mercury and Ozone in the Arctic Boundary Layer Induced by Leads in Sea Ice." *Nature* 506 (7486): 81–84. https://doi.org/10.1038/nature12924.

Nerentorp, Michelle. 2016. "Mercury Cycling in the Global Marine Environment." Chalmers University of Technology. https://research.chalmers.se/en/publication/243105.

Agnan, Y., T. A. Douglas, D. Helmig, J. Hueber, and D. Obrist. 2018. "Mercury in the Arctic Tundra Snowpack: Temporal and Spatial Concentration Patterns and Trace Gas Exchanges." *The Cryosphere* 12 (6): 1939–56. https://doi.org/10.5194/tc-12-1939-2018.

Angot, H., A. Dastoor, F. De Simone, K. Gårdfeldt, C. N. Gencarelli, I. M. Hedgecock, S. Langer, et al. 2016. "Chemical Cycling and Deposition of Atmospheric Mercury in Polar Regions: Review of Recent Measurements and Comparison with Models." *Atmos. Chem. Phys.* 16 (16): 10735–63. https://doi.org/10.5194/acp-16-10735-2016.

Bartels-Rausch, T., G. Krysztofiak, A. Bernhard, M. Schläppi, M. Schwikowski, and M. Ammann. 2011. "Phototoinduced Reduction of Divalent Mercury in Ice by Organic Matter." *Chemosphere* 82: 199–203.

Cheng, Meng-Dawn, and William H. Schroeder. 2000. "Potential Atmospheric Transport Pathways for Mercury Measured in the Canadian High Arctic." *Journal of Atmospheric Chemistry* 35 (1): 101–7. https://doi.org/10.1023/A:1006259625983.

Dastoor, A. P., and D. A. Durnford. 2014. "Arctic Ocean: Is It a Sink or a Source of Atmospheric Mercury?" *Environmental Science and Technology* 48: 1707–17.

Demers, Jason D., Joel D. Blum, and Donald R. Zak. 2013. "Mercury Isotopes in a Forested Ecosystem: Implications for Air-Surface Exchange Dynamics and the Global Mercury Cycle." *Global Biogeochemical Cycles* 27 (1): 222–38. https://doi.org/10.1002/gbc.20021.

DiMento, Brian P., Robert P. Mason, Steven Brooks, and Chris Moore. 2019. "The Impact of Sea Ice on the Air-Sea Exchange of Mercury in the Arctic Ocean." *Deep Sea Research Part I: Oceanographic Research Papers* 144 (February): 28–38. https://doi.org/10.1016/j.dsr.2018.12.001.

Douglas, T. A., M. Sturm, W. R. Simpson, J. D. Blum, L. Alvarez-Aviles, G. J. Keeler, D. K. Perovich, A. Biswas, and K. Johnson. 2008. "Influence of Snow and Ice Crystal Formation and Accumulation on Mercury Deposition to the Arctic." *Environmental Science and Technology* 42: 1542–51.

Douglas, T. A., M. Sturm, W. R. Simpson, S. Brooks, S. E. Lindberg, and D. K. Perovich. 2005. "Elevated Mercury Measured in Snow and Frost Flowers near Arctic Sea Ice Leads." *Geophysical Research Letters* 32 (4). https://doi.org/10.1029/2004GL022132.

Douglas, Thomas A., and Joel D. Blum. 2019. "Mercury Isotopes Reveal Atmospheric Gaseous Mercury Deposition Directly to the Arctic Coastal Snowpack." *Environmental Science & Technology Letters*, March. https://doi.org/10.1021/acs.estlett.9b00131.

Douglas, Thomas A., Lisa L. Loseto, Robie W. Macdonald, Peter Outridge, Aurélien Dommergue, Alexandre Poulain, Marc Amyot, et al. 2012. "The Fate of Mercury in Arctic Terrestrial and Aquatic Ecosystems, a Review." *Environmental Chemistry* 9 (4): 321–55. https://doi.org/10.1071/EN11140.

Douglas, Thomas A, and Matthew Sturm. 2004. "Arctic Haze, Mercury and the Chemical Composition of Snow across Northwestern Alaska." *Atmospheric Environment* 38 (6): 805–20. https://doi.org/10.1016/j.atmosenv.2003.10.042.

5957 Durnford, Dorothy, and Ashu Dastoor. 2011. "The Behavior of Mercury in the Cryosphere: A Review
5958 of What We Know from Observations." *Journal of Geophysical Research: Atmospheres* 116
5959 (D6): D06305. https://doi.org/10.1029/2010JD014809.

5960 Ferrari, C. P., P.-A. Gauchard, K. Aspmo, A. Dommergue, O. Magand, E. Bahlmann, S. Nagorski, et
5961 al. 2005. "Snow-to-Air Exchanges of Mercury in an Arctic Seasonal Snowpack in Ny-Alesund,
5962 Svalbard." *Atmospheric Environment* 39: 7633–45.

5963 Hausmann, M., and U. Platt. 1994. "Spectroscopic Measurement of Bromine Oxide and Ozone in the
5964 High Arctic during Polar Sunrise Experiment 1992." *Journal of Geophysical Research:*
5965 *Atmospheres* 99 (D12): 25399–413. https://doi.org/10.1029/94JD01314.

5966 Jacobi, H. W., D. Voisin, J. L. Jaffrezo, J. Cozic, and T. A. Douglas. 2012. "Chemical Composition of
5967 the Snowpack during the OASIS Spring Campaign 2009 at Barrow, Alaska." *Journal of*
5968 *Geophysical Research: Atmospheres* 117 (D14). https://doi.org/10.1029/2011JD016654.

5969 Jiskra, Martin, Jan Wiederhold, Ulf Skyllberg, Rose-Marie Kronberg, and Ruben Kretzschmar. 2017.
5970 "Source Tracing of Natural Organic Matter Bound Mercury in Boreal Forest Runoff with
5971 Mercury Stable Isotopes." *Environmental Science: Processes & Impacts*.
5972 https://doi.org/10.1039/C7EM00245A.

5973 Johnson, K. P., J. D. Blum, G. J. Keeler, and T. A. Douglas. 2008. "Investigation of the Deposition
5974 and Emission of Mercury in Arctic Snow during an Atmospheric Mercury Depletion Event."
5975 *Journal of Geophysical Research* 113 (D17304). https://doi.org/10.1029/2008JD009893.

5976 Mao, Huiting, Zhuyun Ye, and Charles Driscoll. 2017. "Meteorological Effects on Hg Wet
5977 Deposition in a Forested Site in the Adirondack Region of New York during 2000–2015."
5978 *Atmospheric Environment* 168 (November): 90–100.
5979 https://doi.org/10.1016/j.atmosenv.2017.08.058.

5980 Obrist, Daniel, Yannick Agnan, Martin Jiskra, Christine L. Olson, Dominique P. Colegrove, Jacques
5981 Hueber, Christopher W. Moore, Jeroen E. Sonke, and Detlev Helmig. 2017. "Tundra Uptake of
5982 Atmospheric Elemental Mercury Drives Arctic Mercury Pollution." *Nature* 547 (7662): 201–4.
5983 https://doi.org/10.1038/nature22997.

5984 Pearson, Christopher, Dean Howard, Christopher Moore, and Daniel Obrist. 2019. "Mercury and
5985 Trace Metal Wet Deposition across Five Stations in Alaska: Controlling Factors, Spatial Patterns,
5986 and Source Regions." *Atmospheric Chemistry and Physics* 19 (10): 6913–29.
5987 https://doi.org/10.5194/acp-19-6913-2019.

5988 Poulain, A. J., E. Garcia, M. Amyot, P. G. C. Campbell, and P. A. Ariya. 2007. "Mercury
5989 Distribution, Partitioning and Speciation in Coastal vs. Inland High Arctic Snow." *Geochim.*
5990 *Cosmochim. Acta* 71: 3419–31.

5991 Qin, Caiqing, Yongmin Wang, Yulong Peng, and Dingyong Wang. 2016. "Four-Year Record of
5992 Mercury Wet Deposition in One Typical Industrial City in Southwest China." *Atmospheric*
5993 *Environment* 142 (October): 442–51. https://doi.org/10.1016/j.atmosenv.2016.08.016.

5994 Sanei, H., P. M. Outridge, F. Goodarzi, F. Wang, D. Armstrong, K. Warren, and L. Fishback. 2010.
5995 "Wet Deposition Mercury Fluxes in the Canadian Sub-Arctic and Southern Alberta, Measured
5996 Using an Automated Precipitation Collector Adapted to Cold Regions." *Atmospheric*
5997 *Environment* 44 (13): 1672–81. https://doi.org/10.1016/j.atmosenv.2010.01.030.

5998 Serreze, Mark C., Andrew P. Barrett, Andrew G. Slater, Rebecca A. Woodgate, Knut Aagaard,
5999 Richard B. Lammers, Michael Steele, Richard Moritz, Michael Meredith, and Craig M. Lee.
6000 2006. "The Large-Scale Freshwater Cycle of the Arctic." *Journal of Geophysical Research:*
6001 *Oceans* 111 (C11). https://doi.org/10.1029/2005JC003424.

6002 Sprovieri, F., N. Pirrone, M. Bencardino, F. D'Amore, H. Angot, C. Barbante, E.-G. Brunke, et al.
6003 2017. "Five-Year Records of Mercury Wet Deposition Flux at GMOS Sites in the Northern and
6004 Southern Hemispheres." *Atmos. Chem. Phys.* 17 (4): 2689–2708. https://doi.org/10.5194/acp-17-
6005 2689-2017.

6006 St. Louis, Vincent L., Martin J. Sharp, Alexandra Steffen, Al May, Joel Barker, Jane L. Kirk, David J.
6007 A. Kelly, Shelley E. Arnott, Bronwyn Keatley, and John P. Smol. 2005. "Some Sources and
6008 Sinks of Monomethyl and Inorganic Mercury on Ellesmere Island in the Canadian High Arctic."
6009 *Environmental Science & Technology* 39 (8): 2686–2701. https://doi.org/10.1021/es049326o.

6010 Steffen, A., J. Bottenheim, A. Cole, T. A. Douglas, R. Ebinghaus, U. Friess, S. Netcheva, S. Nghiem,
6011 H. Sihler, and R. Staebler. 2013. "Atmospheric Mercury over Sea Ice during the OASIS-2009
6012 Campaign." *Atmospheric Chemistry and Physics* 13 (14): 7007–21. https://doi.org/10.5194/acp-
6013 13-7007-2013.

6014 Steffen, A., T. Douglas, M. Amyot, P. Ariya, K. Aspmo, T. Berg, J. Bottenheim, et al. 2008. "A
6015 Synthesis of Atmospheric Mercury Depletion Event Chemistry in the Atmosphere and Snow."
6016 *Atmos. Chem. Phys.* 8 (6): 1445–82. https://doi.org/10.5194/acp-8-1445-2008.

6017 Zhou, Hao, Chuanlong Zhou, Philip K. Hopke, and Thomas M. Holsen. 2018. "Mercury Wet
6018 Deposition and Speciated Mercury Air Concentrations at Rural and Urban Sites across New York
6019 State: Temporal Patterns, Sources and Scavenging Coefficients." *Science of The Total*
6020 *Environment* 637–638 (October): 943–53. https://doi.org/10.1016/j.scitotenv.2018.05.047.

6021

6022 Biswas, A., Blum, J. D., Bergquist, B. A., Keeler, G. J., and Xie, Z. Q.: Natural Mercury Isotope
6023 Variation in Coal Deposits and Organic Soils, Environ. Sci. Technol., 42, 8303-8309,
6024 10.1021/es801444b, 2008.

6025 Blum, J. D., Sherman, L. S., and Johnson, M. W.: Mercury Isotopes in Earth and Environmental
6026 Sciences, Annu. Rev. Earth Planet. Sci. Lett., 42, 249-269, 10.1146/annurev-earth-050212-
6027 124107, 2014.

6028 Day, R. D., Roseneau, D. G., Berail, S., Hobson, K. A., Donard, O. F. X., Vander Pol, S. S., Pugh, R.
6029 S., Moors, A. J., Long, S. E., and Becker, P. R.: Mercury Stable Isotopes in Seabird Eggs Reflect
6030 a Gradient from Terrestrial Geogenic to Oceanic Mercury Reservoirs, Environmental Science &
6031 Technology, 46, 5327-5335, 10.1021/es2047156, 2012.

6032 Demers, J. D., Blum, J. D., and Zak, D. R.: Mercury isotopes in a forested ecosystem: Implications for
6033 air-surface exchange dynamics and the global mercury cycle, Global Biogeochem. Cycles, 27,
6034 222-238, Doi 10.1002/Gbc.20021, 2013.

6035 Douglas, T. A., Loseto, L. L., Macdonald, R. W., Outridge, P., Dommergue, A., Poulain, A., Amyot,
6036 M., Barkay, T., Berg, T., Chetelat, J., Constant, P., Evans, M., Ferrari, C., Gantner, N., Johnson,
6037 M. S., Kirk, J., Kroer, N., Larose, C., Lean, D., Nielsen, T. G., Poissant, L., Rognerud, S., Skov,
6038 H., Sorensen, S., Wang, F. Y., Wilson, S., and Zdanowicz, C. M.: The fate of mercury in Arctic
6039 terrestrial and aquatic ecosystems, a review, Environmental Chemistry, 9, 321-355,
6040 10.1071/en11140, 2012.

6041 Douglas, T. A., Sturm, M., Blum, J. D., Polashenski, C., Stuefer, S., Hiemstra, C., Steffen, A., Filhol,
6042 S., and Prevost, R.: A Pulse of Mercury and Major Ions in Snowmelt Runoff from a Small Arctic
6043 Alaska Watershed, Environmental Science & Technology, 10.1021/acs.est.7b03683, 2017.

6044 Douglas, T. A., and Blum, J. D.: Mercury isotopes reveal atmospheric gaseous mercury deposition
6045 directly to the Arctic coastal snowpack, Environmental Science & Technology Letters,
6046 10.1021/acs.estlett.9b00131, 2019.

6047 Gleason, J. D., Blum, J. D., Moore, T. C., Polyak, L., Jakobsson, M., Meyers, P. A., and Biswas, A.:
6048 Sources and cycling of mercury in the paleo Arctic Ocean from Hg stable isotope variations in
6049 Eocene and Quaternary sediments, Geochimica et Cosmochimica Acta, 197, 245-262,
6050 10.1016/j.gca.2016.10.033, 2017.

6051 Jiskra, M., Sonke, J. E., Agnan, Y., Helmig, D., and Obrist, D.: Insights from mercury stable isotopes
6052 on terrestrial–atmosphere exchange of Hg(0) in the Arctic tundra, Biogeosciences, 16, 4051-
6053 4064, 10.5194/bg-16-4051-2019, 2019.

6054 Li, M., Sherman, L. S., Blum, J. D., Grandjean, P., Mikkelsen, B., Weihe, P., Sunderland, E. M., and
6055 Shine, J. P.: Assessing Sources of Human Methylmercury Exposure Using Stable Mercury
6056 Isotopes, Environmental Science & Technology, 48, 8800-8806, 10.1021/es500340r, 2014.

6057 Masbou, J., Point, D., Sonke, J. E., Frappart, F., Perrot, V., Amouroux, D., Richard, P., and Becker, P.
6058 R.: Hg Stable Isotope Time Trend in Ringed Seals Registers Decreasing Sea Ice Cover in the
6059 Alaskan Arctic, Environ Sci Technol, 49, 8977-8985, 10.1021/es5048446, 2015.

6060 Masbou, J., Sonke, J. E., Amouroux, D., Guillou, G., Becker, P. R., and Point, D.: Hg-Stable Isotope
6061 Variations in Marine Top Predators of the Western Arctic Ocean, ACS Earth and Space
6062 Chemistry, 2, 479-490, 10.1021/acsearthspacechem.8b00017, 2018.

6063 Obrist, D., Agnan, Y., Jiskra, M., Olson, C. L., Colegrove, D. P., Hueber, J., Moore, C. W., Sonke, J.
6064 E., and Helmig, D.: Tundra uptake of atmospheric elemental mercury drives Arctic mercury
6065 pollution, Nature, 547, 201-204, 10.1038/nature22997

6066 http://www.nature.com/nature/journal/v547/n7662/abs/nature22997.html#supplementary-information,
6067 2017.

6068 Obrist, D., Kirk, J. L., Zhang, L., Sunderland, E. M., Jiskra, M., and Selin, N. E.: A review of global
6069 environmental mercury processes in response to human and natural perturbations: Changes of
6070 emissions, climate, and land use, Ambio, 47, 116-140, 10.1007/s13280-017-1004-9, 2018.

6071 Olson, C. L., Jiskra, M., Sonke, J. E., and Obrist, D.: Mercury in tundra vegetation of Alaska: Spatial
6072 and temporal dynamics and stable isotope patterns, Science of The Total Environment, 660,
6073 1502-1512, 10.1016/j.scitotenv.2019.01.058, 2019.

6074 Point, D., Sonke, J. E., Day, R. D., Roseneau, D. G., Hobson, K. A., Vander Pol, S. S., Moors, A. J.,
6075 Pugh, R. S., Donard, O. F. X., and Becker, P. R.: Methylmercury photodegradation influenced by
6076 sea-ice cover in Arctic marine ecosystems, Nat. Geosci., 4, 188-194, Doi 10.1038/Ngeo1049,
6077 2011.

6078 Sherman, L. S., Blum, J. D., Johnson, K. P., Keeler, G. J., Barres, J. A., and Douglas, T. A.: Mass-
6079 independent fractionation of mercury isotopes in Arctic snow driven by sunlight, Nat. Geosci., 3,
6080 173-177, 10.1038/ngeo758, 2010.

6081 Sherman, L. S., Blum, J. D., Douglas, T. A., and Steffen, A.: Frost flowers growing in the Arctic
6082 ocean-atmosphere-sea ice-snow interface: 2. Mercury exchange between the atmosphere, snow,
6083 and frost flowers, J. Geophys. Res.-Atmos., 117, D00R10, Artn D00r10

6084 10.1029/2011jd016186, 2012.

6085 Štrok, M., Baya, P. A., and Hintelmann, H.: The mercury isotope composition of Arctic coastal
6086 seawater, Comptes Rendus Geoscience, 347, 368-376, 10.1016/j.crte.2015.04.001, 2015.

6087 Yuan, W., Sommar, J., Lin, C.-J., Wang, X., Li, K., Liu, Y., Zhang, H., Lu, Z., Wu, C., and Feng, X.:
6088 Stable isotope evidence shows re-emission of elemental mercury vapor occurring after reductive
6089 loss from foliage, Environmental Science & Technology, 10.1021/acs.est.8b04865, 2018.

6090

6091 Bartels-Rausch, T.; Krysztofiak, G.; Bernhard, A.; Schläppi, M.; Schwikowski, M.; Ammann, M.
6092 Photoinduced reduction of divalent mercury in ice by organic matter. Chemosphere 2011, 82 (2),
6093 199−203.

6094 Bishop, K. and Y. Lee (1997). "Catchments as a source of mercury/methylmercury in boreal surface
6095 waters." Metal Ions in Biological Systems 34: 113-130.

6096 Biswas, A., Blum, J.D. and Keeler, G. (2008a) A comparison of methods for the estimation of mercury
6097 release from forest fires. Science of the Total Environment doi:10.1029/2008JD009893.

6098 Cheng, M.-D., Schroeder, W. H. (2000) Potential atmospheric transport pathways for mercury
6099 measured in the Canadian high Arctic. Journal of Atmospheric Chemistry 35: 101–107.

6100 Demers, J. D., J. D. Blum and D. R. Zak (2013). "Mercury isotopes in a forested ecosystem:
6101 Implications for air-surface exchange dynamics and the global mercury cycle." Global
6102 Biogeochemical Cycles 27(1): 222-238.

6103 Demers, J. D.; Blum, J. D.; Zak, D. R. Mercury isotopes in a forested ecosystem: Implications for air-
6104 surface exchange dynamics and the global mercury cycle. Global Biogeochemical Cycles. 2013,
6105 27 (1), 222−38.

6106 Dommergue, A.; Ferrari, C. P.; Gauchard, P.-A.; Boutron, C. F.; Poissant, L.; Pilote, M.; Jitaru, P.;
6107 Adams, F. C. The fate of mercury species in a sub-arctic snowpack during snowmelt. Geophys.
6108 Res. Lett. 2003, 30, 1621.

6109 Douglas, T. A.; Loseto, L. L.; Macdonald, R. W.; Outridge, P.; Dommergue, A.; Poulain, A.; Amyot,
6110 M.; Barkay, T.; Berg, T.; Chételat, J.; Constant, P.; et al. The fate of mercury in Arctic terrestrial
6111 and aquatic ecosystems, a review. Environ. Chem. 2012, 9 (4), 321−55.

6112 Douglas, T. A.; Sturm, M.; Blum, J. D.; Polashenski, C.; Stuefer, S.; Hiemstra, C. A.; Steffen, A.; Filhol,
6113 S.; Prevost, R. A pulse of mercury and major ions in snowmelt runoff from a small Arctic Alaska
6114 watershed. Environ. Sci. Technol. 2017, 51, 11145.

6115 Douglas, T. A.; Sturm, M.; Simpson, W. R.; Brooks, S.; Lindberg, S. E.; Perovich, D. K. Elevated
6116 mercury measured in snow and frost flowers near arctic sea ice leads. Geophys. Res. Lett. 2005,
6117 32, L04502.

6118 Douglas, T.; Sturm, M. Arctic haze, mercury and the chemical composition of snow across northwestern
6119 Alaska. Atmos. Environ. 2004, 38 (6), 805−820.

6120 Douglas, T.A., and Blum, J.D. (2019) Mercury isotopes reveal atmospheric gaseous mercury deposition
6121 directly to the Arctic coastal snowpack. Environmental Science and Technology Letters. doi:
6122 10.1021/acs.estlett.9b00131.

6123 Durnford, D.; Dastoor, A. The behavior of mercury in the cryosphere: A review of what we know from
6124 observations. J. Geophys. Res. 2011, 116, 116.

6125 Enrico, M., G. L. Roux, N. Marusczak, L. E. Heimburger, A. Claustres, X. Fu, R. Sun and J. E. Sonke
6126 (2016). "Atmospheric Mercury Transfer to Peat Bogs Dominated by Gaseous Elemental Mercury
6127 Dry Deposition." Environ Sci Technol 50(5): 2405-2412.

6128 Ferrari, C.P., and fifteen others (2005) Snow-to-air exchanges of mercury in an Arctic seasonal snow
6129 pack in Ny-Ålesund, Svalbard. Atmospheric Environment 39: 7633-7645.

6130 Fu, X., X. Yang, X. Lang, J. Zhou, H. Zhang, B. Yu, H. Yan, C.-J. Lin and X. Feng (2016).
6131 "Atmospheric wet and litterfall mercury deposition at urban and rural sites in China." Atmospheric
6132 Chemistry and Physics 16(18): 11547–11562.

6133 Grigal, D. F., R. K. Kolka, J. A. Fleck and E. A. Nater (2000). "Mercury budget of an upland-peatland
6134 watershed." Biogeochemistry 50(1): 95-109.

6135 Guo, L., Cai, Y., Belzile, C. Macdonald, R. (2011) Sources and fluxes of carbon and nutrient species in
6136 the seasonally ice-covered Yukon River. Biogeochemistry, doi:10.1007/s10533-010-9545-z.

6137 Hausmann, M., Platt, U. (1994) Spectroscopic measurement of bromine oxide and ozone in the high
6138 Arctic during Polar Sunrise Experiment 1992. Journal of Geophysical Research 99(D12): 25399-
6139 25413.

6140 Hugelius, G., Strauss, J., Zubrzycki, S., Harden, J. W., Schuur, E. A. G., Ping, C. L., Schirrmeister, L.,
6141 Grosse, G., Michaelson, G. J., Koven, C. D., O'Donnell, J. A., Elberling, B., Mishra, U., Camill,
6142 P., Yu, Z., Palmtag, J., and Kuhry, P.: Estimated stocks of circumpolar permafrost carbon with
6143 quantified uncertainty ranges and identified data gaps, Biogeosciences, 11(23), 6573–6593,
6144 doi:10.5194/bg-11-6573-2014, 2014.

6145 Iverfeldt, Å. (1991). "Mercury in forest canopy throughfall water and its relation to atmospheric
6146 deposition." Water, Air, and Soil Pollution 56: 553-564.

6147 Jacobi HW, Voisin D, Jaffrezo JL, Cozic J, Douglas TA. Chemical composition of the snowpack during
6148 the OASIS spring campaign 2009 at Barrow, Alaska. Journal of Geophysical Research:
6149 Atmospheres. 2012 Jul 27;117(D14).

6150 Jiskra, M., J. G. Wiederhold, U. Skyllberg, R. M. Kronberg, I. Hajdas and R. Kretzschmar (2015).
6151 "Mercury deposition and re-emission pathways in boreal forest soils investigated with Hg isotope
6152 signatures." Environ Sci Technol 49(12): 7188-7196.

6153 Jiskra, M., Sonke, J. E., Agnan, Y., Helmig, D., and Obrist, D.: Insights from mercury stable isotopes
6154 on terrestrial–atmosphere exchange of Hg(0) in the Arctic tundra, Biogeosciences, 16, 4051-4064,
6155 10.5194/bg-16-4051-2019, 2019.

6156 Jiskra, M.; Wiederhold, J. G.; Skyllberg, U.; Kronberg, R. M.; Kretzschmar, R. Source tracing of natural
6157 organic matter bound mercury in boreal forest runoff with mercury stable isotopes. Environmental
6158 Science: Processes & Impacts. 2017, 19 (10), 1235−48.

6159 Johnson, K.P., Blum, J.D., Keeler, G.J., Douglas, T.A. (2008) Investigation of the deposition and
6160 emission of mercury in arctic snow during an atmospheric mercury depletion event. Journal of
6161 Geophysical Research Atmospheres 113(D17304) doi:10.1029/2008JD009893.

6162 Lim, A. G., Jiskra, M., Sonke, J. E., Loiko, S. V., Kosykh, N., and Pokrovsky, O. S.: A revised northern
6163 soil Hg pool, based on western Siberia permafrost peat Hg and carbon observations,
6164 Biogeosciences Discuss., 2020, 1-35, 10.5194/bg-2019-483, 2020.

6165 Lindberg, S., J. Owens and W. Stratton (1994). Application of Throughfall Methods to Estimate Dry
6166 Deposition of Mercury. Mercury Pollution: Integration and Synthesis, Lewis Publishers: 261-271.

6167 McNamara, J. P.; Kane, D. L.; Hinzman, L. D. An analysis of streamflow hydrology in the Kuparuk
6168 River Basin, Arctic Alaska: a nested watershed approach. J. Hydrol. 1998, 206, 39.

6169 Munthe, J., H. Hultberg and Å. Iverfeldt (1995). "Mechanisms of deposition of methylmercury and
6170 mercury to coniferous forests." Water Air and Soil Pollution 80(1-4): 363-371.

6171 Obrist, D., Y. Agnan, M. Jiskra, C. L. Olsen, D. P. Colegrove, J. Hueber, C. W. Moore, J. E. Sonke and
6172 D. Helmig (2017). "Tundra uptake of atmospheric elemental mercury drives arctic mercury
6173 pollution." Nature 547: 201-2014.

6174 Obrist, D.; Agnan, Y.; Jiskra, M.; Olson, C. L.; Colegrove, D. P.; Hueber, J.; Moore, C. W.; Sonke, J.
6175 E.; Helmig, D. Tundra uptake of atmospheric elemental mercury drives Arctic mercury pollution.
6176 Nature 2017, 547 (7662), 201−204.

6177 Obrist D, Johnson DW, Lindberg SW, Luo Y, Hararuk O, Bracho R, Battles JJ, Dail DB, Edmonds RL,
6178 Monson RK, Ollinger SV, Pallardy SG, Pregitzer KS, Todd DE. Mercury distribution across 14
6179 U.S. forests. Part I: Spatial patterns of total Hg concentrations in biomass, litter, and soils.
6180 Environmental Science and Technology, 45, 3974–3981, 2011.

6181 Poulain, A. J.; Garcia, E.; Amyot, M.; Campbell, P. G. C.; Ariya, P. Mercury distribution, partitioning
6182 and speciation in coastal vs. inland high arctic snow. Geochim. Cosmochim. Acta 2007, 71 (14),
6183 3419−3431.

6184 Rea, A., G. Keeler and T. Scherbatskoy (1996). "The deposition of mercury in throughfall and litterfall
6185 in the lake champlain watershed: A short-term study." Atmopsheric Environment 30(19): 3257-
6186 3263.

6187 Rea, A., S. Lindberg and G. Keeler (2001). "Dry deposition and foliar leaching of mercury and selected
6188 trace elements in deciduous forest throughfall." Atmospheric Environment 35(20): 3453-3462.

6189 Simpson WR, Alvarez-Aviles L, Douglas TA, Sturm M, Domine F. Halogens in the coastal snow pack
6190 near Barrow, Alaska: Evidence for active bromine air-snow chemistry during springtime.
6191 Geophysical research letters. 2005 Feb;32(4).

St. Louis, V. L., J. W. M. Rudd, C. A. Kelly, B. D. Hall, K. R. Rolfhus, K. J. Scott, S. E. Lindberg and W. Dong (2001). "Importance of the Forest Canopy to Fluxes of Methyl Mercury and Total Mercury to Boreal Ecosystems." Environmental Science and Technology 35(15): 3089-3098.

St. Louis, V.L., and nine others (2005) Some sources and sinks of monomethyl and inorganic mercury on Ellesmere Island in the Canadian High Arctic. Environmental Science and Technology 39: 2686- 2701.

Steffen A, Douglas T, Amyot M, Ariya P, Aspmo K, Berg T, Bottenheim J, Brooks S, Cobbett F, Dastoor A, Dommergue A. A synthesis of atmospheric mercury depletion event chemistry linking atmosphere, snow and water. Atmospheric Chemistry and Physics Discussions. 2007 Jul 26;7(4):10837-931.

Steffen, A.; Bottenheim, J.; Cole, A.; Douglas, T. A.; Ebinghaus, R.; Friess, U.; Netcheva, S.; Nghiem, S.; Sihler, H.; Staebler, R. Atmospheric mercury over sea ice during the OASIS-2009 campaign. Atmos. Chem. Phys. 2013, 13, 7007−7021.

Wang, X., J. Luo, R. Yin, W. Yuan, C. J. Lin, J. Sommar, X. Feng, H. Wang and C. Lin (2017). "Using Mercury Isotopes To Understand Mercury Accumulation in the Montane Forest Floor of the Eastern Tibetan Plateau." Environ Sci Technol 51(2): 801-809.

Wang, X., Z. Bao, C.-J. Lin, W. Yuan and X. Feng (2016). "Assessment of global mercury deposition through litterfall." Environmental Science and Technology 50(16): 8548–8557.

Wright, L. P., L. Zhang and F. J. Marsik (2016). "Overview of mercury dry deposition, litterfall, and throughfall studies." Atmospheric Chemistry and Physics 16(21): 13399–13416.

Zhang, L., Z. Wu, I. Cheng, L. P. Wright, M. L. Olson, D. A. Gay, M. R. Risch, S. Brooks, M. S. Castro, G. D. Conley, E. S. Edgerton, T. M. Holsen, W. Luke, R. Tordon and P. Weiss-Penzias (2016). "The Estimated Six-Year Mercury Dry Deposition Across North America." Environ Sci Technol 50(23): 12864-12873.

Zheng, W., D. Obrist, D. Weis and B. A. Bergquist (2016). "Mercury isotope compositions across North American forests." Global Biogeochemical Cycles 30(10): 1475-1492.

Zhang Y., Soerensen A. L., Schartup A. T., Sunderland E. M. (2020). A global model for methylmercury formation and uptake at the base of marine food webs, doi: 10.1029/2019GB006348.

Bindler R, Renberg I, Appleby PG et al (2001) Mercury accumulation rates and spatial patterns in lake sediments from West Greenland: a coast to ice margin transect. Environ Sci Technol 35:1736–1741.

Blais, J.M., Kalff, J. (1995). 'The influence of lake morphometry on sediment focussing.' *Limnology and Oceanography*, 40, (3), 582-588.

Bloom, N.S., Preus, E., Katon, J., Hiltner, M. (2003). 'Selective extractions to access the biogeochemically relevant fractionation of inorganic mercury in sediments and soils.' *Analytica Chimica Acta*, 479, 233-248.

Burke, S.M., Zimmerman, C.E., Branfireun, B.A., Koch, J.C., Swanson, H.K. (2018). 'Patterns and controls of mercury accumulation in sediments for three thermokarst lakes on the arctic coastal plain of Alaska.' *Aquatic Sciences*, 80, (1), 1-15.

Carrie, J., Sanei, H., Stern, G. (2012). 'Standardisation of Rock-Eval pyrolysis for the analysis of recent sediments and soils.' *Organic Geochemistry*, 46, 38-53.

Chen, J., Hintelmann, H., Zheng, W., Feng, X., Cai, H., Wang, Z., Yuan, S., Wang, Z. (2016). 'Isotopic evidence for distinct sources of mercury in lake waters and sediments.' *Chemical Geology*, 426, 33-44.

6238 Chételat, J., Amyot, M., Arp, P., Blais, J.M., Depew, D., Emmerton, C.A., Evans, M., Gamberg, M.,
6239 Gantner, N., Girard, C., Graydon, J., Kirk, J., Lean, D., Lehnherr, I., Muir, D., Nasr, M., Poulain,
6240 A.J., Power, M., Roach, P., Stern, G., Swanson, H., van der Velden, S. (2015). 'Mercury in
6241 freshwater ecosystems of the Canadian Arctic: Recent advances on its cycling and fate.' *Science*
6242 *of the Total Environment*, 509-510, 41-66.

6243 Cooke, C.A., Wolfe, A.P., Michelutti, N., Balcom, P.H., Briner, J.P. (2012). 'A holocene perspective
6244 on algal mercury scavenging to sediments of an arctic lake.' *Environmental Science and*
6245 *Technology*, 46, 7135-7141.

6246 Dastoor, A., Ryzhkov, A., Durnford, D., Lehnherr, I., Steffen, A., Morrison, H. (2015). 'Atmospheric
6247 mercury in the Canadian arctic. Part II: Insight from modelling.' *Science of the Total Environment*,
6248 509-510, 16-27.

6249 Deison, R., Smol, J.P., Kokelj, S.V., Pisaric, M.F.J., Kimpe, L.E., Poulain, A.J., Sanei, H., Thienpont,
6250 J.R., Blais, J.M. (2012). 'Spatial and temporal assessment of mercury and organic matter in
6251 thermokarst affected lakes of the Mackenzie Delta Uplands, NT, Canada.' *Environmental Science*
6252 *and Technology*, 46, 8748-8755.

6253

6254 Drevnick, P.E., Yang, H., Lamborg, C.H., Rose, N.L. (2012). 'Net atmospheric mercury deposition to
6255 Svalbard: Estimates from lacustrine sediments.' *Atmospheric Environment*, 59, 509-513.

6256 Fitzgerald WF, Engstrom DR, Lamborg CH et al (2005) Modern and historic atmospheric mercury
6257 fluxes in northern Alaska: Global sources and Arctic depletion. Environ Sci Technol 39:557–568.

6258 Grasby, S.E., Sanei, H., Beauchamp, B., Chen, Z. (2013). 'Mercury deposition through the Permo-
6259 Triassic biotic crisis.' *Chemical Geology*, 351, 209-216.

6260 Goodsite, M.E., Outridge, P.M., Christensen, J.H., Dastoor, A., Muir, D., Travnikov, O., Wilson, S.
6261 (2013). 'How well do environmental archives of atmospheric mercury deposition in the arctic
6262 reproduce rates and trends depicted by atmospheric models and measurements?' *Science of the*
6263 *Total Environment*, 452-453, 196-207.

6264 Jackson, A.K., Evers, D.C., Adams, E.M., Cristol, D.A., Eagles-Smith, C., Edmonds, S.T., Gray, C.E.,
6265 Hoskins, B. et al (2015). 'Songbirds as sentinels of mercury in terrestrial habitats of eastern North
6266 America.' *Ecotoxicology*, 24, 453-467.

6267 Jiang, S., Liu, X., Chen, Q. (2011). 'Distribution of total mercury and methylmercury in lake sediments
6268 in arctic Ny-Alesund.' *Chemosphere*, 83, 1108-1116.

6269 Jiskra, M., Wiederhold, J.G., Skyllberg, U., Kronberg, R.M., Kretzschmar, R. (2017). 'Source tracing
6270 of natural organic matter bound mercury in boreal forest runoff with mercury stable isotopes.'
6271 *Environmental Science: Process and Impacts*, 19, 1235-1248.

6272 Kersten, M., Smedes, F. (2002). 'Normalization procedures for sediment contaminants in spatial and
6273 temporal trend monitoring.' *J. Environ. Monit*., 4, 109-115.

6274 Kim, C.S., Bloom, N.S., Rytuba, J.J., Brown, Jr. G.E. (2003). 'Mercury speciation by X-ray absorption
6275 fine structure spectroscopy and sequential chemical extractions: A comparison of speciation
6276 methods.' *Environmental Science & Technology*, 37, 5102-5108.

6277 Kirk, J.L., Muir, D.C.M., Antoniades, D., Evans, M.S., Jackson, T.A., Kling, H., Lamoureux, S., Lim,
6278 D.S.S., Pienitz, R., Smol, J.P., Stewart, K., Wang, X., Yang, F. (2011). 'Climate Change and
6279 mercury accumulation in Canadian high and subarctic lakes.' *Environmental Science and*
6280 *Technology*, 45, 964-970.

6281 Kirk, J., Gleason, A. (2015). 'Tracking long-range atmospheric transport of contaminants in arctic
6282 regions using lake sediments.' In: J.M. Blais et al (eds.) *Environmental Contaminants,*
6283 *Developments in Paleoenvironmental Research*, **18**, 223-262.

6284 Korosi, J.B., Griffiths, K., Smol, J.P., Blais, J.M. (2018). 'Trends in historical mercury deposition
6285 inferred from lake sediment cores across a climate gradient in the Canadian High Artic.'
6286 *Environmental Pollution*, 241, 459-467.

6287 Le Faucheur, S., Campbell, P.G.C., Fortin, C., Slaveykova, V. (2014). 'Interactions between mercury
6288 and phytoplankton: Speciation, bioavailability and internal handling.' *Environmental Toxicology*
6289 *and Chemistry*, 33, 1211-1224.

6290 Lehnherr, I., St. Louis, V.L., Sharp, M., Gardner, A., Smol, J.P., Schiff, S.L., Muir, D.C.G., Mortimer,
6291 C.A., Michelutti, N., Tarnocai, C., St. Pierre, K.A., Emmerton, C.A., Wiklund, J.A., Köck, G.,
6292 Lamoureux, S.F., Talbot, C.H. (2018). 'The world's largest high arctic lake responds rapidly to
6293 climate warming.' *Nature Communications*, 9: 1290, 1-9.

6294 Lepak, R.F., Yin, R., Krabbenhoft, D.P., Ogorek, J.M., DeWild, J.F., Holsen, T.M., Hurley, J.P. (2015).
6295 'Use of stable isotope signatures to determine mercury sources in Great Lakes. *Environmental*
6296 *Science and Technology Letters*, 2, 335-341.

6297 Lockhart, W.L., Macdonald, R.W., Outridge P.M., Wilkinson, P., DeLaronde, J.B., Rudd, J.W.M.
6298 (2000). 'Tests of the fidelity of lake sediment core records of mercury deposition to known
6299 histories of mercury contamination.' *The Science of the Total Environment*, 260, 171-180.

6300 Loring, D.H. (1991). 'Normalization of heavy-metal data from estuarine and coastal sediments.' *ICES*
6301 *J. Mar. Sci.*, 48, 101-115.

6302 Meyers, P.A., Teranes, J.L. (2001). 'Sediment organic matter.' In: Tracking environmental change
6303 using lake sediments, volume 2, Physical and Geochemical Methods, Eds Last, W.M., Smol, J.P.
6304 Kluwer Academic publishers, The Netherlands.

6305 Michelutti, N., Wolfe, A. P., Vinebrooke, R.D., Rivard, B., Briner, J.P. (2005). 'Recent primary
6306 production increases in arctic lakes.' *Geophysical Research Letters*, 32, 1-4.

6307 Muir, D.C.G., Wang, X., Yang, F., Nguyen, N., Jackson, T.A., Evans, M.S., Douglas, M., Kock, G.,
6308 Lamoureux, S., Pienitz, R., Smol, J.P., Vincent, W.F., Dastoor, A. (2009). 'Spatial trends and
6309 historical deposition of mercury in eastern and northern Canada inferred from lake sediment cores.'
6310 *Environment Science & Technology*, 43, 4802 – 4809.

6311 Obrist, D., Kirk, J.L., Zhang, L., Sunderland, E.M., Jiskra, M., Selin, N.E. (2018). 'A review of global
6312 environmental mercury processes in response to human and natural perturbations: changes of
6313 emissions, climate, and land use.' *Ambio*, 47, 116-140.

6314 Oldfield, F., Appleby, P.G. (1984). 'Empirical testing of ^{210}Pb-dating models for lake sediments.' In:
6315 E.Y. Haworth and J.W. Lund (eds.) *Lake Sediments and Environmental History*, 93-124.

6316 Outridge, P.M., Sanei, H., Stern, G.A., Hamilton, P.B., Goodarzi, F. (2007). 'Evidence for control of
6317 mercury accumulation rates in Canadian high arctic lake sediments by variations of aquatic primary
6318 productivity.' *Environmental Science and Technology*, 41, 5259-5265.

6319 Outridge, P.M., Stern, G.A., Hamilton, P.B., Sanei, H. (2019). 'Algal scavenging of mercury in
6320 preindustrial Arctic lakes.' *Limnology and Oceanography*, 64, 1558-1571.

6321 Perry, E., Norton, S.A., Kamman, N.C., Lorey, P.M., Driscoll, C.T. (2005). 'Deconstruction of historic
6322 mercury accumulation in lake sediments, northeastern United States.' *Ecotoxicology*, 14, 85 – 99.

6323 Roberts, S., Kirk, J.L., Wiklund, J.A., Muir, D.C.G., Yang, F., Gleason, A., Lawson, G. (2019).
6324 'Mercury and metal(loid) deposition to remote Nova Scotia lakes from both local and distant
6325 sources.' *Science of the Total Environment*, 675, 192-202.

6326 Rydberg, J., Klaminder, J., Rosén, P., Bindler, R. (2010). 'Climate driven release of carbon and mercury
6327 from permafrost mires increases mercury loading into sub-arctic lakes.' *Science of the Total*
6328 *Environment*, 408, 4778-4783.

6329 Sanei, H., Outridge, P.M., Dallimore, A., Hamilton, P.B. (2012). 'Mercury-organic matter relationships
6330 in pre-pollution sediments of thermokarst lakes from the Mackenzie River Delta, Canada: the role
6331 of depositional environment.' *Biogeochemistry*, 107, 149-164.

6332 Schartup, A.T., Balcom, P.H., Soerensen, A.L., Gosnell, K.J., Calder, R.S.D., Mason, R.P., Sunderland,
6333 E.M. (2015). 'Freshwater dischargers drive high levels of methylmercury in arctic marine biota.'
6334 *PNAS*, 112, (38), 11789-11794.

6335 St. Louis, V., Graydon, J., Mitchell, C., Oswald, C. (2016). 'Mercury fate and methylation in terrestrial
6336 upland and wetland environments.' In Canada Mercury Science Assessment.

6337 Stern, G.A., Sanei, H., Roach, P., Delaronde, J., Outridge, P.M. (2009). 'Historical interrelated
6338 variations of mercury and aquatic organic matter in lake sediment cores from a subarctic lake in
6339 Yukon, Canada: Further evidence toward the algal-mercury scavenging hypothesis.'
6340 *Environmental Science and Technology*, 43, 7684-7690.

6341 St. Pierre, K.A., St. Louis, V.L., Lehnherr, I., Gardner, A.S., Serbu, J.A., Mortimer, C.A., Muir, D.C.G.,
6342 Wiklund, J.A., Lemire, D., Szostek, L., Talbot, C. (2019). 'Drivers of mercury cycling in the
6343 rapidly changing glacierized watershed of the high Arctic's largest lake by volume (Lake Hazen,
6344 Nunavut, Canada.' *Environmental Science & Technology*, **53**, 1175-1185.

6345 St. Pierre, K.A., St. Louis, V.L., Lehnherr, I., Schiff S,L., Muir, D.C.G., Poulain, A.J., Smol, J.P.,
6346 Talbot, C., Ma, M., Findlay, D.L., Findlay, W.J., Arnott, S.E., Gardner, A.S. (2019).
6347 'Contemporary limnology of the rapidly changing glacierized watershed of the world's largest
6348 High Arctic lake.' *Science Reports*, **9**: 4447, 1-15.

6349 Wiklund, J.A., Kirk, J.L., Muir, D.C.G., Evans, M., Yang, F., Keating, J., Parsons, M.T. (2017).
6350 'Anthropogenic mercury deposition in Flin Flon Manitoba and the Experimental Lakes Area
6351 Ontario (Canada): A multi-lake sediment core reconstruction.' *Science of the Total Environment*,
6352 586, 685 – 695.

6353

6354 AMAP (2011) AMAP Assessment 2011: Mercury in the Arctic. (Arctic Monitoring and Assessment
6355 Programme, Oslo).

6356 Amos HM, Jacob DJ, Kocman D, Horowitz H.M., Zhang Y, et al. (2014) Global biogeochemical
6357 implications of mercury discharges from rivers and sediment burial. Environ Sci Technol
6358 48:9514–9522.

6359 Box, J.E., Colgan, W.T., Christensen, T.R., et al., 2019. Key indicators of Arctic climate change:
6360 1971–2017. Environ. Res. Lett. 14, 045010. doi.org/10.1088/1748-9326/aafc1b.

6361 Brigham, M.E., Wentz, D.A., Aiken, G.R., and Krabbenhoft, D.P., 2009. Mercury cycling in stream
6362 ecosystems. 1. Water column chemistry and transport. Environ. Sci. Technol. 43: 2720–2725.

6363 Cossa D, Heimbürger L-E, Sonke JE, Planquette H, Lherminier P. et al (2019). Sources, cycling and
6364 transfer of mercury in the Labrador Sea (Geotraces-Geovide cruise). Marine Chemistry 198: 64-
6365 69. Doi: 10.1016/j.marchem.2017.11.006.

6366 Dastoor AP, and Durnford DA (2014). Arctic Ocean: Is it a sink or a source of atmospheric mercury?
6367 Environ. Sci. Technol. 48: 1707–1717.

6368 Domagalski J, Majewski MS, Alpers CN, Eckley CS, Eagles-Smith CA, Schenk L, and Wherry S.
6369 (2016). Comparison of mercury mass loading in streams to atmospheric deposition in watersheds
6370 of Western North America: Evidence for non-atmospheric mercury sources. Science of the Total
6371 Environment 568: 638–650.

6372 Durnford D, Dastoor A, Ryzhkov A, Poissant L, Pilote M, and Figueras-Nieto D (2012) How relevant
6373 is the deposition of mercury onto snowpacks? − Part 2: A modeling study. Atmos. Chem. Phys.
6374 12: 9251−9274. DOI: 10.5194/acp-12-9251-2012.

6375 Fisher JA, Jacob DJ, Soerensen AL, Amos HM, Steffen A, and Sunderland EM (2012) Riverine
6376 source of Arctic Ocean mercury inferred from atmospheric observations. Nature Geoscience
6377 5:499–504.

6378 Gleason, J. D., Blum, J. D., Moore, T. C., Polyak, L., Jakobsson, M., Meyers, P. A., and Biswas, A.
6379 2017. Sources and cycling of mercury in the paleo Arctic Ocean from Hg stable isotope
6380 variations in Eocene and Quaternary sediments, Geochimica et Cosmochimica Acta 197: 245-
6381 262. Doi: 10.1016/j.gca.2016.10.033.

6382 Gordon J, Quinton W, Branfireun BA, and Olefeldt D. (2016). Mercury and methylmercury
6383 biogeochemistry in a thawing permafrost wetland complex, Northwest Territories, Canada.
6384 Hydrological *Process. 30: 3627–3638. DOI: 10.1002/hyp.10911.*

6385 Holmes, R.M., J.W. McClelland, S.E. Tank, R.G.M. Spencer, and A.I. Shiklomanov. 2018. Arctic
6386 Great Rivers Observatory. Water Quality Dataset. https://www.arcticgreatrivers.org/data.

6387 Kirk JL, Lehnherr I, Andersson M, Braune BM, Chan L, Dastoor AP, et al. (2012) Mercury in Arctic
6388 marine ecosystems: source, pathways, and exposure. Environ. Res. 119: 64−87. Doi:
6389 10.1016/j.envres.2012.08.012.

6390 Lim AG, Jiskra M, Soenke JE, Loiko SV, Kosykh N, and Pokrovsky OS. (2020). A revised northern
6391 soil Hg pool, based on western Siberia permafrost peat Hg and carbon observations.
6392 Biogeosciences (in press).

6393 Masbou, J., Sonke, J. E., Amouroux, D., Guillou, G., Becker, P. R., and Point, D. 2018. Hg-Stable
6394 Isotope Variations in Marine Top Predators of the Western Arctic Ocean. ACS Earth and Space
6395 Chemistry 2: 479-490. Doi: 10.1021/acsearthspacechem.8b00017.

6396 Mu, C.C., Zhang, F., Chen, X., Ge, S.M., Mu, M., Jia, L., Wu, Q.B., Zhang, T.J. 2019. Carbon and
6397 mercury export from the Arctic rivers and response to permafrost degradation. Water Research
6398 161: 54-60.

6399 Olson, C., Jiskra, M., Biester, H., Chow, J., and Obrist, D. (2018). Mercury in active-layer tundra soils
6400 of Alaska: concentrations, pools, origins, and spatial distribution. Global Biogeochemical Cycles
6401 32: 1058-1073. Doi: 10.1029/2017GB005840.

6402 Outridge PM, Macdonald RW, Wang F, Stern GA, and Dastoor AP (2008) A mass balance inventory
6403 of mercury in the Arctic Ocean. Environ Chem 5: 1–23.

6404 Schuster, P.F., Schaefer, K.M., Aiken, G.R., Antweiler, R.C., Dewild, J.F., Gryziec, J.D., Gusmeroli,
6405 A., Hugelius, G., Jafarov, E., Krabbenhoft, D.P., Liu, L., Herman- Mercer, N., Mu, C., Roth,
6406 D.A., Schaefer, T., Striegl, R.G., Wickland, K.P., Zhang, T. 2018. Permafrost stores a globally
6407 significant amount of mercury. Geophys. Res. Lett. 45: 1463-1471.

6408 Schuster, P.F., Striegl, R.G., Aiken, G.R., Krabbenhoft, D.P., Dewild, J.F., Butler, K., Kamark, B.,
6409 Dornblaser, M. 2011. Mercury export from the Yukon River Basin and potential response to a
6410 changing climate. Environ. Sci. Technol. 45: 9262-9267.

6411 Serreze M C, Barrett A P, Slater A G, Woodgate R A, Aagaard K, Lammers R B, Steele M, Moritz R,
6412 Meredith M and Lee C M. 2006. The large-scale freshwater cycle of the Arctic. Journal of
6413 Geophysical Research-Oceans 111.

6414 Soerensen AL, Jacob DJ, Schartup AT, Fisher JA, Lehnherr I, et al. (2016) A mass budget for
6415 mercury and methylmercury in the Arctic Ocean. Global Biogeochem Cycles 30: 560–575. Doi:
6416 10.1002/2015GB005280

6417 Sonke JE, Teisserenc R, Heimbürger-Boavida L-E, Petrova MV, Marusczak N, et al. (2018) Eurasian
6418 river spring flood observations support net Arctic Ocean mercury export to the atmosphere and
6419 Atlantic Ocean. Proc. Natl. Acad. Sci. 115: E11586–E11594. Doi: 10.1073/pnas.1811957115.

6420 Stein R, and Macdonald RW. 2004. *The Organic Carbon Cycle in the Arctic Ocean.* Springer
6421 Publishing, Berlin.

6422 Walvoord, M.A. and Striegl, R.G. 2007. Increased groundwater to stream discharge from permafrost
6423 thawing in the Yukon River basin: Potential impacts on lateral export of carbon and nitrogen.
6424 Geophys. Res. Lett. 34. L12402. doi.org/10.1029/2007GL030216

6425 Zhang Y, Jacob DJ, S. Dutkiewicz S, Amos HM, and Sunderland EM (2015) Biogeochemical drivers
6426 of the fate of riverine mercury discharged to the global and Arctic oceans. Global Biogeochem
6427 Cycles 29: 854–864.

6428

6429 Couture, N.J., Irrgang, A., Pollard, W., Lantuit, H., and Fritz, M. (2018). Coastal erosion of
6430 permafrost soils along the Yukon coastal plain and fluxes of organic carbon to the Canadian
6431 Beaufort Sea. Journal of Geophysical Research: Biogeosciences 123. Doi:
6432 10.1002/2017JG004166.

6433 Fisher, J.A., Jacob, D.J., Soerensen, A.L., Amos, H.M., Steffen, A., and Sunderland, E.M. (2012).
6434 Riverine source of Arctic Ocean mercury inferred from atmospheric observations. Nature
6435 Geoscience 5: 499–504.

6436 Gibbs, A.E., Ohman, K.A., and Richmond, B.M. (2015). National assessment of shoreline change—A
6437 GIS compilation of vector shorelines and associated shoreline change data for the north coast of
6438 Alaska, U.S.-Canadian border to Icy Cape. U.S. Geological Survey Open-File Report 2015-1030,
6439 Doi: 10.3133/ofr20151030.

6440 Günther, F., Overduin, P.P., Sandakov, A.V., Grosse, G., and Grigoriev, M.N. (2013). Short- and
6441 long-term thermo-erosion of ice-rich permafrost coasts in the Laptev Sea region. Biogeosciences
6442 10: 4297–4318. Doi: 10.5194/bg-10-4297-2013.

6443 Hill, P.R., Blasco, S.M., Harper, J.R., and Fissel, D.B. (1991). Sedimentation on the Beaufort Sea
6444 Shelf. Continental Sea Research 11: 821-842.

6445 Hossain, M.F, Chen, W., and Zhang, Y. (2015) Bulk density of mineral and organic soils in the
6446 Canada's arctic and sub-arctic. Information Processing in Agriculture 2: 183-190. Doi:
6447 10.1016/j.inpa.2015.09.001.

6448 Irrgang, A.M., Lantuit, H., Manson, G.K., Günther, F., Grosse, G., and Overduin, P.P. (2018).
6449 Variability in rates of coastal change along the Yukon coast, 1951 to 2015. Journal of
6450 Geophysical Research: Earth Surface 123: 779-800. Doi: 10.1002/2017JF004326.

6451 Jones, B.M., Arp, C.D., Jorgenson, M.T., Hinkel, K.M., Schmutz, J.A., and Flint, P.L. (2009).
6452 Increase in the rate and uniformity of coastline erosion in Arctic Alaska. Geophysical Research
6453 Letters 36: L03503. Doi: 10.1029/2008GL036205.

6454 Lantuit, H., Overduin, P., Couture, N., Wetterich, S., Aré, F., Atkinson, D., et al. (2012). The Arctic
6455 coastal dynamics database: A new classification scheme and statistics on Arctic permafrost
6456 coastlines. Estuaries and Coasts 35: 383–400. Doi: 10.1007/s12237-010-9362-6.

6457 Leitch, D.R. (2006). Mercury Distribution in Water and Permafrost of the Lower Mackenzie Basin,
6458 Their Contribution to the Mercury Contamination in the Beaufort Sea Marine Ecosystem, and
6459 Potential Effects of Climate Variation. Master of Science thesis, Univ. of Manitoba, Winnipeg.

6460 Lim AG, Jiskra M, Soenke JE, Loiko SV, Kosykh N, and Pokrovsky OS. (2020). A revised northern
6461 soil Hg pool, based on western Siberia permafrost peat Hg and carbon observations.
6462 Biogeosciences (in press).

6463 O'Connor, D., Hou, D., Ok, Y.S., Mulder, J., Duan, L., Wu, Q., Wang, S., Tack, F.M.G., and
6464 Rinklebe J. (2019) Mercury speciation, transformation, and transportation in soils, atmospheric
6465 flux, and implications for risk management: A critical review. Environment International 126:
6466 747–761. Doi: 10.1016/j.envint.2019.03.019.

6467 Olson, C., Jiskra, M., Biester, H., Chow, J., and Obrist, D. (2018). Mercury in active-layer tundra soils
6468 of Alaska: concentrations, pools, origins, and spatial distribution. Global Biogeochemical Cycles
6469 32: 1058-1073. Doi: 10.1029/2017GB005840.

6470 Outridge, P.M., Macdonald, R.W., Wang, F., Stern, G.A., and Dastoor, A.P. (2008). A mass balance
6471 inventory of mercury in the Arctic Ocean. Environment and Chemistry 5: 89–111. Doi:
6472 10.1071/EN08002.

6473 Outridge PM, and Sanei H (2010). Does organic matter degradation affect the reconstruction of pre-
6474 industrial atmospheric mercury deposition rates from peat cores? — A test of the hypothesis
6475 using a permafrost peat deposit in northern Canada. International Journal of Coal Geology 83:
6476 73–81. doi:10.1016/j.coal.2010.04.004.

6477 Overduin, P.P., Strzelecki, M.C., Grigoriev, M.N., Couture, N., Lantuit, H., St-Hilare-Gravel, D.,
6478 Günther F., and Wetterrich, S. (2014). Coastal change in the Arctic. In: Martini, I. P. and
6479 Wanless, H. R. (eds) Sedimentary Coastal Zones from High to Low Latitudes: Similarities and
6480 Differences. Geological Society, London, Special Publication 388. Doi: 10.1144/SP388.13.

6481 Rachold, V., Eicken, H., Gordeev, V.V., Grigoriev, H., Hubberten, H.-W., Lisitzin, A.P. et al. (2004).
6482 Modern terrigeneous organic carbon input to the Arctic Ocean. In: R. Stein and R. W. Macdonald
6483 (eds), The Organic Carbon Cycle in the Arctic Ocean, pp. 33–55, Springer, Berlin.

6484 Schuster, P.F., Schaefer, K.M., Aiken, G.R., Antweiler, R.C., Dewild, J.F., Gryziec, J.D., et al.
6485 (2018). Permafrost stores a globally significant amount of mercury. Geophysical Research
6486 Letters *45*: 1463–1471. Doi: 10.1002/2017GL075571

6487 Soerensen, A.L., Jacob, D.J., Schartup, A.T., Fisher, J.A., Lehnherr, I., St. Louis, V.L., Heimbürger,
6488 L.-E., Sonke, J.E., Krabbenhoft, D.P., and Sunderland, E.M. (2016). A mass budget for mercury
6489 and methylmercury in the Arctic Ocean. Global Biogeochemical Cycles 30: 560–575. Doi:
6490 10.1002/2015GB005280.

6491 St Pierre, K.A., St Louis, V.L., Kirk, J.L., Lehnherr, I., Wang, S., and La Farge, C. (2015).
6492 Importance of open marine waters to the enrichment of total Mercury and monomethylmercury
6493 in lichens in the Canadian High Arctic. Environmental Science & Technology 49: 5930−5938.

6494 Zhang Y, Jacob DJ, Dutiewicz S, Amos HM, Long MS, and Sunderland EM. (2015) Biogeochemical
6495 drivers of the fate of riverine mercury discharged to the global and Arctic oceans. Global
6496 Biogeochemical Cycles 29: 854–864. doi:10.1002/2015GB005124.

6497

6498 Burke, S. M.; Zimmerman, C. E.; Branfireun, B. A.; Koch, J. C.; Swanson, H. K., Patterns and
6499 controls of mercury accumulation in sediments from three thermokarst lakes on the Arctic
6500 Coastal Plain of Alaska. *Aquatic Sciences* **2018,** *80*, (1). doi:10.1007/s00027-017-0553-0

6501 Deison, R.; Smol, J. P.; Kokelj, S. V.; Pisaric, M. F. J.; Kimpe, L. E.; Poulain, A. J.; Sanei, H.;
6502 Thienpont, J. R.; Blais, J. M., Spatial and Temporal Assessment of Mercury and Organic Matter
6503 in Thermokarst Affected Lakes of the Mackenzie Delta Uplands, NT, Canada. Environ. Sci.
6504 Technol. 2012, 46, (16), 8748-8755.

6505 Emmerton, C. A.; Graydon, J. A.; Gareis, J. A. L.; St. Louis, V. L.; Lesack, L. F. W.; Banack, J. K.
6506 A.; Hicks, F.; Nafziger, J., Mercury Export to the Arctic Ocean from the Mackenzie River,
6507 Canada. *Environmental Science & Technology* **2013,** *47*, (14), 7644-7654.

6508 Godin, E.; Fortier, D.; Coulombe, S., Effects of thermo-erosion gullying on hydrologic flow networks,
6509 discharge and soil loss. *Environmental Research Letters* **2014,** *9*, (10), 105010.

6510 Gordon, J.; Quinton, W.; Branfireun, B. A.; Olefeldt, D., Mercury and methylmercury
6511 biogeochemistry in a thawing permafrost wetland complex, Northwest Territories, Canada.
6512 *Hydrological Processes* **2016,** *30*, (20), 3627-3638.

6513 Jorgenson, M. T.; Shur, Y., Evolution of lakes and basins in northern Alaska and discussion of the
6514 thaw lake cycle. *Journal of Geophysical Research: Earth Surface* **2007,** *112*, (F2), F02S17.

6515 Lim, A. G.; Sonke, J. E.; Krickov, I. V.; Manasypov, R. M.; Loiko, S. V.; Pokrovsky, O. S., Enhanced
6516 particulate Hg export at the permafrost boundary, western Siberia. *Environmental Pollution*
6517 **2019,** *254*, 113083.

6518 Olefeldt, D.; Goswami, S.; Grosse, G.; Hayes, D.; Hugelius, G.; Kuhry, P.; McGuire, A. D.;
6519 Romanovsky, V. E.; Sannel, A. B. K.; Schuur, E. A. G.; Turetsky, M. R., Circumpolar
6520 distribution and carbon storage of thermokarst landscapes. *Nature Communications* **2016,** *7*,
6521 13043.

6522 MacMillan, G. A.; Girard, C.; Chételat, J.; Laurion, I.; Amyot, M., High Methylmercury in Arctic and
6523 Subarctic Ponds is Related to Nutrient Levels in the Warming Eastern Canadian Arctic.
6524 *Environmental Science and Technology* **2015,** *49*, (13), 7743-7753.

6525 Northern Contaminants Program Secretariat, Canadian Arctic Contaminants Assessment Report III:
6526 Mercury in Canada's North. Aboriginal Affairs and Northern Development Canada, Ed. **2012**;
6527 307 pp.

6528 Schuster, P. F.; Striegl, R. G.; Aiken, G. R.; Krabbenhoft, D. P.; Dewild, J. F.; Butler, K.; Kamark, B.;
6529 Dornblaser, M., Mercury Export from the Yukon River Basin and Potential Response to a
6530 Changing Climate. *Environ. Sci. Technol.* **2011,** *45*, (21), 9262-9267.

6531 Schuster, P. F.; Schaefer, K. M.; Aiken, G. R.; Antweiler, R. C.; Dewild, J. F.; Gryziec, J. D.;
6532 Gusmeroli, A.; Hugelius, G.; Jafarov, E.; Krabbenhoft, D. P.; Liu, L.; Herman-Mercer, N.; Mu,
6533 C.; Roth, D. A.; Schaefer, T.; Striegl, R. G.; Wickland, K. P.; Zhang, T., Permafrost Stores a
6534 Globally Significant Amount of Mercury. *Geophysical Research Letters* **2018,** *45*, (3), 1463-
6535 1471.

6536 Sonke, J. E.; Teisserenc, R.; Heimbürger-Boavida, L.-E.; Petrova, M. V.; Marusczak, N.; Le Dantec,
6537 T.; Chupakov, A. V.; Li, C.; Thackray, C. P.; Sunderland, E. M.; Tananaev, N.; Pokrovsky, O.
6538 S., Eurasian river spring flood observations support net Arctic Ocean mercury export to the
6539 atmosphere and Atlantic Ocean. *Proceedings of the National Academy of Sciences* **2018,** *115*,
6540 (50), E11586.

6541 St Pierre, K. A.; Zolkos, S.; Shakil, S.; Tank, S. E.; St Louis, V. L.; Kokelj, S. V., Unprecedented
6542 Increases in Total and Methyl Mercury Concentrations Downstream of Retrogressive Thaw
6543 Slumps in the Western Canadian Arctic. *Environmental Science and Technology* **2018,** *52*, (24),
6544 14099-14109.

6545 Vonk, J. E.; Tank, S. E.; Bowden, W. B.; Laurion, I.; Vincent, W. F.; Alekseychik, P.; Amyot, M.;
6546 Billet, M. F.; Canário, J.; Cory, R. M.; Deshpande, B. N.; Helbig, M.; Jammet, M.; Karlsson, J.;
6547 Larouche, J.; MacMillan, G.; Rautio, M.; Walter Anthony, K. M.; Wickland, K. P., Reviews and
6548 syntheses: Effects of permafrost thaw on Arctic aquatic ecosystems. *Biogeosciences* **2015,** *12*,
6549 (23), 7129-7167.

6550 Lim, A. G., Jiskra, M., Sonke, J. E., Loiko, S. V., Kosykh, N., and Pokrovsky, O. S.: A revised
6551 northern soil Hg pool, based on western Siberia permafrost peat Hg and carbon observations,
6552 *Biogeosciences Discussions*, https://doi.org/10.5194/bg-2019-483, in review, 2020.

6553 Pope et al. in review at *Environmental Science and Technology*. [Cape Bounty, NU Hg fluxes]

6554

6555 Agather AM, Bowman KL, Lamborg CH, and Hammerschmidt CR (2019). Distribution of mercury
6556 species in the Western Arctic Ocean (U.S. GEOTRACES GN01). Marine Chemistry 216:
6557 103686. Doi: 10.1016/j.marchem.2019.103686.

6558 Carmack EC, Yamamoto-Kawai M, Haine TWN, Bacon S, Bluhm BA, Lique C, et al (2016).
6559 Freshwater and its role in the Arctic marine system: sources, disposition, storage, export, and
6560 physical and biogeochemical consequences in the Arctic and global oceans. J. Geophys. Res.
6561 Biogeosci. 121: 675–717. Doi:10.1002/2015JG003140.

6562 Cossa D, Heimbürger L-E, Pérez FF, García-Ibáñez MI, Sonke JE, et al (2018). Mercury distribution
6563 and transport in the North Atlantic Ocean along the GEOTRACES-GA01 transect.
6564 Biogeosciences 15: 2309–2323. Doi: 10.5194/bg-15-2309-2018

6565 Cossa D, Heimbürger L-E, Sonke JE, Planquette H, Lherminier P. et al (2019). Sources, cycling and
6566 transfer of mercury in the Labrador Sea (Geotraces-Geovide cruise). Marine Chemistry 198: 64-
6567 69. Doi: 10.1016/j.marchem.2017.11.006.

6568 Roach AT, Aagaard K, Pease CH, Salo SA, Weingartner T, Pavlov V, and Kulakov M. (1995). Direct
6569 measurements of transport and water properties through the Bering Strait. J. Geophys. Res. 100:
6570 18443. Doi:10.1029/95JC01673.

6571 Haine TWN, Curry B, Gerdes R, Hansen E, Karcher M, Lee C, et al. (2015) Arctic freshwater export:
6572 Status, mechanisms, and prospects. Global Planet. Change 125: 13–35.
6573 Doi:10.1016/j.gloplacha.2014.11.013.

6574 Heimbürger, L. E., J. Sonke, D. Cossa, D. Point, C. Lagane, L. Laffont, B. Galfond, M. Nicolaus, B.
6575 Rabe, and M. M. Rutgers van der Loeff (2015). Shallow methylmercury production in the
6576 marginal sea ice zone of the central Arctic Ocean. Sci. Rep., 5, doi:10.1038/srep10318

6577 Lehnherr L, St. Louis V, Hintelmann H, and Kirk JL. 2011. Methylation of inorganic mercury in polar
6578 marine waters. Nature Geoscience DOI: 10.1038/NGEO1134.

6579 Østerhus S, Woodgate R, Valdimarsson H, Turrell B, de Steur L, Quadfasel D, et al. (2019). Arctic
6580 Mediterranean exchanges: a consistent volume budget and trends in transports from two decades
6581 of observations. Ocean Sci. 15: 379–399. Doi: 10.5194/os-15-379-2019.

6582 Outridge PM, Macdonald RW, Wang F, Stern GA, and Dastoor AP (2008). A mass balance inventory
6583 of mercury in the Arctic Ocean. Environ. Chem. 5: 89–111.

6584 Peralta-Ferriz C, and Woodgate RA. (2017). The dominant role of the East Siberian Sea in driving the
6585 oceanic flow through the Bering Strait — Conclusions from GRACE Ocean Mass Satellite data
6586 and in situ mooring observations between 2002 and 2016. Geophysical Research Letters 44:
6587 11472–11481. Doi: 10.1002/2017GL075179.

6588 Rachold, V., H. Eicken, V. V. Gordeev, H. Grigoriev, H.-W. Hubberten, A. P. Lisitzin, L.
6589 Shevchenko, and L. Schirmeister (2004). Modern terrigeneous organic carbon input to the Arctic
6590 Ocean, in The Organic Carbon Cycle in the Arctic Ocean, edited by R. Stein and R. W.
6591 Macdonald, Springer, Berlin. pp. 33–55.

6592 Soerensen, A. L., Jacob, D. J., Schartup, A. T., Fisher, J. A., Lehnherr, I., et al (2016). A mass budget
6593 for mercury and methylmercury in the Arctic Ocean. Global Biogeochem. Cycl. 30: 560–575.
6594 Doi: 10.1002/2015GB005280.

6595 Torres-Valdés S, Tsubouchi T, Bacon S, Naveira-Garabato AC, Sanders R, et al (2013). Export of
6596 nutrients from the Arctic Ocean. Journal of Geophysical Research: Oceans, 118, 1625–1644.
6597 Doi: 10.1002/jgrc.20063.

6598 Tsubouchi **T,** Bacon S, **Aksenov Y,** Naveira Garabato AC, Beszczynska-Möller A. (2018). The Arctic
6599 Ocean seasonal cycles of heat and freshwater fluxes: observation-based inverse
6600 estimates. *Journal of Physical Oceanography.* Doi: 10.1175/JPO-D-17-0239.1.

6601 Wang F, Macdonald RW, Armstrong DA, Stern GA. (2012). Total and methylated mercury in the
6602 Beaufort Sea: the role of local and recent organic remineralization. Environ. Sci. Technol. 46:
6603 11821−11828. Doi: 10.1021/es302882d.

6604 Wang K, Munson KM, Beaupré-Laperrière A, Mucci A, Macdonald RW, and Wang F. 2018.
6605 Subsurface seawater methylmercury maximum explains biotic mercury concentrations in the
6606 Canadian Arctic. Scientific Reports 8:14465. Doi:10.1038/s41598-018-32760-0.

6607 Woodgate RA, Weingartner TJ, and Lindsay, RW (2010). The 2007 Bering Strait oceanic heat flux
6608 and anomalous Arctic sea-ice retreat. Geophysical Research Letters 37: L01602. Doi:
6609 10.1029/2009GL041621.

6610 Woodgate RA (2018). Increases in the Pacific inflow to the Arctic from 1990 to 2015, and insights
6611 into seasonal trends and driving mechanisms from year-round Bering Strait mooring data. Prog.
6612 Oceanogr. 160: 124–154. Doi: 10.1016/j.pocean.2017.12.007, 2018.

Canario, J., L. Poissant, M. Pilote, C. Blaise, P. Constant, J.-F. Ferard, and F. Gagne (2013), Toxicity survey of Canadian Arctic marine sediments. J. Soils Sediments, 14, 196–203, doi:10.1007/s11368-013-0792-1.

Fox, A. L., E. A. Hughes, R. P. Trocine, J. H. Trefry, S. V. Schonberg, N. D. McTigue, B. K. Lasorsa, B. Konar, and L. W. Cooper (2013). Mercury in the northeastern Chukchi Sea: Distribution patterns in seawater and sediments and biomagnification in the benthic food web. Deep Sea Res. Part II, doi:10.1016/j.dsr2.2013.07.012.

Gamboa, A., J.-C. Montero-Serrano, G. St-Onge, A. Rochon, and P.-A. Desiage (2017). Mineralogical, geochemical, and magnetic signatures of surface sediments from the Canadian Beaufort Shelf and Amundsen Gulf (Canadian Arctic). Geochem. Geophys. Geosyst. 18: 488–512. Doi:10.1002/2016GC006477.

Gobeil C, Macdonald RW, and Smith JN. 1999. Mercury profiles in sediments of the Arctic Ocean basins. *Environ. Sci. Technol. 33*: 4194. doi:10.1021/ES990471P.

Graydon, J. A., C. A. Emmerton, L. F. W. Lesack, and E. N. Kelly (2009). Mercury in the Mackenzie River delta and estuary: Concentrations and fluxes during open-water conditions. Sci. Total Environ. 407: 2980–2988.

Hollweg, T. A., C. C. Gilmour, and R. P. Mason (2010). Mercury and methylmercury cycling in sediments of the mid-Atlantic continental shelf and slope. Limnol. Oceanogr. 55: 2703–2722.

Schartup, A. T., U. C. Ndu, P. H. Balcom, R. P.Mason, and E.M. Sunderland (2015). Contrasting effects of marine and terrestrially derived dissolved organic matter on mercury speciation and bioavailability in seawater. Environ. Sci. Technol. 49: 5965–5972. Doi:10.1021/es506274x.

Sunderland, E. M., F. A. P. C. Gobas, B. A. Branfireun, and A. Heyes (2006). Environmental controls on the speciation and distribution of mercury in coastal sediments. Mar. Chem. 102: 111–123. Doi:10.1016/J.Marchem.2005.09.019.

Holmes, R. M., J. W. McClelland, B. J. Peterson, I. A. Shiklomanov, A. I. Shiklomanov, A. V. Zhulidov, V. V. Gordeev, and N. N. Bobrovitskaya (2002). A circumpolar perspective on fluvial sediment flux to the Arctic Ocean. Global Biogeochem. Cycles 16: 1098. Doi:10.1029/2001GB001849,

Macdonald RW and Thomas DJ. 1991. Chemical interactions and sediments of the western Canadian Arctic Shelf. *Cont. Shelf Res.11*, 843. Doi:10.1016/0278-4343(91)90082-H.

Outridge PM, Macdonald RW, Wang F, Stern GA, and Dastoor AP (2008). A mass balance inventory of mercury in the Arctic Ocean. Environ. Chem. 5: 89–111.

Pucko, M., A. Burt, W. Walkusz, F. Wang, R. W. Macdonald, S. Rysgaard, D. G. Barber, J. E. Tremblay, and G. A. Stern (2014). Transformation of mercury at the bottom of the Arctic food web: An overlooked puzzle in the mercury exposure narrative. Environ. Sci. Technol. 48: 7280–7288. doi:10.1021/es404851b.

Rachold, V., H. Eicken, V. V. Gordeev, H. Grigoriev, H.-W. Hubberten, A. P. Lisitzin, L. Shevchenko, and L. Schirmeister (2004). Modern Terrigeneous Organic Carbon Input to the Arctic Ocean, in *The Organic Carbon Cycle in the Arctic Ocean*, edited by R. Stein and R. W. Macdonald, pp. 33-55. Springer, Berlin, Heidelberg.

Soerensen, A. L., Jacob, D. J., Schartup, A. T., Fisher, J. A., Lehnherr, I., et al (2016). A mass budget for mercury and methylmercury in the Arctic Ocean. Global Biogeochem. Cycl. 30: 560–575. Doi: 10.1002/2015GB005280.

Bełdowski, J., Miotk, M., Zaborska, A., Pempkowiak, J. (2015) Distribution of sedimentary mercury off Svalbard, European Arctic. Chemosphere 122, 190-198.

6660 Chesnokova, A., Baraër, M., LaperrièreRobillard, T. and Huh, K. (2020). Linking mountain glacier
6661 retreat and hydrological changes in southwestern Yukon. Water Resources Research, 56,
6662 e2019WR025706.

6663 Christianson, K., Kohler, J., Alley, R.B., Nuth, C. and Van Pelt, W.J.J. (2015) Dynamic perennial firn
6664 aquifer on an Arctic glacier. Geophysical Research Letters, 42 (5), 1418-1426.

6665 Cossa, D., Heimbürger, L.E., Sonke, J.E., Planquette, H., Lherminier, P., García-Ibáñez, M.I., Pérez,
6666 F.F. and Sarthou, G. (2018) Sources, cycling and transfer of mercury in the Labrador Sea
6667 (GEOTRACESGEOVIDE cruise). Marine Chemistry 198, 64–69.

6668 Cook, J., Edwards, A., Takeuchi, N. and Irvine-Fynn, T. (2016) Cryoconite: The dark biological secret
6669 of the cryosphere. Progress in Physical Geography, 40(1), 66–111.

6670 Delaney, I., Bauder, A., Werder, M.A. and Farinotti, D. (2018) Regional and annual variability in
6671 subglacial sediment transport by water for two glaciers in the Swiss Alps. Frontiers in Earth
6672 Sciences 6,175.

6673 Friske, P.W.B., McCurdy, M.W., Day, S.J., Gross, H., Lynch, J.J., Balma, R.G. and Durham, C.C.
6674 (1994). Regional stream sediment and water geochemical reconnaissance data, southwestern
6675 Yukon (parts of NTS 115A and 115B). Geological Survey of Canada, Open File 2859.

6676 Halm, D.R., and Dornblaser, M.M. (2007) Water and sediment quality in the Yukon River and its
6677 tributaries between Atlin, British Columbia, Canada, and Eagle, Alaska, USA, 2004: U.S.
6678 Geological Survey Open-File Report 2007-1197, 120 p.

6679 Hood, E,. Battin, T.J., Fellman, J., O'Neel. S. and Spencer, R.G. (2015) Storage and release of organic
6680 carbon from glaciers and ice sheets. Nature Geoscience 8, 91–96.

6681 Hood, E., Fellman, J., Spencer, R.G.M., Hernes, P.J., Edwards, R., Damore, D., Scott, D. (2009)
6682 Glaciers as a source of ancient and labile organic matter to the marine environment. Nature
6683 462,1044–1047.

6684 Graham, A.M., Aiken, G.R. and Gilmour, C.C. (2012) Dissolved organic matter enhances microbial
6685 mercury methylation under sulfidic conditions. Environmental Science and Technology, 46, 5,
6686 2715-2723.

6687 Kristmannsdóttir, H., Björnsson, A., Pálsson, S. and Sveinbjörnsdóttir, A.E. (1999) The impact of the
6688 1996 subglacial volcanic eruption in Vatnajökull on the river Jökulsá á Fjöllum, North Iceland.
6689 Journal of Volcanology and Geothermal Research 92, 359–372.

6690 Liu, Y, Chai, X, Hao, Y, Gao, X, Lu, Z, Zhao, Y, Zhang, J and Cai M. (2015) Total mercury and
6691 methylmercury distributions in surface sediments from Kongsfjorden, Svalbard, Norwegian
6692 Arctic. Environmental Science and Pollution Research International 22(11), 8603-10.

6693 Milner, A. M., Khamis, K., Battin, T. J., Brittain, J.E., Barrand, N.E., Füreder, L., Cauvy-Fraunié, S.,
6694 Gíslason, G.M. , Jacobseni, D., Hannaha, D.M., Hodson, A.J., Hood, E., Lencioni, V., Ólafsson,
6695 J. S. Robinson, C.T., Tranter, M., and Brown, L.E. (2017) Glacier shrinkage driving global changes
6696 in downstream systems. Proceedings of the National Academy of Sciences 114(37), 9770-9778.

6697 Mouginot, J., Rignot, E., Bjørk, A.A., van den Broeke, M., Millan, R., Morlighem, M., Brice Noël, B.,
6698 Scheuchl, B. and Wood, M. (2019) Forty-six years of Greenland Ice Sheet mass balance from 1972
6699 to 2018. Proceedings of the National Academy of Sciences 116 (19), 9239-9244.

6700 Nagorski, S. A., Engstrom, D. R., Hudson, J. P., Krabbenhoft, D. P., Hood, E., DeWild, J. F. and Aiken,
6701 G.R. (2014) Spatial distribution of mercury in southeastern Alaskan streams influenced by glaciers,
6702 wetlands, and salmon. Environmental Pollution 184, 62–72.

6703

6704 Nasr, M. and Arp, P.A. (2018) Total mercury concentrations in lake and streams sediments related to
6705 wet-area coverage and geogenic sources within upslope basins. Soil and Sediment Contamination
6706 27 (3), 221–248.

6707 Nasr N., Ogilvie J., Castonguay M., Rencz A. and Arp P. A. (2011) Total Hg concentrations in stream
6708 and lake sediments: discerning geospatial patterns and controls across Canada. Applied
6709 Geochemistry 26, 1818–1831.

6710 Overeem, I., Hudson, B. D., Syvitski, J. P. M., Mikkelsen, A. B., Hasholt, B.,van den Broeke, M. R.,
6711 Noël, B. P. Y. and Morlighem, M. (2017) Substantial export of suspended sediment to the global
6712 oceans from glacial erosion in Greenland. Nature Geoscience, 10(11), 859-863.

6713 Overeem, I. and Syvitski, J. P.M. (2008) Changing sediment supply in Arctic rivers, in: Sediment
6714 Dynamics in Changing Environments (Ed. J. Schmidt et al.), International Association of
6715 Hydrological Sciences Publication 325, 391-397.

6716 Søndergaard, J., Tamstorf, M., Elberling, B., Larsen, M. M., Mylius, M. R., Lund, M., Abermann, J.
6717 and Riget, F. (2015) Mercury exports from a High-Arctic river basin in Northeast Greenland (74
6718 degrees N) largely controlled by glacial lake outburst floods. Science of the Total Environment
6719 514, 83−91.

6720 Schartup, A.T., Balcom, P.H., Soerensen, A.L., Gosnell, K.J., Calder, R.S.D., Mason, R.P. and
6721 Sunderland, E.M. (2015) Methylmercury sources in the Arctic. Proceedings of the National
6722 Academy of Sciences 112 (38) 11789-11794.

6723 St.-Louis, V., Sharp, M., Steffen, A., May, A., Barker, J., Kirk J., Kelly, D., Arnott, S., Keatley, B. and
6724 Smol, J. (2005) Some sources and sinks of monomethyl and inorganic mercury on Ellesmere Island
6725 in the Canadian High Arctic. Environmental Science and Technology 39, 2686–2701.

6726 St. Pierre, K.A., St. Louis, V. L., Lehnherr, I., Gardner, A.S., Serbu, J.A., Mortimer, C.A., Muir, D.C.G.,
6727 Wiklund, J.A., Lemire, D., Szostek, L., and Talbot, C. (2019) Environmental Science and
6728 Technology 53 (3), 1175-1185.

6729 Vermilyea, A. W., Nagorski, S. A., Lamborg, C. H., Hood, E. W., Scott, D. and Swarr, G. J. (2017)
6730 Continuous proxy measurements reveal large mercury fluxes from glacial and forested watersheds
6731 in Alaska. Science of the Total Environment 599–600, 145–155.

6732 Wada, T., Chikita, K. A., Kim, Y. and Kudo, I. (2011) Glacial effects on discharge and sediment load
6733 in the subarctic Tanana River Basin, Alaska. Arctic, Antarctic, and Alpine Research 43(4), 632–
6734 648.

6735 Zdanowicz, C., Kruemmel, E., Lean, D., Poulain, A., Yumvihoze, E., Chen, J. and Hintelmann, H.
6736 (2013) Accumulation, storage and release of mercury in a glaciated Arctic catchment, Baffin
6737 Island. Geochimica et Cosmochimica Acta 107, 316–335.

6738 Zdanowicz, C., Karlsson, P., Beckholmen, I., Roach, P., Poulain, A., Yumvihoze, E., Martma, T.,
6739 Ryjkov, A. and Dastoor, A. (2018) Snowmelt, glacial and atmospheric sources of mercury to a
6740 subarctic mountain lake catchment, Yukon, Canada. Geochimica et Cosmochimica Acta 238,
6741 374−393.

6742 Zdanowicz, C. M., Krümmel, E. M., Poulain, A. J., Yumvihoze, E., Chen, J., Štrok, M., Scheer, M. and
6743 Hintelmann, H. (2016), Historical variations of mercury stable isotope ratios in Arctic glacier firn
6744 and ice cores, Global Biogeochemical Cycles, 30, 1324–1347.

6745 Zhang, B., Chen, T., Guo, J., Wu, M., Yang, R., Chen, X., Wu, X., Zhang, W., Kang, S., Liu, G. and
6746 Dyson, P. (2020) Microbial mercury methylation profile in terminus of a high-elevationglacier on
6747 the northern boundary of the Tibetan Plateau. Science of the Total Environment, 708,135226.

6748

6749 Bring, A., and Coauthors, 2016: Arctic terrestrial hydrology: A synthesis of processes, regional effects,
6750 and research challenges. *J. Geophys. Res. G Biogeosciences*, **121**, 621–649,
6751 doi:10.1002/2015JG003131.

6752 Charles, V., K. Tiit, S. D. A., and T. L. J., 2014: A global inventory of lakes based on high-resolution
6753 satellite imagery. *Geophys. Res. Lett.*, **41**, 6396–6402, doi:10.1002/2014GL060641.

6754 Evans, S. G., S. E. Godsey, C. R. Rushlow, and C. Voss, 2020: Water tracks enhance water flow above
6755 permafrost in upland Arctic Alaska hillslopes. *J. Geophys. Res. Earth Surf.*,
6756 doi:10.1029/2019JF005256.

6757

6758 King, T. V., B. T. Neilson, L. D. Overbeck, and D. L. Kane, 2020: A distributed analysis of lateral
6759 inflows in an Alaskan Arctic watershed underlain by continuous permafrost. *Hydrol. Process.*, **34**,
6760 633–648, doi:10.1002/hyp.13611.

6761 Langford, J. E., R. A. Schincariol, R. M. Nagare, W. L. Quinton, and A. A. Mohammed, 2019: Transient
6762 and Transition Factors in Modeling Permafrost Thaw and Groundwater Flow. *Groundwater*,
6763 gwat.12903, doi:10.1111/gwat.12903.

6764 Rey, D. M., M. Walvoord, B. Minsley, J. Rover, and K. Singha, 2019: Investigating lake-area dynamics
6765 across a permafrost-thaw spectrum using airborne electromagnetic surveys and remote sensing
6766 time-series data in Yukon Flats, Alaska. *Environ. Res. Lett.*, **14**, doi:10.1088/1748-9326/aaf06f.

6767 Rushlow, C. R., and S. E. Godsey, 2017: Rainfall-runoff responses on Arctic hillslopes underlain by
6768 continuous permafrost, North Slope, Alaska, USA. *Hydrol. Process.*, **31**, 4092–4106,
6769 doi:10.1002/hyp.11294.

6770 Selroos, J.-O., H. Cheng, P. Vidstrand, and G. Destouni, 2019: Permafrost Thaw with Thermokarst
6771 Wetland-Lake and Societal-Health Risks: Dependence on Local Soil Conditions under Large-Scale
6772 Warming. *Water*, **11**, 574, doi:10.3390/w11030574.

6773 Smith, L. C., Y. Sheng, and G. M. MacDonald, 2007: A first pan-arctic assessment of the influence of
6774 glaciation, permafrost, topography and peatlands on northern hemisphere lake distribution.
6775 *Permafr. Periglac. Process.*, **18**, 201–208, doi:10.1002/ppp.581.

6776 Song, C., G. Wang, T. Mao, J. Dai, and D. Yang, 2019: Linkage between permafrost distribution and
6777 river runoff changes across the Arctic and the Tibetan Plateau. *Sci. China Earth Sci.*,
6778 doi:10.1007/s11430-018-9383-6.

6779 Stone, L. E., X. Fang, K. M. Haynes, M. Helbig, J. W. Pomeroy, O. Sonnentag, and W. L. Quinton,
6780 2019: Modelling the effects of permafrost loss on discharge from a wetland-dominated,
6781 discontinuous permafrost basin. *Hydrol. Process.*, **33**, 2607–2626, doi:10.1002/hyp.13546.

6782 Trochim, E. D., M. T. Jorgenson, A. Prakash, and D. L. Kane, 2016: Geomorphic and biophysical
6783 factors affecting water tracks in northern Alaska. *Earth Sp. Sci.*, **3**, 123–141,
6784 doi:10.1002/2015EA000111.

6785 Walvoord, M. A., and B. L. Kurylyk, 2016: Hydrologic impacts of thawing permafrost—a review.
6786 *Vadose Zo. J.*, **15**, doi:10.2136/vzj2016.01.0010.

6787 Walvoord, M. A., C. I. Voss, B. A. Ebel, and B. J. Minsley, 2019: Development of perennial thaw zones
6788 in boreal hillslopes enhances potential mobilization of permafrost carbon. *Environ. Res. Lett.*, **14**,
6789 doi:10.1088/1748-9326/aaf0cc.

6790 Young-Robertson, J. M., N. Raz-Yaseef, L. R. Cohen, B. Newman, T. Rahn, V. Sloan, C. Wilson, and
6791 S. D. Wullschleger, 2018: Evaporation dominates evapotranspiration on Alaska's Arctic Coastal
6792 Plain. *Arctic, Antarct. Alp. Res.*, **50**, e1435931, doi:10.1080/15230430.2018.1435931.

6793

6794

6795 Appelquist, H., Jensen, K.O., Sevel, T., Hammer, C. 1978. Mercury in the Greenland Ice Sheet.
6796 Nature 273, 657-659, 1978.

6797 AMAP, 1998. AMAP Assessment Report: Arctic Pollution Issues. Arctic Monitoring and Assessment
6798 Programme (AMAP), Oslo, Norway. xii+859 pp.

6799 AMAP, 2005. AMAP Assessment 2002: Heavy Metals in the Arctic. Arctic Monitoring and
6800 Assessment Programme (AMAP), Oslo, Norway. xvi + 265 pp.

6801 AMAP, 2011. AMAP Assessment 2011: Mercury in the Arctic. Arctic Monitoring and Assessment
6802 Programme (AMAP), Oslo, Norway. xiv + 193 pp.

6803 AMAP/UN Environment, 2019. Technical Background Report for the Global Mercury Assessment
6804 2018. Arctic Monitoring and Assessment Programme, Oslo, Norway/UN Environment
6805 Programme, Chemicals and Health Branch, Geneva, Switzerland. viii + 426 pp including E-
6806 Annexes.

6807 AMAP/UNEP, 2008. Technical Background Report to the Global Atmospheric Mercury Assessment.
6808 Arctic Monitoring and Assessment Programme / UNEP Chemicals Branch. 159 pp.

6809 AMAP/UNEP, 2013. Technical Background Report for the Global Mercury Assessment 2013. Arctic
6810 Monitoring and Assessment Programme, Oslo, Norway/UNEP Chemicals Branch, Geneva,
6811 Switzerland. vi + 263 pp

6812 Battye, W. and Battye, R. 2002. Development of Emissions Inventory Methods for Wildland Fire.
6813 Final Report. US-EPA 68-D-98-046, Chapel Hill, NC, USA.

6814 Boutron, C.F., Vandal, G.M., Fitzgerald, W.F. 1998. A forty year record of mercury in central
6815 Greenland snow. Geophysical Research Letters 25 (17) 3315-3318, 1998.

6816 Bullock, D., Johnson, S., 2011. Electric Generating Utility Mercury Speciation Profiles for Clean Air
6817 Mercury Rule, EPA-454/R-11-010. EPA.

6818 Chen, L., Liu, M., Fan, R., Ma, S., Xu, Z., Ren, M., He, Q., 2013. Mercury speciation and emission
6819 from municipal solid waste incinerators in the Pearl River Delta, South China. Science of The
6820 Total Environment 447, 396-402.

6821 Dastoor, A., and Durnford, D.. 2014. Arctic Ocean: Is it a sink or a source of atmospheric mercury?,
6822 Environ. Sci. Technol., 48(3), 1707–1717, 2014.

6823 Evangeliou, N., Balkanski, Y., Hao, W.M., Petkov, A., Silverstein, R.P., Corley, R., Nordgren, B.L.,
6824 Urbanski, S.P., Eckhardt, S., Stohl, A., Tunved, P., Crepinsek, S., Jefferson, A., Sharma, S.,
6825 Nojgaard, J.K., Skov, H. 2016. Wildfires in northern Eurasia affect the budget of black carbon in
6826 the Arctic – a 12 year retrospective synopsis (2002-2013). Atmos. Chem. Phys. 16, 7587-7604.
6827 2016.

6828

* This is Chapter 4 of the AMAP Mercury Assessment*

4. Changes in Arctic mercury levels – Processes affecting mercury fate and biological uptake

Description: Explaining observed trends in terms of processes; focus on processes IN the Arctic leading to mercury uptake by biota, especially the production and loss of methylmercury. Addresses the question: *What are the processes affecting mercury fate and biological uptake?*

Coordinating authors: Michelle Nerentorp (michelle.nerentorp@ivl.se), Feiyue Wang (feiyue.wang@umanitoba.ca)
Co-authors:
Data contributors:
Revisions: First Draft

Note: First authors are identified as lead authors responsible for the section/subsection; co-authors and contributors are in alphabetic order; lead authors and coauthors will evolve based on interest and contributions. Communication/questions to the coordinating author of each section.

7019 **Table of Contents**

7037
7038
7039
7040
7041

4.1 (Introduction) What is the fate of mercury entering the Artic?

Description: Introduction to the chapter

Coordinating authors: Michelle Nerentorp

Contributing authors: Michelle Nerentorp

This chapter deals with the question what happens to the mercury that has transported and deposited into the Arctic environment. Once it has deposited some of the mercury will be transformed into organic methylmercury that bioaccumulates and biomagnifies in Arctic food webs. This chapter begins with describing the transformation processes, uptake routes and driving factors of how mercury is moved from the abiotic environment into biota (Section 4.2), including describing what mercury species are important for biotic uptake (Section 4.2.1), how is mercury methylated and demethylated (Section 4.2.2), mercury uptake pathways into biota (Section 4.2.3) and seasonal driving factors (Section 4.2.4).

Recent research has shown that mercury methylation and biotic uptake varies depending on the type of environment, such as Arctic lakes and wetlands, estuaries, seawater, snow and ice (Section 4.3). How these different environments affect mercury uptake in phytoplankton and zooplankton, at the base of the food chain (Section 4.4.), are important to understand how eventually mercury ends up higher up in the food chain (Section 4.5). The sea ice environment has recently been found to play a role of mercury transformation and biotic uptake in Arctic food chains (Section 4.6). To get the full understanding of how mercury is transported and transformed within the Arctic region, the role of organic matter such as microbes and dissolved organic carbon need to be considered (Section 4.7). A summary of the new understanding of the fate of mercury entering the Arctic environment is provided in Section 4.8.

4.2 How does Hg move from the abiotic environment to biota?

***Description*:** Provide recent update on our understanding of Hg speciation and bioavailability, uptake pathways (including habitat-specific feeding or cross-ecosystem subsidies), seasonality, etc.

Coordinating author: Feiyue Wang

- Highlight: Mercury uptake by biota is determined not just by the amount of mercury emissions to the Arctic, but also by biogeochemical and ecological processes occurring in the Arctic.
- Highlight: Those process affect mercury uptake by biota by affecting the

bioavailability, methylation, uptake, bioaccumulation, and biomagnification of mercury in the ecosystems.

4.2.1 Speciation and bioavailability

***Description*:** What mercury species are relevant for bio uptake? How is bioavailability defined and how is it controlled? What factors are important? Chemical form, physical factors?

Contributing authors: Warren RL Cairns

In its strict sense, bioavailability is "the fraction of an administered dose that reaches the systemic circulation. Thus, by definition, the bioavailability of an intravenously injected chemical is 1 (or 100%)" (Johanson, 2010). In the previous assessment (AMAP, 2011), it was noted that bioavailability of Hg "includes the availability of inorganic Hg forms to microbial populations responsible for Hg methylation and the availability of methyl mercury (MeHg) in prey items to predators within foodwebs". The bioavailability of mercury from the environment is controlled by many factors such as the chemical form or speciation of the mercury ions Hg^{2+} or $MeHg^{+}$, their biochemical reactivity *in situ*, the activity of local microbial communities, and the eventual balance between the dissolved and particulate fractions of the mercury present (AMAP, 2011). A recent review (Bradley et al., 2017) noted that although many risk assessor models assume a 95-100% bioavailability/ assimilation efficiency for MeHg, studies on 25 species of fish found values that ranged from 10 to 100% for MeHg and 2 to 51% for Hg^{2+}, while in humans, 20 studies reported MeHg bioavailabilities ranging from 2 to 100% and 0.2% to 94% for Hg^{2+}. Several factors affected these results such as the Hg source and the nutrients present. For Arctic and non-Arctic populations, a potentially important factor is how the food preparation affected the bioavailability of Hg. They report a reduced bioavailability in humans for total and MeHg in fish after frying, boiling, or grilling and a reduced bioaccessibility after the assumption of coffee of 10-60%, or tea (green or black) of up to 92%.

The relatively new field of metallomics was born to study the uptake and incorporation of elements into biota and the proteome and the biotransformations that occur within organisms. In the environment the cations Hg^{2+} and $MeHg^{+}$ are bound to anions in water to form stable complexes. Mercury is also a thiophile, forming strong bonds with sulfur, especially in biota (Feldmann et al., 2018) (Wang et al., 2012), the bioaccumulation of MeHg in plants is thus driven by binding with sulfur containing proteins via the roots. To further complicate matters, it has been demonstrated that the vegetation of the Arctic tundra

can uptake Hg^0 directly from the atmosphere (Obrist et al., 2017), a phenomenon that has also been observed on the Tibetan plateau (Wang et al., 2020), where evolving vegetation after glacier retreat seems to be acting as an active "pump" drawing down Hg^0 from the atmosphere, increasing the amount of mercury sequestered in areas affected by glacier retreat in a form available to plant life.

In freshwater aquatic ecosystems, the main carrier ligand for MeHg is dissolved organic carbon (DOC) (Tsui and Finlay, 2011), where it has the double role of promoting the solubility and transport of MeHg in surface waters, and attenuating dissolved MeHg uptake by aquatic food webs by limiting transport across cell membranes. This effect also occurs in the Arctic, MeHg accumulation in benthic and planktonic food chains was found to be proportional to the MeHg:DOC ratio in surface waters (Chételat et al., 2018), to the extent that it is reported to be a strong predictor of lake sensitivity to mercury contamination. Going up the food chain, bioaccumulation factors for MeHg in Norwegian fresh water fish reduced as total organic carbon (TOC) levels increased (Braaten et al., 2018), suggesting the formation of Hg complexes in the water column that reduced the bioavailability of MeHg. Methylation of mercury in high Arctic wetland ponds was found to be negatively correlated with DOC levels by decreasing Hg^{2+} availability to methylating microorganisms (Lehnherr et al., 2012), and overall, it was found that: "MeHg concentrations in High Arctic pond waters are controlled by the production of MeHg in sediments, itself controlled by a combination of factors including methylation potential, THg concentrations in sediments, and the anaerobic microbial decomposition of organic matter, as well as photodemethylation in the water column." An 8 month incubation experiment (Yang et al., 2016) has shown MeHg production in Arctic soils can increase by > 10 fold in both organic and mineral rich soil fractions with increased temperatures. The increased availability of stored organic carbon breakdown products such as reducing sugars and ethanol was found to be fundamental in this change. They found that freshly added mercury was more easily methylated and that permafrost thawing driven by climate change could potentially enhance MeHg production by an order of magnitude. This would have a signficiant impact on mercury bioaccumulation and magnification in the Arctic food web.

Efforts have also been taken to further understand mercury speciation and availability in the snowpack. In the snow at Alert, Canada, mercury snow concentrations peak in May (Steffen et al., 2014) when atmospheric reactive gaseous mercury levels peak. Work on polar ice mimics has shown dissolved gaseous mercury can be directly oxidized to Hg^{2+} (O'Concubhair et al., 2012) in the presence of hydrogen peroxide, nitrous acid and the sulfuric acid/ O_2 couple. Using a specific bacterial *mer-lux* biosensor (Larose et al., 2011),

7145 researchers were able to determine the bioavailable fraction of newly deposited Hg to the
7146 snowpack. They report that in surface snow, bioavailable Hg mostly deposited in snowfall
7147 events in higher proportions than deposition provoked by the atmospheric mercury depletion
7148 events (AMDEs; see Chapter 3). They estimate that AMDEs potentially deposit 20 $t.y^{-1}$ of
7149 bioavailable Hg to Arctic surfaces, whereas wet and dry deposition may provide between
7150 135-225 $t.y^{-1}$.

7151 The increasing amounts of bioavailable mercury in surface waters are starting to have an
7152 effect on mercury accumulation at the bottom of Arctic marine food webs (Foster et al.,
7153 2012) with total Hg levels of up to 242 ng g^{-1} in zooplankton. Mercury uptake by sea ice
7154 algae is only limited by the amount of mercury available for uptake when spring blooms
7155 commence (Burt et al., 2013). This is important since ice algae represent 10-60% of annual
7156 primary production in the Arctic and they may become even more abundant under mild
7157 climate conditions. The authors estimate that with the replacement of multi-year sea ice with
7158 first year ice due to climate change, an extra 48 kg/yr of particle bound Hg could enter the
7159 Beaufort Sea in the coming years.

7160

7161 **4.2.2 Methylation/demethylation**

7162 ***Contributing authors:*** Warren RL Cairns

7163 Methylmercury production/destruction pathways.

7164 Methylation and demethylation of mercury is important as it determines the concentration of
7165 MeHg which is the main Hg form that biomagnifies in the aquatic food web. Although it is
7166 well known that MeHg targets the nervous system, it is only now being appreciated that
7167 MeHg is a class of compound that can cause epigenetic effects (Sharavanan et al., 2019).
7168 When MeHg crosses the placental or blood brain barrier, it has been demonstrated to "effect
7169 microRNA expression, histone modifications and DNA methylation globally as well as at
7170 the individual gene level" in exposed brain tissue (Culbreth and Aschner, 2019). These
7171 effects can also be inherited, so MeHg toxic effects can be passed to future generations, this
7172 effect will surely be compounded if those future generations are also exposed as seems to be
7173 happening in Minamata and could well be occurring in the Arctic.

7174 As noted in the previous AMAP report in 2011, the activity of sulfate and iron reducing
7175 bacteria in anoxic sediments was thought to be the main mercury methylation pathway.
7176 Since then there has been enough work to merit several reviews on the subject in the
7177 literature. A review published in 2013 (Li and Cai, 2013) reported progress in understanding

Hg methylation and demethylation in aquatic environments by focusing on the sites and pathways of methylation and demethylation, the bioavailability of Hg species and the potential shown by isotopic studies in estimating net MeHg production. They report that Hg methylation is mostly via biotic pathways with some abiotic processes occurring, with sulfate reducing bacteria (SRB) being the dominant culprit for Hg methylation in aquatic systems followed by iron reducing bacteria and methanogens. Instead, Hg demethylation is mostly a biotic process involving the same methylation bacteria in sediments, but in the water column abiotic photo demethylation is thought to be the dominant process. However, it was unclear which of the demethylation processes was dominant, with OH radicals, singlet oxygen species and MeHg complexation with DOM being implicated. By 2013, most Hg isotopic work was on the use of adding isotopically labelled Hg to systems to estimate methylation and demethylation rates, the authors noted an urgent need for analytical methods able to accurately measure the differences between ambient and spiked Hg species in these experiments. In 2017 recent advances in the study of Hg methylation in aquatic systems (Paranjape and Hall, 2017) were reviewed. The main advance between the two reviews being the identification of the hgcAB gene cluster as the genetic code that enables microbes to methylate Hg. Its identification and tracking through a wide range of environments is now crucial in determining the range of environmental conditions that can support Hg methylation and the individual species that cause it. This review also covered abiotic factors controlling mercury methylation, these factors are mostly those that effect the Hg bioavailability to methylating bacteria, such as the presence of complexing agents, as well as those affecting the activity of methylating bacteria, such as temperature, pH and redox potential.

Two reviews specifically on microbial mercury methylation were published in 2019. One concentrated on mercury methylation by anaerobic organisms (Ma et al., 2019) and reported on the kinds of organisms that can methylate Hg, what uptake pathways are there for Hg^{2+} to microbial cells, the biochemical reactions that happen in the cells and what biochemical factors regulate Hg methylation mechanisms in microorganisms. They report that once Hg has crossed the cytoplasmic membranes either via the Mer-based transport system (a series of membrane bound proteic transporters) or passive diffusion, the acetyl-coenzyme A (acetyl-CoA) pathway has been assumed to be the main biochemical mechanism for producing MeHg since the discovery of the essential role of the HgcAB proteins in Hg methylation. The other review concentrated on Hg methylation in in aquatic environments (Regnell and Watras, 2019), they confirm that the dominant source of MeHg in freshwater systems is methylation of inorganic Hg by anaerobes. The consensus is that MeHg

7213 production rates depend generally on the ability of these organisms to uptake Hg and their
7214 activity in the environment. Current evidence shows that all Hg methylating microbes
7215 possess the *hgcAB* gene pair that codes for proteins essential for MeHg production and that
7216 current knowledge shows that MeHg is released from the cells by unknown mechanisms.
7217 High MeHg production in freshwater systems is linked to high Hg bioavailability through
7218 the formation of $Hg(SH)_2$, HgS nanoparticles and Hg-thiol complexes. Instead, in the open
7219 ocean, the review reports that Hg methylation is not restricted to anoxic environments,
7220 although it mainly occurs in oxygen deficient zones. They hope that future studies will be
7221 able to explain why Me_2Hg is a significant Hg species in marine waters but not in
7222 freshwater.

7223 Biotic and abiotic degradation of MeHg in aquatic ecosystems has been reviewed (Du et al.,
7224 2019) since the methylation and demethylation of Hg is a cycle that determines net MeHg
7225 production. Microbial breakdown of MeHg is by either reductive or oxidative
7226 demethylation, unlike Hg methylation, the genes for Hg demethylation have not yet been
7227 found, some strains are able to methylate and demethylate Hg, while others can only do one
7228 or the other, the authors predict that unravelling this mystery will be the object of future
7229 study. Abiotic demethylation is either by physical or chemical degradation. Physical
7230 degradation is mostly photodegradation in surface waters by 5 main mechanisms that
7231 include direct photo-dissociation, degradation by hydroxyl radicals and direct
7232 photodissociation of MeHg-DOM complexes via intramolecular electron transfers.
7233 However, new mechanisms continue to be found and proposed. Chemical degradation is
7234 thought to be mainly by selenoamino assistant degradation, but progress is limited as few
7235 are working on this subject and it has yet to be observed outside of the laboratory.

7236 Moving towards the Arctic, progress made in understanding microbial mercury methylation
7237 in the cryosphere has been reviewed (Sharma Ghimire et al., 2019). The authors have listed
7238 the microorganisms that have been identified in the cryosphere that can methylate mercury.
7239 Figure 4.1 from this paper reports the main known cellular processes involved in mercury
7240 uptake, methylation and its toxic effect, whilst Figure 4.2 reports the main processes that a
7241 model of Hg methylation in the cryosphere should contain.

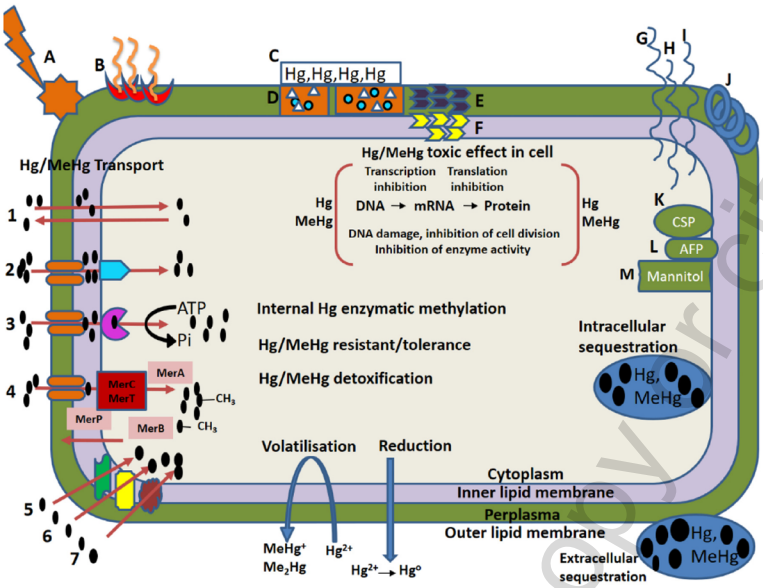

Fig. 3. Combining most probable processes involved (directly/indirectly) in mercury uptake, transport, methylation and their toxic effect in cellular organization. A. Sensor and signaling by cell when Hg is present in the environment, B. Hg binding site at cell surface, C. Hg binding in EPS surface in psychrophiles, D. Presence of EPS and biofilms on psychrophiles cell surface, E. Outer membrane Hg binding site, F. Inner membrane Hg/MeHg binding site, G. Short-chain fatty acid, H. Unsaturated fatty acid, I. Lipopolysaccharide, J. Chaerones, K. Cols shock protein, L. Antifreeze protein, M. Mannitol, 1. Passive diffusion, 2. Facilitated diffusion, 3. Active transport, 4. Mer-mediated transport, 5. P-type ATPase transport system, 6. CBA transporter, 7. CDF Transporter.

7242

7243 **Figure 4.1**. Main known cellular process involved in mercury uptake, methylation and its
7244 toxic effect (Sharma Ghimire et al., 2019) (can we ask permission for these or adapt them
7245 somehow?)

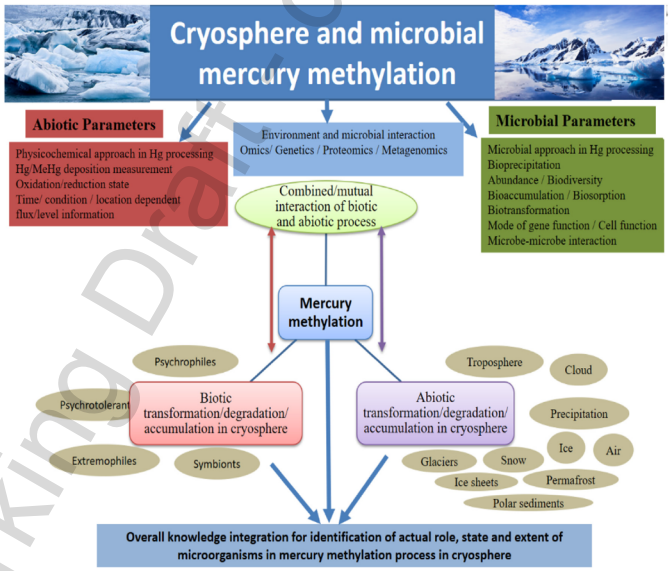

Fig. 4. The workflow of physical, chemical, genomics, proteomics, and omics approach that can contribute toward the development of a model to understand biotic and abiotic Hg methylation and microbial function in the cryosphere. Abiotic parameters: anthropogenic and atmospheric deposition measurement, oxidation/reduction state, time-dependent flux/level information, condition-dependent flux/level information, and location dependent flux/level information. Biotic parameters: measurement of bioprecipitation, cultivation, abundance, biodiversity, bioaccumulation, biosorption, biotransformation, mode of gene function, mode of Cell function, microbe-microbe interaction, genetics, proteomics, metagenomics, genome-scale ecosystem level metabolic network study, comparative and dynamic metabolic network study.

7246

7247 **Figure 4.2**. Main processes that a model of Hg methylation in the cryosphere should
7248 contain. (Sharma Ghimire et al., 2019) (can we ask permission for these or adapt them
7249 somehow?)

7250

7251 **4.2.3 Uptake pathways**

7252 (including habitat-specific feeding or cross-ecosystem subsidies)

7253 ***Contributing authors:***

7254 Transfer pathways for mercury into Arctic food webs.

7255

7256 **4.2.4 Seasonality**

7257 ***Contributing authors:***

7258 How do these processes change with season?

7259

7260 **4.3 How, when and where is Hg methylated in the Arctic?**

7261 ***Description*:** Provide recent update on our understanding of Hg methylation in
7262 lakes/wetlands, estuaries, seawater, snow and sea ice. Synthesis of Arctic GEOTRACES
7263 results on MeHg distribution in Arctic seawater.
7264 ***Coordinating author:*** Feiyue Wang
7265 ***Contributing authors:*** Sofi Jonsson

7266 Methylation and demethylation of Hg are two of the main key processes determining to
7267 what extent Hg remobilized from the environment is available for biological uptake and
7268 magnification as MeHg. Current literature does not support shared formation pathways of
7269 the two products of Hg methylation (i.e. MeHg and DMeHg). Methylation of inorganic Hg
7270 resulting in DMeHg production, was early on recognized as a primarily biotic process
7271 carried out by specific groups of e.g. sulfate and iron reducing bacteria. In 2013, Parks et al.
7272 identified two shared genes among known Hg methylators, the *hgcAB* genes, and
7273 demonstrated that these were needed for the bacterial formation of MeHg in tested bacterial
7274 strain.(Parks *et al.*, 2013) This discovery was a paradigm shift within the field and lead to
7275 the discoveries of new potential Hg methylators (REF) and novel strategies to identify novel
7276 Hg methylators (REF) as well as primary groups within a systems who can do this (ref).
7277 Utilizing existing available microbial metagenomes, Podar et al. identified high *hgcAB*
7278 abundance in thawing permafrost soils(Podar *et al.*, 2015). This is further discussed below.
7279 Methylation of Hg to MeHg is by far the most extensively studied
7280 methylation/demethylation process of Hg followed by MeHg demethylation processes
7281 whereas comparably little has been done on formation and degradation pathways of

DMeHg. Formation of DMHg has been shown previously in bacterial cultures(Baldi, Pepi and Filippelli, 1993; Sommar, Feng and Lindqvist, 1999) and associated with polarmacroalgae(Pongratz and Heumann, 1998) and marine bacteria(Pongratz and Heumann, 1999). Although these work point to synergies between the activity of organism and production of DMHg, there is today no support of it being a biological product. Baldi, et. Al.(Baldi, Pepi and Filippelli, 1993) for example suggested formation of DMeHg in bacterial cultures to be a result of an abiotic reaction between dissolved sulphide and MeHg (via the formation of bismethylmercurysulfide). Recent work has also shown abiotic formation of DMHg from MeHg when MeHg is adsorbed onto organic or inorganic surfaces containing reduced sulphur sites(Jonsson, Mazrui and Mason, 2016).

Discussion about demethylation will be added.

4.3.1 Lakes/wetlands

Contributing authors: Sofi Jonsson

A number of studies have undertaken the challenge to estimate stocks of Hg arctic soils. Schuster et. al. provided the first panarctic estimate of Hg in permafrost soils by multiplying observed Hg:SOC (median ± interquartile range = 1.6 ± 0.9 µg THg/g C) ratios identified in Alaskan soil samples with a Circum-Arctic Soil Carbon Database (CASCD)(Hugelius *et al.*, 2013, 2014; Schuster *et al.*, 2018). This resulted in estimated of 863 ± 501 Gg THg in the active layer and 793 ± 461 Gg THg in the perennially frozen substrate. Subsequent studies covering additional permafrost regions points to lower Hg:SOC ratios in other system, yet supporting substantial storage of Hg in these soils. Olson et al. measured Hg:SOC ratios ranging from 0.27 in organic soils (0 – 30 cm depth) to 0.62 µg THg/g C in mineral soils (30 – 100 cm depth) (Olson *et al.*, 2018). Lim et al (in review) further report Hg:SOC ratios of 0.13 ± 0.12 (median ± interquartile range) from peatlands in the western Siberian lowland suggested revised estimates of Hg:SOC ratios for North America and Eurasia of 0.19 and 0.77 for organic and mineral soils, respectively (Lim et al., in review, 2020). Work from sites in Fennoscandia further supports lower Hg:SOC ratios (ranging from 0.07 ± 0.07 in the peat plateau to 0.10 ± 0.06 and 0.11 ± 0.10 in the distant and collapse fens, respectively) (Tarbier et al, in prep. (S. Jonsson)). Given the large of amounts of Hg that potentially could be released from Arctic soils in a warmer climate, methylation rates in the Arctic terrestrial environment have gained more attention. Thawing of permafrost can result in the collapse of the active soil layer (soil above the frozen permafrost), generating partly wetter and more anoxic conditions that are potentially favourable for Hg methylating bacteria(Yang *et al.*, 2016). Increased Hg methylation in wetter and more anoxic conditions has

been demonstrated in temperate and tropical zones (Hsu-Kim *et al.*, 2018), whereas few studies have covered Hg methylation in zones with thawing permafrost. In previously formed thaw ponds, Lehnherr et al. measured Hg methylation rates similar to rates in already identified Hg methylation 'hot-spots'(Lehnherr *et al.*, 2012; Lehnherr, St. Louis and Kirk, 2012). High concentrations of dissolved MeHg, supposedly from either increased export of MeHg from peat soils, or in situ methylation in pond sediments, has also been shown in thaw Eastern Canadian thaw ponds (MacMillan *et al.*, 2015).

To incorporate:

Increased Hg methylation at higher temperatures has also been demonstrated in laboratory incubation experiments with permafrost soil (Yang *et al.*, 2016).

Increased concentration of MeHg in soil porewater along thaw gradients in Sweden (Fahnestock *et al.*, 2019)

Increased concentration and fraction of MeHg in thawing permafrost soils (collapsed fen) compared to permafrost soil (peat plateau) (Tarbier et al, in prep. (S. Jonsson))

Increased export and pore water concentration of MeHg in fens recently formed from permafrost thaw (Gordon *et al.*, 2016)

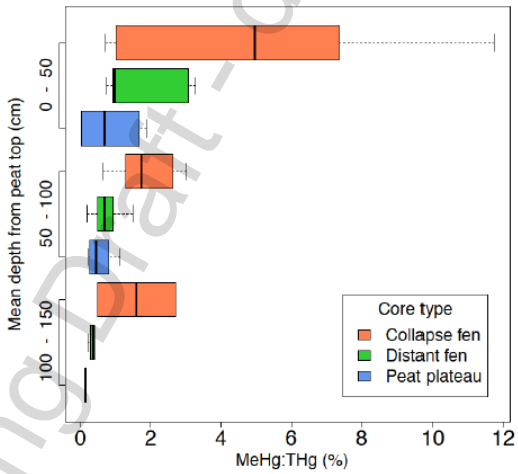

Figure 25. The range and distribution of MeHg:THg data across the five (replicate) study sites, separated by core class and grouped into three categories by the depth from peat-top, 0 – 50 cm, 50 – 100 cm, and 100 – 150 cm; outliers are not shown. The 150 – 200 cm depth category was not included because only certain peat plateau cores had depths greater than 150 cm. MeHg production is highest in the collapse fens and top portions of the cores and tends to decrease with depth across all sites.

	Core class	Min.	Max.	Mean	Median	SD	RSD (%)
MeHg (ng MeHg/g soil)	All	0.006	27.94	1.04	0.34	3.24	310.55
	Peat plateau	0.006	2.43	0.28	0.12	0.49	178
	Collapse fen	0.02	27.94	2.58	0.79	5.68	219.64
	Distant fen	0.008	2.61	0.51	0.26	0.63	122.8

4.3.2 Estuaries

Contributing authors: Sofi Jonsson

Shelf sediments

	MeHg	% MeHg	
Chukchi Sea	0.15 ± 0.07 ng/g d.w	0.43 ± 0.17	(Fox *et al.*, 2014)
Liem et al.	*Fig below*		

Figure 1. Concentrations of HgT and MeHg (ng g^{-1} d.w, average ± 1 SD)

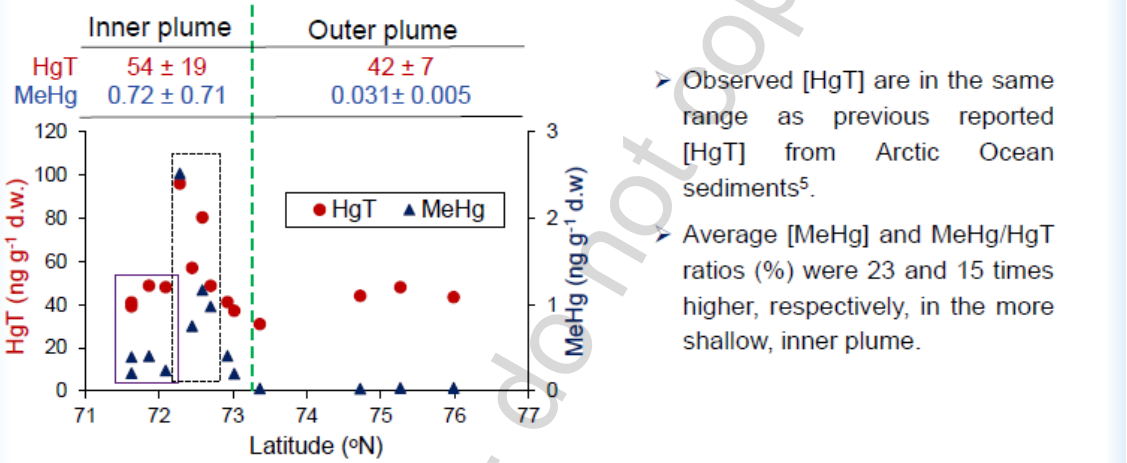

Potential figure from Liem (unpublished)

4.3.3 Seawater

Contributing authors: Feiyue Wang, Sofi Jonsson

Methylation processes in seawater. Relevant processes.

- Highlight: One of the most significant discoveries in the past 10 years is the presence of a methylmercury enrichment layer at shallow depths in Arctic seawater throughout the Arctic Ocean. This methylmercury layer readily explains a long-time mystery of why marine animals in the Western Canadian Arctic take up more mercury than those in the Eastern Canadian Arctic. The origin of this subsurface methylmercury in seawater however remains unknown.

One of the most significant discoveries since the AMAP (2011) report is the presence of a methylmercury enrichment layer at shallow depths in Arctic seawater throughout the Arctic

Ocean (Wang et al., 2012, 2018; Heimbürger et al., 2015; Agather et al., 2019). This methylmercury layer readily explains a long-time mystery of why marine animals in the Western Canadian Arctic take up more mercury than those in the Eastern Canadian Arctic (Wang et al., 2018). The origin of this subsurface methylmercury in seawater however remains unknown.

While a subsurface enrichment of MeHg in seawater has been observed in almost all major ocean basins (UNEP/AMAP 2019), including the Atlantic Ocean (Bowman et al., 2015; Bratkič et al., 2016), Pacific Ocean (Sunderland et al., 2009; Hammerschmidt and Bowman, 2012; Munson et al., 2015; Bowman et al., 2016; Kim et al., 2017), Southern Ocean (Gionfriddo et al., 2016), Mediterranean Sea (Cossa et al., 2009, 2012, 2018), Baltic Sea (Soerensen et al., 2016b) and the Black Sea (Rosati et al., 2018), what differentiates the Arctic Ocean is that the MeHg enrichment occurs at a much shallower depth (100–300 m depth) where dissolved oxygen is well above 75% of the saturation value (Wang et al., 2012, 2018) (Figure 4.3). As this subsurface MeHg maximum lies within the habitat of zooplankton and other lower trophic-level biota, it has been suggested that biological uptake of the subsurface MeHg and subsequent biomagnification explains a long-standing mystery in the Canadian Arctic on why marine animals in the western Arctic have higher mercury levels than those in the east (Wang et al., 2018).

The source of subsurface methylmercury in the Arctic Ocean and other ocean basins in the world remains a subject of debate. Most of the studies have attributed the subsurface methylmercury to in situ mercury methylation in the water column associated with organic matter remineralization (Sunderland et al., 2009; Cossa et al., 2011; Wang et al., 2012; Heimbürger et al., 2015), yet the biotic or abiotic process that responsible for the methylation remains unidentified (Bowman et al., 2019). The recent work in the Canadian Arctic (Wang et al., 2018) shows that the possibility of a shelf sediment methylmercury source with offshore transport cannot be ruled out. This is supported by three lines of evidence: 1) the spatial distribution pattern of subsurface methylmercury in relationship with distinctive water masses (Wang et al., 2018); 2) the lack of known mercury methylators in the highly oxygenated subsurface water; and 3) the problems associated with existing mercury methylation and demethylation rates that were determined using a seawater incubation approach (Wang et al., 2020). This calls for further studies on methylmercury dynamics in the Arctic and global oceans.

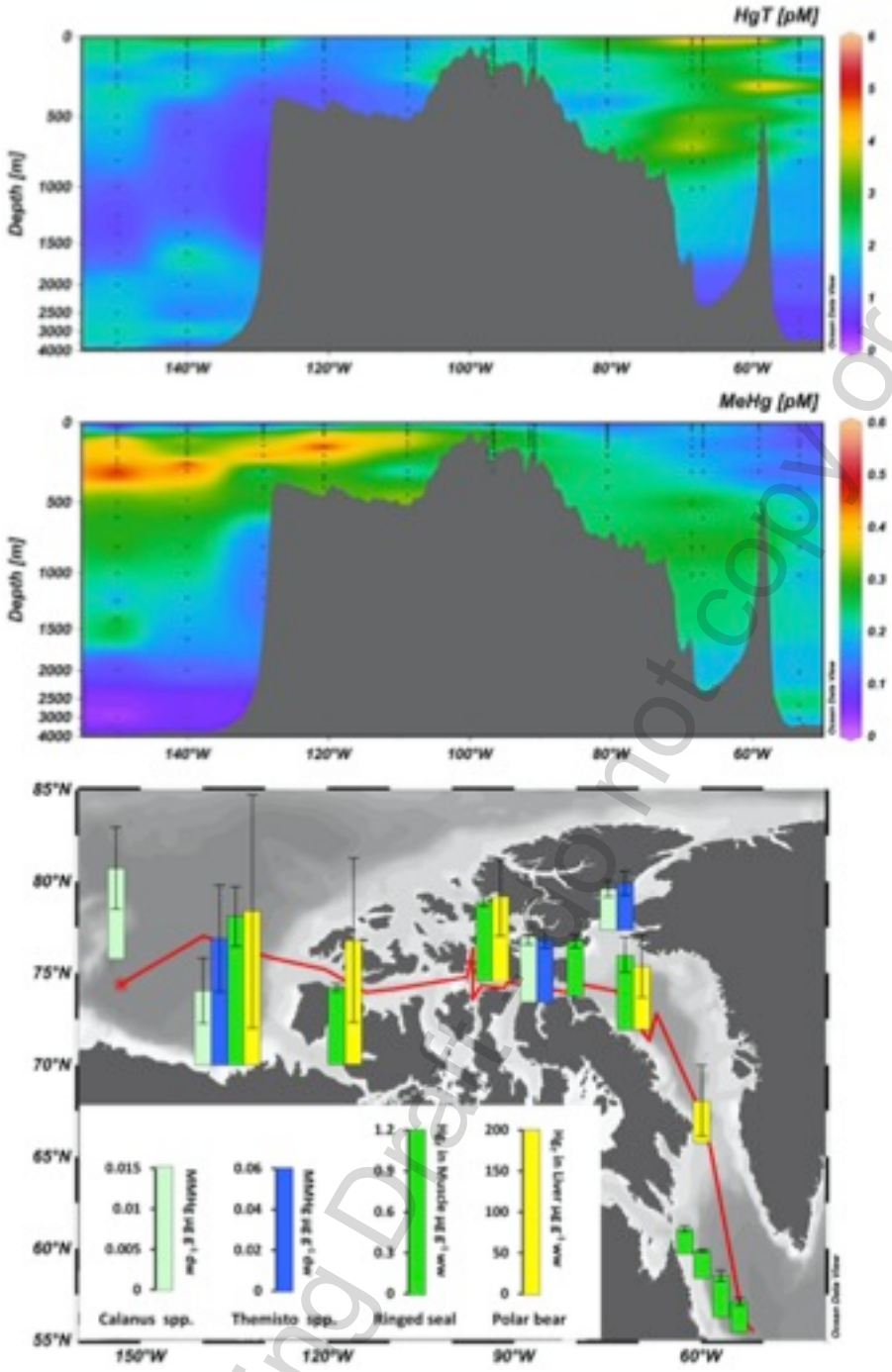

Figure 4.3 Total mercury (HgT) and methylmercury (MeHg) concentrations in seawater (top and middle panels, respectively) and the marine food web (bottom) along a longitudinal (west-to-east) section (the red line in the bottom panel) across the Canadian Arctic and Labrador Sea. The bar charts in the bottom panel show mean concentrations ± one standard deviation of monomethylmercury (MMHg) in Calanus spp. and Themisto spp. collected from 1998 to 2012, HgT in muscle of adult ringed seals collected in 2007 and 2011, and HgT in liver of polar bears collected from 2005 to 2008. Redrawn from Wang et al. (2018).

4.3.4 Snow/sea ice

Contributing authors: Michelle Nerentorp, Warren RL Cairns

- Highlight: The Arctic sea ice environment not only regulates the exchange of mercury between the atmosphere and the ocean, but also acts as a medium where mercury transformation and uptake by biota can take place.

Methylation processes in snow/seawater. Relevant processes.

The sea ice environment is a dynamic system that separates the atmosphere and the Arctic Ocean. It acts both as a barrier against atmospheric deposition and as a cap against evasion of mercury from the sea surface (Nerentorp Mastromonaco et al., 2017; Andersson et al., 2008) , thus influencing the timing and magnitude of net deposited mercury into the Arctic Ocean during atmospheric mercury depletion events (AMDEs) (Schroeder et al., 1998). The presence of sea ice also decrease photodegradation of methylmercury in underlying water (Ebinghaus et al., 2002).

Methylation within snowpack (Larose et al., 2010). Did not contribute to the methylmercury found in sea ice (Gionfriddo et al., 2016; Soerensen et al., 2016).

Mercury is believed to enter snow and sea ice either from atmospheric net deposition or from the under-ice water (Chaulk et al., 2011). Once in the ice, mercury can undergo transformations into other mercury compounds such as methylmercury. Methylation of mercury has earlier been suggested to occur in the anaerobic brine environment or in the lower part of the ice due to the involvement of sulfate-reducing bacteria (Chaulk et al., 2011; Beattie et al., 2014).

Microorganisms that possess the mercury reductive and detoxifying *mer* genes have been identified in the sea ice environment (Bowman et al., 2014; Møller et al. 2011; Møller et al., 2014; Poulain et al., 2007). However, little is known about the processes that control the methylation and biotic uptake of mercury in polar marine systems. It was previously believed that methylating processes of mercury were strictly anerobic (Gilmour et al., 2013), although also aerobic mercury methylation has been observed in surface seawater (Heimbürger et al., 2015; Schartup et al., 2015).

During the Antarctic expedition SIPEX II, Gionfriddo et al. (2016) studied the metagenomic sequence of microbes residing within sea ice, especially focusing on microbial genes encoding the methylating functional genes *hgcA* and *hgcb* and the reductive functional genes *mer*-operon.

The study identified the microaerophilic nitrite oxidizing bacteria *Nitrospina* to be a

potential candidate of methylating mercury within sea ice, as well as Proteobacteria, a potential mercury reductive agent possessing the *mer* operon gene (Gionfriddo et al., 2016).

Surface waters are enriched with mercury due to sea ice melt. This contribution of mercury into the Arctic Ocean could constitute of a biotic source of methylmercury in Arctic surface waters and the methylation of mercury deeper down in the water column (Gionfriddo et al., 2016).

No pattern has been observed of the distribution of methylmercury in Antarctic sea ice (Gionfriddo et al., 2016).

Relationships between methylmercury and chla has been found both in Antarctic and Arctic ice (Cossa et al., 2011; Beattie et al., 2014). Gionfriddo et al. (2016) suggest that se-ice phytoplankton play a role in the stimulation of methylation of oxidized mercury. Strong relationship was found between increased Chla and unique genes for functional subsystems in marine phytoplankton, except for osmotic stress. This shows that primary production is a driver of bacterial activity in sea ice. They also found a covariance of Chla and methylmercury which suggests a microbial mercury methylation and the activity of phytoplankton and phototrophs. Gionfriddo et al. (2016) suggest that microbial methylation of mercury by microbes occurs within the sea ice, carried out by micorarephilic bacteria, such as Nitrospina. The methylation is suggested to occur within brine pockets and periphytic biofilms where organic matter is trapped and decaying. Due to the seasonality in primary production, methylmercury formation could also show seasonal variations. Methylation within sea ice in the Arctic could be a plausible cause of the net input of methyl mercury into the Arctic Ocean.

4.4 What are the processes affecting mercury uptake at the base of the food chain?

***Description*:** Provide recent update on our understanding of processes at the base of the food chain – phytoplankton, zooplankton.

Coordinating author: John Chételat

Contributing authors: John Chételat

Notes and key studies

- Few studies on mercury in Arctic plankton, although new data for marine phytoplankton (Fox et al. 2017), sea ice algae (Burt et al. 2013) and lake seston (Chetelat et al. 2018). Similarly, new data for zooplankton in marine (Pomerleau et

al. 2016, Pucko et al. 2014, Foster et al. 2012) and fresh waters (Lescord et al. 2016, Chetelat et al. 2018, 2012)

- Subsurface maxima of MeHg in the western Arctic Ocean where greater Hg bioaccumulation is observed (Wang et al. 2018)
- Bioaccumulation factors of MeHg are greater for biofilms and seston in low DOC Arctic lakes (Chetelat et al. 2018)
- MeHg accumulation varies among species and trophic levels in the marine plankton food web (Foster et al. 2012),
- Evidence from Hg stable isotopes suggests that atmospherically deposited Hg is a dominant source to Arctic marine food webs (Mabou et al. 2018)
- Little information available for uptake in terrestrial food webs, although coastal lichens (an important food source supporting terrestrial biota) have higher MeHg concentrations than inland (St. Pierre et al. 2015)
- Basal mercury concentrations were higher in Arctic char food webs in lacustrine than marine food webs (van der Velden et al. 2013)
- Freshwater discharges into subarctic coastal waters enhances MeHg bioaccumulation in plankton (Shartup et al. 2015)

4.5 What are the processes affecting mercury bioaccumulation at higher trophic levels?

***Description*:** Including role of food chain length, transfer and physiological/life history influences on bioaccumulation in top predators.

Coordinating author: John Chételat

Contributing authors: John Chételat

Notes and key studies:

- Geographic variation in mercury concentration (e.g., ringed seal, polar bear) related to food chain length (St. Louis et al. 2011, Brown et al. 2016)
- Cross-ecosystem subsidies (e.g., sea-run char, terrestrial mammals feeding in the marine environment) influence mercury concentrations in predatory animals (van der Velden et al. 2013, Bochavar et al. 2013, Hallanger et la. 2019)
- New research on biomagnification rates in Arctic food webs, for example: Northern latitude ecosystems have higher Hg biomagnication rates than tropical regions (Lavoie et al. 2013). Similar biomagnification rates between lacustrine and marine food webs with Arctic char (van der Velden et al. 2013).

- Importance of age (rather than size) in fish (Vander Velden et al. 2011, 2013); demethylation with age in marine mammals (Masbou et al. 2018); increasing Hg with maturity in polar bears (Beschoft et al. 2016).
- Influence of body condition on mercury in polar bear (Beschoft et al. 2016; McKinney et al. 2017).

4.6 What are the effects of the sea ice environment on Hg uptake?

***Description*:** Sea ice as a storage, transformation, and uptake medium for Hg in the Arctic marine ecosystem.

Coordinating author: Michelle Nerentorp

Contributing authors: Michelle Nerentorp

How does Hg enter ice and what happens to it? Transportation and transformation processes of Hg inside the sea ice. Uptake of MeHg from zoo plankton feeding from underneath the ice during winter? Seasonality? Melting sea ice and snow, melt ponds.

Sea ice act as a porous barrier between the atmosphere and the Arctic Ocean. The permeability, and thus the transport of contaminants through the ice, depends on the microstructure and on the presence of brine pockets and channels within the ice. Disregarding the porosity, sea ice has been shown to act as a cap, reducing the re-emission of elemental mercury from sea surfaces and result in supersaturated concentrations of DGM-concentration under the ice (Andersson et al., 2008; Nerentorp Mastromonaco et al., 2017).

It has previously been assumed that sea ice acts as a barrier against net atmospheric deposition, reducing the amounts of mercury entering the marine ecosystem. However, it has been shown that significant amounts of mercury reside within Arctic (Chaulk et al., 2011; Beattie et al., 2014) and Antarctic sea ice (Nerentorp Mastromonaco et al., 2016), leading to the conclusion that sea ice also take up and transports mercury, and other contaminants, through porosities and brine channels between the air-sea-ocean interface.

There are majorly three suggested processes of how contaminants can enter sea ice (Wang et al., 2017);

1. Freeze rejection, where dissolved contaminants in seawater are trapped within brine pockets during sea ice formation, due to freeze rejection of large or charged ions.

2. Particle entrapment of aquatic particles during suspension freezing. This process occurs

typically in shallow shelf waters and is more important for trace metals and organic contaminants that have high affinity to particles.

3. Wet and dry deposition of airborne contaminants onto snow, ice or open leads.

Due to ice drift and freezing and melting processes, contaminants within sea ice are also transported spatially and temporally (Wang et al., 2017).

Studies have observed an enrichment of mercury in sea ice compared to the underlying water (Gionffriddo et al., 2016. Och fler). That can be explained by atmospheric deposition and the temporary

A recent study showed that the melting of multiyear ice in the Arctic Ocean could lead to a release of 2,1 kmol total mercury and 0,21 kmol methylmercury annually (Beattie et al., 2014). The contribution of mercury input from melting sea ice and snow is together with atmospheric deposition the second largest net input of mercury into the Arctic Ocean (Soerensen et al., 2016).

4.7 What are the effects of organic matter on Hg uptake?

***Description*:** How organic matter affects Hg speciation, (de-)methylation, and uptake.
Coordinating author: Michelle Nerentorp
Contributing authors: Gretchen Lescord, Sofi Jonsson

Paragraph 1: Intro

- Introductory statement on the complex relationship between DOM and Hg cycling. Discuss recent Hg-DOM review and its findings in Arctic systems (Lavoie et al., 2019).
- Number of studies in the Arctic and sub-Arctic
- Overview of correlations reported:
    - Hudelson et al., (2019) found that DOC and POC were strong correlates of Arctic char Hg in Resolute Lakes. Lescord et al., (2015) report correlations between DOC (in combination with total nutrient levels) and [THg] in Arctic char, as well as with the rates of mercury biomagnification in the same food webs.
    - Bioaccumulation rates of MeHg in Arctic lakes were correlated with lower

7557 [DOC] (Chételat et al., 2018).

7558 - Other key examples or general correlations.

7559 Paragraph 2: DOM quality and thresholds for bioaccumulation

7560 – Recent work has shown that DOM's effect on Hg bioaccumulation in aquatic biota
7561 may be concentration-dependent.

7562 – Studies report a bell-curve relationship between DOC and MeHg in biota, with ~8-
7563 11 mg/L as the flection point (Braaten et al., 2018; French et al., 2014). Discuss
7564 DOC concentration ranges in Arctic systems. What does this mean for future climate
7565 scenarios?

7566 – These concentration dependant relationships may be due to several factors. For
7567 example:

7568 - Lab-based studies on DOC-Hg equilibrium (Chiasson-Gould et al., 2014).

7569 - Recent sub-arctic work on DOM characterization imply these relationships
7570 may be due changes in the quality of DOM (Lescord et al., 2018).

7571 - In particular, $SUVA_{254}$ (measures of DOM aromaticity) may be important
7572 and cost-accessible measures in future Hg-DOM research (e.g., Burns et al.,
7573 2013; Skyllberg et al., 2009).

7574 Paragraph 3: Permafrost degradation as a source of DOM and Hg

7575 – Warming climate in the Arctic is causing thaw slumps (TSs) in permafrost across
7576 the Arctic and sub-Arctic (Walvoord et al., 2019).

7577 – Define TSs; discuss sources of Hg and DOM in Arctic/sub-Arctic systems (Gordon
7578 et al., 2016; Houben et al., 2016; MacMillan et al., 2015; Mu et al., 2019; Schuster
7579 et al., 2018; St Pierre et al., 2018).

7580 – In fact, the highest ever recorded concentration of total and methyl [Hg] (1,270 ng/
7581 L and 7 ng/L, respectively) in an uncontaminated site were measured downstream of
7582 a permafrost thaw slump in NWT (St Pierre et al., 2018). Other studies show
7583 similarly elevated levels of both Hg measures (Gordon et al., 2016; Houben et al.,
7584 2016; MacMillan et al., 2015).

7585 – What do future warming scenarios mean for TS? Lim et al., (2019) estimate up to a
7586 2-fold increase in Hg and particulate organic carbon (POC) transport into Siberian
7587 waters in the next 10-50 years.

- More work is needed to understand if the Hg released is being methylated and bioaccumulated into food webs. Furthermore, these thaw slumps are likely affecting a wide-range of other biogeochemical processes that will either directly or indirectly alter Hg transport, methylation, or bioaccumulation in receiving waterbodies (e.g., selenium; Pokrovsky et al., 2018).

Paragraph 4: The influence of DOM on the photodemethylation of MeHg

- Define photodemethylation and DOM interactions (UV penetration, etc; Klapstein et al., 2017).
- DOC influences Hg(II) and Hg(0) binding and conversion in sub-arctic sediments (Brazeau et al., 2013).
- Photodemethylation was identified as one of the forces driving MeHg mass balances in high Arctic wetlands (Lehnherr et al., 2012).
- Discuss recent Arctic findings: (Girard et al., 2016); others?
- Dependant on many other factors (e.g.,) and structural characteristics of DOM (Jeremiason et al., 2015).

Uptake of Hg(II) into bacterial cells, carrying the Hg methylating genes, and of MeHg into the base of the food web (i.e. phytoplankton) are key steps linking natural and anthropogenic sources of Hg to its environmental harm. Significant advances has been done in the last 10 years with regard to the effect of organic matter for these two processes. It is generally agreed that primarily dissolved complexes of HgII and MMHg are taken up by Hg methylating bacteria and at the base of aquatic food webs (Drott et al., 2007; Schaefer and Morel, 2009; Chiasson-Gould, Blais and Poulain, 2014). Adsorption of HgII and MMHg to the solid phase are thus important processes limiting their biological uptake (Schartup et al., 2015; Mazrui et al., 2016). However, as shown in our previous work, different dissolved and solid chemical forms of Hg differ in their bioavailability (Jonsson et al., 2012; Mazrui et al., 2016). Although recent terrestrial inputs of HgII and MMHg did not contribute much to the stock of MMHg in the estuarine system, 40 to 70 % of the bioaccumulated Hg pool originated from these recent terrestrial Hg inputs. In these studies, refractory pools of HgII and MMHg were not fully accounted for. In the investigated retrogressive thaw slump (St. Pierre et al., 2018), over 95% of the Hg was released in the particulate phase.

4.8 What characteristics in the Arctic promote Hg bioaccumulation?

***Description*:** Summary, include a summary diagram.

Coordinating author: Michelle Nerentorp

Contributing authors: John Chételat

- Long food chains
- Long-lived fish (Arctic char) in lakes
- Freshwater discharge to coastal areas
- Low DOC in lake waters

(Chételat et al., 2018; Macdonald et al., 2010)

Textbox 4.1: Relationship between Hg(0), inorganic Hg(II), and methylmercury

***Description*:**
Coordinating author: Michelle Nerentorp
Contributing authors:
***Status*:**

4.9 References

Andersson, M. E., Sommar, J., Gårdfeldt, K. & Lindqvist, O. 2008. Enhanced concentrations of dissolved gaseous mercury in the surface waters of the Arctic Ocean. Mar. Chem.110:190–194.

Baldi, F., Pepi, M. and Filippelli, M. (1993) 'Methylmercury Resistance in Desulfovibrio desulfuricans Strains in Relation to Methylmercury Degradation', Applied and Environmental Microbiology, 59(8), pp. 2479–2485.

Beattie, S. A.; Armstrong, D.; Chaulk, A.; Comte, J.; Gosselin, M.; Wang, F. Total and methylated mercury in Arctic multiyear sea ice. Environ. Sci. Technol. 2014, 48:5575−5582.

Bechshoft T, Derocher AE, Richardson E, Lunn NJ, St Louis VL. Hair Mercury Concentrations in Western Hudson Bay Polar Bear Family Groups. Environmental Science and Technology 2016; 50: 5313-5319.

Bidleman TF, Stern GA, Tomy GT, Hargrave BT, Jantunen LM, MacDonald RW. Scavenging amphipods: Sentinels for penetration of mercury and persistent organic chemicals into food webs of the deep Arctic Ocean. Environmental Science and Technology 2013; 47: 5553-5561.

Bocharova N, Treu G, Czirják GA, Krone O, Stefanski V, Wibbelt G, et al. Correlates between Feeding Ecology and Mercury Levels in Historical and Modern Arctic Foxes (Vulpes lagopus). PLoS ONE 2013; 8.

Bowman, J. S., Berthiaume, C. T., Armbrust, E. & Deming, J. W. The genetic potential for key biogeochemical processes in Arctic frost flowers and young sea ice revealed by metagenomic analysis. FEMS Microbiol. Ecol. 89, 376–387 (2014).

Braaten, H.F. V., de Wit, H.A., Larssen, T., Poste, A.E., 2018. Mercury in fish from Norwegian lakes: The complex influence of aqueous organic carbon. Sci. Total Environ. 627, 341–348. https://doi.org/10.1016/j.scitotenv.2018.01.252

Bradley, M.A., Barst, B.D., Basu, N., 2017. A review of mercury bioavailability in humans and fish. Int. J. Environ. Res. Public Health. https://doi.org/10.3390/ijerph14020169

Brazeau, M.L., Blais, J.M., Paterson, A.M., Keller, W., Poulain, A.J., 2013. Evidence for microbially mediated production of elemental mercury (Hg0) in subarctic lake sediments. Appl. Geochemistry 37, 142–148. https://doi.org/10.1016/j.apgeochem.2013.07.020

Brown TM, Fisk AT, Wang X, Ferguson SH, Young BG, Reimer KJ, et al. Mercury and cadmium in ringed seals in the Canadian Arctic: Influence of location and diet. Science of the Total Environment 2016; 545-546: 503-511.

Burns, D.A., Aiken, G.R., Bradley, P.M., Journey, C.A., Schelker, J., 2013. Specific ultra-violet absorbance as an indicator of mercury sources in an Adirondack River basin. Biogeochemistry 113, 451–466. https://doi.org/10.1007/s10533-012-9773-5

Burt, A., Wang, F., Pučko, M., Mundy, C.J., Gosselin, M., Philippe, B., Poulin, M., Tremblay, J.É., Stern, G.A., 2013. Mercury uptake within an ice algal community during the spring bloom in first-year Arctic sea ice. J. Geophys. Res. Ocean. 118, 4746–4754. https://doi.org/10.1002/jgrc.20380

Chaulk, A.; Stern, G. A.; Armstrong, D.; Barber, D. G.; Wang, F. Mercury distribution and transport across the ocean-sea-ice-atmosphere interface in the Arctic Ocean. Environ. Sci. Technol. 2011, 45:1866−1872.

Chételat J, Amyot M, Cloutier L. Shifts in elemental composition, methylmercury content and δ 15N ratio during growth of a High Arctic copepod. Freshwater Biology 2012; 57: 1228-1240.

Chételat J, Poulain AJ, Amyot M, Cloutier L, Hintelmann H. Ecological determinants of methylmercury bioaccumulation in benthic invertebrates of polar desert lakes. Polar Biology 2014; 37: 1785-1796.

Chételat, J., Richardson, M.C., Macmillan, G.A., Amyot, M., Poulain, A.J., 2018. Ratio of Methylmercury to Dissolved Organic Carbon in Water Explains Methylmercury

7686 Bioaccumulation Across a Latitudinal Gradient from North-Temperate to Arctic Lakes.
7687 Environ. Sci. Technol. 52, 79–88. https://doi.org/10.1021/acs.est.7b04180
7688 Chiasson-Gould, S.A., Blais, J.M., Poulain, A.J., 2014. Dissolved organic matter kinetically
7689 controls mercury bioavailability to bacteria. Environ. Sci. Technol. 48, 3153–3161.
7690 https://doi.org/10.1021/es4038484
7691 Clayden MG, Arsenault LM, Kidd KA, O'Driscoll NJ, Mallory ML. Mercury bioaccumulation
7692 and biomagnification in a small Arctic polynya ecosystem. Science of the Total Environment
7693 2015; 509-510: 206-215.
7694 Cossa, D. et al. Mercury in the southern ocean. Geochim. Cosmochim. Acta 75, 4037–4052
7695 (2011).
7696 Culbreth, M., Aschner, M., 2019. Methylmercury Epigenetics. Toxics 7, 56.
7697 https://doi.org/10.3390/toxics7040056
7698 Douglas, T.A., M. Amyot, T. Barkay, T. Berg, J. Chetelat, P. Constant, A. Dommergue, M.
7699 Evans, C. Ferrari, N. Gantner, M. Johnson, J. Kirk, N. Kroer, C. Larose, D. Lean, L. Loseto,
7700 R. Macdonald, D. Muir, T. G. Nielsen, P. Outridge, A. Poulain, L. Poissant, S. Rognerud, H.
7701 Skov, S. Sorensen, F. Wang, C. Zdanowicz, Chapter 3. What is the Fate of Mercury Entering
7702 the Arctic Environment? in AMAP Assessment 2011. Mercury in the Arctic 2011, pp. 45–65
7703 (Arctic Monitoring and Assessment Programme: Oslo, Norway).
7704 Douglas, T.A., Loseto, L.L., MacDonald, R.W., Outridge, P., Dommergue, A., Poulain, A.,
7705 Amyot, M., Barkay, T., Berg, T., Chetelat, J., Constant, P., Evans, M., Ferrari, C., Gantner,
7706 N., Johnson, M.S., Kirk, J., Kroer, N., Larose, C., Lean, D., Nielsen, T.G., Poissant, L.,
7707 Rognerud, S., Skov, H., Sørensen, S., Wang, F., Wilson, S., Zdanowicz, C.M., 2012. The
7708 fate of mercury in Arctic terrestrial and aquatic ecosystems, a review. Environ. Chem.
7709 https://doi.org/10.1071/EN11140
7710 Drott, A. et al. (2007) 'Importance of dissolved neutral mercury sulfides for methyl mercury
7711 production in contaminated sediments', Environmental Science and Technology, 41(7), pp.
7712 2270–2276. doi: 10.1021/es061724z.
7713 Du, H., Ma, M., Igarashi, Y., Wang, D., 2019. Biotic and Abiotic Degradation of Methylmercury
7714 in Aquatic Ecosystems: A Review. Bull. Environ. Contam. Toxicol.
7715 https://doi.org/10.1007/s00128-018-2530-2
7716 Ebinghaus, R. et al. Antarctic springtime depletion of atmospheric mercury. Environ. Sci.
7717 Technol. 36, 1238–1244 (2002).
7718 Fahnestock, M. F. et al. (2019) 'Mercury reallocation in thawing subarctic peatlands',
7719 Geochemical Perspectives Letters, pp. 33–38. doi: 10.7185/geochemlet.1922.
7720 Feldmann, J., Bluemlein, K., Krupp, E.M., Mueller, M., Wood, B.A., 2018. Metallomics Study in
7721 Plants Exposed to Arsenic, Mercury, Selenium and Sulphur, in: Advances in Experimental
7722 Medicine and Biology. Springer New York LLC, pp. 67–100. https://doi.org/10.1007/978-3-
7723 319-90143-5_4
7724 Foster, K.L., Stern, G.A., Pazerniuk, M.A., Hickie, B., Walkusz, W., Wang, F., MacDonald,
7725 R.W., 2012. Mercury biomagnification in marine zooplankton food webs in hudson bay.
7726 Environ. Sci. Technol. 46, 12952–12959. https://doi.org/10.1021/es303434p
7727 Fox AL, Trefry JH, Trocine RP, Dunton KH, Lasorsa BK, Konar B, et al. Mercury
7728 biomagnification in food webs of the northeastern Chukchi Sea, Alaskan Arctic. Deep-Sea
7729 Research Part II: Topical Studies in Oceanography 2017; 144: 63-77.
7730 Fox AL, Hughes EA, Trocine RP, Trefry JH, Schonberg SV, McTigue ND, et al. Mercury in the
7731 northeastern Chukchi Sea: Distribution patterns in seawater and sediments and
7732 biomagnification in the benthic food web. Deep-Sea Research Part II: Topical Studies in
7733 Oceanography 2014; 102: 56-67.
7734 French, T.D., Houben, A.J., Desforges, J.W., Kimpe, L.E., Kokelj, S. V, Poulain, A.J., Smol, J.P.,
7735 Wang, X., Blais, J.M., 2014. Dissolved Organic Carbon Thresholds Affect Mercury
7736 Bioaccumulation in Arctic Lakes. Envirnomental Sci. Technol. 48, 3162–3168.
7737 https://doi.org/10.1021/es403849d

7738 Gilmour, C. C. et al. Mercury methylation by novel microorganisms from new environments.
7739 Environ. Sci. Technol. 47, 11810–11820 (2013).
7740 Gionfriddo, C.M., Tate, M.T., Wick. R.R., Schultz, M.B., Zemla, A., Thelen, M.P., Schofield, R.,
7741 Krappenhoft, D.P., Holt, K.E., Moreau, J.W. 2016, Microbial mercury methylation in
7742 Antarctic sea ice. Nature Microbiology. DOI: 10.1038/nmicrobiol.2016.127
7743 Girard, C., Leclerc, M., Amyot, M., 2016. Photodemethylation of Methylmercury in Eastern
7744 Canadian Arctic Thaw Pond and Lake Ecosystems. Environ. Sci. Technol. 50, 3511–3520.
7745 https://doi.org/10.1021/acs.est.5b04921
7746 Gordon, J., Quinton, W., Branfireun, B.A., Olefeldt, D., 2016. Mercury and methylmercury
7747 biogeochemistry in a thawing permafrost wetland complex, Northwest Territories, Canada.
7748 Hydrol. Process. 30, 3627–3638. https://doi.org/10.1002/hyp.10911
7749 Hallanger IG, Fuglei E, Yoccoz NG, Pedersen ÅØ, König M, Routti H. Temporal trend of
7750 mercury in relation to feeding habits and food availability in arctic foxes (Vulpes lagopus)
7751 from Svalbard, Norway. Science of the Total Environment 2019; 670: 1125-1132.
7752 Heimbürger, L.-E. et al. Shallow methylmercury production in the marginal sea ice zone of the
7753 central Arctic Ocean. Sci. Rep. 5, 10318 (2015).
7754 Houben, A.J., French, T.D., Kokelj, S. V., Wang, X., Smol, J.P., Blais, J.M., 2016. The impacts
7755 of permafrost thaw slump events on limnological variables in upland tundra lakes,
7756 Mackenzie Delta region. Fundam. Appl. Limnol. 11–35.
7757 https://doi.org/10.1127/FAL/2016/0921
7758 Hsu-Kim, H. et al. (2018) 'Challenges and opportunities for managing aquatic mercury pollution
7759 in altered landscapes', Ambio, 47(2). doi: 10.1007/s13280-017-1006-7.
7760 Hudelson, K.E., Muir, D.C.G., Drevnick, P.E., Köck, G., Iqaluk, D., Wang, X., Kirk, J.L., Barst,
7761 B.D., Grgicak-Mannion, A., Shearon, R., Fisk, A.T., 2019. Temporal trends, lake-to-lake
7762 variation, and climate effects on Arctic char (Salvelinus alpinus) mercury concentrations
7763 from six High Arctic lakes in Nunavut, Canada. Sci. Total Environ. 678, 801–812.
7764 https://doi.org/10.1016/j.scitotenv.2019.04.453
7765 Hugelius, G. et al. (2013) 'A new data set for estimating organic carbon storage to 3 m depth in
7766 soils of the northern circumpolar permafrost region', Earth System Science Data, 5(2), pp.
7767 393–402. doi: 10.5194/essd-5-393-2013.
7768 Hugelius, G. et al. (2014) 'Estimated stocks of circumpolar permafrost carbon with quantified
7769 uncertainty ranges and identified data gaps', Biogeosciences, 11(23), pp. 6573–6593. doi:
7770 10.5194/bg-11-6573-2014.
7771 Jeremiason, J.D., Portner, J.C., Aiken, G.R., Hiranaka, A.J., Dvorak, M.T., Tran, K.T., Latch,
7772 D.E., 2015. Photoreduction of Hg(II) and photodemethylation of methylmercury: The key
7773 role of thiol sites on dissolved organic matter. Environ. Sci. Process. Impacts 17, 1892–1903.
7774 https://doi.org/10.1039/c5em00305a
7775 Johanson, G., 2010. Modeling of Disposition. Compr. Toxicol. 153–177.
7776 https://doi.org/10.1016/B978-0-08-046884-6.00108-1
7777 Jonsson, S. et al. (2012) 'Mercury methylation rates for geochemically relevant HgII species in
7778 sediments', Environmental Science and Technology, 46(21). doi: 10.1021/es3015327.
7779 Jonsson, S., Mazrui, N. M. and Mason, R. P. (2016) 'Dimethylmercury Formation Mediated by
7780 Inorganic and Organic Reduced Sulfur Surfaces', Scientific Reports. Nature Publishing
7781 Group, pp. 6:27958, DOI: 10.1038/srep27958. doi: 10.1038/srep27958.
7782 Klapstein, S.J., Ziegler, S.E., O'Driscoll, N.J., 2017. Methylmercury photodemethylation is
7783 inhibited in lakes with high dissolved organic matter. Environ. Pollut. 232, 392–401.
7784 https://doi.org/10.1016/J.ENVPOL.2017.09.049
7785 Larose, C. et al. Springtime changes in snow chemistry lead to new insights into mercury
7786 methylation in the Arctic. Geochim. Cosmochim. Acta 74, 6263–6275 (2010).
7787 Larose, C., Dommergue, A., Marusczak, N., Coves, J., Ferrari, C.P., Schneider, D., 2011.
7788 Bioavailable mercury cycling in polar snowpacks. Environ. Sci. Technol. 45, 2150–2156.
7789 https://doi.org/10.1021/es103016x

7790 Lavoie RA, Jardine TD, Chumchal MM, Kidd KA, Campbell LM. Biomagnification of mercury
7791 in aquatic food webs: A worldwide meta-analysis. Environmental Science and Technology
7792 2013; 47: 13385-13394.
7793 Lavoie, R.A., Amyot, M., Lapierre, J.F., 2019. Global Meta-Analysis on the Relationship
7794 Between Mercury and Dissolved Organic Carbon in Freshwater Environments. J. Geophys.
7795 Res. Biogeosciences 124, 1508–1523. https://doi.org/10.1029/2018JG004896
7796 Lehnherr, I., St. Louis, V.L., Kirk, J.L., 2012. Methylmercury cycling in high arctic wetland
7797 ponds: Controls on sedimentary production. Environ. Sci. Technol. 46, 10523–10531.
7798 https://doi.org/10.1021/es300577e
7799 Lehnherr, I. et al. (2012) 'Methylmercury Cycling in High Arctic Wetland Ponds: Sources and
7800 Sinks', Environmental Science & Technology. American Chemical Society, 46(19), pp.
7801 10514–10522. doi: 10.1021/es300576p.
7802 Lescord, G.L., Emilson, E., Johnston, T., Branfireun, B., Gunn, J., 2018. The optical properties of
7803 dissolved organic matter and their relation to mercury concentrations in water and biota
7804 across a remote freshwater drainage basin. Environ. Sci. Technol. 52, 3344−3353.
7805 https://doi.org/10.1021/acs.est.7b05348
7806 Lescord, G.L., Kidd, K.A., Kirk, J.L., O'Driscoll, N.J., Wang, X., Muir, D.C.G., 2015. Factors
7807 affecting biotic mercury concentrations and biomagnification through lake food webs in the
7808 Canadian high Arctic. Sci. Total Environ. 509–510, 195–205.
7809 https://doi.org/10.1016/j.scitotenv.2014.04.133
7810 Li, Y. Bin, Cai, Y., 2013. Progress in the study of mercury methylation and demethylation in
7811 aquatic environments. Chinese Sci. Bull. https://doi.org/10.1007/s11434-012-5416-4
7812 Lim, A.G., Sonke, J.E., Krickov, I. V., Manasypov, R.M., Loiko, S. V., Pokrovsky, O.S., 2019.
7813 Enhanced particulate Hg export at the permafrost boundary, western Siberia. Environ. Pollut.
7814 254. https://doi.org/10.1016/j.envpol.2019.113083
7815 Ma, M., Du, H., Wang, D., 2019. Mercury methylation by anaerobic microorganisms: A review.
7816 Crit. Rev. Environ. Sci. Technol. 49, 1893–1936.
7817 https://doi.org/10.1080/10643389.2019.1594517
7818 Macdonald RW, Loseto LL. Are Arctic Ocean ecosystems exceptionally vulnerable to global
7819 emissions of mercury? A call for emphasised research on methylation and the consequences
7820 of climate change. Environmental Chemistry 2010; 7: 133-138.
7821 MacMillan, G.A., Girard, C., Chételat, J., Laurion, I., Amyot, M., 2015. High Methylmercury in
7822 Arctic and Subarctic Ponds is Related to Nutrient Levels in the Warming Eastern Canadian
7823 Arctic. Environ. Sci. Technol. 49, 7743–7753. https://doi.org/10.1021/acs.est.5b00763
7824 Masbou J, Sonke JE, Amouroux D, Guillou G, Becker PR, Point D. Hg-Stable Isotope Variations
7825 in Marine Top Predators of the Western Arctic Ocean. ACS Earth and Space Chemistry
7826 2018; 2: 479-490.
7827 Matsuyama, A., Eguchi, T., Sonoda, I., Tada, A., Yano, S., Tai, A., Marumoto, K., Tomiyasu, T.,
7828 Akagi, H., 2011. Mercury speciation in the water of Minamata Bay, Japan. Water. Air. Soil
7829 Pollut. 218, 399–412. https://doi.org/10.1007/s11270-010-0654-z
7830 Mazrui, N. M. et al. (2016) 'Enhanced availability of mercury bound to dissolved organic matter
7831 for methylation in marine sediments', Geochimica et Cosmochimica Acta, 194. doi:
7832 10.1016/j.gca.2016.08.019.
7833 McKinney MA, Atwood TC, Pedro S, Peacock E. Ecological Change Drives a Decline in
7834 Mercury Concentrations in Southern Beaufort Sea Polar Bears. Environmental Science and
7835 Technology 2017; 51: 7814-7822.
7836 McMeans BC, Arts MT, Fisk AT. Impacts of food web structure and feeding behavior on
7837 mercury exposure in Greenland Sharks (Somniosus microcephalus). Science of the Total
7838 Environment 2015; 509-510: 216-225.
7839 Mu, C., Zhang, F., Chen, X., Ge, S., Mu, M., Jia, L., Wu, Q., Zhang, T., 2019. Carbon and
7840 mercury export from the Arctic rivers and response to permafrost degradation. Water Res.
7841 161, 54–60. https://doi.org/10.1016/j.watres.2019.05.082

7842 Møller, A. K. et al. Diversity and characterization of mercury-resistant bacteria in snow,
7843 freshwater and sea-ice brine from the High Arctic. FEMS Microbiol. Ecol. 75, 390–401
7844 (2011).
7845 Møller, A. K. et al. Mercuric reductase genes (merA) and mercury resistance plasmids in High
7846 Arctic snow, freshwater and sea-ice brine. FEMS Microbiol. Ecol. 87, 52–63 (2014).
7847 Nerentorp Mastromonaco, M.G.; Gårdfeldt, K.; Langer, S.; Dommergue, A. 2016. Seasonal study
7848 of mercury species in the Antarctic sea ice environment. Environ. Sci. Technol.50,
7849 23:12705-12712.
7850 Nerentorp Mastromonaco, M.G., Gårdfeldt, K., Langer, S. Mercury flux over west Antarctic Seas
7851 during winter, spring and summer. 2017. Mar. Chem. 193:44-54.
7852 Obrist, D., Agnan, Y., Jiskra, M., Olson, C.L., Colegrove, D.P., Hueber, J., Moore, C.W., Sonke,
7853 J.E., Helmig, D., 2017. Tundra uptake of atmospheric elemental mercury drives Arctic
7854 mercury pollution. Nature 547, 201–204. https://doi.org/10.1038/nature22997
7855 O'Concubhair, R., O'Sullivan, D., Sodeau, J.R., 2012. Dark oxidation of dissolved gaseous
7856 mercury in polar ice mimics. Environ. Sci. Technol. 46, 4829–4836.
7857 https://doi.org/10.1021/es300309n
7858 Olson, C. et al. (2018) 'Mercury in Active-Layer Tundra Soils of Alaska: Concentrations, Pools,
7859 Origins, and Spatial Distribution', Global Biogeochemical Cycles, 32(7), pp. 1058–1073.
7860 doi: 10.1029/2017GB005840.
7861 Paranjape, A.R., Hall, B.D., 2017. Recent advances in the study of mercury methylation in
7862 aquatic systems. FACETS 2, 85–119. https://doi.org/10.1139/facets-2016-0027
7863 Parks, J. M. et al. (2013) 'The genetic basis for bacterial mercury methylation.', Science, 339, pp.
7864 1332–1335, DOI: 10.1126/science.1230667. doi: 10.1126/science.1230667.
7865 Podar, M. et al. (2015) 'Global prevalence and distribution of genes and microorganisms involved
7866 in mercury methylation', (October), pp. 1–13. doi: 10.1126/sciadv.1500675.
7867 Pongratz, R. and Heumann, K. G. (1998) 'Production of methylated mercury and lead by polar
7868 macroalgae - a significant natural source for atmospheric heavy metals in clean room
7869 compartments', Chemosphere, 36(9), pp. 1935–1946. doi: 10.1016/S0045-6535(97)10078-9.
7870 Pongratz, R. and Heumann, K. G. (1999) 'Production of methylated mercury, lead, and cadmium
7871 by marine bacteria as a significant natural source for atmospheric heavy metals in polar
7872 regions', Chemosphere, 39(1), pp. 89–102. doi: 10.1016/S0045-6535(98)00591-8.
7873 Pokrovsky, O.S., Bueno, M., Manasypov, R.M., Shirokova, L.S., Karlsson, J., Amouroux, D.,
7874 2018. Dissolved Organic Matter Controls Seasonal and Spatial Selenium Concentration
7875 Variability in Thaw Lakes across a Permafrost Gradient. Environ. Sci. Technol. 52, 10254–
7876 10262. https://doi.org/10.1021/acs.est.8b00918
7877 Pomerleau C, Stern GA, Pućko M, Foster KL, Macdonald RW, Fortier L. Pan-Arctic
7878 concentrations of mercury and stable isotope ratios of carbon (δ 13 C) and nitrogen (δ 15 N)
7879 in marine zooplankton. Science of the Total Environment 2016; 551-552: 92-100.
7880 Poulain, A. J. et al. Potential for mercury reduction by microbes in the high arctic. Appl. Environ.
7881 Microbiol. 73, 2230–2238 (2007).
7882 Pućko M, Burt A, Walkusz W, Wang F, Macdonald RW, Rysgaard S, et al. Transformation of
7883 mercury at the bottom of the arctic food web: An overlooked puzzle in the mercury exposure
7884 narrative. Environmental Science and Technology 2014; 48: 7280-7288.
7885 Regnell, O., Watras, C.J., 2019. Microbial Mercury Methylation in Aquatic Environments: A
7886 Critical Review of Published Field and Laboratory Studies. Environ. Sci. Technol.
7887 https://doi.org/10.1021/acs.est.8b02709
7888 Ruus A, Øverjordet IB, Braaten HFV, Evenset A, Christensen G, Heimstad ES, et al.
7889 Methylmercury biomagnification in an Arctic pelagic food web. Environmental Toxicology
7890 and Chemistry 2015; 34: 2636-2643.
7891 Schaefer, J. K. and Morel, F. M. M. (2009) 'High methylation rates of mercury bound to cysteine
7892 by Geobacter sulfurreducens', Nature Geoscience. Nature Publishing Group, 2(2), pp. 123–
7893 126. doi: 10.1038/ngeo412.

7894 Schartup AT, Balcom PH, Soerensen AL, Gosnell KJ, Calder RSD, Mason RP, et al. Freshwater
7895 discharges drive high levels of methylmercury in Arctic marine biota. Proceedings of the
7896 National Academy of Sciences of the United States of America 2015; 112: 11789-11794.
7897 Schartup, A. T. et al. (2015) 'Contrasting effects of marine and terrestrially derived dissolved
7898 organic matter on mercury speciation and bioavailability in seawater', Environmental
7899 Science and Technology, 49(10), pp. 5965–5972. doi: 10.1021/es506274x.
7900 Schroeder, W. H.; Anlauf, K. G.; Barrie, L. A.; Lu, J. Y.; Steffen, A.; Schneeberger, D. R.; Berg,
7901 T. Arctic springtime depletion of mercury. Nature 1998, 394, 331–332.
7902 Schuster, P.F., Schaefer, K.M., Aiken, G.R., Antweiler, R.C., Dewild, J.F., Gryziec, J.D.,
7903 Gusmeroli, A., Hugelius, G., Jafarov, E., Krabbenhoft, D.P., Liu, L., Herman-Mercer, N.,
7904 Mu, C., Roth, D.A., Schaefer, T., Striegl, R.G., Wickland, K.P., Zhang, T., 2018. Permafrost
7905 Stores a Globally Significant Amount of Mercury. Geophys. Res. Lett. 45, 1463–1471.
7906 https://doi.org/10.1002/2017GL075571
7907 Sharavanan, V.J., Sivaramakrishnan, M., Sivarajasekar, N., Senthilrani, N., Kothandan, R.,
7908 Dhakal, N., Sivamani, S., Show, P.L., Awual, M.R., Naushad, M., 2019. Pollutants inducing
7909 epigenetic changes and diseases. Environ. Chem. Lett. https://doi.org/10.1007/s10311-019-
7910 00944-3
7911 Sharma Ghimire, P., Tripathee, L., Zhang, Q., Guo, J., Ram, K., Huang, J., Sharma, C.M., Kang,
7912 S., 2019. Microbial mercury methylation in the cryosphere: Progress and prospects. Sci.
7913 Total Environ. https://doi.org/10.1016/j.scitotenv.2019.134150
7914 Skyllberg, U., Westin, M.B., Meili, M., Björn, E., 2009. Elevated concentrations of methyl
7915 mercury in streams after forest clear-cut: A consequence of mobilization from soil or new
7916 methylation? Environ. Sci. Technol. 43, 8535–8541. https://doi.org/10.1021/es900996z
7917 Sommar, J., Feng, X. B. and Lindqvist, O. (1999) 'Speciation of volatile mercury species present
7918 in digester and deposit gases', Applied Organometallic Chemistry, 13(6), pp. 441–445.
7919 Steffen, A., Bottenheim, J., Cole, A., Ebinghaus, R., Lawson, G., Leaitch, W.R., 2014.
7920 Atmospheric mercury speciation and mercury in snow over time at Alert, Canada. Atmos.
7921 Chem. Phys. 14, 2219–2231. https://doi.org/10.5194/acp-14-2219-2014
7922 St. Louis VL, Derocher AE, Stirling I, Graydon JA, Lee C, Jocksch E, et al. Differences in
7923 mercury bioaccumulation between polar bears (ursus maritimus) from the Canadian high-
7924 and sub-arctic. Environmental Science and Technology 2011; 45: 5922-5928.
7925 St. Pierre KA, St. Louis VL, Kirk JL, Lehnherr I, Wang S, La Farge C. Importance of open
7926 marine waters to the enrichment of total mercury and monomethylmercury in lichens in the
7927 canadian high arctic. Environmental Science and Technology 2015; 49: 5930-5938.
7928 St Pierre, K.A., Zolkos, S., Shakil, S., Tank, S.E., St Louis, V.L., Kokelj, S. V., 2018.
7929 Unprecedented Increases in Total and Methyl Mercury Concentrations Downstream of
7930 Retrogressive Thaw Slumps in the Western Canadian Arctic. Environ. Sci. Technol. 52,
7931 14099–14109. https://doi.org/10.1021/acs.est.8b05348
7932 Soerensen, A. L. et al. A mass budget for mercury and methylmercury in the Arctic Ocean.
7933 Global Biogeochem. Cycles 30, 560–575 (2016).
7934 Tsui, M.T.K., Finlay, J.C., 2011. Influence of Dissolved Organic Carbon on Methylmercury
7935 Bioavailability across Minnesota Stream Ecosystems. Environ. Sci. Technol. 45, 5981–5987.
7936 https://doi.org/10.1021/es200332f
7937 Ukonmaanaho, L., Starr, M., Kantola, M., Laurén, A., Piispanen, J., Pietilä, H., Perämäki, P.,
7938 Merilä, P., Fritze, H., Tuomivirta, t., Heikkinen, J., Mäkinen, J., Nieminen, T.M. 2016.
7939 Impacts of forest harvesting on mobilization of Hg and MeHg in drained peatland forests on
7940 black schist or felsic bedrock. Environmental monitoring and assessment, 188(4), 1-22. DOI
7941 10.1007/s10661-016-5210-x
7942 Van der Velden S, Evans MS, Dempson JB, Muir DCG, Power M. Comparative analysis of total
7943 mercury concentrations in anadromous and non-anadromous Arctic charr (Salvelinus
7944 alpinus) from eastern Canada. Science of the Total Environment 2013; 447: 438-449.
7945 Van der Velden S, Dempson JB, Evans MS, Muir DCG, Power M. Basal mercury concentrations
7946 and biomagnification rates in freshwater and marine food webs: Effects on Arctic charr

(Salvelinus alpinus) from eastern Canada. Science of the Total Environment 2013; 444: 531-542.

Walvoord, M.A., Voss, C.I., Ebel, B.A., Minsley, B.J., 2019. Development of perennial thaw zones in boreal hillslopes enhances potential mobilization of permafrost carbon. Environ. Res. Lett 14, 15003. https://doi.org/10.1088/1748-9326/aaf0cc

Wang, F., Pucko, M., Stern, G. 2017. Transport and transformation of contaminants in sea ice. Chapter 19, Sea Ice, Third Edition. Edited by David N. Thomas. John Wiley & Sons, Ltd.

Wang K, Munson KM, Beaupré-Laperrière A, Mucci A, Macdonald RW, Wang F. Subsurface seawater methylmercury maximum explains biotic mercury concentrations in the Canadian Arctic. Scientific Reports 2018; 8.

Wang, X., Luo, J., Yuan, W., Lin, C.-J., Wang, F., Liu, C., Wang, G., Feng, X., 2020. Global warming accelerates uptake of atmospheric mercury in regions experiencing glacier retreat. Proc. Natl. Acad. Sci. 201906930. https://doi.org/10.1073/pnas.1906930117

Yang, Z., Fang, W., Lu, X., Sheng, G.P., Graham, D.E., Liang, L., Wullschleger, S.D., Gu, B., 2016. Warming increases methylmercury production in an Arctic soil. Environ. Pollut. 214, 504–509. https://doi.org/10.1016/j.envpol.2016.04.069

* This is Chapter 5 of the AMAP Mercury Assessment*

5. How does climate change influence mercury in the Arctic environment and in biota?

Leads: Melissa McKinney and John Chételat

Contributors: Marc Amyot, Ashu Dastoor, Thomas A. Douglas, Kyle Elliott, Kim Fernie, Lars-Eric Heimbürger-Boavida, Magali Houde, Jane Kirk, Derek Muir, Ville Junttila, Kimmo Kahilainen, Robert Letcher, Jaakko Mannio, Adam Morris, Nicolas Pelletier, Heli Routti, Henrik Skov, Kyra St Pierre, Liisa Ukonmaanaho, Jussi Vuorenmaa, David Yurkowski

NOTES

- Sections 2a&b, and section 5 still lack content
- The chapter is long (text ~20,000 words). Sections will be edited to reduce length and improve clarity; aiming for brief but comprehensive text.
- There is content that needs to be re-organized (moved to different sections or chapters).
- Figures for the chapter still need to be developed.

Table of Contents

5.1. Introduction

Contributors: John Chételat, Melissa McKinney, Tom Douglas

Global climate change is most pronounced in the Arctic, where surface air temperatures have risen at more than twice the rates elsewhere due to Arctic amplification (Serreze and Barry, 2011). The Paris Accord's stated goal is to limit temperature rise to no more than 2°C (https://unfccc.int/process-and-meetings/the-paris-agreement/the-paris-agreement), and the Intergovernmental Panel on Climate Change (IPCC) SR-15 report suggested further limiting the increase to just 1.5°C rise would reduce multiple impacts of climate change (Bindi et al 2018), yet Arctic temperatures have already risen by more than 2°C (IPCC 2013). Arctic warming is also projected to continue to increase faster than the global mean under future scenarios (IPCC 2013). Resulting physical changes to the Arctic environment are marked: reductions in sea ice extent and thickness, dramatic loss of multiyear ice, a decreased length of ice season in seasonal ice regions, retreating mountain and tidewater glaciers, permafrost thaw and thermokarst development, an altered seasonal snow cover, and increased river runoff and altered nutrient availability (Post et al., 2009; Perovich and Richter-Menge 2012; Bintanja et al., 2017; Box et al., 2019). In lockstep with these cryospheric changes, extensive ecological changes have been documented including increased marine primary production, reduced population sizes of some ice-dependent species, northward range shifts of sub-Arctic and temperate marine and terrestrial species, and altered trophic structuring. (Post et al 2009, 2013, Fossheim et al 2015, Pecl et al 2017). These physical and ecological changes to Arctic ecosystems are likely to have consequences for the long-term cycling and bioaccumulation of mercury (Hg) (Stern et al. 2012).

A paragraph here on how the Arctic is unique because of its' strong seasonality, how that is changing, the altered timing of shoulder seasons like melt and freezeup and what that means for the source, fate, deposition, or migration of Hg. (moved from below): Recent manifestations of climate change vary within the circumpolar Arctic including regional differences in warming and altered snow cover (AMAP 2017). Similarly, climate change is affecting ecological processes on multiple temporal scales, from lengthening of the Arctic growing season (Ernakovich et al. 2014) to continued multi-decadal declines of sea ice and glacier extent (AMAP 2017). Since the last AMAP mercury assessment released in 2011, environmental change in the Arctic has continued to accelerate, and a clearer picture is emerging of the profound shifts in climate and the cryosphere (AMAP 2019, Box et al. 2019, Saros et al. 2019).

Effects of climate-driven environmental change on Hg cycling in the Arctic are complex and interactive because of potential alterations to multiple processes including Hg transport (St. Pierre et al. 2018, Zdanowicz et al. 2018), transformations such as methylmercury (MeHg) production (Yang et al. 2016, MacMillan et al. 2015), biological uptake of MeHg (Poste et al. 2019, Hudelson et al. 2019),

and its transfer through food webs (McKinney et al. 2017, Braune et al. 2014). The environmental change that is currently underway in the Arctic may be unique to particular environments, and therefore, consideration of effects specific to marine, freshwater, or terrestrial ecosystems is warranted. For example, the loss of multi-year sea ice in the marine environment is having profound ecological effects (Post et al. 2013), many of which are not relevant to Arctic freshwater lakes. Further, geographic scope and temporal scale need to be considered in an assessment of climate change impacts on Hg cycling.

This chapter presents an assessment of current evidence for climate change influences on Hg in the Arctic environment and in biota. First, a brief summary is provided on what is known about climate change effects on the physical and ecological processes within Arctic marine, freshwater, and terrestrial ecosystems. Then, the science on connections between physical or ecological changes and the environmental and biological fate of Arctic Hg is integrated to address two key questions: (1) What are the key abiotic and biotic changes currently affecting Arctic Hg?, and (2) How will a projected future warmer climate alter levels of Hg in the Arctic environment and its biota? This chapter draws on climate-related temporal trends of Hg bioaccumulation that were analyzed in chapter 2, as well as the synthesis of processes affecting Arctic environmental Hg in chapters 3 and 4. Finally, conclusions and recommendations for future evaluation of climate change impacts on Hg are provided.

5.2 How has climate change affected the physical and biogeochemical characteristics of Arctic environments?

a. Atmosphere

Contributor: Tom Douglas

Some papers to integrate:

- Bintanja R, Selten FM. Future increases in Arctic precipitation linked to local evaporation and sea-ice retreat. Nature. 2014 May;509(7501):479.
- Cole AS, Steffen A, Pfaffhuber KA, Berg T, Pilote M, Poissant L, Tordon R, Hung H. Ten-year trends of atmospheric mercury in the high Arctic compared to Canadian sub-Arctic and mid-latitude sites. Atmospheric Chemistry and Physics. 2013 Feb 7;13(3):1535-45.
- Friedman CL, Zhang Y, Selin NE. Climate change and emissions impacts on atmospheric PAH transport to the Arctic. Environmental science & technology. 2013 Dec 9;48(1):429-37.
- Handorf D, Jaiser R, Dethloff K, Rinke A, Cohen J. Impacts of Arctic sea ice and continental snow cover changes on atmospheric winter teleconnections. Geophysical Research Letters. 2015 Apr 16;42(7):2367-77.
- Kopec BG, Feng X, Michel FA, Posmentier ES. Influence of sea ice on Arctic precipitation. Proceedings of the National Academy of Sciences. 2016 Jan 5;113(1):46-51.
- There is also the polar regions chapter (Ch. 3) in https://www.ipcc.ch/srocc/
- Or https://www.ipcc.ch/report/ar5/wg2/polar-regions/
- Overland and Wang, 2016
- Notes (Melissa): More precipitation as rain and less as snow (belongs in atmosphere section?), reductions in extreme cold events and small increases in extreme warm events (SWIPA 2017). Likely increases in rain-on-snow (freezing rain) events (Hansen et al 2014). Changes in storm events may occur, and a northward shift in storm tracks in the North Atlantic may be occurring (Collins et al 2013)

b. Marine environments

Contributors: **Lars Eric Heimbürger-Boavida**, Melissa McKinney

(Melissa) The Arctic is particularly sensitive to global climate change, with profound changes documented across marine, terrestrial and freshwater realms. The recent Snow, Water, Ice, and Permafrost in the Arctic (SWIPA) Report concluded that the climate in the Arctic is moving towards a new state, and that enhanced efforts to control greenhouse gas emissions would reduce further loss, but that the system will not return to earlier conditions during the course of this century (AMAP,

2017). The enhanced susceptibility to warming in this region is refered to as Arctic amplification and a positive feedback loop connected to sea ice loss is thought to be largely responsible (Serreze and Barry, 2011). That is, decreased ice cover means more open water, which better absorbs solar radiation, which in turn leads to higher temperatures and further reductions in ice cover (Pistone et al., 2014; Screen and Simmonds, 2010). In fact, sea ice loss, as documented by satellite records over the past four decades, has been identified as one of the most noticeable indications of GCC thus far (IPCC, 2013). There is much interannual variability in sea ice extent, but overall declining trends since 1979, which are projected to continue. Declines in extent are significant in all months of the year, and estimated at -0.4 and -0.9 million km^2 per decade in winter (March) and summer (September), with some evidence of small recent accelerations in ice loss (SWIPA 2017). The declines are also found across nearly all regions, but show regional variability in magnitude, with the Beaufort and Chukchi seas showing the greatest reductions (SWIPA 2017). The Arctic Ocean is expected to become seasonally ice free in the coming decades, with some estimates suggesting as early as the next decade (2030s) (SWIPA 2017).

(Melissa) In addition to changes in extent of sea ice/open water, there have also been changes in sea ice thickness, multiyear ice, ice timing, distribution, mobility, and snow depth over the ice. Sea ice thickness and volume over the Arctic basin have declined by two-thirds from the 1980s to 2010s (Overland and Wang 2013; Lindsay and Schweiger 2015). After 2005, sea ice in the Arctic switched from predominantly multi-year cover, to coverage dominated by annual ice (AMAP SWIPA 2017). The ice-covered season is becoming shorter, with earlier melt onset and later freeze-up (Barber et al 2015). The drift speed of sea ice has increased by around 10% per decade related to a weaker ice pack being more susceptible to increases in wind speeds (1-2% per decade) (Vihma et al. 2012). Likely due to later formation of sea ice in the fall, snow depth on the sea ice has shown consistent declines (Webster et al 2014), with possible connections to rising proportions of first-year ice.

(Melissa) Additional shifts in the marine environment have been recorded related to ocean temperatures and circulation, freshwater fluxes, and sea levels. Along with warming surface air temperatures in the Arctic, sea surface temperatures have generally increased (Chukchi, Kara, East Siberian, and Laptev, but not Barents) (Timmermans and Proshutinsky 2014), and so have waters at lower depths, due to warmer waters entering from the North Atlantic and North Pacific (AMAP SWIPA 2017). Increased river discharge and melting glaciers have led to a 50% increase in freshhwater flux in less than two decades off south Greenland (Bamber et al 2012). Because salinity is an important driver of ocean currents, this increased flux has been suggested to have played a role in recently observed reductions in the Atlantic Meridional Overturning Circulation (Ramstorf et al 2015).

(Melissa) Other aspects to cover:
- sea level rise
- seasonality of changes. also note that it is the colder times (night, winter) that are warming the most.
- extreme weather –sea ice protected the region from storms?
- increased iceberg discharge (Bigg et al 2014)

(Lars-Eric) It is difficult to find evidence for change in seawater Hg species composition due to the lack of observations. Wang et al. 2012 provided first off-shore data on the Canadian Arctic Archipelago. Heimbürger et al. 2015 provide the first 4 profiles in the central Arctic Ocean (2011 cruise). Both studies find a surface enrichment in total Hg and a shallow total MeHg peak at the lower halocline (200m-depth compared to 1000m in the Northatlantic), which might be responsible for the high biota Hg levels in the Arctic. The GEOTRACES programme organized the first pan-Arctic survey with 2 Canadian (2015 CAA & Labrador Sea, Wang et al. 2018), 2 German (2015 central Arctic, 2016 Fram Strait; Petrova et al. in review) and 1 American cruise (2015 central Arctic; Agather et al., 2019, Dimento et al., 2019). The new Hg species data is comparable to the 2011 observations and includes now dimethylHg. It is not surprising to see no difference 5 years later because the expected changes are little (Soerensen et al., 2016) and require longer observation series.

Perspectives:

- Reduced sea ice extent and thickness will allow more sea-air exchange of gaseous Hg species
- Reduced sea ice extent will promote photochemical reactions (Point et al. 2009)
- Loss of MYI will impact MeHg budget
- More stratification may further enhance shallow MeHg peak
- Changes in phytoplankton abundance and species might affect MeHg peak (Heimbürger et al. 2010)
- Changes in particle export flux (the only mechanism to remove Hg from the ocean) are expected and will impact the Hg budget and species (Tesan et al. in review)

c. Terrestrial environments

Contributors: **Tom Douglas**, John Chetelat

Arctic amplification is causing enhanced warming in Earth's Polar Regions compared to lower latitudes (Screen and Simmonds, 2010; Serreze et al., 2011) This is leading to profound physical changes in Arctic terrestrial environments. Of particular relevance to Arctic terrestrial mercury processes include a longer summer growing season (Tagesson et al., 2012), changing precipitation patterns with an increase in summer (wet) precipitation (Zhang et al., 2013; Bintanja and Andry,

2017), an altered seasonality (Vihma, 2014), and increasing instability of the cryosphere, particularly permafrost thaw (AMAP 2017, 2019). Total annual precipitation is increasing, such as in coastal Greenland where meteorological observations are available for the period since 1890 (Mernild et al. 2015) and more broadly across the Arctic in recent decades (Box et al. 2019). Currently, much of the Arctic's annual precipitation falls as snow, which is released from terrestrial environments during spring melt. Climate modelling predicts a long-term shift towards precipitation predominantly in the form of rain instead of snow during the 21st century (Bintanja et al. 2017), and the frequency of freezing rain and rain-on-snow events are increasing (Hartman et al. 2013, Liston and Hiemstra 2011). Snow cover duration is decreasing, with a trend in earlier onset of snowmelt in spring (AMAP 2017). Further, warmer temperatures are contributing to altered watershed hydrology, with greater streamflow in winter (Spence et al. 2014, Dery et al. 2009). These shifts in the water cycle are may be significant for mercury cycling, given the critical role of water in the transport of mercury within the Arctic.

For soild and ecosystem processes the largest change in the Arctic attributable to rising temperatures is an increase in permafrost thaw degradation and the melting of land ice (Liljedahl et al., 2016). Permafrost is warming around the circumpolar Arctic (Biskaborn et al. 2019), which is leading to the formation of thermokarst features on the landscape such as sinkholes and thermokarst lakes (AMAP 2017). For example, Lewkowicz and Way (2019) found, using satellite imagery, a 60-fold increase in retrogressive thaw slumps (large catastrophic thaw features) on Banks Island (Northwest Territories, Canada) between 1984 and 2015. The destabilization and slumping of permafrost is releasing sediment to downstream lakes and waterways as well as to the Arctic Ocean from coastal erosion (Lewkowicz and Way 2019, Kokelj et al. 2015, Lantuit and Pollard 2008). Thermokarst responses to climate warming are not uniform, however, and vary regionally within the circumpolar Arctic in relation to local landscape factors (AMAP 2017).

The greatest stores of land ice (e.g., glaciers, ice sheets, ice caps, ice fields) are in Greenland, the Russian Arctic, the northern Canadian Arctic, and Alaska, and all regions are losing ice mass at an accelerating rate due to anthropogenic climate warming (Box et al., 2018, AMAP 2017, 2019). Melting Arctic land ice is contributing to sea level rise, and transporting nutrients, particulates, and contaminants to downstream freshwater and marine environments (Sondergaard et al. 2015, Zdanowicz et al. 2018, Anderson et al. 2018). Together, these large-scale changes in the terrestrial cryosphere have important implications for mercury cycling and transport in the Arctic.

A recent study establishing Hg stocks in permafrost soils calculates that permafrost stores twice as much Hg as all other soils, the oceans, and the atmosphere combined (Schuster et al., 2018). The study establishes mean and median values for thousands of permafrost soils which allows for

identification of potential hot spots of elevated Hg in different regions or types of soil. The upper 0 to 1 m of soils typically have lower concentrations than soils from 1 to 3 m depth. Schuster et al. (2018) provide maps of total Hg in Northern Hemisphere permafrost soils, however, no clear patterns exist to establish whether specific types of permafrost or unique locations in the Arctic have statistically significantly elevated Hg stores. Clearly more studies need to be done to establish whether permafrost Hg hot spots exist and to identify potential pathways of the Hg cycle in high latitude coils that could promote the transport or accumulation of Hg. From this a better projection can be made of what permafrost Hg is most vulnerable to liberation if/when permafrost thaws.

Add Schuster et al. Figure 3 of N. hemisphere Hg stores?

Uncited key reference:

Bring, A.; Fedorova, I.; Dibike, Y.; Hinzman, L.; Mård, J.; Mernild, S. H.; Prowse, T.; Semenova, O.; Stuefer, S. L.; Woo, M. K., Arctic terrestrial hydrology: A synthesis of processes, regional effects, and research challenges. J. Geophys. Res. Biogeosci. 2016, 121, (3), 621-649.

Loranty MM, Abbott BW, Blok D, Douglas TA, Epstein HE, Forbes BC, Jones BM, Kholodov AL, Kropp H, Malhotra A, Mamet SD. Reviews and syntheses: Changing ecosystem influences on soil thermal regimes in northern high-latitude permafrost regions. Biogeosciences. 2018 Aug 31;15(17):5287-313.

d. Freshwater environments

Contributors: **Kimmo Kahilainen**, Kyra St Pierre, John Chetelat, Jussi Vuorenmaa, Liisa Ukonmaanaho

Number of freshwater systems:

(K.S.) Changes to the hydrological cycle in response to Arctic warming have had important implications for the number of lakes and ponds dotting Arctic tundra landscapes. While the number of lakes and ponds may be increasing downstream of retreating glaciers (Stokes et al. 2007, Milner et al. 2017), increasing evaporation and thermokarst evolution has led to dramatic declines in the number and surface area of lakes and ponds in non-glacierized regions (Carroll et al. 2011, Finger Higgins et al. 2019).

(J.C) Watershed geomorphology can play a role in recent changes to water surface area, which appear to be regional in nature within the Arctic (Carroll et al. 2018). Water surface area has increased in parts of Alaska with warming lowland permafrost (Pastick et al. 2018) while it has decreased in lakes

of the Northwest Territories that are situated on bedrock and likely isolated from groundwater (Carroll et al 2018).

Ice cover and lake surface temperatures:

In Arctic environments, ice up to two metres thick can cover lakes for as much as ten months of the year and is a critical feature regulating the physics, chemistry and biology of these ecosystems. With warming, lake ice melt and the day at which complete lake ice melt occurs has been happening earlier in the summer (Surdu et al. 2016), and the onset of lake ice formation has been delayed (Lehnherr et al. 2018), trends which are predicted to continue into the future (Brown and Duguay 2011). These shifts in ice phenology have occurred in concert with the warming of surface waters during the summer months (O'Reilly et al. 2015). The loss of lake ice over a longer period has the potential to increase light availability in, as well as atmospheric deposition to, surface waters, with implications for biological productivity, carbon processing (Cory et al. 2014) and contaminant cycling there (Outridge et al. 2007).

Fennoscandian hydrology:

(Jussi Vuorenmaa) Long-term hydrological records of ice phenology from subarctic region of Finland show clear changes in the winter and spring climatic seasonal conditions (Korhonen, 2019). The ice seasonality (dates of ice freeze and break-up) from River Tornionjoki, which is a border river between northern Sweden and Finland, has been recorded since 1693 i.e. over the past 300 years, thus providing empirical evidence for the centuries timescale climatic changes and variations in the northern latitudes (Korhonen 2006; Sharma et al., 2016; Korhonen 2019). It has been asserted that break-up dates are even better climatic indicators than the air temperature itself (e.g. Livingstone, 1997). The trend towards earlier break-ups in 1693–2002 was 4.3 days per 100 years (Korhonen, 2006), but trend has become stronger during the past two decades, being 4.65 day per 100 years between 1693–2018 (Korhonen, 2019). The prevalence of extreme events, defined as extremely warm springs with ice-break dates prior to calendar day 124 (early May), has also been increasing. The River Tornionjoki experienced nine extreme events in the 14-year period between 2000–2013 and 10 in the 207-year period between 1693–1899, also suggesting that trend towards earlier break-ups has become stronger in the 21st century (Sharma et al. 2016). Corresponding trend has been reported elsewhere in Arctic rivers (Cooley and Pavelsky, 2016). The effect of climate warming has also been reported by parallel data of air temperature and ice seasonality for the River Tornionjoki between 1802–2002, which show clear correspondence between river ice break-up dates and spring temperatures (Helama et al., 2013).

Significant long-term trends towards earlier break-ups, later freeze-ups and shorter durations of ice cover have been reported also for larger subarctic lakes in Finland (Korhonen, 2002). The average

trends between 1885–2002 for earlier breaks-up, later freeze-up and shorter duration of ice cover were 7.5, 4.6, and 12.8 days per 100 years, respectively. Similarly, with subarctic and Arctic rivers, lakes in northern Finland and elsewhere in Arctic have shown stronger trends towards earlier break-ups, later freeze-ups and shorter ice cover periods in the 21st century than earlier (Lei et al. 2012; Šmejkalová et al., 2016; Korhonen, 2019). Climate change has also affected to maximum ice thickness in large Finnish subarctic lakes. Records since early 1950s until 2000/2002 showed general increasing trend in maximum ice thickness, but since then increasing trends have disappeared (Korhonen, 2006, 2019). Corresponding trend analysis for the period 1971–2016 showed significant decrease in maximum lake ice thicknesses (Korhonen and Koskela, 2017).

Climate change has affected to seasonal distribution and long-term trend pattern of river discharge in North Finland, which have a large effect on northern hydrology (Korhonen and Kuusisto, 2010; Veijalainen et al. 2012; Korhonen, 2019). Long-term records of discharge between 1911–2004 showed increases in winter and spring discharges, which were focused on late winter and early spring, respectively, suggesting that trends can be accounted for by the warming of winter and spring and the earlier snowmelt (Korhonen and Kuusisto, 2010). These seasonal trends have become even stronger when data was extended until 2017 (1911–2017), due to the increasing number of mild winters during the 2000s and 2010s (Korhonen, 2019). Results of simulated future changes in discharges on annual and seasonal scales for northern rivers in Finland between 1911–2099 showed that consistently in different climate scenarios, seasonal changes, most importantly the increases in winter and spring discharge, are anticipated in the future (Veijalainen et al., 2012).

Lake thermal stratification:

(J.C) Arctic lakes tend to remain well-mixed or weakly stratified during the open-water season (Vincent et al. 2009, Priet-Mahao et al. 2019). With rising temperatures, warmer waters and a longer ice-free period, thermal stratification patterns in lakes are expected to change by strengthening of the temperature gradient in the water column and lengthening the stratification period (Gebre et al. 2014, Prowse et al. 2006). Little information is available, however, on the extent that thermal stratification patterns are changing in Arctic lakes, likely because few long-term high-frequency measurements are available for lake water columns. However, recent studies in Greenland indicate that warming and processes which affect water transparency are likely to affect lake stratification (Saros et al. 2016, Cadieux et al. 2017). These shifts in water column mixing are important because thermal stratification has a major influence on the biogeochemistry of lakes.

Organic matter and solute loading:

DOC loading:

(Jussi Vuorenmaa, Liisa Ukonmaanaho, Kimmo Kahilainen) Increasing leaching of dissolved organic matter (DOM) from terrestrial catchments, often estimated by dissolved organic carbon (DOC), has been detected from boreal to Arctic regions (Monteith et al., 2007; Garmo et al., 2014, deWit et al. 2016; Räike et al. 2016, Wauthy et al. 2018), resulting in widespread browning of lakes and rivers. A trend assessment from almost 500 lakes, rivers and streams in Norway, Sweden and Finland showed largest trends in boreal region, but significant long-term increase in concentrations of DOC has been common also in subarctic freshwaters (de Wit et al., 2016). Browning in the 1990s and early 2000s has been attributed dominantly to improved air chemistry i.e. substantially decreased acid sulphate deposition and variations in sea-salt deposition, acting through chemically-controlled organic matter solubility in catchment soils (de Wit et al., 2007; Monteith et al., 2007; Evans et al., 2012; Oulehle et al., 2013; Valinia et al., 2015). Recently, changes in climatic conditions, such as increased precipitation and discharge, are exerting greater influence on variation and increasing DOC concentrations in surface waters (Räike et al., 2012; de Wit et al., 2016; Zwart et al., 2017). Increased vegetation i.e. greening of catchments, intensive land-use (e.g. forestry activity and peat mining) and elevated run-off will jointly increase DOC in subarctic Fennoscandian watercourses (Finstad et al. 2016; Räike et al. 2016). Forestry is the most important land-use form in southern part of subarctic Finland and intensive forestry practises have influence on DOC and mercury flows from catchments to watercourse (Box XX; case study). In addition to direct effect of changes in hydrological regimes, climate change has been observed to browning lakes in Arctic and subarctic regions through thawing of permafrost and deepening of active layer thickness, introducing more DOM to freshwaters (Vonk et al., 2015; Wauthy et al., 2018) and increasing organic carbon (OC) export in large Arctic rivers (Mu et al., 2018). On the other hand, declining concentrations of DOC throughout 2000s have been observed in Arctic lakes in Greenland (Saros et al., 2015). Nevertheless, many studies have addressed various aspects of DOM in Arctic rivers (Cory et al., 2014; O'Donnell et al., 2016; Kaiser et al., 2017) and lakes (Cory et al., 2014; Osburn et al., 2017; Jiang et al., 2020), and reported that DOM derived from terrestrial environments is abundant and widely distributed in Arctic surface waters.

<<<<<<<<<<<<<<<<<<<<<<<<<<<<<<<<<<<<<<<<<<<<<<<<<<<<<<<<<<<<<<<<<<<<<<<

BOX XX.

Case study: Forest harvesting impact on mobilization of mercury and methylmercury in peatland forests. (Liisa Ukonmaanaho, Luke)

Wetlands, which include mix of peatlands as well rivers, lakes and shallow bays, are the main ecosystem type in the Arctic region covering up to 60% of the total surface area (Ramsar 2014). Wetlands are also important storage of the mercury (Hg), which has accumulated to the soil and sediments during centuries. Mercury has a strong affinity to organic substances and therefore organic soils play an important role in mobilization and transport of Hg from the soils to the water bodies.

Furthermore, peatlands, which are organic soils have typically, high ground water level which creates anoxic conditions, promoting Hg methylation to methylmercury (MeHg) (Grigal 2002). Soil disturbance such as forest harvesting may increase the mineralization of organic matter, mobilization of dissolved carbon (DOC) and runoff fluxes (Nieminen et al. 2015) and could therefore promote the exports of Hg and MeHg to the surface waters. If more intensified harvesting methods such as whole-tree harvesting with stump lifting (WTHs) is practiced, leaching of stored Hg and MeHg to recipient water bodies can potentially increase.

We studied impacts of intensified forest harvesting on the mobilization of Hg and MeHg in drained peatland forests in Northern Finland (Ukonmaanaho et al. 2016), study included eight peatland dominated small catchments. Study indicated that Hg concentrations in ditch water increased after intensified harvesting (WTHs) and stem only harvesting (SOH), however MeHg concentrations increased clearly only at the WTHs sites, indicating that stump lifting with soil disturbance increased MeHg leaching (Fig. 1). The higher MeHg concentrations were typical at the end of the summer when the soil was at its warmest, which is a great concern because of predicted climate warming. Results showed also that the annual Hg and DOC concentration in ditch water correlated positively (Fig. 2), suggesting that Hg is leaching is related to the DOC and organic matter leaching, which usually increase after soil disturbance. However, such correlation was not found between MeHg and DOC.

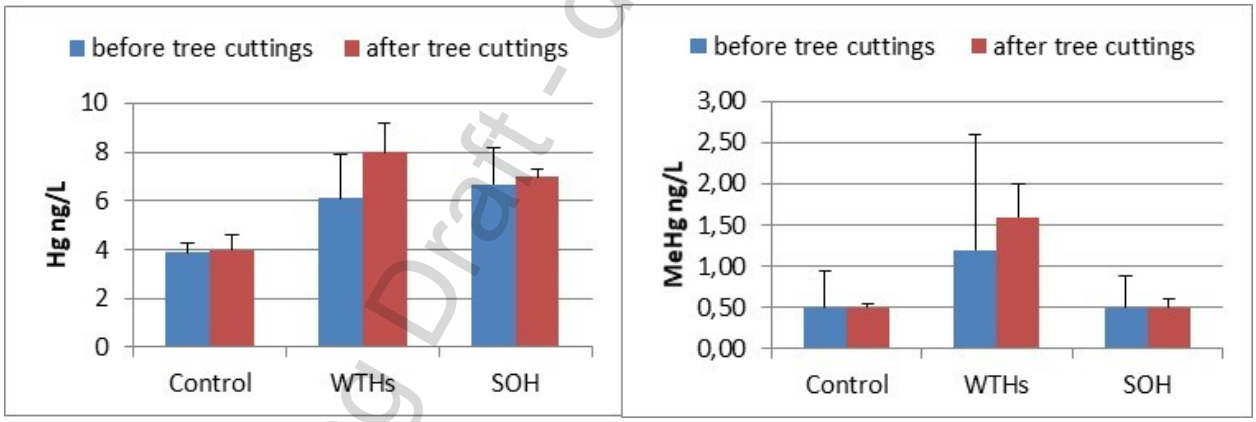

Fig. 1. Hg and MeHg concentrations before tree cuttings and after tree cuttings in two control, four whole-tree harvesting sites (WTHs) and two stem-only-harvesting (SOH) sites (2008-2012).

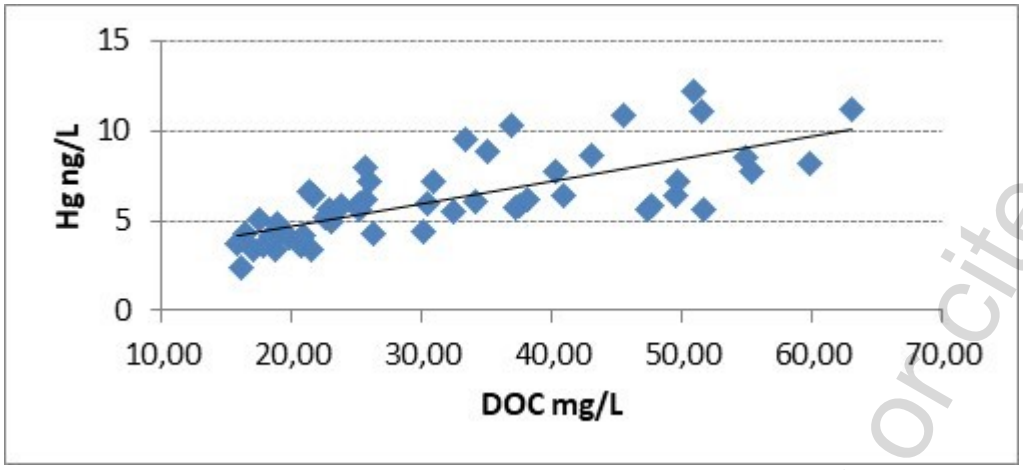

8421

8422 **Fig 2.** Correlation of DOC and Hg in ditch waters (r=0.72, p<0.05) (2008-2012).

8423

8424 Hg and MeHg load followed pattern of concentrations, although load is also depended on run-off and
8425 precipitation. Cumulative Hg and MeHg load indicated that both Hg and MeHg load increased more
8426 in treated sites than in control sites (Fig. 3). However, in case of MeHg there was only a slight
8427 difference in the load between control and stem-only harvested sites. Based on the results above it is
8428 possible that in a future warmer and more rainy subarctic area, as has predicted, mobilizing of Hg and
8429 MeHg from the soil will increase, especially in case of simultaneous forestry actions.

8430

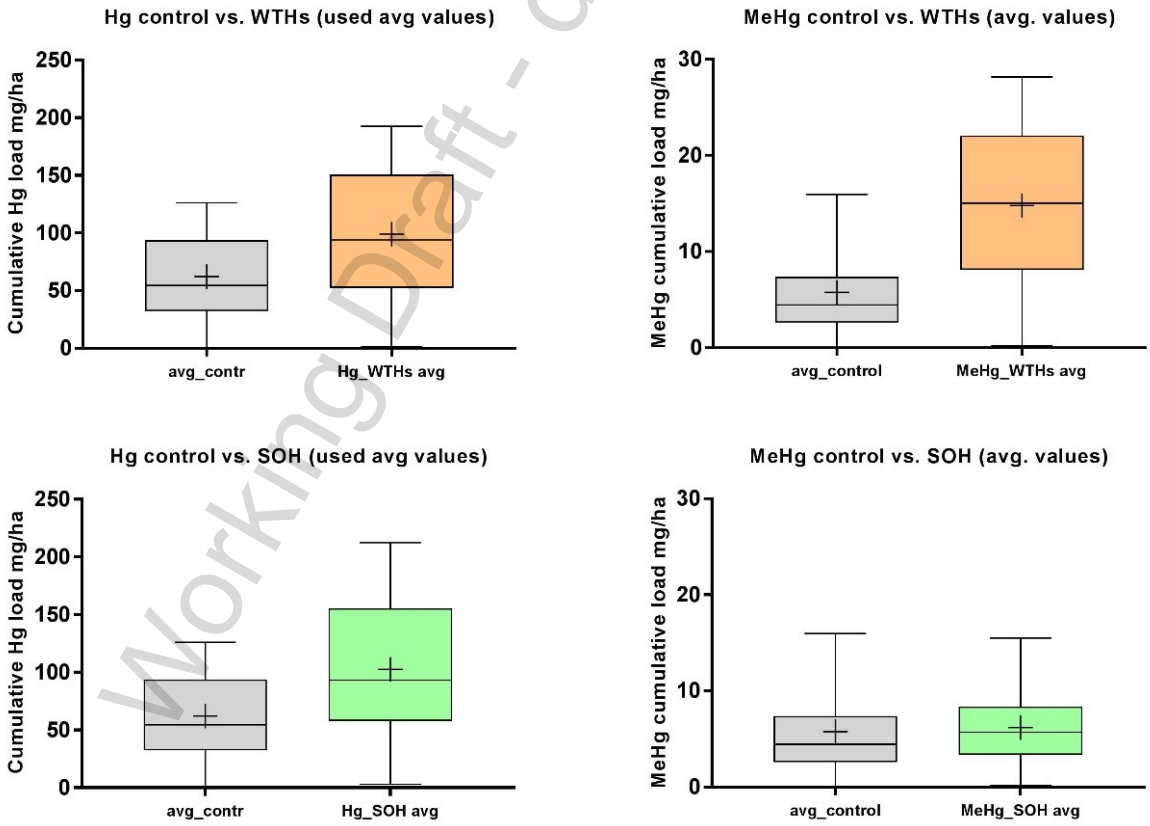

8431

Fig. 3. Cumulative average load of Hg and MeHg in ditch water (2008-2012), in control sites (n=2) and whole tree harvesting + stem lifting (WTHs) sites (n=4) and stem only harvesting (SOH) sites (n=2).

<<<<<<<<<<<<<<<<<<<<<<<<<<<<<<<<<<<<<<<<<<<<<<<<<<<<<<<<<<<<<<<<<<<<<<<<<<

Browning of surface waters from increasing terrestrial dissolved organic carbon (DOC) concentrations is a serious environmental concern e.g. in terms of biogeochemical mercury (Hg) cycling in Arctic and subarctic ecosystems. Organic matter (OM) as dissolved organic carbon (DOC) is the main transport vector for Hg and methylmercury (MeHg) from catchment soils to surface waters (Grigal, 2002). DOC is known to affect the Hg cycle in aquatic environments due to its overriding influence on complexation, photochemical, and microbial processes. Positive correlation between Hg and DOC concentration in water and biota is often observed, however DOC quality and age maybe important factor behind these correlations (Lescord et al. 2018; Poste et al. 2019). Arctic and subarctic lakes are often characterized by clear water with low DOC (Henriksen et al., 1997; Pienitz et al., 1997a,b; Lim et al., 2001; Forsström et al. 2015), but many of these systems are browning (Macdonald et al., 2005; Wauthy et al. 2018) that may add to the existing high Hg burdens. Browning of lakes is also known to enhance thermal stratification (Snucins et al., 2000), and thereby weaken aeration of hypolimnion and promoting anoxia (Couture et al., 2015), which is reported to enhance in-lake methylation of inorganic Hg and accumulation of MeHg to biota in small temperate and boreal lakes (Watras et al., 1995, Eckley et al., 2005, Rask et al., 2010, Verta et al., 2010). Climate change-induced browning of lakes and oxygen-related MeHg production in the hypolimnion and its bioaccumulation may be a concern also in northern lakes. Browning of lakes will shift primary production towards secondary bacterial production that is linked to elevated Hg levels in boreal watercourses (Forsström et al. 2013; Lescord et al. 2018). Furthermore, increasing DOC will decrease the penetration of UV-radiation in water column and reduce demethylation processes in surface water (DiMento & Mason 2017; Williamsson et al. 2019).

Soils in the Arctic and subarctic permafrost contain substantial reservoirs of OC (Tarnocai et al., 2009; Schuur et al., 2015) and Hg bound with organic matter (Schuster et al., 2018). Arctic and subarctic ecosystems are now undergoing rapid change due to climate warming, which has accelerated mobilizing of OC and Hg from soils to surface waters and will likely increase as permafrost thaws under predicted climate warming scenarios (Mu et al., 2018; Schuster et al., 2018). Northern Hemisphere permafrost soils contain nearly twice as much Hg as all other soils, the ocean, and the atmosphere combined. The turnover time associated with the microbial decay of frozen organic matter is ~14,000 years (Schuster et al., 2018), making the Hg locked in permafrost effectively stable on human time scales. However, projections indicate a 30–99% reduction in near surface permafrost by 2100, and, once thawed, the turnover time for microbial decay drops to ~70

8469 years (Koven et al., 2013; Schaefer et al., 2014), making stores of Hg in permafrost soils susceptible
8470 to release over the next century. There is a need to take Arctic permafrost regions in the global Hg
8471 cycle (Schuster et al., 2018).

5.3 How has climate change affected Arctic ecosystems?

a. Marine ecosystems

Contributor: **Kyle Elliott**

(Kyle) The Arctic Ocean and related water bodies make up about 4% of the Earth's surface. Arctic marine ecosystems are characterized by low primary productivity over much of the year when seas are covered by ice with a pulse in productivity in surface waters associated with sea ice melt in the late spring. Biodiversity of many taxa is low, especially under the multi-year ice of high latitudes, which especially limits breath-hold divers such as many birds and mammals. Many of taxa in Arctic ecosystems are pagophilic ('ice-loving') and require ice at least part of the year (Post et al. 2013). A variety of physical changes are impacting oceans worldwide, including increasing temperature, changing acidity and altered freshwater inputs; these changes are also occurring in the Arctic but, because of the importance of pagophilic species, responses to ice, unique to polar seas, often overwhelm other changes (Post et al. 2013).

Changes in arctic marine ecosystems in response to a changing climate will ultimately be responses to changes in physical processes listed in section 2b, but can be compounded by the emergent processes occurring in complex food webs (i.e. trophic cascades, food web topologies; Zarnetske et al. 2012). Thus, responses to climate change include both direct responses (thermal or acidity tolerance) and indirect responses (top-down, bottom-up and horizontal processes). Direct responses affect the fundamental niche, the range of possible environments in which the species can exist, leading to changes in species distributions. Indirect responses affect the realized niche, as biotic interactions often greatly reduce the actual niche possible for a species.

Perhaps the greatest direct impact of climate change on marine species is loss of ice. Pagophilic species require ice to survive, and their loss can have an impact on their population growth rates. For example, polar bears require ice to capture their preferred prey, ringed seal pups. Similarly, under ice algae require ice as a substrate to grow. Sea acidification can also directly impact species, especially calciferous benthic fauna. Finally, many Arctic animals may be unable to tolerate warmer waters. As most Arctic species are cold-adapted even relative 'cool' temperatures may be a challenge. For example, Arctic cod do not reproduce effectively in waters above about 4ºC. Similarly, thick-billed murres experience heat stress that are mundane for their more southerly congeners, with many dying from overheating in warm summers. Thus, a warmer, more acid, ice-free ocean may alter the fundamental niche of many Arctic species northwards.

Changing fundamental niches of predators can lead to complex bottom-up 'trophic surges' or temporal mismatches. For example, lack of under-ice algae, a preferred food of copepods, can lead to reduced populations of Arctic cod and consequently top predators that prefer cod (Gaston et al. 2003; Yurkowski et al. 2017, 2018). Indeed, reductions in accessible, sympagic Arctic cod are a common theme across the Arctic with reductions in Arctic cod in the diet of many marine predators; the cod may still be there but may be difficult to detect if they are not associated with readily visible ice (Gaston et al. 2003; Gaston & Elliott 2014; Divoky et al. 2015, 2016). The match-mismatch hypothesis is a classic mechanism for bottom-up regulation associated with climate change (Thomas et al. 2003). Marine ectotherms can respond rapidly to changes in temperature and phytoplankton availability (Gremillet et al. 2015; Amelineau et al. 2019). Marine endotherms, such as seabirds and marine mammals, often respond in a more complex fashion to a hormonal pathway closely tied to photoperiod. Thus, although the timing of ice-off has advanced by over a month in Hudson Bay, the timing of breeding of seabirds has only advanced by a few days. As a consequence, seabirds are nourishing their offspring after Arctic cod, their preferred prey, is no longer accessible, leading to smaller chicks (Gaston et al. 2009; Gaston & Elliott 2014; Divoky et al. 2015, 2016). Presumably these changes are also happening in other taxa that are more difficult to directly monitor.

In contrast to bottom-up regulation, top-down regulation occurs when enemies (predators or parasites) cause changes in prey populations. If these changes affect animal distributions at least two trophic levels below the predator, these changes are termed 'trophic cascades'. A classic example of such a cascade occurred in response to the 1977-2008 regime shift towards warmer waters in Alaska. Reduced sea lion populations (due to altered diet) caused killer whales to switch to eating sea otters. Fewer sea otters led to more sea urchins, less kelp, reduced rockfish populations and increased consumption of waterbirds by eagles (due to fewer fish available). Other examples of top-down regulation include (1) the punctuated arrival of killer whales in the Arctic during longer ice-free summers, with potential impacts on beluga and narwhale populations (Higdon & Ferguson 2011) and (2) increased polar bear predation on terrestrial food during the ice-free period. In the latter case, because the ice-free period now overlaps to a greater degree with seabird breeding, hungry polar bears are switching to feed on bird eggs, occasionally even eating adults (Gaston & Elliott 2013; Harwood et al. 2015; Divoky et al. 2015). In some cases, bears eat tens of thousands of birds, causing colony declines and dispersion into smaller colonies. Parasites can also cause top-down regulation, with the classic example being caribou migrations driven by avoidance of biting flies. Warm summers in recent years have increased black flies and mosquitoes in some regions, leading to reproductive failure by birds (Gaston & Elliott 2013). Thus, top-down effects from both predators and parasites are having strong impacts on Arctic marine ecosystems.

The various impacts have led to changes in species distributions, which is one of the most widely documented impacts of climate change on ecosystems (Post et al. 2009; Wassmann et al. 2011; Pecl et al. 2017). Sometimes such distributions include southerly invasive species moving north and outcompeting 'Arctic' species. For example, razorbills have moved into Hudson Bay following increased sand lance, leading to potential competition with 'native' seabirds. Increasingly, ecosystems are changing from benthic towards pelagic species, with energy flows becoming more pelagic. Food web link and length alterations likely vary among regions (Bartley et al. 2019). Ultimately, these changes lead to altered gene diversity and gene function, at both the species and population levels.

b. Terrestrial ecosystems

Contributor: **Heli Routti**

(Heli) Arctic tundra biome comprises about 5% of the Earth's terrestrial surface and the majority of it is located on coast within 100 km of seas seasonally covered by ice (Ims et al., 2013). The longevity of sea ice may thus have a strong influence on temperature and climate and consequently the productivity of Arctic tundra ecosystems (Bhatt et al., 2010). Terrestrial Arctic ecosystems are characterized by low primary productivity, which restricts the length and complexity of food webs and decomposer webs (Ims et al., 2013).

Responses of Arctic terrestrial ecosystems to climate change show generally large variation among areas, which is related to a large spatial variation in climate change itself (Ims et al., 2013). Most research has focused effects of climate change on one trophic level at a time. Both monitoring and experimental studies in the circumpolar Arctic suggest that both grass and grass-like plants and shrubs respond positively to warming and their abundance is likely to increase over time (Bjorkman et al., 2020; Elmendorf et al., 2012). Although some studies showed earlier leaf emergence and flowering with rising temperatures, there is no consistent responses in plant flowering or leaf emergence or senescence (Bjorkman et al., 2020). Lemmings are a key herbivores of Arctic tundra ecosystems due to their important role in transferring energy from plants to mammalian and avian predators (Gilg et al., 2003). Although climate warming has been documented to negatively affect low arctic lemming populations, which co-occur with boreal voles, there is no consistent global declining trend for lemmings in the Arctic (Ehrich et al., 2020). *Rangifer* subspecies, including reindeers and caribous are the most abundant large terrestrial herbivore of Arctic terrestrial ecosystems. Their large range from woodlands to the High Arctic indicates that they are able to cope with differing environmental conditions, which is also a possible source of resilience to climate change. Overall, studies focusing on effects of climate change on reindeer and caribou suggest that the responses are varied in across their circumpolar distribution (Mallory and Boyce, 2017). Contrasting responses may also occur at local scale. Warm spells and rain-on-snow events that entirely encapsulate short-growing vegetation

across large areas of high-Arctic tundra (Peeters et al., 2019) occur more and more frequently in the High Arctic (Bintanja and Andry, 2017). These events have been shown to negatively affect vital rates of high-arctic tundra herbivores and have further consequences on the abundance of arctic carnivores (Hansen et al., 2013). However, higher summer temperatures are also beneficial to reindeers. Net effects of climate change were negative to a coastal reindeer population and positive for a continental reindeer population (Hansen et al., 2019b). Also, behavioural changes and alternative use of landscape and food resources may buffer environmental change (Hansen et al., 2019a; Loe et al., 2016). For example, proportion of Svalbard reindeers feeding along the shoreline partly on kelp has increased along with icier winters (Hansen et al., 2019a). Relatively large changes have been observed in tundra bird populations. Opposing trends have been observed for waders and waterfowl at the circumpolar Arctic: over half of wader taxa are declining and almost half of all waterfowl are increasing (Smith et al., 2020). Peregrine falcon and gyrfalcon populations are generally stable (Franke et al., 2020), whereas ptarmigans population trends vary regionally (Fuglei et al., 2020).

Climate change has also been documented to affect structure and functioning of Arctic terrestrial food webs. A study on seven Arctic terrestrial food webs indicates that food webs are more complex and diverse and have stronger predation of small herbivores in warmer locations compared to colder locations (Legagneux et al., 2014). A study from Canadian High Arctic (Juhasz et al.) showed that reproduction of snow geese increased with increasing precipitation and temperature, whereas lemmings were not affected by local or regional climate. Arctic fox breeding success was also positively related to reproduction of snow geese. Harsher winter conditions decreased arctic fox breeding success likely through effects on their body condition and stress.

c. Freshwater ecosystems

Contributor: Kimmo Kahilainen

(Kimmo) Major impacts of climate change in Arctic region are related on strong increase of temperature and productivity in both terrestrial catchment and aquatic ecosystems (e.g. de Wit et al. 20 16; AMAP 2017). These joint effects have ubiquitous effects across ecosystems, communities, populations and individuals (e.g. Post et al. 2009; Scheffers et al. 2016; Rolls et al. 2017). Pronounced glacial melting will increase concentrations and seasonal exposure on suspended solids that has pronounced effects reducing light penetration, lowering temperature and increased conductivity (Lento et al. 2019). At the broad level, permafrost thaw and increasing rain will obviously bring more nutrients, carbon and catchment stored mercury into lakes and rivers (de Wit et al. 2016; AMAP 2017; Schuster et al. 2018; Lento et al. 2019). In streams, increased amount of terrestrial vegetation and dissolved organic carbon (DOC) will have shading effects limiting benthic algal production. In lakes increased DOC and nutrients will also have shading effects that are shifting benthic algae

fuelled food webs towards increasingly pelagic phytoplankton and bacterial energy driven systems (Forsström et al. 2013). In subarctic lakes, this shift could be even pronounced via pelagic-benthic coupling where increased pelagic phytoplankton production starts to settle over benthic habitats and subsequently start to fuel benthic consumers too (Hayden et al. 2019). Small and shallow lakes are reacting changes much faster than more resilient large and deep lakes with thermal refuges and volumetric buffer against abrupt changes to alternative state (Scheffer & Carpenter 2003; Hayden et al. 2019). Such shift towards pelagic energy fuelled food webs may elevate mercury accumulation (Power et al. 2002: Thomas et al. 2016).

In food web and community levels, warming will enhance range expansion of warmer adapted new species (Post et al. 2009; Rolls et al. 2017). Such effects can be very fast in taxa with high dispersal abilities via wind and waterbirds (plankton, benthic invertebrates, macrophytes), but dispersal of fish requires connectivity of watercourses or salt tolerance when colonizing Arctic islands (Laske et al. 2020; Lau et al. 2020). New colonizers often initially increase the links in food webs, but may also have strong competitive and predatory interactions with native fauna with potential alterations of energy and mercury flows in food webs (Hayden et al. 2014a; Thomas et al. 2016; Rolls et al. 2017). In primary producers, algal communities are likely change from diatom dominated fauna towards increasingly importance of blue-green algae and heterotrophic bacteria along increasing productivity potentially elevating basal mercury concentrations (Forsström et al. 2013; Taipale et al. 2016; Przytulska et al. 2017; Kozak et al. 2020). Increasing open-water period and temperature tend to favour short lived filter feeding cladocerans, such as *Daphnia* and *Bosmina*, zooplankton over the lipid rich and long lifecycle copepods especially in lake ecosystems (e.g. Hampton et al. 2017; Hayden et al. 2017). Shift towards cladoceran dominated zooplankton fauna (especially *Daphnia*) in lakes and ponds has been often related to elevated mercury levels (Chetelat & Amyot 2009). However, such shifts in zooplankton fauna in Arctic ponds are less evident as they often lack fish predators and pond food webs are governed by persistence e.g. water level in winter and summer (Rautio et al. 2011; Schartau et al. 2020). Freshwater fishes in Arctic often compose of generalist and cold-water adapted salmonid species (e.g. Arctic charr; *Salvelinus alpinus*, whitefish *Coregonus* spp.) using both pelagic and benthic resources based on their seasonal abundance influencing on mercury concentrations in muscle and liver tissues (e.g. Kahilainen et al. 2016; Keva et al. 2017). Both *Salvelinus* and *Coregonus* are prone to diverge into sympatric morphs (or subspecies) using different prey items ranging from zooplankton, benthic macroinvertebrates or fish that has clear effect on mercury content that often peaks in planktivorous or piscivorous morphs (Kahilainen et al. 2017; Braaten et al. 2020). Range expansions of warmer adapted species, such as percids, sticklebacks and cyprinids, are usually related to immigration of more specialized species and increasing share of pelagic reliant species those could elevate pelagic derived mercury (Hayden et al. 2017). There is also tendency that fish communities will change from autumn or winter spawning species (salmonids,

burbot; *Lota lota*) towards spring-spawning species (northern pike; *Esox lucius*, yellow perch; *Perca flavescens*, European perch; *Perca fluviatilis*, cyprinids) dominated lakes (Reist et al. 2006; Rolls et al. 2017). Furthermore, increasing temperatures are generally related to decreasing size, earlier maturation and shorter longevity in fish (Heibo et al. 2005; Blanck & Lamouroux 2007; Hayden et al. 2017). Many Arctic regions contain anadromous fish species (Arctic charr, lake trout, Dolly Varden), those are likely to retreat from warm southern regions or start to form stationary freshwater populations along increasing temperature and productivity (Finstad & Hein 2012). These stationary freshwater populations will usually have elevated mercury than anadromous populations (van der Velden et al. 2013; Braaten et al. 2020). Decreasing winter ice and snow in Arctic freshwaters could have negative effects on native fauna via range of abiotic and biotic effects those will likely to change year-round mercury dynamics in consumer tissues (Helland et al. 2011; Shuter et al. 2012; Hampton et al. 2017; Keva et al. 2017).

5.4 What influence has climate change had on Hg transport processes?

a. Atmospheric deposition

Contributors: Ashu Dastoor, Henrik Skov

(Ashu) The concurrent impacts of changes in climate, chemical composition, land-use, and primary and secondary mercury emissions on mercury temporal trends make it difficult to detect the influence of changes in anthropogenic emissions in observed temporal trends. Despite increases in global anthropogenic emissions over the past several decades (Streets et al., 2011), Arctic atmospheric Hg levels have decreased or remained constant (Cole and Steffen, 2010; Cole et al., 2013, Berg et al. 2013). Implications of climate change related factors such as rise in air temperatures (particularly in spring) and reduced sea ice extent and thickness to the mercury levels in the Arctic ecosystems are complex and multidirectional (Stern et al., 2012; Bekryaev et al., 2010; Cavalieri et al., 2012).

Fisher et al. (2013) investigated the factors controlling Hg(0) trends in the Arctic from 1979-2008 using global historical anthropogenic emissions inventory of Streets et al. (2011) using GEOS-Chem. The model simulated a small increasing trend in Hg(0) concentrations over 30 years mainly reflecting the growth in emissions. The model captured the springtime interannual variability in Hg(0) concentrations at Arctic sites with moderate skill and found it to be more significant compared to the temporal trend. The model reproduced the observed shift in minimum Hg(0) concentrations from May during 1995–2001 to April in 2002–2007 at Alert and attributed this shift to local cooling in April along with warming in May confirming Cole and Steffen (2010). However, shift in minimum Hg(0) concentrations at Alert was not found to be a characteristic of the Arctic as a whole. The study concluded that high temperatures and low sea ice fraction in spring decrease the frequency and intensity of AMDEs, while high solar radiation in spring enhances the photo-reduction and re-emission of Hg deposited to snowpack. During summer, the same environmental changes drive increased photo-reduction of Hg(II) in the ocean and enhanced evasion of Hg(0) to the atmosphere. Thus, Fisher et al. (2013) suggested that climate warming may lead to decreased fluxes of Hg from the atmosphere to the cryosphere and increased Hg(0) concentrations in the Arctic.

Chen et al. (2015) extended the study by Fisher et al. (2013) to quantitatively determine the contributions of changes in environmental variables (i.e., surface air temperature, sea surface temperature, sea ice fraction, sea ice lead occurrence, melting of multiyear sea ice, planetary boundary layer depth, net short wave radiation, surface wind speed, freshwater discharge, and net primary productivity) and anthropogenic emissions to Hg trends in the Arctic using anthropogenic emission inventories from AMAP/UNEP for the years 2000, 2005, and 2010. The model captured most of the seasonality in observed trends, especially the increasing trends in spring and fall; however, failed to

reproduce the increasing trends in July at Alert and in October at Ny-Ålesund. In addition to confirming the results by Fisher et al. (2013) in spring and summer, the study found that decrease in Atlantic ocean evasion of Hg at lower latitudes contributed to the decrease in Hg(0) concentrations in the Arctic from November–March.

Dastoor et al. (2015) assessed the impact of changing anthropogenic emissions and meteorology on Hg(0) concentrations and deposition in the Canadian Arctic from 1990-2005 using GEM-MACH-Hg and AMAP anthropogenic emissions (AMAP, 2011). Interannual variability in air concentration and deposition of Hg was found to be driven by interannual variability in meteorology. Changes in meteorology and anthropogenic emissions were found to contribute equally to the decrease in surface air Hg(0) concentrations in the Canadian Arctic with an overall decline of ~12% from 1990-2005 in agreement with measurements at Alert (Cole and Steffen, 2010; Cole et al., 2013). In contrast, the model simulated 15% increase and 5% decrease in net deposition in the High Arctic due to changes in meteorology and decline in emissions in North America and Europe, respectively, resulting in an overall increase of 10% in Hg deposition over a period of 1990-2005. Increasing regions of snowpack over first year sea ice led to a decreasing trend in mercury re-emission fluxes from snowpack which resulted in increased net Hg deposition in the model. Halogen-enriched snowpacks over first year sea ice supress reduction and re-emission of mercury from snow. Additionally, decrease in snow cover extent and a small increase in precipitation contributed to a small increase in deposition. Although the link between Hg deposition and lake sediment fluxes is not fully understood, an increase in deposition of mercury in the Arctic appears to be consistent with observed increases in Hg fluxes in some Arctic lake sediments in recent decades (Goodsite et al., 2013).

Despite modelling differences, all studies suggested a dominant role of climate warming related changes in environmental factors on Hg trends in the Arctic. Current mercury models lack a complete representation of the complexity of climate sensitive Hg processes. For example, Fisher at al. (2013) and Chen et al. (2015) did not consider the impact of changing snow characteristics, i.e., halogen content in sea-ice and snowpack, on reduction and re-emission of Hg from snow; whereas, Dastoor et al. (2015) study neglected changes in ocean Hg evasion. Fully interactive atmosphere-land-ocean biogeochemical mercury models including detailed representation of sea-ice dynamics are required to close the gap in modelling results.

(H.S.) The concentration levels of GEM in the atmosphere is controlled by its source strength (both anthropogenic and natural), the atmospheric relaxation time, transport, its chemical reactions and the final fate removing mercury into reservoirs (ref). All these processes except anthropogenic emission have a climate component that might affect the dynamics of future mercury dynamics.

The relaxation time of atmospheric mercury is dependent on the oxidation of GEM to GOM and PM as GOM and PM are fast removed by either wet or dry deposition. The final fate of mercury is also depenent on the reduction of oxidized mercury back in e.g. the water column back to elemental mercury (Skov et al. 2020). The reaction kinetic of Hg^0 in the atmosphere is temperature dependent (Goodsite et al 2004, 2012, Dibble's group, Donohoue et al. 2006), where oxidation is decreasing with increasing temperature, and thus GOM and PM formation is expected to decrease in a future warmer climate. The deposition is dependent on the stability of the atmosphere, wind speed and the surface properties (Skov et al. 2006) and thus the distribution between atmosphere, and land surfaces is climate dependent and the deposition will most likely increase as e.g. the aerodynamic resistance will decrease and snow covered areas will decrease as well as sea ice areas.

The transport from mid latitudes is dependent on the position of the major weather systems and it is predicted to change with changing climate (IPCC 2019). The polar front will be weakened (references) and thus Arctic will be more exposed to air masses from Hg source regions at mid latitudes.

Effect of climate on Hg uptake in food web
Effect of type of copepods on uptake and on bioaccumulation
Effect of permafrost melt and erosion on Hg in Arctic Ocean
…..

Conclusion: It is at present impossible to predict the future exposure of mercury for the Arctic terrestrial and marine biota. Until now the main reason for observed levels and trends in the different Arctic matrixes have been the source strengths and geographical locality of sources. In future, the effect of temperature increase will be more important. It will lead to changes in the distribution between matrixes (Air waters and biota) and in the bioaccumulation due changes of species e.g. low latitude copepods will migrate northward and replace the Arctic species.

- Baya, P. A.; Gosselin, M.; Lehnherr, I.; St. Louis, V. L.; Hintelmann, H., Determination of monomethylmercury and dimethylmercury in the arctic marine boundary layer. *Environmental Science and Technology* **2015,** *49*, (1), 223-232
- Dommergue, A.; Martinerie, P.; Courteaud, J.; Witrant, E.; Etheridge, D. M., A new reconstruction of atmospheric gaseous elemental mercury trend over the last 60 years from Greenland firn records. *Atmospheric Environment* **2016,** *136*, 156-164.

- Douglas, T. A.; Blum, J. D., Mercury Isotopes Reveal Atmospheric Gaseous Mercury Deposition Directly to the Arctic Coastal Snowpack. *Environmental Science and Technology Letters* **2019,** *6*, (4), 235-242.
- Hansen, K. M.; Christensen, J. H.; Brandt, J., The influence of climate change on atmospheric deposition of mercury in the arctic—A model sensitivity study. *International Journal of Environmental Research and Public Health* **2015,** *12*, (9), 11254-11268
- Obrist, D.; Agnan, Y.; Jiskra, M.; Olson, C. L.; Colegrove, D. P.; Hueber, J.; Moore, C. W.; Sonke, J. E.; Helmig, D., Tundra uptake of atmospheric elemental mercury drives Arctic mercury pollution. *Nature* **2017,** *547*, (7662), 201-204
- Obrist, D.; Kirk, J. L.; Zhang, L.; Sunderland, E. M.; Jiskra, M.; Selin, N. E., A review of global environmental mercury processes in response to human and natural perturbations: Changes of emissions, climate, and land use. *Ambio* **2018,** *47*, (2), 116-140
- Olson, C. L.; Jiskra, M.; Sonke, J. E.; Obrist, D., Mercury in tundra vegetation of Alaska: Spatial and temporal dynamics and stable isotope patterns. *Science of the Total Environment* **2019,** *660*, 1502-1512
- Pankratov, F. F.; Konoplev, A. V.; Makhura, A.; Kats, O. V., Analysis of the data of long-term monitoring of atmospheric mercury content and meteorological parameters at Amderma polar station. *Russian Meteorology and Hydrology* **2013,** *38*, (6), 405-413
- Zdanowicz, C.; Kruemmel, E.; Lean, D.; Poulain, A.; Kinnard, C.; Yumvihoze, E.; Chen, J.; Hintelmann, H., Pre-industrial and recent (1970-2010) atmospheric deposition of sulfate and mercury in snow on southern Baffin Island, Arctic Canada. *Science of the Total Environment* **2015,** *509-510*, 104-114\
- Zheng, J., Archives of total mercury reconstructed with ice and snow from Greenland and the Canadian High Arctic. *Science of the Total Environment* **2015,** *509-510*, 133-144
- Pearson C, Howard D, Moore C, Obrist D. Mercury and trace metal wet deposition across five stations in Alaska: controlling factors, spatial patterns, and source regions. Atmospheric Chemistry and Physics, 19, 6913-6929, 2019.
- Obrist D, Pearson C, Moore C. Mercury and other trace element wet deposition in Alaska: spatial patterns, controlling factors, and source regions. A draft report to the Alaska Department of Environmental Conservation. https://dec.alaska.gov/media/10511/aktracemetals-dri-report-092016.pdf
- Jaeglé, L.: Atmospheric long-range transport and deposition of mercury to Alaska, Department of Atmospheric Sciences, University of Washington, Seattle, A report to the Alaska Department of Environmental Conservation, 2010.
- Douglas, T. A. and Sturm, M.: Arctic haze, mercury and the chemical composition of snow across northwestern Alaska, Atmos. Environ., 38, 805–820, 2004.

- Douglas, T. A., Loseto, L. L., Macdonald, R.W., Outridge, P., Dommergue, A., Poulain, A., Amyot, M., Barkay, T., Berg, T., Chetelat, J., Constant, P., Evans, M., Ferrari, C., Gantner, N., Johnson, M. S., Kirk, J., Kroer, N., Larose, C., Lean, D., Nielsen, T. G., Poissant, L., Rognerud, S., Skov, H., Sorensen, S., Wang, F., Wilson, S., and Zdanowicz, C. M.: The fate of mercury in Arctic terrestrial and aquatic ecosystems, a review, Environ. Chem., 9, 321–355, https://doi.org/10.1071/en11140, 2012.
- Moore, C. W., Obrist, D., Steffen, A., Staebler, R. M., Douglas, T. A., Richter, A., & Nghiem, S. V. (2014). Convective forcing of mercury and ozone in the arctic boundary layer induced by leads in sea ice. Nature, 506(7486), 81–84. https://doi.org/10.1038/nature12924
- Angot, H., Dastoor, A., De Simone, F., Gårdfeldt, K., Gencarelli, C. N., Hedgecock, I. M., Langer, S., Magand, O., Mastromonaco, M. N., Nordstrøm, C., Pfaffhuber, K. A., Pirrone, N., Ryjkov, A., Selin, N. E., Skov, H., Song, S., Sprovieri, F., Steffen, A., Toyota, K., Travnikov, O., Yang, X., and Dommergue, A.: Chemical cycling and deposition of atmospheric mercury in polar regions: review of recent measurements and comparison with models, Atmos. Chem. Phys., 16, 10735–10763, https://doi.org/10.5194/acp-16- 10735-2016, 2016a.
- Angot, H., Magand, O., Helmig, D., Ricaud, P., Quennehen, Gallée, H., Del Guasta, M., Sprovieri, F., Pirrone, N., Savarino, J., and Dommergue, A.: New insights into the atmospheric mercury cycling in central Antarctica and implications on a continental scale, Atmos. Chem. Phys., 16, 10735–10763, https://doi.org/10.5194/acp-16-10735- 2016, 2016a.,
- Angot, H., Magand, O., Helmig, D., Ricaud, P., Quennehen, B., Gallée, H., Del Guasta, M., Sprovieri, F., Pirrone, N., Savarino, J., and Dommergue, A.: New insights into the atmospheric mercury cycling in central Antarctica and implications on a continental scale, Atmos. Chem. Phys., 16, 8249–8264, https://doi.org/10.5194/acp-16-8249-2016, 2016b.
- Fitzgerald, W. F., Engstrom, D. R., Lamborg, C. H., Tseng, C.-M., Balcom, P. H., and Hammerschmidt, C. R.: Modern and historic atmospheric mercury fluxes in Northern Alaska: global sources and arctic depletion, Environ. Sci. Technol., 39, 557–568, https://doi.org/10.1021/es049128x, 2005.
- Van Dam, B., Helmig, D., Burkhart, J. F., Obrist, D., and Oltmans, S. J.: Springtime boundary layer O3 and GEM depletion at Toolik Lake, Alaska, J. Geophys. Res.-Atmos., 118, 3382–3391, https://doi.org/10.1002/jgrd.50213, 2013.

b. Catchment transport

Contributors: **Kyra St Pierre**, Nicolas Pelletier, Jane Kirk

(K.S.) Understanding the impacts of climate change on catchment transport remains complex due to the often synergistic and/or antagonistic effects of these varying processes. We highlight the way that

these consequences of climate change - namely snowmelt and precipitation changes, permafrost degradation, forest fires, and glacial melt - may have already affected and may continue to influence Hg transport across watersheds. We then integrate these changes in catchment transport, by summarizing recent (post AMAP 2011) work on lake sediment archives.

- Fitzgerald, W. F.; Hammerschmidt, C. R.; Engstrom, D. R.; Balcom, P. H.; Lamborg, C. H.; Tseng, C. M., Mercury in the Alaskan Arctic. In *Alaska's Changing Arctic: Ecological Consequences for Tundra, Streams, and Lakes*, 2014.
- Carrie, J.; Stern, G. A.; Sanei, H.; Macdonald, R. W.; Wang, F. Determination of mercury biogeochemical fluxes in the remote Mackenzie River Basin, northwest Canada, using speciation of sulfur and organic carbon. Appl. Geochem. 2012, 27 (4), 815−824.
- Zdanowicz, C.; Karlsson, P.; Beckholmen, I.; Roach, P.; Poulain, A.; Yumvihoze, E.; Martma, T.; Ryjkov, A.; Dastoor, A., Snowmelt, glacial and atmospheric sources of mercury to a subarctic mountain lake catchment, Yukon, Canada. Geochim. Cosmochim. Acta 2018, 238, 374-393.
- Braaten, de Wit, Fjeld, Rognerud, Lydersen, Larssen, 2014. Environmental factors influencing mercury speciation in subarctic and boreal lakes. Science of the Total Environment, 476-477, 336-345.

Snowmelt

- Agnan, Y.; Douglas, T. A.; Helmig, D.; Hueber, J.; Obrist, D., Mercury in the Arctic tundra snowpack: Temporal and spatial concentration patterns and trace gas exchanges. *Cryosphere* **2018,** *12*, (6), 1939-1956
- Douglas, T. A.; Sturm, M.; Blum, J. D.; Polashenski, C.; Stuefer, S.; Hiemstra, C.; Steffen, A.; Filhol, S.; Prevost, R., A Pulse of Mercury and Major Ions in Snowmelt Runoff from a Small Arctic Alaska Watershed. *Environmental Science and Technology* **2017,** *51*, (19), 11145-11155.
- Durnford, D.; Dastoor, A.; Ryzhkov, A.; Poissant, L.; Pilote, M.; Figueras-Nieto, D., How relevant is the deposition of mercury onto snowpacks?-Part 2: A modeling study. *Atmospheric Chemistry and Physics* **2012,** *12*, (19), 9251-9274.
- Dommergue, A.; Larose, C.; Faïn, X.; Clarisse, O.; Foucher, D.; Hintelmann, H.; Schneider, D.; Ferrari, C. P., Deposition of Mercury Species in the Ny-Ålesund Area (79°N) and Their Transfer during Snowmelt. Environ. Sci. Technol. 2010, 44 (3), 901- 907.

Permafrost (and active-layer soil?) degradation

(K.S.) Soils in permafrost regions store an estimated 1,656±962 Gg of Hg, or more Hg than all other soils, atmosphere and oceans combined (Schuster et al. 2018 GRL). With a loss of between 6 and 29% of high latitude permafrost predicted for each 1°C of warming (Koven et al. 2013 JClim.), climate change-induced permafrost thaw could mobilize a vast amount of Hg, hitherto stored in frozen soils. The fate of this Hg will depend on eventually depend on the type of thermokarst terrain (i.e., lake, wetland or hillslope thermokarst; Olefledt et al. 2016), and climatic factors controlling transport to downstream ecosystems.

(K.S.) Permafrost thaw across the Arctic results in the creation of small thermokarst lakes, ponds and wetlands (French et al. 2017 EST; Olefeldt et al. 2016 Nat. Commun.; Gordon et al. 2016). These highly productive systems are shallow, have high inputs of organic matter and nutrients and are microbially active, making them excellent environments for the production of MMHg (MacMillan et al. 2015 EST; Gordon et al. 2016). When these ponds drain following slumping, further permafrost degradation or erosion, they may then become an important source of MMHg to nearby rivers (e.g., Fortier et al. 2007, PPP). Changes to thermokarst along the edges of small sub-arctic lakes have led to increased Hg deposition, with potentially important implications for the production of MMHg (Rydberg et al. 2010 STOTEN).

(K.S.) One of the most striking consequences of permafrost degradation in parts of the Arctic subject to hillslope thermokarst is the development of retrogressive thaw slumps, a form of mass wasting characteristic of hilly regions underlain by ice-rich permafrost. These features, which can be up to 40 ha in area, can release large quantities of sediments and solutes to lakes, rivers and coastal waters (Kokelj et al. 2013 JGR Earth. Surf.). Concentrations of Hg_T and MMHg in streams draining slumps in the western Canadian Arctic have been recorded as high as 1,270 ng/L and 7 ng/L, respectively (St. Pierre et al. 2018 EST). High sedimentation rates in slump-affected lakes have been hypothesized to dilute Hg deposition in these environments (Deison et al. 2014 EST), but monitoring of these sites is needed to understand the long-term impact of these events. At present, Hg mobilization through the streams draining slump-affected areas is transport-limited (i.e., sediment supply exceeds water volume); however, during high flow events, like the spring freshet, or if predictions of a wetter Arctic are realized (Bintanja and Andry 2017 Nat. Geosci.), such conditions could enable the mobilization of vast quantities of Hg to downstream ecosystems.

- Mercury levels skyrocket thanks to Arctic warm up. *Nature* **2018,** *564*, (7735), 164
- Halbach, K.; Mikkelsen, Ø.; Berg, T.; Steinnes, E., The presence of mercury and other trace metals in surface soils in the Norwegian Arctic. *Chemosphere* **2017,** *188*, 567-574

- Olson, C.; Jiskra, M.; Biester, H.; Chow, J.; Obrist, D., Mercury in Active-Layer Tundra Soils of Alaska: Concentrations, Pools, Origins, and Spatial Distribution. *Global Biogeochemical Cycles* **2018,** *32*, (7), 1058-1073 Lim, A. G.; Sonke, J. E.; Krickov, I. V.; Manasypov, R. M.; Loiko, S. V.; Pokrovsky, O. S., Enhanced particulate Hg export at the permafrost boundary, western Siberia. *Environmental Pollution* **2019,** *254*, 113083.
- Friedli, H. R., Radke, L. F., Payne, N. J., McRae, D. J., Lynham, T. J., & Blake, T. W. (2007). Mercury in vegetation and organic soil at an upland boreal forest site in Prince Albert National Park, Saskatchewan, Canada. Biogeosciences, 112(G1), G01004.
- Hararuk, O., Obrist, D., & Luo, Y. (2013). Modelling the sensitivity of soil mercury storage to climate-induced changes in soil carbon pools. Biogeosciences, 10(4), 2393–2407. https://doi.org/10.5194/bg-10-2393-2013
- Douglas, T. A., Sturm, M., Blum, J. D., Polashenski, C., Stuefer, S., Hiemstra, C., Steffen, A., Filhol, S., and Prevost, R.: A pulse of mercury and major ions in snowmelt runoff from a small arctic Alaska watershed, Environ. Sci. Technol., 51, 11145–11155,https://doi.org/10.1021/acs.est.7b03683, 2017.
- Barker, A. J., Douglas, T. A., Jacobson, A. D., McClelland, J. W., Ilgen, A. G., Khosh, M. S., Lehn, G. O., and Trainor, T. P.: Late season mobilization of trace metals in two small Alaskan arctic watersheds as a proxy for landscape scale permafrost active layer dynamics, Chem. Geol., 381, 180–193, https://doi.org/10.1016/j.chemgeo.2014.05.012, 2014.
- Klaminder, J., Yoo, K., Rydberg, J., & Giesler, R. (2008). An explorative study of mercury export from a thawing palsa mire. Journal of Geophysical Research, 113, G04034. https://doi.org/10.1029/2008JG000776
- Pogojeva, Yakushev, Ilinskaya, Polukhin, Braaten, Kristiansen, 2018. Experimental study of the influence of thawing permafrost on the chemical properties of sea water. Russian Journal of Earth Sciences, 18.
- Kokelj, S. V.; Lacelle, D.; Lantz, T. C.; Tunnicliffe, J.; Malone, L.; Clark, I. D.; Chin, K. S., Thawing of massive ground ice in mega slumps drives increases in stream sediment and solute flux across a range of watershed scales. *Journal of Geophysical Research: Earth Surface* 2013**,** *118*, (2), 681-692.

Forest fires

(K.S) Hg dynamics across the Arctic region are affected by fires occurring both locally and further afield. Gaseous elemental mercury (GEM), typically considered the dominant species emitted by fire, can be transported over long distances from source regions (Fraser et al. 2018). Meanwhile, particulate-bound mercury (PBM) has a relatively shorter residence time and is typically deposited closer to the emission source (Fraser et al. 2018). Over the past 50 years, the frequency and severity of

wildfires across the Northern Hemisphere have increased concomitantly with summer air temperatures and lengthening dry periods (Gillet et al. 2004; French et al. 2015). Model estimates (GEOS-CHEM) suggest that ~10% of total annual Hg deposition (15 Mg) to the Arctic originates from forest fires, largely from the large swaths of boreal forests in Eurasia (Kumar and Wu 2019).

(K.S) Characterized by low temperatures and little available biomass, Arctic tundra has historically not been prone to intense and expansive fires (Hu et al. 2015). Local wildfires within the Arctic, though, have become increasingly common during the summer and early fall, especially within the discontinuous and sporadic permafrost zones (French et al. 2015). The susceptibility of tundra ecosystems to fire largely depends on the crossing of certain temperature and precipitation thresholds (the "threshold effect"), predicted to occur more often with climate change (Hu et al. 2015). In Alaska, for example, the average annual area burned is projected to double by 2100, and the probability of extreme seasons are projected to increase by 13-23%, relative to the 1950-2009 period (Hu et al. 2015). Fires in permafrost zones typically result in the substantial loss of soil organic matter, increased active layer water storage, and soil temperatures (Nossov et al. 2013), all of which can influence the biogeochemical cycling of Hg through northern ecosystems.

(K.S) Aside from the direct deposition of GEM and PBM to the landscape, local wildfires may also indirectly enhance the mobilization of Hg stored in soils through permafrost degradation, active layer deepening/ warming, and thermokarst feature development (Jones et al. 2015; Gibson et al. 2018). In particular, wildfires are estimated to be responsible for 2200±1500 km^2 of thermokarst bog formation over a 400,000 km^2 area of the sporadic-discontinuous permafrost zone in sub-arctic Canada (Gibson et al. 2018). Thermokarst development may then promote the mobilization and production of neurotoxic methylmercury (see above, MacMillan et al. 2015). However, the impact of wildfires on the transport of Hg by streams and rivers across burned landscapes, remains largely unexplored. Recent work suggests that wildfires may not affect watershed yields of dissolved Hg in the sporadic/discontinuous permafrost zones, though particulate Hg – an important by-product of wildfire, especially close to the source (Fraser et al. 2018; Obrist et al. 2018) - was not specifically measured (Hutchins et al. *in prep*).

(K.S) Global climate models predict both an increase in fire season length of more than 20 days for high latitude northern regions by 2100 (Flannigan et al. 2013), and an increased incidence of extreme or large fire seasons (Hu et al. 2015), emphasizing the role that fire could play in the Arctic moving forwards. Understanding the impacts of fire on Hg dynamics through Arctic ecosystems, particularly on watershed connectivity and stream/river transport to downstream systems, will be critical.

Impact of climate change on recent and future wildfire activity in Canada – implications for mercury
(Nicolas Pelletier) Wildfires are an important process for global and local mercury cycling because biomass burning releases Hg accumulated in terrestrial ecosystems over millennia (Giesler et al., 2017). The Arctic Hg loading could be affected in at least two ways by the changes in wildfire activity caused by climate change. First, wildfires are appearing in the Arctic tundra, where they historically have been very rare, with consequences on the local release of Hg, the long-term Hg sink capacity of the tundra and other indirect changes on local Hg cycling caused by changes in ecosystems properties. Second, the Arctic will receive Hg emitted by wildfire occurring at lower latitudes (temperate and subarctic), by atmospheric and riverine transport.

Tundra ecosystems are characterized by a low wildfire occurrence because of low temperatures, short snow-free seasons and the lack of flammable biomass (Hu et al., 2015; Wein, 1976). However, climate warming will affect multiple environmental parameters that are predicted to increase fire activity in this biome. Lake sediment charcoal records revealed that wildfires use to only occurs in the driest and warmest regions of the tundra, such as Western Alaska and Northeastern Siberia, but since 2007, some fires occurred in area where fire have been absent for the last 6500 to 35000 years (Chipman et al., 2015). Models predicting the likelihood of wildfires across the Tundra find summer temperature and annual moisture availability as the most influential controls of historical fire regimes (Balshi et al., 2009; Young et al., 2017). However, non-linear responses have been identified between climate variable and Tundra fire activity (Hu et al., 2015; Young et al., 2017). For example, Young et al. (2017) identified an important threshold occurring at an average July temperature of 13.4°C and below an annual moisture availability of approximately 150 mm. Considering climatic variables only and using available scenario for future climate, Hu et al., (2015) predicted a doubling of the burned area in Alaska by 2100 whereas Young et al. (2017) predicted a fourfold increase in the 30-years probability of fire occurrence by 2100 for the same region.

Other changes directly caused by a warmer climate could exacerbate the likelihood of fire activity in the Tundra, such as changes in vegetation cover, lightning activity, fire season length and land connectivity caused by the shrinkage and disappearance of Arctic ponds (Coogan et al., 2019; Hu et al., 2015; Riordan et al., 2006; Smith et al., 2005). The tundra is currently experiencing an increase in shrub growth and dominance, gradually replacing herbaceous tundra vegetation (Box et al., 2019; Myers-Smith et al., 2015). In paleo-environmental records, similar changes in northcentral Alaska between 14,000 and 10,000 years ago were associated with an important increase in wildfire activity, where the birch-dominated landscapes burned as frequently as the current boreal forest (Higuera et al., 2008). However, it is difficult to separate the influence of vegetation and climate in such records and uncertainties persist regarding the direct influence the change in vegetation type in the tundra on fire regimes. The recent increase in air temperature and precipitations in the tundra are also directly

correlated to an increase in lightning activity, by far the main ignition source for tundra and boreal wildfires (Hanes et al., 2019; Veraverbeke et al., 2017). In the Northwest Territories and Alaska, lightning activity have increased between 1970 and 2014 and led to exceptionally high levels of burning near the northern treeline in 2014 and 2015 (Veraverbeke et al., 2017). Paleo-records and modelling indicate that Arctic sea ice is moderately correlated with tundra area burned in some areas such as Alaska (Hu et al., 2010, 2015). A decrease in sea-ice extent, and the associated changes in precipitation patterns could therefore influence wildfire activity in some areas of the tundra.

The important role of the Tundra biome as accumulator of atmospheric mercury has been recognized from recent work on soils and vegetation stable Hg isotopes (Obrist et al., 2017). An increase in wildfire activity in the tundra could lead to a relatively rapid release of terrestrial mercury accumulated over long-term. Terrestrial Hg loss caused by arctic tundra fires are currently not well quantified, but based on measured carbon loss following wildfires and the important association between soil carbon and mercury, tundra fires could constitute a major source of Hg to the atmosphere. In 2007, a single wildfire on the Alaskan Arctic slope released about 30% of the carbon reservoir in the affected area, an amount of carbon similar in magnitude to the annual net C sink for the entire Arctic tundra biome (Mack et al., 2011). Research is still lacking to quantify the proportion of soil Hg released by tundra wildfires and the speciation of the released Hg. Wildfires in permafrost regions could also have indirect effect on Hg cycling by accelerating permafrost thaw in sensitive areas (Gibson et al., 2018). Thawing of permafrost can lead to important landscape disturbances including the creation of thermokarst ponds and wetlands, active-layer detachments and greater exports of particulate and dissolved organic carbon to aquatic environments (Box et al., 2019). Altogether, the increased Hg release from tundra wildfires and the landscape changes they cause could diminish the gaseous atmospheric Hg sink capacity of the tundra, with consequences on both local and global Hg cycling.

The Arctic receives atmospheric Hg (gaseous and particulate) from wildfires occurring in the temperate and subarctic latitudes, including the boreal forest (Fraser et al., 2018). The predicted changes in the boreal forest fire regime are important for global Hg cycling since boreal forest are a large Hg reservoir with a naturally short fire-return interval. A recent study measuring Hg accumulation in a chronosequence of forest soils with different fire history highlighted the potential for Hg accumulation during millennia in the absence of wildfire in boreal forests of Sweden (Giesler et al., 2017). Human-induced climate warming and drying has led to an increase in fuel available for burning and an increase in yearly burned area in North America boreal forest ecosystems since at least the 1960s (Abatzoglou & Williams, 2016; Gillett, 2004; Kirchmeier-Young et al., 2018). It is estimated that human-caused climate warming is responsible of ~50% of all area burned since 1984 in the western United States (Abatzoglou & Williams, 2016) and 86%-91% of all area burned in British

Columbia during 2017 (Kirchmeier-Young et al., 2018). In Canada, the only region with a negative trend in fire area burned over the last 30 years is the Atlantic Maritime, contributing to only ~0.01% of the total area burned in Canada (Coops et al., 2018). The number of large fires (>200 ha) have approximately doubled over the last 57 years in Canada (Hanes et al., 2019) and has increased at a rate of seven additional large fire per year in the western United States between 1984 and 2011 (Dennison et al., 2014). Since fire size is directly correlated to burning temperature and height of convective plumes, increasing fire size in the boreal forest could lead to changes in the ratio of Hg released by wildfire and the range of the Hg transported in the atmosphere.

Because of climate warming, the fire season typically starts one week earlier and finishes one week later in Canada on average since 1958 (Hanes et al., 2019; Jain et al., 2017). A similar trend is observed in the western US (Dennison et al., 2014) and in-line with the ~19% increase in global fire average fire season length between 1979 and 2013 (Jolly et al., 2015). The lengthening of the fire season could participate in the increase in fire size and severity since early-season fires occur at a time where vegetation can be more flammable (Coogan et al., 2019). Increasing lightning activity is also widespread in North America (Hanes et al., 2019; Veraverbeke et al., 2017). For example, it is predicted that period of elevated risk of lightning-caused wildfire will increase by >50% by 2050 in northern Ontario, Canada (Woolford et al., 2014).

Changes in wildfire activity in the North-American and Eurasian continents lead to greater release of terrestrial Hg that can be deposited at variable distance from the fires depending on atmospheric transport and fire conditions. A modelling experiment by Kumar et al. (2018) suggest that climate change between 2000 and 2050 could increase Hg emissions by 8% in North America and 14% in Eurasia. A recent model of atmospheric Hg transport for Canadian wildfires suggest that the majority of the Hg emitted by Canadian wildfires is deposited in temperate to subarctic latitudes. However, plumes from intense wildfire seasons like summer 2014 in the Northwest-Territories have reached the high Arctic pass the 70° latitude, including the West coast of Greenland (Fraser et al., 2018). The amount of Hg deposited by wildfires in the Northwest-Territories, Nunavut and Yukon exhibit a lot of spatial and temporal heterogeneity and varied between 0.05 and 2.5 µg m-2 yr-1 according to the same transport model (Fraser et al., 2018). A recent estimation from lake sediment collected north of Great Slave Lake (Northwest Territories, Canada) estimate that charcoal deposition from wildfire since the late 1800s co-occurred with excess deposition of Hg to the lakes varying between 0 and 9 µg m^{-2} yr^{-1} (Pelletier et al., in preparation). Future research need to provide additional direct measurements for the amount and speciation of Hg released from wildfires in a variety of settings. Modelers require a better prediction of the propensity of boreal peatlands to burn in the future (Fraser et al., 2018). Peatlands are an important sink for organic matter and Hg in the circumboreal regions and models including the burning of peat-rich soils could lead to significantly greater estimates of Hg

release (Turetsky et al., 2006). A better estimation of the net proportion of gaseous Hg to particulate Hg produced by wildfires in different contexts is also crucial to ameliorate the accuracy wildfire plume Hg transport models. The proportion of Hg released as gaseous elemental Hg in wildfires varies between 50 and 95% based on aircraft measurements (Friedli et al., 2003; Friedli et al., 2001), satellite measurements (Finley et al., 2009) and laboratory experiments (Kohlenberg et al., 2018; Obrist et al., 2008). Few studies have investigated the environmental control on the partitioning of Hg speciation in wildfire plumes (e.g., Obrist et al., 2008). River input are the most important source of Hg to the Arctic Ocean (Fisher et al., 2012) and wildfires can release terrestrial Hg to streams (Abraham et al., 2017) that could ultimately increase the riverine input of Hg to the Arctic Ocean. While the link between stream Hg loading and wildfires is understood, the impact of boreal and tundra wildfires on Artic riverine Hg inputs have currently not been explored. The combination of legacy contamination from anthropogenic emissions and greater fire frequency could lead to greater mercury release from contemporary and future fires than historical fires (Biswas et al., 2007; Obrist et al., 2018), but research clearly demonstrating this hypothesis is still lacking.

Therefore, Artic Hg cycling will be impacted by changes in wildfire activity caused by climate change in three ways; (1) the appearance of tundra fires, which will release terrestrial Hg to the atmosphere and streams locally, (2) the transport of wildfire-derived Hg from lower latitude via the atmosphere, and possibly via rivers. Recent research has demonstrated that wildfires are a major process for Hg cycling and that fire activity also have consequences for Hg loading in areas where fire are historically rare or absent, including the Arctic.

- Olson CL, Jiskra M, Sonke JE, Obrist D. Spatial and temporal dynamics of mercury in tundra vegetation. The Science of the Total Environment, Mercury in tundra vegetation of Alaska: Spatial and temporal dynamics and stable isotope patterns. The Science of the Total Environment, 660, 1502-1512, 2019.

Glacier melt

(K.S.) Within many glacierized catchments in the Arctic, glacier melt currently accounts for the largest source of both water and Hg to downstream ecosystems (Zdanowicz et al. 2018 GCA, St. Pierre et al. 2019 EST). Glacial meltwaters integrate two principle sources of Hg: 1) legacy and modern Hg archived in glacial ice and snow; and, 2) geogenic Hg transported by meltwaters as they flow across poorly consolidated proglacial landscapes (Zdanowicz et al. 2013 GCA). Hg deposition to glaciers has varied substantially over time in response to changes in both natural (e.g., volcanic eruptions) and anthropogenic sources (Beal et al. 2015 EST). We would therefore expect the Hg contribution from ice and snow to change over time, in concert with the loss of older ice and the simultaneous contributions from modern depositional processes. In many cases, however, geogenic

contributions of Hg within the sediment-laden meltwaters could be as important, if not more, than those of melting ice and snow (Zdanowicz et al. 2013 GCA). Large, periodic fluctuations in meltwater volume, including glacial lake outburst floods, can mobilize substantial quantities of Hg from the surrounding landscape. In the Zackenberg River of northeast Greenland, for example, glacial lake outburst floods are responsible for between 5-10% of the river discharge in years when they occur, but 15-31% of the Hg export (Søndergaard et al. 2015 STOTEN). These extreme meltwater discharge events may become increasingly common with climate change (Harrison et al. 2018, Cryo.; Nilsson et al. 2015 Fresh. Biol.), with the potential for substantial mobilization of Hg across landscapes.

(K.S.) Although glacial meltwaters typically contain very little (<0.1 ng/L) MMHg (Zdanowicz et al. 2013 GCA, St. Pierre et al. 2019 ES&T), little attention has been paid to Hg dynamics in subglacial channels or within cryoconite on glacier surfaces, both of which could support methylation. Subglacial meltwaters can become anoxic and contain enough bioavailable carbon to support significant production of methane, similar conditions required for Hg methylation (e.g., Lamarche-Gagnon 2019 Nature). Higher concentrations of MMHg (1.0 ng/g) have been detected in cryoconite of the Tibetan Plateau, suggesting either the preferential accumulation of MMHg there or active methylation (Huang et al. 2019 ES&T).

- Calleja, M. L.; Kerhervé, P.; Bourgeois, S.; Kędra, M.; Leynaert, A.; Devred, E.; Babin, M.; Morata, N., Effects of increase glacier discharge on phytoplankton bloom dynamics and pelagic geochemistry in a high Arctic fjord. *Progress in Oceanography* **2017,** *159*, 195-210
- Kim, H., Kwon, S.Y., Lee, K. et al. Input of terrestrial organic matter linked to deglaciation increased mercury transport to the Svalbard fjords. Sci Rep 10, 3446 (2020). https://doi.org/10.1038/s41598-020-60261-6

Lake sediment

(K.S) Lake sediments are excellent archives with which to assess both climate-related changes in catchment transport and atmospheric deposition of Hg in relation to ecosystem function over time (Chételat 2015). However, given that these two processes overlap in time, disentangling the relative contribution of each can be challenging (Korosi et al. 2018). Whereas post-industrial increases in Hg deposition, largely due to anthropogenic activities, are reported across most northern lakes, the impacts of climate change on catchments are much more variable and depends on local characteristics, such as catchment to lake area ratio (Drevnick et al. 2012), the presence of glaciers or susceptibility to different thermokarst landform types (Burke et al. 2018).

Enhanced algal scavenging of Hg, as a result of climate-induced increases in lake primary production (Outridge et al. 2007), is supported by positive correlations between algal-derived organic carbon (S2) and Hg concentrations in sediment cores from some lakes (Brazeau et al. 2013, Korosi et al. 2018).

However, multiple studies have shown that while this process may explain recent increases in Hg accumulation of the sediments of some lakes, the dominance of algal scavenging may not be as widespread as previously thought (Kirk et al. 2011, Cooke et al. 2012, Korosi et al. 2018, Burke et al. 2018).

Increasingly, changes in catchment transport processes are being reflected in Hg deposition rates in lake sediment cores, especially in watersheds undergoing dramatic change as a result of permafrost thaw and glacial melt. Lehnherr et al. (2018) report an 8-times higher sedimentation rate in Lake Hazen, relative to the 1948 baseline, since the post-2007 acceleration of glacial melt across the watershed, translating to Hg deposition rates up to 180 $\mu g\ m^{-2}\ yr^{-1}$. Indeed, annual Hg sedimentation rates from cores collected from Lake Hazen matched well with THg mass balance of the lake, suggesting that the sediment cores were a good archive of interannual variability in catchment inputs (St. Pierre et al. 2019). Deison et al. (2012) collected lake sediment cores in a lake affected by a retrogressive thaw slump and attributed reduced Hg concentrations to increased inorganic sedimentation rates by slump materials. Korosi et al. (2015) report the post-1970 subsidence of permafrost-associated peatlands resulted in changes to terrestrial organic matter transport to downstream lakes, but not necessarily to Hg enrichment. In a meta-analysis of lakes across the Arctic and Alaska, Burke et al. (2018) found that lakes with catchments susceptible to thermokarst development were more likely to have high, but variable Hg accumulation rates. Fire may also play an important role in transforming watersheds and Hg depositional regimes, especially within the Sub-Arctic region, by mobilizing Hg previously stored in plant material and catalyzing the permafrost degradation (Brazeau et al. 2013, Korosi et al. 2015).

In rapidly changing Arctic catchments, monotonic trends in lake sediment Hg accumulation may not always be detectable (Burke et al. 2018). Instead, episodic increases in Hg accumulation rates from singular large events (active layer detachments, extremely warm periods, large rainfall or snowmelt) characteristic of the current climate regime may instead punctuate the record (Burke et al. 2018). Collectively, these studies highlight that catchment changes may affect Hg cycling in more complex ways than directly increasing transport alone (e.g., changing organic matter sources, loss or reorganization of Hg pools through fire).

(Jane Kirk) Hg diel, seasonal, and inter-annual hydrological transport dynamics and annual fluxes were determined from a long term sampling program (2007-2017) in paired High Arctic rivers (unofficially named East and West) which have experience localized permafrost disturbances (ALDs) and hydroclimatic change. East and West rivers are located at the Cape Bounty Arctic Watershed Observatory (CBAWO; 74°54'N, 109°35'W), a remote site on southern Melville Island, Nunavut. East and west rivers are physiographically similar, second order (East: 11.6 km^2, West: 8.0 km^2)

rivers with subtle variations in topographic relief that generate broadly similar seasonal runoff, solute and sediment exports (Lewis et al., 2012). Prolonged warm temperatures and a major rainfall event in July 2007 resulted in 1.2 and 2.7% of the East and West catchments, respectively, being disturbed by ALDs (Lamoureux and Lafrenière, 2017). ALDs varied from small, isolated patches on slopes to long, linear features that directly coupled with the river channels. Further permafrost degradation led to the exposure of massive ice along a length of the West River channel bank by late 2008, leading to enhanced undercutting and bank erosion until 2012 (Favaro and Lamoureux, 2015). In contrast, in the East River catchment, few ALDs coupled with the main fluvial channel network and no ice was exposed along the channel banks.

Mean THg concentrations varied considerably between years, with the highest concentrations in 2009 following the ALDs, and the lowest in 2012, but were generally comparable between the rivers. Hg in both rivers was predominantly particulate-bound as pTHg (4.2± 4.1 ng L^{-1}, or 31-73% of the total) and was significantly related with total suspended solids (TSS) concentrations (East: r^2=0.68, n=71, $p<0.05$; West: r^2=0.76, n=75, $p<0.05$) and fractions of organic carbon (Figure X). Concentrations of fTHg (2.0± 1.4 ng L^{-1}) and MeHg (0.05± 0.03 ng L^{-1}; range <0.008 - 0.11 ng L^{-1}) concentrations were generally low and comparable in both rivers and weakly increased with increasing THg concentrations. Hydrologic discharge from disturbed sub-catchments had higher mean THg concentrations compared to that draining an undisturbed sub-catchment in all years, with highest THg (58 ng L^{-1}) observed from the most disturbed sub-catchment (Big Slide). In the years following the initial permafrost disturbance (2007), mean THg concentration in discharge from the disturbed Ptarmigan subcatchment declined (34.0 ng L^{-1} in 2009 to 15.1 ng L^{-1} in 2017). However, by 2016 and 2017, mean THg concentrations remained significantly higher in Q from the disturbed sub-catchments (mean 8.4 ng L^{-1}) compared with that from the undisturbed (Goose) subcatchment (mean 4.2 ng L^{-1}) (t-test, $\alpha = 0.05$; n = 44, $p<0.05$).

Highest THg concentrations were typically observed during the nival period (ranging between 6.8-21.3 ng L^{-1}) and declined rapidly during baseflow (1.1-11.7 ng L^{-1}), when hydrological connectivity to slopes was diminished. Elevated THg concentrations (up to 9.7 ng L^{-1}) were also observed during the limited number of stormflow events we were able to sample (Figure X).Seasonal patterns in THg concentrations at CBAWO are similar to those in streams elsewhere in the High Arctic (Cornwallis Island, Nunavut; Loseto et al., 2004; Semkin et al., 2005). However, due to the abundance of mineral sediment in our study rivers (Beel et al., 2018), mean THg concentrations are substantially higher than other small High Arctic rivers (e.g., 9.3 ng L^{-1} in West River vs. 1.4 ng L^{-1} in streams of Cornwallis Island; Semkin et al., 2005). Our seasonal results also broadly agree with results from other large, sediment rich sub-Arctic rivers, such as the Yukon (mean THg = 15.0 ng L^{-1}; Schuster et al., 2011) and Mackenzie rivers (mean THg = 14.6 ng L-1; Emmerton et al., 2013).

High frequency sampling during high flow events of 2017 showed that concentrations of THg, pTHg, and fTHg had pronounced diel variability and hysteresis related to Q during both stormflow and nival periods (Figure X). THg and pTHg concentrations rapidly increased and peaked before maximum daily discharge (Figure X). In contrast, concentrations of fTHg showed the opposite pattern, with peak fTHg concentration occurring on the falling limb of Q (Figure X). Similarly, in the Mackenzie River, pTHg concentrations peaked before Q while fTHg peaked during waning flow (Leitch et al., 2007). These data clearly show that higher frequency Hg sampling is required during periods of variable Q to accurately characterize Hg concentrations and particulate-dissolved partitioning (Figure X).

Annual THg fluxes from both rivers were estimated using the TSS-THg regressions. However, Hg was often lower than expected based on the TSS-THg relationship during peak TSS so uncapped and capped fluxes were calculated using a maximum observed THg concentration of 21 ng L^{-1}. Annual Hg fluxes ranged widely between the East and West rivers (East: 1.8-14.2 g (uncapped: 1.8-14.4 g); West: 3.7-11.3 g (3.7-15.8 g)) (Figure X), with the highest THg fluxes occurring in years with high cumulative runoff and sediment supply from landscape disturbances. For example, the 2008 THg fluxes in the West River were some of the highest we measured (11.4 g (12.4 g)), suggesting that landscape disturbance had an immediate impact on THg flux through the mobilization and transport of previously stored terrestrial Hg to the downstream aquatic environment. This is not surprising given that 100+ ALDs formed at CBAWO in late July 2007 (Lamoureux and Lafrenière, 2017) and immediately increased the subsequent 2008 nival sediment flux. Permafrost disturbances such as ALDs and RTSs have been shown to increase dissolved and particulate biogeochemical fluxes in other Arctic watersheds (Bowden et al., 2008; Kokelj et al., 2013; Rudy et al., 2017; St. Pierre et al., 2018). Research recently demonstrated high TSS exports from active RTSs, which also generated exceptionally high THg concentrations and fluxes (St. Pierre et al., 2018) in the Peel Plateau region, Northwest Territories, Canada. However, it is important to distinguish the sustained disturbance associated with RTSs, often for years or decades, from the short lived activity (several years at most) of ALDs that occurred at CBAWO. Hence, while both types of permafrost disturbance appear to readily mobilize TSS and THg, the intensity and longevity of disturbance associated with RTSs is substantially higher than that of ALDs.

To directly compare the multi-year river fluxes, we normalized with respect to catchment area and runoff (mm). Runoff normalized specific THg fluxes (g km^{-2} mm^{-1}) were broadly similar between rivers and years, except in 2008-2009 immediately following the ALDs and substantial stormflow events (Figure X). For example, in July 2009, stormflow events (41 mm total; Beel et al., 2018) transferred an estimated 63% (73%) and 51% (63%) of the total seasonal THg flux from the East and

West catchments, respectively. Collectively these stormflow events transported more THg (East: 4.5 g (7.5 g), West: 6.2 g (10.0 g)) than the entire 2010 season in both rivers (5.1 g) (Figure X). Overall, our results show that the diel and seasonal timing and intensity of runoff was a dominant driver of THg flux in all years, with the majority of discharge and peak THg and MeHg concentrations occurring during either the brief nival freshet or uncommon late season rainfall events. These results are consistent with Hg transport patterns elsewhere in the Arctic, where episodic, high intensity Q events, such as rainfall and glacial outburst floods, are responsible for the majority of terrestrial Hg fluxes (Søndergaard, et al., 2015).

However, after the rainfall induced mobilization of sediment and THg, exhaustion of sediment suggests that, at a catchment scale, the sediment and THg downstream impact of the 2007 disturbances was largely complete (Beel et al., 2018). Analysis of variance of the West River TSS-THg relationships show that 2008 and 2009 were statistically similar ($p<0.05$) while 2010 shows a significant reduction in TSS-THg regression slope, implying a change in sediment and THg source relationships. Specific THg fluxes in both rivers show little inter seasonal variability post-2010, and suggest that localized exposed channel ice and associated bank erosion was not a major Hg source (Figure X). Alternatively, results suggest that channel sediment storage has the capacity to buffer localized increases in pTHg supply from catchment sources. Soil Hg profiles from elsewhere in the Arctic show that Hg concentrations in the surface and organic horizons are higher than deeper mineral soils (St. Pierre et al., 2018; Obrist et al., 2017), suggesting that deeper mineral soil accessed through bank erosion may contribute proportionately less Hg than shallow ALDs. However, detailed soil profiles are needed to confirm this.

The consistency of the specific THg flux in both rivers over multiple years after 2010 suggests that at a catchment scale, THg flux largely reached equilibrium with respect to both landscape disturbance and hydroclimatic changes. Given the disproportionate sediment transport response to the major 2009 rainfall, we speculate that the 2009 rainfall event contributed to subsequent stabilization of THg fluxes by flushing the channel system of pTHg sourced from the ALDs. These results are in contrast to the disturbed sub-catchment results from 2016 and 2017 that showed there was only a partial recovery from disturbance, with elevated THg and TSS concentrations. Hence, we infer that ongoing delivery of Hg from disturbed slopes is either diminished or retained in downstream river channel as pTHg in storage. Notably, in the absence of hydrological coupling, thermal perturbation of the active layer (Lafrenière and Lamoureux, 2013) appears to have little effect on THg flux. Summer mean temperatures in 2011 and 2012 were the warmest on record (since 1948), and led to widespread, active layer deepening. This deep thaw was linked to a notable increase in solute flux from the catchments and accumulation in downstream lakes (Roberts et al., 2017). However, given that the 2012 THg flux was the lowest observed in the sampling period for both rivers (East: 1.8 g (1.8 g),

West: 3.7 g (3.7 g)) there is no evidence that active layer deepening increased Hg flux from the landscape. Limited winter snowfall prior to runoff in 2012 (Favaro and Lamoureux, 2015) further reduced TSS and pTHg fluxes due to decreased Q, yet by comparison, the 2012 THg specific flux remains consistent to other years. These results suggest the importance of hydrogeomorphic controls over Hg fluxes from disturbances to downstream systems, and the contrast between localized impacts and larger catchment response. At longer timescales, results show a short-lived (1-2 year) elevated catchment THg flux following the formation of permafrost disturbances in 2007. At the hillslope scale, Q from disturbed sub-catchments continue to have elevated Hg concentrations 10 years after the initial physical permafrost disturbance. Perhaps most notably, despite record deep thermal perturbation (thaw) in 2011 and 2012, there was no observable effect on THg flux at the catchment scale.

In addition to climate-induced permafrost perturbation, the Arctic is predicted to become both warmer and wetter, particularly through increased frequency of late-season rainfall events (Bintanja and Andry, 2017). Based on the results from this study, projected increased rainfall is a potentially important mechanism for altering THg flux due to the erosional susceptibility of soils and channel sediments during the summer. The strong runoff and sediment transport response in 2009 suggests the potential to flush Hg stored in the channel system. As the Arctic shifts to an increasingly pluvially-dominated hydrological system (Bintanja, 2018), the frequency of high magnitude Q events will increase and the timing of flow will shift to conditions that are expected to be more conducive to higher sediment flux (Lewis and Lamoureux, 2010; Beel et al., 2018). This will likely increase the flux of Hg from Arctic rivers though enhanced Q, sediment transport and mobilization of pTHg. Thus, the combination of permafrost disturbance and projected climate and hydrological changes point to a future increase in the magnitude of riverine Hg to the Arctic Ocean from this region.

- Outridge, P. M.; Stern, G. A.; Hamilton, P. B.; Sanei, H., Algal scavenging of mercury in preindustrial Arctic lakes. *Limnology and Oceanography 0*, (0) 2019
- Muir, D. C. G.; Wang, X.; Yang, F.; Nguyen, N.; Jackson, T. A.; Evans, M. S.; Douglas, M.; Köck, G.; Lamoureux, S.; Pienitz, R.; Smol, J. P.; Vincent, W. F.; Dastoor, A., Spatial trends and historical deposition of mercury in eastern and northern Canada inferred from lake sediment cores. Environ. Sci. Technol. 2009, 43, (13), 4802-4809.
- Outridge, P. M.; Sanei, H.; Courtney Mustaphi, C. J.; Gajewski, K., Holocene climate change influences on trace metal and organic matter geochemistry in the sediments of an Arctic lake over 7,000 years. Appl. Geochemi. 2017, 78, 35-48.
- Drevnick, P. E.; Cooke, C. A.; Barraza, D.; Blais, J. M.; Coale, K. H.; Cumming, B. F.; Curtis, C. J.; Das, B.; Donahue, W. F.; Eagles-Smith, C. A.; Engstrom, D. R.; Fitzgerald, W.

F.; Furl, C. V.; Gray, J. E.; Hall, R. I.; Jackson, T. A.; Laird, K. R.; Lockhart, W. L.; Macdonald, R. W.; Mast, M. A.; Mathieu, C.; Muir, D. C. G.; Outridge, P. M.; Reinemann, S. A.; Rothenberg, S. E.; Ruiz-Fernández, A. C.; Louis, V. L. S.; Sanders, R. D.; Sanei, H.; Skierszkan, E. K.; Van Metre, P. C.; Veverica, T. J.; Wiklund, J. A.; Wolfe, B. B., Spatiotemporal patterns of mercury accumulation in lake sediments of western North America. *Science of The Total Environment* **2016,** *568*, 1157-1170.

- Chételat, J.; Amyot, M.; Arp, P.; Blais, J. M.; Depew, D.; Emmerton, C. A.; Evans, M.; Gamberg, M.; Gantner, N.; Girard, C.; Graydon, J.; Kirk, J.; Lean, D.; Lehnherr, I.; Muir, D.; Nasr, M.; J. Poulain, A.; Power, M.; Roach, P.; Stern, G.; Swanson, H.; van der Velden, S., Mercury in freshwater ecosystems of the Canadian Arctic: Recent advances on its cycling and fate. *Sci. Total Environ.* **2015,** *509*, 41-66.
- Lewis, T. and Lamoureux, S.F., 2010. Twenty-first century discharge and sediment yield predictions in a small high Arctic watershed. Global and Planetary Change, 71(1-2), pp.27-41.
- Schuster, P.F., Schaefer, K.M., Aiken, G.R., Antweiler, R.C., Dewild, J.F., Gryziec, J.D., Gusmeroli, A., Hugelius, G., Jafarov, E., Krabbenhoft, D.P. and Liu, L., 2018. Permafrost stores a globally significant amount of mercury. Geophysical Research Letters, 45(3), pp.1463-1471.

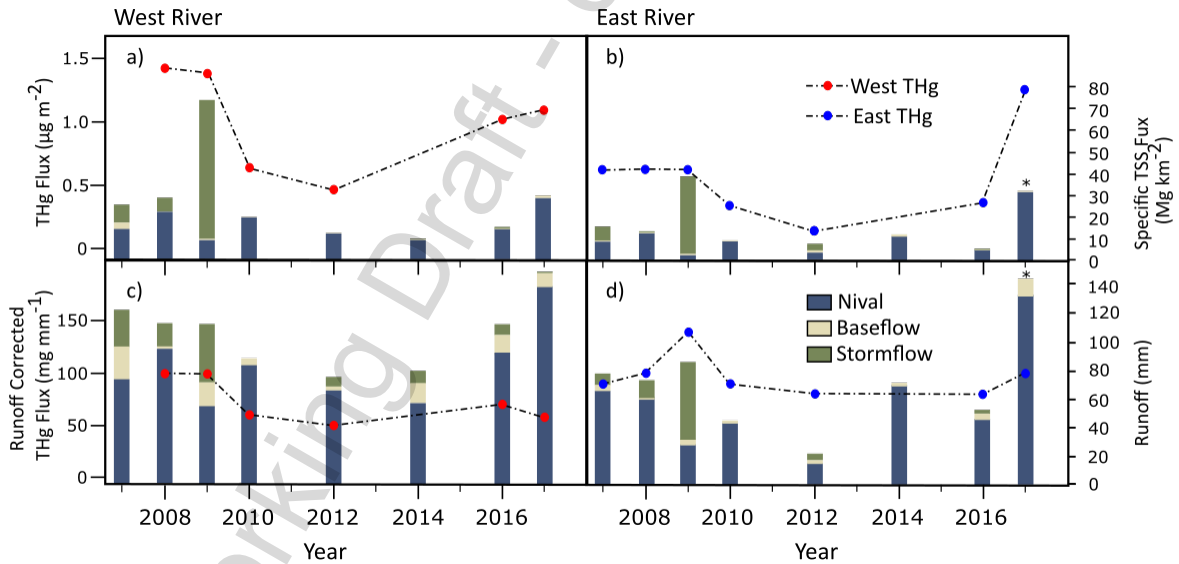

Figure X. Area-runoff corrected sediment (TSS) flux from West (a) and East river (b) (bars) and annual West (c) and East river (d) runoff during different hydrological phases. Area corrected THg flux, a) and b) and runoff corrected THg flux, c) and d) (mg mm^{-1}). Asterix (*) indicates incomplete discharge data during late season stormflow preventing calculation of THg fluxes.

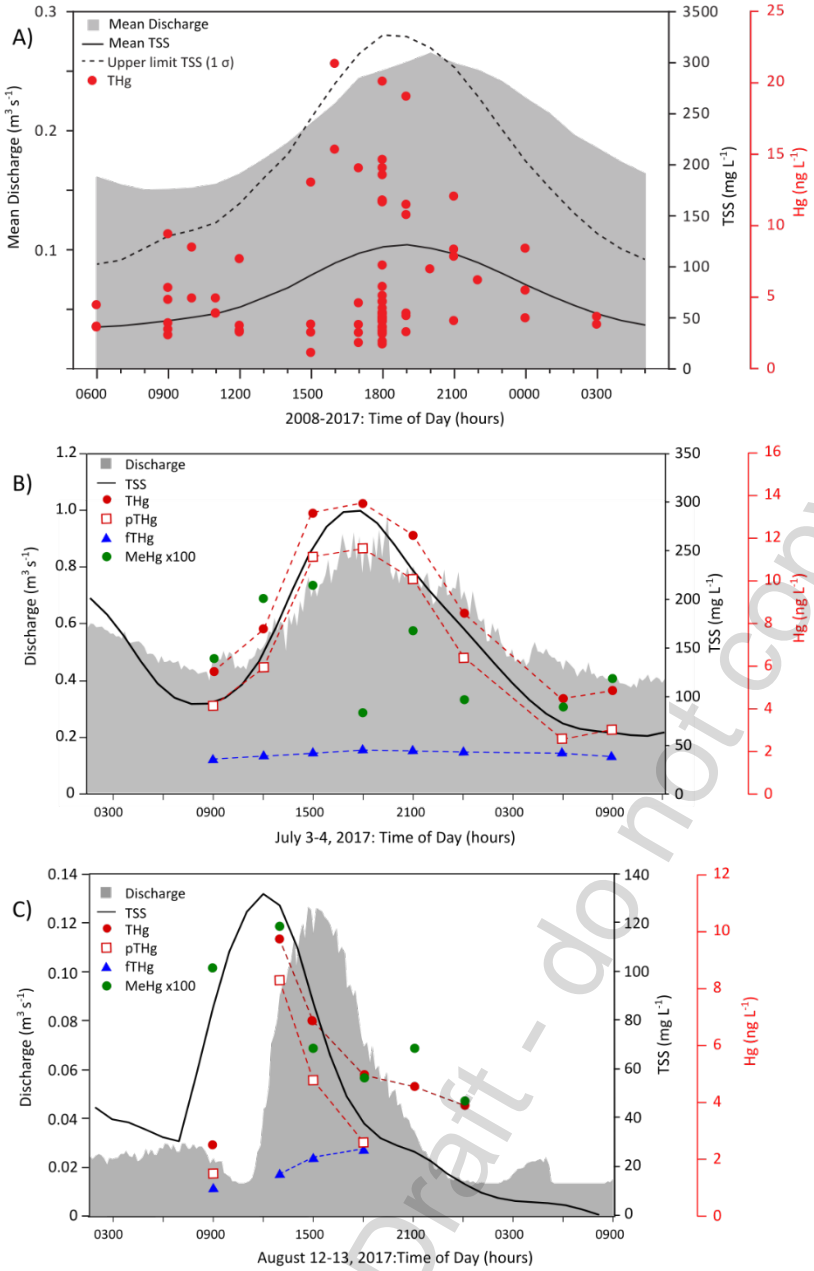

Figure X. Distribution of mercury (Hg), total suspended solids (TSS), and hydrological parameters in West River over different time periods: a) time of day compilation of all data (2008-2017); b) nival discharge period (July 3-4, 2017 shown); and c) stormflow event August, 12-13, 2017.

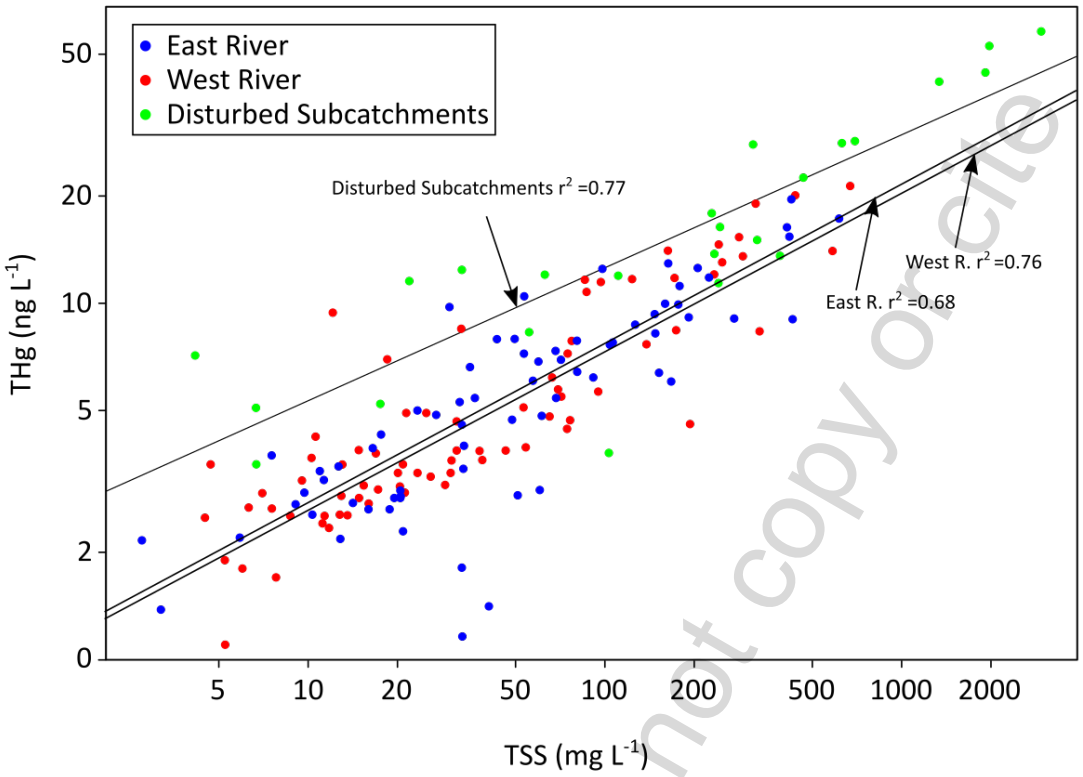

9393

9394 **Figure X.** Significant ($p<0.05$) regression relationships between concentrations of THg and TSS
9395 regressions for West River 2008-2017 (red circles), East River 2007-2017 (blue circles), and disturbed
9396 sub-catchments (Big Slide, Ptarmigan, ALD-05, Caribou) in 2009, 2016, and 2017 (green circles).
9397 Adjusted r^2 for each group indicated.

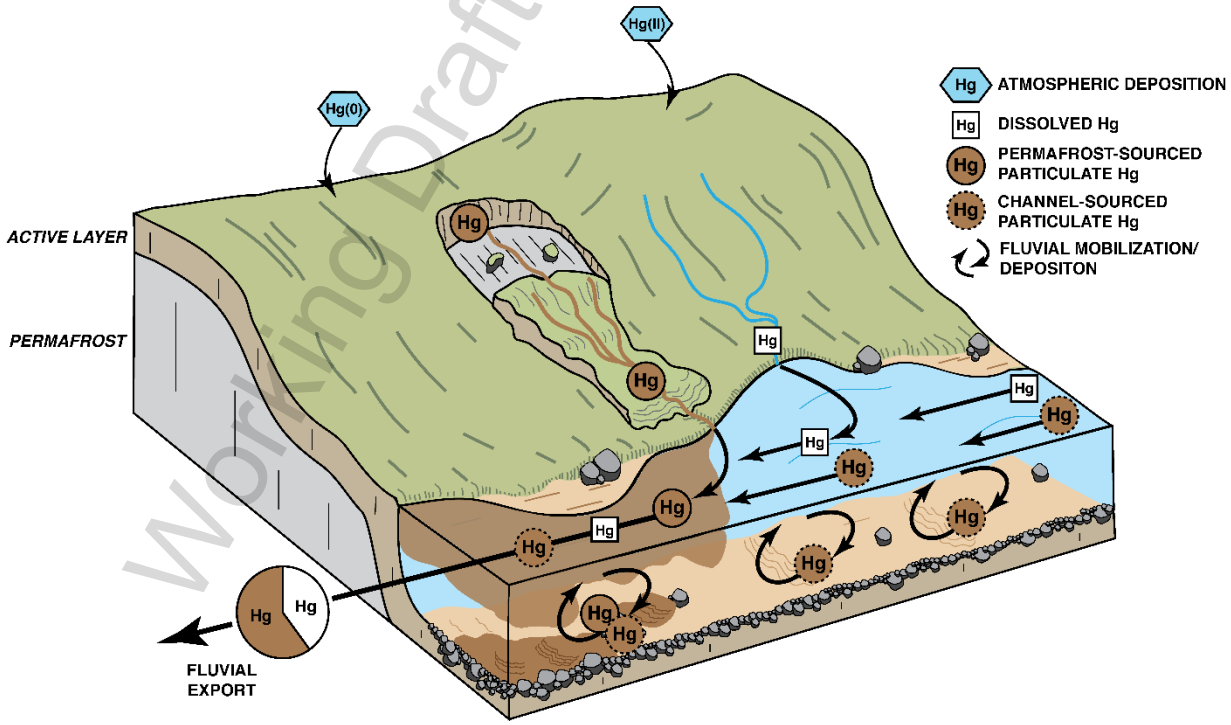

9398

Figure X. Caption to come

c. River transport

Contributors: **Kyra St Pierre**, Ville Junttila, Jaakko Mannio

(K.S.) As glaciers melt, permafrost thaws and precipitation patterns change across the Arctic, one of the principle consequences of these changes is for the transport of Hg by rivers. Rivers integrate changes happening throughout their catchments, acting as conduits for previously archived Hg mobilized by increased precipitation, active layer deepening (and other modes of permafrost thaw) and glacial melt to downstream freshwater and marine ecosystems. As rivers are one of the primary sources of Hg to the Arctic Ocean (Fisher et al. 2012 Nat Geosci.), such changes have potentially important implications for the transformation and accumulation of Hg through food webs in aquatic ecosystems (Schartup et al. 2015 PNAS).

(K.S.) The dramatic transformation of Arctic landscapes in response to climate change may lead to an increase in the transport of particulate-bound Hg. The transition from sporadic to discontinuous permafrost is associated with maximal particulate-bound Hg mobilization (Lim et al. 2019, Environ. Pollut.). Similarly, high temporal variability in the dynamics of glacial meltwater rivers across poorly consolidated High Arctic landscapes also results in Hg fluxes dominated by the particle-bound fraction (Søndergaard et al. 2015 STOTEN, St. Pierre et al. 2019 EST). The predicted climatic changes across the regions may lead to substantial changes in landscape stability, especially in regions susceptible to hillslope thermokarst (Olefeldt et al. 2016 Nat. Commun.). In these areas, we might expect to see enhanced mobilization and transport of particulate-bound Hg. Whether this Hg is then available to organisms in downstream ecosystems remains to be seen (but see Gagnon and Fisher 1997 EST).

Table 5x. Total Hg and MMHg yield estimates from Arctic rivers.

River	Basin area (km^2)	Water Source [a]	Years	Annual discharge ($km^{3)}$	THg yield (g km^{-2} yr^{-1})	MMHg yield (g $km^{-2}yr^{-1}$)	Study
SMALL RIVERS							
Eastern Canadian Arctic							
Abbé	390	S, G	2015-16	0.38-1.56	0.61-2.63	0.002-0.008	St. Pierre et al. 2019
Gilman	992	S, G	2015-16	0.44-1.93	0.72-3.30	0.003-0.010	St. Pierre et al. 2019

H. Nesmith	1274	S, G	2015-16	0.59-2.29	0.98-3.88	0.003-0.012	St. Pierre et al. 2019
Snow Goose	222	S, G	2015-16	0.30-1.18	0.61-1.96	0.003-0.007	St. Pierre et al. 2019
Turnabout	678	S, G	2015-16	0.35-1.20	0.57-2.04	0.002-0.007	St. Pierre et al. 2019
Very	1035	S, G	2015-16	0.77-1.60	1.32-2.91	0.004-0.009	St. Pierre et al. 2019
Greenland							
Kobbefjord	32	S, R, P	2008-10	0.02-0.04	0.20-0.45	-	Søndergaard et al. 2012
Zackenberg	514	S, G	2009-13	0.15 – 0.23+	1.4–3.1	-	Søndergaard et al. 2015
Sub-Arctic							
Churchill	281	S, R, P	2003-07	17	25-224	17-32	Kirk/St. Louis 2009 ES&T
Nelson	892	S, R, P	2003-07	112	70-192	0.59-7.04	Kirk/St. Louis 2009 ES&T
Finland							
Pallasjoki	107	S,R	2005–2018	0.036–0.064	0.127–2.56		Junttila et al. unpubl.
Tornionjoki	39 383	S, R	2001–2019	8.64–18.7	0,347–1,86		Junttila et al. unpubl.
Paatsjoki	14 481	S,R	2001–2008	3.4–13	0.413–4.65		Junttila et al. unpubl.
ARCTIC GREAT RIVERS							
Kolyma	0.65 x 10^6	S, R, P	1999-2017	77.6-154			Mu et al. 2019
Lena	2.4 x 10^6	S, R, P	1999-2017	457-681			Mu et al. 2019
Mackenzie	1.8 x 10^6	S, R, P	2007-10	312-346	1.3-2.4	0.008-0.013	Emmerton et al. 2013
			1999-2017	250-333			Mu et al. 2019

Ob'	2.95 x 10^6	S, R, P	1999-2017	300-547			Mu et al. 2019
Yenisey	2.5 x 10^6	S, R, P	1999-2017	447-687			Mu et al. 2019
Yukon	0.83 x 10^6	S, R, P	2001-05	203	5.2		Schuster et al. 2011
			2002-17	177-246			Mu et al. 2019

[a]Water source: G, glacial; S, snow; R, rain; P, permafrost.

Table calculations and Finnish river description text below by Ville Junttila and Jaakko Mannio: Finnish Hg inputs are based on results of Finland's environmental administration database and calculated according to the instructions provided by HELCOM (2019). Total mercury was analysed with CVAF from 2001 and ICP-MS from 2015 (both with LOQ of 0.002 µg L^{-1})

Paatsjoki

145 km long Paatsjoki is the outlet of the Lake Inarinjärvi which discharges to the Barents Sea. 71% of the Finnish catchment area (14 500 km^2) is forested and 14% wetlands. Urban areas cover 0.4% of the river basin and two wastewater treatment plants, which receive influents from 4 700 inhabitants, discharge effluents to the Lake Inarijärvi.

Tornionjoki

520 km long Tornionjoki discharges to the Bothnian Bay of the Baltic Sea. 74% of the catchment area is forested and 14% wetlands. Urban areas cover 1% of the river basin and 5 small sized wastewater treatment plants discharges effluents directly to the Tornionjoki.

Pallasjoki.

20 km long Pallasjoki is outlet of the Lake Pallasjärvi which discharges to the River Ounasjoki and further to the River Kemijoki, which discharges to the Bothinan Bay of the Baltic sea. The flow and Hg concentrations are measured at the outlet of the Lake Pallasjärvi. 69% of the catchment area (107 km^2) is forested and 7% wetlands. Urban areas cover 0.5% of the river basin but no permanent inhabitants exist.

HELCOM 2019. Guidelines for the annual and periodical compilation and reporting of waterborne pollution inputs to the Baltic Sea.

- Rigét, F.; Tamstorf, M. P.; Larsen, M. M.; Søndergaard, J.; Asmund, G.; Falk, J. M.; Sigsgaard, C., Mercury (Hg) transport in a high arctic river in northeast Greenland. *Water, Air, and Soil Pollution* **2011,** *222*, (1-4), 233-242
- Zhang, Y.; Jacob, D. J.; Dutkiewicz, S.; Amos, H. M.; Long, M. S.; Sunderland, E. M., Biogeochemical drivers of the fate of riverine mercury discharged to the global and Arctic oceans. *Global Biogeochemical Cycles* **2015,** *29*, (6), 854-864
- Sonke, J. E.; Teisserenc, R.; Heimbürger-Boavida, L.-E.; Petrova, M. V.; Marusczak, N.; Le Dantec, T.; Chupakov, A. V.; Li, C.; Thackray, C. P.; Sunderland, E. M.; Tananaev, N.; Pokrovsky, O. S., Eurasian river spring flood observations support net Arctic Ocean mercury export to the atmosphere and Atlantic Ocean. Proc. Nat. Acad. Sci. 2018, 115, (50), E11586.
- Zolkos, S.; Krabbenhoft, D.; Suslova, A.; Tank, S.; McClelland, J.; Spencer, R. G. M.; Shiklomanov, A.; Zhulidov, A.; Gurtovaya, T.; Zimov, N.; Zimov, S.; Mutter, E.; Kutny, L/; Amos, E.; Holmes, R., Mercury Export from Arctic Great Rivers. (In review)

d. Ocean currents

Contributor: Lars-Eric Heimbürger-Boavida

The largest oceanic fluxes occurs at Fram Strait (REF) and has a strong seasonal variability (Tsubouchi et al. 2018), drives the largest oceanic Hg in and outflow (Soerensen et al. 2016). Only little change of those Hg fluxes are expected (Petrova et al. in review).

- Fisher, J. A.; Jacob, D. J.; Soerensen, A. L.; Amos, H. M.; Corbitt, E. S.; Streets, D. G.; Wang, Q.; Yantosca, R. M.; Sunderland, E. M., Factors driving mercury variability in the Arctic atmosphere and ocean over the past 30 years. *Global Biogeochemical Cycles* **2013,** *27*, (4), 1226-1235
- Soerensen, A. L.; Jacob, D. J.; Schartup, A. T.; Fisher, J. A.; Lehnherr, I.; St Louis, V. L.; Heimbürger, L. E.; Sonke, J. E.; Krabbenhoft, D. P.; Sunderland, E. M., A mass budget for mercury and methylmercury in the Arctic Ocean. *Global Biogeochemical Cycles* **2016,** *30*, (4), 560-575
- Tsubouchi, T., Bacon, S., Aksenov, Y., Garabato, A. C. N., Beszczynska-Möller, A., Hansen, E., et al. (2018). The arctic ocean seasonal cycles of heat and freshwater fluxes: Observation-based inverse estimates. *Journal of Physical Oceanography*, *48*(9), 2029–2055. https://doi.org/10.1175/JPO-D-17-0239.1

9490

5.5 What are the impacts of climate change on Hg biogeochemical processes?

Notes:
Kimmo & Daniel: Organize mercury redox and methylation sections by phases/matrices such as seawater, fresh water, snow, soil, sediment
Marc: I tried to follow the notes from Kimmo and Daniel, organizing the sections by matrices; I have put info as bullet points as for now and make it as a text soon. A short overview of known processes is first given, and climate-related statements conclude each section.

The main biogeochemical processes affecting Hg cycling in the Arctic landscape are redox reactions between divalent and elemental Hg, and methylation/demethylation reactions. These reactions can occur to different extent in a variety of matrices, including freshwater, seawater, snow, sea ice, soils and sediments. They may be biotic or abiotic in nature, and are driven by environmental variables such as temperature, exposure to solar radiation, organic matter, nutrients and chloride concentrations. All these variables are expected to be modified by climate change. The effect of climate change on these two sets of reactions will be explored for key environmental compartments of the North, excluding the atmosphere.

a. Inorganic mercury redox processes

Contributor: **Marc Amyot**

Freshwater

- Mercury redox reactions in freshwater can occur through photochemical, abiotic and microbial processes (Moller et al., 2011). The relative importance of these processes varies with depth and light penetration. The dominant process is usually a net photoreduction of Hg(II) in surface waters, although there is a scarcity of data on Hg reduction and oxidation in Arctic freshwaters. One special case of Hg reduction is the photoreduction of MeHg (Chandan et al., 2014).
- Climate may alter the flux of organic matter and particulate matter to freshwater systems. This may decrease net photoreduction of Hg(II) to Hg(0) because of lower light penetration and because of interactions between DOC and reducible Hg(II) (O'Driscoll et al. 2018). Decreased net photoreduction would lead to lower Hg evasion from lake surfaces. However, this may be offset by a longer season with no ice-cover and therefore longer solar irradiation of surface waters.

- In low-DOM systems, influx of DOM may initially promote redox processes because of its role as a photosensitizer, before hampering them, and a bell-shaped response curve is likely (Girard et al. 2016).
- Dark abiotic and microbial Hg reduction occurring in bottom anoxic waters (Gu et al., 2011) is likely to increase in freshwater systems impacted by eutrophication.
- Chandan, P.; Ghosh S.; Bergquist, B.A. Mercury isotope fractionation during aqueous photoreduction of monomethylmercury in the presence of dissolved organic matter. Environmental Science and Technology 2014, 49, 259-267.
- Girard C., Leclerc M, Amyot M. 2016. Photodemethylation of Methylmercury in Eastern Canadian Arctic Thaw Pond and Lake Ecosystems. Environ. Sci. Technol. 50: 3511-3520.
- Gu, B.; Bian, Y.; Miller, C.L.; Dong, W.; Jiang, X.; Liang, L. Mercury reduction and complexation by natural organic matter in anoxic environments. Proceedings of the National Academy of Sciences of the United States of America 2011, 108(4) 1479-1483.
- Luo H.W.; Yin, X.; Jubb, A.M.; Chen, H.; Lu, X.; Zhang, W.; Lin, H.; Yu, H.Q.; Liang, L.; Sheng, G.P.; Gu, B. Photochemical reactions between mercury (Hg) and dissolved organic matter decrease Hg bioavailability and methylation. Environmental Pollution, 2017, 220, 1359-1365.
- Moller, A.K.; Barkay, T.; Al-Soud, W.A.; Sorensen, S.J.; Skov, H.; Kroer, N. Diversity and characterization of mercury-resistant bacteria in snow, freshwater and sea-ice brine from the High Arctic. FEMS Microbiology Ecology 2011 75, 390-401.
- O'Driscoll, N,J,; Vost, E.; Mann, E.; Klapstein, S.; Tordon, R.; Lukeman, M. Mercury photoreduction and photooxidation in lakes: effects of filtration and dissolved organic carbon concentration. Journal of Environmental Sciences 2018, 68, 151-159.

Seawater

- In seawater, the presence of chloride promotes Hg(0) photooxidation and can lead to a lower net photoreduction. With depth, photoredox processes are no longer significant, and microbial reduction may dominate, as indicated by the presence of the *mer*-mediated reduction (Poulain et al., 2007).
- There is no new study directly on redox transformations in seawater, but some on photodemethylation, which end-product may be Hg(0). There is however important information on Hg(0) measurements from the U.S. Arctic GEOTRACES cruise (Dimento et al., 2019) and other cruises. They reported near-saturation Hg(0) levels in ice-free waters but highly-enriched levels under ice, an indication of under-ice Hg reduction.

- Hg(II) reduction in coastal seawater can also be stimulated by riverine inputs of organic matter (Douglas et al., 2012). This should lead to increased Hg evasion in systems receiving such inputs.
- In general, longer periods of ice-free surface seawater will increase the role of Hg photoreduction in promoting Hg evasion from sea surface.
- Batrakova, N.; Travnikov, O.; Rozovskaya, O. Chemical and physical transformations of mercury in the ocean: a review. Ocean Science 2014, 10, 1047-1063.
- Poulain, A.J.; Chadhain, S.M.N.; Ariya, P.A.; Amyot, M.; Garcia, E.; Campbell, P.G.C., Zylstra, G.J.; Barkay, T. Potential for mercury reduction by microbes in the High Arctic. Applied and Environmental Microbiology 2007, 2230-2238.

Sediments

- Hg(II) can be reduced in sediments either abiotically (by interacting with DOM) or microbially.
- There is growing evidence of the presence of *merA* genes in high latitude sediments and that the effective population size of these genes is varying as a function of anthropogenic Hg inputs (Ruuskanen et al., 2019).
- In aquatic systems that will receive additional inputs of Hg linked to the thawing of permafrost, this mer-mediated reduction could increase.
- Further, inputs of OM and nutrients to sediments could also promote abiotic reduction and non-mer microbial reduction.
- Ruuskanen, M.O.; Aris-Brosou, S.; Poulain, A.J. Swift evolutionary response of microbes to a rise in anthropogenic mercury in the Northern Hemisphere. The ISME Journal 2019, https://doi.org/10.1038/s41396-019-0563-0

Snow and sea ice

- Hg(II) deposited on snow can be rapidly photoreduced and revolatilized. This process may decrease the overall impact of AMDEs (Ferrari et al. 2008; Sherman et al., 2010). The fraction of Hg remaining in snow may be highly bioavailable (Brooks et al, 2006). Deeper in the snowpack, dark oxidation occasionally occurs (Faïn et al., 2013).
- Snow and frost flowers associated with sea ice leads are characterized by high chloride levels and can retain high levels of Hg (Douglas et al., 2005), likely because of a shift in balance between Hg reduction and oxidation, favoring the latter (Mann et al., 2015). Frost flowers may also trap Hg recently re-emitted from the snowpack (Sherman et al., 2012). Overall, frost flowers may increase Hg loading to the Arctic Ocean.

- The presence of salt in melting snow will further promote a shift from particulate to dissolved Hg, likely increasing its mobility (Mann et al., 2011). Also, crystallographic history of snow and crystals will affect Hg concentrations (Douglas et al., 2008).
- Other variables impacting photoredox Hg transformations in snow include temperature, the presence of forest canopy, DOM, snowpacks oxidants (produced from DOM photolysis or from halogen chemistry) (Mann et al. 2014).
- Mercury-resistant bacteria are found in Arctic snow and sea-ice brine, and could contribute to reducing Hg(II) to Hg (0), particularly in deeper layers (Moller et al., 2011).
- Predictive models rely on simplistic reaction mechanisms or on set Hg(0) reemission percentages due to incomplete understanding of Hg redox transformations in snow/ice (Mann et al. 2014; Durnsford et al., 2012). There is a need to at least have good sets of redox reaction rates and their dependance to key variables (temperature, irradiation, snowpack chemistry). One such study is the one by Mann et al. (2015), which assessed Hg photoreaction kinetics in frozen and melted Arctic snow. They saw lower total photoreduced Hg at lower light intensity and concluded that, with climate change, earlier snowmelt periods may result in less Hg loss to the atmosphere from snowpacks.
- Another prediction emerging from recent work regards the effect of chloride on Hg retention in snow. Since there are projections for greater snowpack chloride loading, more Hg could be delivered to Arctic aquatic systems by melted snow (Steffen et al., 2013; Mann et al. 2018).

- Brooks, S. B., Saiz-Lopez, A., Skov, H., Lindberg, S. E., Plane, J. M. C., and Goodsite, M. E.: The mass balance of mercury in the springtime arctic environment, Geophys. Res. Lett., 33, L13812, https://doi.org/10.1029/2005GL025525, 2006.
- DiMento, B. P.; Mason, R. P.; Brooks, S.; Moore, C., The impact of sea ice on the air-sea exchange of mercury in the Arctic Ocean. *Deep-Sea Research Part I: Oceanographic Research Papers* **2019,** *144*, 28-38.
- Douglas, T. A. and Sturm, M.: Arctic haze, mercury and the chemical composition of snow across northwestern Alaska, Atmos. Environ., 38, 805–820, https://doi.org/10.1016/j.atmosenv.2003.10.042, 2004.
- Douglas, T. A., Sturm, M., Simpson, W. R., Brooks, S., Lindberg, S. E., and Perovich, D. K.: Elevated mercury measured in snow and frost flowers near Arctic sea ice leads, Geophys. Res. Lett., 32, L04502, https://doi.org/10.1029/2004GL022132, 2005.
- Douglas, T. A., Sturm, M., Simpson, W. R., Blum, J. D., Alvarez-Aviles, L., Keeler, G. J., Perovich, D. K., Biswas, A., and Johnson, K.: Influence of snow and ice crystal formation and accumulation on mercury deposition to the Arctic, Environ. Sci. Technol., 42, 1542–1551, https://doi.org/10.1021/es070502d, 2008.

- Douglas, T. A., Loseto, L. L., Macdonald, R.W., Outridge, P., Dommergue, Poulain, A., Amyot, M., Barkay, T., Berg, T., Chételat, J., Constant, P., Evans, M., Ferrari, C., Gantner, N., Johnson, M. S., Kirk, J., Kroer, N., Larose, C., Lean, D., Nielsen, T.G., Poissant, L., Rognerud, S., Skov, H., Sørensen, S., Wang, F., Wilson, S., and Zdanowicz, C. M.: The fate of mercury in arctic terrestrial and aquatic ecosystems, a review, Environ. Chem., 9, 321–355, https://doi.org/10.1071/EN11140, 2012.
- Faïn, X., Helmig, D., Hueber, J., Obrist, D., and Williams, M. W.: Mercury dynamics in the Rocky Mountain, Colorado, snowpack, Biogeosciences, 10, 3793–3807, https://doi.org/10.5194/bg-10- 3793-2013, 2013.
- Faïn, X., Grangeon, S., Bahlmann, E., Fritsche, J., Obrist, D., Dommergue, A., Ferrari, C. P., Cairns, W., Ebinghaus, R., Barbante, C., Cescon, P., and Boutron, C.: Diurnal production of gaseous mercury in the alpine snowpack before snowmelt, J. Geophys. Res., 112, D21311, https://doi.org/10.1029/2007JD008520, 2007.
- Ferrari, C. P., Padova, C., Faïn, X., Gauchard, P.-A., Dommergue, A., Aspmo, K., Berg, T., Cairns, W., Barbante, C., Cescon, P., Kaleschke, L., Richter, A., Wittrock, F., and Boutron, C.: Atmospheric mercury depletion event study in Ny-Ålesund (Svalbard) in spring 2005, Deposition and transformation of Hg in surface snow during springtime, Sci. Total Environ., 397, 167–177, https://doi.org/10.1016/j.scitotenv.2008.01.064, 2008.
- Mann, E.; Ziegler, S.; Mallory, M.; O'Driscoll, N., Mercury photochemistry in snow and implications for Arctic ecosystems. *Environmental Reviews* **2014,** *22*, (4), 331-345
- Mann, E. A.; Ziegler, S. E.; Steffen, A.; O'Driscoll, N. J., Increasing chloride concentration causes retention of mercury in melted Arctic snow due to changes in photoreduction kinetics. *Journal of Environmental Sciences (China)* **2018,** *68*, 122-129
- Mann, E., Meyer, T., Mitchell, C. P. J., and Wania, F.: Mercury fate in ageing and melting snow: development and testing of a controlled laboratory system, J. Environ. Monit., 13, 2695–2702, https://doi.org/10.1039/C1EM10297D, 2011.
- Mann, E. A., Mallory, M. L., Ziegler, S. E., Tordon, R., and O'Driscoll, N. J.: Mercury in Arctic snow: quantifying the kinetics of photochemical oxidation and reduction, Sci. Total Environ., 509–510, 115–132, https://doi.org/10.1016/j.scitotenv.2014.07.056, 2015.
- Moller, A.K.; Barkay, T.; Al-Soud, W.A.; Sorensen, S.J.; Skov, H.; Kroer, N. Diversity and characterization of mercury-resistant bacteria in snow, freshwater and sea-ice brine from the High Arctic. FEMS Microbiology Ecology 2011 75, 390-401.
- Moore, C. W., Obrist, D., Steffen, A., Staebler, R. M., Douglas, T. A., Richter, A., and Nghiem, S. V.: Convective forcing of mercury and ozone in the Arctic boundary layer induced by leads in sea ice, Nature, 506, 81–84, https://doi.org/10.1038/nature12924, 2014.

- Sherman, L. S., Blum, J. D., Douglas, T. A., and Steffen, A.: Frost flowers growing in the Arctic ocean-atmosphere-sea-snow interface: 2. Mercury exchange between the atmosphere, snow, and frost flowers, J. Geophys. Res., 117, D00R10, 10.1029/2011jd016186, 2012a.
- Sherman, L. S., Blum, J. D., Johnson, K. P., Keeler, G. J., Barres, J. A., and Douglas, T. A.: Mass-independent fractionation of mercury isotopes in Arctic snow driven by sunlight, Nat. Geosci., 3, 173-177, 10.1038/ngeo758, 2010.
- Steffen, A., Bottenheim, J., Cole, A., Douglas, T. A., Ebinghaus, R., Friess, U., Netcheva, S., Nghiem, S., Sihler, H., and Staebler, R.: Atmospheric mercury over sea ice during the OASIS-2009 campaign, Atmos. Chem. Phys., 13, 7007–7021, https://doi.org/10.5194/acp-13-7007-2013, 2013.
- Wang, F.; Pućko, M.; Stern, G., Transport and transformation of contaminants in sea ice. In *Sea Ice: Third Edition*, 2016; pp 472-491

Soils/ecosystems

(very little work available from arctic ecosystems – I hence listed largely work from temperate sites):

- Demers, J. D., Blum, J. D., & Zak, D. R. (2013). Mercury isotopes in a forested ecosystem: Implications for air-surface exchange dynamics and the global mercury cycle. Global Biogeochemical Cycles, 27, 222–238. https://doi.org/10.1002/gbc.20021
- Jiskra, M., Wiederhold, J. G., Skyllberg, U., Kronberg, R. M., Hajdas, I., & Kretzschmar, R. (2015). Mercury deposition and re-emission pathways in boreal forest soils investigated with Hg isotope signatures. Environmental Science & Technology, 49(12), 7188–7196. https://doi.org/ 10.1021/acs.est.5b00742
- Wang, X., et al. (2017). "Using Mercury Isotopes To Understand Mercury Accumulation in the Montane Forest Floor of the Eastern Tibetan Plateau." Environmental Science & Technology 51(2): 801-809.
- Obrist, D., Kirk, J. L., Zhang, L., Sunderland, E. M., Jiskra, M., and Selin, N. E.: A review of global environmental mercury processes in response to human and natural perturbations: Changes of emissions, climate, and land use, Ambio, 47, 116-140, 10.1007/s13280-017-1004-9, 2018.
- Obrist, D., Pokharel, A. K., and Moore, C.: Vertical profile measurements of soil air suggest immobilization of gaseous elemental mercury in mineral soil, Environ. Sci. Technol., 48, 2242-2252, 10.1021/es4048297, 2014.
- Obrist, D., Agnan, Y., Jiskra, M., Olson, C. L., Colegrove, D. P., Hueber, J., Moore, C. W., Sonke, J. E., and Helmig, D.: Tundra uptake of atmospheric elemental mercury drives Arctic mercury pollution, Nature, 547, 201–204, https://doi.org/10.1038/nature22997, 2017.

- Demers, J. D., Blum, J. D., and Zak, D. R.: Mercury isotopes in a forested ecosystem: Implications for air-surface exchange dynamics and the global mercury cycle, Global Biogeochem. Cycles, 27, 222-238, 5 Doi 10.1002/Gbc.20021, 2013.
- Yu, B., Fu, X., Yin, R., Zhang, H., Wang, X., Lin, C. J., Wu, C., Zhang, Y., He, N., Fu, P., Wang, Z., Shang, L., Sommar, J., Sonke, J. E., Maurice, L., Guinot, B., and Feng, X.: Isotopic Composition of Atmospheric Mercury in China: New Evidence for Sources and Transformation Processes in Air and in Vegetation, Environ Sci Technol, 50, 9262-9269, 10.1021/acs.est.6b01782, 2016.
- Yuan, W., Sommar, J., Lin, C.-J., Wang, X., Li, K., Liu, Y., Zhang, H., Lu, Z., Wu, C., and Feng, X.: Stable isotope evidence shows re-emission of elemental mercury vapor occurring after reductive loss from foliage, Environmental Science & Technology, 10.1021/acs.est.8b04865, 2018.
- Zheng, W., Demers, J., Lu, X., Bergquist, B. A., Anbar, A. D., Blum, J. D., and Gu, B.: Mercury stable isotope fractionation 25 during abiotic dark oxidation in the presence of thiols and natural organic matter, Environmental Science Technology,10.1021/acs.est.8b05047, 2018.
- Zheng, W., Obrist, D., Weis, D., and Bergquist, B. A.: Mercury isotope compositions across North American forests, Global Biogeochem. Cycles, 30, 1475-1492, 10.1002/2015gb005323, 2016.

b. Methylmercury production and decomposition

Contributor: **Marc Amyot**

- DiMento, B. P.; Mason, R. P., Factors controlling the photochemical degradation of methylmercury in coastal and oceanic waters. *Marine Chemistry* **2017,** *196*, 116-125
- Góngora, E., Braune, B.M. and Elliott, K.H., 2018. Nitrogen and sulfur isotopes predict variation in mercury levels in Arctic seabird prey. Marine pollution bulletin, 135, pp.907-914.
- Heimburger, L. E.; Sonke, J. E.; Cossa, D.; Point, D.; Lagane, C.; Laffont, L.; Galfond, B. T.; Nicolaus, M.; Rabe, B.; Van Der Loeff, M. R., Shallow methylmercury production in the marginal sea ice zone of the central Arctic Ocean. *Scientific Reports* **2015,** *5*
- Lehnherr, I., Methylmercury biogeochemistry: A review with special reference to Arctic aquatic ecosystems. *Environmental Reviews* **2014,** *22*, (3), 229-243
- Lehnherr, I.; St. Louis, V. L.; Emmerton, C. A.; Barker, J. D.; Kirk, J. L., Methylmercury cycling in high arctic wetland ponds: Sources and sinks. *Environmental Science and Technology* **2012,** *46*, (19), 10514-10522.

- Lehnherr, I.; St. Louis, V. L.; Kirk, J. L., Methylmercury cycling in high arctic wetland ponds: Controls on sedimentary production. *Environmental Science and Technology* **2012,** *46*, (19), 10523-10531.
- Macdonald, R. W.; Loseto, L. L., Are Arctic Ocean ecosystems exceptionally vulnerable to global emissions of mercury? A call for emphasised research on methylation and the consequences of climate change. *Environmental Chemistry* **2010,** *7*, (2), 133-138
- Munson, K. M.; Lamborg, C. H.; Boiteau, R. M.; Saito, M. A., Dynamic mercury methylation and demethylation in oligotrophic marine water. *Biogeosciences* **2018,** *15*, (21), 6451-6460
- Soerensen, A. L.; Schartup, A. T.; Skrobonja, A.; Björn, E., Organic matter drives high interannual variability in methylmercury concentrations in a subarctic coastal sea. *Environmental Pollution* **2017,** *229*, 531-538
- St. Pierre, K. A.; Chételat, J.; Yumvihoze, E.; Poulain, A. J., Temperature and the sulfur cycle control monomethylmercury cycling in high arctic coastal marine sediments from Allen Bay, Nunavut, Canada. *Environmental Science and Technology* **2014,** *48*, (5), 2680-2687
- St. Pierre, K. A.; St. Louis, V. L.; Kirk, J. L.; Lehnherr, I.; Wang, S.; La Farge, C., Importance of open marine waters to the enrichment of total mercury and monomethylmercury in lichens in the canadian high arctic. *Environmental Science and Technology* **2015,** *49*, (10), 5930-5938
- Wang, F.; MacDonald, R. W.; Armstrong, D. A.; Stern, G. A., Total and methylated mercury in the beaufort sea: The role of local and recent organic remineralization. *Environmental Science and Technology* **2012,** *46*, (21), 11821-11828
- Yang, Z.; Fang, W.; Lu, X.; Sheng, G. P.; Graham, D. E.; Liang, L.; Wullschleger, S. D.; Gu, B., Warming increases methylmercury production in an Arctic soil. *Environmental Pollution* **2016,** *214*, 504-509
- Poste, Braaten (joint first authors), Sørensen, de Wit, Larssen, 2015. Effects of photodemethylation on the methylmercury budget of boreal Norwegian lakes. Environmental Toxicology & Chemistry, 34, 6, 1213-1223.
- Girard C., Leclerc M, Amyot M. 2016. Photodemethylation of Methylmercury in Eastern Canadian Arctic Thaw Pond and Lake Ecosystems. Environ. Sci. Technol. 50: 3511-3520. *Notes:* (from Kimmo): increasing temperature effects in snow, soil, water, in lakes: complex interactions among increased temperature, browning, eutrophication and UV

5.6 How has climate change altered Hg exposure in Arctic biota?

- Wang, F. et al. How closely do mercury trends in fish and other aquatic wildlife track those in the atmosphere? – Implications for evaluating the effectiveness of the Minamata Convention. Sci. Total Environ. 674, 58-70, (2019).
- AMAP, 2019. AMAP Assessment 2018: Biological Effects of Contaminants on Arctic Wildlife and Fish.
- Braaten, Åkerblom, Kahilainen, Poste, Rask, Vuorenmaa, Malinen, Lydersen, Amundsen, Kashulin, Kashulina, Terentyev, Christensen, de Wit, 2019. Improved environmental status: 50 years of declining fish mercury levels in boreal and subarctic Fennoscandia. Environmental Science & Technology, 53, 4, 1834-1843.
- Poste, Pastukhov, Braaten, Ozersky, Moore, 2018. Seal teeth document the rise and fall of mercury contamination in the food web of Lake Baikal. Environmental Toxicology & Chemistry. DOI: 10.1002/etc.4095.
- Ruus, Øverjordet, Braaten, Evenset, Christensen, Heimstad, Gabrielsen, Borgå, 2015. Methylmercury biomagnification in an Arctic pelagic food web. Environmental Toxicology & Chemistry, 34, 11, 2636-2643.
- Braaten, Harman, Øverjordet, Larssen, 2014. Effects of sample preparation on methylmercury concentrations in Arctic organisms. International Journal of Environmental Analytical Chemistry, 94, 9, 863-873.

a. Marine biota

Contributors: **Melissa McKinney**, Magali Houde, Derek Muir, Heli Routti, Kyle Elliott/Kim Fernie, Robert Letcher, Adam Morris, Dave Yurkowski,

(Magali, Derek) The ringed seal (*Phoca hispida*) has been a key biomonitoring animal for evaluating trends of contaminants in the Arctic. Temporal trends of total mercury (THg) in ringed seals from the Canadian Arctic were evaluated in relation with climate parameters such as precipitation, climatic indices and ice-coverage (Houde, Muir, et al, In prep). More than 1,500 ringed seals from regions of the Beaufort Sea, Central Arctic, Eastern Baffin Island, Hudson Bay and Ungava/Nunatsiavut were collected with the help of northerners between 1972 and 2017. Results indicated that THg concentrations in liver increased with age of seals, in a site-specific manner, to about 15 years of age and no differences in accumulation were found between sexes. Mercury concentrations did not significantly change through time in seal liver, however, levels of muscle THg decreased significantly over the time period in seals from East Baffin Island (-3.1%) and Ungava/Nunatsiavut (-3.9%). THg concentrations in both tissues were found to significantly increase with nitrogen stable isotope

(δ15N), indicative of trophic levels, in seal muscle. An increase in δ15N values overtime was also found in seals from the Central Arctic. Moreover, carbon stable isotope (δ13C) values in muscle of seals decreased significantly at all sites through time suggesting a shift in diet towards pelagic and/or offshore preys.

When comparing with climate factors, results indicated that the mean air temperature was negatively related to mercury levels in muscle of all seals from the Central Arctic and Baffin island; lower THg accumulation in seal tissues were observed at these sites in years with warmer temperatures (Figure X). Precipitations (including rain and snow) were associated with higher Hg concentrations in liver of seals from the Beaufort Sea during the studied period and negatively correlated with muscle levels in two regions (Beaufort Sea and Central Arctic).

The Arctic Oscillation (AO) recorded during the year of, or preceding, the sampling was in general positively correlated with Hg in seals from different Canadian Arctic regions (Figure X). The relationships were, however, negative in Hudson Bay seals for climate data collected on the year of capture. Similar observations were made between Hg concentrations in both tissues and the North Atlantic Oscillation (NAO) (Figure X). Mercury tissue levels associations with the Pacific/North America Pattern (PNA) data were overall negatively associated with levels of THg in seals at multiple sites. Analyses indicated that the total annual sea-ice coverage recorded the year of, or preceding, the hunts was negatively linked with Hg levels in muscle and liver of seals from the Beaufort Sea. These results suggest that the loss of ice coverage could contribute to higher accumulation of mercury in seals. The type of ice could also be of importance in the accumulation of Hg in seals as new-ice coverage was significantly related to THg in muscle as compared to first-year ice and multi-year ice (Houde et al prep).

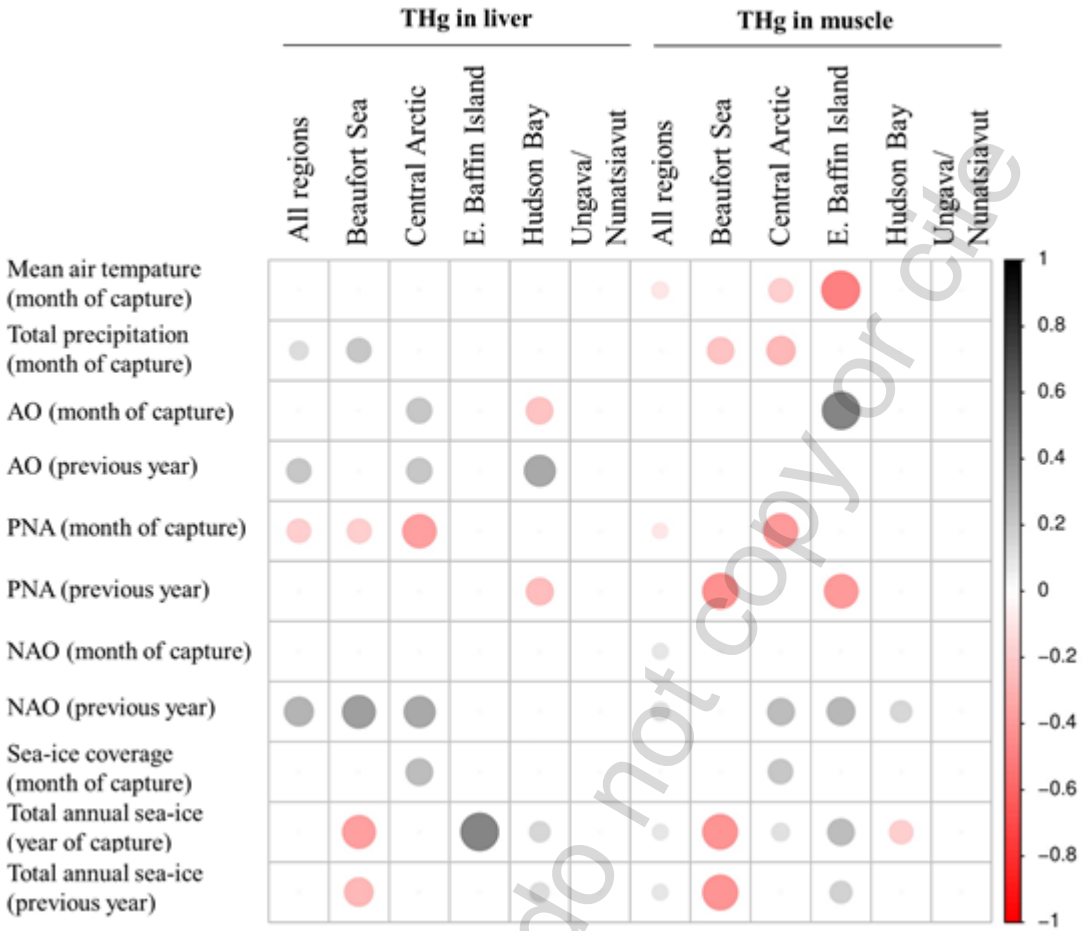

Figure X.

(Adam and Rob) Linear regressions of THg concentrations (***μ***g g^{-1} dw) versus year of sampling were not significant in liver of southern (2008–2016) or western (2007–2015) Hudson Bay polar bears (SHB and WHB respectively), thick-billed murre eggs from Coats Island (1993–2015, Northern HB, THg was normalized to the mean δ^{15}N = 14.2 ‰), or kidney of caribou from the Qamanirjuaq herd (2006–2015, normalized to the mean age = 6.2 yr) also in the WHB region (Table 1) (Morris et al., 2020). In Morris et al.(2020), contaminant concentrations in murres were normalized to the mean δ^{15}N to compensate for the significant decrease observed from 1993 to 2015 (r^2 = 0.16, p = 0.0008, n = 65, slope = -0.029 ‰ yr^{-1}), as also previously observed at both Coats Island and High Arctic murre colonies (Braune et al., 2014). The δ^{15}N and δ^{13}C ratios in the polar bears did vary by year, with diet previously identified as a significant factor affecting contaminant concentrations in WHB bears (McKinney et al., 2009; McKinney et al., 2010); however, the extent of the data did not allow for dietary normalization in both subpopulations which would be necessary for comparison. Regardless these changes are important to consider as they have not been uniform over time. In the SHB, the δ^{13}C appeared to have increased (r^2 = 0.021, p = 0.14, n = 101, slope = +0.037 ‰ yr^{-1}) from spring 2010 to spring 2016 while the δ^{15}N appears to have decreased (r^2 = 0.0021, p = 0.65, n = 100, slope =

-0.022 ‰ yr^{-1}) though interpretation is limited as those regressions were not significant (Morris et al. 2020). Like the SHB, the $\boldsymbol{\delta}^{15}N$ signatures may have decreased in the WHB from fall 2007 to fall 2015 (r^2 = 0.0084, p = 0.42, n = 78, slope = -0.059 ‰ yr^{-1}), however, only the $\boldsymbol{\delta}^{13}C$ changed significantly, decreasing over that period (r^2 = 0.11, p = 0.0037, n = 78, slope = -0.059 ‰ yr^{-1}) (Morris et al., 2020), indicating changes in the opposite direction of the SHB bears and possibly a greater influence of terrestrial/inland resources and/or changes in prey species of seal as previously observed (McKinney et al., 2009).

General linear models (GLMs) were also used to test the combined effects of year, a range of climate and weather variables (time-lagged zero to 3-yrs) and their interactions on THg concentrations in the same populations of animals (Morris et al., 2020). Sea ice exhibited significant relationships with concentrations of THg in caribou and SHB polar bears, but not in the WHB bears or the murres (Morris et al.2020). More sea ice in the eastern HB (later break up dates, shorter ice-free periods, or greater fall sea ice coverage) was consistently associated with greater concentrations of THg in liver of SHB polar bears (Table 1). The two strongest models for caribou found that concentrations of THg increased when the 1-yr and 2-yr time-lagged ordinal dates of sea ice freeze up were later (calculated based on 50 % and 90 % coverage, respectively). Compensating for the freeze up date 1-yr prior to sampling also produced a significant trend with year (4.4 % yr^{-1}) in the multivariate model with sea ice in caribou (Morris et al., 2020) (Table 1). It has been previously shown that greater ice coverage, shorter ice-free periods and later break up times allow polar bears to effectively hunt high trophic level prey such as seals for longer periods of time (Derocher et al., 2004). MacDonald et al. (2005) also put forth more sea ice would limit mercury volatilization and increase bioavailability to the marine food web, both of which could increase levels of mercury as observed in the Morris et al. (2020) study. Conversely, greater concentrations of THg in caribou with later freeze up dates could be due to greater volatilization and deposition of Hg from HB waters to nearshore lichens (and theoretically other vegetation), as observed in the high Arctic (St Pierre et al., 2015).

Morris et al.(2020) also found that concentrations of THg in murre eggs and caribou were related to June and summer AO values 3-yrs prior to sampling (Table 1). In these models, AO+ conditions 3-yrs prior to sampling were associated with lower concentrations of THg in both species (Table 1). The latitude of the HB study sites situates them between zones of influence of the oscillation indices and directly in the latitude of the westerly winds and the Jetstream, which strengthen under AO+ conditions. In murre eggs, higher annual sea level pressures 1-yr prior to sampling were associated with greater concentrations of THg (Table 1), corroborating the June AO model, as in the AO- phase, sea level pressure is greater at greater latitudes, and THg concentrations tended to be greater in that phase of the AO.

Morris et al. (2020) also reported that greater precipitation levels in the summer or fall 1-yr prior to sampling resulted in greater tissue residues of THg in WHB polar bears and caribou, which is a logical result of greater atmospheric scavenging and deposition associated with more precipitation (Macdonald et al., 2005). Greater fall and annual wind speeds (3-yr time-lag) were related to lower concentrations of Hg in murre eggs, but greater winter wind speeds (no time lag) were related to greater concentrations in WHB polar bear livers (Table 1) (Morris et al., 2020). Differences in time-lags, wind direction, and the status of the oscillation indices would all affect how contaminants are delivered or dispersed by greater wind speeds depending on the source region, which may explain these differences between the species.

Morris et al.(2020) also found that SHB bears exhibited significant positive relationships between THg and forest fire extent (total hectares burned annually) in the Northwest Territories and Manitoba. These relationships could be due to emissions of Hg or, for example, from enrichment of the HB food web due to increased nutrient inputs and productivity after fires, which resulted in greater concentrations of Hg in high trophic position lake fish (Kelly et al., 2006).

Table 1. Results of general linear model[a] tests of weather and climate factors with concentrations of total mercury (THg, μg g^{-1} dry weight) in kidney of caribou from the Qamanirjuaq herd, eggs of thick-billed murres, and liver of southern and western Hudson Bay (SHB and WHB) polar bears. Constants ($\boldsymbol{\beta}_0$) are shown with the coefficients ($\boldsymbol{\beta}_x$), listed in the order in the formula given in the model. Models are listed in order of lowest to highest Akaike Information Criterion corrected for small sample sizes (AIC_C).

Models	n	$\boldsymbol{\beta}_0$	$\boldsymbol{\beta}_1$	$\boldsymbol{\beta}_2$	AICc	MSE[b]	r^2_{ADJ}	*p*-value
Caribou (kidney)[c]								
Year	10	-63	0.032	--	11.2	0.11	0.0023	0.34
2 -Yr lagged Central HB > 90% freeze up	10	-10	0.034	--	2.08	0.040	0.60	0.0053
Year + 1-Yr lagged NW HB > 50% freeze up	10	-104	0.043	0.060	3.03	0.032	0.72	0.0047
3 -Yr lagged summer AO	10	1.4	-0.52	--	6.20	0.054	0.39	0.031
1-Yr lagged fall precipitation[d]	7	-0.83	0.012	--	--	--	0.58	0.029
Thick-billed murre (egg)[e]								
Year	13	-16	0.0079	--	-14.54	0.013	0.11	0.139
1-yr lagged annual sea level pressure	13	-104	0.10	--	-23.97	0.006	0.57	0.0017
3-Yr lagged fall wind speeds	13	0.20	-0.029	--	-17.51	0.010	0.29	0.032
3-Yr lagged June AO	13	-0.30	-0.12	--	-17.41	0.012	0.29	0.034

3-Yr lagged annual wind speeds	13	1	-0.072	--	-17.34	0.012	0.29	0.035
Western Hudson Bay bears (liver)								
Year	8	-58	0.031	--	8.59	0.060	-0.013	0.38
Winter wind speeds	8[f]	0.57	0.12	--	0.027	0.028	0.65	0.0094
3-Yr lagged fall air temperature	8	3.4	0.12	--	3.34	0.036	0.47	0.035
1-Yr lagged summer precipitation	5	2.4	0.0045	--	--	--	0.93	0.0057
Southern Hudson Bay bears (liver)								
Year	7	-86	0.044	--	6.31	0.035	0.30	0.1187
1-yr lagged NT total ha burned (fire)	7	2.90	1.5E-07	--	0.32	0.027	0.70	0.0116
Eastern HB < 30 % break up date	7	1.3	0.0098	--	0.39	0.027	0.70	0.0119
Eastern HB ice free days[g]	7	4.2	-0.0072	--	1.01	0.026	0.67	0.0150
Eastern HB summer sea ice coverage (%)	7	2.8	0.013	--	1.05	0.029	0.67	0.0152
Eastern HB fall sea ice coverage (%)	7	2.8	0.20	--	1.42	0.031	0.65	0.0175
2-yr lagged MB total ha burned (fire)	7	2.9	4.2E-07	--	2.28	0.15	0.61	0.0242

[a] The GLMs used a backwards stepwise procedure to find the model with the lowest AIC_C from the basic formula LN [THg µg g^{-1} dry weight] = $\boldsymbol{\beta}_0$ + $\boldsymbol{\beta}_1$.Year + $\boldsymbol{\beta}_2$.Climate/Weather factor + $\boldsymbol{\beta}_3$.(Year x Climate/Weather factor).

[b] MSE = mean squared error from leave-one out cross validation procedures; the MSE values indicated that the models were consistent, though the exact rankings did differ from those based on the AIC_C.

[c] Caribou THg concentrations were normalized to a mean age of 6.2 years prior to GLM modeling.

[d] AIC_C values are not shown for precipitation due to multiple missing values, which prohibits comparisons as only models with equal n values can be compared using their AIC_C.

[e] Concentrations of THg in murre eggs were normalized to a mean $d^{15}N$ of 14.2 ‰.

[f] One of the winter wind speed values was missing and was imputed in order to facilitate comparisons using AIC_C.

[g] This ice-free period was calculated as the number of days between the date of < 30 % sea ice coverage at break up and the > 10 % coverage at freeze up.

(Dave - paper in revision; also a work in progress, can add a figure or 2 if needed) Polar bears (*Ursus maritimus*) and ringed seals (*Pusa hispida*) form a strong Arctic predator-prey relationship and are experiencing habitat loss with decreasing sea ice extent and harmful dietary exposure to total mercury (THg) and other pollutants. The spring sea ice period is important for both polar bears and ringed seals, as polar bears use sea ice as a hunting platform during spring before sea ice break-up, while ringed seals use the sea ice for pupping and their annual molt prior to feeding intensively during the

open water period. Both species are opportunistic foragers and consume a wide variety of prey items, but no study has investigated whether both polar bears and ringed seals inhabiting the same geographic area are responding to ecosystem changes similarly by exhibiting similar temporal patterns in THg concentration, niche dynamics, and body fat condition.

Polar bear hair (n = 590) and adipose (n = 429) samples, as well as ringed seal muscle (n = 294) samples were collected from 2003-2016 in southwestern Hudson Bay (Yurkowski et al 2020 ES&T). Inter-annual changes in polar bear $\delta^{15}N$ values were strongly correlated with ringed seal $\delta^{15}N$ indicating that temporal changes in polar bear $\delta^{15}N$ values are dependent on ringed seal $\delta^{15}N$ values suggesting that mechanisms which influence inter-annual variability in food chain dynamics lower in the food web may affect both polar bears and ringed seals similarly. A decline in THg concentration (by 3.8% per year) and $\delta^{13}C$ (by 1.5‰ over 13 years) occurred in ringed seals suggesting a change in feeding habits and increased use of phytoplankton carbon versus benthic or sympagic carbon over time, whereas no changes occurred in polar bears. This trend was also observed in western Hudson Bay beluga whale (*Delphinapterus leucas*) where both THg concentration and $\delta^{13}C$ declined from 1984-2008 likely due to increased consumption of more-offshore or pelagic-associated prey (Gaden et al. 2010).

Contrasting temporal patterns of 3-dimensional niche size, which incorporates $\delta^{13}C$, $\delta^{15}N$ and THg concentration, and $\delta^{13}C$ range between ringed seals and polar bears occurred where niche size significantly decreased in polar bears but not in ringed seals and $\delta^{13}C$ range significantly decreased in polar bears, whereas a significant increase occurred in ringed seals. These contrasting patterns suggest that both species are likely responding differently to temporal changes in carbon production between pelagic, sympagic and benthic pathways, and inter-annual changes in prey availability.

In addition, the $\delta^{13}C$ spacing between niches of both species increased by approximately 1.5x suggesting different responses to annual changes in sympagic-pelagic carbon source production. The changing foraging ecologies for both polar bears and ringed seals suggest a weakening of this predator-prey relationship where polar bears still derive most of their carbon energy from sympagic sources (~80%; Brown et al. 2018) as opposed to ringed seals who are now more-associated with pelagic carbon. Indications of the polar bear-ringed seal relationship weakening with climate change is apparent in East Greenland (McKinney et al. 2013) and Svalbard (Hamilton et al. 2018) and is likely also occurring in western Hudson Bay. These trends are only likely to continue with our current greenhouse gas emissions resulting in the continual deterioration of polar bear and ringed seal habitats (Castro de la Guardia et al. 2013).

(Melissa; work in progress) In the Arctic marine environment, studies assessing how climate change-linked variation in diet or food web composition affects THg (and persistent organic pollutant) levels in biota have recently been reviewed (McKinney et al 2015). Reports came from marine mammals and seabirds in the Canadian Arctic, Greenland, and Svalbard, Norway. At that time, no such reports for THg in marine invertebrate or fish had been published, and no data was available from the Alaskan or Russian Arctic regions.

The first empirical evaluation of these relationships was a study on ringed seals sampled in the western Canadian Arctic community of Ulukhaktok, NWT (Gaden et al 2009). Levels of THg were found to be higher in the years that followed both shorter and longer ice-free seasons relative to years following more average-type ice-free season length. It was suggested that such variation in environmental conditions influenced the abundance and age classes of ringed seal prey, in particular, Arctic cod (*Boreogadus saida*), and hence ringed seal exposures to THg. Markers of dietary variation, δ15N and δ13C did not show associations with length of ice-free season, but this may have been a consequence of varying turnover rates between THg and δ15N and δ13C. No overall temporal trends were found over the study period from 1973 to 2007. Further east, THg temporal trends in central West, Northwest and central East Greenland ringed seals in were assessed in relation to climate metrics, including water temperature, sea ice coverage, and Arctic Oscillation (AO) index (Rigét et al 2012). From the early 1980s to 2010, THg levels rose by 10% and 2% per year in central East Greenland (Ittoqqortoormiit) and Northwest Greenland (Avanersuaq), respectively. In addition to other factors such as year, age, and trophic position, the THg levels in all three regions were explained by the winter AO index. That is, levels of THg were higher when the AO was higher, i.e., when conditions enhanced transport of air masses from North America and Europe to the region and when precipitation was higher. The authors thus suggested that higher THg levels may be found in ringed seal under climate change due to greater atmospheric and fluvial transport. From the mid-1980s or 1990s to 2000s in Hudson Bay and Foxe Basin, Canada, levels of THg declined in beluga whale, but not in Atlantic walrus and narwhal (Gaden and Stern 2010). Ratios of δ13C also decline in beluga, suggesting the possibility of a shift in their prey type or habitat, but only weak associations of δ13C and the NAO index were found. As well, no associations were found between δ15N or THg with NAO. IIn another study on beluga whales, THg levels increased from 1981 to 2002, but then declined or stabilized through to 2012 in individuals from the Beaufort Sea (Loseto et al 2015). Climate indices, such as the Pacific Decadal Oscillation (PDO) with an eight-year time lag, better explained variation in THg levels than did δ13C or δ15N ratios.

For seabirds, at two locations in Svalbard, black-legged kittiwakes (Rissa tridactyla) and little auks (Alle alle) THg levels and δ15N ratios were compared between 2008 and 2009 (Øverjordet et al., 2015). For kittiwakes, levels of THg were lower when they were feeding at a lower trophic position

and showed different feeding habits. These lower trophic position years had less ice, and thus less access to Arctic cod, which are at a higher trophic position than other prey prey. However, THg was not affected by trophic position in little auks, which exhibit more specialized feeding behaviours on invertebrates, relative to the more opportunistic feeding behaviour on various fish and invertebrates exhibited by kittiwakes. In the low and high Canadian Arctic, thick-billed murres (Uria lomvia) links between THg trends and diets and/or sea ice conditions were investigated (Braune et al., 2014). Increases in fish versus invertebrate prey have been found in the high Arctic (Provencher et al., 2012), and here, THg levels increased at a faster rate than when adjusted for diet change (using δ15N). Increases in lower trophic level capelin versus Arctic cod prey have been found in the low Arctic in association with sea ice declines, and here, THg levels did not show trends, while δ15N-adjusted trends increased. These findings may be partly be explained by the co-occurring shift to lower trophic level prey, but it was suggested that changes in Hg cycles and bioavailability and other factors related to climate change, may also have played a role.

Additional work has been published subsequent to the review (McKinney et al 2015). For polar bears from the southern Beaufort Sea, Alaska, as the sea ice has declined both spatially and temporally, the proportion of the subpopulation spending an extended period of time (more than 21 days per year) onshore during the reduced ice season has risen (Atwood et al 2016). While onshore, these polar bears consume the remains of subsistence-harvested bowhead whales and possibly other prey (Schiebe et al 2008; Rogers et al 2015, McKinney et al 2017a, Bourque et al 2020). Levels and trends of THg were investigated in this polar bear subpopulation over a period of increasing land use from 2004 to 2001 (McKinney et al 2017b). Levels of THg declined in spring-sampled polar bears by 13% per year, mainly driven by declines in adult males. Lower THg concentrations were associated with higher body mass index (BMI) and higher proportional consumption of lower trophic position prey. Trends in THg adjusted for BMI showed non-significant declines, suggesting that altered feeding and condition, not declining environmental concentrations of mercury, were responsible for these short-term declines in THg concentrations. As longer-term studies of this (Rode et al 2010, 2014) and some other polar bear populations have conversely shown declines in polar bear body condition, McKinney et al (2017b) suggested that body condition declines should, in fact, drive up circulating levels of THg.

Shifts in the composition of forage fish communities in the Arctic may also have implications for THg or MeHg levels in top predators. Need to describe Pedro et al 2017, Pedro et al 2019** ***

(Heli; Svalbard polar bears) Temporal trends of mercury in relation to variation in carbon, nitrogen and sulphur isotopes were investigated in 177 hair samples from adult female polar bears sampled from Svalbard 1995-2016 (Lippold et al. in revision). Temporal decline in δ13C and δ34S values

measured in hair indicated an increasing proportion of terrestrial diet items from terrestrial sources over time. Alternatively, changes in δ34S may reflect increasing sulfate reduction rate, leading to higher MeHg concentrations in the environment. THg concentrations increased with increasing δ13C and δ34S values, which suggested that polar bears with more mixed diet were more exposed to Hg than those with solely marine diet. Concentrations of tHg increased between 1995 and 2016 with a steeper increase after 2000. When tHg concentrations were corrected for δ13C or δ34S, the increase in the later period was steeper. This suggests that the change of diet towards more terrestrial food items exposes polar bears to lower concentrations of Hg.

(Heli; Growth and bioenergetics - mammals and birds)
Arctic marine mammals go through seasonal changes in body fatness. For example, polar bears generally feed extensively in spring and early summer, when ringed seals are pupping and moulting on sea ice. During sea ice free periods, polar bears have reduced if any access to food and they thus fast. Pregnant females spend winter in den, so they can fast up to eight months in a row. Variation in polar bear body condition in the Beaufort Sea has been related to hair mercury concentrations, with higher levels in thinner individuals (McKinney et al., 2017). McKinney et al. suggested that MeHg deposition in the fur may be increased in fasting polar bears that catabolize proteins and thus mobilize MeHg into the blood circulation. However, the relationships may also be related to changes in diet, as body condition, diet and Hg were all inter-related. Lippold et al. (in revision) reported also a negative, although non-significant, trend between body condition and hair THg in female polar bears from Svalbard. As the body condition was not confounded with diet, increased Hg deposition during fasting is a likely explanation for higher Hg concentrations in thinner bears. Similarly to the polar bear studies, feather Hg concentrations were negatively related to body condition in little auks from East Greeland (Amélineau et al., 2019). A contrasting relationships was found for blood Hg concentrations and eider body condition (Provencher et al., 2016). Body condition of arctic foxes was not related to their body fatness (Hallanger et al., 2019).

Blevin et al. (2017) hypothesized that Hg among other pollutants would affect metabolic rate through changes in thyroid hormone levels in kittiwakes from Svalbard. The results showed, however, that Hg was not related to metabolic rate neither in males or females (Blévin et al., 2017).

(From Kim Fernie and AMAP POPs-CC report): For thick-billed murres breeding in Hudson Bay, early results suggest that higher circulating concentrations of total mercury were related to lower circulating triiodothyronine that in turn was related to increased time diving under water when foraging for prey; however, these relationships were evident during the course of this study, only when ice conditions were average (2016) or poor for the birds (2017; ice disappeared early), and not

when there was much ice available later in the breeding season for the birds to forage from for prey (2018) (K. Fernie (ECCC) and K. Elliott (McGill University), pers. comm.).

- Foster, K.L., Braune, B.M., Gaston, A.J., Mallory, M.L. Climate influence on mercury in arctic seabirds (in submission?)
- Routti, H., Letcher, R.J., Born, E.W., Branigan, M., Dietz, R., Evans, T.J., McKinney, M.A., Peacock, E., Sonne, C., 2012. Influence of carbon and lipid sources on variation of mercury and other trace elements in polar bears (Ursus maritimus). Environmental Toxicology and Chemistry 31, 2739–2747. 10.1002/etc.2005
- Fort et al. 2016 Does temporal variation of mercury levels in Arctic seabirds reflect changes in global environmental contamination, or a modification of Arctic marine food web functioning? Env. Pollut. DOI: 10.1016/j.envpol.2015.12.061
- Ruus et al. 2015 Methylmercury biomagnification in an Arctic pelagic food web. Env Tox Chem DOI: 10.1002/etc.3143
- Pomerleau, C., Matthews, C.J.D., Gobeil, C., Stern, G.A., Ferguson, S.H., Macdonald, R.W., 2018. Mercury and stable isotope cycles in baleen plates are consistent with year-round feeding in two bowhead whale (Balaena mysticetus) populations. Polar Biology 41, 1881-1893. 10.1007/s00300-018-2329-y
- Rigét, F. F., Vorkamp, K. & Muir, D. C. G. Temporal trends of contaminants in arctic char (Salvelinus alpinus) from a small lake, southwest Greenland during a warming climate. J. Environ. Monit 12, 2252-2258, (2010).
- Carrie, J. et al. Increasing contaminant burdens in an arctic fish, burbot (Lota lota), in a warming climate. Environ. Sci. Technol 44, 316-322, (2010).
- Burt, A. et al. Mercury uptake within an ice algal community during the spring bloom in first-year Arctic sea ice. Journal of Geophysical Research: Oceans 118, 4746-4754, (2013).

b. Terrestrial biota

Contributors: **Heli Routti**

(Heli) Some species, like the Arctic fox is a terrestrial species, but it also feeds on marine food webs at coastal tundra areas (Dalerum et al., 2012; Ehrich et al., 2015; Eide et al., 2005). Variation in arctic foxes' diet may have further consequences to their mercury exposure as terrestrial prey such as reindeers, geese and ptarmigans have lower levels of Hg than marine prey species such as seals and seabirds (Aastrup et al., 2000; Braune and Malone, 2006; Fant et al., 2001; Jæger et al., 2009; Pacyna et al., 2018; Pedersen et al., 2006). Coastal Arctic foxes that feed on marine prey items have considerable higher levels of Hg than inland foxes that mostly feed on terrestrial food items

(Bocharova et al., 2013). Also, studies using stable isotopes of carbon and nitrogen as dietary tracers indicate that Hg concentrations increase with higher intake of high trophic level marine food items (Hallanger et al., 2019). Climate-related changes in the physical environment may change prey availability for arctic foxes. For example, Arctic foxes need sea ice to scavenge remains of seals killed by polar bears or hunt new-born ringed seal pups (Gjertz and Lydersen, 1986). Furthermore, rain-on-snow events, that encapsulate tundra vegetation in ice (Peeters et al., 2019), are connected to reindeer mortality and thus the number of available reindeer carcasses for arctic foxes (Hansen et al., 2013). Changes in food availability has been shown to have consequences to mercury exposure in Arctic foxes. Concentrations of Hg increased the more sea ice was available and decreased with increasing reindeer mortality (Hallanger et al., 2019). Long-term temporal trends (1997-2014) on young Arctic foxes (n=109) from Svalbard shows that the temporal increase in liver Hg levels was slightly faster, 7.2% (95% CI: 2.3, 9.6) per year when the concentrations were adjusted for variation in diet proxies (stable isotopes of nitrogen and carbon) and food availability (availability of sea ice and reindeer mortaility), whereas yearly change of the measured concentrations was 3.5% (CI:−0.11, 7.2) (Hallanger et al., 2019).

There is generally little knowledge how mercury exposure of terrestrial herbivores are affected by climate changes. Generally, concentrations of mercury in reindeer are low (Aastrup et al., 2000; Pacyna et al., 2018). A study from the Canadian Arctic suggests that proximity to open marine waters throughout year leads to increased concentrations of mercury in terrestrial herbivores (St Pierre et al., 2015). Mercury concentrations in lichens were enriched at coastal sites adjacent to polynyas compared to sites locked in by sea ice for the majority of the year. It could be thus hypothesized that decline in sea ice may lead to increased mercury exposure in terrestrial herbivores using coastal areas. Furthermore, for example Svalbard reindeers have been documented to feed increasingly on shoreline along with icier winters (Hansen et al., 2019). High intake of washed-ashore kelp among reindeers using shoreline (Hansen et al., 2019) may lead to higher mercury exposure compared to animals feeding on terrestrial plants due to higher mercury concentrations in kelp compared to terrestrial plants (Chan et al., 1995; Olson et al., 2019; Wojtun et al., 2013). Effects of changing vegetation to mercury uptake and cycling in Arctic tundra ecosystems is currently unknown.

c. Freshwater biota

Contributors: **Kimmo Kahilainen,** John Chételat

(Kimmo) Methylmercury is uptaken by the primary producers at the base of food webs (Morel et al. 1998). In lakes, regime shift towards pelagic dominated energy pathways tend to increase mercury accumulation in food webs as phytoplankton is more prone to absorb methylmercury from water column compared to benthic algae (Watras 1998; Pickhardt & Fisher 2007). Pelagic food webs tend to

accumulate mercury more efficiently than benthic ones, potentially via longer and more chain type of food webs (Power et al. 2002; Thomas et al. 2016). Melting snow and subsequently formatted melting ponds could be very important sources of methylmercury draining into lakes, where this substance is quickly taken up via phytoplankton. Overall, increasing precipitation is correlated with DOC leaching from catchment to freshwater that transport also mercury and promote bacterial production in lakes (Forsström et al. 2013; de Wit et al. 2016; Poste et al. 2019). In lakes, increasing temperature and productivity may also lead to anoxia in deep profundal habitat and sediments promoting within lake methylation processes by bacteria (e.g. Morel et al. 1998). However, development of anoxic conditions are highly dependent on lake productivity, morphometry, regional temperature and wind exposure, where change in stratification is prone to alter mercury uptake in lake food webs (Rask et al. 2010). Role of filter feeding *Daphnia* in methylmercury uptake and transfer from phytoplankton to fishes has been recognized and may get even more efficient in future when the distribution range of this cladoceran is likely to increase (e.g. Chetelat & Amyot 2009; Kahilainen et al. 2016).

Marine and freshwater habitats are well-connected via anadromous fish, in which marine foraging is related on lower mercury exposure due to lower Hg in saltwater prey (Van der Velden et al. 2013; Tran et al. 2019; Braaten et al. 2020). Within lakes, shift from benthic invertebrates to pelagic zooplankton prey often lead to elevated mercury content in fish (Kahilainen et al. 2016; Keva et al. 2017; Kahilainen et al. 2017). Another important dietary shift is related to piscivory i.e. fish feeding that elevate trophic level and Hg content (Cabana & Rasmussen 1994). In subarctic lakes, increasing trophic level and use of pelagic energy sources increase the mercury concentrations within species and potentially also in food webs (Kidd et al. 2012; Thomas et al. 2016; Ahonen et al. 2018; Kozak et al. 2020). The new immigrating pelagic species are prone to increase the food chain length leading to elevated mercury in top predators (Thomas et al. 2016). However, many top predators feed on both pelagic and benthic prey fish compromising their mercury content. Mercury concentrations in river resident fish and food webs can be variable, but generally plankton based food chains are missing that often means lower mercury content in rivers than lakes.

Arctic lakes are often know of their relative large adult fish composing of few year classes and potentially having very high age (>20 years). In such highly seasonal systems, most fish are in adult stage and use significant part of their energy to gonad growth (Hayden et al. 2014b; McMeans et al. 2015). In slow growing European whitefish (*Coregonus lavaretus*) year-round study indicated a continuum of summer growth dilution at and winter condensation of mercury due to spawning and starvation under long ice-covered period (Keva et al. 2017). In these adult and thus mature fish, very little somatic growth is observed and year-round mercury variation exceeds annual bioaccumulation of mercury. Winter condensation of Hg in fish muscle seems to be the case in several other freshwater species including both autumn and spring spawning species (Kahilainen et al. 2020). Experimental

thinning of dense subarctic brown trout (*Salmo trutta*) population indicated that decreasing longevity and improved growth are lowering mercury concentration in muscle, liver and kidney tissues (Milardi et al. 2020).

Diet-growth interactions in lake-dwelling Arctic char in the eastern Canadian Arctic: (John Chételat) Arctic char (*Salvelinus alpinus*) is a slow-growing, long-lived salmonid species that is widely distributed in cold, unproductive lakes across the circumpolar Arctic (Power et al. 2009). Climate change effects such as warmer temperatures and increased aquatic productivity are anticipated to improve growth conditions for Arctic freshwater fishes, and it has been suggested that faster growth rates may reduce mercury concentrations through somatic biodilution (Stern et al. 2012). However, recent research has demonstrated that age and dietary mercury exposure are the dominant factors controlling mercury concentrations in Arctic char in northern Canada (van der Velden et al. 2013a,b; Chételat et al., in prep). Anadromous char typically have lower mercury concentrations in their muscle than lake-dwelling char, and they are also often larger in size for a given age (van der Velden et al. 2013a; Swanson et al. 2011). A comparison of paired marine and lacustrine food webs in the eastern Canadian Arctic indicated that basal methylmercury concentrations explained differences in muscle concentrations between anadromous and lake-dwelling char, rather than growth rate or trophic level (Velden et al. 2013b,c). Among lake-dwelling char, age better explained muscle mercury concentrations than growth rate (determined by length-at-age), and faster-growing fish did not have lower mercury concentrations (van der Velden et al. 2012, Chételat et al., in prep). This lack of a growth dilution effect is, in part, due to the higher trophic level of some faster growing lacustrine Arctic char (Chetelat et al., in prep). Thus, while piscivory infers an advantage for growth through greater caloric intake, it also results in greater intake of mercury from eating higher trophic level prey. These findings suggest environmental change in the Arctic that affects food web exposure to methylmercury (e.g., methylmercury production, uptake at the base of the food web, food web structure) is more likely to have a long-term impact on mercury bioaccumulation in Arctic char than improved growth from warmer temperatures or increased lake productivity.

- Chételat, J.; Richardson, M. C.; Macmillan, G. A.; Amyot, M.; Poulain, A. J., Ratio of Methylmercury to Dissolved Organic Carbon in Water Explains Methylmercury Bioaccumulation Across a Latitudinal Gradient from North-Temperate to Arctic Lakes. *Environmental Science and Technology* **2018,** *52*, (1), 79-88
- French, T. D.; Houben, A. J.; Desforges, J. P. W.; Kimpe, L. E.; Kokelj, S. V.; Poulain, A. J.; Smol, J. P.; Wang, X.; Blais, J. M., Dissolved organic carbon thresholds affect mercury bioaccumulation in Arctic lakes. *Environmental Science and Technology* **2014,** *48*, (6), 3162-3168.

10220 • Hudelson, K. E. et al. Temporal trends, lake-to-lake variation, and climate effects on Arctic
10221 char (Salvelinus alpinus) mercury concentrations from six High Arctic lakes in Nunavut,
10222 Canada. Sci. Total Environ. 678, 801-812, (2019).

10223 **5.7 Conclusions and recommendations**

10224 Contributors: John Chételat, Melissa McKinney, Tom Douglas,

10225 References:

References

(Sections 1-6, as of 02 MARCH 2020)

Aastrup P, Riget F, Dietz R, Asmund G. Lead, zinc, cadmium, mercury, selenium and copper in Greenland caribou and reindeer (Rangifer tarandus). Sci. Total Environ. 2000; 245: 149-159.

Abatzoglou, J. T., & Williams, A. P. (2016). Impact of anthropogenic climate change on wildfire across western US forests. Proceedings of the National Academy of Sciences of the United States of America, 113(42), 11770–11775. https://doi.org/10.1073/pnas.1607171113

Abraham, J., Dowling, K., & Florentine, S. (2017). Risk of post-fire metal mobilization into surface water resources: A review. Science of The Total Environment, 599–600, 1740–1755. https://doi.org/10.1016/j.scitotenv.2017.05.096

Agather, A. M., Bowman, K. L., Lamborg, C. H., & Hammerschmidt, C. R. (2019). Distribution of mercury species in the Western Arctic Ocean (U.S. GEOTRACES GN01). Marine Chemistry, 216, 103686. https://doi.org/10.1016/j.marchem.2019.103686

Agnan, Y.; Douglas, T. A.; Helmig, D.; Hueber, J.; Obrist, D., Mercury in the Arctic tundra snowpack: Temporal and spatial concentration patterns and trace gas exchanges. Cryosphere 2018, 12, (6), 1939-1956

Ahonen, S.A., Hayden, B., Leppänen, J.J. & Kahilainen, K.K. 2018: Climate and productivity affect total mercury concentration and bioaccumulation rate of fish along a spatial gradient of subarctic lakes. Science of the Total Environment 637-638: 1586- 1596.

Alsos, I. G. et al. Frequent long-distance plant colonization in the changing arctic. Science 316, 1606-1609, (2007).

AMAP, 2018. AMAP Assessment 2018: Arctic Ocean Acidification. Arctic Monitoring and Assessment Programme (AMAP), Tromsø, Norway. Vi+187pp

AMAP, 2019. AMAP Assessment 2018: Biological Effects of Contaminants on Arctic Wildlife and Fish.

AMAP, 2019. AMAP Climate Change Update 2019: An Update to Key Findings of Snow, Water, Ice and Permafrost in the Arctic (SWIPA) 2017. Arctic Monitoring and Assessment Programme (AMAP), Oslo, Norway. 12 pp.

AMAP. Snow, Water, Ice and Permafrost in the Arctic (SWIPA) 2017. 269 pp (Oslo, Norway, 2017).

Amélineau F, Grémillet D, Harding AMA, Walkusz W, Choquet R, Fort J. Arctic climate change and pollution impact little auk foraging and fitness across a decade. Scientific Reports 2019; 9: 1014.

Anderson et al. (2018)?

Angot, H., Dastoor, A., De Simone, F., Gårdfeldt, K., Gencarelli, C. N., Hedgecock, I. M., Langer, S., Magand, O., Mastromonaco, M. N., Nordstrøm, C., Pfaffhuber, K. A., Pirrone, N., Ryjkov, A., Selin, N. E., Skov, H., Song, S., Sprovieri, F., Steffen, A., Toyota, K., Travnikov, O., Yang, X., and Dommergue, A.: Chemical cycling and deposition of atmospheric mercury in polar regions: review of recent measurements and comparison with models, Atmos. Chem. Phys., 16, 10735–10763, https://doi.org/10.5194/acp-16- 10735-2016, 2016a.

Angot, H., Magand, O., Helmig, D., Ricaud, P., Quennehen, B., Gallée, H., Del Guasta, M., Sprovieri, F., Pirrone, N., Savarino, J., and Dommergue, A.: New insights into the atmospheric mercury cycling in central Antarctica and implications on a continental scale, Atmos. Chem. Phys., 16, 8249–8264, https://doi.org/10.5194/acp-16-8249-2016, 2016b.

Atwood, T. C. et al. Rapid environmental change drives increased land use by an Arctic marine predator. PLoS ONE 11, e0155932, (2016).

Balshi, M. S., McGuire, A. D., Duffy, P., Flannigan, M., Walsh, J., & Melillo, J. (2009). Assessing the response of area burned to changing climate in western boreal North America using a Multivariate Adaptive Regression Splines (MARS) approach. Global Change Biology, 15(3), 578–600. https://doi.org/10.1111/j.1365-2486.2008.01679.x

Barker, A. J., Douglas, T. A., Jacobson, A. D., McClelland, J. W., Ilgen, A. G., Khosh, M. S., Lehn, G. O., and Trainor, T. P.: Late season mobilization of trace metals in two small Alaskan arctic

watersheds as a proxy for landscape scale permafrost active layer dynamics, Chem. Geol., 381, 180–193, https://doi.org/10.1016/j.chemgeo.2014.05.012, 2014.
Bartley, T. J. et al. Food web rewiring in a changing world. Nature Ecology & Evolution 3, 345-354, (2019).
Batrakova, N.; Travnikov, O.; Rozovskaya, O. Chemical and physical transformations of mercury in the ocean: a review. Ocean Science 2014, 10, 1047-1063.
Baya, P. A.; Gosselin, M.; Lehnherr, I.; St. Louis, V. L.; Hintelmann, H., Determination of monomethylmercury and dimethylmercury in the arctic marine boundary layer. Environmental Science and Technology 2015, 49, (1), 223-232
Beal, S. A.; Osterberg, E. C.; Zdanowicz, C. M.; Fisher, D. A., Ice Core Perspective on Mercury Pollution during the Past 600 Years. Environ. Sci. Technol. 2015, 49, (13), 7641-7647.
Beel, C.R., Lamoureux, S.F., Orwin, J.F., 2018. Fluvial response to a period of hydrometeorological change and landscape disturbance in the Canadian High Arctic. Geophysical Research Letters, 45, doi:10.10292018GL079660
Bhatt US, Walker DA, Raynolds MK, Comiso JC, Epstein HE, Jia G, et al. Circumpolar Arctic tundra vegetation change is linked to sea ice decline. Earth Interactions 2010; 14: 1-20.
Bindi, S. et al. in Global Warming of 1.5°C. An IPCC Special Report on the impacts of global warming of 1.5°C above pre-industrial levels and related global greenhouse gas emission pathways, in the context of strengthening the global response to the threat of climate change, sustainable development, and efforts to eradicate poverty (eds V. Masson-Delmotte et al.) (2018).
Bintanja R, Andry O. Towards a rain-dominated Arctic. Nature Climate Change. 2017 Apr;7(4):263.
Bintanja, R., 2018. The impact of Arctic warming on increased rainfall. Scientific Reports, 8, 16001.
Biskaborn BK, Smith SL, Noetzli J, Matthes H, Vieira G, Streletskiy DA, et al. Permafrost is warming at a global scale. Nature Communications 2019; 10.
Biswas, A., Blum, J. D., Klaue, B., & Keeler, G. J. (2007). Release of mercury from Rocky Mountain forest fires. Global Biogeochemical Cycles, 21(1). https://doi.org/10.1029/2006GB002696
Bjorkman AD, García Criado M, Myers-Smith IH, Ravolainen V, Jónsdóttir IS, Westergaard KB, et al. Status and trends in Arctic vegetation: Evidence from experimental warming and long-term monitoring. Ambio 2020; 49: 678-692.
Blanck, A. & Lamouroux, N. 2007: Large-scale intraspecific variation in life-history traits of European freshwater fish. Journal of Biogeography 34: 862-875.
Blévin P, Tartu S, Ellis HI, Chastel O, Bustamante P, Parenteau C, et al. Contaminants and energy expenditure in an Arctic seabird: Organochlorine pesticides and perfluoroalkyl substances are associated with metabolic rate in a contrasted manner. Environ. Res. 2017; 157: 118-126.
Bocharova N, Treu G, Czirják GÁ, Krone O, Stefanski V, Wibbelt G, et al. Correlates between feeding ecology and mercury levels in historical and modern Arctic foxes (Vulpes lagopus). PLOS ONE 2013; 8: e60879.
Bourque, J., Atwood, T. C., Divoky, G. J., Stewart, C. & McKinney, M. A. Fatty acid-based diet estimates suggest ringed seal remain the main prey of southern Beaufort Sea polar bears despite recent use of onshore food resources. Ecol. Evol. 10, 2093-2103, (2020).
Bowden, W.B., Gooseff, M.N., Balser, A., Green, A., Peterson, B.J. and Bradford, J., 2008. Sediment and nutrient delivery from thermokarst features in the foothills of the North Slope, Alaska: Potential impacts on headwater stream ecosystems. Journal of Geophysical Research: Biogeosciences, 113.
Box, J. E., Colgan, W. T., Christensen, T. R., Schmidt, N. M., Lund, M., Parmentier, F.-J. W., Brown, R., Bhatt, U. S., Euskirchen, E. S., Romanovsky, V. E., Walsh, J. E., Overland, J. E., Wang, M., Corell, R. W., Meier, W. N., Wouters, B., Mernild, S., Mård, J., Pawlak, J., & Olsen, M. S. (2019). Key indicators of Arctic climate change: 1971–2017. Environmental Research Letters, 14(4), 045010. https://doi.org/10.1088/1748-9326/aafc1b
Braaten, Åkerblom, Kahilainen, Poste, Rask, Vuorenmaa, Malinen, Lydersen, Amundsen, Kashulin, Kashulina, Terentyev, Christensen, de Wit, 2019. Improved environmental status: 50 years of

declining fish mercury levels in boreal and subarctic Fennoscandia. Environmental Science & Technology, 53, 4, 1834-1843.
Braaten, de Wit, Fjeld, Rognerud, Lydersen, Larssen, 2014. Environmental factors influencing mercury speciation in subarctic and boreal lakes. Science of the Total Environment, 476-477, 336-345.
Braaten, H.F.V., Christensen, G.N., Rosten, C., Thaulow, J., Kahilainen, K.K. & Hawley, K.L. 2020: Mercury bioaccumulation in populations of Arctic charr (Salvelinus alpinus) from subarctic and Arctic Norway – effect of life-history strategies. In preparation.
Braaten, Harman, Øverjordet, Larssen, 2014. Effects of sample preparation on methylmercury concentrations in Arctic organisms. International Journal of Environmental Analytical Chemistry, 94, 9, 863-873.
Braune BM, Gaston AJ, Hobson KA, Gilchrist HG, Mallory ML. Changes in food web structure alter trends of mercury uptake at two seabird colonies in the Canadian Arctic. Environmental science & technology 2014; 48: 13246-52.
Braune BM, Malone BJ. Organochlorines and mercury in waterfowl harvested in Canada. Environ. Monit. Assess. 2006; 114: 331-359.
Braune, B. M., Gaston, A. J., Hobson, K. A., Gilchrist, H. G. & Mallory, M. L. Changes in food web structure alter trends of mercury uptake at two seabird colonies in the Canadian Arctic. Environ. Sci. Technol 48, 13246-13252, (2014).
Brazeau, M. L.; Poulain, A. J.; Paterson, A. M.; Keller, W.; Sanei, H.; Blais, J. M., Recent changes in mercury deposition and primary productivity inferred from sediments of lakes from the Hudson Bay Lowlands, Ontario, Canada. Environ. Pollut. 2013, 173, (0), 52-60.
Brooks, S. B., Saiz-Lopez, A., Skov, H., Lindberg, S. E., Plane, J. M. C., and Goodsite, M. E.: The mass balance of mercury in the springtime arctic environment, Geophys. Res. Lett., 33, L13812, https://doi.org/10.1029/2005GL025525, 2006.
Brown, L.C; Duguay, C.R. The fate of lake ice in the North American Arctic. The Cryosphere, (2011), 869-892.
Burke, S. M.; Zimmerman, C. E.; Branfireun, B. A.; Koch, J. C.; Swanson, H. K., Patterns and controls of mercury accumulation in sediments from three thermokarst lakes on the Arctic Coastal Plain of Alaska. Aquatic Sciences 2018, 80, (1)
Burt, A. et al. Mercury uptake within an ice algal community during the spring bloom in first-year Arctic sea ice. Journal of Geophysical Research: Oceans 118, 4746-4754, (2013).
Cabana, G. & Rasmussen, J.B. 1994: Modelling food chain structure and contaminant bioaccumulation using stable nitrogen isotopes. Nature 372: 255-257.
Cadieux SB, White JR, Pratt LM. Exceptional summer warming leads to contrasting outcomes for methane cycling in small Arctic lakes of Greenland. Biogeosciences 2017; 14: 559-574.
Calleja, M. L.; Kerhervé, P.; Bourgeois, S.; Kędra, M.; Leynaert, A.; Devred, E.; Babin, M.; Morata, N., Effects of increase glacier discharge on phytoplankton bloom dynamics and pelagic geochemistry in a high Arctic fjord. Progress in Oceanography 2017, 159, 195-210
Carrie, J. et al. Increasing contaminant burdens in an arctic fish, burbot (Lota lota), in a warming climate. Environ. Sci. Technol 44, 316-322, (2010).
Carrie, J.; Stern, G. A.; Sanei, H.; Macdonald, R. W.; Wang, F. Determination of mercury biogeochemical fluxes in the remote Mackenzie River Basin, northwest Canada, using speciation of sulfur and organic carbon. Appl. Geochem. 2012, 27 (4), 815−824.
Carroll ML, Loboda TV. The sign, magnitude and potential drivers of change in surface water extent in Canadian tundra. Environmental Research Letters 2018; 13.
Carroll, M. L., Townshend, J. R. G., Dimiceli, C. M., Loboda, T., & Sohlberg, R. A. (2011). Shrinking lakes of the Arctic: Spatial relationships and trajectory of change. Geophysical Research Letters, 38, L20406.
Chan HM, Kim C, Khoday K, Receveur O, Kuhnlein HV. Assessment of Dietary Exposure to Trace Metals in Baffin Inuit Food. Environ. Health Perspect. 1995; 103: 740-746.

10375 Chandan, P.; Ghosh S.; Bergquist, B.A. Mercury isotope fractionation during aqueous photoreduction of
10376 monomethylmercury in the presence of dissolved organic matter. Environmental Science and
10377 Technology 2014, 49, 259-267.
10378 Cherry, J. E., Déry, S. J., Cheng, Y., Stieglitz, M., Jacobs, A. S., and Pan, F.: Climate and
10379 hydrometeorology of the Toolik Lake region and the Kuparuk River basin, in: Alaska's changing
10380 arctic: ecological consequences for tundra, streams, and lakes, edited by: Hobbie, J. E. and Kling, G.
10381 W., 21–60, Oxford University Press, New York, 2014.
10382 Chetelat, J. & Amyot, M. 2009: Elevated methylmercury in High Arctic Daphnia and the role of
10383 productivity in controlling their distribution. Global Change Biology 15: 706-718.
10384 Chételat, J. et al. (in prep, manuscript submission in spring 2020). Diet-growth interactions and their
10385 influence on mercury concentrations in two salmonid species from lakes in the eastern Canadian
10386 Arctic.
10387 Chételat, J.; Amyot, M.; Arp, P.; Blais, J. M.; Depew, D.; Emmerton, C. A.; Evans, M.; Gamberg, M.;
10388 Gantner, N.; Girard, C.; Graydon, J.; Kirk, J.; Lean, D.; Lehnherr, I.; Muir, D.; Nasr, M.; J. Poulain,
10389 A.; Power, M.; Roach, P.; Stern, G.; Swanson, H.; van der Velden, S., Mercury in freshwater
10390 ecosystems of the Canadian Arctic: Recent advances on its cycling and fate. Sci. Total Environ.
10391 2015, 509, 41-66.
10392 Chételat, J.; Richardson, M. C.; Macmillan, G. A.; Amyot, M.; Poulain, A. J., Ratio of Methylmercury to
10393 Dissolved Organic Carbon in Water Explains Methylmercury Bioaccumulation Across a Latitudinal
10394 Gradient from North-Temperate to Arctic Lakes. Environmental Science and Technology 2018, 52,
10395 (1), 79-88
10396 Cheung, W. W. L. et al. Projecting global marine biodiversity impacts under climate change scenarios.
10397 Fish Fish. 10, 235-251, (2009).
10398 Chipman, M.L., Hudspith, V., Higuera, P.E., Duffy, P.A., Kelly, R., Oswald, W.W., Hu, F.S.
10399 Spatiotemporal patterns of tundra fires: Late-Quaternary charcoal records from Alaska. (2015)
10400 Biogeosciences, 12 (13), pp. 4017-4027.
10401 Coogan, S. C. P., Robinne, F.-N., Jain, P., & Flannigan, M. D. (2019). Scientists' warning on wildfire —
10402 a Canadian perspective. Canadian Journal of Forest Research, 49(9), 1015–1023.
10403 https://doi.org/10.1139/cjfr-2019-0094
10404 Cooke, C. A.; Wolfe, A. P.; Michelutti, N.; Balcom, P. H.; Briner, J. P., A holocene perspective on algal
10405 mercury scavenging to sediments of an Arctic lake. Environmental Science and Technology 2012,
10406 46, (13), 7135-7141.
10407 Cooley, S.W. and T.M. Pavelsky, 2016. Spatial and temporal patterns in Arctic river ice breakup revealed
10408 by automated ice detection from MODIS imagery. Remote Sensing of Environment, 175: 310–322.
10409 Coops, N. C., Hermosilla, T., Wulder, M. A., White, J. C., & Bolton, D. K. (2018). A thirty year, fine-
10410 scale, characterization of area burned in Canadian forests shows evidence of regionally increasing
10411 trends in the last decade. PLOS ONE, 13(5), e0197218.
10412 https://doi.org/10.1371/journal.pone.0197218
10413 Cory, R.M., C.P. Ward, B.C. Crump and G.W. and G.W. Kling, 2014. Sunlight controls water column
10414 processing of carbon in arctic fresh waters. Science, 345: 925–928.
10415 Couture, R.M., H.A. de Wit, K. Tominaga, P. Kiuru and I. Markelov, 2015. Oxygen dynamics in a boreal
10416 lake responds to long-term changes in climate, ice phenology, and DOC inputs. Journal of
10417 Geophysical Research: Biogeosciences, 120: 2441–2456.
10418 Dalerum F, Perbro A, Magnusdottir R, Hersteinsson P, Angerbjorn A. The Influence of coastal access on
10419 isotope variation in Icelandic Arctic foxes. Plos One 2012; 7: 8.
10420 de Wit, H.A., J. Mulder, A. Hindar and L. Hole, 2007. Long-term increase in dissolved organic carbon in
10421 streamwaters in Norway is response to reduced acid deposition. Environmental Science &
10422 Technology, 41: 7706–7713.
10423 de Wit, H.A., S. Valinia, G.A. Weyhenmeyer, M.N. Futter, P. Kortelainen, K. Austnes, D.O. Hessen, A.
10424 Räike, H. Laudon and J. Vuorenmaa, 2016. Current Browning of Surface Waters Will Be Further

Promoted by Wetter Climate. Environmental Science and Technology Letters, 12 (3): 430–435. doi: 10.1021/acs.estlett.6b00396.

Deison, R.; Smol, J. P.; Kokelj, S. V.; Pisaric, M. F. J.; Kimpe, L. E.; Poulain, A. J.; Sanei, H.; Thienpont, J. R.; Blais, J. M., Spatial and Temporal Assessment of Mercury and Organic Matter in Thermokarst Affected Lakes of the Mackenzie Delta Uplands, NT, Canada. Environ. Sci. Technol. 2012, 46, (16), 8748-8755.

Demers, J. D., Blum, J. D., & Zak, D. R. (2013). Mercury isotopes in a forested ecosystem: Implications for air-surface exchange dynamics and the global mercury cycle. Global Biogeochemical Cycles, 27, 222–238. https://doi.org/10.1002/gbc.20021

Dennison, P. E., Brewer, S. C., Arnold, J. D., & Moritz, M. A. (2014). Large wildfire trends in the western United States, 1984-2011. Geophysical Research Letters, 41(8), 2928–2933. https://doi.org/10.1002/2014GL059576

Derocher AE, Lunn NJ, Stirling I. Polar bears in a warming climate. Integrative and Comparative Biology 2004; 44: 163-176.

Déry SJ, Stahl K, Moore RD, Whitfield PH, Menounos B, Burford JE. Detection of runoff timing changes in pluvial, nival, and glacial rivers of western Canada. Water Resources Research 2009; 45.

DiMento, B. P.; Mason, R. P.; Brooks, S.; Moore, C., The impact of sea ice on the air-sea exchange of mercury in the Arctic Ocean. Deep-Sea Research Part I: Oceanographic Research Papers 2019, 144, 28-38.

DiMento, B.P. & Mason, R.P. 2017. Factors controlling the photochemical degradation of methylmercury in coastal and oceanic waters. Marine Chemistry 196: 116-125.

Divoky, G.J., Douglas, D.C. and Stenhouse, I.J., 2016. Arctic sea ice a major determinant in Mandt's black guillemot movement and distribution during non-breeding season. Biology letters, 12(9), p.20160275.

Divoky, G.J., Lukacs, P.M. and Druckenmiller, M.L., 2015. Effects of recent decreases in arctic sea ice on an ice-associated marine bird. Progress in Oceanography, 136, pp.151- 161.

Dommergue, A.; Larose, C.; Faïn, X.; Clarisse, O.; Foucher, D.; Hintelmann, H.; Schneider, D.; Ferrari, C. P., Deposition of Mercury Species in the Ny-Ålesund Area (79°N) and Their Transfer during Snowmelt. Environ. Sci. Technol. 2010, 44 (3), 901- 907.

Dommergue, A.; Martinerie, P.; Courteaud, J.; Witrant, E.; Etheridge, D. M., A new reconstruction of atmospheric gaseous elemental mercury trend over the last 60 years from Greenland firn records. Atmospheric Environment 2016, 136, 156-164.

Donohoue, D. L.; Bauer, D.; Cossairt, B.; Hynes, A. J., Temperature and pressure dependent rate coefficients for the reaction of Hg with Br and the reaction of Br with Br: A pulsed laser photolysis-pulsed laser induced fluorescence study. J. Phys. Chem. A 2006, 110 (21), 6623-6632.

Douglas, T. A. and Sturm, M.: Arctic haze, mercury and the chemical composition of snow across northwestern Alaska, Atmos. Environ., 38, 805–820, https://doi.org/10.1016/j.atmosenv.2003.10.042, 2004.

Douglas, T. A., Loseto, L. L., Macdonald, R.W., Outridge, P., Dommergue, A., Poulain, A., Amyot, M., Barkay, T., Berg, T., Chetelat, J., Constant, P., Evans, M., Ferrari, C., Gantner, N., Johnson, M. S., Kirk, J., Kroer, N., Larose, C., Lean, D., Nielsen, T. G., Poissant, L., Rognerud, S., Skov, H., Sorensen, S., Wang, F., Wilson, S., and Zdanowicz, C. M.: The fate of mercury in Arctic terrestrial and aquatic ecosystems, a review, Environ. Chem., 9, 321–355, https://doi.org/10.1071/en11140, 2012.

Douglas, T. A., Sturm, M., Blum, J. D., Polashenski, C., Stuefer, S., Hiemstra, C., Steffen, A., Filhol, S., and Prevost, R.: A pulse of mercury and major ions in snowmelt runoff from a small arctic Alaska watershed, Environ. Sci. Technol., 51, 11145–11155,https://doi.org/10.1021/acs.est.7b03683, 2017.

Douglas, T. A., Sturm, M., Simpson, W. R., Blum, J. D., Alvarez-Aviles, L., Keeler, G. J., Perovich, D. K., Biswas, A., and Johnson, K.: Influence of snow and ice crystal formation and accumulation on mercury deposition to the Arctic, Environ. Sci. Technol., 42, 1542–1551, https://doi.org/10.1021/es070502d, 2008.

Douglas, T. A., Sturm, M., Simpson, W. R., Brooks, S., Lindberg, S. E., and Perovich, D. K.: Elevated mercury measured in snow and frost flowers near Arctic sea ice leads, Geophys. Res. Lett., 32, L04502, https://doi.org/10.1029/2004GL022132, 2005.

Douglas, T. A.; Blum, J. D., Mercury Isotopes Reveal Atmospheric Gaseous Mercury Deposition Directly to the Arctic Coastal Snowpack. Environmental Science and Technology Letters 2019, 6, (4), 235-242.

Drevnick, P. E.; Cooke, C. A.; Barraza, D.; Blais, J. M.; Coale, K. H.; Cumming, B. F.; Curtis, C. J.; Das, B.; Donahue, W. F.; Eagles-Smith, C. A.; Engstrom, D. R.; Fitzgerald, W. F.; Furl, C. V.; Gray, J. E.; Hall, R. I.; Jackson, T. A.; Laird, K. R.; Lockhart, W. L.; Macdonald, R. W.; Mast, M. A.; Mathieu, C.; Muir, D. C. G.; Outridge, P. M.; Reinemann, S. A.; Rothenberg, S. E.; Ruiz-Fernández, A. C.; Louis, V. L. S.; Sanders, R. D.; Sanei, H.; Skierszkan, E. K.; Van Metre, P. C.; Veverica, T. J.; Wiklund, J. A.; Wolfe, B. B., Spatiotemporal patterns of mercury accumulation in lake sediments of western North America. Science of The Total Environment 2016, 568, 1157-1170.

Durnford, D.; Dastoor, A.; Ryzhkov, A.; Poissant, L.; Pilote, M.; Figueras-Nieto, D., How relevant is the deposition of mercury onto snowpacks?-Part 2: A modeling study. Atmospheric Chemistry and Physics 2012, 12, (19), 9251-9274.

Eckley, C.S., C.J. Watras, H. Hintelmann, K. Morrison, A.D. Kent and O. Regnell, 2005. Mercury methylation in the hypolimnetic waters of lakes with and without connection to wetlands in northern Wisconsin. Canadian Journal of Fisheries and Aquatic Sciences, 62: 400–411.

Ehrich D, Ims R, Yoccoz N, Lecomte N, Killengreen S, Fuglei E, et al. What can stable isotope analysis of top predator tissues contribute to monitoring of tundra ecosystems? Ecosystems 2015; 18: 404-416.

Ehrich D, Schmidt NM, Gauthier G, Alisauskas R, Angerbjörn A, Clark K, et al. Documenting lemming population change in the Arctic: Can we detect trends? Ambio 2020; 49: 786-800.

Eide NE, Eid PM, Prestrud P, Swenson JE. Dietary responses of arctic foxes Alopex lagopus to changing prey availability across an Arctic landscape. Wildl. Biol. 2005; 11: 109-121.

Elmendorf SC, Henry GH, Hollister RD, Bjork RG, Bjorkman AD, Callaghan TV, et al. Global assessment of experimental climate warming on tundra vegetation: heterogeneity over space and time. Ecol Lett 2012; 15: 164-75.

Emmerton CA, Graydon JA, Gareis JA, St. Louis VL, Lesack LF, Banack JK, Hicks F, Nafziger J., 2013. Mercury export to the Arctic Ocean from the Mackenzie River, Canada. Environmental Science & Technology, 47(14), pp. 7644-7654.

Emmerton, C. A.; Graydon, J. A.; Gareis, J. A. L.; St. Louis, V. L.; Lesack, L. F. W.; Banack, J. K. A.; Hicks, F.; Nafziger, J., Mercury Export to the Arctic Ocean from the Mackenzie River, Canada. Environ. Sci. Technol. 2013, 47 (14), 7644-7654.

Ernakovich, J. G. et al. Predicted responses of arctic and alpine ecosystems to altered seasonality under climate change. Global Change Biol. 20, 3256-3269, (2014).

Evans, C.D., T.G. Jones, A. Burden, N. Ostle, P. Zielinski, M.D.A. Cooper, M. Peacock, J.M. Clark, F. Oulehle, D. Cooper and F. Freeman, 2012. Acidity controls on dissolved organic carbon mobility in organic soils. Global Change Biology, 18: 3317–3331.

Faïn, X., Grangeon, S., Bahlmann, E., Fritsche, J., Obrist, D., Dommergue, A., Ferrari, C. P., Cairns, W., Ebinghaus, R., Barbante, C., Cescon, P., and Boutron, C.: Diurnal production of gaseous mercury in the alpine snowpack before snowmelt, J. Geophys. Res., 112, D21311, https://doi.org/10.1029/2007JD008520, 2007.

Faïn, X., Helmig, D., Hueber, J., Obrist, D., and Williams, M. W.: Mercury dynamics in the Rocky Mountain, Colorado, snowpack, Biogeosciences, 10, 3793–3807, https://doi.org/10.5194/bg-10-3793-2013, 2013.

Fant ML, Nyman M, Helle E, Rudback E. Mercury, cadmium, lead and selenium in ringed seals (Phoca hispida) from the Baltic Sea and from Svalbard. Environmental pollution (Barking, Essex : 1987) 2001; 111: 493-501.

10526 Favaro, E.A. and Lamoureux, S.F., 2015. Downstream patterns of suspended sediment transport in a High
10527 Arctic river influenced by permafrost disturbance and recent climate change. Geomorphology, 246,
10528 pp.359-369.
10529 Ferrari, C. P., Padova, C., Faïn, X., Gauchard, P.-A., Dommergue, A., Aspmo, K., Berg, T., Cairns, W.,
10530 Barbante, C., Cescon, P., Kaleschke, L., Richter, A., Wittrock, F., and Boutron, C.: Atmospheric
10531 mercury depletion event study in Ny-Ålesund (Svalbard) in spring 2005, Deposition and
10532 transformation of Hg in surface snow during springtime, Sci. Total Environ., 397, 167–177,
10533 https://doi.org/10.1016/j.scitotenv.2008.01.064, 2008.
10534 Finger Higgens, R. A.; Chipman, J. W.; Lutz, D. A.; Culler, L. E.; Virginia, R. A.; Ogden, L. A.,
10535 Changing Lake Dynamics Indicate a Drier Arctic in Western Greenland. J. Geophys. Res. Biogeosci.
10536 2019, 124, (4), 870-883.
10537 Finley, B. D., Swartzendruber, P. C., & Jaffe, D. A. (2009). Particulate mercury emissions in regional
10538 wildfire plumes observed at the Mount Bachelor Observatory. Atmospheric Environment, 43(38),
10539 6074–6083. https://doi.org/10.1016/j.atmosenv.2009.08.046
10540 Finstad, A.G. & Hein, C.L. 2012: Migrate of stay: terrestrial primary productivity and climate drive
10541 anadromy in Arctic charr. Global Change Biology 18: 2487-2497.
10542 Finstad, A.G., Andersen, T., Larsen, S., Tominaga, K., Blumenrath, S., de Wit, H.A., Tømmervik, H. and
10543 Hesen, D.O. 2016. From greening to browning: catchment vegetation development and reduced S-
10544 deposition promote organic carbon load on decadal time scales in Nordic lakes. Scientific reports 6:
10545 31944.
10546 Fisher, J. A., Jacob, D. J., Soerensen, A. L., Amos, H. M., Steffen, A., & Sunderland, E. M. (2012).
10547 Riverine source of Arctic Ocean mercury inferred from atmospheric observations. Nature
10548 Geoscience, 5(7), 499–504. https://doi.org/10.1038/ngeo1478
10549 Fisher, J. A.; Jacob, D. J.; Soerensen, A. L.; Amos, H. M.; Corbitt, E. S.; Streets, D. G.; Wang, Q.;
10550 Yantosca, R. M.; Sunderland, E. M., Factors driving mercury variability in the Arctic atmosphere
10551 and ocean over the past 30 years. Global Biogeochemical Cycles 2013, 27, (4), 1226-1235
10552 Fitzgerald, W. F., Engstrom, D. R., Lamborg, C. H., Tseng, C.-M., Balcom, P. H., and Hammerschmidt,
10553 C. R.: Modern and historic atmospheric mercury fluxes in Northern Alaska: global sources and arctic
10554 depletion, Environ. Sci. Technol., 39, 557–568, https://doi.org/10.1021/es049128x, 2005.
10555 Fitzgerald, W. F.; Hammerschmidt, C. R.; Engstrom, D. R.; Balcom, P. H.; Lamborg, C. H.; Tseng, C.
10556 M., Mercury in the Alaskan Arctic. In Alaska's Changing Arctic: Ecological Consequences for
10557 Tundra, Streams, and Lakes, 2014.
10558 Flannigan, M.; Cantin, A. S.; de Groot, W. J.; Wotton, M.; Newbery, A.; Gowman, L. M., Global
10559 wildland fire season severity in the 21st century. Forest Ecology and Management 2013, 294, 54-61.
10560 Forsström, L., Roiha, T. & Rautio, M. 2013: Responses of microbial food web to increased allochthonous
10561 DOM in an oligotrophic subarctic lake. Aquatic Microbial Ecology 68: 171-184.
10562 Forstsström, L., Rautio, M., Cusson, M., Sorvari, S., Albert, R-L., Kumagai, M. and Korhola, A. 2015.
10563 Dissolved organic matter concentration, optical parameters and attenuation of solar radiation in high-
10564 latitude lakes across three vegetation zones. Ecoscience 22: 17-31.
10565 Fort et al. 2016 Does temporal variation of mercury levels in Arctic seabirds reflect changes in global
10566 environmental contamination, or a modification of Arctic marine food web functioning? Env. Pollut.
10567 DOI: 10.1016/j.envpol.2015.12.061
10568 Fortier, D.; Allard, M.; Shur, Y., Observation of rapid drainage system development by thermal erosion of
10569 ice wedges on Bylot Island, Canadian Arctic Archipelago. Permafrost and Periglacial Processes
10570 2007, 18, (3), 229-243.
10571 Fosheim, M. et al. 2015: Recent warming leads to a rapid borealization of fish communities in the Arctic.
10572 Nature Climate Change 5: 673-677.
10573 Foster, K. L., Braune, B. M., Gaston, A. J. & Mallory, M. L. Climate influence on mercury in Arctic
10574 seabirds. Sci. Total Environ. 693, 133569, (2019).

10575 Frainer A, Primicerio R, Kortsch S, Aune M, Dolgov AV, Fossheim M, Aschan MM. 2017 Climate-
10576 driven changes in functional biogeography of Arctic marine fish communities. Proc. Natl Acad. Sci.
10577 USA 114, 12 202–12 207. (doi:10.1073/pnas.1706080114)
10578 Franke A, Falk K, Hawkshaw K, Ambrose S, Anderson DL, Bente PJ, et al. Status and trends of
10579 circumpolar peregrine falcon and gyrfalcon populations. Ambio 2020; 49: 762-783.
10580 Fraser, A., Dastoor, A., & Ryjkov, A. (2018). How important is biomass burning in Canada to mercury
10581 contamination? Atmospheric Chemistry and Physics, 18(10), 7263–7286.
10582 https://doi.org/https://doi.org/10.5194/acp-18-7263-2018
10583 French, N. H. F.; Jenkins, L. K.; Loboda, T. V.; Flannigan, M.; Jandt, R.; Bourgeau-Chavez, L. L.;
10584 Whitley, M., Fire in arctic tundra of Alaska: past fire activity, future fire potential, and significance
10585 for land management and ecology. International Journal of Wildland Fire 2015, 24, (8), 1045-1061.
10586 French, T. D.; Houben, A. J.; Desforges, J. P. W.; Kimpe, L. E.; Kokelj, S. V.; Poulain, A. J.; Smol, J. P.;
10587 Wang, X.; Blais, J. M., Dissolved organic carbon thresholds affect mercury bioaccumulation in
10588 Arctic lakes. Environmental Science and Technology 2014, 48, (6), 3162-3168.
10589 Friedli, H R, Radke, L. F., Lu, J. Y., Banic, C. M., Leaitch, W. R., & MacPherson, J. I. (2003). Mercury
10590 emissions from burning of biomass from temperate North American forests: laboratory and airborne
10591 measurements. Atmospheric Environment, 37(2), 253–267. https://doi.org/10.1016/S1352-
10592 2310(02)00819-1
10593 Friedli, H. R., Radke, L. F., Payne, N. J., McRae, D. J., Lynham, T. J., & Blake, T. W. (2007).
10594 Mercury in vegetation and organic soil at an upland boreal forest site in Prince Albert National Park,
10595 Saskatchewan, Canada. Biogeosciences, 112(G1), G01004.
10596 Friedli, Hans R, Radke, L. F., & Lu, J. Y. (2001). Mercury in smoke from biomass fires. Geophysical
10597 Research Letters, 28(17), 3223–3226. https://doi.org/10.1029/2000GL012704
10598 Fuglei E, Henden J-A, Callahan CT, Gilg O, Hansen J, Ims RA, et al. Circumpolar status of Arctic
10599 ptarmigan: Population dynamics and trends. Ambio 2020; 49: 749-761.
10600 Gaden, A. & Stern, G. A. Temporal Trends in Beluga, Narwhal and Walrus Mercury Levels: Links to
10601 Climate Change. In: A little less Arctic: Top predators in the world's largest northern inland sea,
10602 Hudson Bay (eds S.H. Ferguson, L.L. Loseto, & M.L. Mallory) Ch. 10, 197-216 (Springer, 2010).
10603 Gaden, A., Ferguson, S. H., Harwood, L., Melling, H. & Stern, G. A. Mercury trends in ringed seals
10604 (Phoca hispida) from the western Canadian Arctic since 1973: Associations with length of ice-free
10605 season. Environ. Sci. Technol 43, 3646-3651, (2009).
10606 Gagnon, C.; Fisher, N. S., Bioavailability of Sediment-Bound Methyl and Inorganic Mercury to a Marine
10607 Bivalve. Environmental Science & Technology 1997, 31, (4), 993-998.
10608 Garmo, Ø.A., B.L. Skjelkvåle, H.A. de Wit, L. Colombo, C. Curtis, J. Fölster, A. Hoffmann, J. Hruška, T.
10609 Høgåsen, D.S. Jeffries, W.B. Keller, P. Krám, V. Majer, D.T. Monteith, A.M. Paterson, M. Rogora,
10610 D. Rzychon, S. Steingruber, J.L. Stoddard, J. Vuorenmaa and A. Worsztynowicz, 2014. Trends in
10611 Surface Water Chemistry in Acidified Areas in Europe and North America from 1990 to 2008.
10612 Water, Air, & Soil Pollution, 225 (3): 1–14.
10613 Gaston, A.J. and Elliott, K.H., 2013. Effects of climate-induced changes in parasitism, predation and
10614 predator-predator interactions on reproduction and survival of an Arctic marine bird. Arctic, 66, 43-
10615 51.
10616 Gaston, A.J. and Elliott, K.H., 2014. Seabird diet changes in northern Hudson Bay, 1981-2013, reflect the
10617 availability of schooling prey. Marine Ecology Progress Series, 513, pp.211-223.
10618 Gaston, A.J., Gilchrist, H.G. and Hipfner, J.M., 2005. Climate change, ice conditions and reproduction in
10619 an Arctic nesting marine bird: Brunnich's guillemot (Uria lomvia L.). Journal of Animal Ecology,
10620 74(5), pp.832-841.
10621 Gebre S, Boissy T, Alfredsen K. Sensitivity to climate change of the thermal structure and ice cover
10622 regime of three hydropower reservoirs. Journal of Hydrology 2014; 510: 208-227.
10623 Gibson, C. M., Chasmer, L. E., Thompson, D. K., Quinton, W. L., Flannigan, M. D., & Olefeldt, D.
10624 (2018). Wildfire as a major driver of recent permafrost thaw in boreal peatlands. Nature
10625 Communications, 9(1). https://doi.org/10.1038/s41467-018-05457-1

10626 Giesler, R., Clemmensen, K. E., Wardle, D. A., Klaminder, J., & Bindler, R. (2017). Boreal Forests
10627 Sequester Large Amounts of Mercury over Millennial Time Scales in the Absence of Wildfire.
10628 Environmental Science & Technology, 51(5), 2621–2627. https://doi.org/10.1021/acs.est.6b06369
10629 Gilg O, Hanski I, Sittler B. Cyclic dynamics in a simple vertebrate predator-prey community. Science
10630 2003; 302: 866-868.
10631 Gillett, N. P. (2004). Detecting the effect of climate change on Canadian forest fires. Geophysical
10632 Research Letters, 31(18), L18211. https://doi.org/10.1029/2004GL020876
10633 Girard C., Leclerc M, Amyot M. 2016. Photodemethylation of Methylmercury in Eastern Canadian Arctic
10634 Thaw Pond and Lake Ecosystems. Environ. Sci. Technol. 50: 3511-3520.
10635 Gjertz I, Lydersen C. Polar bear predation on ringed seals in the fast-ice of Hornsund, Svalbard. Polar
10636 Res. 1986; 4: 65-68.
10637 Góngora, E., Braune, B.M. and Elliott, K.H., 2018. Nitrogen and sulfur isotopes predict variation in
10638 mercury levels in Arctic seabird prey. Marine pollution bulletin, 135, pp.907- 914.
10639 Goodsite, M. E.; Plane, J. M. C.; Skov, H., A theoretical study of the oxidation of Hg-0 to HgBr2 in the
10640 troposphere. Environ. Sci. Technol. 2004, 38 (6), 1772-1776.
10641 Gordon, J.; Quinton, W.; Branfireun, B. A.; Olefeldt, D., Mercury and methylmercury biogeochemistry in
10642 a thawing permafrost wetland complex, Northwest Territories, Canada. Hydrological Processes
10643 2016, 30, (20), 3627-3638
10644 Grémillet, D., Fort, J., Amélineau, F., Zakharova, E., Le Bot, T., Sala, E. and Gavrilo, M., 2015. Arctic
10645 warming: nonlinear impacts of sea-ice and glacier melt on seabird foraging. Global change biology,
10646 21(3), pp.1116-1123.
10647 Griffith et al 2019 Nature Climate Change Ecological resilience
10648 Grigal, D.F. 2002. Inputs and outputs of mercury form terrestrial watersheds: a review. Environ. Rev.
10649 10:1-39. DOI: 10.1139/A01-013.
10650 Gu, B.; Bian, Y.; Miller, C.L.; Dong, W.; Jiang, X.; Liang, L. Mercury reduction and complexation by
10651 natural organic matter in anoxic environments. Proceedings of the National Academy of Sciences of
10652 the United States of America 2011, 108(4) 1479-1483.
10653 Halbach, K.; Mikkelsen, Ø.; Berg, T.; Steinnes, E., The presence of mercury and other trace metals in
10654 surface soils in the Norwegian Arctic. Chemosphere 2017, 188, 567-574
10655 Hallanger IG, Fuglei E, Yoccoz NG, Pedersen ÅØ, König M, Routti H. Temporal trend of mercury in
10656 relation to feeding habits and food availability in arctic foxes (Vulpes lagopus) from Svalbard,
10657 Norway. Sci. Total Environ. 2019; 670: 1125-1132.
10658 Hampton, S.E. et al. 2017: Ecology under lake ice. Ecology Letters 20: 98-111.
10659 Hanes, C. C., Wang, X., Jain, P., Parisien, M. A., Little, J. M., & Flannigan, M. D. (2019). Fire-regime
10660 changes in canada over the last half century. Canadian Journal of Forest Research, 49(3), 256–269.
10661 https://doi.org/10.1139/cjfr-2018-0293
10662 Hansen BB, Grotan V, Aanes R, Saether BE, Stien A, Fuglei E, et al. Climate events synchronize the
10663 dynamics of a resident vertebrate community in the High Arctic. Science 2013; 339: 313-315.
10664 Hansen BB, Lorentzen JR, Welker JM, Varpe O, Aanes R, Beumer LT, et al. Reindeer turning maritime:
10665 Ice-locked tundra triggers changes in dietary niche utilization. Ecosphere 2019a; 10.
10666 Hansen BB, Pedersen ÅØ, Peeters B, Le Moullec M, Albon SD, Herfindal I, et al. Spatial heterogeneity
10667 in climate change effects decouples the long-term dynamics of wild reindeer populations in the high
10668 Arctic. Global Change Biol. 2019b; 25: 3656-3668.
10669 Hansen, K. M.; Christensen, J. H.; Brandt, J., The influence of climate change on atmospheric deposition
10670 of mercury in the arctic—A model sensitivity study. International Journal of Environmental
10671 Research and Public Health 2015, 12, (9), 11254-11268
10672 Hararuk, O., Obrist, D., & Luo, Y. (2013). Modelling the sensitivity of soil mercury storage to
10673 climate-induced changes in soil carbon pools. Biogeosciences, 10(4), 2393–2407.
10674 https://doi.org/10.5194/bg-10-2393-2013
10675 Harrison, S.; Kargel, J. S.; Huggel, C.; Reynolds, J.; Shugar, D. H.; Betts, R. A.; Emmer, A.; Glasser, N.;
10676 Haritashya, U. K.; Klimeš, J.; Reinhardt, L.; Schaub, Y.; Wiltshire, A.; Regmi, D.; Vilímek, V.,

Climate change and the global pattern of moraine-dammed glacial lake outburst floods. The Cryosphere 2018, 12, (4), 1195-1209.

Hartmann, D.L., A.M.G. Klein Tank, M. Rusticucci, L.V. Alexander, S. Brönnimann, Y. Charabi, F.J. Dentener, E.J. Dlugokencky, D.R. Easterling, A. Kaplan, B.J. Soden, P.W. Thorne, M. Wild and P.M. Zhai, 2013: Observations: Atmosphere and Surface. In: Climate Change 2013: The Physical Science Basis. Contribution of Working Group I to the Fifth Assessment Report of the Intergovernmental Panel on Climate Change [Stocker, T.F., D. Qin, G.-K. Plattner, M. Tignor, S.K. Allen, J. Boschung, A. Nauels, Y. Xia, V. Bex and P.M. Midgley (eds.)]. Cambridge University Press, Cambridge, United Kingdom and New York, NY, USA, pp. 159–254, doi:10.1017/CBO9781107415324.008.

Harwood, L.A., Smith, T.G., George, J.C., Sandstrom, S.J., Walkusz, W. and Divoky, G.J., 2015. Change in the Beaufort Sea ecosystem: diverging trends in body condition and/or production in five marine vertebrate species. Progress in Oceanography, 136, pp.263-273.

Hayden, B., et al. 2014: Lake morphometry and resource polymorphism determine niche segregation between cool and cold-water adapted fish. Ecology 95: 538-552.

Hayden, B., et al. 2017: Climate and productivity shape fish and invertebrate community structure in subarctic lakes. Freshwater Biology 62: 990-1003.

Hayden, B., et al. 2019: From clear lakes to murky waters - tracing the functional response of high-latitude lake communities to concurrent 'greening' and 'browning'. Ecology Letters 22: 807-816.

Hayden, B., Harrod, C. & Kahilainen, K.K. 2014a: Lake morphometry and resource polymorphism determine niche segregation between cool and cold-water adapted fish. Ecology 95: 538-552.

Hayden, B., Harrod, C. & Kahilainen, K.K. 2014b: Dual-fuels: intra-annual variation in the relative importance of benthic and pelagic resources to maintenance, growth and reproduction in a generalist salmonid fish. Journal of Animal Ecology 83: 1501-1512.

Heibo, E., Magnhagen, C., Vøllestad, L.A. 2005: Latitudinal variation in life-history traits in Eurasian perch. Ecology 86: 3377-3386.

Heimbürger, L.E., Sonke, J. E., Cossa, D., Point, D., Lagane, C., Laffont, L., et al. (2015). Shallow methylmercury production in the marginal sea ice zone of the central Arctic Ocean. Sci. Rep., 5(1), 10318. https://doi.org/10.1038/srep10318

Helama, S., J. Jiang, J. Korhonen, J. Holopainen and T. Timonen, 2013. Quantifying temporal changes in Tornionjoki river ice breakup dates and spring temperatures in Lapland since 1802. Journal of Geographical Sciences, 23(6): 1069–1079.

Helland, I.P., Finstad, A.G., Forseth, T., Hesthagen, T. & Ugedal, O. 2011: Ice-cover effects on competitive interactions between two fish species. Journal of Animal Ecology 80: 539-547.

Henriksen, A., J. Mannio, A. Wilander, T. Moiseenko, T. Traaen, B.L. Skjelkvåle, E. Fjeld and J. Vuorenmaa, 1997. Regional lake surveys in the Barents region of Finland, Norway, Sweden and Russian Kola, 1995. Results. Acid Rain Research Report 45/97. NIVA Report SNO 3633-97, Oslo. 36 pp.

Higuera, P. E., Brubaker, L. B., Anderson, P. M., Brown, T. A., Kennedy, A. T., & Hu, F. S. (2008). Frequent Fires in Ancient Shrub Tundra: Implications of Paleorecords for Arctic Environmental Change. PLOS ONE, 3(3), e0001744. https://doi.org/10.1371/journal.pone.0001744

Hu, F. S., Higuera, P. E., Duffy, P., Chipman, M. L., Rocha, A. V, Young, A. M., Kelly, R., & Dietze, M. C. (2015). Arctic tundra fires: natural variability and responses to climate change. Frontiers in Ecology and the Environment, 13(7), 369–377. https://doi.org/10.1890/150063

Hu, F. S., Higuera, P. E., Walsh, J. E., Chapman, W. L., Duffy, P. A., Brubaker, L. B., & Chipman, M. L. (2010). Tundra burning in Alaska: Linkages to climatic change and sea ice retreat. Journal of Geophysical Research: Biogeosciences, 115(G4). https://doi.org/10.1029/2009JG001270

Huang, J.; Kang, S.; Ma, M.; Guo, J.; Cong, Z.; Dong, Z.; Yin, R.; Xu, J.; Tripathee, L.; Ram, K.; Wang, F., Accumulation of Atmospheric Mercury in Glacier Cryoconite over Western China. Environmental Science & Technology 2019, 53, (12), 6632-6639.

10727 Hudelson, K. E. et al. Temporal trends, lake-to-lake variation, and climate effects on Arctic char
10728 (Salvelinus alpinus) mercury concentrations from six High Arctic lakes in Nunavut, Canada. Sci.
10729 Total Environ. 678, 801-812, (2019).
10730 Hutchins, R., Tank, S.E., Olefeldt, D., Quinton, W.L., Spence, C., Dion, N., Mengitsu, S.G. Wildfires in
10731 subarctic Canada have no impact on downstream mercury transport but cause decreased delivery of
10732 dissolved carbon and nutrients. In prep.
10733 Ims R, A., Ehrich D, Forbes BC, Huntley B, Walker DA, Wookey PA. Terrestrial Ecosystems (Chapter
10734 12). In: Meltofte H, editor. Arctic biodiversity assessment. Status and trends in Arctic biodiversity.
10735 Conservation of Arctic Flora and Fauna, Akureyri, 2013.
10736 IPCC. Climate Change 2013: The Physical Science Basis. Contribution of Working Group I to the Fifth
10737 Assessment Report of the Intergovernmental Panel on Climate Change. 1-1535 (Cambridge, UK,
10738 2013).
10739 Jæger I, Hop H, Gabrielsen GW. Biomagnification of mercury in selected species from an Arctic marine
10740 food web in Svalbard. Sci. Total Environ. 2009; 407: 4744-4751.
10741 Jaeglé, L.: Atmospheric long-range transport and deposition of mercury to Alaska, Department of
10742 Atmospheric Sciences, University of Washington, Seattle, A report to the Alaska Department of
10743 Environmental Conservation, 2010.
10744 Jain, P., Wang, X., & Flannigan, M. D. (2017). Trend analysis of fire season length and extreme fire
10745 weather in North America between 1979 and 2015. International Journal of Wildland Fire, 26(12),
10746 1009. https://doi.org/10.1071/WF17008
10747 Jiang, T., D. Wang, B. Meng, J. Chi, H. Laudon and J. Liu, 2020. The concentrations and characteristics
10748 of dissolved organic matter in high-latitude lakes determine its ambient reducing capacity. Water
10749 Research, 169: 115217.
10750 Jiskra, M., Wiederhold, J. G., Skyllberg, U., Kronberg, R. M., Hajdas, I., & Kretzschmar, R. (2015).
10751 Mercury deposition and re-emission pathways in boreal forest soils investigated with Hg isotope
10752 signatures. Environmental Science & Technology, 49(12), 7188–7196. https://doi.org/
10753 10.1021/acs.est.5b00742
10754 Jolly, W. M., Cochrane, M. A., Freeborn, P. H., Holden, Z. A., Brown, T. J., Williamson, G. J., &
10755 Bowman, D. M. J. S. (2015). Climate-induced variations in global wildfire danger from 1979 to
10756 2013. Nature Communications, 6. https://doi.org/10.1038/ncomms8537
10757 Jones, B. M.; Grosse, G.; Arp, C. D.; Miller, E.; Liu, L.; Hayes, D. J.; Larsen, C. F., Recent Arctic tundra
10758 fire initiates widespread thermokarst development. Scientific Reports 2015, 5, (1), 15865.
10759 Kahilainen, K.K. Thomas, S.M., Keva, O., Hayden, B., Knudsen R., Eloranta A.P., Tuohiluoto, K.,
10760 Amundsen P-A., Malinen, T. &; Järvinen, A. 2016: Seasonal dietary shift to zooplankton influences
10761 stable isotope ratios and total mercury concentrations in Arctic charr (Salvelinus alpinus (L.)).
10762 Hydrobiologia 783: 47-63.
10763 Kahilainen, K.K., Keva, O., Harrod, C. & Hayden, B. 2020: Mercury dynamics in fish muscle during
10764 winter and summer in subarctic lakes. In preparation.
10765 Kahilainen, K.K., Thomas, S.M., Nystedt, E.K.M., Keva, O., Malinen, T. & Hayden, B. 2017:
10766 Ecomorphological divergence drives differential mercury bioaccumulation of polymorphic European
10767 whitefish (Coregonus lavaretus) populations of subarctic lakes. Science of the Total Environment
10768 599-600: 1768-1778.
10769 Kaiser, K., M. Canedo-Oropeza, R. McMahon and R.M.W. Amon, 2017. Origins and transformations of
10770 dissolved organic matter in large Arctic rivers. Scientific Reports, 7: 13064.
10771 Kane, E. S. (2012). Squeezing the arctic carbon balloon: Ecosystem carbon storage. Nature Climate
10772 Change, 2(12), 841–842. https://doi.org/10.1038/nclimate1764
10773 Kelly EN, Schindler DW, St Louis VL, Donald DB, Vladicka KE. Forest fire increases mercury
10774 accumulation by fishes via food web restructuring and increased mercury inputs. Proceedings of the
10775 National Academy of Sciences of the United States of America 2006; 103: 19380-5.

10776 Keva, O., Hayden, B., Harrod, C. & Kahilainen, K.K. 2017: Total mercury concentrations in liver and
10777 muscle of European whitefish (Coregonus lavaretus (L.)) in a subarctic lake - assessing the factors
10778 driving year-round variation. Environmental Pollution 231: 1518-1528.
10779 Kidd, K.A., Muir, D.C.G., Evans, M.S., Wang, X., Whittle, M., Swanson, H.K., Johston, T., Guildford, S.
10780 2012: Biomagnification of mercury through lake trout (Salvelinus namaycush) food webs of lakes
10781 with different physical, chemical and biological characteristics. Science of Total Environment 438:
10782 135-143.
10783 Kirchmeier-Young, M. C., Gillett, N. P., Zwiers, F. W., Cannon, A. J., & Anslow, F. S. (2018).
10784 Attribution of the influence of human-induced climate change on an extreme fire season. Earth's
10785 Future, 2018EF001050. https://doi.org/10.1029/2018EF001050
10786 Kirk, J. L.; Muir, D. C. M.; Antoniades, D.; Douglas, M. S. V.; Evans, M. S.; Jackson, T. A.; Kling, H.;
10787 Amoureux, S.; Lim, D. S. S.; Pienitz, R.; Smolo, J. P.; Stewart, K.; Wang, X.; Yang, F., Climate
10788 change and mercury accumulation in canadian high and subarctic lakes. Environmental Science and
10789 Technology 2011, 45, (3), 964-970
10790 Klaminder, J., Yoo, K., Giesler, R., Teknisk-naturvetenskapliga, f., Umeå, u., &; ekologi, m. o. g. I. f.
10791 (2009). Soil carbon accumulation in the dry tundra: Important role played by precipitation. Journal of
10792 Geophysical Research, 114, G04005. https://doi.org/10.1029/2009JG000947
10793 Klaminder, J., Yoo, K., Rydberg, J., & Giesler, R. (2008). An explorative study of mercury export
10794 from a thawing palsa mire. Journal of Geophysical Research, 113, G04034.
10795 https://doi.org/10.1029/2008JG000776
10796 Kohlenberg, A. J., Turetsky, M. R., Thompson, D. K., Branfireun, B. A., & Mitchell, C. P. J. (2018).
10797 Controls on boreal peat combustion and resulting emissions of carbon and mercury. Environmental
10798 Research Letters, 13(3), 35005. https://doi.org/10.1088/1748-9326/aa9ea8
10799 Kokelj, S. V.; Lacelle, D.; Lantz, T. C.; Tunnicliffe, J.; Malone, L.; Clark, I. D.; Chin, K. S., Thawing of
10800 massive ground ice in mega slumps drives increases in stream sediment and solute flux across a
10801 range of watershed scales. Journal of Geophysical Research: Earth Surface 2013, 118, (2), 681-692.
10802 Kokelj, S. V.; Tunnicliffe, J.; Lacelle, D.; Lantz, T. C.; Chin, K. S.; Fraser, R. Increased precipitation
10803 drives mega slump development and destabilization of ice-rich permafrost terrain, northwestern
10804 Canada. Global Planet. Change 2015, 129, 56−68.
10805 Korhonen, J. and E. Kuusisto, 2010. Long-term changes in the discharge regime in Finland. Hydrology
10806 Research, 41(3-4): 253–268.
10807 Korhonen, J. and J.J. Koskela, 2017. Inconsistencies in Finnish hydrological observations. In: Proceeding
10808 of 21st Northern Research Basins symposium and Workshop: Cold-region hydrology in a non-
10809 stationary world. Yakutsk, Russia, 6–12 August, 2017. Melnikov Permafrost Institute Press,
10810 Yakutsk. pp. 58–66.
10811 Korhonen, J., 2006. Long-term changes in lake ice cover in Finland. Nordic Hydrology, 37(4-5): 347–
10812 363.
10813 Korhonen, J., 2019. Long-term changes and variability of the winter and spring season hydrological
10814 regime in Finland 2019. Report Series in Geophysics No 79, University of Helsinki, 83 pp.
10815 Korosi, J. B.; Griffiths, K.; Smol, J. P.; Blais, J. M., Trends in historical mercury deposition inferred from
10816 lake sediment cores across a climate gradient in the Canadian High Arctic. Environmental Pollution
10817 2018, 241, 459-467
10818 Korosi, J. B.; McDonald, J.; Coleman, K. A.; Palmer, M. J.; Smol, J. P.; Simpson, M. J.; Blais, J. M.,
10819 Long-term changes in organic matter and mercury transport to lakes in the sporadic discontinuous
10820 permafrost zone related to peat subsidence. Limnol. Oceanogr. 2015, 60, (5), 1550-1561.
10821 Kortsch S, Primicerio R, Fossheim M, Dolgov AV, Aschan M. 2015 Climate change alters the structure
10822 of arctic marine food webs due to poleward shifts of boreal generalists. Proc. R. Soc. B 282,
10823 20151546. (doi:10.1098/rspb.2015.1546)
10824 Kortsch, S., Primicerio, R., Beuchel, F., Renaud, P. E., Rodrigues, J., Lønne, O. J., & Gulliksen, B.
10825 (2012). Climate-driven regime shifts in Arctic marine benthos. Proceedings of the National Academy
10826 of Sciences, 109(35), 14052-14057.

Koven, C. D., W.J. Riley and A. Stern, 2013. Analysis of permafrost thermal dynamics and response to climate change in the CMIP5 Earth system models. Journal of Climate, 26(6): 1877–1900.

Koven, C.D., Riley, W.J., Stern, A. Analysis of permafrost thermal dynamics and response to climate change in the CMIP5 earth system models. Journal of Climate 2013, 26, 1877-1900.

Kozak, N., Ahonen, S.A., Keva, O., Østbye, K., Taipale, S.J., Hayden, B. & Kahilainen K.K. 2020: Changing mercury biomagnification in subarctic food webs along climatic and productivity gradients. In preparation.

Kumar, A., Wu, S., Huang, Y., Liao, H., & Kaplan, J. O. (2018). Mercury from wildfires: Global emission inventories and sensitivity to 2000–2050 global change. Atmospheric Environment, 173, 6–15. https://doi.org/10.1016/j.atmosenv.2017.10.061

Kumar, A.; Wu, S., Mercury Pollution in the Arctic from Wildfires: Source Attribution for the 2000s. Environmental Science & Technology 2019, 53, (19), 11269-11275.

Lafrenière, M.J. and Lamoureux, S.F., 2013. Thermal perturbation and rainfall runoff have greater impact on seasonal solute loads than physical disturbance of the active layer. Permafrost and Periglacial Processes, 24(3), pp.241-251.

Laidre, K. L. et al. Quantifying the sensitivity of arctic marine mammals to climate-induced habitat change. Ecol. Appl 18, S97-S125, (2008).

Lamarche-Gagnon, G.; Wadham, J. L.; Sherwood Lollar, B.; Arndt, S.; Fietzek, P.; Beaton, A. D.; Tedstone, A. J.; Telling, J.; Bagshaw, E. A.; Hawkings, J. R.; Kohler, T. J.; Zarsky, J. D.; Mowlem, M. C.; Anesio, A. M.; Stibal, M., Greenland melt drives continuous export of methane from the ice-sheet bed. Nature 2019, 565, (7737), 73-77.

Lamoureux, S.F. and Lafrenière, M.J., 2017. More than just snowmelt: integrated watershed science for changing climate and permafrost at the Cape Bounty Arctic Watershed Observatory. Wiley Interdisciplinary Reviews: Water, 5(1), e1255.

Lantuit H, Pollard WH. Fifty years of coastal erosion and retrogressive thaw slump activity on Herschel Island, southern Beaufort Sea, Yukon Territory, Canada. Geomorphology 2008; 95: 84-102.

Laske, S.M., Amundsen, P-A., Christoffersen, K.S., Erkinaro, J., Gudbergsson, G., Hayden, B., Heino, J., Holmgren, K., Kahilainen, K.K., Lento, J., Orell, P., Östergren, J., Power, M., Rafikov, R., Romakkaniemi, A., Svenning, M.A., Swanson, H., Whitman, M., & Zimmerman, C.E. 2020: Circumpolar patterns of Arctic freshwater fish diversity – A baseline for monitoring. Freshwater Biology. Early view. Doi: 10.1111/fwb.13405

Lau, D.C.P., Goedkoop, W., Schartau, A.K., Hayden, B., Erkinaro, J., Karlsson, J., Heino, J., Ruuhijärvi, J., Holmgren, K., Kahilainen, K.K., Christoffersen, K., Forsström, L., Kahlert, M., Mjelde, M., Svenning, M., Liljaniemi, P., Karjalainen, S.M., Hellsten, S., Sandøy, S., Vrede, T. 2020: Multitrophic biodiversity patterns and environmental descriptors of sub-Arctic lakes in northern Europe. Freshwater Biology. Early view. Doi: 10.1111/fwb.13477

Lee, R. E. Jr. (2015). In J. E. Hobbie & G.W. Kling (Eds.), Alaska's changing Arctic: Ecological consequences for tundra, streams, and lakes, (p. 1170). Middletown: American Library Association CHOICE.

Legagneux P, Gauthier G, Lecomte N, Schmidt NM, Reid D, Cadieux MC, et al. Arctic ecosystem structure and functioning shaped by climate and herbivore body size. Nature Climate Change 2014; 4: 379-383.

Lehnherr, I., Methylmercury biogeochemistry: A review with special reference to Arctic aquatic ecosystems. Environmental Reviews 2014, 22, (3), 229-243

Lehnherr, I.; St. Louis, V. L.; Emmerton, C. A.; Barker, J. D.; Kirk, J. L., Methylmercury cycling in high arctic wetland ponds: Sources and sinks. Environmental Science and Technology 2012, 46, (19), 10514-10522.

Lehnherr, I.; St. Louis, V. L.; Kirk, J. L., Methylmercury cycling in high arctic wetland ponds: Controls on sedimentary production. Environmental Science and Technology 2012, 46, (19), 10523-10531.

Lehnherr, I.; St. Louis, V. L.; Muir, D. C. G.; Sharp, M. J.; Gardner, A. S.; Lamoureux, S.; Smol, J. P.; St. Pierre, K. A.; Michelutti, N.; Schiff, S. L.; Emmerton, C. A.; Tarnocai, C.; Talbot, C., The

10878 world's largest High Arctic lake responds rapidly to climate warming. Nat. Commun. 2018, 9,
10879 1290.
10880 Lehnherr, I.; St. Louis, V. L.; Muir, D. C. G.; Sharp, M. J.; Gardner, A. S.; Lamoureux, S.; Smol, J. P.; St.
10881 Pierre, K. A.; Michelutti, N.; Schiff, S. L.; Emmerton, C. A.; Tarnocai, C.; Talbot, C., The world's
10882 largest High Arctic lake responds rapidly to climate warming. Nat. Commun. 2018, 9, 1290.
10883 Lei, R., M. Leppäranta, B. Cheng, P. Heil and Z. Li, 2012. Changes in ice-season characteristics of a
10884 European Arctic lake from 1964 to 2008. Climatic Change, 115(3): 725–739.
10885 Lento, J., et al.2019: CAFF Circumpolar Biodiversity Monitoring Program State of Arctic Freshwater
10886 Biodiversity Report. Conservation of Arctic Flora and Fauna. Arctic Council. 170 p.
10887 Lescord, G.L., Emilson, E.J.S., Johnston, T.A., Branfireun, B.A. and Gunn, J.M. 2018: Optical properties
10888 of dissolved organic matter and their relation to mercury concentration in water and biota across a
10889 remote freshwater drainage basin. Environmental Science & Technology 52: 3344-3353.
10890 Lewis, T. and Lamoureux, S.F., 2010. Twenty-first century discharge and sediment yield predictions in a
10891 small high Arctic watershed. Global and Planetary Change, 71(1-2), pp.27-41.
10892 Lewis, T., Lafrenière, M.J. and Lamoureux, S.F., 2012. Hydrochemical and sedimentary responses of
10893 paired High Arctic watersheds to unusual climate and permafrost disturbance, Cape Bounty, Melville
10894 Island, Canada. Hydrological Processes, 26(13), pp.2003-2018.
10895 Lewkowicz AG, Way RG. Extremes of summer climate trigger thousands of thermokarst landslides in a
10896 High Arctic environment. Nature Communications 2019; 10
10897 Liljedahl AK, Boike J, Daanen RP, Fedorov AN, Frost GV, Grosse G, Hinzman LD, Iijma Y, Jorgenson
10898 JC, Matveyeva N, Necsoiu M. Pan-Arctic ice-wedge degradation in warming permafrost and its
10899 influence on tundra hydrology. Nature Geoscience. 2016 Apr;9(4):312-8.
10900 Lim, A. G.; Sonke, J. E.; Krickov, I. V.; Manasypov, R. M.; Loiko, S. V.; Pokrovsky, O. S., Enhanced
10901 particulate Hg export at the permafrost boundary, western Siberia. Environmental Pollution 2019,
10902 254, 113083.
10903 Lim, D.S.S., M.S.V. Douglas, J.P. Smol and D.R.S. Lean, 2001. Physical and chemical limnological
10904 characteristics of 38 lakes and ponds on Bathurst Island, Nunavut, Canadian High Arctic.
10905 International Review of Hydrobiology, 86: 1−22.
10906 Liston GE, Hiemstra CA. The changing cryosphere: Pan-Arctic snow trends (1979-2009). Journal of
10907 Climate 2011; 24: 5691-5712.
10908 Livingstone, D.M., 1997. Break-up dates of alpine lakes as proxy data for local and regional mean surface
10909 air temperatures. Climatic Change, 37(2): 407–439.
10910 Loe LE, Hansen BB, Stien A, D. Albon S, Bischof R, Carlsson A, et al. Behavioral buffering of extreme
10911 weather events in a high-Arctic herbivore. Ecosphere 2016; 7: e01374.
10912 Loseto, L. L., Stern, G. A. & Macdonald, R. W. Distant drivers or local signals: Where do mercury trends
10913 in western Arctic belugas originate? Sci. Total Environ 509-510, 226-236, (2015).
10914 Loseto, L.L., Lean, D.R.S. and Siciliano, S.D., 2004. Snowmelt Sources of Methylmercury to High Arctic
10915 Ecosystems. Environmental Science and Technology, 38, pp. 3004-3010.
10916 Luo H.W.; Yin, X.; Jubb, A.M.; Chen, H.; Lu, X.; Zhang, W.; Lin, H.; Yu, H.Q.; Liang, L.; Sheng, G.P.;
10917 Gu, B. Photochemical reactions between mercury (Hg) and dissolved organic matter decrease Hg
10918 bioavailability and methylation. Environmental Pollution, 2017, 220, 1359-1365.
10919 Macdonald RW, Harner T, Fyfe J. Recent climate change in the Arctic and its impact on contaminant
10920 pathways and interpretation of temporal trend data. The Science of the Total Environment 2005; 342:
10921 5-86.
10922 Macdonald, R. W.; Loseto, L. L., Are Arctic Ocean ecosystems exceptionally vulnerable to global
10923 emissions of mercury? A call for emphasised research on methylation and the consequences of
10924 climate change. Environmental Chemistry 2010, 7, (2), 133-138
10925 Mack, M. C., Bret-Harte, M. S., Hollingsworth, T. N., Jandt, R. R., Schuur, E. A. G., Shaver, G. R., &
10926 Verbyla, D. L. (2011). Carbon loss from an unprecedented Arctic tundra wildfire. Nature, 475(7357),
10927 489–492. https://doi.org/10.1038/nature10283

MacMillan, G. A.; Girard, C.; Chételat, J.; Laurion, I.; Amyot, M., High Methylmercury in Arctic and Subarctic Ponds is Related to Nutrient Levels in the Warming Eastern Canadian Arctic. Environmental Science and Technology 2015, 49, (13), 7743-7753

Mallory CD, Boyce MS. Observed and predicted effects of climate change on Arctic caribou and reindeer. Environ. Rev. 2017; 26: 13-25.

Mann, E. A., Mallory, M. L., Ziegler, S. E., Tordon, R., and O'Driscoll, N. J.: Mercury in Arctic snow: quantifying the kinetics of photochemical oxidation and reduction, Sci. Total Environ., 509–510, 115–132, https://doi.org/10.1016/j.scitotenv.2014.07.056, 2015.

Mann, E. A.; Ziegler, S. E.; Steffen, A.; O'Driscoll, N. J., Increasing chloride concentration causes retention of mercury in melted Arctic snow due to changes in photoreduction kinetics. Journal of Environmental Sciences (China) 2018, 68, 122-129

Mann, E., Meyer, T., Mitchell, C. P. J., and Wania, F.: Mercury fate in ageing and melting snow: development and testing of a controlled laboratory system, J. Environ. Monit., 13, 2695–2702, https://doi.org/10.1039/C1EM10297D, 2011.

Mann, E.; Ziegler, S.; Mallory, M.; O'Driscoll, N., Mercury photochemistry in snow and implications for Arctic ecosystems. Environmental Reviews 2014, 22, (4), 331-345

McKinney MA, Peacock E, Letcher RJ. Sea ice-associated diet change increases the levels of chlorinated and brominated contaminants in polar bears. Environmental Science and Technology 2009; 43: 4334-9.

McKinney MA, Stirling I, Lunn NJ, Peacock E, Letcher RJ. The role of diet on long-term concentration and pattern trends of brominated and chlorinated contaminants in western Hudson Bay polar bears, 1991-2007. The Science of the Total Environment 2010; 408: 6210-22.

McKinney, M. A. et al. A review of ecological impacts of global climate change on persistent organic pollutant and mercury pathways and exposures in arctic marine ecosystems. Curr. Zool. 61, 617-628, (2015).

McKinney, M. A. et al. Global change effects on the long-term feeding ecology and contaminant exposures of East Greenland polar bears. Global Change Biol. 19, 2360-2372, (2013).

McKinney, M. A., Atwood, T. C., Pedro, S. & Peacock, E. Ecological change drives a decline in mercury concentrations in southern Beaufort Sea polar bears. Environ. Sci. Technol. 51, 7814-7822, (2017).

McKinney, M. A., Atwood, T., Iverson, S. J. & Peacock, E. Temporal complexity of southern Beaufort Sea polar bear diets during a period of increasing land use. Ecosphere 8, e01633, (2017a).

McMeans, B.C., McCann, K.S., Humpries, M., Rooney, N. & Fisk, A.T. 2015: Food web structure in temporally-forced ecosystems. Trends in Ecology and Evolution 30: 662-672.

Mercury levels skyrocket thanks to Arctic warm up. Nature 2018, 564, (7735), 164

Mernild, S. H.; Hanna, E.; McConnell, J. R.; Sigl, M.; Beckerman, A. P.; Yde, J. C.; Cappelen, J.; Malmros, J. K.; Steffen, K., Greenland precipitation trends in a long-term instrumental climate context (1890–2012): evaluation of coastal and ice core records. Int. J. Climatol. 2015, 35, (2), 303-320.

Milardi, M., Keva, O. & Kahilainen, K.K. 2020: Measuring mercury concentration of a whole fish population in a subarctic lake - seasonal and annual bioaccumulation patterns in brown trout (Salmo trutta) tissues. In preparation.

Milner, A. M.; Khamis, K.; Battin, T. J.; Brittain, J. E.; Barrand, N. E.; Füreder, L.; Cauvy- Fraunié, S.; Gíslason, G. M.; Jacobsen, D.; Hannah, D. M.; Hodson, A. J.; Hood, E.; Lencioni, V.; Ólafsson, J. S.; Robinson, C. T.; Tranter, M.; Brown, L. E., Glacier shrinkage driving global changes in downstream systems. Proc. Nat. Acad. Sci. 2017, 114, (37), 9770-9778.

Moller, A.K.; Barkay, T.; Al-Soud, W.A.; Sorensen, S.J.; Skov, H.; Kroer, N. Diversity and characterization of mercury-resistant bacteria in snow, freshwater and sea-ice brine from the High Arctic. FEMS Microbiology Ecology 2011 75, 390-401.

Monteith, D.T., J.L. Stoddard, C.D. Evans, H.A. de Wit, M. Forsius, T. Høgåsen, A. Wilander, B.L. Skjelkvale, D.S. Jeffries, J. Vuorenmaa, B. Keller, J. Kopácek and J. Vesely, 2007. Dissolved

organic carbon trends resulting from changes in atmospheric deposition chemistry. Nature 2007, 450: 537–540.

Moore, C. W., Obrist, D., Steffen, A., Staebler, R. M., Douglas, T. A., Richter, A., & Nghiem, S. V. (2014). Convective forcing of mercury and ozone in the arctic boundary layer induced by leads in sea ice. Nature, 506(7486), 81–84. https://doi.org/10.1038/nature12924

Moore, S. E. & Huntington, H. P. Arctic marine mammals and climate change: Impacts and resilience. Ecol. Appl 18, S157-S165, (2008).

Morel, F.M.M., Kraepel, A.M.L. & Amyot, M. 1998: The chemical cycle and bioaccumulation of mercury. Annual Review of Ecology and Systematics 29: 543-566.

Morris AD, Letcher RJ, Braune B, Gamberg M, Stow J. Climate, weather and time: Factors of influence on concentrations of priority contaminants in terrestrial, avian and marine wildlife from the Hudson Bay. Science of the Total Environment 2020; In final preparation.

Mu, C., F. Zhang, X. Chen, S. Ge, M. Mu, L. Jia, Q. Wu and T. Zhang, 2018. Carbon and mercury export from the Arctic rivers and response to permafrost degradation. Water Research, 161: 54–60.

Muir, D. C. G.; Wang, X.; Yang, F.; Nguyen, N.; Jackson, T. A.; Evans, M. S.; Douglas, M.; Köck, G.; Lamoureux, S.; Pienitz, R.; Smol, J. P.; Vincent, W. F.; Dastoor, A., Spatial trends and historical deposition of mercury in eastern and northern Canada inferred from lake sediment cores. Environ. Sci. Technol. 2009, 43, (13), 4802-4809.

Munson, K. M.; Lamborg, C. H.; Boiteau, R. M.; Saito, M. A., Dynamic mercury methylation and demethylation in oligotrophic marine water. Biogeosciences 2018, 15, (21), 6451-6460

Myers-Smith, I. H. et al. Shrub expansion in tundra ecosystems: Dynamics, impacts and research priorities. Environmental Research Letters 6, (2011).

Myers-Smith, I. H., Elmendorf, S. C., Beck, P. S. A., Wilmking, M., Hallinger, M., Blok, D., Tape, K. D., Rayback, S. A., Macias-Fauria, M., Forbes, B. C., Speed, J. D. M., Boulanger-Lapointe, N., Rixen, C., Lévesque, E., Schmidt, N. M., Baittinger, C., Trant, A. J., Hermanutz, L., Collier, L. S., … Vellend, M. (2015). Climate sensitivity of shrub growth across the tundra biome. Nature Climate Change, 5(9), 887–891. https://doi.org/10.1038/nclimate2697

Natali, S. M., Schuur, E. A. G., Webb, E. E., Pries, C. E. H., & Crummer, K. G. (2014). Permafrost degradation stimulates carbon loss from experimentally warmed tundra. Ecology, 95(3), 602–608. https://doi.org/10.1890/13-0602.1

Nieminen, M., Koskinen, M., Sarkkola, S., Laurén, A., Kaila, A., Kiikkilä, O., Nieminen, T.M., Ukonmaanaho, L. 2015. Dissolved organic carbon export from harvested peatland forests with differing site characteristics. Water Air and soil Pollution 226:181. DOI 10.1007/s11270-015-2444-0

Nilsson, C.; Polvi, L. E.; Lind, L., Extreme events in streams and rivers in arctic and subarctic regions in an uncertain future. Freshwater Biology 2015, 60, (12), 2535-2546.

Nossov, D. R.; Torre Jorgenson, M.; Kielland, K.; Kanevskiy, M. Z., Edaphic and microclimatic controls over permafrost response to fire in interior Alaska. Environmental Research Letters 2013, 8, (3), 035013.

Notes: (From Kyra): (changing hydrological cycle (timing of key events, magnitude of fluxes, water sources), impacts of a changing cryosphere (permafrost thaw and glacial melt)

O'Donnell, J.A., G.R. Aiken, D.K. Swanson, S. Panda, K.D. Butler and A.P. Baltensperger, 2016. Dissolved organic matter composition of Arctic rivers: linking permafrost and parent material to riverine carbon. Global Biogeochemical Cycles, 30: 1811–1826.

O'Reilly, C.; et al. Rapid and highly variable warming of lake surface waters around the globe. Geophys. Res. Lett. 2015, 42, 10773– 10781.

Obrist D, Pearson C, Moore C. Mercury and other trace element wet deposition in Alaska: spatial patterns, controlling factors, and source regions. A draft report to the Alaska Department of Environmental Conservation. https://dec.alaska.gov/media/10511/aktracemetals-dri-report-092016.pdf

Obrist, D., Agnan, Y., Jiskra, M., Olson, C. L., Colegrove, D. P., Hueber, J., Moore, C. W., Sonke, J. E., and Helmig, D.: Tundra uptake of atmospheric elemental mercury drives Arctic mercury pollution, Nature, 547, 201–204, https://doi.org/10.1038/nature22997, 2017.

Obrist, D., Kirk, J. L., Zhang, L., Sunderland, E. M., Jiskra, M., & Selin, N. E. (2018). A review of global environmental mercury processes in response to human and natural perturbations: Changes of emissions, climate, and land use. Ambio, 47(2), 116–140. https://doi.org/10.1007/s13280-017-1004-9

Obrist, D., Moosmüller, H., Schürmann, R., Chen, L.-W. A., & Kreidenweis, S. M. (2008). Particulate-Phase and Gaseous Elemental Mercury Emissions During Biomass Combustion: Controlling Factors and Correlation with Particulate Matter Emissions. Environmental Science & Technology, 42(3), 721–727. https://doi.org/10.1021/es071279n

Obrist, D., Pokharel, A. K., and Moore, C.: Vertical profile measurements of soil air suggest immobilization of gaseous elemental mercury in mineral soil, Environ. Sci. Technol., 48, 2242-2252, 10.1021/es4048297, 2014.

O'Driscoll, N,J,; Vost, E.; Mann, E.; Klapstein, S.; Tordon, R.; Lukeman, M. Mercury photoreduction and photooxidation in lakes: effects of filtration and dissolved organic carbon concentration. Journal of Environmental Sciences 2018, 68, 151-159.

Olefeldt, D.; Goswami, S.; Grosse, G.; Hayes, D.; Hugelius, G.; Kuhry, P.; McGuire, A. D.; Romanovsky, V. E.; Sannel, A. B. K.; Schuur, E. A. G.; Turetsky, M. R., Circumpolar distribution and carbon storage of thermokarst landscapes. Nature Communications 2016, 7, 13043.

Olson CL, Jiskra M, Sonke JE, Obrist D. Mercury in tundra vegetation of Alaska: Spatial and temporal dynamics and stable isotope patterns. Sci. Total Environ. 2019; 660: 1502-1512.

Olson, C.; Jiskra, M.; Biester, H.; Chow, J.; Obrist, D., Mercury in Active-Layer Tundra Soils of Alaska: Concentrations, Pools, Origins, and Spatial Distribution. Global Biogeochemical Cycles 2018, 32, (7), 1058-1073

Osburn, C.L., N.J. Anderson, C.A. Stedmon, M.E. Giles, E.J. Whiteford, T.J. McGenity, A.J. Dumbrell and G.J.C. Underwood, 2017. Shifts in the source and composition of dissolved organic matter in Southwest Greenland lakes along a regional hydroclimate gradient. Journal of Geophysical Research: Biogeosciences, 122: 3431–3445.

Oulehle, F., T.G. Jones, A. Burden, M.D.A. Cooper, I. Lebron, P. Zielinski and C.D. Evans, 2013. Soil-solution partitioning of DOC in acid organic soils: results from a UK field acidification and alkalization experiment. European Journal of Soil Science, 64: 787–796.

Outridge, P. M.; Sanei, H.; Courtney Mustaphi, C. J.; Gajewski, K., Holocene climate change influences on trace metal and organic matter geochemistry in the sediments of an Arctic lake over 7,000 years. Appl. Geochemi. 2017, 78, 35-48.

Outridge, P. M.; Sanei, H.; Stern, G. A.; Hamilton, P. B.; Goodarzi, F., Evidence for control of mercury accumulation rates in Canadian High Arctic lake sediments by variations of aquatic primary productivity. Environmental Science & Technology 2007, 41, (15), 5259-5265.

Outridge, P. M.; Stern, G. A.; Hamilton, P. B.; Sanei, H., Algal scavenging of mercury in preindustrial Arctic lakes. Limnology and Oceanography 0, (0) 2019

Øverjordet, I. B. et al. Effect of diet, location and sampling year on bioaccumulation of mercury, selenium and cadmium in pelagic feeding seabirds in Svalbard. Chemosphere 122, 14-22, (2015).

Pacyna AD, Koziorowska K, Chmiel S, Mazerski J, Polkowska Z. Svalbard reindeer as an indicator of ecosystem changes in the Arctic terrestrial ecosystem. Chemosphere 2018; 203: 209-218.

Pankratov, F. F.; Konoplev, A. V.; Makhura, A.; Kats, O. V., Analysis of the data of long-term monitoring of atmospheric mercury content and meteorological parameters at Amderma polar station. Russian Meteorology and Hydrology 2013, 38, (6), 405-413

Pastick NJ, Jorgenson MT, Goetz SJ, Jones BM, Wylie BK, Minsley BJ, et al. Spatiotemporal remote sensing of ecosystem change and causation across Alaska. Global Change Biology 2019; 25: 1171-1189.

11077 Pearson C, Howard D, Moore C, Obrist D. Mercury and trace metal wet deposition across five stations in
11078 Alaska: controlling factors, spatial patterns, and source regions. Atmospheric Chemistry and Physics,
11079 19, 6913-6929, 2019.
11080 Pecl, G. T. et al. Biodiversity redistribution under climate change: Impacts on ecosystems and human
11081 well-being. Science 355, 1389, (2017).
11082 Pedersen HC, Fossøy F, Kålås JA, Lierhagen S. Accumulation of heavy metals in circumpolar willow
11083 ptarmigan (Lagopus l. lagopus) populations. Sci. Total Environ. 2006; 371: 176-189.
11084 Pedro, S. et al. Limited effects of changing prey fish communities on food quality for aquatic predators in
11085 the eastern Canadian Arctic in terms of essential fatty acids, methylmercury and selenium.
11086 Chemosphere 214, 855-865, (2019).
11087 Pedro, S. et al. Mercury and persistent organic pollutants in native and invading forage species of the
11088 Canadian Arctic: Consequences for food web dynamics. Environ. Pollut. 229, 229-240, (2017).
11089 Peeters B, Pedersen AO, Loe LE, Isaksen K, Veiberg V, Stien A, et al. Spatiotemporal patterns of rain-
11090 on-snow and basal ice in high Arctic Svalbard: detection of a climate-cryosphere regime shift.
11091 Environ. Res. Lett. 2019; 14.
11092 Perovich, D. K. & Richter-Menge, J. A. Loss of sea ice in the Arctic. Ann. Rev. Mar. Sci 1, 417-441,
11093 (2009).
11094 Pickhardt, P.C. & Fisher, N.S. 2007: Accumulation of inorganic and methylmercury by freshwater
11095 phytoplankton in two contrasting water bodies. Environmental Science and Technology 41: 125-131.
11096 Pienitz, R., J.P. Smol and D.R.S. Lean, 1997a. Physical and chemical limnology of 59 lakes located
11097 between the southern Yukon and the Tuktoyaktuk Peninsula, Northwest Territories (Canada).
11098 Canadian Journal of Fisheries and Aquatic Sciences, 54: 330−346.
11099 Pogojeva, Yakushev, Ilinskaya, Polukhin, Braaten, Kristiansen, 2018. Experimental study of the influence
11100 of thawing permafrost on the chemical properties of sea water. Russian Journal of Earth Sciences,
11101 18.
11102 Pomerleau, C., Matthews, C.J.D., Gobeil, C., Stern, G.A., Ferguson, S.H., Macdonald, R.W., 2018.
11103 Mercury and stable isotope cycles in baleen plates are consistent with year-round feeding in two
11104 bowhead whale (Balaena mysticetus) populations. Polar Biology 41, 1881-1893. 10.1007/s00300-
11105 018-2329-y
11106 Post, E. et al. 2009: Ecological dynamics across the Arctic associated with recent climate change. Science
11107 325, 1355-1358.
11108 Post, E. et al. Ecological consequences of sea-ice decline. Science 341, 519-524, (2013).
11109 Poste, A.E., Hoel, C.S., Andersen, T., Arts, M.T., Frærøvig, P-J. and Borgå, K. 2019: Terrestrial organic
11110 matter increases zooplankton methylmercury accumulation in a brown-water boreal lake. Science of
11111 the Total Environment 674: 9-18.
11112 Poste, Braaten (joint first authors), Sørensen, de Wit, Larssen, 2015. Effects of photodemethylation on the
11113 methylmercury budget of boreal Norwegian lakes. Environmental Toxicology & Chemistry, 34,
11114 6, 1213-1223.
11115 Poste, Pastukhov, Braaten, Ozersky, Moore, 2018. Seal teeth document the rise and fall of mercury
11116 contamination in the food web of Lake Baikal. Environmental Toxicology & Chemistry. DOI:
11117 10.1002/etc.4095.
11118 Poulain, A.J.; Chadhain, S.M.N.; Ariya, P.A.; Amyot, M.; Garcia, E.; Campbell, P.G.C., Zylstra, G.J.;
11119 Barkay, T. Potential for mercury reduction by microbes in the High Arctic. Applied and
11120 Environmental Microbiology 2007, 2230-2238.
11121 Power M, Reist JD, Dempson JB. Fish in high-latitude Arctic lakes. Polar Lakes and Rivers: Limnology
11122 of Arctic and Antarctic Aquatic Ecosystems, 2009.
11123 Power, M., Klein, G.M., Guiguer, K.R.R.A. & Kwan, M.K.H. 2002: Mercury accumulation in the fish
11124 community of a sub-Arctic lake in relation to trophic position and carbon sources. Journal of Applied
11125 Ecology 39: 819-830.
11126 Priet-Mahéo MC, Ramón CL, Rueda FJ, Andradóttir HÓ. Mixing and internal dynamics of a medium-size
11127 and deep lake near the Arctic Circle. Limnology and Oceanography 2019; 64: 61-80.

Provencher JF, Forbes MR, Hennin HL, Love OP, Braune BM, Mallory ML, et al. Implications of mercury and lead concentrations on breeding physiology and phenology in an Arctic bird. Environ. Pollut. 2016; 218: 1014-1022.

Prowse TD, Wrona FJ, Reist JD, Gibson JJ, Hobbie JE, Lévesque LMJ, et al. Climate change effects on hydroecology of arctic freshwater ecosystems. Ambio 2006; 35: 347-358.

Przytulska, A. et al. 2017: Increased risk of cyanobacterial blooms in northern high- latitude lakes through climate warming and phosphorus enrichment. Freshwater Biology 62: 1986-1996.

Räike, A., Kortelainen, P., Mattsson, T. and Thomas, D.N. 2016. Long-term trends (1975-2014) in the concentrations and export of carbon from Finnish rivers to the Baltic Sea: organic and inorganic components compared. Aquatic Sciences 78: 505-523.

Räike, A., P. Kortelainen, T. Mattsson and D.N. Thomas, 2012. 36 year trends in dissolved organic carbon export from Finnish rivers to the Baltic Sea. Science of the Total Environment, 435: 188–201.

Ramsar. 2014. "Ramsar focuses on Arctic wetlands." Press. Ramsar Convention on Wetlands. Web 30.01.2020:http://saconenvis.nic.in/e_bulletin_dec_2014_files/ramsar.htm

Rantala, M.V. et al. 2016: Sources and controls of organic carbon in lakes across the subarctic treeline. Biogeochemistry 129: 235-253.

Rask, M., M. Korhonen, S. Salo, M. Forsius, M. Kiljunen, R.I. Jones and M. Verta, 2010. Does thermocline change affect methyl mercury concentrations in fish in small boreal lakes? Biogeochemistry, 101: 311–322.

Rautio, M., Dufresne, F., Laurion, I., Bonilla, S., Vincent, W.F. & Christoffersen, K.S. 2011: Shallow freshwater ecosystems of the circumpolar Arctic. Ecoscience 18: 204-222.

Reist, J., F. Wrona, T. Prowse, M. Power, J. Dempson, R. Beamish, J. King, T. Carmichael, and C. Sawatzky. 2006. General effects of climate change on Arctic fishes and fish populations. Ambio 35:370–380.

Rigét, F. F., Dietz, R. & Hobson, K. A. Temporal trends of mercury in Greenland ringed seal populations in a warming climate. J. Environ. Monit 14, 3249-3256, (2012).

Rigét, F. F., Vorkamp, K. & Muir, D. C. G. Temporal trends of contaminants in arctic char (Salvelinus alpinus) from a small lake, southwest Greenland during a warming climate. J. Environ. Monit 12, 2252-2258, (2010).

Rigét, F.; Tamstorf, M. P.; Larsen, M. M.; Søndergaard, J.; Asmund, G.; Falk, J. M.; Sigsgaard, C., Mercury (Hg) transport in a high arctic river in northeast Greenland. Water, Air, and Soil Pollution 2011, 222, (1-4), 233-242

Riordan, B., Verbyla, D., & McGuire, A. D. (2006). Shrinking ponds in subarctic Alaska based on 1950–2002 remotely sensed images. Journal of Geophysical Research: Biogeosciences, 111(G4). https://doi.org/10.1029/2005JG000150

Roberts, K.E., Lamoureux, S.F., Kyser, T.K., Muir, D.C.G., Lafrenière, M.J., Iqaluk, D., Pieńkowski, A.J. and Normandeau, A., 2017. Climate and permafrost effects on the chemistry and ecosystems of High Arctic Lakes. Scientific reports, 7(1), p.13292.

Rode, K. D.; Amstrup, S. C.; Regehr, E. V. Reduced body size and cub recruitment in polar bears associated with sea ice decline. Ecol. Appl. 2010, 20, 768−782.

Rode, K. D.; Regehr, E. V.; Douglas, D. C.; Durner, G.; Derocher, A. E.; Thiemann, G. W.; Budge, S. M. Variation in the response of an Arctic top predator experiencing habitat loss: feeding and reproductive ecology of two polar bear populations. Global Change Biol. 2014, 20,76−88.

Rogers, M. C., Peacock, E., Simac, K., O'Dell, M. B. & Welker, J. M. Diet of female polar bears in the southern Beaufort Sea of Alaska: Evidence for an emerging alternative foraging strategy in response to environmental change. Polar Biol. 38, 1035-1047, (2015).

Rolls, R.J., et al. 2017: Conceptualising the interactive effects of climate change and biological invasions on subarctic freshwater fish. Ecology and Evolution 7: 4109-4128.

Routti, H., Letcher, R.J., Born, E.W., Branigan, M., Dietz, R., Evans, T.J., McKinney, M.A., Peacock, E., Sonne, C., 2012. Influence of carbon and lipid sources on variation of mercury and other trace

elements in polar bears (Ursus maritimus). Environmental Toxicology and Chemistry 31, 2739–2747. 10.1002/etc.2005

Rudy, A.C.A., Lamoureux, S.F., Kokelj, S.V., Smith, I.R. and England, J.H., 2017. Accelerating Thermokarst Transforms Ice-Cored Terrain Triggering a Downstream Cascade to the Ocean. Geophysical Research Letters, 44(21), pp.11-080.

Ruus, Øverjordet, Braaten, Evenset, Christensen, Heimstad, Gabrielsen, Borgå, 2015. Methylmercury biomagnification in an Arctic pelagic food web. Environmental Toxicology & Chemistry, 34, 11, 2636-2643.

Ruuskanen, M.O.; Aris-Brosou, S.; Poulain, A.J. Swift evolutionary response of microbes to a rise in anthropogenic mercury in the Northern Hemisphere. The ISME Journal 2019, https://doi.org/10.1038/s41396-019-0563-0

Rydberg, J.; Klaminder, J.; Rosén, P.; Bindler, R., Climate driven release of carbon and mercury from permafrost mires increases mercury loading to sub-arctic lakes. Science of the Total Environment 2010, 408, (20), 4778-4783

Saros JE, Anderson NJ, Juggins S, McGowan S, Yde JC, Telling J, et al. Arctic climate shifts drive rapid ecosystem responses across the West Greenland landscape. Environmental Research Letters 2019; 14.

Saros JE, Northington RM, Osburn CL, Burpee BT, John Anderson N. Thermal stratification in small arctic lakes of southwest Greenland affected by water transparency and epilimnetic temperatures. Limnology and Oceanography 2016; 61: 1530-1542.

Saros, J.E., C.L. Osburn, R.M. Northington, S.D. Birkel, J.D. Auger, C.A. Stedmon and N.J. Anderson, 2015. Recent decrease in DOC concentrations in Arctic lakes of southwest Greenland. Geophysical Research Letters, 42: 6703–6709, doi:10.1002/2015GL065075.

Schaefer, K., H. Lantuit, V.E. Romanovsky, E.A.G. Schuur and R. Witt, 2014. The impact of the permafrost carbon feedback on global climate. Environmental Research Letters, 9(8): 085003.

Schartau, A.K., Christoffersen, K., Mariash, H., Einarsson, A., Hayden, B., Hrafnsdottir, T., Kahilainen, K.K., Rautio, M., Ruhland, K., Smol, J. & Vrede, T. 2020: First circumpolar assessment of Arctic freshwater phytoplankton and zooplankton diversity: spatial patterns and environmental drivers. Freshwater Biology.

Schartup, A. T.; Balcom, P. H.; Soerensen, A. L.; Gosnell, K. J.; Calder, R. S. D.; Mason, R. P.; Sunderland, E. M.; St. Louis, V. L., Freshwater discharges drive high levels of methylmercury in Arctic marine biota. Proceedings of the National Academy of Sciences of the United States of America 2015, 112, (38), 11789-11794

Scheffer & Carpenter, S.R. 2003: Catastrophic regime shifts in ecosystems: linking theory to observation. Trends in Ecology and Evolution 18: 648–656.

Scheffers, B.R. et al. 2016: The broad footprint of climate change from genes to biomes to people. Science 354: aaf7671.

Schliebe, S. et al. Effects of sea ice extent and food availability on spatial and temporal distribution of polar bears during the fall open-water period in the Southern Beaufort Sea. Polar Biol. 31, 999-1010, (2008).

Schuster, P. F.; Schaefer, K. M.; Aiken, G. R.; Antweiler, R. C.; Dewild, J. F.; Gryziec, J. D.; Gusmeroli, A.; Hugelius, G.; Jafarov, E.; Krabbenhoft, D. P.; Liu, L.; Herman-Mercer, N.; Mu, C.; Roth, D. A.; Schaefer, T.; Striegl, R. G.; Wickland, K. P.; Zhang, T., Permafrost Stores a Globally Significant Amount of Mercury. Geophysical Research Letters 2018, 45, (3), 1463-1471

Schuster, P. F.; Striegl, R. G.; Aiken, G. R.; Krabbenhoft, D. P.; Dewild, J. F.; Butler, K.; Kamark, B.; Dornblaser, M. Mercury Export from the Yukon River Basin and Potential Response to a Changing Climate. Environ. Sci. Technol. 2011, 45 (21), 9262−9267.

Schuur, E. A. G., Abbott, B., & Permafrost Carbon, N. (2011). High risk of permafrost thaw. Nature, 480(7375), 32–33. https://doi.org/10.1038/ 480032a

11227 Schuur, E.A.G., A.D. Mcguire, C. Schädel, G. Grosse, J.W. Harden, D.J. Hayes, G. Hugelius, C.D.
11228 Koven, P. Kuhry and D.M. Lawrence, 2015. Climate change and the permafrost carbon feedback,
11229 Nature 520 (7546): 171–179.
11230 Screen, J. A., & Simmonds, I. (2010). The central role of diminishing sea ice in recent Arctic temperature
11231 amplification. Nature, 464(7293), 1334-1337.
11232 Semkin, R.G., Mierle, G. and Neureuther, R.J., 2005. Hydrochemistry and mercury cycling in a High
11233 Arctic watershed. Science of the Total Environment, 342(1-3), pp.199-221.
11234 Serreze MC, Barry RG. Processes and impacts of Arctic amplification: A research synthesis. Global and
11235 planetary change. 2011 May 1;77(1-2):85-96.
11236 Sharma, S., J.J. Magnuson, R.D. Batt, L.A. Winslow, J. Korhonen and Y. Aono, 2016. Direct
11237 observations of ice seasonality reveal changes in climate over the past 320–570 years. Scientific
11238 Reports, 6: 25061.
11239 Sherman, L. S., Blum, J. D., Douglas, T. A., and Steffen, A.: Frost flowers growing in the Arctic ocean-
11240 atmosphere-sea-snow interface: 2. Mercury exchange between the atmosphere, snow, and frost
11241 flowers, J. Geophys. Res., 117, D00R10, 10.1029/2011jd016186, 2012a.
11242 Sherman, L. S., Blum, J. D., Johnson, K. P., Keeler, G. J., Barres, J. A., and Douglas, T. A.: Mass-
11243 independent fractionation of mercury isotopes in Arctic snow driven by sunlight, Nat. Geosci., 3,
11244 173-177, 10.1038/ngeo758, 2010.
11245 Shuter, B.J., Finstad, A.G., Helland, I.P., Zweimuller, I. & Hölker, F. 2012: The role of winter phenology
11246 in shaping the ecology of freshwater fish and their sensitivities to climate change. Aquatic Sciences
11247 74: 637-657.
11248 Skov, H. Hjorth J. Nordstrøm, C. Jensen, B. Christoffersen, C. Poulsen, M.B. Liisberg, J.B. and Dall'Osto
11249 M, 2020. The variability of ozone and mercury at Villum Research Station, Station Nord in North
11250 Greenland from 1995 to 2017. ACPD, doi.org/10.5194/acp-2019-912.
11251 Smith PA, McKinnon L, Meltofte H, Lanctot RB, Fox AD, Leafloor JO, et al. Status and trends of tundra
11252 birds across the circumpolar Arctic. Ambio 2020; 49: 732-748.
11253 Smith, L. C., Sheng, Y., MacDonald, G. M., & Hinzman, L. D. (2005). Disappearing Arctic Lakes.
11254 Science, 308(5727), 1429 LP – 1429. https://doi.org/10.1126/science.1108142
11255 Smol, J. P. et al. Climate-driven regime shifts in the biological communities of arctic lakes. Proceedings
11256 of the National Academy of Sciences of the United States of America 102, 4397-4402, (2005).
11257 Snucins, E. and G. John, 2000. Interannual variation in the thermal structure of clear and colored lakes.
11258 Limnology and Oceanography, 45: 1639–1646.
11259 Soerensen, A. L., Jacob, D. J., Schartup, A. T., Fisher, J. A., Lehnherr, I., St. Louis, V. L., et al. (2016). A
11260 mass budget for mercury and methylmercury in the Arctic Ocean. Global Biogeochemical Cycles,
11261 30(4), 560–575. https://doi.org/10.1002/2015GB005280
11262 Soerensen, A. L.; Schartup, A. T.; Skrobonja, A.; Björn, E., Organic matter drives high interannual
11263 variability in methylmercury concentrations in a subarctic coastal sea. Environmental Pollution 2017,
11264 229, 531-538
11265 Søndergaard, J., Tamstorf, M., Elberling, B., Larsen, M.M., Mylius, M.R., Lund, M., Abermann, J. and
11266 Rigét, F., 2015. Mercury exports from a High-Arctic river basin in Northeast Greenland (74 N)
11267 largely controlled by glacial lake outburst floods. Science of the Total Environment, 514, pp.83-91.
11268 Søndergaard, J.; Riget, F.; Tamstorf, M. P.; Larsen, M. M. Mercury Transport in a Low- Arctic River in
11269 Kobbefjord, West Greenland (64A degrees N). Water, Air, Soil Pollut. 2012, 223 (7), 4333−4342.
11270 Sonke, J. E.; Teisserenc, R.; Heimbürger-Boavida, L.-E.; Petrova, M. V.; Marusczak, N.; Le Dantec, T.;
11271 Chupakov, A. V.; Li, C.; Thackray, C. P.; Sunderland, E. M.; Tananaev, N.; Pokrovsky, O. S.,
11272 Eurasian river spring flood observations support net Arctic Ocean mercury export to the atmosphere
11273 and Atlantic Ocean. Proc. Nat. Acad. Sci. 2018, 115, (50), E11586.
11274 Spence C, Kokelj SA, Kokelj SV, Hedstrom N. The process of winter streamflow generation in a
11275 subarctic Precambrian Shield catchment. Hydrological Processes 2014; 28: 4179-4190.

11276 St Pierre KA, St Louis VL, Kirk JL, Lehnherr I, Wang S, La Farge C. Importance of Open Marine Waters
11277 to the Enrichment of Total Mercury and Monomethylmercury in Lichens in the Canadian High
11278 Arctic. Environ. Sci. Technol. 2015; 49: 5930-5938.
11279 St Pierre KA, Zolkos S, Shakil S, Tank SE, St Louis VL, Kokelj SV. Unprecedented Increases in Total
11280 and Methyl Mercury Concentrations Downstream of Retrogressive Thaw Slumps in the Western
11281 Canadian Arctic. Environmental Science and Technology 2018; 52: 14099-14109.
11282 St Pierre, K. A.; St Louis, V. L.; Lehnherr, I.; Gardner, A. S.; Serbu, J. A.; Mortimer, C. A.; Muir, D. C.
11283 G.; Wiklund, J. A.; Lemire, D.; Szostek, L.; Talbot, C., Drivers of Mercury Cycling in the Rapidly
11284 Changing Glacierized Watershed of the High Arctic's Largest Lake by Volume (Lake Hazen,
11285 Nunavut, Canada). Environmental Science and Technology 2019, 53, (3), 1175-1185
11286 St. Pierre, K. A.; Chételat, J.; Yumvihoze, E.; Poulain, A. J., Temperature and the sulfur cycle control
11287 monomethylmercury cycling in high arctic coastal marine sediments from Allen Bay, Nunavut,
11288 Canada. Environmental Science and Technology 2014, 48, (5), 2680-2687
11289 Steffen, A., Bottenheim, J., Cole, A., Douglas, T. A., Ebinghaus, R., Friess, U., Netcheva, S., Nghiem, S.,
11290 Sihler, H., and Staebler, R.: Atmospheric mercury over sea ice during the OASIS-2009 campaign,
11291 Atmos. Chem. Phys., 13, 7007–7021, https://doi.org/10.5194/acp-13-7007-2013, 2013.
11292 Stern, G. A. et al. How does climate change influence arctic mercury? Sci. Total Environ 414, 22-42,
11293 (2012).
11294 Stokes, C. R.; Popovnin, V.; Aleynikov, A.; Gurney, S. D.; Shahgedanova, M., Recent glacier retreat in
11295 the Caucasus Mountains, Russia, and associated increase in supraglacial debris cover and supra-
11296 /proglacial lake development. Annals of Glaciology 2007, 46, 195-203.
11297 Surdu, C. M.; Duguay, C. R.; Prieto, D. F., Evidence of recent changes in the ice regime of lakes in the
11298 Canadian High Arctic from spaceborne satellite observations. The Cryosphere 2016, 10, 941-960.
11299 Swanson H, Gantner N, Kidd KA, Muir DCG, Reist JD. Comparison of mercury concentrations in
11300 landlocked, resident, and sea-run fish (Salvelinus spp.) from Nunavut, Canada. Environmental
11301 Toxicology and Chemistry 2011; 30: 1459-1467.
11302 Tagesson T, Mastepanov M, Tamstorf MP, Eklundh L, Schubert P, Ekberg A, Sigsgaard C, Christensen
11303 TR, Ström L. High-resolution satellite data reveal an increase in peak growing season gross primary
11304 production in a high-Arctic wet tundra ecosystem 1992–2008. International Journal of Applied Earth
11305 Observation and Geoinformation. 2012 Aug 1;18:407-16.
11306 Taipale, S.J., et al. 2016: Lake eutrophication and brownification downgrade availability and transfer of
11307 essential fatty acids for human consumption. Environment International 96: 156-166.
11308 Tarnocai, C., J.G. Canadell, E.A.G. Schuur, P.Kuhry, G.Mazhitova and S. Zimov , 2009. Soil organic
11309 carbon pools in the northern circumpolar permafrost region. Global Biogeochemical Cycles, 23(2):
11310 GB2023.
11311 Thomas, S.M., Kiljunen, M., Malinen, T., Eloranta, A.P., Amundsen, P-A., Lodenius, M. & Kahilainen,
11312 K.K. 2016: Food-web structure and mercury dynamics in a large subarctic lake following multiple
11313 species introductions. Freshwater Biology 61: 500-517.
11314 Tran, L., Reist, J. D., Gallagher, C. P. & Power, M. 2019: Comparing total mercury concentrations of
11315 northern Dolly Varden, Salvelinus malma malma, in two Canadian Arctic rivers 1986–1988 and
11316 2011–2013. Polar Biol. 42: 865-876.
11317 Tsubouchi, T., Bacon, S., Aksenov, Y., Garabato, A. C. N., Beszczynska-Möller, A., Hansen, E., et al.
11318 (2018). The arctic ocean seasonal cycles of heat and freshwater fluxes: Observation-based inverse
11319 estimates. Journal of Physical Oceanography, 48(9), 2029–2055. https://doi.org/10.1175/JPO-D-17-
11320 0239.1
11321 Turetsky, M. R., Harden, J. W., Friedli, H. R., Flannigan, M., Payne, N., Crock, J., & Radke, L. (2006).
11322 Wildfires threaten mercury stocks in northern soils. Geophysical Research Letters, 33(16), L16403.
11323 https://doi.org/10.1029/2005GL025595
11324 Turetsky, M. R., Kane, E. S., Harden, J. W., Ottmar, R. D., Manies, K. L., Hoy, E., & Kasischke, E. S.
11325 (2011). Recent acceleration of biomass burning and carbon losses in Alaskan forests and peatlands.
11326 Nature Geoscience, 4(1), 27–31. https://doi.org/10.1038/ngeo1027

Ukonmaanaho, L., Starr, M., Kantola, M., Laurén, A., Piispanen, J., Pietilä, H., Perämäki, P., Merilä, P., Fritze, H., Tuomivirta, t., Heikkinen, J., Mäkinen, J., Nieminen, T.M. 2016. Impacts of forest harvesting on mobilization of Hg and MeHg in drained peatland forests on black schist or felsic bedrock. Environmental monitoring and assessment, 188(4), 1-22. DOI 10.1007/s10661-016-5210-x

Valinia, S., M.N. Futter, B.J. Cosby, P. Rosén and J. Fölster, 2015. Simple Models to Estimate Historical and Recent Changes of Total Organic Carbon Concentrations in Lakes. Environmental Science & Technology, 49: 386–394.

Van Dam, B., Helmig, D., Burkhart, J. F., Obrist, D., and Oltmans, S. J.: Springtime boundary layer O3 and GEM depletion at Toolik Lake, Alaska, J. Geophys. Res.-Atmos., 118, 3382–3391, https://doi.org/10.1002/jgrd.50213, 2013.

van der Velden S, Evans MS, Dempson JB, Muir DCG, Power M. Comparative analysis of total mercury concentrations in anadromous and non-anadromous Arctic charr (Salvelinus alpinus) from eastern Canada. Science of the Total Environment 2013; 447: 438-449.

van der Velden S, Reist JD, Babaluk JA, Power M. Biological and life-history factors affecting total mercury concentrations in Arctic charr from Heintzelman Lake, Ellesmere Island, Nunavut. Science of the Total Environment 2012; 433: 309-317.

van der Velden, S., Dempson, J. B. & Power, M. Comparing mercury concentrations across a thirty year time span in anadromous and non-anadromous Arctic charr from Labrador, Canada. Sci. Total Environ. 509-510, 165-174, (2015).

van der Velden, S., Dempson, J.B., Evans, M.S., Muir, D.C.G. & Power, M. 2013: Basal mercury concentrations and biomagnification rates in freshwater and marine food webs: Effects on Arctic charr (Salvelinus alpinus) from eastern Canada. Science of Total Environment 444: 531-542.

Veijalainen, N., J. Korhonen, B. Vehviläinen and H. Koivusalo, 2012. Modelling and statistical analysis of catchment water balance and discharge in Finland in 1951–2099 using transient climate scenarios. Journal of Water and Climate Change, 3(1): 55–78.

Veraverbeke, S., Rogers, B. M., Goulden, M. L., Jandt, R. R., Miller, C. E., Wiggins, E. B., & Randerson, J. T. (2017). Lightning as a major driver of recent large fire years in North American boreal forests. Nature Climate Change, 7(7), 529–534. https://doi.org/10.1038/nclimate3329

Verta, M., S. Salo, M. Korhonen, P. Porvari, A. Paloheimo and J. Munthe, 2010. Climate induced thermocline change has an effect on the methyl mercury cycle in small boreal lakes. Science of the Total Environment, 408: 3639–3647.

Vihma T. Effects of Arctic sea ice decline on weather and climate: a review. Surveys in Geophysics. 2014 Sep 1; 35(5):1175-214.

Vincent WF, MacIntyr S, Spigel RH, Laurion I. The physical limnology of high-latitude lakes. Polar Lakes and Rivers: Limnology of Arctic and Antarctic Aquatic Ecosystems, 2009.

Vonk, J.E., S.E. Tank, P.J. Mann, R.G.M. Spencer, C.C. Treat, R.G. Striegl, B.W. Abbott and K.P. Wickland, 2015. Biodegradability of dissolved organic carbon in permafrost soils and aquatic systems: a meta-analysis. Biogeosciences, 12 (23): 6915–6930.

Wang, F. et al. How closely do mercury trends in fish and other aquatic wildlife track those in the atmosphere? – Implications for evaluating the effectiveness of the Minamata Convention. Sci. Total Environ. 674, 58-70, (2019).

Wang, F., MacDonald, R. W., Armstrong, D. A., & Stern, G. A. (2012). Total and methylated mercury in the Beaufort sea: The role of local and recent organic remineralization. Environmental Science and Technology, 46(21), 11821–11828. https://doi.org/10.1021/es302882d

Wang, F.; Pućko, M.; Stern, G., Transport and transformation of contaminants in sea ice. In Sea Ice: Third Edition, 2016; pp 472-491

Wang, K., Munson, K. M., Beaupré-Laperrière, A., Mucci, A., Macdonald, R. W., & Wang, F. (2018). Subsurface seawater methylmercury maximum explains biotic mercury concentrations in the Canadian Arctic. Scientific Reports, 8(1), 14465. https://doi.org/10.1038/s41598-018-32760-0

Wang, X., et al. (2017). "Using Mercury Isotopes To Understand Mercury Accumulation in the Montane Forest Floor of the Eastern Tibetan Plateau." Environmental Science & Technology 51(2): 801-809.

Wassmann, P., Duarte, C. M., Agusti, S. & Sejr, M. K. Footprints of climate change in the Arctic marine ecosystem. Global Change Biol. 17, 1235-1249, (2011).

Watras, C.J., Back, R.C., Halvorsen, S., Hudson, R.J.M., Morrison, K.A. & Wente, S.P. 1998: Bioaccumulation of mercury in pelagic freshwater food webs. Science of Total Environment 219: 183-208.

Watras, C.J., N.S. Bloom, S.A. Claas, K.A. Morrison, C.C. Gilmour and S.R. Graig, 1995. Methylmercury production in the anoxic hypolimnion of a dimictic seepage lake. Water, Air, and Soil Pollution, 80: 735–45.

Wauthy, M., M. Rautio, K.S. Christoffersen, L. Forsström, I. Laurion, H. L. Mariash, S. Peura, W.F. Vincent, 2018. Increasing dominance of terrigenous organic matter in circumpolar freshwaters due to permafrost thaw. Limnology and Oceanography Letters, 3: 186–198.

Wein, R. W. (1976). Frequency and Characteristics of Arctic Tundra Fires. Arctic, 29(4), 213–222. http://www.jstor.org/stable/40508760

Williams, J. W., Jackson, S. T. & Kutzbacht, J. E. Projected distributions of novel and disappearing climates by 2100 AD. Proc. Natl. Acad. Sci. USA 104, 5738-5742, (2007).

Williamsson, C.E., Neale, P.J., Hylander, S., Rose, K.C., Figueroa, F.L., Robinson, S.A., Häder, D-P., Wängberg, S-Å. and Worrest, R.C. 2019. The interactive effects of stratospheric ozone depletion, UV radiation, and climate change on aquatic ecosystems. Photochemical & Photobiological Sciences 18: 717.

Wisz MS et al. 2015 Arctic warming will promote Atlantic-Pacific fish interchange. Nat. Clim. Change 5, 261–265. (doi:10.1038/nclimate2500)

Wojtun B, Samecka-Cymerman A, Kolon K, Kempers AJ, Skrzypek G. Metals in some dominant vascular plants, mosses, lichens, algae, and the biological soil crust in various types of terrestrial tundra, SW Spitsbergen, Norway. Polar Biol. 2013; 36: 1799-1809.

Woolford, D. G., Dean, C. B., Martell, D. L., Cao, J., & Wotton, B. M. (2014). Lightning-caused forest fire risk in Northwestern Ontario, Canada, is increasing and associated with anomalies in fire weather. Environmetrics, 25(6), 406–416. https://doi.org/10.1002/env.2278

Yang, Z.; Fang, W.; Lu, X.; Sheng, G. P.; Graham, D. E.; Liang, L.; Wullschleger, S. D.; Gu, B., Warming increases methylmercury production in an Arctic soil. Environmental Pollution 2016, 214, 504-509

Young, A. M., Higuera, P. E., Duffy, P. A., & Hu, F. S. (2017). Climatic thresholds shape northern high-latitude fire regimes and imply vulnerability to future climate change. Ecography, 40(5), 606–617. https://doi.org/10.1111/ecog.02205

Yu, B., Fu, X., Yin, R., Zhang, H., Wang, X., Lin, C. J., Wu, C., Zhang, Y., He, N., Fu, P., Wang, Z., Shang, L., Sommar, J., Sonke, J. E., Maurice, L., Guinot, B., and Feng, X.: Isotopic Composition of Atmospheric Mercury in China: New Evidence for Sources and Transformation Processes in Air and in Vegetation, Environ Sci Technol, 50, 9262-9269, 10.1021/acs.est.6b01782, 2016.

Yuan, W., Sommar, J., Lin, C.-J., Wang, X., Li, K., Liu, Y., Zhang, H., Lu, Z., Wu, C., and Feng, X.: Stable isotope evidence shows re-emission of elemental mercury vapor occurring after reductive loss from foliage, Environmental Science & Technology, 10.1021/acs.est.8b04865, 2018.

Yurkowski, D. et al. Contrasting temporal patterns of mercury, niche dynamics, and body fat indices of polar bears and ringed seals in a melting icescape. Environ. Sci. Technol., (2020).

Yurkowski, D.J., N.E. Hussey, A.T. Fisk, K.L. Imrie, R.F. Tallman and S.H. Ferguson. 2017. Temporal shifts of forage fish availability decrease intraguild predation pressure between beluga whales and Greenland halibut in a warming Arctic. Biology Letters 13: 20170433

Yurkowski, D.J., N.E. Hussey, S.H. Ferguson, and A.T. Fisk. 2018. A temporal shift in trophic diversity among a predator assemblage in a changing Arctic. Royal Society Open Science 5: 180259.

Zarnetske, P. L., Skelly, D. K. & Urban, M. C. Biotic multipliers of climate change. Science 336, 1516-1518, (2012).

Zdanowicz C, Karlsson P, Bekholmen I, Roach P, Poulain A, Yumvihoze E, et al. Snowmelt, glacial and atmospheric sources of mercury to a subarctic mountain lake catchment, Yukon, Canada. Geochimica et Cosmochimica Acta 2018; 238: 374-393.

Zdanowicz, C.; Kruemmel, E.; Lean, D.; Poulain, A.; Kinnard, C.; Yumvihoze, E.; Chen, J.; Hintelmann, H., Pre-industrial and recent (1970-2010) atmospheric deposition of sulfate and mercury in snow on southern Baffin Island, Arctic Canada. Science of the Total Environment 2015, 509-510, 104-114\

Zdanowicz, C.; Krümmel, E. M.; Lean, D.; Poulain, A. J.; Yumvihoze, E.; Chen, J.; Hintelmann, H., Accumulation, storage and release of atmospheric mercury in a glaciated Arctic catchment, Baffin Island, Canada. Geochimica et Cosmochimica Acta 2013, 107, 316-335

Zhang X, He J, Zhang J, Polyakov I, Gerdes R, Inoue J, Wu P. Enhanced poleward moisture transport and amplified northern high-latitude wetting trend. Nature Climate Change. 2013 Jan;3(1):47.

Zhang, Y.; Jacob, D. J.; Dutkiewicz, S.; Amos, H. M.; Long, M. S.; Sunderland, E. M., Biogeochemical drivers of the fate of riverine mercury discharged to the global and Arctic oceans. Global Biogeochemical Cycles 2015, 29, (6), 854-864

Zheng, J., Archives of total mercury reconstructed with ice and snow from Greenland and the Canadian High Arctic. Science of the Total Environment 2015, 509-510, 133-144

Zheng, W., Demers, J., Lu, X., Bergquist, B. A., Anbar, A. D., Blum, J. D., and Gu, B.: Mercury stable isotope fractionation 25 during abiotic dark oxidation in the presence of thiols and natural organic matter, Environmental Science Technology,10.1021/acs.est.8b05047, 2018.

Zheng, W., Obrist, D., Weis, D., and Bergquist, B. A.: Mercury isotope compositions across North American forests, Global Biogeochem. Cycles, 30, 1475-1492, 10.1002/2015gb005323, 2016.

Zolkos, S.; Krabbenhoft, D.; Suslova, A.; Tank, S.; McClelland, J.; Spencer, R. G. M.; Shiklomanov, A.; Zhulidov, A.; Gurtovaya, T.; Zimov, N.; Zimov, S.; Mutter, E.; Kutny, L/; Amos, E.; Holmes, R., Mercury Export from Arctic Great Rivers. (In review)

Zwart, J.A., S.D. Sebestyen, C.T. Solomon and S.E. Jones, 2017. The influence of hydrologic residence time on lake carbon cycling dynamics following extreme precipitation events. Ecosystems, 20: 1000–1014

Additional Notes

Section 2a

- *Changing timing of shoulder seasons; increases in rain and major precipitation events ().*
- *Notes: (from Kimmo)* elevation of greenhouse gases (CO2, CH4, H20…), change in cloudiness, change in UV intensity, change in large scale weather patterns (Arctic Oscillation, NAO)
- *(from Kyle)* increased wind and major storm events (to my mind, the largest change in Hudson Bay is that it has gone from being a dry, sunny, Arctic ocean to a wet, stormy, North Atlantic ocean).
- *(from Hans)* -(lack of) change in atmospheric loading of Hg
- *More……. Needs chem modeling results and temp results and ways to link increasing atmos temps with changing atmos chem processes?*

Section 2b

- *Notes:* (from Kimmo, edits by Kyle) increase of DOC in estuaries, methane release in coastal areas, decrease of sea ice extent, quality and thickness, major change in light conditions (under ice vs open water), elevated water temperatures, especially at the surface, including altered thermoclines, changes in sea currents, some parts decreased salinity due to ice melting, acidification of Arctic seas

Section 2c

- Notes: (from Kimmo) permafrost thaw, change in snow cover, change in precipitation (direction may vary among Arctic regions), increased air and soil temperature, change in run-off and erosion. Yes to all of this! Change in timing of spring runoff. Arctic coastal retreat as a particulate, POC, and perhaps Hg cycling game changer along coasts and estuaries.
- Weave in Schuster et al. (2018) Hg stocks in permafrost but identify that stocks and fate/transport/deposition are quite different animals. The same processes that lead to Hg storage can be undone with thaw. Is there any work linking Hg to C or pH or some other biogeochemical signature? Provide a schematic Figure or the one from Schuister with the different compartments and their Hg stocks. From there identify what is most vulnerable is this can be identified.
- What is new and novel from the 2012 assessment/paper?

Section 2d

- *Notes:* (from Kyra): (ice cover, changes to the hydrological cycle (inputs and fluxes), thermokarst pond development/drying, proglacial lake and river development)
  (from Kimmo): changes (above) in catchment properties such as permafrost thaw and increased run-off via higher precipitation will have significant effects on freshwater environments (rivers, lakes, ponds), changes in ice-type and snow cover, extended open water season, increased DOC from catchment: joint effects of browning and eutrophication,decreased light and UV in water column due to increased DOC, increased primary production of lakes have potential to increase anoxic conditions especially in ice-covered winter
- Lakes/ponds versus streams and rivers. Spring melt as a major event for fluxes of C and perhaps Hg?
- Results from the large rivers like the Yukon and Russian Rivers AND results from smaller watersheds. What is different or the same?
- What is new and novel from the 2012 assessment/paper?

Section 3a

- *Notes:* (from Kimmo, edits by Kyle) change in species distributions (Barents Sea for example), changes in realized niches, change from benthic towards pelagic species and energy flows, food web link and length alterations that likely vary among regions, sea acidification and response of

calciferous benthic fauna, drastic reduction of ice-dependent species (e.g. from ice-algae to polar cod/polar bear) (from Kyle) (might be worth adding 'bottom-up and top-down changes to food web structure, including trophic cascades' which is partly but not completely captured above), heat stress and changing fundamental niches, changes in gene diversity and gene function,

Section 3b

- *Notes:* (from Kimmo) change in species distributions, decrease of snow dependent species, increased primary producers extent (e.g. extending treelines), general greening, change in food web complexity and length (likely varies among regions), change in species migrations (caribou, birds), asynchrony of population cycling increases (lemmings, geometric moths)

Section 3c

- *Notes:* (from Kimmo) energy sources shift from benthic algae towards phytoplankton, longevity and size of animals decrease, change in species distribution: cold-water species decrease, cool and warm water species increase, Spring spawning species increase, food web complexity change, habitat availability change and pelagic species will increase, initially increasing number of species

Section 4c

- Eurasian, Yulkon and Mackenzie studies versus smaller rivers/catchments. What can this comparison tell us?

Section 5b

- *Notes:* (from Kimmo): increasing temperature effects in snow, soil, water, in lakes: complex interactions among increased temperature, browning, eutrophication and UV

Section 6b

- *Notes:* (from Kimmo) terrestrial: shifts from tundra to shrub, bush and trees; marine: increasingly pelagic phytoplankton driven food webs
- *Notes:* (from Kimmo):Terrestrial: diet shifts in opportunistic species crows, gulls, foxes

Section 6c

- *Notes:* (from Kimmo) lakes: important role of phytoplankton in initial uptake. Shift of primary consumers from lipid rich copepods to cladocerans (e.g. Daphnia), lakes: shift towards more pelagic phytoplankton driven food webs may elevate base level, complex patterns in biomagnification in lake food webs as elevated productivity also dilutes methylmercury to higher primary producer biomass and in edible species (larger blue-green algae),
- *Notes:* (from Kimmo): - lakes: generalist fish will shift towards zooplankton diet and diet diversity will decrease; lakes: pelagic food web will be strengthened and littoral one is weakened. Pelagic energy start to drive benthic food webs too; lakes: resource polymorphism is frequent in Arctic (e.g. Arctic charr, whitefish, lake trout) as has influence to diet and habitat considerations as well as food webs; Lakes: habitat diversity of food webs will decrease due to browning and eutrophication: share of pelagic and profundal increase; Lakes: New zooplanktivorous species will increase pelagic prey for piscivores;
- *Notes:* (from Kimmo) growth dilution – starvation cycles, decreasing seasonal cycles due to shorter winter length, decreased longevity of species decrease top concentrations, different responses of spring and autumn spawning fish species, elevated excretion of mercury?

* This is Chapter 6 of the AMAP Mercury Assessment*

12000

12001 **6. What are the toxicological effects of mercury in Arctic biota?**

12002 **Leads:** Rune Dietz and Robert J. Letcher

12003 **Co-authors:** Josh Ackermann, Benjamin Barst, Niladri Basu, Olivier Chastel, John Chetelát, Sam
12004 Dastnau, Jean-Pierre Desforges, Collin A. Eagles-Smith, Igor Eulaers, Jérôme Fort, C. Alex Hartman,
12005 Christian Sonne and Simon Wilson

12006 **Data and sample contributors:** Birgitta Andreassen, Aqqalu R. Asvid, Claus Bech, Pierre Blevin,
12007 David Boertmann, Jan Ove Bustnes, Tomasz M. Ciesielski, Sarah Dxxx, Maria Dam, Krishna Das Mark
12008 Evans, Anita Evenset, Geir Wing Gabrielsen, Mary Gamberg, Paul F. Hoekstra, Mary Gamberg, Xx
12009 Gartner et al, Ingeborg G. Hallanger, Mads P. Heide-Jørgensen, Lisa B. Helgason, Mark P. Herzog,
12010 Michael Houde, Kathrin Hoydal, Karista? Hudelson, Bjørn M. Jenssen, Audrey Jæger, Sarah Leclaire,
12011 Ulf Lindstrøm, Lisa Loseto, Cecilie Miljeteig, Børge Moe, Anders Mosbech, Derek C.G. Muir, Anders
12012 Mosbech, Nynne H. Nielsen, Sanna T. Nielsen, Sara H. Peterson, Marianna Pinzone, Poste, Frank F.
12013 Rigét, Anna Roos, Heli Routti, Halvor Saunes, Ursula Siebert, Gary Stenson, Gary Stern, Jakob Strand,
12014 Jens Søndergaard, Swanson and Kidd (2010), Phil Thomas, Gabriel Treu, Cortney Watt, Gisli
12015 Vikingson, van der Velden et al., Scott Hatch, Jóhannis Danielsen, Sébastien Descamps, Kyle Elliott,
12016 Kjell Einar Erikstad, Alexey Ezhov, Maria Gavrilo, Grant Gilchrist, Olivier Gilg, David Grémillet,
12017 Elena Golubova, Erpur Hansen, Nicholas Per Huffeldt, Jon Einar Jónsson, Alexander Kitaysky, Yuri
12018 Krasnov, Erlend Lorentzen, Mark Mallory, Flemming Merkel, Willam A. Montevecchi, Anders
12019 Mosbech, Bergur Olsen, Rachael Orben, Jennifer Provencher, Gregory J. Robertson, Kjetil Sagerup,
12020 Hallvard Strøm,Tone Kristin Reiertsen, Torkel Lindberg Tórarinsson, Grigori Tertitski, Katarzyna
12021 Wojczulanis-Jakubas, Dariusz Jakubas, Elena Tolmacheva, Sindri Gíslason, Heather Renner, Marc
12022 Romano, Nora Rojek, Glenn Yannic

12023
12024
12025
12026
12027
12028
12029
12030
12031
12032

12033 **Table of Contents**

12034

12054

12055

12056 **6.1. Introduction**

12057 The circumpolar Arctic has been subject to minimal direct production, use and emission of industrial
12058 contaminants such mercury (Hg). However, methylmercury (MeHg) biomagnifies in Arctic organisms
12059 due to long, lipid-rich Arctic marine food webs, which are based on atmospheric and sea-current, long-
12060 range transport of Hg. Thus,there is concern for the health of exposed wildlife and for indigenous human
12061 populations that largely depend on marine wildlife as part of their traditional diet. In 2017, an
12062 international treaty for the regulation of Hg (UNEP's Minamata Convention on Mercury) entered into
12063 force world-wide (Evers et al., 2016). Among the eight Arctic countries (Canada,
12064 Denmark/Greenland/Faroes Islands, Finland, Iceland, Norway, Russia, Sweden and the USA),
12065 collaborating on pollution issues within the Arctic Monitoring and Assessment Programme (AMAP,
12066 Arctic Council), most effect studies on wildlife and fish have been historically available from the North
12067 Atlantic between Greenland and Svalbard (Norway). In these regions, tissue concentrations of
12068 organohalogen contaminants (OHCs) and other persistent organic pollutants (POPs) are found to be the
12069 highest in wildlife and fish as was evidenced in the previous three AMAP reports on POPs and metals
12070 (AMAP, 1998, 2004, 2016; Letcher et al., 2010; Dietz et al., 2013a).
12071
12072 The latest Hg assessments for the Arctic have provided specific insights into the transport, geographical
12073 trends, links to climate change, and human health for Hg (Dietz et al., 2013a; Outridge et al., 2011a,
12074 2011b). The last combined POP and Hg effect assessment was a detailed review on risks using five
12075 exposure risk categories for marine and terrestrial mammals as well as for marine and freshwater-
12076 feeding birds and birds of prey. Although fish were included in the 2011 AMAP Hg assessment, risk
12077 categories used in the present assessment are for the first time included in an AMAP assessment, which
12078 is true for invertebrates as well. Concurrent with the present study, a comparative assessment is being
12079 conducted for the Baltic region with inclusion of Hg results from subsamples of Arctic fish and bivalve
12080 species, which also range into the Arctic (Dietz et al., submitted). This comparative assessment also
12081 includes marine mammals, seabirds and birds of prey in the Baltic and adjacent waters as well as for
12082 the Arctic region.
12083
12084 Many of the recent Hg effect studies reported for fish and other Arctic wildlife, including the
12085 measurement of strategic biomarker endpoints, *in vitro* experiments for top predator species, and
12086 pathological studies on fish around Arctic mining sites, have been reported previously in detail by
12087 AMAP (2018) and Dietz et al. (2019). Hence, a summary of these results are not repeated in the present
12088 Hg effects chapter. Also not dealt with in the present chapter are the numerous natural (ecological and
12089 physiological) and anthropogenic factors, including climate change, invasive species and pathogens,
12090 changes in food web dynamics and predator-prey interactions that influence and confound the exposure
12091 to and effects of contaminants. This information is detailed in Chapter 4 on climate change effects
12092 (Macdonald et al., 2003, 2005; UNEP/AMAP, 2011; Jenssen et al., 2015; McKinney et al., 2015).

The present Hg effects assessment also does not address temporal trends of Hg in Arctic biota since is reported elsewhere in Rigét et al. (2011) as well as recently in Chapter 2, which provides almost an additional 10 years of data compared to the last Hg assessments (Outridge et al. 2011/AMAP 2011). With respect to effects studies, the last comprehensive AMAP reports provide detailed reviews on Hg health effect studies up to 2010 time frame (Dietz et al., 2013a; Outridge et al., 2011a, 2011b). Here we review the literature on the biological effects of Hg from 2010 and up to 2019, providing the most up to date risk assessment for Hg and for more species than in the last effect assessments (AMAP 2018; Dietz et al. 2019). We explicitly address important knowledge gaps identified in previous AMAP reports regarding regions with a lack of data like the Russian Arctic (at least for seabirds). Contaminant levels are used for Arctic species in a circumpolar risk analysis, as was first carried out by Ackerman et al. (2016) for North American birds.

To our knowledge, there has been little effort to quantify population level effects of Hg exposure despite multiple health effects that have been reported in field studies of Arctic species (Dietz et al., 2019; Routti et al., 2019). Establishing links between contaminant exposure and health outcomes is a difficult task (Rodriguez-Estival and Mateo, 2019). Such information is however extremely important to determine in order to manage and conserve wildlife populations. It is critical to measure individual impacts and for use to estimate population-level effects using various modeling approaches, which take into account effects on reproduction, immune and endocrine functioning as well as energy demands (Svensson et al., 2011). This also requires a combination of *in vitro* dose-response studies and when possible *in vivo* studies on key species as has been reported in the Baltic as reference populations from other areas including pristine areas such as the Arctic (Desforges et al., 2016, 2017, 2018a, 2018b, 2018c).

The 2018 AMAP assessment of biological effects of POPs and Hg reported on results from recent wildlife studies including Hg measurements in different tissues and organs in order to assess related health effects. The present Hg assessment will refer to that work, but with minimal repetition of the content in the 2018 AMAP report, and instead focuses on additional effects information including Hg in additional body compartment types e.g. hair and feathers. A total of 20 newly published journal papers were found in the literature since 2018. There is also a substantial amount of new seabird Hg data from the ArcTox project (https://arctox.univ-lr.fr/) and included in the present assessment.

The earlier 2011 AMAP Hg assessment called for work to explore the effects of multiple stressors including chemical, environmental and nutritional factors on the toxicity of Hg in Arctic biota. Subsequently, the more recent 2018 AMAP POPs and Hg assessment identified methods that could be extended in their application to provide additional information on Hg toxicity in the anticipated 2021 AAR4 Hg assessment.

6.2 Combined effects of chemical stressors

6.2.1. What is known about the combined effects of mercury and other contaminants, and additional types of environmental stressors?

Arctic animals possess physiological mechanisms and processes that impart varying degrees of tolerance (robustness) to environmental stressors and while maintaining normal health. Environmental stress can be in the form of depleted or changing food resources as a consequence of habitat perturbation or loss and in relation to global warming. Combined with exposure to OHC and Hg chemical stressors, documented physiological perturbations include the alteration of homeostasic circulating levels of thyroid hormone, corticosterone and vitamin A, and neurotransmitter function (Dietz et al., 2019; Letcher et al., 2010; Sonne, 2010). These homeostatic perturbation can in turn can influence important fitness/health parameters as have been documented for polar bears through modulations of immune functioning, reproductive success, neuro-endocrine related behavior and bone/calcium homeostasis. Expanding further to the population level, for the various polar bear (*Ursus maritimus*) subpopulations this may result in a reduction of bear numbers, changes in their circumpolar distribution pattern, and possibly subpopulation extirpation (Sonne et al., 2015). Likewise, energetic stress (food depletion) and poorer body condition are known to reduce normal functioning of immune and reproductive systems. The use of peripheral adipose tissue to compensate for the lower energy intake will release bioavailable contaminants including Hg into the blood stream increasing the risk of neuro-endocrine disruption, which together with a poorer body condition can decrease reproductive rates and increase mortality.

Studies have suggested that global warming will induce a shift in the micro-pathogen composition towards higher virulence (Price et al., 2019) and the combination of this and an impaired immune and reproductive system will add further stress to Arctic top predators (Desforges et al., 2016, 2017, 2018a, 2018b). Climate change leading to increasing temperature and humidity could result in unforeseen changes in the distribution of pathogens, where for example ticks are a vector for their expansion northward (Sonenshine and Mather, 1994; Kutz, 2009; Lindgren and Gustafson, 2001). In addition, it is clear that zoonosis (diseases transmitted between humans and animals) are a threat to Arctic animals and human populations, and especially because environmental contaminants such as PCBs and Hg are immune-suppressive (Desforges et al., 2016).

Global warming is also changing the food web dynamics and exposure pathways, and leading for example to high Hg and PCB exposure in Arctic fish and polar bears (Desforges et al., 2018c; McKinney et al., 2013; Schartup et al., 2019). Depleted sea ice coverage and earlier dates of ice break-up have changed and/or reduced the quality of the habitat of Arctic animals such as polar bears, seals and toothed whales. Such ice changes are also having an impact on the metabolic and energetic profiles of these animals due to changes in home range and feeding opportunities (Pagano et al., 2018; Routti et al.,

2016; Tartu et al., 2017). In addition to this, decreased sea ice coverage scenarios means polar bears need to spend more time on land and thereby increasing the probability of human interactions (Atwood et al., 2016). Ultimately, these factors will likely increase bear mortalities, and the regional conditions will depend on the specific sea ice reductions. In addition, increased oil exploration, mining, and tourism activities in the Arctic will increase the polar bear-human interactions, which will increase the occurrence of self-defense kills, which will add further stress to the affected animals (Stirling and Ross, 2011). These polar bear-human interactions are all likely to increase as a result of sea-ice decreases.

From an ecotoxicological point of view, it is not environmentally relevant to evaluate OHC and Hg exposure separately as the real-world reality is that organisms are exposed to complex chemical mixtures of anthropogenic origin. In general, the adverse health effects of chemical mixtures exposure and the associated cumulative effects are poorly understood including in Arctic biota (AMAP, 2018). Further complexities to the understanding of chemical mixtures are the biochemical changes in exposed organisms as part of the toxicokinetic mechanisms and pathways and toxicodynamics. Alternately, this is not necessarily correct as the real-world situation is a complex mixture of chemicals and more or less unknown synergistic interactions of chemical groups and their multiple congeners. It is currently unknown how climate change and the combined effects from OHC and Hg exposure lead to e.g. oxidative stress and neuro-endocrine disruption effects in Arctic animals including polar bears (Dietz et al., 2013, 2019; Letcher et al., 2010; Sonne, 2010). One can only guess as to whether polar bears are adative and robust enough to sustain themselves, e.g. relying solely on terrestrial alternative food sources, which are lower in adipose tissue (than seals) and thereby energy (Pagano et al., 2018).

In the Arctic climate change hotspot of Hudson Bay, severe sea-ice reductions have been documented with effects on polar bear behaviour and survival (Castro de la Guardia et al., 2013; Durner et al., 2017; McCall et al., 2015). Yurkowski et al. (2020) very recently reported on the temporal patterns in Hg concentrations in western Hudson Bay polar bears (hair) and ringed seals (*Pusa hispida*) (muscle), niche dynamics, and body fat indices. They found a decline in THg concentrations in ringed seals suggesting a change in feeding habits and carbon source use over time, whereas no significant changes occurred in polar bears. Ringed seal body fat index was higher in years of earlier sea ice breakup with no change occurring in polar bears. They suggested that these species have different responses to annual and climate change related changes in sympagic-pelagic carbon source production. One may view the Hudson Bay polar bears as an early warning subpopulation for the consequences of depleted sea ice scenarios. In fact, it has been estimated that all Arctic summer sea-ice will be gone by year 2040 and that will affect polar bear survival and reproductive rates (Molnár et al., 2011; Stroeve and Notz et al., 2018). A complete population collapse and quite possibly species extinction from loss of sea-ice alone proposed 10 years ago (Amstrup et al., 2010). However, the fact that Hudson Bay polar bears live in relatively southern habitats makes it difficult to extrapolate to other polar bear subpopulations. For

example, North Greenland polar bears may be favoured by the Polar Basin ice conditions and ringed seal breeding habitats. A similar situation is possible for the four or five high-Arctic Canadian polar bear subpopulations. Therefore, the survival of the most southern polar bear subpopulations in general depends on the bears exhibiting the necessary adaptions including migrating north, or changes in feeding strategies that include a diet of terrestrial mammals (high terrestrial productivity) and/or access to marine mammals including carcasses.

6.2.2. What role does mercury speciation play in uptake and toxic effects?

The uptake of organic Hg passing the intestinal mucosa occurs in the range of 70-90 % or more, which is significantly higher compared to inorganic mercury of which 15-40 % is absorbed (Berlin, 1986). Most Hg in muscle is in the form of organic MeHg, while liver and kidney Hg is mostly in the form of an inorganic mercury-selenide complex (Dietz et al., 2013). Therefore, the mechanisms of MeHg and HgSe uptake differ and so does the amount of Hg absorbed. In addition, the toxicity of organic and inorganic Hg speciation differs as organic Hg entering the circulatory system reaches and passes the blood-brain-barrier (BBB) thereby resulting in high toxicity (Aschner and Aschner, 1990). The target tissues upregulate subcellular synthesis of methallothionein and selenide complex binding thereby detoxifying Hg as it becomes inert (Dietz et al., 2013, 2019; Raymond and Ralston, 2004). Therefore, looking at the molar ratio of Hg:Se is important as it gives the information if Se is in surplus and thereby capable of detoxifying Hg by forming tiemanite complexes (Dietz et al., 2013, 2019). In the marine ecosystem, Se is in surplus while it is not always the case in freshwater systems. Therefore, Hg exposure will pose a greater threat to terrestrial species with risk through oxidative stress and neuro-endocrine disruption. Toothed whales in comparison to polar bears have a reduced ability to demethylate MeHg and with excretion through hair, which results in higher body burdens as well as increasing risk of toxic Hg exposure (Sonne et al., 2018). This is exemplified by a recent study of pilot whales where Hg scavenged Se leading to the risk of deficiencies in the bioavailable Se pool, and thereby increasing the risk of toxic effects due to reduced Se-bound proteins and oxidative stress (Gajdosechova et al., 2016a, 2016b, 2018; Tinggi, 2003). Likewise, birds excrete Hg through feathers, which also helps to reduce the risk of MeHg effects on the central nervous system (Basu et al.. 2009). Selenium containing enzymes also include deiodinase, which is important in the activation of the thyroid hormone and thereby potentially linked to endocrine disruption from Hg exposure (Hawkes and Keim, 2003). A recent study by Albert et al. (2019) provided a detailed overview of Hg contamination in the feathers and blood of Arctic seabirds and concluded that important interspecific variations in Hg blood concentrations according to seabird trophic status, but all the reported Hg concentrations are below the admitted toxicity thresholds. Hg concentrations in feathers follow similar trends.

6.3. Does evidence exist for mercury concentrations in tissues that are harmful to Arctic biota (exposure in relation to effect thresholds)?

12241 **6.3.1 Methodology**

12242 ***6.3.1.1. Study design***

12243 The present assessment study design is based on a review of the existing literaturefor post-2000 reports
12244 of Hg exposure in marine mammals, seabirds, birds of prey, fish and bivalves from the Baltic Sea, North
12245 Sea and North Atlantic, and, where possible, the raw data was extracted. In addition, Hg analyses were
12246 conducted within the projects BONUS BALTHEALTH and ARCTOX. Data was also obtained from
12247 the ICES (Extract conducted by Hans Mose Jensen, ICES) and Swedish EPA databases
12248 (https://dvsb.ivl.se/MetaInfo) for the following ICES ecoregions: Greenland Sea, Norwegian Sea,
12249 Barents Sea, Icelandic Waters, Faroese Waters, Greater North Sea and the Baltic Sea.
12250

12251 ***6.3.1.2. Mercury data and analysis***

12252 Reference is made to peer-reviewed articles (SI Tables 1-4) for the respective analytical methods used
12253 to generate published Hg data that contributed to the current assessment. New and unpublished Hg data
12254 included in the present report was generated at the accredited Trace Element Lab of the Aarhus
12255 University as well as at the University of la Rochelle. Briefly, both labs used a Milestone DMA-80
12256 Direct Mercury Analyzer (Sorisole, Italy) for the analysis of dried tissue samples for total Hg (referred
12257 to as Hg throughout this article) (Sorisole, Italy) following the U.S. EPA Method 7473 (EPA 1998).
12258 Details on the analytical procedure and quality assurance for the analyses at Aarhus University are
12259 provided in Sonne et al. (2020/this issue) and Dietz et al. (2019). Details of unpublished results from
12260 ArcTox, University of la Rochelle have previously been described by Fort et al. (2016).
12261

12262 ***6.3.1.3. Risk analysis***

12263 The risk analysis in the present assessment for potential Hg-associated health effects was based on five
12264 risk level categories: no risk, low risk, moderate risk, high risk and severe risk (Table 1). These risk
12265 thresholds reflect effects on reproduction and adverse effects on condition, behaviour and productivity.
12266 For marine mammals, the hepatic Hg threshold values were used according to Ronald et al. (1977) and
12267 Dietz et al. (2019). For terrestrial mammals, hepatic Hg threshold values were used as determined for
12268 mink (*Mustela vison*) (Wobeser et al., 1976; Wren et al., 1987). For birds, the assessment methodology
12269 presented earlier by Ackerman et al. (2016) was adapted for liver, blood, egg and body feather
12270 concentrations.
12271

12272 Similar risk categories were established for fish based on two key papers by Dillon et al. (2010) and
12273 Peterson et al. (2004). Using the latter study, whole-body Hg burdens were converted to equivalent
12274 muscle Hg concentrations.
12275

12276 **Table 1.** Estimated risk to total mercury (Hg) exposure on the health effects in wildlife and fish and
12277 risk categories for the human consumption of bivalves (as no risk data for bivalve exposure exists.

		No risk	Low risk	Moderate risk	High risk	Severe risk	Reference
Marine mamm	Liver (µg/g)	<16.00	16.0–64.0	64.0–83.0	83.0–123.0	≥123.0	Ronald et al. 1977
Marine bird	Egg (µg/g)	<0.11	0.11–0.47	0.47–1.30	1.30–1.70	≥1.70	Ackermann et al. 2016
	Liver (µg/g)	<1.40	1.40–7.30	7.30–22.70	22.70–30.50	≥30.50	Ackermann et al. 2016
	Blood equivale	<0.20	0.20–1.00	1.00–3.00	3.00–4.00	≥4.00	Ackermann et al. 2016
	Body feather (	<1.58	0.58-7.92	7.92-23.8	23.8-31.7	≥31.7	Ackermann et al. 2016
Bird of prey	Body feather (	<1.58	0.58-7.92	7.92-23.8	23.8-31.7	≥31.7	Ackermann et al. 2016
Fish	Muscle (µg/g)	<0.10	0.10-0.30	0.30-0.50	0.50-2.00	≥2.00	Dillon et al. 2010

12278
12279 **6.3.2. Marine mammals**
12280 ***6.3.2.1 Liver related effects of mercury on Arctic marine mammals***
12281 The Hg risk evaluation for marine mammals is an update of a similar exercise conducted for the previous
12282 assessments (AMAP, 2018; Dietz et al., 2019). In the 2018, we reported on 70 species, regions and age
12283 groups with an overall number of 2371 individuals. The present assessment is based on an increase to
12284 111 species, regions and age groups (59 % increase) with a total number of 3572 individuals (51 %
12285 increase). However, 15 of the species, regions and age groups in the present assessment were from
12286 regions outside the Arctic with 127 individuals of ringed seals and harbour porpoises. Overall 29
12287 species, regions and age groups (30.2 %) were within the two highest risk categories, of which 18 groups
12288 (18.8 %) had individuals in the Severe risk category (> 126 µg/g ww) and an additional 11 groups (11.5
12289 %) had individuals in the High risk category (83-126 µg/g ww). The 29 species, regions and age groups
12290 from the two highest risk categories accounted for only 200 individuals (5.8 %) out of a total of 3445
12291 individuals analysed for their Hg loads. As for the Severe risk category, this accounted for
12292 approximately 102 individuals (3.0 %) and the High risk category accounted for the remaining 98
12293 individuals (2.8 %) (Fig. 6.3.2.1; Annex Table 6.1). The ten highest exposed animal groups (evaluated
12294 by percentage in the Severe risk category (SRC)) are in the following decreasing order: 1) adult hooded
12295 seals from the Denmark Strait (SRC: 57.0 %; 154.8 µg/g (61.49–358.2 µg/g)), 2) adult male hooded
12296 seals from Greenland Sea/Denmark Strait (SRC: 45.0 %; 120.8 µg/g (13.2-320.6 µg/g)), 3) adult polar
12297 bears from the Northern Beaufort Sea (SRC: 41.0 %; 122.1 µg/g (35.0–414.3 µg/g)), 4) juvenile polar
12298 bears from Qaanaaq NW Greenland (SRC: 33.3 %; 45.3 µg/g (21.3–351.2)µg/g)), 5) adult killer whales
12299 from E. Greenland, Iceland and Faroe Islands (SRC: 33.4 %; 112.1 µg/g (26.7–199.8 µg/g)), 6) adult
12300 long-finned pilot whales from the Faroe Islands (SRC: 27.4 %; 76.7 µg/g (3.52-574 µg/g)), 7) juvenile
12301 polar bears from Lancaster/Jones Sound (SRC: 20.0 %; 67.9 µg/g (39.1–149.8 µg/g)), 8) subadult long-
12302 finned pilot whale from the Faroe Islands (SRC: 20.0 %; 34.8 µg/g (24.4-153 µg/g)), 9) adult female
12303 ringed seals from Sachs Harbor (SRC: 11.5 %; 35.6 µg/g (0.62-320.3 µg/g)) and 10) adult male ringed
12304 seals from Sachs Harbor (SRC: 7.8 %; 36.0 µg/g (0.45-145.9 µg/g)) (Fig. 6.3.2.1; Annex Table 6.1).
12305
12306 The ten least exposed animal groups (Arctic regions with all 100 % in the No risk category) are in the
12307 following increasing order: 1) yearling harp seals from the Greenland Sea (Median: 0.17 µg/g; 0.05-0.7

µg/g), 2) foetus killer whales from E. Greenland, Iceland and Faroe Islands (Median: 0.18 µg/g; 0.11–0.47 µg/g), 3) subadult harbour porpoises from the Barents Sea (Median: 0.49 µg/g; 0.13-2.27 µg/g), 4) adult male harbour porpoises from the Barents Sea (Median: 0.58 µg/g; 0.18-10.2 µg/g), 5) subadult harbour porpoises from the Norwegian Coast (Median: 0.69 µg/g; 0.17-3.42 µg/g), 6) subadult harp seals from the Greenland Sea/Denmark Strait (Median: 0.69 µg/g; 0.23-2.74 µg/g), 7) adult female harp seals from the Greenland Sea/Denmark Strait (Median: 0.76 µg/g; 0.19-7.98 µg/g), 8) adult harp seals from Ittoqqortoormiit (Median: 0.78 µg/g; 0.14–8.9 µg/g), 9) juvenile ringed seals from Qeqertarssuaq (Median: 0.92 µg/g; 0.18-8.19 µg/g); 10) juvenile ringed seals from Kangiqsujuaq (Median: 0.92 µg/g; 0.367-2.0 µg/g) (Fig. 6.3.2.1a, b; Annex Table 6.1).

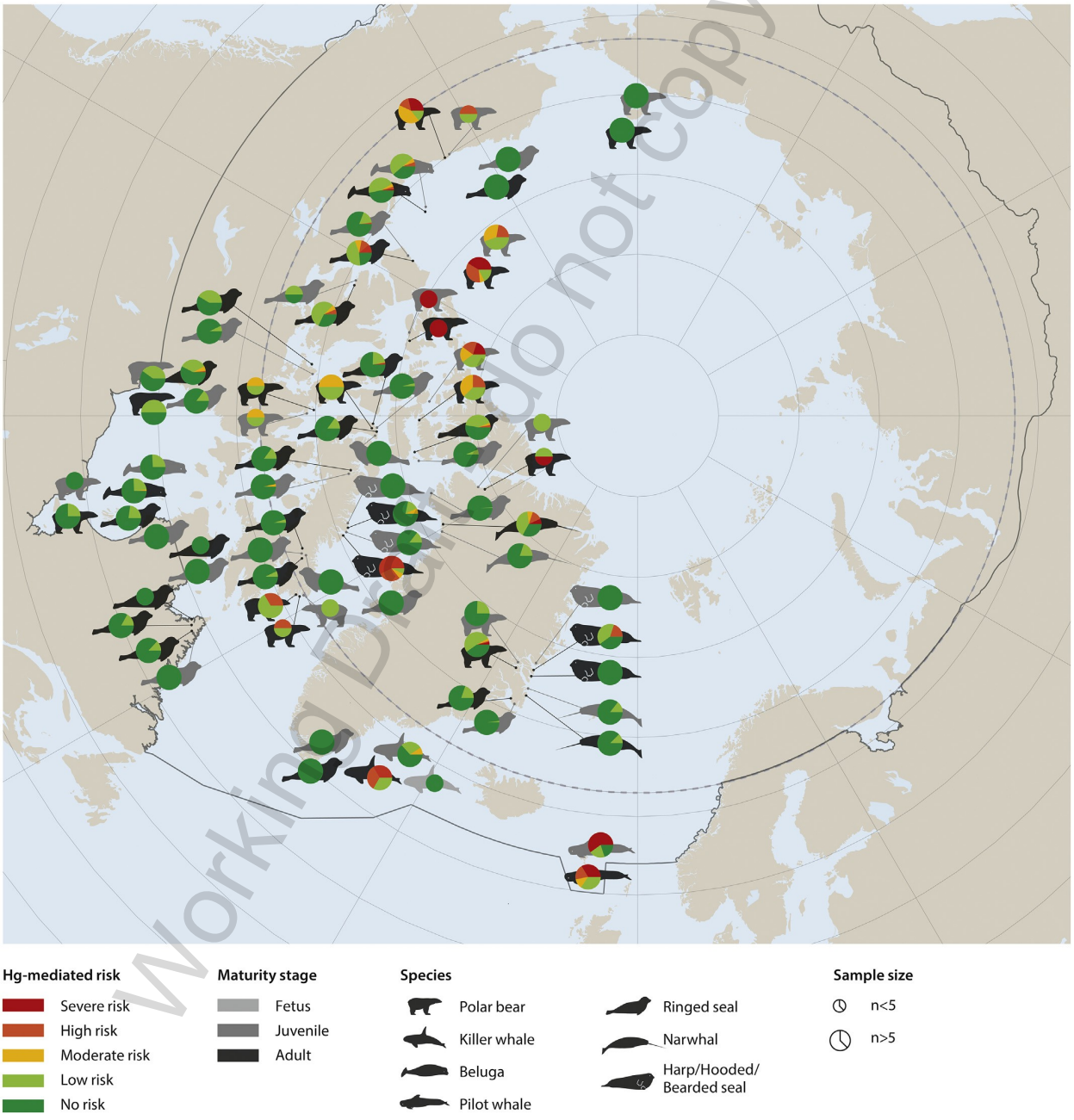

12320 **Figure 6.3.2.1.** Geographical overview of the proportion of individuals of specific Arctic marine
12321 mammal populations that are at risk of Hg-mediated health effects; based on post-2000 monitoring data
12322 grouped according to maturity where possible. The five risk categories are defined using effect threshold
12323 categories observed for harp seals (Ronald et al., 1977). See SI Table 2 for the detailed information
12324 upon which this summary graphic is based. To be updated and similar map figures produced for other
12325 species groups
12326

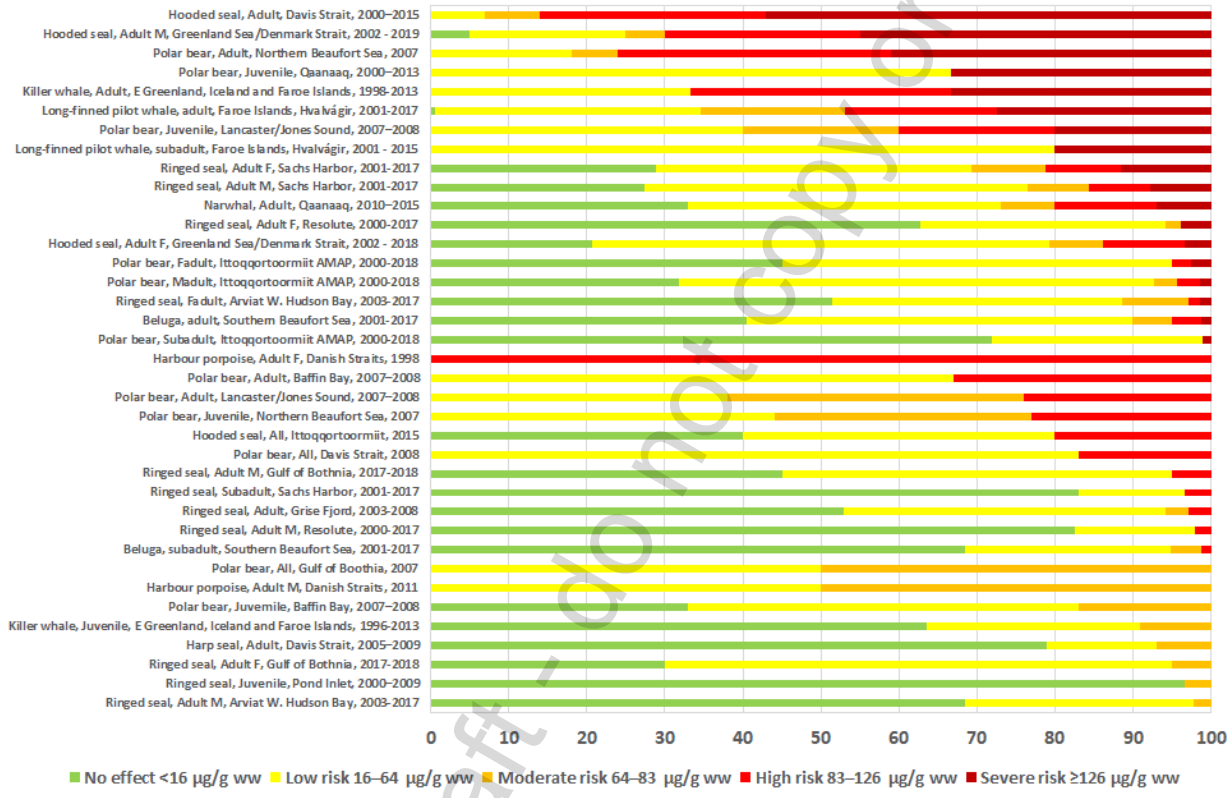

12327

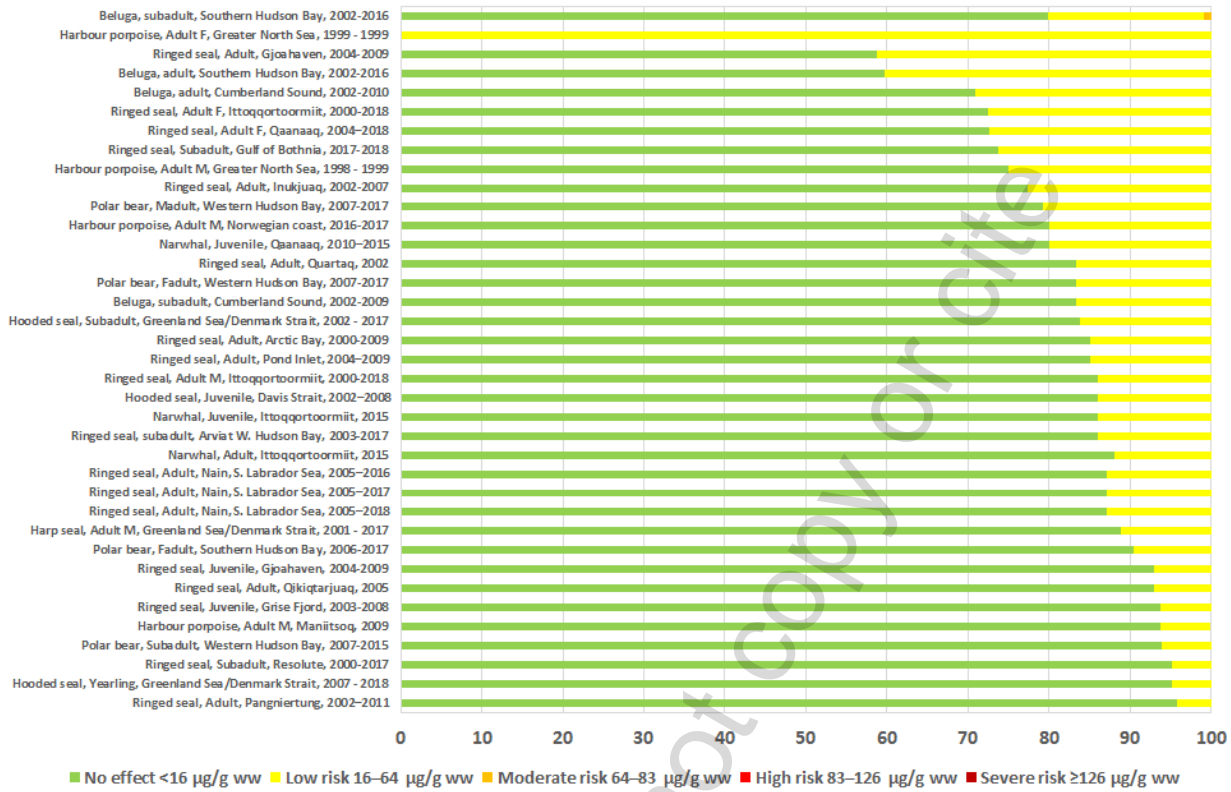

12328

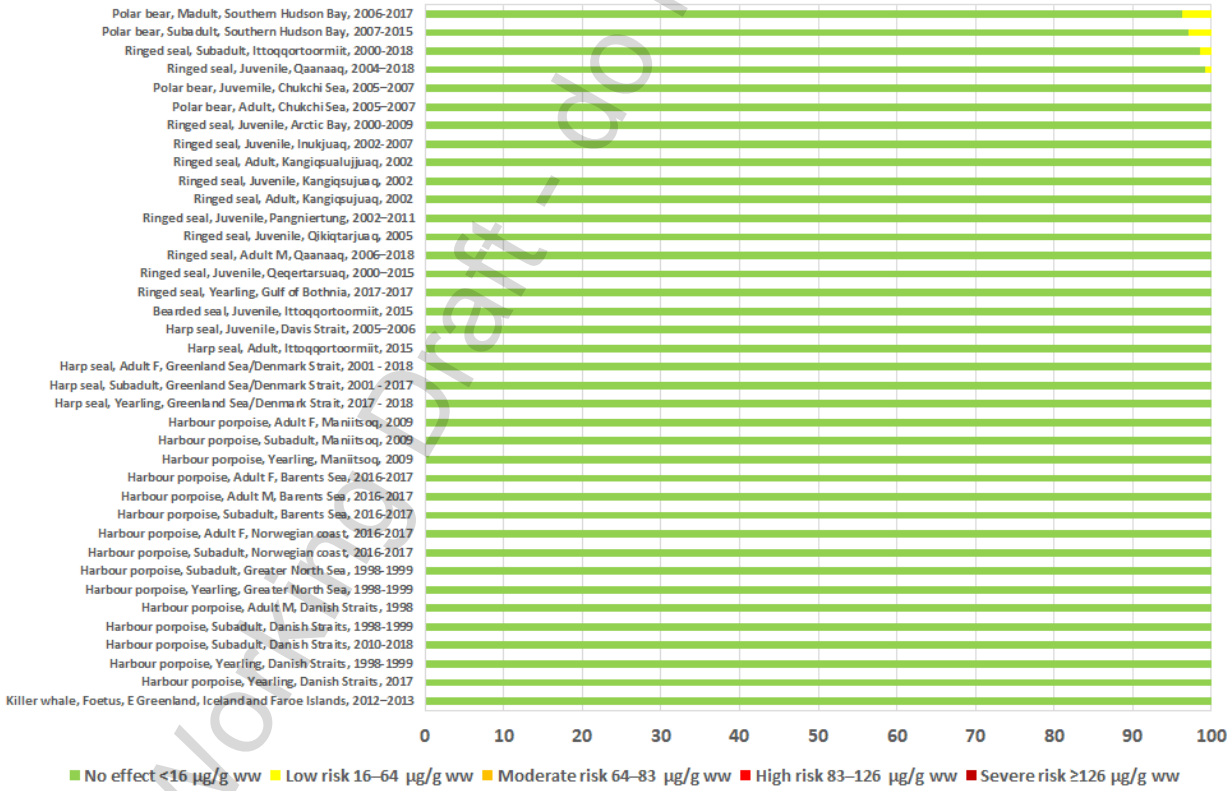

12329

12330 **Figure 6.3.2.2.** Ranked overview (from highest to lowest risk) of the proportion of marine mammal
12331 livers, per region from the Arctic, that are at risk for Hg-mediated health effects (categorised in five risk
12332 categories based upon liver Hg effect thresholds).

12333

12334 ***6.3.2.3 Comparison of marine mammal hair concentrations with effect guidelines***

12335 In the AMAP (2018) and Dietz et al. (2019) effect assessments, only liver samples were used. However,
12336 as hair samples are often used to evaluate human risk and exposure to Hg, we conducted an assessment
12337 of the regional risk of polar bears based on polar bear hair samples collected from the hunt as well as
12338 from the extensive satellite tagging activities conducted across the Arctic. Some hair samples were also
12339 available from seals, but as the liver to hair conversion was considered to rather inaccurate, the seal
12340 samples and data were not included in this exercise. Most hair samples are hence available from polar
12341 bears that were routinely collected during tagging studies. However, hair samples collected before 2000
12342 were included in this effect exercise in order to obtain a better spatial coverage. The hair samples
12343 revealed that bears from three populations in the northeastern Canadian Arctic had concentrations in
12344 the Severe risk category (> 48.1 µg/g dw), namely Viscount Melville Sound (30.0 %; median
12345 concentrations of 22.1 µg/g (16.7-85.2 µg/g)), Norwegian Bay (8.0 %; median concentrations of 25.2
12346 µg/g (13.8-90.0 µg/g)), and Lancaster Sound (3.6 %; median concentrations of 16.0 µg/g (3.1-72.7
12347 µg/g)). The corresponding percentages of bears from these three populations in the High risk category
12348 (31.7-48.1 µg/g) were 0.0, 20.0 and 7.4 %, respectively. As all the populations were samples before
12349 year 2000, it is uncertain what the present risk patterns are. It is however, important to conclude that
12350 concern for the Hg exposure of the polar bears has been expressed based on liver concentrations from
12351 the same regions (AMAP 2018; Dietz et al. 2013, 2019).
12352
12353 This Figure will be made in collaboration with Simon Wilson after the National Assessment
12354
12355 **Figure 6.3.2.3.** Geographical overview of the proportion of polar bear sub population groups that are
12356 at risk of Hg-mediated health effects; based on pre- and post-2000 monitoring data grouped according
12357 to maturity where possible. The five risk categories are defined using effect threshold categories
12358 observed for harp seals (Ronald et al., 1977) converted into hair concentrations by the East Greenland
12359 correlation between these two matrices. See SI Table 2 for the detailed information upon which this
12360 summary graphic is based.
12361

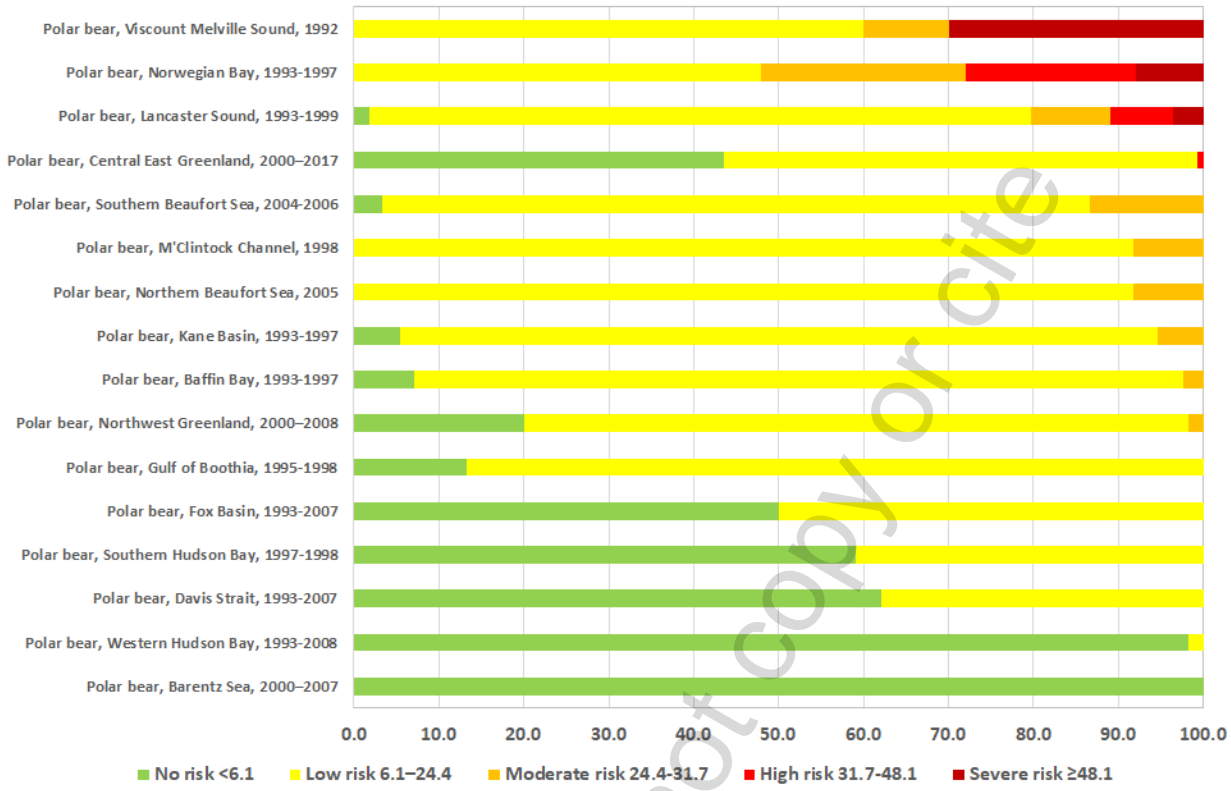

Figure 6.3.2.4. Ranked overview (from highest to lowest risk) of the proportion of polar bears, per region from the Arctic, that are at risk for Hg-mediated health effects (categorised in five risk categories based upon tissue-specific Hg effect thresholds).

6.3.3. Terrestrial mammals

The majority of Hg concentrations in terrestrial mammals fell within the two lowest risk categories for Hg-mediated health effects (No risk and Low risk, see Fig. 6.3.3.1). Icelandic Arctic fox (*Vulpes lagopus*) however, had 9 % of the adult population being at Severe risk, 35 % in the Moderate risk, 22 % in the Low risk and 35 % in the No risk category. The juvenile Arctic foxes were somehow lower exposed as the majority of the foxes (67 %) in this age group fell in the No risk category and 8 and 25 % fell in the Low risk and Moderate risk categories, respectively. Juvenile Arctic foxes from Arviat and Svalbard had 98 % and 100 % in the No risk category respectively, which does not raise any concern (Figure 6.3.3.1 and Annex Table 6.3). For sheep (*Ovis aries*) on the Faroe Islands, as much as 15 % were found in the Moderate risk category, which is higher than expected and could be attributed to agricultural fertilization by fish remains or eutrophication by bird droppings (from the extensive seabird colonies on the islands) as suggested by AMAP (2018) and Dietz et al. (2019). The remaining 85 % of the sheep fell in the No risk category. All (100 %) seven Caribou/reindeer (*Rangifer tarandus*) populations and age groups were all in the No risk group with median Hg concentrations ranging from 0.12 to 1.24 µg/g ww (Figure 6.3.3.1 and Annex Table 6.3).

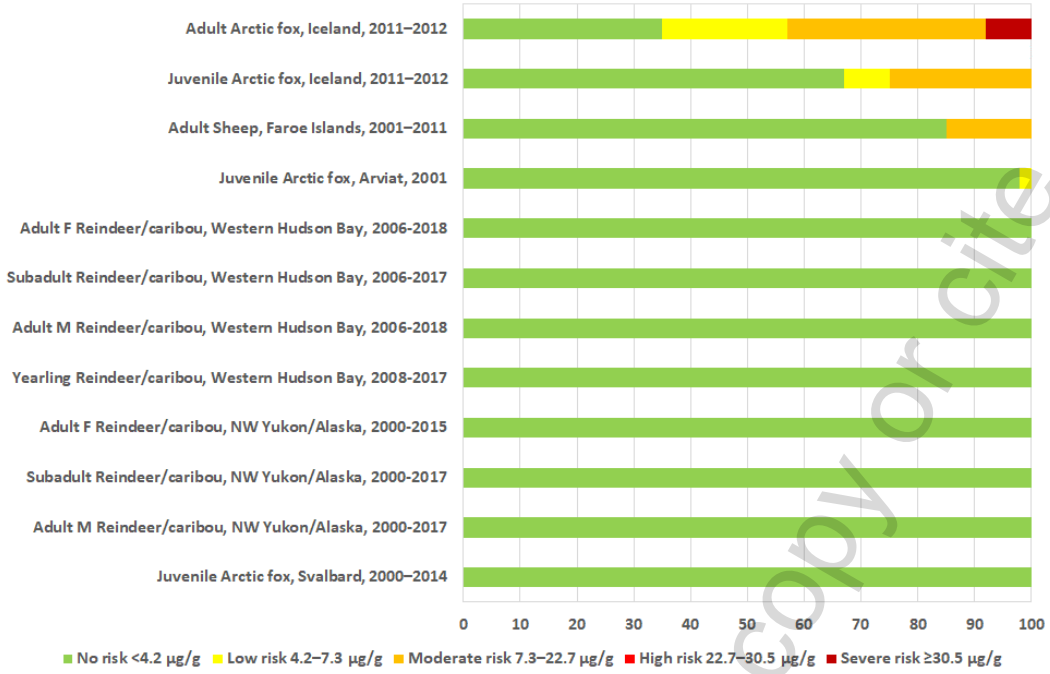

Fig. 6.3.3.1. Ranked overview (from highest to lowest risk) of the proportion of individuals, where possible grouped according to maturity, of specific Arctic terrestrial mammal populations that are at risk of total Hg-mediated health effects. Following 2000–2015 hepatic concentrations, five risk categories are reported based upon effect threshold categories observed for mink (Wobeser et al., 1976; Wren et al., 1987).

6.3.4. Marine and terrestrial birds

Authors: Joshua T. Ackerman, Olivier Chastel, Jérôme Fort

Methylmercury is known to have numerous detrimental effects on birds (Scheuhammer et al. 2007, Ackerman et al. 2016*b*). Avian reproduction is especially sensitive to methylmercury toxicity, with even low levels of exposure leading to adverse health effects (Wiener et al. 2003, Heinz et al. 2009). Aquatic birds typically have the highest exposures to environmental mercury contamination (Ackerman et al. 2016*b*), although more terrestrial birds, like riparian songbirds, are also known to bioaccumulate methylmercury to potentially harmful levels (Cristol et al. 2008, Ackerman et al. 2019). Within the Arctic, birds are primarily exposed to elevated levels of methylmercury in pelagic (Provencher et al. 2014, Braune et al. 2015, Peck et al. 2016, Burnham et al. 2018, Albert et al. 2019) and coastal shoreline and wetland foraging habitats (Hargreaves et al. 2011, McCloskey et al. 2013, Perkins et al. 2016, Sun et al. 2019). Peregrine falcon *Falco peregrinus* from Northwest Greenland also showed a high mercury contamination despite its terrestrial habitat and diet (Burnham et al. 2018).

We reviewed and assessed the potential for methylmercury toxicity in Artic birds using the available data (**Annex Tables 4A-C**). To assess risk, we used methylmercury toxicity benchmarks previously established for bird blood (Ackerman et al. 2016*b*), and converted these values into equivalent concentrations in other bird tissues that are also commonly sampled in the arctic, such as eggs, liver, and contour feathers. Blood-equivalent mercury concentrations <0.2 µg/g ww are below the lowest-observed effect levels, whereas birds are generally considered to be at low risk when blood mercury concentrations are 0.2-1.0 µg/g ww, moderate risk at 1.0-3.0 µg/g ww, high risk at 3.0-4.0 µg/g ww, and severe risk at >4.0 µg/g ww (Ackerman et al. 2016*b*). We converted these toxicity benchmarks in bird blood into equivalent concentrations in eggs, based on a review paper which established a general bird maternal transfer equation of mercury from females to their eggs (Ackerman et al. 2020). Similarly, we converted blood to liver mercury concentrations using an intra-tissue correlation equation built for four species of birds (Eagles-Smith et al. 2008). Because many of the Arctic bird data for mercury exposure have been sampled using bird feathers (Albert et al. 2019), we also converted these toxicity benchmarks for bird blood into body feather mercury concentrations. Unlike the other equations, intra-tissue correlations for feathers and internal tissues, such as with blood or eggs, tend to be poor (Evers et al. 1998, Eagles-Smith et al. 2008, Ackerman et al. 2016*a*). Feather molt represents a major excretion pathway in bird during which 60-90% of accumulated mercury is excreted (Honda et al. 1986, Lewis et al. 1993, Braune and Gaskin 1987, Braune 1987, Agusa et al. 2005). Mercury in feathers becomes stable once they have grown (Appelquist et al. 1984). Since feathers have often grown months before they are collected, the existing temporal and spatial mismatch in mercury concentrations between feathers and other tissues is exacerbated. In addition, feather mercury concentrations can be difficult to interpret, due to the complex timing and location of feather molt (Pyle 2008, Pyle et al. 2018), differences among feather tracts (such as head vs body feather; Braune and Gaskin 1987, Ackerman et al. 2016*a*, Fort et al. 2016), the large scale movements of birds, often migratory species exposed to mercury over different regions (Fleishman et al. 2019), and the extreme variability in mercury concentrations in some species both within and among individual feathers from the same individual bird (Peterson et al. 2019).

Because of these complexities, feathers are typically not recommended for mercury biomonitoring programs if detailed information about bird species biology is lacking (Ackerman et al. 2016*b*, Chételat et al. 2020) such as their precise feather molt timing or their distribution over their annual cycle (Ackerman et al. 2012, Albert et al. 2019). In these specific cases, feathers can be a useful sampling tool to represent mercury exposure, such as in remote oceanic locations where birds are difficult to sample. For example, nape feathers of red-legged kittiwakes (*Rissa brevirostris*) are thought to be grown at the end of the wintering period and were sampled on their breeding grounds where birds can be more easily captured on their nest (Fleishman et al. 2019). This sampling strategy coupled together with geolocation dataloggers demonstrated that kittiwakes wintering at more southern latitudes within

12442 the North Pacific Ocean had higher mercury concentrations than birds wintering at more northern
12443 latitudes (Fleishman et al. 2019). Similarly, head feathers of little auks (*Alle alle*) which grow on the
12444 wintering grounds were used to demonstrate that birds were 3.5 times more contaminated when outside
12445 of their Arctic breeding locations, indicating that methylmercury acquired at non-arctic wintering areas
12446 in the northwest Atlantic can be transported to Artic breeding areas by migratory birds and has the
12447 potential to affect reproductive success (Fort et al. 2014). Hence, feathers were useful to demonstrate
12448 that non-Arctic regions that were used by the Arctic avian community for several months per year, when
12449 birds travel thousands of kilometers between their Arctic breeding site and non-Arctic non-breeding
12450 grounds (e.g. Egevang et al. 2010), are of high concern due to higher mercury contamination
12451 experienced during winter (Albert et al. unpublished).
12452
12453 Based on these toxicity benchmarks, we found that 50% of birds had tissue mercury concentrations that
12454 were above the no adverse health effects level (a blood-equivalent mercury concentration of 0.2 µg/g
12455 ww) and that 1% of birds were either at high or severe risk (**Annex Tables 4A-C**). In particular,
12456 northern fulmar (*Fulmarus glacialis*), ivory gull (*Pagophila eburnea*), glaucous-winged gull (*Larus*
12457 *glaucescens*), glaucous gull (*Larus hyperboreus*), lesser black-backed gull (*Larus fuscus*), black-legged
12458 kittiwake (*Rissa tridactyla*), red-legged kittiwake (*Rissa brevirostris*), atlantic puffin (*Fratercula*
12459 *arctica*), thick-billed murre (Brünnich's guillemot, *Uria lomvia*), black guillemot (*Cepphus grille*),
12460 pigeon guillemot (*Cepphus Columba*), rhinoceros auklet (*Cerorhinca monocerata*), double-crested
12461 cormorant (*Phalacrocorax auratus*), and ruddy turnstone (*Arenaria interpres*) had at least 5% of the
12462 individuals sampled with mercury concentrations at levels considered to be at moderate or higher risk
12463 to toxicity (**Annex Tables 4A-C**). Mercury concentrations in birds tended to increase historically within
12464 the Arctic, but trends have flattened recently in several Arctic regions (Braune et al. 2001, 2006, 2016,
12465 Braune 2007, Bond et al. 2015, but see Fort et al. 2016 in East Greenland). As is common, bird mercury
12466 concentrations differed widely among sites in the Arctic due to differences in bioaccumulation
12467 pathways and processes (Braune et al. 2002, 2014*b*). Braune et al. (2014*a*) found that thick-billed
12468 murres breeding at two high arctic colonies tended to have higher mercury concentrations than murres
12469 breeding at three low arctic locations. In contrast, birds wintering at more southern latitudes generally
12470 had higher methylmercury exposure (Fort et al. 2014, Fleishman et al. 2019). In general, the XXX
12471 portion of the Arctic tended to have birds with higher methylmercury exposure (**Figure X**) with a
12472 tendency for higher concentrations measured in the Canadian Arctic and Western Greenland than in the
12473 European Arctic and Russia (Fort et al. unpublished). The following sections detail the recent work
12474 which has demonstrated effects of methylmercury on Arctic bird health.
12475
12476 ***6.3.4.1 Vitamins, oxidative stress, and telomeres***
12477 Vitamins A, D, and E are essential nutrients and play a fundamental role in growth, development,
12478 reproduction, bone mineral homeostasis, protection against tissue damage, and immune and endocrine

function (Debier and Larondelle, 2005). Because of their key physiological importance, changes in these vitamins have been considered as pertinent biomarkers of contaminant exposure and effects in Arctic wildlife (for persistent organic pollutants (POPs) see Helgason et al. 2010, Braune et al. 2011, Verreault et al., 2013). Since 2010, few studies addressing the relationships between mercury and vitamins in Arctic seabirds have been conducted. In the ivory gull (*Pagophila eburnea*), a year-round and significantly contaminated resident of the Arctic (Bond et al. 2015, Lucia et al. 2015), eggs from Svalbard and the Russian Arctic populations were sampled to investigate relationships between whole egg mercury content (0.06 - 0.30 µg/g ww), eggshell thinning, vitamin A, and vitamin E (Miljeteig et al., 2012). No associations between mercury levels, eggshell thinning and the two vitamins were found in this study.

Regarding the effects of contaminants on wildlife, one biochemical mechanism thought to be particularly important is oxidative stress because of its potential detrimental effects on key fitness traits, such as cellular homeostasis or reproduction (Costantini 2014). Since 2010, most studies on contaminants-oxidative stress relationships have concentrated on organic compounds (OCs, PCBs, PFASs) and showed that increased molecular oxidative damage and disruption of antioxidant defenses was found in the most contaminated individuals from several Arctic bird species, although strength of the relations varied greatly according to species and locations (birds of prey: Sletten et al. 2016; seabirds: Wayland et al. (2010) Bourgeon et al. 2012, Costantini et al. 2018).

For mercury, however, only a handful of studies are available. Investigations on temperate or Antarctic seabirds have reported some associations between mercury and oxidative stress (Costantini et al. 2014; Gibson et al. 2014; Hoffman et al 2011). For Arctic seabirds, Wayland et al. (2010) investigated glaucous gulls (*Larus hyperboreus*) from the Canadian Arctic and found associations between some oxidative markers (thiols, lipid peroxidation) and mercury burden. In Svalbard, there was no association between blood mercury levels (1.96-4.82 µg/g dw) and several oxidative status markers for kittiwakes (*Rissa tridactyla*) (Chastel, Costantini, Gabrielsen, Blévin, unpublished). Similarly, Fenstad et al. (2016) found no association between mercury burden and total antioxidant capacity in Baltic and Svalbard common eiders.

Oxidative stress is considered as one of the mechanisms involved in the shortening of telomeres, which are repeated sequences of non-coding DNA located at the terminal ends of chromosomes (Blackburn 2005). Following the discoveries of telomeres and their implications for maintaining chromosome stability, health, and ageing, there has been a growing interest into the study of telomere dynamics in relation to contaminant exposure (Angelier et al. 2018). Since 2010, a few studies have explored telomeres-contaminants relationships in Arctic free living birds and, for oxidative stress, these studies have mainly addressed OCPs, PCBs and PFAS (Sletten et al; 2016, Blévin et al.2016, 2017, Eckbo et

al. 2019). Regarding mercury, only one study has been conducted, and they found that absolute telomere length was positively associated, but weakly, with blood mercury levels in Svalbard kittiwakes (Angelier et al. 2018). Thus, there is a current data gap for our understanding of the relationship between mercury and telomeres.

6.3.4.2 Endocrinology

In order to maximize fitness, individuals must make behavioral decisions on their reproduction depending on environmental conditions (e.g., whether to breed or not, when to breed, what level of parental investment). These behavioral decisions are mediated by hormones: such as luteinizing hormone, a pituitary hormone involved in the onset of breeding (Goutte et al. 2011); stress hormones (corticosterone, Wingfield and Sapolski 2003); and prolactin, a pituitary hormone involved in the expression of parental care (Angelier and Chastel 2009). Because mercury is a known endocrine disruptor (Tan et al, 2009), mercury may impair breeding decisions (Hartman et al. 2019) and more generally alter the ability of Arctic seabirds to adequately respond to ongoing environmental changes (Jenssen 2006). Since 2010, Arctic seabird studies have greatly advanced our knowledge of the impact of mercury as an endocrine disruptor for wildlife.

Research conducted on Svalbard black-legged kittiwakes has shown that mercury (range: 0.91–3.08 mg/g dw) appear to target pituitary hormones. For example, during the pre-laying period, high mercury concentrations in blood were related to a decreasing luteinizing hormone secretion (Tartu et al. 2013). Additionally, experimental challenges with exogenous GnRH (gonadotropin-releasing hormone) were conducted to test the ability of the pituitary to release luteinizing hormone in relation to mercury concentrations. These investigations suggested that mercury disrupted LH secretion by suppressing GnRH input to the pituitary and that elevated mercury concentrations were linked to skipped reproduction (Tartu et al. 2013). A similar pattern was observed for Antarctic seabirds (Tartu et al. 2014a). As for LH, mercury seems to impact another pituitary hormone: prolactin which is known to play a key role in the expression of avian parental care (Angelier & Chastel 2009).In black-legged kittiwakes from Svalbard as well as in Antarctic seabirds, high mercury exposure appeared to be associated with lower plasma prolactin levels and poor incubation behavior (Tartu et al. 2015a, 2016). The effect of mercury on stress hormones secretion is less clear (Herring et al. 2012 for temperate seabird nestlings, Provencher et al. 2016a on common eider duck (*Somateria mollissima*). In Svalbard kittiwakes, baseline and stress-induced corticosterone levels were unrelated to mercury concentrations (range: 0.82-2.96 µg/g dw). In this population, exacerbated baseline and stress-induced corticosterone levels appeared rather triggered by organic compounds (PCBs), possibly via a stimulation of adrenocorticotropic hormone (ACTH) receptors (Tartu et al. 2015b).

6.3.4.3 Genotoxicity

Alterations in the genetic material may have severe consequences for individuals and populations. Since 2010 some studies have investigated the genotoxic effects of environmental exposure to pollutants in Arctic seabirds (e.g.; organohalogen contaminants: Haarr et al. 2017). Fenstad et al. (2016) assessed the impact of blood concentrations of mercury on DNA double-strand break (DSB) frequency, in blood cells of a high-exposed Baltic (mercury: 0.43–1.71 nmol/gww) , and lower exposed Arctic population (Svalbard, mercury: 0.31–0.98 nmol/gww) of common eiders. Significant positive relationships between mercury and DNA DSB frequency were found in Baltic, but not in Svalbard eiders.

6.3.4.4 Immunology

Exposure to mercury has been associated with depressed avian immune responses (Fallacara et al. 2011; Lewis et al., 2013) and this may pose an additional threat to Arctic birds since climate change could favor the emergence of new infectious diseases or a higher prevalence of parasites in the Arctic (Eagles-Smith et al. 2018; Lee et al. 2020). Since 2010, few studies have investigated immune responses to mercury in free-living species. For Arctic seabirds, Provencher et al. (2016a) did not find association between mercury blood levels and immunoglobulinY (IgY) in female eider ducks from the Canadian Arctic. Similarly, in an experimental study of Svalbard barnacle geese (*Branta leucopsis*), it was found that exposure to mercury from a historic coal mine area had little impact on four innate immune parameters (haemolysis, haemagglutination, haptoglobin-like activity, and nitric oxide) in goslings (de Jong et al. 2017). Within the general framework of the effects of contaminants on immunity, there has been an interest in the study of contaminant-parasite interactions in recent years. Indeed, contaminants and parasites may negatively affect wildlife health and reproduction either additively or synergistically (Marcogliese and Pietrock, 2011). To date, only one study on Common Eider from the Canadian Arctic indicated that mercury (breast muscle levels: 0.63 ± 0.24 µg/g) and gastro-intestinal parasites may potentially influence each other (Provencher et al. 2016b).

6.3.4.5 Neurology

The concentrations of receptors in the brain for neurotransmitters such as acetylcholine and glutamate, can be affected by exposure to methylmercury in birds and mammals. Thus, concentrations of receptors in the brain can be used as biomarkers of methylmercury effects in wildlife (Basu et al., 2006; Scheuhammer et al., 2015). However, Braune et al. (2012) found no relation between mercury concentration and density of specifc neuroreceptors in brain tissue from thick-billed murre (*Uria lomvia*) and Arctic tern (*Sterna paradisea*) embryos (mercury concentrations: 0–3.2 µg/g ww for the murre embryos and 0–1.6 µg/g ww for the tern embryos).

6.3.4.6 Bioenergetics-energy expenditure-thyroids hormones

Basal metabolic rate (BMR), the minimal energetic cost of living in endotherms, is known to be influenced by thyroid hormones (THs) which are known to stimulate in vitro oxygen consumption of

tissues in birds and mammals. Several environmental contaminants may act on energy expenditure through their thyroid hormone-disrupting properties. However, the effect of mercury on BMR is still poorly documented for wildlife. Blévin et al. (2017) investigated the relationships between three groups of contaminants (organochlorines (OCs), perfluoroalkyl substances (PFASs), and mercury) with metabolic rate (MR), considered here as a proxy of BMR, and also with circulating total THs (thyroxine (TT4) and triiodothyronine (TT3)) in adult black-legged kittiwakes from Svalbard, during the chick rearing period. This study indicated that, contrary to some OC and PFASs (Blévin et al. 2017; Melnes et al. 2018 for glaucous gull), metabolic rate and thyroid hormones (T3) were not associated with mercury blood levels.

6.3.4.7 Parental behavior

In birds, incubation-related behaviors are influenced by hormonal regulation. In some Antarctic seabirds, Tartu et al. (2015a) showed that mercury concentrations were associated with reduced egg-incubation effort. However, relatively little is known about the effect of contaminants on incubation temperature for wild birds (Hartman et al. 2019, Taylor et al. 2018). By using temperature thermistors placed into artificial eggs, Blévin et al. (2018) investigated relationships between three groups of contaminants (organochlorines (OCs), perfluoroalkyl substances (PFASs), and mercury) with incubation temperature and also with prolactin concentrations and brood patch size in incubating Svalbard black-legged kittiwakes. This study revealed that, contrary to OC, mercury concentrations in blood (2.004±0.591 mg/g dw in males; 1.426±0.377mg/g dw in females) were not related to the minimum incubation temperature, the size of the brood patch, nor to hatching probability. Incubation does not solely imply the active warming of the eggs but also the active turning of eggs to facilitate albumen absorption by the embryo, reduce the likelihood of an embryo being malpositioned for hatch (Herring et al. 2010), and prevents the embryo from adhering to the inner shell membrane. Using the same egg-logger in the same population of black-legged kittiwake, Blévin et al. (2020) found that, contrary to PCBs and PFASs, blood mercury concentrations were unrelated to egg-turning behavior, similar to studies on egg turning in seabirds at temperate latitudes (Taylor et al. 2018).

6.3.4.8 Reproductive performances and demographic responses

Research conducted since 2010 on arctic marine and terrestrial birds have revealed several links between mercury exposure and endocrine pathways, immune response, genetic material, and parental care behaviors. Thus, chronic exposure to methylmercury might compromise survival rate and long-term reproductive outputs (Evers et al. 2008, Scheuhammer et a. 2012), thus potentially leading to population declines. Here, we review studies conducted during the 2010-2019 that have addressed the effects of mercury on reproductive performances and long-term demographic responses in terrestrial and marine birds in the Arctic.

Reproductive performances: Exposure to methylmercury is known to alter avian sexual and mating behaviors (Frederick et al. 2011). For Arctic birds, very few information is available: contrary to some legacy chlorinated POPs (Blévin et al. 2013), mercury concentrations in Svalbard kittiwakes did not appear to be associated with carotenoid-based sexual ornamentations, carotenoid concentrations in plasma, nor to paring success (Blévin, Costantini, Bustamante, Gabrielsen, Chastel unpublished). Further, the high frequency of abnormal sperm cells observed in this species in Svalbard (Humann-Guilleminot et al. 2018) was unrelated to mercury blood concentrations (Blévin eta. in prep). On the other hand, Amélineau et al. (2019) reported that adult little auks (*Alle alle*) with high mercury concentrations were in reduced body condition. Skipped breeding behavior (non-breeding by individuals that previously bred), is a common occurrence in long-lived birds (Cubaynes et a. 2011; Goutte et al. 2011). Investigations conducted in Svalbard have shown that the probability of skipped breeding was associated with high mercury concentrations in pre-laying kittiwakes, whereas laying date and clutch size were not related to mercury concentrations (Tartu et al. 2013). In Greenland, female little auks that have been more contaminated with mercury during winter (measured in feathers) were found to lay smaller eggs (Fort et al. 2014). In another study of Svalbard kittiwakes, mercury concentration was negatively related to breeding success (probably to raise at least one chick) in males (Tartu et al. 2016). Hargreaves et al. (2010) studied potential effects of mercury in three biparental shorebird species nesting in Nunavut, Canada: ruddy turnstones (*Arenaria interpres*), grey plovers (*Pluvialis squatarola*), and semipalmated plovers (*Charadrius semipalmatus*). Maximum mercury concentrations in blood approached those associated with toxicological effects in other bird species and it was found that reproductive success was negatively correlated with paternal mercury concentrations. The negative effect of mercury exposure on egg hatchability was experimentally tested in Brunnich guillemots and Arctic terns by injecting a range of environmentally relevant concentrations (0–6.4 µg/g ww) of methylmercury chloride (MeHgCl). This study by Braune et al. (2012) demonstrated the relative sensitivity of the developing embryos to methylmercury in these two arctic seabird species (Braune et al., 2012). Finally, in Greenland little auks, chicks with the highest mercury concentrations hatched with a body mass reduced by approximately 30% compared to those with the lowest concentrations, although no impact was further observed on their growth and fledging success (Kerric et al. unpublished). Nevertheless, Amélineau et al. (2019) found that the long-term increase in mercury contamination of this same population was associated with decreased chick growth rate during the last decade.

Demographic responses: Our understanding of the ultimate consequences of mercury exposure on long-term fitness is still limited in free-living Arctic birds because of the paucity of long-term data sets that would be required to address this topic. During the 2010-2019 period, a few long-term capture-mark-recaptures studies on Antarctic (wandering albatross *Diomedea exulans*; Goutte et al. 2014a, subantarctic and south polar skuas *Catharacta lonnbergi*, *C. maccormicki* Goutte et al. 2014b) and

Arctic seabirds (Svalbard: Glaucous gull and black-legged kittiwake Erikstad et al. 2013; Goutte et al. 2015; Greenland: Little auk, Amélineau et al. 2019, Northern Norway: Common, eider Bardsen et a. 2018) have estimated the impact of contaminants on long-term breeding probability, reproductive success, and adult survival. These studies, based on long-term ringing programs have mainly focused on legacy chlorinated POPs, but some of them have included blood and feather mercury concentrations into demographic models (Goutte et al. 2014 a,b; 2015, 2018, Bårdsen et al. 2018; Amélineau et al. 2019). Regarding Arctic seabirds, a long-term study on Svalbard kittiwakes found reduced breeding probability with higher mercury concentrations, but the overall impact of mercury on demographic parameters was modest compared to that of some legacy chlorinated POPs (Goutte et al. 2015). Importantly, all these long-term studies revealed no effect of mercury on adult survival, a key parameter for seabird population dynamics, despite a wide range in blood mercury concentrations (little auks: 0.89 µg/g dw, black-legged; kittiwakes: 2.09±0.46 µg/g dw; south polar skua: 2.15 ± 0.17 mg/g dw; subantarctic skua: 8.22 ± 0.24 µg/g dw; wandering albatross: 7.7 ± 3.6 µg/g dw)

These demographical investigations need to be extended to other species (especially terrestrial ones) and other Arctic regions. Further, Arctic birds are exposed to multiple stressors and the impacts of mercury probably act in concert with both natural and other anthropogenic stressors (e.g. diseases, parasites, disturbance, climate-related environmental changes). Thus, even mercury concentrations considered as posing low or moderate risks to birds, may cause adverse effects if they co-occur with increased levels of other stressors (Fort et al. 2015, Tartu et al. 2016; Amélineau et al. 2019). Future investigations should also incorporate other types of contaminants (legacy chlorinated and brominated POPs, PFAS, other non-essential trace elements such as Selenium) in demographical models to better assess the specific impacts of mercury. Many Arctic birds leave the Arctic after the breeding period and some are long distance migrants, spending the winter in sub-Arctic, temperate, tropical and Antarctic areas (e.g., Egevang et al. 2010; Gilg et al. 2013). Environmental stressors (harsh weather, food shortage) and mercury uptake experienced outside the breeding season can result in sub-lethal to lethal effects and contribute to large bird mortality by impacting their body condition (Fort et al. 2015). They can also result in non-lethal effects that will be carried later to the next breeding season (Fort et al. 2014, Fleishman et al. 2019). Such direct and carry-over effects (Norris 2005) can strongly impact fitness and population dynamics. Combining miniaturized tracking systems (e.g., geolocators to document migratory movements and wintering areas) with measurements of mercury levels (Fort et al. 2014, Fleishman et al. 2019), other environmental stressors and detailed demographical surveys should provide relevant information on the global impact of mercury on Arctic birds.

6.3.5. Shorebirds

Authors:'Marie Perkins and Nil Basu

This work intends to identify regions within the terrestrial Arctic and shorebird species at the greatest risk for Hg exposure and to elucidate factors influencing Hg concentrations in shorebirds. 2,478 blood and feather samples were analyzed collected from 12 breeding shorebird species during 2012 and 2013. Sampling locations included five sites in Alaska located near Nome, Cape Krusenstern, Barrow, and the Ikpikpuk and Colville rivers; and four sites in Canada located on the Mackenzie River Delta, Bylot Island, Igloolik, and East Bay. Blood Hg concentrations in individual shorebirds ranged from 0.01 – 3.52 μg/g, with an overall mean of 0.30 ± 0.27 μg/g.

This study was in collaboration with the Arctic Shorebird Demographics Network (ASDN), a large-scale network currently researching shorebirds across the North American Arctic, and the Biodiversity Research Institute (BRI, Portland, Maine, USA), a non-profit organization specializing in Hg exposure in wildlife. Collaborating study sites in 2012 included five sites in Alaska located near Nome, Cape Krusenstern, Barrow, the Ikpikpuk River, and the Colville River, and three sites in Canada near the Mackenzie River Delta, Bylot Island, and East Bay (Figure 2.1). An additional Canadian study site, Igloolik, was included with the previously sampled sites in 2013. The ASDN biologists collected blood and feather samples for Hg analysis from adult shorebirds (hatched the prior summer or earlier) captured while conducting routine fieldwork during the breeding season.

6.3.6 Marine fish and freshwater fish

Author: Benjamin D. Barst

Additional data contributors: Derek Muir, Nikolaus Gantner, Michael Power, Frank F. Rigét, Heidi Swanson

In the context of MeHg research, fish have been studied as vectors for MeHg transfer to wildlife and humans, with little focus on the deleterious effects of MeHg to the fish themselves (Wiener and Spry 1996; Scheuhammer et al. 2007; Sandheinrich and Wiener 2011). Most of the early laboratory studies that investigated the health effects of MeHg exposures to fish, involved aqueous exposures at high concentration, rather than more realistic dietary exposures at environmentally relevant levels (Scheuhammer et al. 2007). Most of the relevant research effort regarding the effects of dietary MeHg exposures to fish have been conducted over about the last 20 years. Clear effects on fish growth and survival occur at high tissue Hg concentrations (5 to 20 μg/g wet weight in muscle) that are generally associated with point source contamination (Sandheinrich and Wiener 2011). Perhaps the clearest example that environmental organic Hg exposure results in toxic effects in wild fish is that of Minamata Bay, where fish tissue Hg levels reached ~10 to 20 μg/g wet weight and fish "rotated continuously and floated belly-up to the surface" (Harada 1995). Locations that receive Hg through atmospheric deposition rather than through direct point source contamination typically have fish with muscle Hg concentrations well below those that result in overt toxicity (Depew et al. 2013; Eagles-Smith et al.

2016; Barst et al. 2019). Nevertheless, growing evidence provided by laboratory and field research indicates that the Hg concentrations found commonly in wild fish are sufficient to cause sublethal toxic effects (Dillon et al. 2010; Sandheinrich and Wiener 2011).

The toxicity of MeHg may be linked to its ability to penetrate cellular membranes (Bridges and Zalups 2010) and interact with sensitive subcellular sites (Benjamin D. Barst et al. 2016). Within cells, MeHg overwhelms antioxidant defenses resulting in oxidative stress, altered gene expression, biochemical changes, and tissue damage in fish exposed to MeHg naturally or in the laboratory (Sandheinrich and Wiener 2011). Altered predator avoidance behavior has been reported for fish exposed to MeHg in the laboratory (Webber and Haines 2003). Moreover, survival skills related to foraging and predator evasion behaviors were impaired in juvenile fish exposed to MeHg through maternal transfer (Alvarez et al. 2006). Laboratory studies demonstrate that environmentally relevant concentrations of dietary MeHg impair fish reproduction through reductions in circulating sex hormones, reduced fecundity, and altered reproductive behavior (Hammerschmidt et al. 2002; Drevnick and Sandheinrich 2003; Drevnick et al. 2006; Sandheinrich and Miller 2006).

Effects data produced from laboratory exposures provide the basis for modeled MeHg residue-effect levels for fish (Beckvar et al. 2005; Dillon et al. 2010). The toxic effect level generated by Beckvar et al. (2005; 0.33 µg/g wet weight in edible muscle) is based on laboratory studies that assessed sublethal endpoints including behavior, development, reproduction and growth. The toxic effect level developed by Dillon et al. (2010; 0.5 µg/g wet weight in edible muscle) is based on laboratory studies with endpoints most relevant to ecological risk assessment including lethal developmental abnormalities, reproductive success, mortality, and survival. The residue-effect level reported by Dillon et al. (2010), is consistent with the value set by Sandheinrich and Wiener (2011), which was based on both laboratory and field studies. The dose-response model developed by Dillon et al. (2010) may be particularly useful as it is based on endpoints of interest to risk assessors and can predict percent injury across a range of tissue Hg concentrations.

Comparing Hg concentrations of wild fish to residue-effect levels is a relatively quick way to assess the potential for toxic effects in a population of interest. This approach has been used to screen large amounts of Hg data (~43,000 Hg measurements) for fish in the Great Lakes region of the United States (Sandheinrich et al. 2011). A similar approach was recently carried out to assess potential risks of MeHg for non-anadromous Arctic char (those that are restricted to lakes and rivers) (Barst et al. 2019). This screening-level risk assessment included 1569 non-anadromous Arctic char that were sampled from 83 sites, which ranged from locations in the boreal forest to those from the High Arctic. Site-specific mean total Hg concentrations in muscle tissue varied from 0.01 to 1.13 µg/g wet weight. A comparison between site-specific mean total Hg concentrations in muscle and the lower residue-effect level

12775 (0.33 µg/g wet weight) suggests that 21% of the populations of non-anadromous Arctic char are at risk
12776 for MeHg toxicity. Populations of non-anadromous Arctic char that exceeded 0.33 µg/g wet weight
12777 were located in Greenland (7 populations) and Canada (10 populations), almost exclusively in regions
12778 of discontinuous or continuous permafrost. The percentage of populations at risk decreased to 13%
12779 when considering the higher residue-effect level of 0.5 µg/g wet weight. Collectively, the results of the
12780 screening-level risk assessment suggest that certain populations of non-anadromous Arctic char may be
12781 at risk for MeHg toxicity, especially those located in regions containing discontinuous or continuous
12782 permafrost soils (Barst et al. 2019).
12783
12784 We built upon this initial effort to assess the potential for MeHg in arctic freshwater and marine fish by
12785 using available Hg data (Table XX) and a dose-response model that predicts injury across a range of
12786 Hg concentrations (Dillon et al. 2010). To simplify our comparisons, we converted whole-body residue
12787 effects concentrations (the basis for the dose-response model) to muscle concentrations using a
12788 conversion factor (Peterson et al. 2004). From the dose-response model we created five risk categories.
12789 Based on comparisons to the dose-response model, a higher proportion of freshwater fish had Hg levels
12790 in the high and severe risk categories (above 0.5 µg/g wet weight) as compared with the marine fish.
12791 The freshwater fish dataset was biased towards a larger number of non-anadromous Arctic char
12792 populations (n=XX). Of these, approximately XX populations had individuals at high or severe risk for
12793 MeHg toxicity. Sea run Arctic char tended to have lower concentrations of Hg and were therefore
12794 categorized as lower risk, with the exception of fish collected from the Faroe Islands. Marine fish in the
12795 ling family tended to have the highest Hg concentrations potentially placing them at risk for MeHg
12796 toxicity.
12797
12798 Despite the relative simplicity of screening-level assessments, there are various limitations related to
12799 the use of this approach for predicting MeHg toxicity in fish populations of interest. These limitations
12800 have been discussed elsewhere, both in general terms (Dillon et al. 2010) and in the context of non-
12801 anadromous Arctic char (Barst et al. 2019). As studies that focus on the direct effects of MeHg exposure
12802 to arctic fish are lacking, the screening-level approach is particularly useful.
12803
12804 A field study from the Canadian High Arctic aimed to assess potential health effects of MeHg exposure
12805 to landlocked Arctic char. Arctic char (n=114) were sampled in 2011 and 2012 from four lakes (Small,
12806 9-Mile, North, Amituk) on Cornwallis Island (Nunavut, Canada) that span a gradient of Hg
12807 contamination (Barst et al. 2016). Total Hg concentrations in muscle tissue were greatest in char form
12808 Amituk Lake, intermediate in char from North Lake and 9-Mile Lake, and lowest in char from Small
12809 Lake. Total Hg concentrations in livers were two to five times greater than in muscle, with a maximum
12810 of 6.5 µg/g wet weight for an individual from Amituk Lake. For all livers, total Hg was mainly present
12811 as MeHg (51 to 90%). A subcellular partitioning procedure based on differential centrifugation was

carried out to separate liver cells from Small and Amituk Arctic char into six operationally defined fractions. These subcellular fractions were assigned to one of two groups, including a potentially sensitive compartment (mitochondria + heat-denatured proteins (HDP) including enzymes + microsomes and lysosomes) and a detoxified compartment (peptides and heat-stable proteins (HSP) including metallothionein + granule-like concretions. Total Hg analyses of the various fractions revealed that the sensitive compartments contributed 73 and 61% of the contributions of total Hg in Small and Amituk livers, suggesting that Hg is not effectively detoxified in the livers of these fish. Histological investigation revealed hepatic fibrosis, predominately in the livers of Amituk Lake Arctic char. A significantly greater number of individuals from Amituk Lake (83%) exhibited this abnormality than individuals from the other study lakes. Evidence of fibrosis was also found in individuals from 9-Mile (29%) and North Lake (27%). Although, Hg exposure may have resulted in the observed hepatic fibrosis, the role of other factors (parasites, other contaminants) cannot be excluded (Barst et al. 2016).

6.3.7 Invertebrates

Few dosing studies have been conducted on invertebrates to determine critical body residues of Hg-associated toxicological effects (Flanders et al., 2019; Gimbert et al., 2016). Furthermore, much of the toxicological information is based on short-term Hg dosing to water, even though the diet is the primary route of MeHg exposure for invertebrates (Williams et al., 2010; Tsui and Wang, 2007; Fisher and Hook, 2002). Therefore, only a preliminary risk analysis of Hg toxicity to Arctic invertebrates could presently be conducted, and invertebrates were not included in the broader risk analysis for vertebrates. Published data were compiled from 13 marine studies and 12 freshwater studies from the last two decades to characterize the ranges of Hg and MeHg concentrations in Arctic aquatic invertebrates. Hg concentrations varied an order of magnitude among invertebrate taxa (Figure 6.3.6). Though sometimes not reported, the proportion of Hg as MeHg was also variable among invertebrates when data were available. For example, the percent MeHg in benthic fauna ranged from 9-73 % in the Chukchi Sea (Fox et al., 2017). Hg and MeHg concentrations of invertebrates were typically low with the majority of measurements < 0.2 µg/g dry weight for marine taxa and < 0.5 µg/g dry weight for freshwater taxa (Figure XX). A recent examination of over 6000 Hg measurements of marine bivalves in the Baltic Sea found that 99 % of samples had concentrations < 1 µg/g dry weight (0.1 µg/g wet weight) (Dietz et al., 2020). The maximum Hg and MeHg concentrations reported in the published literature were 3.5 µg Hg/g for benthic invertebrates from a Fennoscandian Lake (Kahilainen et al., 2017) and 0.87 µg MeHg/g for epibenthic shrimp in the Canadian high Arctic (Pedro et al., 2019).

Dosing studies have demonstrated that inorganic Hg and MeHg exposure are only lethal to aquatic invertebrates at extremely high water concentrations (Overjordet et al., 2014; Fisher and Hook, 2002; Borgmann et al., 1993), which are well above conditions observed in Arctic environments. Similarly, published values for critical body residues of Hg (on a dry weight basis) associated with lethality are

12849 well above concentrations found in Arctic invertebrates, such as 33.3 µg/g for the cladoceran *Daphnia*
12850 (Tsui and Wang, 2004), 48.8 µg/g for blue mussel (*Mytilus edulis*, Pelletier, 1988), 90 µg/g for the
12851 freshwater amphipod *Hyallela azteca* (Borgmann et al., 1993), 15.2 µg/g for the marine amphipod
12852 *Bathyporeia pilosa* (Khayrallah, 1985), and >10 µg/g for marine copepods (*Calanus* spp., Overjordet
12853 et al., 2014). Those threshold values associated with lethality are at least 2-3 orders of magnitude higher
12854 than concentrations observed in Arctic invertebrates (Figure XX). Reduced reproductive success or
12855 growth are associated with elevated mercury body burdens of 16.4 ± 32.9 µg/g (Biesinger et al., 1982,
12856 Gimbert et al., 2016). One exception was a study of reproductive success in the marine copepod *Acartia*,
12857 where egg production was inhibited at a much lower body Hg concentration of 0.5 µg/g (Hook and
12858 Fisher, 2002). Arctic marine copepods have lower Hg concentrations (0.057 ± 0.058 µg/g, n=16) than
12859 that threshold, although the study does suggest that sublethal effects of mercury could potentially occur
12860 in contaminated environments (Fisher and Hook, 2002). Based on the limited toxicological information
12861 available, Hg concentrations in aquatic invertebrates from Arctic environments are not likely to pose a
12862 toxicological risk to invertebrates.

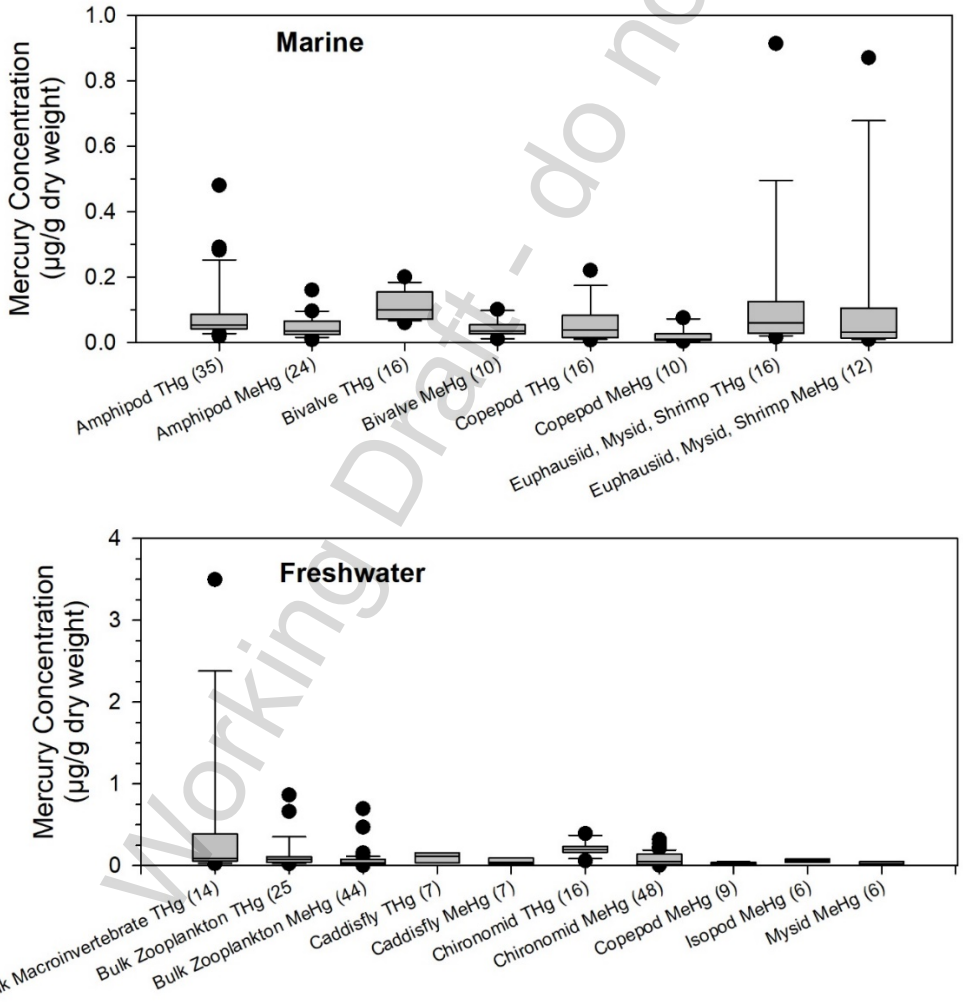

12863

12864 **Figure 6.3.6.** Total mercury (THg) and methylmercury (MeHg) concentrations of common marine and
12865 freshwater invertebrates from published studies in the circumpolar Arctic over the last two decades.
12866 Sample sizes (in parentheses) are the number of sites where measurements were made.
12867
12868 **6.4 Estimating population effects from mercury loads in highly exposed wildlife**
12869 Assessing the impact of Hg exposure and accumulation at the population-level is challenging for any
12870 species, but especially so for species living in remote areas like the Arctic. Such assessments require
12871 long term population monitoring to determine the link between observed tissue Hg levels and relevant
12872 long-term fitness metrics such as adult survival, reproductive success and recruitment (i.e. offspring
12873 survival to reproductive age), and ultimately population growth rates. For the Arctic, only a few studies
12874 in Arctic seabirds have been published to tackle this difficult question (see sea bird Reproductive
12875 performances and demographic responses section for summary). Despite reported effects on
12876 reproductive performance linked to Hg exposure, these studies report only modest effects on
12877 demographic parameters and no effect on adult survival (Goutte et al. 2014 a,b; 2015, 2018, Bårdsen
12878 et al. 2018; Amélineau et al. 2019). For all other Arctic species included in this report, little to no
12879 information is available on the population impacts of Hg.
12880
12881 It is because of this paucity of information that we currently undertook the pan-Arctic Hg risk
12882 assessment. The risk categories outlined here represent the best available information on mercury
12883 effects in a broad range of relevant species across vertebrate taxa. The high and severe risk categories
12884 are of potential concern regarding impacts at the population-level, given the observed effects in the
12885 reference toxicity studies. The most comprehensive toxicity data are available for birds, for which
12886 dozens of studies across multiple species, life-stages, and experimental designs (e.g. laboratory
12887 exposures to ecological studies) were summarized to establish the risk categories. Here, expected effects
12888 for populations in the high risk category include moderately reduced reproductive performance in the
12889 form of reduced hatching success and occasional failed reproduction, as well as reduced immune-
12890 competence. Severe risk includes severe reproductive impairment (low hatching success and offspring
12891 survival), oxidative stress, neurotoxicity, and ultimate increased adult mortality. The available data for
12892 marine and terrestrial mammals are much less comprehensive and derived from few captive feeding
12893 studies in harp seal and mink, respectively (Table 1). For harp seals, no data was reported for
12894 reproductive performance, but high risk includes potential for organ lesions (kidney, liver), anorexia,
12895 and reduced growth, while severe risk includes severe impacts on organ function (i.e. kidney failure),
12896 weight loss, and ultimately increased mortality. For mink, observed effects in the high risk category
12897 included reduced litter size and offspring growth rate, and severe risk included brain lesions, reduced
12898 growth, anorexia, and increased adult mortality. *Fish and invertebrates?*.
12899

Given the direct consequences on reproduction and survival for the high and severe risk categories, two endpoints of key concern for potential population impacts, concern is warranted for select populations of hooded seals, killer whales, and pilot whales, as well as Lancaster Sound and Northern Beaufort Sea polar bears and harbour porpoises in the Danish Straits. Here, >20% of sampled individuals within these populations (and up to 60-90%) had concerning tissue mercury levels; impacts in such a large proportion of the population has the potential to meaningfully affect demographic rates and overall population fitness. For polar bears in the highly exposed region like the Lancaster Sound and Jones Sound the populations trends are data deficient (Vongraven & York, 2014; Dietz et al. 2015). From areas like the S. Beaufort Sea and the Baffin Bay the populations are declining, but the effect of climate change are likely to play a major role in these areas (*Ibid*.). The pilot whales occurring Faroese and Greenlandic waters) are likely to represent vagrants from the North Atlantic population, which numbers several 100 thousands individuals (NAMMCO 2018a). To the Faroese hunt on pilot whales the increasing hunt on pilot whales in Greenland due to climate change should be added to evaluate the cumulative effects of these threat at the population level relative to the populations being harvested (Pinierneq 2019). Similarly, a large portion of the Arctic fox population in Iceland is at high and severe risk for potential population relevant impacts. **Info for birds**

Is in important to again note that the above population assessment, at least for marine and terrestrial mammals, is based on toxicity data from only one relevant species for each group (e.g. harp seal and mink). Care must be taken to extrapolate effects across species because of potential inter-species differences in Hg toxicokinetics (e.g. uptake and distribution) and toxicodynamics (e.g. species sensitivity to effects). Because such differences are unknown at this time and difficult to assess, the current risk exercise provides the best available evidence-based assessment of potential impacts across Arctic species. Further, these Arctic species of concern for mercury effects are also potentially impacted at the population-level through similar effects on reproduction and adult survival due to habitat changes linked to climate warming effects linked to POPs and other contaminants and hunting (e.g. Laidre et al., 2015 Dietz et al. 2015; 2019). Teasing out the effects of Hg from other stressors such as climate change remains a challenge for wildlife studies, though it is expected that these stressors act in concert to increase the overall stress of individuals and populations. Overall, more work on exact risk benchmark values for different species and regions are recommended as well as population effect studies in relation to Hg and other contaminant loads as conducted for killer whales by Desforges et al. (2018).

6.5 Geographical trends and Hg hotspots for wildlife, fish, invertebrates and abiotic matrices

It is clear from risk categorizations that have already been presented that there are “hot spot” species populations and regions with respect to Hg exposure. For marine mammals, Fig. 6.3.2.1 shows that the most highly Hg exposed species and populations are adult hooded seals from the Denmark Strait, adult

male hooded seals from Greenland Sea/Denmark Strait, adult polar bears from the Northern Beaufort Sea, juvenile polar bears from Qaanaaq NW Greenland, adult killer whales from E. Greenland, Iceland and Faroe Islands, adult long-finned pilot whales from the Faroe Islands, juvenile polar bears from Lancaster/Jones Sound, subadult long-finned pilot whale from the Faroe Islands, adult female ringed seals from Sachs Harbor and adult male ringed seals from Sachs Harbor. For terrestrial mammals, Fig. 6.3.3.1 shows that the most highly Hg exposed species and populations are Icelandic Arctic fox. Terrestrial mammals in general are at a much less exposure risk than marine mammals. For invertebrates, Fig. 6.3.6 shows that from various marine and freshwater invertebrate studies that Hg risk is an order of magnitude lower than for vertebrates, and Hg as MeHg were also variable among invertebrates.

Previous publications have considered geographical hotspots with respect to Hg biomangnification and adverse biological effects. These have been carried out on sediments, Arctic char, sea birds, ringed seals, as well as polar bears (e.g. AMAP 1998; Albert et al. In review; Dietz et al. 1998, 2000b, 2013a, this assessment, Rigét et al. 2005; Routti et al. 2011, 2012; *sediment paper*). Most of these surveys have shown a hotspot for Hg depletion and exposure in the northeastern Canadian Arctic and northwestern Greenland The ideal way to determine hotspot areas is to conduct the analyses on only recent datasets e.g. 2015-2020, using same age/sex group meanwhile correcting for dietary confounding using stable N and C isotopic analyses.

Recent analyses of Arctic Alcids suggest the Western Arctic in Canada to have the highest biomagnified concentrations and is supported by circumpolar studies of ringed seals (Albert et al. In review; Rigét et al. 2005). Studies of polar bears also points towards the Canadian Arctic as a hotspot adjusted adjusted for sex and age (Dietz et al 2000b; Routti et al. 2011) based on liver analyses, and that study was later adjusted for differences in feeding ecology by adjusting for the influence of carbon and lipid measurements (Routti et al. 2012). Less information is available from fish, however, according to Dietz et al. (2013), Hg levels in land-locked chard was highest in the Canadian Arctic compared to e.g. Greenland. As for the abiotic media Hg depletion, brome-oxide measurements sediment, Hg in the waterbodies and sediment cores will be explored in detail (Christensen in Brooks et al. 2002, Wang et al. 2019??).

We will during the revision stage include graphical illustrations as shown below Fig 6.5. These includes heat mapping, graphical differences including longitudes and latitudes (not just longitude as that may bias the results if there is a north/south difference) and %- of the lowest concentrations in each matrices/species for each area. These graphics represents the idea of the hotspot discussion. Longitudes are not adjusted and all data may be combined in one heatmap with both longitude and latitudes.

12974

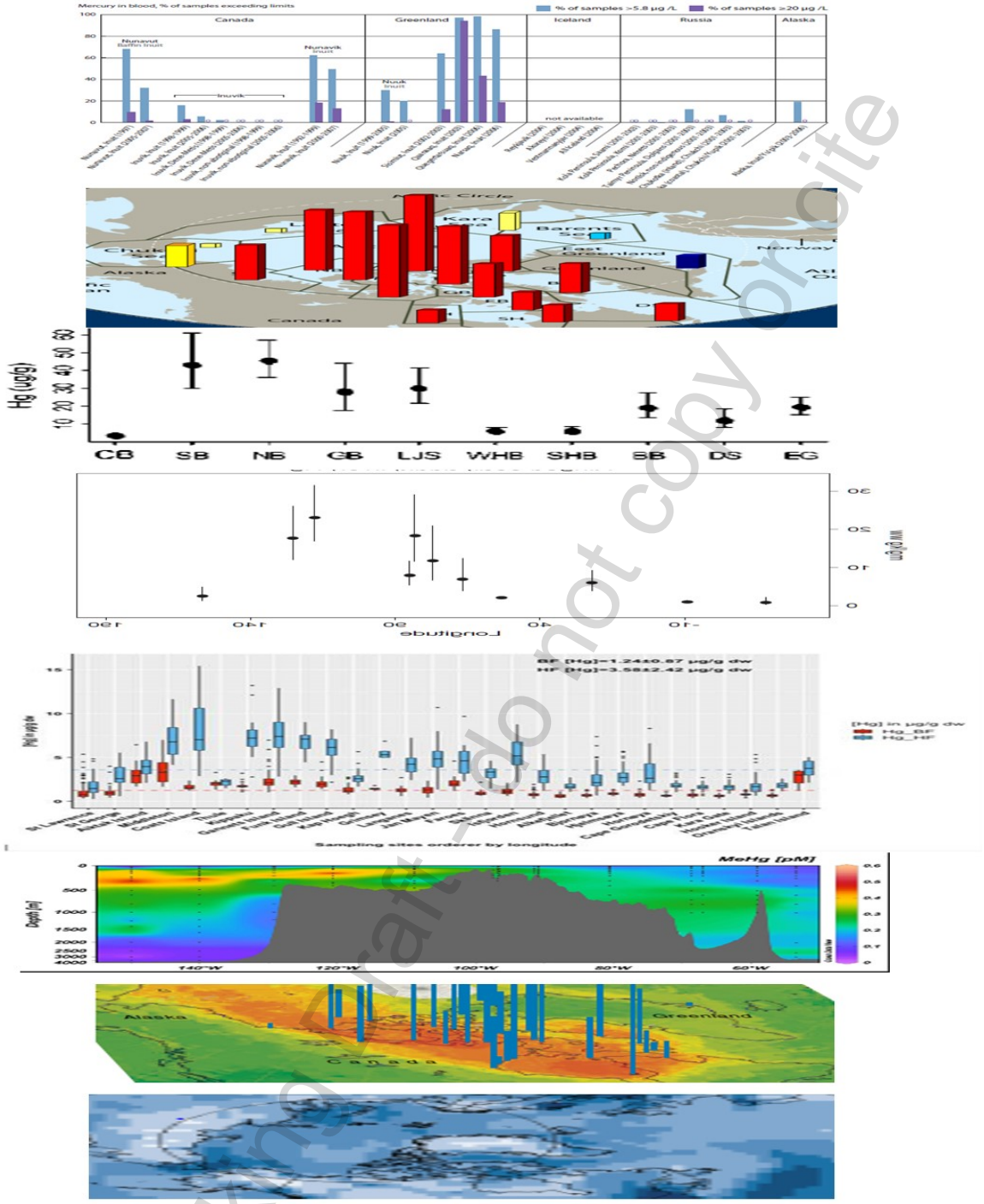

12975

12976

12977 **Figure XX.** Geographical patterns of (from the bottom) DEHM model estimates of total mercury
12978 deposition with mercury depletion, satellite-derived BrO concentration averages for March and May
12979 2000, methyl mercury in the ocean, mercury in feathers of common guillemot, mercury in ringed seal
12980 livers, mercury in polar bear livers, mercury in blood of Arctic Inuits. (Albert et al. In review;
12981 Christensen in Brooks et al. 2002, Dietz et al. this assessment, Rigét et al. 2005, Routti et al. 2011,
12982 Wang et al. 2019??)

12983 **6.6 Conclusions and recommendations**

12984

12985 **References**

12986 Ackerman, J. T., C. A. Eagles-Smith, M. P. Herzog, and C. A. Hartman. 2016*a*. Maternal transfer of
12987 contaminants in birds: Mercury and selenium concentrations in parents and their eggs.
12988 Environmental Pollution 210:145–154.
12989 Ackerman, J. T., C. A. Eagles-Smith, M. P. Herzog, C. A. Hartman, S. H. Peterson, D. C. Evers, A.
12990 K. Jackson, J. E. Elliott, S. S. Vander Pol, and C. E. Bryan. 2016*b*. Avian mercury exposure and
12991 toxicological risk across western North America: A synthesis. Science of the Total Environment
12992 568:749–769.
12993 Ackerman, J. T., C. A. Hartman, and M. P. Herzog. 2019. Mercury contamination in resident and
12994 migrant songbirds and potential effects on body condition. Environmental Pollution 246:797–
12995 810. Elsevier Ltd.
12996 Ackerman, J.T., Eagles-Smith, C.A., Herzog, M.P., Hartman, C.A., Peterson, S.H., Evers, D.C.,
12997 Jackson, A.K., Elliott, J.E., Vander Pol, S.S., Bryan, C.E., 2016. Avian mercury exposure and
12998 toxicological risk across western North America: a synthesis. Sci. Total Environ. 568, 749–769.
12999 Ackerman, JT, CT Overton, ML Casazza, JY Takekawa, CA Eagles-Smith, RA Keister, and MP
13000 Herzog. 2012. Does mercury contamination reduce body condition of endangered California
13001 clapper rails? Environmental Pollution 162:439-448.
13002 Ackerman, JT, MP Herzog, DC Evers, DA Cristol, KP Kenow, GH Heinz, RA Lavoie, RL Brasso,
13003 ML Mallory, JF Provencher, BM Braune, A Matz, JA Schmutz, CA Eagles-Smith, LJ Savoy,
13004 MW Meyer, and CA Hartman. 2020. Synthesis of maternal transfer of mercury in birds:
13005 implications for altered toxicity risk. Environmental Science and Technology on line.
13006 Agusa, T., Matsumoto, T., Ikemoto, T., Anan, Y., Kubota, R., Yasunaga, G., Kunito, T., Tanabe, S.,
13007 Ogi, H., Shibata, Y., 2005. Body distribution of trace elements in Black- tailed gulls from Rishiri
13008 Island, Japan: age-dependent accumulation and transfer to feathers and eggs. Environ. Toxicol.
13009 Chem. 24, 2107.
13010 Albert et al. In review. Céline Albert[a], Hàlfdàn Helgi Helgason, Maud Brault-Favrou, Françoise
13011 Amélineau, Signe Christensen-Dalsgaard, Johannis Danielson, Sébastien Descamps, Rune
13012 Dietz[c], Kyle Elliott, Kjell Einar Erikstad, Igor Eulaers[c], Alexei Ezhov, Maria Gavrilo, Elena
13013 Golubova, David Grémillet, Erpur Snær Hansen, Scott Hatch, Dariusz Jakubas, Sacha Kitaysky,
13014 Yann Kolbeinsson, Yuri Krasnov, Magdalene Langset, Sarah Leclaire, Svein-Håkon Lorentsen,
13015 Erlend Lorentzen, Mark L. Mallory, Benjamin Merkel, Flemming Ravn Merkel, Bill
13016 Montevecchi, Anders Mosbech[c], Bergur Olsen, Alisson Patterson, Nicolas Per Huffeldt,
13017 Christine Plumejeaud[a], Isabeau Pratte, Tone Kristin Reiertsen, Heather Renner, Greg Robertson,
13018 Nora Rojek, Marc Romano, Hallvard Strøm, Geir Helge Systad, Torkell Lindberg Tórarinsson,
13019 Alexis Will, Katarzyna Wojczulanis-Jakubas, Paco Bustamante[a], Jérôme Fort[a] (in review) The role
13020 of winter on the mercury contamination of Arctic seabirds: a pan-Arctic approach. OR
13021 Importance of the winter period on the mercury contamination of Arctic alcids - a pan-Arctic
13022 scale study.
13023 Albert, C., M. Renedo, P. Bustamante, and J. Fort. 2019. Using blood and feathers to investigate
13024 large-scale Hg contamination in Arctic seabirds: A review. Environmental Research 177:108588.
13025 Alvarez M del C, Murphy CA, Rose KA, McCarthy ID, Fuiman LA. 2006. Maternal body burdens of
13026 methylmercury impair survival skills of offspring in Atlantic croaker (Micropogonias undulatus).
13027 Aquat Toxicol. doi:10.1016/j.aquatox.2006.09.010.
13028 AMAP, 1998. Arctic Pollution Issues. Arctic Monitoring and Assessment Programme (AMAP), Oslo,
13029 Norway.
13030 AMAP, 2004. AMAP Assessment 2002: Persistent Organic Pollutants in the Arctic. Arctic Monitoring
13031 and Assessment Programme (AMAP, Oslo, Norway.
13032 AMAP, 2011. AMAP Assessment 2011: Mercury in the Arctic. Arctic Monitoring and As- sessment
13033 Programme (AMAP), Oslo, Norway.
13034 AMAP, 2016. AMAP Assessment 2015: Temporal Trends in Persistent Organic Pollutants in the Arctic.
13035 Arctic Monitoring and Assessment Programme (AMAP), Oslo, Norway (pp. vi+71pp).
13036 AMAP, 2018

13037 Amélineau F, Grémillet D, Harding AM, Walkusz W, Choquet R, Fort J. 2019. Arctic climate change
13038 and pollution impact little auk foraging and fitness across a decade. Scientific Reports 9:1014
13039 Amstrup Sc, DeWeaver ET, Douglas DC, Marcot BG, Durner GM, Bitz CM, Bailey DA. 2010.
13040 Greenhouse gas mitigation can reduce sea-ice loss and increase polar bear persistence. Nature
13041 468:955-958.
13042 Angelier F, Chastel O. 2009. Stress, prolactin and parental investment in birds: a review. General and
13043 Comparative Endocrinology 163: 142-148.
13044 Angelier F, Costantini D, Blévin P, Chastel O. 2018. Do glucocorticoids mediate the link between
13045 environmental conditions and telomere dynamics in wild vertebrates? A review. General and
13046 Comparative Endocrinology 256: 99-111
13047 Appelquist, H., Asbirk, S., Drabæk, I., 1984. Mercury monitoring: mercury stability in bird feathers.
13048 Mar. Pollut. Bull. 15, 22–24.
13049 Aschner M, Aschner JL. 1990. Mercury neurotoxicity: mechanisms of blood-brain barrier transport.
13050 Neurosci Biobehav Rev 14:169-176.
13051 Atwood TC, Peacock E, McKinney MA, Lillie K, Wilson R, Douglas DC, Miller S, Terletzky P. 2016.
13052 Rapid environmental change drives increased land use by an arctic marine predator. PLoS One
13053 11:e0155932.
13054 Bardsen JB, Hanssen SA, Bustnes JO. 2018. Multiple stressors: modeling the effect of pollution,
13055 climate, and predation on viability of a sub-arctic marine bird. Ecosphere 9(7) e02342
13056 Barst B.D., Rosabal M, Campbell PGC, Muir DGC, Wang X, Köck G, Drevnick PE. 2016. Subcellular
13057 distribution of trace elements and liver histology of landlocked Arctic char (Salvelinus alpinus)
13058 sampled along a mercury contamination gradient. Environ Pollut. 212.
13059 doi:10.1016/j.envpol.2016.03.003.
13060 Barst BD, Drevnick PE, Muir DCG, Gantner N, Power M, Köck G, Chéhab N, Swanson H, Rigét F,
13061 Basu N. 2019. Screening-level risk assessment of methylmercury for non-anadromous Arctic
13062 char (Salvelinus alpinus). Environ Toxicol Chem. doi:10.1002/etc.4341.
13063 Barst Benjamin D., Rosabal M, Campbell PGC, Muir DGC, Wang X, Köck G, Drevnick PE. 2016.
13064 Subcellular distribution of trace elements and liver histology of landlocked Arctic char
13065 (Salvelinus alpinus) sampled along a mercury contamination gradient. Environ Pollut.
13066 doi:10.1016/j.envpol.2016.03.003.
13067 Basu N, Scheuhammer AM, Rouvinen-Watt K, Grochowina N, Klenavic K, Evans RD, Chan HM.
13068 2006. Methylmercury impairs components of the cholinergic system in captive mink (Mustela
13069 vison). Toxicological Sciences 91: 202-9.
13070 Basu N, Scheuhammer AM, Sonne C, Letcher RJ, Dietz R. 2009. Is dietary mercury of
13071 neurotoxicological concern to wild polar bears (*Ursus maritimus*)? Environ Toxicol Chem
13072 28:133-140.
13073 Beckvar N, Dillon TM, Read LB. 2005. Approaches for linking whole-body fish tissue residues of
13074 mercury or DDT to biological effects thresholds. Environ Toxicol Chem. doi:10.1897/04-
13075 284R.1.
13076 Berlin M. 1986. Mercury. In: Friberg, L., G.F. Nordberg & V.B. Vouk (eds.): Handbook on the
13077 toxicology of metals. Elsevier Science Publishers 1986; Amsterdam. Vol. II: 187-445.
13078 Biesinger, K.E., Anderson, L.E., Eaton, J.G., 1982. Chronic effects of inorganic and organic mercury
13079 on Daphnia magna: Toxicity, accumulation, and loss. Archives of Environmental Contamination
13080 and Toxicology 11, 769-774.
13081 Blackburn EH. 2005. Telomeres and telomerase: their mechanisms of action and the effects of
13082 altering their functions. FEBS Letter 579: 859-862.
13083 Blévin P, Angelier F, Tartu S, Bustamante P, Herzke D, Moe B, Bech C, Gabrielsen GW, Bustnes JO,
13084 Chastel O. 2017. Perfluorinated substances and telomeres in an Arctic seabird: Cross-sectional
13085 and longitudinal approaches. Environmental Pollution 230: 360-367.
13086 Blévin P, Angelier F, Tartu S, Ruault S, Bustamante P, Herzke D, Moe B, Bech C, Gabrielsen GW,
13087 Bustnes JO, Chastel O. 2016. Exposure to oxychlordane is associated with shorter telomeres in
13088 arctic breeding kittiwakes. Science of the Total Environment 563-564: 125-130.
13089 Blévin P, Shaffer SA, Bustamante P, Angelier F, Picard B, Herzke D, Moe B, Gabrielsen GW,
13090 Bustnes JO, Chastel O.2018. Organochlorines, perfluoroalkyl substances, mercury, and egg
13091 incubation temperature in an Arctic seabird: Insights from data loggers. Environmental

13092 Toxicology and Chemistry 37: 2881-2894.
13093 Blévin P, Shaffer SA, Bustamante P, Angelier F, Picard B, Herzke D, Moe B, Gabrielsen GW,
13094 Bustnes JO, Chastel O. 2020. Contaminants, prolactin and parental care in an Arctic seabird:
13095 Contrasted associations of perfluoroalkyl substances and organochlorine compounds with egg-
13096 turning behavior. General and Comparative Endocrinology 291: 113420.
13097 Blévin P, Tartu S, Angelier F, Leclaire S, Bustnes JO, Moe B, Herzke D, Gabrielsen GW, Chastel O.
13098 2014. Integument colouration in relation to persistent organic pollutants and body condition in
13099 arctic breeding black-legged kittiwakes (Rissa tridactyla). Science of the Total Environment 470:
13100 248-254.
13101 Blévin P, Tartu S, Ellis HI, Chastel O, Bustamante P, Parenteau C, Herzke D, Angelier F, Gabrielsen
13102 GW. 2017. Contaminants and energy expenditure in an Arctic seabird: Organochlorine pesticides
13103 and perfluoroalkyl substances are associated with metabolic rate in a contrasted manner.
13104 Environmental Research 157: 118-126.
13105 Bond AL, Hobson KA, Branfireun BA. 2015. Rapidly increasing methyl mercury in endangered Ivory
13106 Gull (Pagophila eburnea) feathers over a 130 year record. Proceeding of the Royal Society B
13107 282:20150032.
13108 Borgmann, U., Norwood, W.P., Clarke, C., 1993. Accumulation, regulation and toxicity of copper, zinc,
13109 lead and mercury in Hyalella azteca. Hydrobiologia 259, 79-89.
13110 Braune BM, Scheuhammer AM, Crump D, Jones S, Porter E, Bond D. 2012. Toxicity of
13111 methylmercury injected into eggs of thick billed murres and arctic terns. Ecotoxicology 21:
13112 2143-2152.
13113 Braune, B. M. 2007. Temporal trends of organochlorines and mercury in seabird eggs from the
13114 Canadian Arctic, 1975-2003. Environmental Pollution 148:599–613.
13115 Braune, B. M., A. J. Gaston, and M. L. Mallory. 2016. Temporal trends of mercury in eggs of five
13116 sympatrically breeding seabird species in the Canadian Arctic. Environmental Pollution
13117 214:124–131. Elsevier Ltd.
13118 Braune, B. M., A. J. Gaston, H. G. Gilchrist, M. L. Mallory, and J. F. Provencher. 2014*a*. A
13119 geographical comparison of mercury in seabirds in the eastern Canadian Arctic. Environment
13120 International 66:92–96. Elsevier B.V.
13121 Braune, B. M., A. J. Gaston, K. A. Hobson, H. G. Gilchrist, and M. L. Mallory. 2014*b*. Changes in
13122 food web structure alter trends of mercury uptake at two seabird colonies in the Canadian Arctic.
13123 Environmental Science and Technology 48:13246–13252.
13124 Braune, B. M., and D. E. Gaskin. 1987. Mercury levels in Bonaparte's gulls (*Larus philadelphia*)
13125 during autumn molt in the Quoddy region, New Brunswick, Canada. Archives of Environmental
13126 Contamination and Toxicology 549:539–549.
13127 Braune, B. M., G. M. Donaldson, and K. a Hobson. 2001. Contaminant residues in seabird eggs from
13128 the Canadian Arctic. Part I. Temporal trends 1975-1998. Environmental Pollution 114:39–54.
13129 Braune, B. M., G. M. Donaldson, and K. A. Hobson. 2002. Contaminant residues in seabird eggs from
13130 the Canadian Arctic. II. Spatial trends and evidence from stable isotopes for intercolony
13131 differences. Environmental Pollution 117:133–145.
13132 Braune, B. M., J. Chételat, M. Amyot, T. Brown, M. Clayden, M. Evans, A. Fisk, A. Gaden, C.
13133 Girard, A. Hare, J. Kirk, I. Lehnherr, R. Letcher, L. Loseto, R. Macdonald, E. Mann, B.
13134 McMeans, D. Muir, N. O'Driscoll, A. Poulain, K. Reimer, and G. Stern. 2015. Mercury in the
13135 marine environment of the Canadian Arctic: Review of recent findings. Science of The Total
13136 Environment 509–510:67–90. Elsevier B.V.
13137 Braune, B. M., M. L. Mallory, and H. G. Gilchrist. 2006. Elevated mercury levels in a declining
13138 population of ivory gulls in the Canadian Arctic. Marine Pollution Bulletin 52:969–987.
13139 Braune, B.M., 1987. Comparison of total mercury levels in relation to diet and molt for nine species
13140 of marine birds. Arch. Environ. Contam. Toxicol. 16, 217–224.
13141 Bridges CC, Zalups RK. 2010. Transport of inorganic mercury and methylmercury in target tissues and
13142 organs. J Toxicol Environ Heal - Part B Crit Rev. doi:10.1080/10937401003673750.
13143 Burnham, J.H., Burnham, K.K., Chumchal, M.M., Welker, J.M. and Johnson, J.A., 2018.
13144 Correspondence between mercury and stable isotopes in high Arctic marine and terrestrial avian
13145 species from northwest Greenland. Polar Biology, 41(7), pp.1475-1491.

13146 Castro de la Guardia L, Derocher AE, Myers PG, Terwisscha van Scheltinga AD, Lunn NJ. 2013. Future
13147 sea ice conditions in Western Hudson Bay and consequences for polar bears in the 21st century.
13148 Global Change Biol 19:2675-2687.
13149 Chételat, J., J. T. Ackerman, C. A. Eagles-Smith, and C. E. Hebert. 2020. Methylmercury exposure in
13150 wildlife: A review of the ecological and physiological processes affecting contaminant
13151 concentrations and their interpretation. Science of the Total Environment 711.
13152 Chételat, J., Poulain, A.J., Amyot, M., Cloutier, L., Hintelmann, H., 2014. Ecological determinants of
13153 methylmercury bioaccumulation in benthic invertebrates of polar desert lakes. Polar Biology 37,
13154 1785-1796.
13155 Chételat, J., Richardson, M.C., Macmillan, G.A., Amyot, M., Poulain, A.J., 2018. Ratio of
13156 methylmercury to dissolved organic carbon in water explains methylmercury bioaccumulation
13157 across a latitudinal gradient from north-temperate to Arctic lakes. Environmental Science and
13158 Technology 52, 79-88.
13159 Costantini D, Blévin P, Herzke D, Moe B, Gabrielsen GW, Bustnes JO, Chastel O. 2018. Higher
13160 plasma oxidative damage and lower plasma antioxidant defences in an Arctic seabird exposed to
13161 longer perfluoroalkyl acids. Environmental Research 168: 278-285.
13162 Costantini D, Meillère A, Carravieri A, Lecomte V, Sorci G, Faivre B, Weimerskirch H, Bustamante
13163 P, Labadie P, Budzinski H, Chastel O. 2014 Oxidative stress in relation to reproduction,
13164 contaminants, gender and age in a long-lived seabird. Oecologia 175: 1107-1116.
13165 Costantini, D. 2014. Oxidative Stress and Hormesis in Evolutionary Ecology and Physiology.
13166 Springer
13167 Cristol, D. A., R. L. Brasso, A. M. Condon, R. E. Fovargue, S. L. Friedman, K. K. Hallinger, A. P.
13168 Monroe, and A. E. White. 2008. The movement of aquatic mercury through terrestrial food webs.
13169 Science 320:335–335.
13170 Cubaynes S, Doherty PF, Schreiber EA, Gimenez O. 2011 To breed or not to breed: a seabird's
13171 response to extreme climatic events. Biology Letters 7: 303-306.
13172 de Jong ME, Scheiber IBR, van den Brink NW, Braun A, Matson KD, Komdeur J, Loonen MJJE.
13173 2017. Indices of stress and immune function in Arctic barnacle goslings (Branta leucopsis) were
13174 impacted by social isolation but not a contaminated grazing environment. Science of the Total
13175 Environment 601-602: 132-141
13176 Debier C, Larondelle Y. 2005. Vitamins A and E: metabolism, roles and transfer to offspring. British
13177 Journal of Nutrition 93: 153-174.
13178 Depew DC, Burgess NM, Anderson MR, Baker R, Bhavsar SP, Bodaly RA (Drew., Eckley CS, Evans
13179 MS, Gantner N, Graydon JA, et al. 2013. An overview of mercury concentrations in freshwater
13180 fish species: A national fish mercury dataset for Canada. Can J Fish Aquat Sci. doi:10.1139/cjfas-
13181 2012-0338.
13182 Desforges JP, Bandoro C, Shehata L, Sonne C, Dietz R, Puryear WB, Runstadler JA. 2018a.
13183 Environmental contaminant mixtures modulate in vitro influenza infection. Sci Total Environ
13184 634:20-28.
13185 Desforges JP, Hall A, McConnell B, Rosing Asvid A, Barber JL, Brownlow A, De Guise S, Eulaers I,
13186 Jepson PD, Letcher RJ, Levin M, Ross PS, Samarra F, Víkingson G, Sonne C, Dietz R. 2018c.
13187 Predicting global killer whale population collapse from PCB pollution. Science 361:1373-1376.
13188 Desforges JP, Levin M, Jasperse L, De Guise S, Eulaers I, Letcher RJ, Acquarone M, Nordøy E, Folkow
13189 LP, Jensen TH, Grøndahl C, Bertelsen MF, St. Leger J, Almunia J, Sonne C, Dietz R. 2017. The
13190 in vitro effects of polar bear and killer whale blubber-derived contaminant 'cocktail' mixtures on
13191 marine mammal immune cells. Environ Sci Technol 51:11431-11439.
13192 Desforges JP, Levin M, Jasperse L, De Guise S, Jensen TH, Grøndahl C, Bertelsen MF, Sonne C, Dietz
13193 R. 2018b. Immune function in Arctic mammals: Natural killer (NK) cell activity in polar bear,
13194 muskox and reindeer. Vet Immun Immunopathol 195:72-75.
13195 Desforges JPW, Sonne C, Levin M, Siebert U, De Guise S, Dietz R. 2016. Immunotoxic effects of
13196 environmental pollutants in marine mammals. Environ Int 86:126-139.
13197 Dietz R, Basu N, Braune B, O'Hara T, Scheuhammer TM, Sonne C, Andersen M, Andreasen C,
13198 Andriashek D, Asmund G, Aubail A, Baagøe H, Born EW, Chan HM, Derocher AE, Grandjean
13199 P, Knott K, Kirkegaard M, Lunn N, Messier F, Obbard M, Olsen MT, Peacock E, Renzoni A,

13200 Rigét F, Skaare JU, Stern G, Stirling I, Taylor M, Wiig Ø, Aars J. 2013. What are the
13201 toxicological effects of mercury in Arctic biota? Sci Total Environ 443:775-790.
13202 Dietz R, C Sonne, J-P Desforges, I Eulaers, A Rosing Asvid, R. Letcher, P. Jepson 2019. Killer whales
13203 calls for further protection. Environment International 126: 443-444.
13204 https://doi.org/10.1016/j.envint.2019.02.060
13205 Dietz R, K Gustavson, C Sonne, J-P Desforges, FF Rigét, V Pavlova, MA McKinney, RJ. Letcher 2015.
13206 Physiologically-based pharmacokinetic modelling of immune, reproductive and carcinogenic
13207 effects from contaminant exposure in polar bears (*Ursus maritimus*) across the Arctic.
13208 Environmental Research 140: 45–55.
13209 Dietz R, R Letcher, J-P Desforges, I Eulaers, C Sonne, S Wilson, E Andersen-Ranberg, N Basu, BD
13210 Barst, JO Bustnes, J Bytingsvik, TM Ciesielski, PE Drevnick, GW Gabrielsen, A Haarr, K
13211 Hylland, BM Jenssen, M Levin, MA McKinney, RD Nørregaard, KE Pedersen, J Provencher, B
13212 Styrishave, S Tartu, J Aars, JT Ackerman, A Rosing-Asvid, R Barrett, A Bignert, EW Born, M
13213 Branigan, B Braune, CE Bryant, M Dam, CA Eagles-Smith, M Evans, TJ Evans, AT Fisk, M
13214 Gamberg, K Gustavson, CA Hartman, B Helander, MP Herzog, PF Hoekstra, M Houde, K
13215 Hoydal, AK Jackson, , J Kucklickt , E Lie, L Loseto, ML Mallory, C Miljeteig, A Mosbech,
13216 DCG Muir, ST Nielsen, E Peacock, S Pedro, SH Peterson, A Polder, FF Rigét, P Roach, H
13217 Saunes, M-HS. Sinding, M, JU. Skaare, J Søndergaard, G Stenson, G Stern, G Treu, SS Schuurtt,
13218 G Víkingsson 2019. Current State of Knowledge on Biological Effects from Contaminants on
13219 Arctic Wildlife and Fish. Science of the Total Environment 696: 133792, 1-39.
13220 Dietz, R. F. Riget and E.W. Born 2000b. Geographical differences of zinc, cadmium, mercury and
13221 selenium in polar bears (*Ursus maritimus*) from Greenland. The Science of the Total
13222 Environment 245: 25-48.
13223 Dietz, R., J. Pacyna, D.J. Thomas, G. Asmund, V. Gordeev, P. Johansen, V. Kimstach, L. Lockhart,
13224 S.L. Pfirman, F. F. Riget, G. Shaw, R. Wagemann, M.White 1998a. Chapter 7: Heavy metals.
13225 In: AMAP Assessment Report: Arctic Pollution Issues. Arctic Monitoring and Assessment
13226 Programme. Oslo, Norway: 373-524.
13227 Dietz, R.; Riget, F.; Born, E.W. 2000a. An assessment of selenium to mercury in Greenland marine
13228 animals. The Science of the Total Environment 245: 15 – 24.
13229 Dillon T, Beckvar N, Kern J. 2010. Residuebased mercury dose-response in fish: An analysis using
13230 lethalityequivalent test endpoints. Environ Toxicol Chem. doi:10.1002/etc.314.
13231 Drevnick PE, Sandheinrich MB, Oris JT. 2006. Increased ovarian follicular apoptosis in fathead
13232 minnows (Pimephales promelas) exposed to dietary methylmercury. Aquat Toxicol.
13233 doi:10.1016/j.aquatox.2006.05.007.
13234 Drevnick PE, Sandheinrich MB. 2003. Effects of dietary methylmercury on reproductive endocrinology
13235 of fathead minnows. Environ Sci Technol. doi:10.1021/es034252m.
13236 Durner GM, Douglas DC, Albeke SE, Whiteman JP, Amstrup SC, Richardson E, Wilson RR, Ben-
13237 David M 2017. Increased Arctic sea ice drift alters adult female polar bear movements and
13238 energetics. Global Change Bio, 23:3460-3473.
13239 Eagles-Smith CA, Ackerman JT, Willacker JJ, Tate MT, Lutz MA, Fleck JA, Stewart AR, Wiener JG,
13240 Evers DC, Lepak JM, et al. 2016. Spatial and temporal patterns of mercury concentrations in
13241 freshwater fish across the Western United States and Canada. Sci Total Environ.
13242 doi:10.1016/j.scitotenv.2016.03.229.
13243 Eagles-Smith, C. A., J. T. Ackerman, T. L. Adelsbach, J. Y. Takekawa, A. K. Miles, and R. A.
13244 Keister. 2008. Mercury correlations among six tissues for four waterbird species breeding in San
13245 Francisco Bay, California, USA. Environmental Toxicology and Chemistry 27:2136–2153.
13246 Eckbo N, Le Bohec C, Planas-Bielsa V, Warner NA, Schull Q, Herzke D, Zahn S, Haarr A,
13247 Gabrielsen GW, Borgå K. 2019. Individual variability in contaminants and physiological status
13248 in a resident Arctic seabird species. Environmental Pollution 249: 191-199.
13249 Egevang, C., Stenhousec, Iain J., Phillips, R.A., Petersene, A., Fox, J.W., Silkd, J.R.D., 2010.
13250 Tracking of Arctic terns Sterna paradisaea reveals longest animal migration. Proceedings of the
13251 National Academy of Sciences 107 (5), 2078–2081.
13252 Erikstad KE, Sandvik H., Reiertsen TK, Bustnes JO, Strøm H. 2013. Persistent organic pollution in a
13253 high-Arctic top predator: sex-dependent thresholds in adult survival. Proceedings of the Royal
13254 Society B 280:20131483.

13255 Evers DC, Savoy LJ, Desorbo CR, Yates DE, Hanson W, Taylor KM, Siegel LS, Cooley JH, Bank
13256 MS, Major A, Munney K, Mower BF, Vogel HS, Schoch N, Pokras M, Goodale MW, Fair J.
13257 2008 Adverse effects from environmental mercury loads on breeding common loons.
13258 Ecotoxicology 17: 69-81.
13259 Evers et al., 2016).
13260 Evers, D., J. Kaplan, M. Meyer, P. Reaman, W. Braselton, A. Major, N. Burgess, and A. M.
13261 Scheuhammer. 1998. Geographic trend in mercury measured in common loon feathers and blood.
13262 Environmental Toxicology and Chemistry 17:173–183.
13263 Fallacara DM, Halbrook RS, French JB. 2011. Toxic effects of dietary methylmercury on immune
13264 function and hematology in American kestrels (Falco sparverius). Environmental Toxicology and
13265 Chemistry 30: 1320-1327.
13266 Fenstad AA, Jenssen BM, Moe B, Hanssen SA, Bingham C, Herzke D, Bustnes JO, Krokje A. 2016.
13267 DNA double-strand breaks in incubating female common eiders (Somateria mollissima):
13268 Comparison between a low and a high polluted area. Environmental Research 151: 297-303.
13269 Fenstad AA, Moody AJ, Öst M, Jaatinen K, Bustnes JO, Moe B, Hanssen SA, Gabrielsen KM,
13270 Herzke D, Lierhagen S, Jenssen BM, Krøkje Å. 2016. Antioxidant Responses in Relation to
13271 Persistent Organic Pollutants and Metals in a Low- and a High-Exposure Population of Seabirds.
13272 Environmental Science and Technology 50: 4817-4825
13273 Fisher, N.S., Hook, S.E., 2002. Toxicology tests with aquatic animals need to consider the trophic
13274 transfer of metals. Toxicology 181-182, 531-536.
13275 Flanders, J.R., Long, G., Reese, B., Grosso, N.R., Clements, W., Stahl, R.G., 2019. Assessment of
13276 potential mercury toxicity to native invertebrates in a high-gradient stream. Integrated
13277 Environmental Assessment and Management 15, 374-384.
13278 Fleishman, A. B., R. A. Orben, N. Kokubun, A. Will, R. Paredes, J. T. Ackerman, A. Takahashi, A. S.
13279 Kitaysky, and S. A. Shaffer. 2019. Wintering in the Western Subarctic Pacific Increases Mercury
13280 Contamination of Red-Legged Kittiwakes. Environmental Science and Technology 53:13398–
13281 13407.
13282 Fort J, Lacoue-Labarthe T, Nguyen Hanh L, Boué A, Spitz J & Bustamante P (2015) Mercury in
13283 wintering seabirds, an aggravating factor to winter wrecks? Science of the Total Environment,
13284 527-528C:448-454
13285 Fort J, Robertson GJ, Grémillet D, Traisnel G, Bustamante P. 2014. Spatial ecotoxicology: Migratory
13286 arctic seabirds are exposed to mercury contamination while overwintering in the northwest
13287 Atlantic. Environmental Science & Technology 48: 11560-11567.
13288 Fort, J., D. Grémillet, G. Traisnel, F. Amélineau, and P. Bustamante. 2016. Does temporal variation of
13289 mercury levels in Arctic seabirds reflect changes in global environmental contamination, or a
13290 modification of Arctic marine food web functioning? Environmental Pollution 211:382–388.
13291 Foster, K.L., Stern, G.A., Pazerniuk, M.A., Hickie, B., Walkusz, W., Wang, F., MacDonald, R.W.,
13292 2012. Mercury biomagnification in marine zooplankton food webs in Hudson Bay.
13293 Environmental Science and Technology 46, 12952-12959.
13294 Fox, A.L., Trefry, J.H., Trocine, R.P., Dunton, K.H., Lasorsa, B.K., Konar, B., Ashjian, C.J., Cooper,
13295 L.W., 2017. Mercury biomagnification in food webs of the northeastern Chukchi Sea, Alaskan
13296 Arctic. Deep-Sea Research Part II: Topical Studies in Oceanography 144, 63-77.
13297 Frederick P, Jayasena N. 2011. Altered pairing behaviour and reproductive success in white ibises
13298 exposed to environmentally relevant concentrations of methylmercury. Proceedings of the Royal
13299 Society B 278: 1851-1857.
13300 Gajdosechova Z, Brownlow A, Cottin NT, Fernandes M, Read FL, Urgast DS, Raab A, Feldmann J,
13301 Krupp EM. Possible link between Hg and Cd accumulation in the brain of long-finned pilot
13302 whales (*Globicephala melas*). Sci Total Environ. 2016 Mar 1;545-546:407-13. doi:
13303 10.1016/j.scitotenv.2015.12.082. Epub 2015 Dec 31.
13304 Gajdosechova Z, Lawan MM, Urgast DS, Raab A, Scheckel KG, Lombi E, Kopittke PM, Loeschner K,
13305 Larsen EH, Woods G, Brownlow A, Read FL, Feldmann J, Krupp EM 2016. In vivo formation
13306 of natural HgSe nanoparticles in the liver and brain of pilot whales. Sci Rep. 28;6:34361.
13307 Gajdosechova Zuzana, Zoltan Mester, Jorg Feldmann, Eva M. Krupp. 2018. The role of selenium in
13308 mercury toxicity e Current analytical techniques and future trends in analysis of selenium and
13309 mercury interactions in biological matrices. Trends in Analytical Chemistry 104 (2018) 95e109.

13310 Gibson LA, Lavoie RA, Bissegger S, Campbell LM, Langlois VS. 2014. A positive correlation
13311 between mercury and oxidative stress-related gene expression (GPX3 and GSTM3) is measured
13312 in female double-crested cormorant blood. Ecotoxicology 23: 1004-1014.
13313 Gimbert, F., Geffard, A., Guédron, S., Dominik, J., Ferrari, B.J.D., 2016. Mercury tissue residue
13314 approach in Chironomus riparius: Involvement of toxicokinetics and comparison of subcellular
13315 fractionation methods. Aquatic Toxicology 171, 1-8.
13316 Goutte A, Barbraud C, Herzke D, Bustamante P, Angelier F, Tartu S, Clément-Chastel C, Moe B,
13317 Bech C, Gabrielsen GW, Bustnes JO, Chastel O. 2015. Survival rate and breeding outputs in a
13318 high Arctic seabird exposed to legacy persistent organic pollutants and mercury. Environmental
13319 Pollution 200: 1-9.
13320 Goutte A, Barbraud C, Meillère A, Carravieri A, Bustamante P, Labadie P, Budzinski H, Delord K,
13321 Cherel Y, Weimerskirch H, Chastel O. 2014b. Demographic consequences of heavy metals and
13322 persistent organic pollutants in a vulnerable long-lived bird, the wandering albatross. Proceedings
13323 of the Royal Society B 281:20133313.
13324 Goutte A, Bustamante P, Barbraud C, Delord K, Weimerskirch H, Chastel O. 2014a. Demographic
13325 responses to mercury exposure in two closely related Antarctic top predators. Ecology 95: 1075-
13326 1086.
13327 Goutte A, Kriloff M, Weimerskirch H, Chastel O. 2011. Why do some adult birds skip breeding? A
13328 hormonal investigation in a long-lived bird. Biology Letters 7: 790-792.
13329 Goutte A, Meillère A, Barbraud C, Budzinski H, Labadie P, Peluhet L, Weimerskirch H, Delord K,
13330 Chastel O. 2018. Demographic, endocrine and behavioral responses to mirex in the South polar
13331 skua. Science of the Total Environment 631-632: 317-325
13332 Haarr A, Hylland K, Eckbo N, Gabrielsen GW, Herzke D, Bustnes JO, Blevin P, Chastel O, Moe B,
13333 Hanssen SA, Sagerup K, Borgå K. 2017. DNA damage in arctic seabirds: baseline, sensitivity to
13334 a genotoxic stressor and association to organohalogen contaminants: Genotoxicity and
13335 organohalogens in Arctic avian wildlife. Environmental Toxicology and Chemistry
13336 37:10.1002/etc.4035.
13337 Hammerschmidt CR, Sandheinrich MB, Wiener JG, Rada RG. 2002. Effects of dietary methylmercury
13338 on reproduction of fathead minnows. Environ Sci Technol. doi:10.1021/es011120p.
13339 Harada M. 1995. Minamata disease: Methylmercury poisoning in Japan caused by environmental
13340 pollution. Crit Rev Toxicol. doi:10.3109/10408449509089885.
13341 Hargreaves AL, Whiteside DP, Gilchrist G. 2010. Concentrations of 17 elements, including mercury,
13342 and their relationship to fitness measures in arctic shorebirds and their eggs. Science of the Total
13343 Environment. 408: 3153-3161
13344 Hartman, CA, JT Ackerman, and MP Herzog. 2019. Mercury exposure and altered parental nesting
13345 behavior in a wild songbird. Environmental Science and Technology 53:5396-5405.
13346 Hawkes WC1, Keim NL 2003. Dietary selenium intake modulates thyroid hormone and energy
13347 metabolism in men. J Nutr 133:3443-3448.
13348 Heinz, G. H., D. J. Hoffman, J. D. Klimstra, K. R. Stebbins, S. L. Kondrad, and C. A. Erwin. 2009.
13349 Species differences in the sensitivity of avian embryos to methylmercury. Archives of
13350 Environmental Contamination and Toxicology 56:129–138.
13351 Helgason LB, Verreault J, Braune BM, Borgå K, Primicerio R, Jenssen BM, Gabrielsen GW. 2010.
13352 Relationship between persistent halogenated organic contaminants and TCDD toxic equivalents
13353 on EROD activity and retinoid and thyroid hormone status in northern fulmars. Science of the
13354 Total Environment 408: 6117-6123.
13355 Herring G, Ackerman JT, Eagles-Smith CA. 2010. Embryo malposition as a potential mechanism for
13356 mercury-induced hatching failure in bird eggs. Environmental Toxicology and Chemistry 29:
13357 1788-1794.
13358 Herring G, Ackerman JT, Herzog MP. 2012. Mercury exposure may suppress baseline corticosterone
13359 levels in juvenile birds. Environmental Science and Technology 46: 6339-6346.
13360 Hoffman DJ, Eagles-Smith CA, Ackerman JT, Adelsbach TL, Stebbins KR. 2011. Oxidative stress
13361 response of Forster's terns (Sterna forsteri) and Caspian terns (Hydroprogne caspia) to mercury
13362 and selenium bioaccumulation in liver, kidney, and brain. Environmental Toxicology and
13363 Chemistry 30: 920-929.
13364 Honda K, Min BY, Tatsukawa R. 1986. Distribution of heavy metals and their age-related changes in

13365 the Eastern Great White Egret, Egretta alba modesta, in Korea. Arch Environ Contam Toxicol
13366 15:185–197.
13367 Hook, S.E., Fisher, N.S., 2002. Relating the reproductive toxicity of five ingested metals in calanoid
13368 copepods with sulfur affinity. Marine Environmental Research 53, 161-174.
13369 Humann-Guilleminot S, Blévin P, Azou-Barré A, Yacoumas A, Gabrielsen GW, Chastel O,
13370 Helfenstein F. 2018. Sperm collection in Black-legged Kittiwakes and characterization of sperm
13371 velocity and morphology. Avian Research 9:24: DOI:10.1186/s40657-018-0117-6.
13372 Jenssen BM. 2006. Endocrine-disrupting chemicals and climate change: A worst-case combination for
13373 Arctic marine mammals and seabirds? Environmental Health Perspectives 114: 76-80.
13374 Jenssen et al., 2015;
13375 Kahilainen, K.K., Thomas, S.M., Nystedt, E.K.M., Keva, O., Malinen, T., Hayden, B., 2017.
13376 Ecomorphological divergence drives differential mercury bioaccumulation in polymorphic
13377 European whitefish (*Coregonus lavaretus*) populations of subarctic lakes. Science of the Total
13378 Environment 599-600, 1768-1778.
13379 Khayrallah, N.H., 1985. The tolerance of Bathyporeia pilosa Lindstrom (Amphipoda: *Haustoriidae*) to
13380 organic and inorganic salts of mercury. Marine Environmental Research 15, 137-151.
13381 Kutz S. 2009. The Arctic as a model for anticipating, preventing, and mitigating climate change impacts
13382 on host-parasite interactions. Vet Parasitol 163:217-228.
13383 Laidre, K. L., H. Stern, K. M. Kovacs, L. Lowry, S. E. Moore, E. V Regehr, S. H. Ferguson, et al. 2015.
13384 Arctic marine mammal population status, sea ice habitat loss, and conservation recommendations
13385 for the 21st century. Conservation Biology 00:1–14.
13386 Lee MM, Jaspers VLB, Gabrielsen GW, Jenssen BM, Ciesielski TM, Mortensen ÅK, Lundgren ST,
13387 Waugh CA. 2020. Evidence of avian influenza virus in seabirds breeding on a Norwegian high-
13388 Arctic archipelago. BMC Veterinary Research 16:48
13389 Letcher RJ, Bustnes JO, Dietz R, Jenssen BM, Jørgensen EH, Sonne C, Verreault J, Vijayan MM,
13390 Gabrielsen GW. 2010. Effects Assessment of Persistent Organohalogen Contaminants in Arctic
13391 Wildlife and Fish. Sci Total Environ 408:2995-3043.
13392 Lewis CA, Cristol DA, Swaddle JP, Varian-Ramos CW, Zwollo P. 2013. Decreased immune response
13393 in zebra finches exposed to sublethal doses of mercury. Archives of Environmental
13394 Contamination and Toxicology 64: 327-336
13395 Lewis SA, Becker PH, Furness RW. 1993. Mercury levels in eggs, tissues, and feathers of herring
13396 gulls Larus argentatus from the German Waddden Sea coast. Environ Pollut 80:293–299.
13397 Lindgren, E., Gustafson, R., 2001. Tick-borne encephalitis in Sweden and climate change. Lancet
13398 358:16-18.
13399 Lucia M, Verboven N, Strøm H, Miljeteig C, Gavrilo MV, Braune BM, Boertmann D & Gabrielsen
13400 GW (2015) Circumpolar contamination in eggs of the high-arctic ivory gull Pagophila eburnea.
13401 Environmental Toxicology and Chemistry.
13402 Macdonald et al., 2003,
13403 Macdonald et al., 2005;
13404 Marcogliese DJ, Pietrock M. 2011. Combined effects of parasites and contaminants on animal health:
13405 parasites do matter. Trends in Parasitology 27: 123-130.
13406 McCall AG, Derocher AE, Lunn AJ. 2015. Home range distribution of polar bears in western Hudson
13407 Bay. Polar Biol 38:343-355.
13408 McCloskey, M., S. Robinson, P. A. Smith, and M. Forbes. 2013. Mercury concentration in the eggs of
13409 four Canadian Arctic-breeding shorebirds not predicted based on their population statuses.
13410 SpringerPlus 2:567.
13411 McKinney et al., 2015
13412 McKinney MA, Iverson SJ, Fisk AT, Sonne C, Rigét FF, Letcher RJ, Arts MT, Born EW, Rosing-Asvid
13413 A, Rune Dietz. 2013. Global change effects on the long-term feeding ecology and contaminant
13414 exposures of East Greenland polar bears. Global Change Biol 19:2360-2372.
13415 McMeans, B.C., Arts, M.T., Fisk, A.T., 2015. Impacts of food web structure and feeding behavior on
13416 mercury exposure in Greenland Sharks (*Somniosus microcephalus*). Science of the Total
13417 Environment 509-510, 216-225.
13418 Melnes M, Gabrielsen GW, Herzke D, Sagerup K, Jenssen BM. 2017. Dissimilar effects of
13419 organohalogenated compounds on thyroid hormones in glaucous gulls. Environmental Research

158: 350–357.
Miljeteig C, Gabrielsen GW, Strom H, Gavrilo MV, Lie E, Jenssen BM. 2012. Eggshell thinning and decreased concentrations of vitamin E are associated with contaminants in eggs of ivory gulls. Science of the Total Environment 431: 92-99.
Molnár PK, Derocher AE, Klanjscek T, Lewis MA. 2011. Predicting climate change impacts on polar bear litter size. Nat Commun 2:186.
Norris DR. 2005. Carry-over effects and habitat quality in migratory populations. Oikos 109: 178-186.
Notz D, Stroeve J. 2016. Observed Arctic sea-ice loss directly follows anthropogenic CO2 emission. Science 354:747-750.
Outridge et al. 2011
Outridge et al., 2011a,
Outridge et al., 2011b
Øverjordet, I.B., Altin, D., Berg, T., Jenssen, B.M., Gabrielsen, G.W., Hansen, B.H., 2014. Acute and sub-lethal response to mercury in Arctic and boreal calanoid copepods. Aquatic Toxicology 155, 160-165.
Pagano AM, Durner GM, Rode KD, Atwood TC, Atkinson SN, Peacock E, Costa DP, Owen MA, Williams TM. 2018. High-energy, high-fat lifestyle challenges an Arctic apex predator, the polar bear. Science. 2018 Feb 2;359(6375):568-572.
Peck, L.E., Gilchrist, H.G., Mallory, C.D., Braune, B.M. and Mallory, M.L., 2016. Persistent organic pollutant and mercury concentrations in eggs of ground-nesting marine birds in the Canadian high Arctic. Science of the Total Environment, 556, pp.80-88.
Pedro, S., Fisk, A.T., Ferguson, S.H., Hussey, N.E., Kessel, S.T., McKinney, M.A., 2019. Limited effects of changing prey fish communities on food quality for aquatic predators in the eastern Canadian Arctic in terms of essential fatty acids, methylmercury and selenium. Chemosphere 214, 855-865.
Pelletier, E., 1988. Acute toxicity of some methylmercury complexes to *Mytilus edulis* and lack of selenium protection. Marine Pollution Bulletin 19, 213-219.
Perkins, M. 2018. "Exposure Science to Investigate Factors Influencing Mercury Concentrations in Non-piscivorous Birds" https://escholarship.mcgill.ca/concern/theses/hq37vq93w
Perkins, M., L. Ferguson, R. B. Lanctoct, I. J. Stenhouse, S. Kendall, S. Brown, H. R. R. Gates, J. O. Hall, K. Regan, D. C. D. C. Evers, R. B. Lanctot, I. J. Stenhouse, S. Kendall, S. Brown, H. R. R. Gates, J. O. Hall, K. Regan, D. C. D. C. Evers, R. B. Lanctoct, I. J. Stenhouse, S. Kendall, S. Brown, H. R. R. Gates, J. O. Hall, K. Regan, and D. C. D. C. Evers. 2016. Mercury exposure and risk in breeding and staging Alaskan shorebirds. The Condor 118:571–582.
Peterson SA, Van Sickle J, Hughes RM, Schacher JA, Echols SF. 2004. A biopsy procedure for determining filet and predicting whole-fish mercury concentration. Arch Environ Contam Toxicol. doi:10.1007/s00244-004-0260-4.
Peterson, S. H., J. T. Ackerman, M. Toney, and M. P. Herzog. 2019. Mercury concentrations vary within and among individual bird feathers: A critical evaluation and guidelines for feather use in mercury monitoring programs. Environmental Toxicology and Chemistry 38:1164–1187. John Wiley & Sons, Ltd.
Peterson, S.A., Van Sickle, J., Hughes, R.M., Schacher, J.A., and Echols, S.F. 2004. A biopsy procedure for determining filet and predicting whole-fish mercury concentration. Arch. Environ. Contam. Toxicol. 48, 99–107. doi: 10.1007/s00244-004-0260-4. PMID: 1565781
Price SJ, Leung WTM, Owen CJ, Puschendorf R, Sergeant C, Cunningham AA, Balloux F, Garner TWJ, Nichols RA. 2019. Effects of historic and projected climate change on the range and impacts of an emerging wildlife disease. Glob Change Biol 25:2648-2660.
Provencher JF, Forbes MR, Hennin HL, Love OP, Braune BM, Mallory ML, Gilchrist HG. 2016a. Implications of mercury and lead concentrations on breeding physiology and phenology in an Arctic bird. Environmental Pollution 218: 1014-1022.
Provencher JF, Gilchrist HG, Mallory ML, Mitchell GW, Forbes MR. 2016b. Direct and indirect causes of sex differences in mercury concentrations and parasitic infections in a marine bird. Science of the Total Environment 551–552: 506–512
Provencher, J. F., M. L. Mallory, B. M. Braune, M. R. Forbes, and H. G. Gilchrist. 2014. Mercury and

13475 marine birds in Arctic Canada: effects, current trends, and why we should be paying closer
13476 attention. ENVIRONMENTAL REVIEWS 22:244–255.
13477 Pyle, P. 2008. Identification Guide to North American Birds Part II. Slate Creek Press, Point Reyes
13478 Station, California, USA.
13479 Pyle, P., J. F. Saracco, and D. F. DeSante. 2018. Evidence of widespread movements from breeding to
13480 molting grounds by North American landbirds. Auk 135:506–520.
13481 Raymond LJ, Ralston NV. 2004. Mercury: selenium interactions and health implications. SMDJ 7:72-
13482 77.
13483 Rigét et al. 2005. Science of the Total Environment 351–352 (2005) 312– 322.
13484 Rigét FF, Braune B, Bignert A, Wilson S, Aars J, Andersen M, Asmund G, Aubail A, Dam M, Dietz
13485 R, Evans M, Evans T, Gamberg M, Gantner N, Green N, Gunnlaugsdóttir H, Kannan K, Letcher
13486 RJ, Muir D, Ólafsdóttir K, Renzoni A, Roach P, Sonne C, Stern G, Wiig Ø 2011. Temporal trends
13487 of Hg in Arctic biota, an update. Sci Total Environ. 409:3520–3526.
13488 Ronald, K., Tessaro, S.V., Uthe, J.F., Freeman, H.C., Frank, R., 1977. Methylmercury poisoning in the
13489 harp seal (*Pagophilus groenlandicus*). Sci. Total Environ. 8, 1–11.
13490 Routti et al. 2011. J. Environ. Monit., 2011, 13, 2260.
13491 Routti H, Atwood T, Bechshøft T, Boltunov A, Ciesielski T, Desforges JP, Dietz R, Gabrielsen GW,
13492 Jenssen BM, Letcher RJ, McKinney M, Morris A, Rigét FF, Sonne C, Styrishave B, Tartu S
13493 (2019): State of knowledge on current exposure, fate and potential health effects of contaminants
13494 in polar bears from the circumpolar Arctic. Sci Total Environ 664:1063-1083.
13495 Routti H, Letcher RJ, Born EW, Branigan M, Dietz R, Evans TJ, Fisk AT, Peacock E, Sonne C 2011.
13496 Spatio-temporal trends of selected trace elements in liver tissue from polar bears (*Ursus*
13497 *maritimus*) from Alaska, Canada and Greenland. J Environ Monitor 13: 2260-2267.
13498 Routti H, Lille-Langøy R, Berg MK, Fink T, Harju M, Kristiansen K, Rostkowski P, Rusten M, Sylte
13499 I, Øygarden L, Goksøyr A. 2016a. Environmental chemicals modulate polar bear (*Ursus*
13500 *maritimus*) peroxisome proliferator-activated receptor gamma (PPARG) and adipogenesis in
13501 vitro. Environ Sci Technol 50:10708-10720.
13502 Routti, Hi; Letcher, RJ; Born, EW; Branigan, M; Dietz, R; Evans, TJ; McKinney MA; Peacock, E;
13503 Sonne, C 2012. Influence of carbon and lipid sources on variation of mercury and other trace
13504 elements in polar bears (*Ursus maritimus*). Environmental Toxicology and Chemistry 31, 12,
13505 2739–2747.
13506 Sandheinrich MB, Bhavsar SP, Bodaly RA, Drevnick PE, Paul EA. 2011. Ecological risk of
13507 methylmercury to piscivorous fish of the Great Lakes region. Ecotoxicology.
13508 doi:10.1007/s10646-011-0712-3.
13509 Sandheinrich MB, Miller KM. 2006. Effects of dietary methylmercury on reproductive behavior of
13510 fathead minnows (Pimephales promelas). Environ Toxicol Chem. doi:10.1897/05-641R.1.
13511 Sandheinrich MB, Wiener JG. 2011. Methylmercury Freshwater Fish : Recent Advances in Assessing
13512 Toxicity and Environmentally Relevant Exposures. Environ Contam Biota.
13513 Schartup et al., 2019. Climate change and overfishing increase neurotoxicant in marine predators.
13514 Nature 572:648-650.
13515 Scheuhammer A, Braune B, Chan HM, Frouin H, Krey A, Letcher R, Loseto L, Noël M, Ostertag S,
13516 Ross P, Wayland M. 2015. Recent progress on our understanding of the biological effects of
13517 mercury in fish and wildlife in the Canadian Arctic. Science of the Total Environment 509: 91-
13518 103.
13519 Scheuhammer AM, Basu N, Evers DC, Heinz GH, Sandheinrich M, Bank MS. 2012. Toxicology of
13520 mercury in fish and wildlife: recent advances. In: Bank MS, editor. Mercury in the Environment:
13521 Pattern and Process. Berkley: University of California Press.
13522 Scheuhammer AM, Meyer MW, Sandheinrich MB, Murray MW. 2007. Effects of environmental
13523 methylmercury on the health of wild birds, mammals, and fish. In: Ambio.
13524 Scheuhammer, A. M., M. W. Meyer, M. B. Sandheinrich, and M. W. Murray. 2007. Effects of
13525 environmental methylmercury on the health of wild birds, mammals, and fish. Ambio 36:12–18.
13526 Sletten S, Bourgeon S, Badsen BJ, Herzke D, Criscuolo F, Massemin S, Zahn S, Johnsen TV, Bustnes
13527 JO. 2016. Organohalogenated contaminants in white-tailed eagle (Haliaeetus albicilla) nestlings:
13528 An assessment of relationships to immunoglobulin levels, telomeres and oxidative stress. Science
13529 of the Total Environment 539: 337-349

13530 Sonenshine DE, Mather TN. 1994. Ecological Dynamics of Tick-Borne Zoonoses. Oxford University
13531 Press.
13532 Sonne C, Dyck M, Rigét FF, Bech-Jensen JE, Hyldstrup L, Letcher RJ, Gustavson K, Gilbert MTP,
13533 Dietz R. 2015. Penile density and globally used chemicals in Canadian and Greenland polar
13534 bears. Environ Res 137:287-291.
13535 Sonne C, Jepson PD, Desforges JP, Alstrup AKO, Olsen MT, Eulaers I, Hansen M, Letcher RJ,
13536 McKinney MA, Dietz R. 2018. Pollution threatens toothed whales. SCIENCE 361:1208.
13537 Sonne C. 2010). Health effects from long-range transported contaminants in Arctic top predators: An
13538 integrated review based on studies of polar bears and relevant model species. Environment
13539 International 36:461-491.
13540 Stirling I, Ross JE 2011. Observations of cannibalism by polar bears (*Ursus maritimus*) on summer and
13541 autumn sea ice at Svalbard, Norway. Arctic 64:478-482.
13542 Sun, J., Bustnes, J.O., Helander, B., Bårdsen, B.J., Boertmann, D., Dietz, R., Jaspers, V.L., Labansen,
13543 A.L., Lepoint, G., Schulz, R. and Søndergaard, J., 2019. Temporal trends of mercury differ
13544 across three northern white-tailed eagle (Haliaeetus albicilla) subpopulations. Science of the total
13545 environment, 687, pp.77-86.
13546 Tan SW, Meiller JC, Mahaffey KR. 2009. The endocrine effects of mercury in humans and wildlife.
13547 Critical Reviews in Toxicology 39: 228-269.
13548 Tartu S, Bustamante P, Angelier F, Lendvai AZ, Moe B, Blévin P, Bech C, Gabrielsen GW, Bustnes
13549 JO, Chastel O. 2016. Mercury exposure, stress and prolactin secretion in an Arctic seabird: An
13550 experimental study. Functional Ecology, 30:596-604.
13551 Tartu S, Goutte A, Bustamante P, Angelier F, Moe B, Clément-Chastel C, Bech C, Gabrielsen GW,
13552 Bustnes JO, and Chastel O .2013. To breed or not to breed: endocrine response to mercury
13553 contamination by an Arctic seabird. Biology Letters 9
13554 Tartu S, Lendvai ÁZ, Blévin P, Herzke D, Bustamante P, Moe B, Gabrielsen GW, Bustnes JO,
13555 Chastel O. 2015b. Increased adrenal responsiveness and delayed hatching date in relation to
13556 polychlorinated biphenyl exposure in Arctic-breeding black-legged kittiwakes (Rissa tridactyla).
13557 General and Comparative Endocrinology 219: 165-172.
13558 Tartu S, Lille-Langoy R, Storseth TR, Bourgeon S, Brunsvik A, Aars J, Goksoyr A, Jenssen BM, Polder
13559 A, Thiemann GW, Torget V, Routti, H. 2017a. Multiple stressor effects in an apex predator:
13560 combined influence of pollutants and sea ice decline on lipid metabolism in polar bears. Sci Rep
13561 7:16487.
13562 Tartu S, Wingfield JC, Bustamante P, Angelier F, Budzinski H, Labadie P, Bustnes JO, Weimerskirch
13563 H, Chastel O. 2015a. Corticosterone, prolactin and egg neglect behaviour in relation to mercury
13564 and legacy POPs in a long-lived Antarctic bird. Science of the Total Environment, 505, 180–188.
13565 Tartu, S., Bustamante, P., Goutte, A., Cherel, Y., Weimerskirch. H., Bustnes J.O., Chastel, O. 2014.
13566 Age-related mercury contamination and relationship with luteinizing hormone in a long-lived
13567 Antarctic bird. PLoS ONE, 9(7): e103642
13568 Taylor, GT, JT Ackerman, and SA Shaffer. 2018. Egg turning behavior and incubation temperature in
13569 Forster's terns in relation to mercury contamination. PLoS ONE 13(2):e0191390.
13570 Thompson, D.R., Bearhop, S., Speakman, J.R. and Furness, R.W., 1998. Feathers as a means of
13571 monitoring mercury in seabirds: insights from stable isotope analysis. Environmental Pollution,
13572 101(2), pp.193-200.
13573 Tinggi U. 2003. Essentiality and toxicity of selenium and its status in Australia: a review. Toxicol Lett
13574 137:103-110.
13575 Tsui, M.T.K., Wang, W.X., 2004. Maternal transfer efficiency and transgenerational toxicity of
13576 methylmercury in Daphnia magna. Environmental Toxicology and Chemistry 23, 1504-1511.
13577 Tsui, M.T.K., Wang, W.X., 2007. Biokinetics and tolerance development of toxic metals in Daphnia
13578 magna. Environmental Toxicology and Chemistry 26, 1023-1032.
13579 UNEP/AMAP, 2011;
13580 Verreault J, Helgason LB, Gabrielsen GW, Dam M, Braune BM. 2013. Contrasting retinoid and
13581 thyroid hormone status in differentially-contaminated northern fulmar colonies from the
13582 Canadian Arctic, Svalbard and the Faroe Islands. Environment International,52: 29-40.

13583 Wang, K., Munson, K.M., Beaupré-Laperrière, A., Mucci, A., Macdonald, R.W., Wang, F., 2018.
13584 Subsurface seawater methylmercury maximum explains biotic mercury concentrations in the
13585 Canadian Arctic. Scientific Reports 8.
13586 Webber HM, Haines TA. 2003. Mercury effects on predator avoidance behavior of a forage fish, golden
13587 shiner (Notemigonus crysoleucas). Environ Toxicol Chem. doi:10.1897/1551-
13588 5028(2003)22<1556:MEOPAB>2.0.CO;2.
13589 Wiener JG, Spry DJ. 1996. Toxicological significance of mercury in freshwater fish. Environ Contam
13590 Wildl.
13591 Wiener, J. G., D. P. Krabbenhoft, G. H. Heinz, and A. M. Scheuhammer. 2003. Ecotoxicology of
13592 mercury. Pages 409–463 *in* D. J. Hoffman, B. A. Rattner, G. A. J. Burton, and J. J. Cairns,
13593 editors. Handbook of Ecotoxicology, second edition. CRC Press LCC, Boca Raton, Florida,
13594 USA.
13595 Williams, J.J., Dutton, J., Chen, C.Y., Fisher, N.S., 2010. Metal (As, Cd, Hg, and CH3Hg)
13596 bioaccumulation from water and food by the benthic amphipod *Leptocheirus plumulosus*.
13597 Environmental Toxicology and Chemistry 29, 1755-1761.
13598 Wingfield JC, Sapolsky RM. 2003. Reproduction and resistence to stress: When and how. Journal of
13599 Neuroendocrinology 15: 711-724.
13600 Wobeser, G., Nielsen, N.O., Schiefer, B., 1976. Mercury and mink II. Experimental methyl mercury
13601 intoxication. Can. J. Comp. Med. 40, 34–45.
13602 Wren, C.D., Hunter, D.B., Leatherland, J.F., Stokes, P.M., 1987. The effects of polychlorinated biphenyls
13603 and methylmercury, singly and in combination, on mink. I: uptake and toxic responses. Arch.
13604 Environ. Contam. Toxicol. 16, 441–447.
13605 Yurkowski, D.J., Richardson, E.S., Lunn, N.J., Muir, D.C.G., Johnson, A.C., Derocher, A.E., Ehrman,
13606 A.D., Houde, M., Young, B.G., Debets, C.D., Sciullo, L., Thiemann, G.W., Ferguson, S.H. 2020.
13607 Contrasting temporal patterns of mercury, niche dynamics, and body fat indices of polar bears
13608 and ringed seals in a melting icescape. Environ. Sci. Technol. ASAP on-line Feb. 21 (DOI:
13609 10.1021/acs.est.9b06656).
13610
13611

Annex Tables

Annex Table 6.1. Contemporary (post 2000) Hg exposure and potential health risk for Arctic marine mammals. Individuals are categorised per study region, maturity and sex, and assigned to five risk categories based upon liver tissue-specific Hg effect thresholds. Grey shaded populations are from regions outside the Arctic.

Species	Region	Maturity	Matrix	Years	n	Hg concentration	Risk category					Reference
						Liver, µg/g	<16	16–64	64–83	83–126	≥126	
						Median (Min–Max)	No	Low	Moderate risk	High risk	Severe risk	
Polar bear	Baffin Bay	Juvenile	Liver, ww	2007–2008	6	46.79 (4.55–67.7)	33.0	50.0	17.0	0.0	0.0	Routti et al. 2012
Ursus maritimus		Adult	Liver, ww	2007–2008	6	52.15 (34.07–106.8)	0.0	67.0	0.0	33.0	0.0	
	Chukchi Sea	Juvenile	Liver, ww	2005–2007	5	6.09 (4.20–15.6)	100.0	0.0	0.0	0.0	0.0	
		Adult	Liver, ww	2005–2007	7	5.10 (3.93–12.7)	100.0	0.0	0.0	0.0	0.0	
	Davis Strait	All	Liver, ww	2008	6	28.85 (16.90–93.6)	0.0	83.0	0.0	17.0	0.0	
	Gulf of Boothia	All	Liver, ww	2007	6	60.77 (38.16–79.1)	0.0	50.0	50.0	0.0	0.0	
	Lancaster/Jones Sound	Juvenile	Liver, ww	2007–2008	5	67.93 (39.05–149.8)	0.0	40.0	20.0	20.0	20.0	
		Adult	Liver, ww	2007–2008	8	66.38 (24.67–95.0)	0.0	38.0	38.0	25.0	0.0	
	Northern Beaufort Sea	Juvenile	Liver, ww	2007	9	68.69 (22.08–115.1)	0.0	44.0	33.0	22.0	0.0	
		Adult	Liver, ww	2007	17	122.13 (34.96–414.3)	0.0	18.0	6.0	35.0	41.0	
	Southern Hudson Bay	Fadult	Liver, ww	2006-2017	21	7.38 (3.46-18.57)	90.5	9.5	0.0	0.0	0.0	Letcher and co-workers, pers. comm.
		Madult	Liver, ww	2006-2017	80	6.94 (3.03-17.44)	96.3	3.8	0.0	0.0	0.0	Letcher and co-workers, pers. comm.
		Subadult	Liver, ww	2007-2015	34	5.01 (1.44-17.15)	97.1	2.9	0.0	0.0	0.0	Letcher and co-workers, pers. comm.
	Western Hudson Bay	Fadult	Liver, ww	2007-2017	18	8.58 (4.12-19.13)	83.3	16.7	0.0	0.0	0.0	Letcher and co-workers, pers. comm.
		Madult	Liver, ww	2007-2017	48	12.12 (2.4-28.7)	79.2	20.8	0.0	0.0	0.0	Letcher and co-workers, pers. comm.
		Subadult	Liver, ww	2007-2015	33	6.7 (1.63-22.04)	93.9	6.1	0.0	0.0	0.0	Letcher and co-workers, pers. comm.
	Qaanaaq	Juvenile	Liver, ww	2000–2013	6	45.34 (21.32–351.2)	0.0	66.7	0.0	0.0	33.3	Dietz and co-workers, pers. comm.
	Ittoqqortoormiit AMAP	Fadult	Liver, ww	2000-2018	40	17.25 (2.37-127.4)	45.0	50.0	0.0	2.5	2.5	Dietz and co-workers, pers. comm.
		Madult	Liver, ww	2000-2018	69	18.71 (6.54-186.84)	31.9	60.9	2.9	2.9	1.5	Dietz and co-workers, pers. comm.
		Subadult	Liver, ww	2000-2018	96	11.91 (1.08-5962)	71.9	27.1	0.0	0.0	1.0	Dietz and co-workers, pers. comm.
Ringed seal	Arctic Bay	Juvenile	Liver, ww	2000-2009	18	2.03 (0.24–8.4)	100.0	0.0	0.0	0.0	0.0	Muir and Houde, pers. comm.
Pusa hispida		Adult	Liver, ww	2000-2009	41	7.16 (1.68–58.0)	85.0	15.0	0.0	0.0	0.0	
	Arviat W. Hudson Bay	Fadult	Liver, ww	2003-2017	70	15.7 (0.16-254.86)	51.4	37.1	8.6	1.4	1.4	
		Madult	Liver, ww	2003-2017	89	10.4 (0.07-79.69)	68.5	29.2	2.3	0.0	0.0	
		subadult	Liver, ww	2003-2017	86	3.84 (0.29-54.09)	86.1	14.0	0.0	0.0	0.0	
	Gjoahaven	Juvenile	Liver, ww	2004-2009	14	0.85 (0.176–25.7)	92.9	7.1	0.0	0.0	0.0	
		Adult	Liver, ww	2004-2009	17	8.45 (0.201–40.0)	58.8	41.2	0.0	0.0	0.0	
	Grise Fjord	Juvenile	Liver, ww	2003-2008	16	0.95 (0.351–19.8)	93.8	6.3	0.0	0.0	0.0	
		Adult	Liver, ww	2003-2008	34	15.74 (0.24–87.0)	52.9	41.2	2.9	2.9	0.0	
	Inukjuaq	Juvenile	Liver, ww	2002-2007	15	1.05 (0.308–4.5)	100.0	0.0	0.0	0.0	0.0	
		Adult	Liver, ww	2002-2007	22	4.73 (0.931–60.0)	77.3	22.7	0.0	0.0	0.0	
	Kangiqsualujjuaq	Adult	Liver, ww	2002	4	4.82 (1.516–7.8)	100.0	0.0	0.0	0.0	0.0	
	Kangiqsujuaq	Juvenile	Liver, ww	2002	5	0.92 (0.367–2.0)	100.0	0.0	0.0	0.0	0.0	
		Adult	Liver, ww	2002	4	1.68 (0.616–4.1)	100.0	0.0	0.0	0.0	0.0	
	Nain, S. Labrador Sea	Adult	Liver, ww	2005–2016	32	4.66 (0.553–40.6)	87.1	12.9	0.0	0.0	0.0	
		Adult	Liver, ww	2005–2017	33	4.66 (0.553–40.6)	87.1	12.9	0.0	0.0	0.0	
		Adult	Liver, ww	2005–2018	34	4.66 (0.553–40.6)	87.1	12.9	0.0	0.0	0.0	
	Pangnirtung	Juvenile	Liver, ww	2002–2011	24	2.32 (0.156–15.8)	100.0	0.0	0.0	0.0	0.0	
		Adult	Liver, ww	2002–2011	24	2.41 (0.265–31.5)	95.8	4.2	0.0	0.0	0.0	
	Pond Inlet	Juvenile	Liver, ww	2000–2009	29	1.44 (0.314–69.8)	96.6	0.0	3.4	0.0	0.0	
		Adult	Liver, ww	2004–2009	20	5.36 (0.434–34.3)	85.0	15.0	0.0	0.0	0.0	
	Qiliqtarjuaq	Juvenile	Liver, ww	2005	6	3.98 (3.022–5.2)	100.0	0.0	0.0	0.0	0.0	
		Adult	Liver, ww	2005	14	8.89 (3.894–45.4)	92.9	7.1	0.0	0.0	0.0	
	Quartaq	Adult	Liver, ww	2002	6	5.35 (3.274–26.7)	83.3	16.7	0.0	0.0	0.0	
	Resolute	Adult F	Liver, ww	2000-2017	51	11.1 (0.47-228)	62.8	31.4	2.0	0.0	3.9	
		Adult M	Liver, ww	2000-2017	97	7.42 (0.61-96.4)	82.5	15.5	0.0	2.1	0.0	
		Subadult	Liver, ww	2000-2017	83	3.19 (0.14-23.4)	95.2	4.8	0.0	0.0	0.0	
	Sachs Harbor	Adult F	Liver, ww	2001-2017	52	35.55 (0.62-320.31)	28.9	40.4	9.6	9.6	11.5	
	Eastern Beaufort Sea	Adult M	Liver, ww	2001-2017	51	36.02 (0.45-145.93)	27.5	49.0	7.8	7.8	7.8	
		Subadult	Liver, ww	2001-2017	59	1.65 (0.34-117.68)	83.1	13.6	0.0	3.4	0.0	
	Ittoqqortoormiit	Adult F	Liver (ww)	2000-2018	40	10.08 (1.02-38.55)	72.5	27.5	0.0	0.0	0.0	Rigét and co-workers, pers. comm.
		Adult M	Liver (ww)	2000-2018	57	8.51 (1.95-37.18)	86.0	14.0	0.0	0.0	0.0	
		Subadult	Liver (ww)	2000-2018	139	4.54 (0.08-20.6)	98.6	1.4	0.0	0.0	0.0	
	Qaanaaq	Juvenile	Liver, ww	2004–2018	140	2.66 (0.20–23.2)	99.3	0.7	0.0	0.0	0.0	
		Adult F	Liver, ww	2004–2018	11	7.87 (1.41–39.0)	72.7	27.2	0.0	0.0	0.0	
		Adult M	Liver, ww	2006–2018	10	3.04 (2.07–12.5)	100.0	0.0	0.0	0.0	0.0	
	Qeqertarsuaq	Juvenile	Liver, ww	2000–2015	203	0.92 (0.18-8.19)	100	0	0	0	0	
	Gulf of Bothnia	Adult F	Liver (ww)	2017-2018	20	29.18 (3.06-82.08)	30.0	65.0	5.0	0.0	0.0	Dietz et al. submitted
		Adult M	Liver (ww)	2017-2018	20	22.68 (4.51-110.21)	45.0	50.0	0.0	5.0	0.0	
		Subadult	Liver (ww)	2017-2018	19	6.56 (0.51-20.62)	73.7	26.3	0.0	0.0	0.0	
		Yearling	Liver (ww)	2017-2017	19	0.52 (0.14-0.95)	100.0	0.0	0.0	0.0	0.0	

13619 **Annex Table 1.** Continued

Species	Region	Maturity	Matrix	Years	n	Hg concentration	Risk category					Reference
						Liver, µg/g	<16	16–64	64–83	83–126	≥126	
						Median (Min–Max)	No	Low	Moderate risk	High risk	Severe risk	
Bearded seal *Erignathus barbatus*	Ittoqqortoormiit	Juvenile	Liver, ww	2015	7	1.82 (1.17–8.4)	100.0	0.0	0.0	0.0	0.0	Dietz and co-workers, pers. comm.
Harp seal *Pagophilus groenlandicus*	Davis Strait	Juvenile	Liver, ww	2005–2006	6	1.88 (0.59–4.2)	100.0	0.0	0.0	0.0	0.0	Dietz and co-workers, pers. comm.
		Adult	Liver, ww	2005–2009	14	11.10 (1.81–77.7)	79.0	14.0	7.0	0.0	0.0	
	Ittoqqortoormiit	Adult	Liver, ww	2015	6	0.78 (0.14–8.9)	100.0	0.0	0.0	0.0	0.0	
	Greenland Sea/ Denmark Strait	Adult F	Liver, ww	2001 - 2018	16	0.76 (0.19-7.98)	100.0	0.0	0.0	0.0	0.0	Pinzone and co-workers, pers. comm.
		Adult M	Liver, ww	2001 - 2017	9	0.72 (0.46-23.97)	88.9	11.1	0.0	0.0	0.0	
		Subadult	Liver, ww	2001 - 2017	15	0.69 (0.23-2.74)	100.0	0.0	0.0	0.0	0.0	
		Yearling	Liver, ww	2017 - 2018	19	0.17 (0.05-0.7)	100.0	0.0	0.0	0.0	0.0	
Hooded seal *Cystophora cristata*	Davis Strait	Juvenile	Liver, ww	2002–2008	7	3.01 (0.64–16.6)	86.0	14.0	0.0	0.0	0.0	Dietz and co-workers, pers. comm.
		Adult	Liver, ww	2000–2015	14	154.78 (61.49–358.2)	0.0	7.0	7.0	29.0	57.0	
	Ittoqqortoormiit	All	Liver, ww	2015	5	23.06 (14.13–100.6)	40.0	40.0	0.0	20.0	0.0	
	Greenland Sea/ Denmark Strait	Adult F	Liver, ww	2002 - 2018	29	30.4 (0.31-162.78)	20.7	58.6	6.9	10.3	3.5	Pinzone and co-workers, pers. comm.
		Adult M	Liver, ww	2002 - 2019	20	120.76 (13.24-320.62)	5.0	20.0	5.0	25.0	45.0	
		Subadult	Liver, ww	2002 - 2017	31	6.11 (0.21-20.56)	83.9	16.1	0.0	0.0	0.0	
		Yearling	Liver, ww	2007 - 2018	21	0.44 (0.16-59.62)	95.2	4.8	0.0	0.0	0.0	
Harbour porpoise *Phocoena phocoena*	Maniitsoq	Adult F	Liver, ww	2009	16	5.20 (1.3-15.25)	100.0	0.0	0.0	0.0	0.0	Dietz and co-workers, pers. comm.
		Adult M	Liver, ww	2009	14	5.65 (0.44-21.18)	93.8	6.2	0.0	0.0	0.0	
		Subadult	Liver, ww	2009	9	4.52 (0.24-9.74)	100.0	0.0	0.0	0.0	0.0	
		Yearling	Liver, ww	2009	3	4.63 (4.37-7.38)	100.0	0.0	0.0	0.0	0.0	
	Barents Sea	Adult F	Liver (ww)	2016-2017	22	2.14 (0.34-11.31)	100.0	0.0	0.0	0.0	0.0	Ciesielski and co-workers pers. comm.
		Adult M	Liver (ww)	2016-2017	28	0.58 (0.18-10.23)	100.0	0.0	0.0	0.0	0.0	
		Subadult	Liver (ww)	2016-2017	27	0.49 (0.13-2.27)	100.0	0.0	0.0	0.0	0.0	
	Norwegian coast	Adult F	Liver (ww)	2016-2017	10	9.00 (1.00-17.05)	100.0	0.0	0.0	0.0	0.0	
		Adult M	Liver (ww)	2016-2017	18	6.49 (1.11-11.84)	80.0	20.0	0.0	0.0	0.0	
		Subadult	Liver (ww)	2016-2017	22	0.69 (0.17-3.42)	100.0	0.0	0.0	0.0	0.0	
	Greater North Sea	Adult F	Liver (ww)	1999 - 1999	2	27.30 (21.80-32.80)	0.0	100.0	0.0	0.0	0.0	Strand et al. 2005
		Adult M	Liver (ww)	1998 - 1999	4	12.70 (3.60-23.30)	75.0	25.0	0.0	0.0	0.0	
		Subadult	Liver (ww)	1998-1999	5	3.60 (0.50-7.50)	100.0	0.0	0.0	0.0	0.0	
		Yearling	Liver (ww)	1998-1999	4	0.70 (0.40-0.90)	100.0	0.0	0.0	0.0	0.0	
	Danish Straits	Adult F	Liver (ww)	1998	1	92.00	0.0	0.0	0.0	100.0	0.0	Strand et al. 2005
		Adult M	Liver (ww)	1998	2	8.53 (8.12-8.94)	100.0	0.0	0.0	0.0	0.0	Strand et al. 2005
		Adult M	Liver (ww)	2011	2	68.40 (61.30-75.50)	0.0	50.0	50.0	0.0	0.0	Present study
		Subadult	Liver (ww)	1998-1999	7	1.70 (1.00-2.30)	100.0	0.0	0.0	0.0	0.0	Strand et al. 2005
		Subadult	Liver (ww)	2010-2018	11	1.12 (0.66-2.16)	100.0	0.0	0.0	0.0	0.0	Present study
		Yearling	Liver (ww)	1998-1999	10	0.60 (0.20-2.10)	100.0	0.0	0.0	0.0	0.0	Strand et al. 2005
		Yearling	Liver (ww)	2017	1	1.20	100.0	0.0	0.0	0.0	0.0	Present study
Beluga *Delphinapterus leucas*	Southern Beaufort Sea	adult	Liver, ww	2001-2017	336	19.8 (0-143.74)	40.5	49.4	5.1	3.9	1.2	Loseto and co-workers, pers. comm.
		subadult	Liver, ww	2001-2017	76	10.1 (0-102.63)	68.4	26.3	4.0	1.3	0.0	
	Southern Hudson Bay	adult	Liver, ww	2002-2016	67	10.8 (0.19-53.04)	59.7	40.3	0.0	0.0	0.0	Ferguson and co-workers, pers. comm.
		subadult	Liver, ww	2002-2016	114	7.32 (0.14-75.88)	79.8	19.3	0.9	0.0	0.0	
	Cumberland Sound	adult	Liver, ww	2002-2010	31	12 (0.48-37.77)	71.0	29.0	0.0	0.0	0.0	Watt and co-workers, pers. comm.
		subadult	Liver, ww	2002-2009	12	4.35 (0.63-23.24)	83.3	16.7	0.0	0.0	0.0	
Narwhal *Monodon monoceros*	Qaanaaq	Juvenile	Liver, ww	2010–2015	5	1.38 (0.65–20.7)	80.0	20.0	0.0	0.0	0.0	Dietz and co-workers, pers. comm.
		Adult	Liver, ww	2010–2015	15	30.14 (0.16–132.1)	33.0	40.0	7.0	13.0	7.0	
	Ittoqqortoormiit	Juvenile	Liver, ww	2015	14	3.29 (0.62–32.5)	86.0	14.0	0.0	0.0	0.0	
		Adult	Liver, ww	2015	8	11.48 (0.42–18.1)	88.0	13.0	0.0	0.0	0.0	
Long-finned pilot whale *Globicephala* spp.	Faroe Islands	adult	Liver, ww	2001-2017	179	76.7 (3.52-574)	0.6	34.1	18.4	19.6	27.4	Andreasen and co-workers, pers. comm.
	Hvalvágir	subadult	Liver, ww	2001 - 2015	10	34.8 (24.4-153)	0.0	80.0	0.0	0.0	20.0	
Killer whale *Orcinus orca*	E Greenland, Iceland and Faroe Islands	Foetus	Liver, ww	2012–2013	3	0.18 (0.11–0.47)	100.0	0.0	0.0	0.0	0.0	Dietz and co-workers, pers. comm.
		Juvenile	Liver, ww	1996-2013	11	2.54 (0.53–22.81)	63.6	27.3	9.1	0.0	0.0	
		Adult	Liver, ww	1998-2013	6	112.05 (26.71–199.78)	0.0	33.0	0.0	33.0	33.0	

13620

13621 **Annex Table 2.** Contemporary (post 2000) Hg exposure and potential health risk for polar bear hair samples. Individuals are categorised per study region,
13622 maturity and sex, and assigned to five risk categories based upon liver tissue-specific Hg effect thresholds.
13623

Species	Region	Age group	Matrix	Years	n	Hg concentration	Risk category					Reference
						Hair, µg/g	<6.1	6.1–24.4	24.4-31.7	31.7-48.1	≥48.1	
						Median (Min–Max)	No	Low risk	Moderate risk	High risk	Severe risk	
Polar bear	Kane Basin	All	Hair, dw	1993-1997	37	11.8 (5.3-36.9)	5.4	89.2	5.4	0.0	0.0	Dietz and co-workers, pers. comm.
Polar bear	Baffin Bay	All	Hair, dw	1993-1997	42	9.9 (4.6-25.3)	7.1	90.5	2.4	0.0	0.0	
Polar bear	Davis Strait	All	Hair, dw	1993-2007	29	5.5 (3.7-15.2)	62.1	37.9	0.0	0.0	0.0	
Polar bear	Fox Basin	All	Hair, dw	1993-2007	10	5.8 (4.5-17.0)	50.0	50.0	0.0	0.0	0.0	
Polar bear	Gulf of Boothia	All	Hair, dw	1995-1998	15	9.2 (5.1-18.5)	13.3	86.7	0.0	0.0	0.0	
Polar bear	Lancaster Sound	All	Hair, dw	1993-1999	54	16.0 (3.1-72.7)	1.9	77.8	9.3	7.4	3.7	
Polar bear	M'Clintock Channel	All	Hair, dw	1998	12	21.9 (8.7-18.6)	0.0	91.7	8.3	0.0	0.0	
Polar bear	Northern Beaufort Sea	All	Hair, dw	2005	31	19.5 (6.4-31.0)	0.0	91.7	8.3	0.0	0.0	
Polar bear	Norwegian Bay	All	Hair, dw	1993-1997	25	25.2 (13.8-90.0)	0.0	48.0	24.0	20.0	8.0	
Polar bear	Southern Beaufort Sea	All	Hair, dw	2004-2006	30	12.6 (5.6-28.3)	3.3	83.3	13.4	0.0	0.0	
Polar bear	Southern Hudson Bay	All	Hair, dw	1997-1998	22	5.0 (2.4-13.2)	59.1	40.9	0.0	0.0	0.0	
Polar bear	Western Hudson Bay	All	Hair, dw	1993-2008	59	4.1 (2.6-8.7)	98.3	1.7	0.0	0.0	0.0	
Polar bear	Viscount Melville Sound	All	Hair, dw	1992	10	22.1 (16.7-85.2)	0.0	60.0	10.0	0.0	30.0	
Polar bear	Northwest Greenland	All	Hair, dw	2000–2008	55	7.9 (3.2-26.4)	20.0	78.2	1.8	0.0	33.3	Dietz et al. 2011
Polar bear	Central East Greenland	All	Hair, dw	2000–2017	149	6.4 (1.7-35.0)	43.6	55.7	0.0	0.7	0.0	Dietz and co-workers, pers. comm.
Polar bear	Barentz Sea	All	Hair, dw	2000–2007	58	1.8 (0.7-2.8)	100.0	0.0	0.0	0.0	0.0	Lippold et al. in prep

13624
13625
13626

13627 **Annex Table 3.** Contemporary (post 2000) Hg exposure and potential health risk for Arctic terrestrial mammals. Individuals are categorised per study
13628 region, maturity and sex, and assigned to five risk categories based upon liver tissue-specific Hg effect thresholds.
13629

Species	Region	Maturity	Matrix	Years	n	Hg concentration	Risk category					Reference
						Liver, µg/g	<4.2	4.2–7.3	7.3–22.7	22.7–30.5	≥30.5	
							No risk	Low risk	Moderate risk	High risk	Severe risk	
Arctic fox *Vulpes lagopus*	Arviat	Juvenile	Liver, ww	2001	50	0.12 (0.03–4.7)	98.0	2.0	0.0	0.0	0.0	Hoekstra et al. 2003
	Iceland	Juvenile	Liver, ww	2011–2012	12	2.81 (0.44–11.4)	67.0	8.0	25.0	0.0	0.0	Treu and co-workers, pers. comm.
		Adult	Liver, ww	2011–2012	23	5.82 (0.28–46.2)	35.0	22.0	35.0	0.0	9.0	
	Svalbard	Juvenile	Liver, ww	2000–2014	90	0.12 (0.01–1.1)	100.0	0.0	0.0	0.0	0.0	Hallanger et al. 2019
Reindeer/caribou	NW Yukon/Alaska	Adult F	Liver, ww	2000-2015	52	0.46 (0.18–1.58)	100.0	0.0	0.0	0.0	0.0	Gamberg and co-workers, pers. comm.
	Porcupine	Adult M	Liver, ww	2000-2017	238	0.19 (0.046–2.35)	100.0	0.0	0.0	0.0	0.0	
		Subadult	Liver, ww	2000-2017	19	0.34 (0.082–0.74)	100.0	0.0	0.0	0.0	0.0	
	Western Hudson Bay	Adult F	Liver, ww	2006-2018	119	1.24 (0.29–2.82)	100.0	0.0	0.0	0.0	0.0	
	Qamanirjuaq	Adult M	Liver, ww	2006-2018	80	0.84 (0.31–2.67)	100.0	0.0	0.0	0.0	0.0	
		Subadult	Liver, ww	2006-2017	26	0.93 (0.29–2.20)	100.0	0.0	0.0	0.0	0.0	
		Yearling	Liver, ww	2008-2017	9	0.63 (0.34–1.44)	100.0	0.0	0.0	0.0	0.0	
Sheep *Ovis aries*	Faroe Islands	Adult	Liver, ww	2001–2011	13	0.01 (0.01–29.9)	85.0	0.0	15.0	0.0	0.0	Hoydal and Dam 2005, 2009; Nielsen et al. 2014

13630
13631

13632 **Annex Table 4A.** Contemporary (post 2000) Hg exposure and potential health risk for Arctic seabirds blood values. Individuals are categorised per study
13633 region, age group (mainly adult birds) and assigned to five risk categories based upon blood tissue-specific Hg effect thresholds.

Species	Region	Maturity	Matrix	Years	n	Hg concentration	Risk category					
						Egg, µg/g fww	<0.10	0.10–0.37	0.37–0.91	0.91–1.16	≥1.16	
						Liver, µg/g ww	<0.53	0.53–2.26	2.26-6.10	6.10-7.91	≥7.91	
						Blood equivalent, µg/g ww	<0.2	0.2–1.0	1.0–3.0	3.0–4.0	≥4.0	
						Body feather, µg/g dw	<1.62	1.62-4.53	4.53-9.14	9.14-10.99	≥10.99	
						Median (Min-Max)	No effect	Low risk	Moderate risk	High risk	Severe risk	Reference
Glaucous-winged gull *Larus glaucescens*	Western North America	Adult	Blood eq, ww	2000–2015	30	0.23 (0.14–1.0)	33	67	0	0	0	Ackermann et al. 2016
Pigeon guillemot *Cepphus columba*	Western North America	Adult	Blood eq, ww	2000–2015	27	1.99 (0.90–3.8)	0	11	59	26	4	Ackermann et al. 2016
Double-crested cormorant *Phalacrocorax auritus*	Western North America	Adult	Blood eq, ww	2000–2015	310	0.66 (0.12–4.0)	13	56	23	3	5	Ackermann et al. 2016
King eider *Somateria spectabilis*	Western North America	Adult	Blood eq, ww	2000–2015	143	0.21 (0.08–0.5)	47	53	0	0	0	Ackermann et al. 2016
Northern fulmar *Fulmarus glacialis*	Baffin Island	Adult	Blood eq, ww	2018	24	0.22 (0.07–0.56)	50	50	0	0	0	Fort and co-workers, pers. comm.
	Iceland	Adult	Blood eq, ww	2015-2018	112	0.55 (0.19–1.32)	2	96	2	0	0	Fort and co-workers, pers. comm.
	Jan Mayen	Adult	Blood eq, ww	2015-2018	84	0.30 (0.15–0.79)	12	88	0	0	0	Fort and co-workers, pers. comm.
	Qaanaaq	Adult	Blood eq, ww	2015	10	0.41 (0.07–1.72)	20	70	10	0	0	Fort and co-workers, pers. comm.
	Svalbard	Adult	Blood eq, ww	2015-2017	63	0.17 (0.07–0.41)	65	35	0	0	0	Fort and co-workers, pers. comm.
	Western North America	Adult	Blood eq, ww	2000–2015	13	2.07 (0.79–4.2)	0	23	54	8	15	Ackermann et al. 2016
Glaucous gull *Larus hyperboreus*	Coats Island	Adult	Blood eq, ww	2015-2018	10	1.01 (0.73–2.38)	0	60	40	0	0	Fort and co-workers, pers. comm.
	Franz Josef Land	Adult	Blood eq, ww	2016-2017	39	0.54 (0.25–1.94)	0	92	8	0	0	Fort and co-workers, pers. comm.
	Iceland	Adult	Blood eq, ww	2016-2018	28	0.29 (0.18–0.52)	11	89	0	0	0	Fort and co-workers, pers. comm.
	Jan Mayen	Adult	Blood eq, ww	2016	1	0.46 (0.46–0.46)	0	100	0	0	0	Fort and co-workers, pers. comm.
	Qaanaaq	Adult	Blood eq, ww	2015	33	0.42 (0.12–2.20)	15	76	9	0	0	Fort and co-workers, pers. comm.
	Svalbard	Adult	Blood eq, ww	2015-2017	53	0.26 (0.11–0.66)	26	74	0	0	0	Fort and co-workers, pers. comm.
	Western North America	Adult	Blood eq, ww	2000–2015	61	0.28 (0.13–0.5)	21	77	2	0	0	Ackermann et al. 2016
Herring gull *Larus argentatus*	Iceland	Adult	Blood eq, ww	2016-2018	13	0.11 (0.07–0.18)	100	0	0	0	0	Fort and co-workers, pers. comm.
Ivory gull *Pagophila eburnea*	Station Nord	Adult	Blood eq, ww	2018	6	0.70 (0.37–1.42)	0	83	17	0	0	Fort and co-workers, pers. comm.
Common murre *Uria aalge*	Gorodetskiy Cape	Adult	Blood eq, ww	2015	6	0.21 (0.19–0.30)	50	50	0	0	0	Fort and co-workers, pers. comm.
	Hornøya	Adult	Blood eq, ww	2016-2017	35	0.20 (0.15–0.27)	60	40	0	0	0	Fort and co-workers, pers. comm.
	Iceland	Adult	Blood eq, ww	2015-2018	85	0.17 (0.08–0.45)	76	24	0	0	0	Fort and co-workers, pers. comm.
	Jan Mayen	Adult	Blood eq, ww	2015-2018	91	0.17 (0.06–0.38)	73	27	0	0	0	Fort and co-workers, pers. comm.
	Newfoundland	Adult	Blood eq, ww	2015-2017	92	0.50 (0.27–0.84)	0	100	0	0	0	Fort and co-workers, pers. comm.
	Saint Lawrence Island	Adult	Blood eq, ww	2016-2017	26	0.08 (0.04–0.17)	100	0	0	0	0	Fort and co-workers, pers. comm.
	Svalbard	Adult	Blood eq, ww	2015-2017	51	0.17 (0.10–0.26)	92	8	0	0	0	Fort and co-workers, pers. comm.
	Western North America	Adult	Blood eq, ww	2000–2015	239	0.24 (0.03–0.7)	40	59	1	0	0	Ackermann et al. 2016

13634

13635

Annex Table 4A. Continued.

Black-legged kittiwake *Rissa tridactyla*	Baffin Island	Adult	Blood eq, ww	2018	14	0.31 (0.18–0.39)	14	86	0	0	0	Fort and co-workers, pers. comm.
	Franz Josef Land	Adult	Blood eq, ww	2015-2017	48	0.22 (0.10–0.33)	46	54	0	0	0	Fort and co-workers, pers. comm.
	Hornøya	Adult	Blood eq, ww	2017	15	0.24 (0.15–0.47)	27	73	0	0	0	Fort and co-workers, pers. comm.
	Iceland	Adult	Blood eq, ww	2015-2018	52	0.28 (0.10–0.70)	23	67	0	0	0	Fort and co-workers, pers. comm.
	Kippaku	Adult	Blood eq, ww	2017	25	0.13 (0.09–0.19)	100	0	0	0	0	Fort and co-workers, pers. comm.
	Western North America	Adult	Blood eq, ww	2016-2017	41	0.27 (0.18–0.50)	7	93	0	0	0	Fort and co-workers, pers. comm.
	Newfoundland	Adult	Blood eq, ww	2017	20	0.22 (0.12–0.36)	45	55	0	0	0	Fort and co-workers, pers. comm.
	Pribilofs	Adult	Blood eq, ww	2017	8	0.50 (0.31–0.66)	0	100	0	0	0	Fort and co-workers, pers. comm.
	Qaanaaq	Adult	Blood eq, ww	2015	18	0.20 (0.08–0.38)	56	44	0	0	0	Fort and co-workers, pers. comm.
	Rittenlank	Adult	Blood eq, ww	2015	10	0.17 (0.13–0.23)	90	10	0	0	0	Fort and co-workers, pers. comm.
	Saint Lawrence Island	Adult	Blood eq, ww	2016-2017	16	0.24 (0.06–0.36)	19	81	0	0	0	Fort and co-workers, pers. comm.
	Scoresby Sund	Adult	Blood eq, ww	2017	25	0.19 (0.13–0.41)	60	40	0	0	0	Fort and co-workers, pers. comm.
	Svalbard	Adult	Blood eq, ww	2015-2018	132	0.27 (0.08–0.55)	51	49	0	0	0	Fort and co-workers, pers. comm.
	Svalbard	Adult (pre-laying)	Blood eq, ww	2000-2016	211	1.91 (0.91-3.50)	0	0	97	2	0	Chastel, Bustnes, Gabrielsen and co-workers, Tartu et al. 2016; Goutte et al. 2015; Blévin et al. 2018, 2019
	Svalbard	Adult (incubation)	Blood eq, ww	2000-2016	345	1.45 (0.68-3.29)	0	14	85	1	0	Chastel, Bustnes, Gabrielsen and co-workers, Tartu et al. 2013, 2017
	Svalbard	Adult (chick-rearing)	Blood eq, ww	2000-2016	493	1.04 (0.36-2.83)	0	46	54	0	0	Chastel, Bustnes, Gabrielsen and co-workers, Tartu et al. 2013, 2018
Thick-billed murre *Uria lomvia*	Baffin Island	Adult	Blood eq, ww	2018	20	0.84 (0.52–1.23)	0	85	15	0	0	Fort and co-workers, pers. comm.
	Coats Island	Adult	Blood eq, ww	2015-2018	72	0.27 (0.10–1.47)	18	81	1	0	0	Fort and co-workers, pers. comm.
	Franz Josef Land	Adult	Blood eq, ww	2015-2017	37	0.17 (0.08–0.27)	81	19	0	0	0	Fort and co-workers, pers. comm.
	Gorodetskiy Cape	Adult	Blood eq, ww	2015-2017	10	0.16 (0.10–0.23)	90	10	0	0	0	Fort and co-workers, pers. comm.
	Hornøya	Adult	Blood eq, ww	2016-2017	64	0.18 (0.12–0.27)	78	22	0	0	0	Fort and co-workers, pers. comm.
	Iceland	Adult	Blood eq, ww	2015-2018	65	0.10 (0.04–0.19)	100	0	0	0	0	Fort and co-workers, pers. comm.
	Jan Mayen	Adult	Blood eq, ww	2015-2018	85	0.27 (0.15–0.54)	20	80	0	0	0	Fort and co-workers, pers. comm.
	Kippaku	Adult	Blood eq, ww	2016	30	0.30 (0.15–0.65)	13	87	0	0	0	Fort and co-workers, pers. comm.
	Newfoundland	Adult	Blood eq, ww	2015-2018	41	0.45 (0.28–0.69)	0	100	0	0	0	Fort and co-workers, pers. comm.
	Novaya Zemlya	Adult	Blood eq, ww	2016	4	0.10 (0.09–0.11)	100	0	0	0	0	Fort and co-workers, pers. comm.
	Pribilofs	Adult	Blood eq, ww	2017	7	0.11 (0.06–0.20)	100	0	0	0	0	Fort and co-workers, pers. comm.
	Qaanaaq	Adult	Blood eq, ww	2015	19	0.46 (0.10–0.82)	5	95	0	0	0	Fort and co-workers, pers. comm.
	Saint Lawrence Island	Adult	Blood eq, ww	2016-2017	40	0.08 (0.02–0.53)	67	33	0	0	0	Fort and co-workers, pers. comm.
	Svalbard	Adult	Blood eq, ww	2015-2017	106	0.06 (0.01–0.23)	98	2	0	0	0	Fort and co-workers, pers. comm.
	Western North America	Adult	Blood eq, ww	2000–2015	141	0.12 (0.02–0.6)	65	35	0	0	0	Ackermann et al. 2016
Little auk *Alle alle*	Franz Josef Land	Adult	Blood eq, ww	2015-2017	87	0.07 (0.04–0.19)	100	0	0	0	0	Fort and co-workers, pers. comm.
	Qaanaaq	Adult	Blood eq, ww	2015	19	0.13 (0.08–0.18)	100	0	0	0	0	Fort and co-workers, pers. comm.
	Scoresby Sund	Adult	Blood eq, ww	2015-2017	88	0.17 (0.11–0.27)	83	17	0	0	0	Fort and co-workers, pers. comm.
	Svalbard	Adult	Blood eq, ww	2015-2018	172	0.08 (0.04–0.15)	100	0	0	0	0	Fort and co-workers, pers. comm.

13640 **Annex Table 4A.** Continued

Rhinoceros auklet *Cerorhinca monocerata*	Western North America	Adult	Blood eq, ww	2017	20	0.32 (0.19–0.46)	15	85	0	0	0	Fort and co-workers, pers. comm.
	Western North America	Adult	Blood eq, ww	2000–2015	21	0.94 (0.46–2.0)	0	52	48	0	0	Ackermann et al. 2016
Crested auklet *Aethia cristatella*	Saint Lawrence Island	Adult	Blood eq, ww	2016-2017	52	0.04 (0.01–0.08)	100	0	0	0	0	Fort and co-workers, pers. comm.
Least auklet *Aethia pusilla*	Saint Lawrence Island	Adult	Blood eq, ww	2016-2017	27	0.03 (0.01–0.06)	100	0	0	0	0	Fort and co-workers, pers. comm.
Red-legged kittiwake *Rissa brevirostris*	Pribilofs	Adult	Blood eq, ww	2017	4	0.51 (0.41–0.59)	0	100	0	0	0	Fort and co-workers, pers. comm.
Atlantic puffin *Fratercula arctica*	Hornøya	Adult	Blood eq, ww	2016-2017	56	0.17 (0.10–0.25)	84	16	0	0	0	Fort and co-workers, pers. comm.
	Iceland	Adult	Blood eq, ww	2016-2018	77	0.32 (0.17–0.63)	12	88	0	0	0	Fort and co-workers, pers. comm.
	Newfoundland	Adult	Blood eq, ww	2015-2018	98	0.27 (0.13–0.44)	19	81	0	0	0	Fort and co-workers, pers. comm.
	Seven Island	Adult	Blood eq, ww	2017	20	0.19 (0.13–0.25)	75	25	0	0	0	Fort and co-workers, pers. comm.
	Svalbard	Adult	Blood eq, ww	2015-2017	35	0.12 (0.06–0.24)	86	14	0	0	0	Fort and co-workers, pers. comm.
Common eider Somateria mollissima	East Bay Island	Adult	Blood eq, ww	2016	23	0.24 (0.16–0.38)	26	74	0	0	0	Fort and co-workers, pers. comm.
	Faroe Islands	Adult	Blood eq, ww	2018	11	0.08 (0.02–0.14)	100	0	0	0	0	Fort and co-workers, pers. comm.
	Iceland	Adult	Blood eq, ww	2017-2018	31	0.12 (0.07–0.56)	87	13	0	0	0	Fort and co-workers, pers. comm.
	Qaanaaq	Adult	Blood eq, ww	2015	2	0.11 (0.10–0.13)	100	0	0	0	0	Fort and co-workers, pers. comm.
	Scoresby Sund	Adult	Blood eq, ww	2015	10	0.13 (0.10–0.26)	90	10	0	0	0	Fort and co-workers, pers. comm.
	Svalbard	Adult	Blood eq, ww	2016-2017	68	0.11 (0.05–0.34)	99	1	0	0	0	Fort and co-workers, pers. comm.
	Tromsø	Adult	Blood eq, ww	2016-2017	64	0.06 (0.04–0.10)	100	0	0	0	0	Fort and co-workers, pers. comm.
	Western North America	Adult	Blood eq, ww	2000–2015	102	0.17 (0.07–0.5)	80	20	0	0	0	Ackermann et al. 2016
Ruddy turnstone *Arenaria interpres*	Western North America	Adult	Blood eq, ww	2000–2015	14	0.23 (0.15–1.9)	29	57	7	7	0	Ackermann et al. 2016

13641

13642

13643 **Annex Table 4B.** Contemporary (post 2000) Hg exposure and potential health risk for Arctic seabirds feather values. Individuals are categorised per
13644 study region, age group (mainly adult birds) and assigned to five risk categories based upon feather tissue-specific Hg effect thresholds.
13645

Species	Region	Maturity	Matrix	Years	n	Hg concentration	Risk category					
						Egg, µg/g fww	<0.10	0.10–0.37	0.37–0.91	0.91–1.16	≥1.16	
						Liver, µg/g ww	<0.53	0.53–2.26	2.26-6.10	6.10-7.91	≥7.91	
						Blood equivalent, µg/g ww	<0.2	0.2–1.0	1.0–3.0	3.0–4.0	≥4.0	
						Body feather, µg/g dw	<1.62	1.62-4.53	4.53-9.14	9.14-10.99	≥10.99	
						Median (Min-Max)	No effect	Low risk	Moderate risk	High risk	Severe risk	Reference
Northern fulmar *Fulmarus glacialis*	Faroe Islands	Adult	Body feathers, ww	2015-2017	28	2.80 (1.17–6.75)	4	92	4	0	0	Fort and co-workers, pers. comm.
	Iceland	Adult	Body feathers, ww	2015-2017	76	2.94 (0.82–6.85)	9	82	9	0	0	Fort and co-workers, pers. comm.
	Jan Mayen	Adult	Body feathers, ww	2015-2017	60	2.45 (0.78–6.40)	17	76	7	0	0	Fort and co-workers, pers. comm.
	Qaanaaq	Adult	Body feathers, ww	2015	10	1.96 (0.34–8.23)	30	60	10	0	0	Fort and co-workers, pers. comm.
	Svalbard	Adult	Body feathers, ww	2015-2017	75	1.19 (0.33–4.99)	70	29	1	0	0	Fort and co-workers, pers. comm.
Glaucous winged gull *Larus glaucescens*	Aleutian Islands	Adult	Body feathers, ww	2017	12	7.29 (2.14–14.95)	0	17	58	8	17	Fort and co-workers, pers. comm.
Glaucous gull *Larus hyperboreus*	Coats Island	Adult	Body feathers, ww	2015	1	6.11 (6.11–6.11)	0	0	100	0	0	Fort and co-workers, pers. comm.
	Franz Josef Land	Adult	Body feathers, ww	2015-2017	41	5.32 (2.41–11.51)	0	29	69	2	0	Fort and co-workers, pers. comm.
	Iceland	Adult	Body feathers, ww	2016-2017	17	3.21 (1.37–7.83)	18	64	18	0	0	Fort and co-workers, pers. comm.
	Qaanaaq	Adult	Body feathers, ww	2015	12	13.30 (5.30–23.25)	0	0	17	12	71	Fort and co-workers, pers. comm.
	Svalbard	Adult	Body feathers, ww	2015-2017	67	3.36 (1.01–8.36)	10	58	32	0	0	Fort and co-workers, pers. comm.
Herring gull *Larus argentatus*	Hornøya	Adult	Body feathers, ww	2017	9	1.56 (0.83–4.24)	56	44	0	0	0	Fort and co-workers, pers. comm.
	Iceland	Adult	Body feathers, ww	2015-2017	16	0.69 (0.36–1.84)	94	6	0	0	0	Fort and co-workers, pers. comm.
	Solovetsky Archipelago	Adult	Body feathers, ww	2015-2017	42	2.06 (1.24–4.91)	17	81	2	0	0	Fort and co-workers, pers. comm.
Lesser black-backed gull *Larus fuscus*	Faroe Islands	Adult	Body feathers, ww	2015-2016	23	1.85 (0.61–13.67)	39	35	22	0	4	Fort and co-workers, pers. comm.
	Iceland	Adult	Body feathers, ww	2015-2017	8	1.71 (0.25–3.08)	37	63	0	0	0	Fort and co-workers, pers. comm.
	Solovetsky Archipelago	Adult	Body feathers, ww	2015-2017	36	3.08 (0.81–5.34)	19	73	8	0	0	Fort and co-workers, pers. comm.
Little auk *Alle alle*	Franz Josef Land	Adult	Body feathers, ww	2015-2017	69	0.76 (0.39–1.57)	100	0	0	0	0	Fort and co-workers, pers. comm.
	Qaanaaq	Adult	Body feathers, ww	2015	19	0.62 (0.37–0.86)	100	0	0	0	0	Fort and co-workers, pers. comm.
	Scoresby Sund	Adult	Body feathers, ww	2015-2017	64	1.20 (0.79–2.75)	77	23	0	0	0	Fort and co-workers, pers. comm.
	Svalbard	Adult	Body feathers, ww	2015-2017	73	0.79 (0.30–1.92)	99	1	0	0	0	Fort and co-workers, pers. comm.

13646
13647

Annex Table 4B. Continued

Common murre *Uria aalge*	Faroe Islands	Adult	Body feathers, ww 2016-2017	8	1.93 (1.18–4.58)	0	87	13	0	0	Fort and co-workers, pers. comm.
	Gorodetskiy Cape	Adult	Body feathers, ww 2015-2017	47	0.64 (0.42–1.06)	100	0	0	0	0	Fort and co-workers, pers. comm.
	Iceland	Adult	Body feathers, ww 2016-2017	37	1.09 (0.59–2.69)	92	8	0	0	0	Fort and co-workers, pers. comm.
	Jan Mayen	Adult	Body feathers, ww 2015-2017	63	0.87 (0.41–1.77)	95	5	0	0	0	Fort and co-workers, pers. comm.
	Newfoundland	Adult	Body feathers, ww 2015-2017	96	2.09 (1.02–4.48)	17	83	0	0	0	Fort and co-workers, pers. comm.
	Pribilofs	Adult	Body feathers, ww 2015	12	0.57 (0.43–0.82)	100	0	0	0	0	Fort and co-workers, pers. comm.
	Saint Lawrence Island	Adult	Body feathers, ww 2016-2017	36	0.55 (0.33–0.96)	100	0	0	0	0	Fort and co-workers, pers. comm.
	Svalbard	Adult	Body feathers, ww 2015-2017	48	0.64 (0.45–0.99)	100	0	0	0	0	Fort and co-workers, pers. comm.
	Okhotsk Sea	Adult	Body feathers, ww 2017	1	0.88 (0.88–0.88)	100	0	0	0	0	Fort and co-workers, pers. comm.
Black-legged kittiwake *Rissa tridactyla*	Cape Krutik	Adult	Body feathers, ww 2015-2017	73	1.56 (0.65–10.29)	49	44	5	1	1	Fort and co-workers, pers. comm.
	Faroe Islands	Adult	Body feathers, ww 2015	3	2.99 (2.94–5.56)	0	67	33	0	0	Fort and co-workers, pers. comm.
	Franz Josef Land	Adult	Body feathers, ww 2015-2017	80	3.58 (1.34–9.09)	5	56	39	0	0	Fort and co-workers, pers. comm.
	Hornøya	Adult	Body feathers, ww 2015-2017	73	1.93 (0.57–3.86)	44	56	0	0	0	Fort and co-workers, pers. comm.
	Iceland	Adult	Body feathers, ww 2015-2016	38	3.05 (1.25–8.63)	10	74	16	0	0	Fort and co-workers, pers. comm.
	Kippaku	Adult	Body feathers, ww 2015	26	3.29 (1.71–6.27)	0	88	12	0	0	Fort and co-workers, pers. comm.
	Western North America	Adult	Body feathers, ww 2016-2017	41	3.49 (1.23–7.11)	10	58	32	0	0	Fort and co-workers, pers. comm.
	Newfoundland	Adult	Body feathers, ww 2017	20	4.90 (3.68–7.07)	0	35	65	0	0	Fort and co-workers, pers. comm.
	Novaya Zemlya	Adult	Body feathers, ww 2015-2016	23	1.81 (0.87–12.93)	43	35	9	0	13	Fort and co-workers, pers. comm.
	Pribilofs	Adult	Body feathers, ww 2016-2017	41	3.36 (1.62–8.44)	0	83	17	0	0	Fort and co-workers, pers. comm.
	Qaanaaq	Adult	Body feathers, ww 2015	17	0.96 (0.39–1.82)	94	6	0	0	0	Fort and co-workers, pers. comm.
	Rittenlank	Adult	Body feathers, ww 2015	10	1.83 (1.37–3.88)	40	60	0	0	0	Fort and co-workers, pers. comm.
	Saint Lawrence Island	Adult	Body feathers, ww 2016-2017	32	4.50 (2.09–10.33)	0	56	41	3	0	Fort and co-workers, pers. comm.
	Scoresby Sund	Adult	Body feathers, ww 2017	20	6.05 (2.51–9.36)	0	30	65	5	0	Fort and co-workers, pers. comm.
	Svalbard	Adult	Body feathers, ww 2015-2017	199	3.49 (1.08–13.06)	33	44	20	3	0	Fort and co-workers, pers. comm.

Annex Table 4B. Continued

Thick-billed murre *Uria lomvia*	Coats Island	Adult	Body feathers, ww 2015	20	1.51 (1.20–2.36)	70	30	0	0	0	Fort and co-workers, pers. comm.
	Franz Josef Land	Adult	Body feathers, ww 2015-2017	61	0.73 (0.35–1.31)	100	0	0	0	0	Fort and co-workers, pers. comm.
	Gorodetskiy Cape	Adult	Body feathers, ww 2015-2017	29	0.70 (0.53–1.09)	100	0	0	0	0	Fort and co-workers, pers. comm.
	Hornøya	Adult	Body feathers, ww 2015-2017	60	0.73 (0.37–1.39)	100	0	0	0	0	Fort and co-workers, pers. comm.
	Iceland	Adult	Body feathers, ww 2015-2017	46	1.41 (0.95–1.91)	80	20	0	0	0	Fort and co-workers, pers. comm.
	Jan Mayen	Adult	Body feathers, ww 2015-2017	65	1.59 (0.91–2.34)	54	46	0	0	0	Fort and co-workers, pers. comm.
	Kippaku	Adult	Body feathers, ww 2016	20	1.71 (1.10–3.19)	25	75	0	0	0	Fort and co-workers, pers. comm.
	Newfoundland	Adult	Body feathers, ww 2015-2017	41	2.10 (1.27–5.90)	7	86	7	0	0	Fort and co-workers, pers. comm.
	Novaya Zemlya	Adult	Body feathers, ww 2015-2017	74	0.64 (0.28–1.32)	100	0	0	0	0	Fort and co-workers, pers. comm.
	Pribilofs	Adult	Body feathers, ww 2015-2017	42	0.64 (0.43–1.35)	100	0	0	0	0	Fort and co-workers, pers. comm.
	Qaanaaq	Adult	Body feathers, ww 2015	19	2.20 (0.46–3.91)	21	79	0	0	0	Fort and co-workers, pers. comm.
	Saint Lawrence Island	Adult	Body feathers, ww 2016-2017	40	0.71 (0.32–1.92)	98	2	0	0	0	Fort and co-workers, pers. comm.
	Svalbard	Adult	Body feathers, ww 2015-2017	114	0.59 (0.29–2.11)	97	3	0	0	0	Fort and co-workers, pers. comm.
Rhinoceros auklet *Cerorhinca monocerata*	Western North America	Adult	Body feathers, ww 2016-2017	42	2.20 (0.91–6.96)	24	62	14	0	0	Fort and co-workers, pers. comm.
Crested auklet *Aethia cristatella*	Aleutian Islands	Adult	Body feathers, ww 2017	4	1.19 (0.72–2.10)	75	25	0	0	0	Fort and co-workers, pers. comm.
	Okhotsk Sea	Adult	Body feathers, ww 2017	4	0.70 (0.38–1.49)	100	0	0	0	0	Fort and co-workers, pers. comm.
	Saint Lawrence Island	Adult	Body feathers, ww 2016-2017	33	0.71 (0.33–2.40)	91	9	0	0	0	Fort and co-workers, pers. comm.
Least auklet *Aethia pusilla*	Pribilofs	Adult	Body feathers, ww 2015-2017	65	0.95 (0.23–3.99)	75	25	0	0	0	Fort and co-workers, pers. comm.
	Saint Lawrence Island	Adult	Body feathers, ww 2016-2017	34	1.31 (0.33–5.36)	53	44	3	0	0	Fort and co-workers, pers. comm.
Parakeet auklet *Aethia psittacula*	Aleutian Islands	Adult	Body feathers, ww 2017	4	2.84 (1.91–4.00)	0	100	0	0	0	Fort and co-workers, pers. comm.
	Okhotsk Sea	Adult	Body feathers, ww 2017	13	1.67 (1.00–3.80)	46	54	0	0	0	Fort and co-workers, pers. comm.
Ancient murrelet *Synthliboramphus antiquus*	Aleutian Islands	Adult	Body feathers, ww 2017	2	1.94 (1.42–2.46)	50	50	0	0	0	Fort and co-workers, pers. comm.
	Okhotsk Sea	Adult	Body feathers, ww 2017	12	2.74 (0.94–4.75)	13	87	0	0	0	Fort and co-workers, pers. comm.
Red-legged kittiwake *Rissa brevirostris*	Pribilofs	Adult	Body feathers, ww 2015-2017	61	5.27 (2.35–8.05)	0	28	72	0	0	Fort and co-workers, pers. comm.
	Sampled at St. George Island, Alaska. Feathers grown in Northern Pacific Ocean	Adult	Nape feathers, dw 2011-2017	78	4.66 (2.84-6.46)	0	40	60	0	0	Ackerman and co-workers, pers. comm.

13655 **Annex Table 4B.** Continued

Tufted puffin *Fratercula cirrhata*	Aleutian Islands	Adult	Body feathers, ww 2017	14	2.93 (1.68–6.44)	29	71	0	0	0	Fort and co-workers, pers. comm.
	Okhotsk Sea	Adult	Body feathers, ww 2017	2	2.68 (1.99–3.37)	50	50	0	0	0	Fort and co-workers, pers. comm.
Horned puffin *Fratercula corniculata*	Aleutian Islands	Adult	Body feathers, ww 2017	1	4.61 (4.61–4.61)	0	0	100	0	0	Fort and co-workers, pers. comm.
Atlantic puffin *Fratercula arctica*	Faroe Islands	Adult	Body feathers, ww 2015	3	2.96 (2.67–4.62)	0	67	33	0	0	Fort and co-workers, pers. comm.
	Hornøya	Adult	Body feathers, ww 2015-2017	40	1.04 (0.47–2.34)	95	5	0	0	0	Fort and co-workers, pers. comm.
	Iceland	Adult	Body feathers, ww 2015-2016	47	3.58 (1.09–8.94)	2	79	19	0	0	Fort and co-workers, pers. comm.
	Newfoundland	Adult	Body feathers, ww 2015-2016	36	3.80 (1.99–9.14)	0	78	22	0	0	Fort and co-workers, pers. comm.
	Seven Island	Adult	Body feathers, ww 2015-2016	28	0.86 (0.35–2.26)	96	4	0	0	0	Fort and co-workers, pers. comm.
	Svalbard	Adult	Body feathers, ww 2015-2016	32	2.19 (0.57–5.88)	38	53	9	0	0	Fort and co-workers, pers. comm.
Common eider Somateria mollissima	Aleutian Islands	Adult	Body feathers, ww 2017	1	1.33 (1.33–1.33)	100	0	0	0	0	Fort and co-workers, pers. comm.
	East Bay Island	Adult	Body feathers, ww 2016	23	0.99 (0.63–3.81)	9	91	0	0	0	Fort and co-workers, pers. comm.
	Faroe Islands	Adult	Body feathers, ww 2015-2017	78	0.71 (0.21–12.30)	82	13	3	1	1	Fort and co-workers, pers. comm.
	Iceland	Adult	Body feathers, ww 2015-2017	71	0.84 (0.31–2.39)	93	7	0	0	0	Fort and co-workers, pers. comm.
	Scoresby Sund	Adult	Body feathers, ww 2015	10	0.87 (0.55–2.53)	80	20	0	0	0	Fort and co-workers, pers. comm.
	Seven Island	Adult	Body feathers, ww 2015	1	0.48 (0.48–0.48)	100	0	0	0	0	Fort and co-workers, pers. comm.
	Solovetsky Archipelago	Adult	Body feathers, ww 2015-2017	69	1.08 (0.49–3.46)	88	12	0	0	0	Fort and co-workers, pers. comm.
	Svalbard	Adult	Body feathers, ww 2015-2017	69	1.00 (0.44–2.41)	94	6	0	0	0	Fort and co-workers, pers. comm.
	Tromsø	Adult	Body feathers, ww 2015-2017	75	0.61 (0.25–4.62)	99	1	0	0	0	Fort and co-workers, pers. comm.

13656

13657

13658 **Annex Table 4C.** Contemporary (post 2000) Hg exposure and potential health risk for Arctic seabirds egg and liver values. Individuals are categorised
13659 per study region, age group (mainly adult birds) and assigned to five risk categories based upon egg and liver tissue-specific Hg effect thresholds.

Species	Region	Maturity	Matrix	Years	n	Hg concentration	Risk category				
						Egg, µg/g fww	<0.10	0.10–0.37	0.37–0.91	0.91–1.16	≥1.16
						Liver, µg/g ww	<0.53	0.53–2.26	2.26-6.10	6.10-7.91	≥7.91
						Blood equivalent, µg/g ww	<0.2	0.2–1.0	1.0–3.0	3.0–4.0	≥4.0
						Body feather, µg/g dw	<1.62	1.62-4.53	4.53-9.14	9.14-10.99	≥10.99
						Median (Min-Max)	No effect	Low risk	Moderate risk	High risk	Severe risk	Reference
Northern fulmar *Fulmarus glacialis*	Prince Leopold Is.	Foetus	Egg, ww	2003–2015	57	0.90 (0.54–1.3)	0	0	100	0	0	Braune 2015; Braune et al. 2016
	Qaanaaq	All	Liver, ww	2015	10	2.61 (0.25–5.3)	20	80	0	0	0	Dietz and co-workers, pers. comm.
	Svalbard	All	Liver, ww	2005–2006	10	2.54 (1.64–3.4)	0	100	0	0	0	Jæger et al. 2009
Glaucous-winged gull *Larus glaucescens*	Bering Sea	Foetus	Egg, ww	2005–2009	11	0.12 (0.06–0.2)	45	55	0	0	0	Ackermann et al. 2016
	Gulf of Alaska	Foetus	Egg, ww	2005	6	0.13 (0.01–0.4)	0	100	0	0	0	
Glaucous gull *Larus hyperboreus*	Bering Sea	Foetus	Egg, ww	2005–2009	8	0.15 (0.11–0.2)	0	100	0	0	0	Ackermann et al. 2016
	Bering Strait	Foetus	Egg, ww	2005–2008	13	0.13 9 (0.01–0.4)	46	54	0	0	0	
	Norton Sound	Foetus	Egg, ww	2005–2009	40	0.13 (0.01–0.6)	18	80	3	0	0	
	Qaanaaq	All	Liver, ww	2015	10	1.87 (1.06–3.0)	50	50	0	0	0	Dietz and co-workers, pers. comm.
	Svalbard	All	Liver, ww	2005–2006	9	1.13 (0.40–2.0)	67	33	0	0	0	Jæger et al. 2009
Herring gull *Larus argentatus*	Hornøya	Foetus	Egg, ww	2003	5	0.07 (0.06–0.2)	80	20	0	0	0	Helgason et al. 2008
	Lofoten	Foetus	Egg, ww	2003	5	0.07 (0.04–0.2)	60	40	0	0	0	
Ivory gull *Pagophila eburnea*	Nagurskoe	Foetus	Egg, ww	2006	6	0.24 (0.08–0.2)	17	83	0	0	0	Miljeteig et al. 2009
	Cape Kluyv	Foetus	Egg, ww	2006	7	0.20 (0.16–0.5)	0	71	14	14	0	
	Domashny	Foetus	Egg, ww	2006	12	0.11 (0.03–0.3)	33	58	8	0	0	
Black-legged kittiwake *Rissa tridactyla*	Qaanaaq	All	Liver, ww	2015	10	0.35 (0.20–0.6)	100	0	0	0	0	Dietz and co-workers, pers. comm.
	Svalbard	All	Liver, ww	2005–2006	10	0.97 (0.53–1.4)	100	0	0	0	0	Jæger et al. 2009
	Svalbard	Foetus	Egg, ww	2003	5	0.14 (0.07–0.2)	20	80	0	0	0	Helgason et al. 2011
	Hornøya	Foetus	Egg, ww	2003	5	0.07 (0.06–0.1)	80	20	0	0	0	Helgason et al. 2008
	Lofoten	Foetus	Egg, ww	2003	5	0.09 (0.07–0.1)	80	20	0	0	0	
Thick-billed murre *Uria lomvia*	Aleutian Islands	Foetus	Egg, ww	2000–2010	34	0.11 (0.01–0.4)	44	56	0	0	0	Ackermann et al. 2016
	Bering Sea	Foetus	Egg, ww	2000–2010	39	0.04 (0.01–0.2)	97	3	0	0	0	
	Bering Strait	Foetus	Egg, ww	2002–2008	32	0.13 (0.01–0.4)	94	6	0	0	0	
	Gulf of Alaska	Foetus	Egg, ww	2001–2010	36	0.14 (0.02–0.6)	25	75	0	0	0	
	Prince Leopold Is.	Foetus	Egg, ww	2003–2014	55	0.85 (0.47–1.5)	0	0	96	4	0	Braune et al. 2016
	Coats Is.	Foetus	Egg, ww	2003–2015	55	0.50 (0.32–0.8)	0	36	64	0	0	Braune et al. 2014, 2016; Braune 2015
	Qaanaaq	All	Liver, ww	2015	10	1.06 (0.66–1.5)	90	10	0	0	0	Dietz and co-workers, pers. comm.
	Svalbard	All	Liver, ww	2005–2006	10	0.34 (0.26–0.6)	100	0	0	0	0	Jæger et al. 2009
	Svalbard	Foetus	Egg, ww	2003	5	0.03 (0.02–0.2)	80	20	0	0	0	Helgason et al. 2011
Common murre *Uria aalge*	Aleutian Islands	Foetus	Egg, ww	2005	5	0.04 (0.02–0.1)	80	20	0	0	0	Ackermann et al. 2016
	Bering Sea	Foetus	Egg, ww	2004–2010	30	0.03 (0.01–0.2)	97	3	0	0	0	
	Bering Strait	Foetus	Egg, ww	2002–2008	13	0.06 (0.02–0.1)	85	15	0	0	0	
	Gulf of Alaska	Foetus	Egg, ww	2001–2010	83	0.13 (0.01–0.4)	12	88	0	0	0	
	Norton Sound	Foetus	Egg, ww	2002–2013	35	0.13 (0.05–0.6)	43	57	0	0	0	
Little auk *Alle alle*	Qaanaaq	All	Liver, ww	2015	10	0.25 (0.16–0.4)	100	0	0	0	0	Dietz and co-workers, pers. comm.
	Svalbard	All	Liver, ww	2005–2006	11	0.22 (0.02–0.5)	100	0	0	0	0	Jæger et al. 2009
Black guillemot *Cepphus grylle*	Faroe Islands	Foetus	Egg, ww	2000–2012	142	0.43 (0.14–1.3)	0	56	43	1	0	Hoydal and Dam 2005, 2009; Nielsen et al. 2014
		Juvenile	liver (ww)	2002–2011	65	0.90 (0.49–2.5)	75	25	0	0	0	
	Qaanaaq	All	Liver, ww	2015	10	0.64 (0.43–1.3)	100	0	0	0	0	Dietz and co-workers, pers. comm.
Atlantic puffin *Fraterculaarctica*	Hornøya	Foetus	Egg, ww	2003	5	0.10 (0.09–0.1)	60	40	0	0	0	Helgason et al. 2008
	Lofoten	Foetus	Egg, ww	2003	5	0.11 (0.08–0.1)	40	60	0	0	0	
Common eider Somateria mollissima	Svalbard	All	Liver, ww	2008–2009	40	0.49 (0.23–1.4)	98	3	0	0	0	Saunes 2011

13660

13661

13662 **Annex Table 5A.** Contemporary (post 2000) Hg exposure and potential health risk of Arctic shorebirds blood values. Individuals are categorised per
13663 study region, age group (mainly adult birds) and assigned to five risk categories based upon blood-specific Hg effect thresholds.

Species	Region	Maturity	Matrix	Years	n	Hg concentration	Risk category					
						Egg, µg/g fww	<0.10	0.10–0.37	0.37–0.91	0.91–1.16	≥1.16	
						Liver, µg/g ww	<0.53	0.53–2.26	2.26-6.10	6.10-7.91	≥7.91	
						Blood equivalent, µg/g ww	<0.2	0.2–1.0	1.0–3.0	3.0–4.0	≥4.0	
						Body feather, µg/g dw	<1.62	1.62-4.53	4.53-9.14	9.14-10.99	≥10.99	
						Median (Min-Max)	No effect	Low risk	Moderate risk	High risk	Severe risk	Reference
American Golden-Plover	Barrow		Blood	2012	20	0.20 0.10 - 0.40	62.0	38.0	0.0	0.0	0.0	Perkins et al.2018.
	Barrow		Blood	2013	14	0.16 0.09 - 0.35	62.0	38.0	0.0	0.0	0.0	
	Bylot Island		Blood	2012	23	0.13 0.06 - 0.30	96.0	4.0	0.0	0.0	0.0	
	Bylot Island		Blood	2013	24	0.11 0.08 - 0.22	96.0	4.0	0.0	0.0	0.0	
	Igloolik		Blood	2013	9	0.20 0.10 - 0.32	56.0	44.0	0.0	0.0	0.0	
Baird's Sandpiper	Igloolik		Blood	2013	1	0.11 .	100.0	0.0	0.0	0.0	0.0	
Black Turnstone	Cape Krusenstern		Blood	2012	15	0.20 0.11 - 0.63	63.0	38.0	0.0	0.0	0.0	
	Cape Krusenstern		Blood	2013	1	0.20 .	63.0	38.0	0.0	0.0	0.0	
Black-bellied Plover	East Bay		Blood	2012	6	0.33 0.25 - 0.41	0.0	100.0	0.0	0.0	0.0	
	East Bay		Blood	2013	2	0.40 0.36 - 0.44	0.0	100.0	0.0	0.0	0.0	
Dunlin	Nome		Blood	2012	1	0.33 .	0.0	100.0	0.0	0.0	0.0	
	Cape Krusenstern		Blood	2012	13	0.15 0.09 - 0.21	94.0	6.0	0.0	0.0	0.0	
	Cape Krusenstern		Blood	2013	19	0.13 0.03 - 0.27	94.0	6.0	0.0	0.0	0.0	
	Barrow		Blood	2012	32	0.31 0.15 - 0.76	13.0	83.0	3.0	0.0	0.0	
	Barrow		Blood	2013	57	0.33 0.09 - 0.70	13.0	83.0	3.0	0.0	0.0	
	Ikpikpuk River		Blood	2012	21	0.06 0.01 - 0.12	100.0	0.0	0.0	0.0	0.0	
	Ikpikpuk River		Blood	2013	11	0.11 0.07 - 0.19	100.0	0.0	0.0	0.0	0.0	
	Colville River		Blood	2012	12	0.17 0.13 - 0.24	80.0	20.0	0.0	0.0	0.0	
	Colville River		Blood	2013	13	0.18 0.13 - 0.31	80.0	20.0	0.0	0.0	0.0	
Long-billed Dowitcher	Barrow		Blood	2012	23	0.68 0.39 - 1.01	0.0	61.0	22.0	17.0	0.0	
	Barrow		Blood	2013	13	0.87 0.49 - 1.49	0.0	61.0	22.0	17.0	0.0	
Pectoral Sandpiper	Nome		Blood	2012	5	0.23 0.16 - 0.41	40.0	60.0	0.0	0.0	0.0	
	Barrow		Blood	2012	34	0.58 0.20 - 2.04	0.0	72.0	18.0	10.0	0.0	
	Barrow		Blood	2013	26	0.54 0.23 - 1.09	0.0	72.0	18.0	10.0	0.0	
	Mackenzie River Delta		Blood	2013	7	0.36 0.15 - 0.66	29.0	71.0	0.0	0.0	0.0	
	Bylot Island		Blood	2013	1	0.32 .	0.0	100.0	0.0	0.0	0.0	
Red Phalarope	Barrow		Blood	2012	36	0.42 0.12 - 1.12	10.0	74.0	12.0	4.0	0.0	
	Barrow		Blood	2013	32	0.54 0.20 - 1.60	10.0	74.0	12.0	4.0	0.0	
	Ikpikpuk River		Blood	2012	19	0.07 0.04 - 0.16	100.0	0.0	0.0	0.0	0.0	
	Ikpikpuk River		Blood	2013	13	0.14 0.09 - 0.19	100.0	0.0	0.0	0.0	0.0	
	Colville River		Blood	2012	13	0.26 0.11 - 0.38	23.0	77.0	0.0	0.0	0.0	
	East Bay		Blood	2013	10	0.52 0.28 - 0.66	0.0	100.0	0.0	0.0	0.0	
Red-necked Phalarope	Nome		Blood	2012	16	0.11 0.07 - 0.18	91.0	7.0	0.0	2.0	0.0	
	Nome		Blood	2013	28	0.19 0.04 - 1.55	91.0	7.0	0.0	2.0	0.0	
	Cape Krusenstern		Blood	2012	10	0.17 0.07 - 0.30	70.0	30.0	0.0	0.0	0.0	
	Barrow		Blood	2012	10	0.48 0.26 - 1.43	0.0	93.0	0.0	7.0	0.0	
	Barrow		Blood	2013	4	0.34 0.29 - 0.46	0.0	93.0	0.0	7.0	0.0	
	Ikpikpuk River		Blood	2012	15	0.07 0.03 - 0.17	96.0	4.0	0.0	0.0	0.0	
	Ikpikpuk River		Blood	2013	12	0.15 0.08 - 0.49	96.0	4.0	0.0	0.0	0.0	
	Colville River		Blood	2013	8	0.26 0.13 - 0.39	38.0	63.0	0.0	0.0	0.0	
	Mackenzie River Delta		Blood	2012	15	0.24 0.13 - 0.45	13.0	87.0	0.0	0.0	0.0	
	Mackenzie River Delta		Blood	2013	23	0.37 0.21 - 0.64	13.0	87.0	0.0	0.0	0.0	
Ruddy Turnstone	Colville River		Blood	2013	12	0.61 0.13 - 3.52	33.0	50.0	0.0	17.0	0.0	
	East Bay		Blood	2012	14	0.38 0.16 - 1.00	13.0	81.0	0.0	6.0	0.0	
	East Bay		Blood	2013	2	0.50 0.46 - 0.55	13.0	81.0	0.0	6.0	0.0	
Semipalmated Sandpiper	Nome		Blood	2012	21	0.17 0.05 - 0.44	73.0	27.0	0.0	0.0	0.0	
	Nome		Blood	2013	16	0.16 0.05 - 0.33	73.0	27.0	0.0	0.0	0.0	
	Cape Krusenstern		Blood	2012	34	0.18 0.11 - 0.27	76.0	24.0	0.0	0.0	0.0	
	Cape Krusenstern		Blood	2013	8	0.17 0.13 - 0.24	76.0	24.0	0.0	0.0	0.0	
	Barrow		Blood	2012	34	0.70 0.18 - 1.53	1.0	59.0	24.0	15.0	0.0	
	Barrow		Blood	2013	40	0.61 0.25 - 1.56	1.0	59.0	24.0	15.0	0.0	
	Ikpikpuk River		Blood	2012	46	0.08 0.03 - 0.20	90.0	10.0	0.0	0.0	0.0	
	Ikpikpuk River		Blood	2013	31	0.16 0.10 - 0.32	90.0	10.0	0.0	0.0	0.0	
	Colville River		Blood	2012	14	0.25 0.17 - 0.41	38.0	63.0	0.0	0.0	0.0	
	Colville River		Blood	2013	2	0.18 0.17 - 0.19	38.0	63.0	0.0	0.0	0.0	
	Mackenzie River Delta		Blood	2012	16	0.19 0.12 - 0.27	64.0	36.0	0.0	0.0	0.0	
	Mackenzie River Delta		Blood	2013	20	0.19 0.11 - 0.28	64.0	36.0	0.0	0.0	0.0	
	Igloolik		Blood	2013	7	0.43 0.26 - 0.79	0.0	86.0	14.0	0.0	0.0	
Western Sandpiper	Nome		Blood	2012	15	0.26 0.16 - 0.48	57.0	43.0	0.0	0.0	0.0	
	Nome		Blood	2013	13	0.11 0.03 - 0.30	57.0	43.0	0.0	0.0	0.0	
	Cape Krusenstern		Blood	2012	28	0.21 0.11 - 0.35	57.0	43.0	0.0	0.0	0.0	
	Cape Krusenstern		Blood	2013	21	0.17 0.09 - 0.23	57.0	43.0	0.0	0.0	0.0	
	Barrow		Blood	2012	17	0.43 0.27 - 0.73	0.0	94.0	0.0	0.0	0.0	
	Barrow		Blood	2013	16	0.40 0.24 - 0.58	0.0	94.0	0.0	0.0	0.0	

13664

13665 **Annex Table 5B.** Contemporary (post 2000) Hg exposure and potential health risk of Arctic shorebirds feather values. Individuals are categorised per
13666 study region, age group (mainly adult birds) and assigned to five risk categories based upon feather-specific Hg effect thresholds.

Species	Region	Maturity	Matrix	Years	n	Hg concentration			Risk category			
						Egg, µg/g fww	<0.10	0.10–0.37	0.37–0.91	0.91–1.16	≥1.16	
						Liver, µg/g ww	<0.53	0.53–2.26	2.26-6.10	6.10-7.91	≥7.91	
						Blood equivalent, µg/g ww	<0.2	0.2–1.0	1.0–3.0	3.0–4.0	≥4.0	
						Body feather, µg/g dw	<1.62	1.62-4.53	4.53-9.14	9.14-10.99	≥10.99	
						Median (Min-Max)	No effect	Low risk	Moderate risk	High risk	Severe risk	Reference
American Golden-Plover	Barrow		Feather	2012	20	0.60 0.37 - 1.41	0.0	100.0	0.0	0.0	0.0	Perkins et al.2018.
	Barrow		Feather	2013	16	0.75 0.23 - 1.71	0.0	100.0	0.0	0.0	0.0	
	Bylot Island		Feather	2012	26	0.92 0.31 - 2.27	0.0	94.0	6.0	0.0	0.0	
	Bylot Island		Feather	2013	25	1.27 0.34 - 4.34	0.0	94.0	6.0	0.0	0.0	
	Igloolik		Feather	2013	15	1.41 0.35 - 5.83	0.0	87.0	13.0	0.0	0.0	
Baird's Sandpiper	Igloolik		Feather	2013	1	2.38 .	0.0	100.0	0.0	0.0	0.0	
Black Turnstone	Cape Krusenstern		Feather	2012	14	1.69 0.51 - 4.69	0.0	84.0	16.0	0.0	0.0	
	Cape Krusenstern		Feather	2013	5	1.32 0.39 - 4.27	0.0	84.0	16.0	0.0	0.0	
Black-bellied Plover	East Bay		Feather	2012	6	1.70 0.29 - 2.61	0.0	100.0	0.0	0.0	0.0	
	East Bay		Feather	2013	6	0.86 0.31 - 1.55	0.0	100.0	0.0	0.0	0.0	
Dunlin	Nome		Feather	2012	2	0.88 0.59 - 1.17	0.0	100.0	0.0	0.0	0.0	
	Cape Krusenstern		Feather	2012	14	1.17 0.47 - 2.54	0.0	94.0	3.0	3.0	0.0	
	Cape Krusenstern		Feather	2013	19	1.41 0.49 - 6.38	0.0	94.0	3.0	3.0	0.0	
	Barrow		Feather	2012	24	1.66 0.10 - 5.34	0.0	82.0	18.0	0.0	0.0	
	Barrow		Feather	2013	60	1.72 0.57 - 4.87	0.0	82.0	18.0	0.0	0.0	
	Colville River		Feather	2012	12	1.36 0.80 - 2.72	0.0	83.0	17.0	0.0	0.0	
	Colville River		Feather	2013	17	1.92 0.86 - 4.96	0.0	83.0	17.0	0.0	0.0	
	Ikpikpuk River		Feather	2012	21	1.02 0.49 - 1.87	0.0	100.0	0.0	0.0	0.0	
	Ikpikpuk River		Feather	2013	11	1.32 0.92 - 1.81	0.0	100.0	0.0	0.0	0.0	
Long-billed Dowitcher	Barrow		Feather	2012	22	2.19 0.31 - 12.14	0.0	92.0	6.0	3.0	0.0	
	Barrow		Feather	2013	14	1.07 0.31 - 2.42	0.0	92.0	6.0	3.0	0.0	
Pectoral Sandpiper	Nome		Feather	2012	7	1.66 0.66 - 3.40	0.0	86.0	14.0	0.0	0.0	
	Barrow		Feather	2012	40	2.31 0.56 - 6.67	0.0	70.0	30.0	0.0	0.0	
	Barrow		Feather	2013	33	3.21 0.94 - 7.37	0.0	70.0	30.0	0.0	0.0	
	Mackenzie River Delta		Feather	2013	8	2.23 0.88 - 3.94	0.0	88.0	13.0	0.0	0.0	
	Bylot Island		Feather	2013	1	1.91 .	0.0	100.0	0.0	0.0	0.0	
Red Phalarope	Barrow		Feather	2012	51	0.68 0.14 - 4.00	0.0	99.0	1.0	0.0	0.0	
	Barrow		Feather	2013	40	0.50 0.21 - 0.84	0.0	99.0	1.0	0.0	0.0	
	Colville River		Feather	2012	13	0.51 0.21 - 1.54	0.0	100.0	0.0	0.0	0.0	
	Ikpikpuk River		Feather	2012	19	0.53 0.24 - 1.19	0.0	100.0	0.0	0.0	0.0	
	Ikpikpuk River		Feather	2013	16	0.54 0.22 - 1.20	0.0	100.0	0.0	0.0	0.0	
	East Bay		Feather	2013	15	0.77 0.37 - 1.33	0.0	100.0	0.0	0.0	0.0	
Red-necked Phalarope	Nome		Feather	2012	44	1.03 0.30 - 2.42	0.0	100.0	0.0	0.0	0.0	
	Nome		Feather	2013	33	0.60 0.24 - 2.17	0.0	100.0	0.0	0.0	0.0	
	Cape Krusenstern		Feather	2012	9	0.70 0.34 - 1.33	0.0	100.0	0.0	0.0	0.0	
	Barrow		Feather	2012	12	0.46 0.24 - 0.71	0.0	100.0	0.0	0.0	0.0	
	Barrow		Feather	2013	5	0.46 0.26 - 0.80	0.0	100.0	0.0	0.0	0.0	
	Colville River		Feather	2013	8	0.43 0.27 - 1.02	0.0	100.0	0.0	0.0	0.0	
	Ikpikpuk River		Feather	2012	15	0.50 0.18 - 1.03	0.0	100.0	0.0	0.0	0.0	
	Ikpikpuk River		Feather	2013	16	0.61 0.24 - 2.30	0.0	100.0	0.0	0.0	0.0	
	Mackenzie River Delta		Feather	2013	23	0.68 0.21 - 1.78	0.0	100.0	0.0	0.0	0.0	
Ruddy Turnstone	Colville River		Feather	2013	14	2.25 0.84 - 7.29	0.0	71.0	29.0	0.0	0.0	
	East Bay		Feather	2012	14	1.15 0.27 - 3.29	0.0	95.0	5.0	0.0	0.0	
	East Bay		Feather	2013	5	0.73 0.49 - 0.93	0.0	95.0	5.0	0.0	0.0	
Semipalmated Sandpiper	Nome		Feather	2012	38	0.93 0.28 - 3.66	0.0	99.0	1.0	0.0	0.0	
	Nome		Feather	2013	35	0.97 0.18 - 2.54	0.0	99.0	1.0	0.0	0.0	
	Cape Krusenstern		Feather	2012	34	0.79 0.17 - 2.70	0.0	100.0	0.0	0.0	0.0	
	Cape Krusenstern		Feather	2013	27	0.72 0.18 - 2.10	0.0	100.0	0.0	0.0	0.0	
	Barrow		Feather	2012	55	0.96 0.24 - 9.25	0.0	99.0	1.0	1.0	0.0	
	Barrow		Feather	2013	81	0.86 0.07 - 2.90	0.0	99.0	1.0	1.0	0.0	
	Colville River		Feather	2012	14	0.80 0.34 - 1.83	0.0	100.0	0.0	0.0	0.0	
	Colville River		Feather	2013	2	0.83 0.72 - 0.94	0.0	100.0	0.0	0.0	0.0	
	Ikpikpuk River		Feather	2012	46	0.71 0.18 - 5.18	0.0	98.0	2.0	0.0	0.0	
	Ikpikpuk River		Feather	2013	36	0.85 0.27 - 4.79	0.0	98.0	2.0	0.0	0.0	
	Mackenzie River Delta		Feather	2012	17	1.04 0.14 - 2.01	0.0	100.0	0.0	0.0	0.0	
	Mackenzie River Delta		Feather	2013	20	0.61 0.13 - 1.73	0.0	100.0	0.0	0.0	0.0	
	Igloolik		Feather	2013	11	0.59 0.30 - 2.10	0.0	100.0	0.0	0.0	0.0	
Western Sandpiper	Nome		Feather	2012	38	0.97 0.17 - 2.44	0.0	99.0	1.0	0.0	0.0	
	Nome		Feather	2013	30	1.03 0.15 - 4.68	0.0	99.0	1.0	0.0	0.0	
	Cape Krusenstern		Feather	2012	27	1.74 0.13 - 10.24	0.0	86.0	12.0	2.0	0.0	
	Cape Krusenstern		Feather	2013	30	1.46 0.12 - 4.42	0.0	86.0	12.0	2.0	0.0	
	Barrow		Feather	2012	19	1.64 0.19 - 6.21	0.0	81.0	17.0	2.0	0.0	
	Barrow		Feather	2013	33	1.93 0.17 - 10.13	0.0	81.0	17.0	2.0	0.0	

13667

13668 **Annex Table 6.** Contemporary (post 2000) Hg exposure and potential health risk of Arctic marine fish. Individuals are categorised per study region and
13669 assigned to five risk categories based upon muscle-specific Hg effect thresholds. Grey shaded populations are from regions outside the Arctic.

13670

						Hg concentration	Risk category					
						Muscle (µg/g)	<0.10	0.10-0.30	0.30-0.50	0.5-2.0	≥2.00	
Species	**Region**	**Maturity**	**Matrix**	**Years**	***n***	Median (Min–Max)	No effect	Low risk	Moderate risk	High risk	Severe risk	**Reference**
Atlantic cod	Barents Sea	All F+M	Muscle (ww)	2000-2018	866	0.03 (0.01-0.29)	97.3	2.7	0.0	0.0	0.0	ICES Data Centre 2020
Gadus morhua	Norwegian Sea	All F+M	Muscle (ww)	2000-2018	686	0.08 (0.01-1.87)	67.2	27.3	3.9	1.6	0.0	
	Icelandic Waters	All F+M	Muscle (ww)	2000-2018	47	0.03 (0.02-0.2)	93.6	6.4	0.0	0.0	0.0	
	Faroes Island	All F+M	Muscle (ww)	2000-2016	252	0.04 (0.01-0.21)	97.6	2.4	0.0	0.0	0.0	
	Mýlingsgrunnur	All F+M	Muscle (ww)	2000-2017	266	0.03 (0.01-0.21)	97.7	2.3	0.0	0.0	0.0	BirgittaA
	Baltic Sea	All F+M	Muscle (ww)	2000-2018	223	0.03 (0-0.11)	99.6	0.5	0.0	0.0	0.0	ICES Data Centre 2020
	Celtic Seas	All F+M	Muscle (ww)	2000-2016	42	0.08 (0.03-0.39)	57.1	40.5	2.4	0.0	0.0	
	Greater North Sea	All F+M	Muscle (ww)	2000-2018	2828	0.1 (0.01-1.46)	48.5	41.5	7.9	2.1	0.0	
Common dab	Icelandic Waters	All F+M	Muscle (ww)	2000-2000	1	0.07 (0.07-0.07)	100.0	0.0	0.0	0.0	0.0	ICES Data Centre 2020
Limanda limanda	Baltic Sea	All F+M	Muscle (ww)	2007-2016	90	0.03 (0-0.12)	97.8	2.2	0.0	0.0	0.0	
	Celtic Seas	All F+M	Muscle (ww)	2000-2018	858	0.13 (0.01-0.54)	34.0	61.7	4.2	0.1	0.0	
	Greater North Sea	All F+M	Muscle (ww)	2000-2018	2016	0.09 (0.01-1.1)	59.1	39.8	0.9	0.3	0.0	
European plaice	Barents Sea	All F+M	Muscle (ww)	2000-2011	56	0.02 (0.01-0.08)	100.0	0.0	0.0	0.0	0.0	ICES Data Centre 2020
Pleuronectes platessa	Norwegian Sea	All F+M	Muscle (ww)	2000-2011	53	0.03 (0.01-0.18)	92.5	7.6	0.0	0.0	0.0	
Arctic char	Bjørnøya	All F+M	Muscle (ww)	2001-2015	178	0.13 (0.03-0.83)	33.7	43.8	14.6	7.9	0.0	Poste_Evenset_Blevin
Salvelinus alpinus	Faroes Island	All F+M	Muscle (ww)	2001-2014	169	0.24 (0.12-0.67)	0.0	75.7	19.5	4.7	0.0	ICES Data Centre 2020
(anadromous, sea run)	Greenland Sea	All F+M	Muscle (ww)	2004-2018	45	0.71 (0.17-3.56)	0.0	4.4	11.1	80.0	4.4	
	Queen Maud Gulf	All F+M	Muscle (ww)	2004-2018	155	0.06 (0.01-0.36)	93.6	5.8	0.7	0.0	0.0	Evans_ECCC
Lake trout	GSL-East Arm	All F+M	Muscle (ww)	2000-2018	227	0.16 (0.03-0.58)	20.3	70.5	8.8	0.4	0.0	Evans_ECCC
Salvelinus namaycush	GSL-West Basin	All F+M	Muscle (ww)	2000-2018	212	0.2 (0.08-0.51)	4.7	81.1	13.7	0.5	0.0	

13671
13672
13673
13674
13675

Annex Table 7. Contemporary (post 2000) Hg exposure and potential health risk of Arctic freshwater fish. Individuals are categorised per study region and assigned to five risk categories based upon muscle-specific Hg effect thresholds.

						Hg concentration	Risk category					
						Muscle (µg/g)	<0.10	0.10-0.30	0.30-0.50	0.5-2.0	≥2.00	
Species	**Region**	**Maturity**	**Matrix**	**Years**	***n***	Median (Min–Max)	No effect	Low risk	Moderate risk	High risk	Severe risk	**Reference**
Northern pike	GSL-West Basin	All F+M	Muscle (ww)	2000-2018	266	0.24 (0.09-0.87)	1.9	66.9	28.6	2.6	0.0	Evans_ECCC
Esox lucius	Storvindeln	All F+M	Muscle (ww)	2000-2017	160	0.27 (0.11-0.65)	0.0	65.0	31.3	3.8	0.0	SarahD
Burbot	Fort Good Hope	All F+M	Muscle (ww)	2000-2018	671	0.36 (0-1.04)	1.0	31.2	50.4	17.4	0.0	Stern
Lota lota	GSL-East Arm	All F+M	Muscle (ww)	2000-2018	192	0.13 (0.04-0.36)	22.4	76.6	1.0	0.0	0.0	Evans_ECCC
	GSL-West Basin	All F+M	Muscle (ww)	2000-2018	223	0.16 (0.06-0.51)	10.8	85.2	3.6	0.5	0.0	Evans_ECCC
Brown trout	Leitisvatn	All F+M	Muscle (ww)	2017-2017	13	0.35 (0.15-0.71)	0.0	38.5	46.2	15.4	0.0	BirgittaA
Salmo trutta	Mjáuvøtn	All F+M	Muscle (ww)	2017-2017	7	0.08 (0.06-0.31)	71.4	14.3	14.3	0.0	0.0	BirgittaA
Arctic char	Á Mýrunum	All F+M	Muscle (ww)	2000-2014	197	0.23 (0.1-0.67)	0.0	74.6	22.3	3.1	0.0	BirgittaA
Salvelinus alpinus	Amituk Lake	All F+M	Muscle (ww)	2001-2018	144	1.14 (0.1-3.87)	0.0	5.6	6.3	73.6	14.6	Muir_Hudelson
	Char Lake	All F+M	Muscle (ww)	2000-2018	85	0.42 (0.08-1.03)	3.5	34.1	20.0	42.4	0.0	
	Isortoq AMAP	All F+M	Muscle (ww)	2004-2018	123	0.85 (0.17-3.56)	0.0	2.4	6.5	85.4	5.7	Riget
	Lake Hazen	All F+M	Muscle (ww)	2001-2018	314	0.13 (0.02-1.63)	40.5	35.7	14.7	9.2	0.0	Muir_Hudelson
	North Lake	All F+M	Muscle (ww)	2000-2018	181	0.21 (0.08-1.38)	2.8	72.4	15.5	9.4	0.0	
	Resolute Lake	All F+M	Muscle (ww)	2000-2018	272	0.15 (0.06-0.53)	13.6	76.8	9.2	0.4	0.0	
	Small Lake	All F+M	Muscle (ww)	2011-2012	30	0.09 (0.04-0.19)	100.0	0.0	0.0	0.0	0.0	Barst et al. 2016
	9-Mile Lake	All F+M	Muscle (ww)	2011-2012	30	0.12 (0.06-0.39)	30.0	63.3	6.7	0.0	0.0	
	Boomerang Lake	All F+M	Muscle (ww)	2012-2012	15	0.14 (0.09-0.54)	13.3	66.7	13.3	6.7	0.0	
	East Lake	All F+M	Muscle (ww)	2008-2009	17	0.1 (0.05-0.29)	52.9	47.1	0.0	0.0	0.0	
	West Lake	All F+M	Muscle (ww)	2008-2009	26	0.16 (0.05-0.44)	30.8	61.5	7.7	0.0	0.0	
	Aquiatusuk Lake	All F+M	Muscle (ww)	#VALUE!	15	0.59 (0.16-1.03)	0.0	26.7	13.3	60.0	0.0	
	Saphire Lake	All F+M	Muscle (ww)	2001-2001	9	0.36 (0.16-1.07)	0.0	22.2	55.6	22.2	0.0	Muir et al. (2005)
	Tasialuk	All F+M	Muscle (ww)	2007-2007	10	0.13 (0.08-0.17)	10.0	90.0	0.0	0.0	0.0	Gantner et al. (2010)
	Coady's Pond	All F+M	Muscle (ww)	2007-2007	10	0.1 (0.07-0.12)	50.0	50.0	0.0	0.0	0.0	
	Little Nauyuk	All F+M	Muscle (ww)	2006-2006	10	0.11 (0.07-0.22)	40.0	60.0	0.0	0.0	0.0	
	Radar	All F+M	Muscle (ww)	1999-1999	8	0.91 (0.23-1.92)	0.0	12.5	12.5	75.0	0.0	
	Herbert	All F+M	Muscle (ww)	1999-1999	8	0.35 (0.21-2.34)	0.0	50.0	12.5	25.0	12.5	
	12-Mile Lake	All F+M	Muscle (ww)	2006-2006	10	0.14 (0.1-0.2)	20.0	80.0	0.0	0.0	0.0	
	Coady's Pond #2	All F+M	Muscle (ww)	2007-2007	20	0.12 (0.06-0.21)	25.0	75.0	0.0	0.0	0.0	van der Velden et al. (2013)
	Heintzelman Lake	All F+M	Muscle (ww)	2001-2001	119	0.11 (0.03-0.32)	45.4	52.9	1.7	0.0	0.0	van der Velden et al. (2012)
	Tasiapik Lake	All F+M	Muscle (ww)	2009-2010	31	0.1 (0.06-0.26)	51.6	48.4	0.0	0.0	0.0	
	Esker Lake	All F+M	Muscle (ww)	2008-2008	20	0.07 (0.04-0.86)	80.0	15.0	0.0	5.0	0.0	
	Upper Nakvak Lake	All F+M	Muscle (ww)	2007-2007	20	0.07 (0.03-0.49)	60.0	30.0	10.0	0.0	0.0	
	Tasiapik Lake	All F+M	Muscle (ww)	2009-2010	31	0.1 (0.06-0.26)	51.6	48.4	0.0	0.0	0.0	
	Crazy Lake	All F+M	Muscle (ww)	2010-2010	47	0.06 (0.03-1.03)	78.7	12.8	6.4	2.1	0.0	
	Iqalugaarjuit Lake	All F+M	Muscle (ww)	2004-2004	20	0.11 (0.07-0.3)	45.0	55.0	0.0	0.0	0.0	
	Unnamed Lake	All F+M	Muscle (ww)	2010-2010	18	0.19 (0.08-0.42)	11.1	55.6	33.3	0.0	0.0	
	Lake A (Qaqortoq)	All F+M	Muscle (ww)	1994-1995	50	0.6 (0.07-3.73)	2.0	2.0	26.0	66.0	4.0	Rigét et al. (2000)
	Lake B (Qaqortoq)	All F+M	Muscle (ww)	1995-1995	22	0.48 (0.15-1.71)	0.0	22.7	31.8	45.5	0.0	
	Lake C (Qaqortoq)	All F+M	Muscle (ww)	1995-1995	25	0.54 (0.22-1.32)	0.0	8.0	32.0	60.0	0.0	
	Lake D (Qaqortoq)	All F+M	Muscle (ww)	1995-1995	22	0.57 (0.23-2.01)	0.0	4.6	31.8	59.1	4.6	
	Avanersuaq	All F+M	Muscle (ww)	1994-1995	26	0.21 (0.04-0.5)	23.1	50.0	26.9	0.0	0.0	
	Hovaktok	All F+M	Muscle (ww)	2006-2006	7	0.05 (0.02-0.08)	100.0	0.0	0.0	0.0	0.0	Swanson and Kidd (2010)
	Lake 10	All F+M	Muscle (ww)	2006-2006	7	0.05 (0.03-0.08)	100.0	0.0	0.0	0.0	0.0	Barst et al. 2019
	Lake 32	All F+M	Muscle (ww)	2006-2006	12	0.08 (0.02-0.23)	75.0	0.0	25.0	0.0	0.0	
	Nauyuk	All F+M	Muscle (ww)	2006-2006	18	0.04 (0.02-0.16)	83.3	16.7	0.0	0.0	0.0	Swanson and Kidd (2010)
	Gavia Faeces	All F+M	Muscle (ww)	2006-2006	8	0.08 (0.05-0.51)	75.0	0.0	12.5	12.5	0.0	Swanson et al. (2011)
	Keyhole	All F+M	Muscle (ww)	2006-2006	7	0.1 (0.03-0.27)	42.9	57.1	0.0	0.0	0.0	
	Notgordie	All F+M	Muscle (ww)	2006-2006	5	0.19 (0.15-0.34)	0.0	60.0	40.0	0.0	0.0	
	Roberts	All F+M	Muscle (ww)	2006-2006	34	0.01 (0.01-0.04)	100.0	0.0	0.0	0.0	0.0	Swanson and Kidd (2010)
Lake trout	Lake Kusawa	All F+M	Muscle (ww)	2001-2018	179	0.31 (0.1-1.31)	0.0	48.6	35.8	15.6	0.0	Gamberg
Salvelinus namaycush	Lake Laberge	All F+M	Muscle (ww)	2000-2018	188	0.42 (0.1-1.36)	0.5	24.5	42.6	32.5	0.0	Gamberg

* This is Chapter 7 of the AMAP Mercury Assessment*

7. What is the Impact of Mercury Contamination on Human Health in the Arctic? 2021 Update.

Coordinating Authors: Pal Weihe, Nil Basu

Contributing Authors: Eva Kruemmel, Khaled Abass, Arja Rautio

Table of Contents

7.1. Introduction

Contemporaneous concerns over mercury pollution in the Arctic nears 50 years with past AMAP reports having examined in great detail the evidence of mercury exposure and effects on Arctic populations (AMAP 1998, 2003, 2009, 2011). These reports illustrate that human populations in the Arctic remain amongst the most exposed and impacted worldwide, and they also demonstrate that the impacts of mercury extend beyond classic toxicological effects and also encompass broader issues of social and cultural well-being and food security. This chapter extends upon these works to provide an update of the scientific information since the last report published in 2011 (AMAP 2011). Non-Indigenous residents in the Arctic may also be exposed to mercury though the exposure levels tend to be lower than the region's Indigenous Peoples, and thus the current chapter tends to focus on the latter group.

Since the last AMAP report, the entry into force of the Minamata Convention on Mercury in 2017 signalled the world's commitment by governments to reduce the use and environmental release of mercury in order to protect human health and the environment (Article 1). As described in detail in the introduction, information on mercury in the Arctic from AMAP and involvement from Arctic Indigenous Peoples and Arctic countries were crucial in the negotiations of the Minamata Convention on Mercury. This is particularly visible in the preamble (page 5) of the Minamata Convention, which makes reference to "the particular vulnerabilities of Arctic ecosystems and Indigenous communities". As part of the 2018 UN Global Mercury Assessment, a systematic assessment of mercury exposures worldwide demonstrated "Arctic populations who consume fish and marine mammals" as one of four priority groups of concern (Basu et al., 2018).

Arctic populations, and most notably Indigenous communities, are particularly vulnerable to mercury pollution for several reasons. As elaborated elsewhere in this report (REF), a range of global factors that span from socioeconomic patterns to biogeochemical processes make the Arctic a major sink for mercury pollution. As a result, some traditional country food items (i.e., tissues of certain marine mammals and some freshwater fish in certain geographic locations) may have relatively high levels of mercury, as detailed below. Avoiding such food items is not an option in many cases or communities as traditional food items have great nutritional and cultural benefit, and are far superior nutritionally and affordable compared to store-bought options and are therefore promoted by regional health officials. Further, the harvesting, sharing, and consuming traditional foods support cultural, social, and spiritual health in communities. Finally, critical aspects of mercury pollution, food systems, and northern life are inter-linked and further pressured due to climate change (Berner et al.; Nilsson et al.).

This chapter summarizes information on the impacts of mercury on human health taken primarily from the most recent AMAP human health assessment (AMAP, 2015), with some additional updates from recent studies. In answering the primary question of this chapter – What is the impact of mercury contamination on

human health in the Arctic? – the following sections illustrate links between findings presented in the rest of this assessment and their implications for human health.

7.2. Global influences on mercury exposure in the North

Earlier chapters discuss in detail the most important sources of mercury to the Arctic (Chapter X), biogeochemical factors that drive mercury's movement to the region and also within the region (Chapter X), and the influence of climate change on these processes as well as future scenarios (Chapter X).

As detailed in Chapter X, approximately XX% of the current mercury in Arctic wildlife, some of which represent key food items for Arctic Indigenous Peoples, is estimated to originate from anthropogenic activities in southern latitudes. Even though local and regional characteristics may influence mercury exposure in these species, global anthropogenic activities are ultimately driving exposures to Arctic Peoples. Exposures are further being driven by global drivers such as changes to hydrology or land us as well as the introduction of invasive species, which in turn alter the structure of food webs and ecosystem energetics and ultimately the accumulation and biomagnification of mercury (Eagles Smith et al.)

The impact of climate change on mercury cycling and ultimately human exposures is multi-dimensional and profound. Here we extend upon some examples shared earlier in Chapter X. Which examples? Let's see what that chapter puts forth before expanding here.

Another global phenomenon influencing mercury exposures in the Arctic is the industrialization of many country economies which in turn influences international food markets and trade. As such, and elaborated upon further below, a nutrition transition is well underway in many Arctic communities in that store-bought foods are being increasingly supplemented by certain store-bought foods of low nutritional value that also tend to exemplify a western diet. While such a shift may reduce human exposures to mercury (i.e., less consumption of local fish and wildlife), the shift is also associated with a poorer and unhealthy diet that largely consists of refined carbohydrates and saturated fatty acids with limited content of nutrients, vitamins, and unsaturated fatty acids.

7.3. Dietary influences on mercury exposure in the North

Arctic Indigenous Peoples are largely exposed to mercury through their diet. Here we detail what is known about key foods and factors that may influence exposure, the nutrition transition underway across Arctic communities, and modelling approaches to gauge exposures.

7.3.1 Exposure to mercury contaminated traditional foods

The amount of mercury in traditional and/or local foods can be gleaned from a review of information presented other chapters (Chapter X). The data presented in those chapters demonstrates that the levels of mercury can differ widely across Arctic biota (and even within a species); mercury levels vary greatly across space and time, and are also influenced by factors such as food web position, sex, and age. These in turn have tremendous implications for human exposures especially since many of these biota (or their parts) represent key dietary sources. For example, mercury levels in landlocked Arctic char can vary 100-fold (0.01 to 1.13 µg/g; Barst et al.) and mercury levels in ringed seal liver can vary 4,500-fold based on a review of the min-max data from Chapter X (Biota chapter data). Further, mercury levels within an organism can vary across tissues (REF), and such information is important when developing dietary advisories. Finally, most monitoring and research studies tend to present data on total mercury levels though the percent that is MeHg can vary widely across species and tissues (REF) and is not always characterized. From a human health perspective, the MeHg component is what is most bioavailable (Bradley et al. REF).

Mercury has been measured in thousands of fish samples from across the Arctic region. To help put some of these data into perspective we note that the US EPA has a consumption value of 0.3 µg/g, Health Canada's limit for mercury in the edible portion of retail fish is 0.5 µg/g as is the value proposed by the European Commission (REF), and the World Health Organization has set 1µg/g (REF). An analysis of Hg levels in muscle from 1,569 landlocked Arctic char from across 83 sites found that mercury levels exceeded 0.3 µg/g (ww) in 21% of the sites (Barst et al. REF). In Alaska, Jewett and Duffy (2007) measured muscle mercury in 2,692 samples spanning 17 freshwater species and 24 anadromous and marine fish species. The highest levels were found in northern pike (often exceeded guidelines), and were relatively low in the most frequently consumed species including salmon, cod, halibut, and herring.

The mercury levels in mammalian tissues are often much higher than in fish, and usually these exceed aforementioned guideline values. For example, from the Faroe Islands, mercury levels in cod (a stable food source on the island) are about 0.02 µg/g versus 2 µg/g which may be found in the muscle of pilot whales (REF). The median level of liver mercury in ringed seals from across several studies was almost always above 1 µg/g (Biota Chapter).

A number of dietary surveys have demonstrated that ingestion of some traditional and/or local foods, especially from certain fish and marine mammals, drive exposure to mercury. For example, in a study of children from Nunavut (Canada), the top contributors of mercury exposure were beluga muktuk (33%) followed by narwhal muktuk (26%) and ringed seal liver (15%). When coupled with fish (11%), caribou meat (6%) and ringed seal meat (5%), these food items accounted for over 95% of the total Hg intake. From the Inuit Health Survey (2,074 adults from 36 communities) in Canada, ringed seal liver was the largest source of mercury exposure (59%) followed by Arctic char (8.4%) (Laird et al. 2013b). In fact, ten food

items accounted for ~90% of the mercury intake while the remaining 72 accounted for only 10%. These ten food items include:

ringed seal liver, arctic char meat, beluga muktuk (skin only), beluga muktuk (skin + fat), ringed seal meat, caribou meat, narwhal muktuk (skin + fat), dried caribou meat, narwhal muktuk (skin only), and beluga meat. A study of 2,2224 Inuit adults from Greenland between 2005 and 2008 related dietary information (25 traditional and 43 imported food items) with whole blood mercury levels, and found that seal consumption was the largest contributor of mercury exposure (REF).

[Above information into a table based on below and here: https://academic.oup.com/jn/article/143/6/923/4571735#supplementary-data]

ONLINE SUPPORTING MATERIAL

Supplemental Table 2. Output concentration of Hg, Se, EPA, and DHA from Crystal Ball™ model from the di assessment for IPY Inuit Health Survey participants.[1,2]

Food	Mercury[3], *ng/g*	Selenium[3], *ng/g*	EPA[3], *µg/g*	DHA[3], *µg/g*
Seagull eggs	356 ± 279	594 ± 171	4.82 ± 3.54	207 ± 198
Duck	138 ± 131	387 ± 190	172 ± 193	175 ± 193
Ptarmigan	0.923 ± 0.717	46.2 ± 64.4	67.7 ± 41.5	4.84 ± 3.58
Loon	127 ± 100	385 ± 187	174 ± 194	176 ± 195
Canada goose	11.2 ± 8.82	194 ± 47	95.6 ± 69.4	77.5 ± 59.3
Goose or Eider duck eggs	357 ± 280	342 ± 19.5	4.78 ± 3.53	208 ± 198
Goose eggs	354 ± 279	342 ± 19.5	4.83 ± 3.57	205 ± 194
Eider duck eggs	352 ± 275	342 ± 19.5	4.83 ± 3.57	205 ± 194
Pigeon eggs	356 ± 281	341 ± 19.5	4.84 ± 3.56	207 ± 198
Tern eggs	275 ± 218	342 ± 19.6	4.82 ± 3.56	208 ± 199
Brown duck eggs	354 ± 277	342 ± 19.5	4.89 ± 3.61	206 ± 197
Other eggs	353 ± 279	342 ± 19.5	4.84 ± 3.57	205 ± 197
Willow ptarmigan	6.29 ± 4.96	46.6 ± 66	67.4 ± 41.6	4.85 ± 3.58
Rock ptarmigan	0.918 ± 0.719	47.7 ± 66.3	67.7 ± 41.9	4.81 ± 3.58
Tern	276 ± 219	387 ± 189	174 ± 194	175 ± 194
Swan	12.9 ± 10.2	386 ± 189	174 ± 194	300 ± 275
Lesser Canada goose	16.2 ± 12.7	194 ± 47	96.6 ± 70.6	77.7 ± 59.7
Arctic loon	127 ± 101	384 ± 186	173 ± 194	175 ± 195
Red throated loon	127 ± 101	386 ± 189	175 ± 193	175 ± 196
Eider duck	128 ± 102	384 ± 186	174 ± 195	174 ± 191
Fish eggs	763 ± 606	618 ± 356	8950 ± 3580	11700 ± 4690
Arctic char	119 ± 93.6	260 ± 140	6780 ± 3200	5320 ± 3280
Trout	65.5 ± 51.3	280 ± 156	2130 ± 987	4980 ± 1500
Lake trout	319 ± 252	300 ± 132	2130 ± 985	4990 ± 1590
Salmon	109 ± 85.8	365 ± 91	4340 ± 2200	7530 ± 3060
Whitefish	208 ± 163	236 ± 130	2750 ± 2020	3170 ± 2500
Sculpin	67.2 ± 52.8	604 ± 137	912 ± 722	917 ± 722
Capelin	66.2 ± 52.6	415 ± 69.8	4870 ± 2820	6950 ± 3620
Rock cod	112 ± 88.3	377 ± 36	384 ± 280	1270 ± 499
Dried cod	111 ± 87.4	1350 ± 1060	99.8 ± 79.2	3850 ± 3050
Brook trout	65 ± 51.7	278 ± 154	2130 ± 983	4960 ± 1480
Cod	112 ± 88	138 ± 134	383 ± 277	1280 ± 501
Atlantic cod	113 ± 88.8	377 ± 36.1	379 ± 274	1270 ± 497
Turbot	23.7 ± 18.8	415 ± 69.9	5980 ± 1000	4470 ± 757
Halibut	230 ± 182	415 ± 70.1	2260 ± 1890	3000 ± 1280
Herring	118 ± 93	322 ± 129	9500 ± 2070	8830 ± 1630
Smelts	66.8 ± 52.7	415 ± 70.3	4830 ± 2810	3850 ± 3040

The accessibility and bioavailablity of mercury from a given food item into an individual may be influenced by a range of factors. A body of emerging research suggests that mercury may be less than 100% bioavailable from food items to human consumers (Bradley REF). For example, Laird et al. (2009) used an in vitro system to calculate that the bioaccessibility of mercury from the small intestine may range between 1

and 93% for 16 fish, wild game, and marine mammal samples typically consumed by Inuit. While these in vitro results suggest that not all the ingested mercury is taken up, to our knowledge such a finding has yet to be proven in a human population study and thus the emerging science should be viewed cautiously. There remains long interest on the potential protective role of selenium against mercury risk, and while experimental studies tend to suggest a protective role for selenium few population studies have provided convincing and consistent evidence. For example, consideration of selenium in two waves of the Faroe Islands birth cohort studies found no evidence for a protective role for selenium (Choi et al. 2008) though a study of adults from the Inuit Health Survey from Canada found some cardioprotective effects of selenium in relation to mercury exposure (REF).

7.3.2 Nutrition transition

The nature of mercury exposures across the Arctic is changing, and diet is playing a major role in this change. From the 2007-2008 Inuit Health Survey of 36 Canadian Arctic Communities, researchers calculated a 50% decline in the consumption of fish, whale, seal meat and birds and were able to associate this with a significant decrease in essential nutrients such as zinc and vitamin D (Rosol et al. 2016). Interviews with Inuit community members in Nunavut (Canada) that included elders and hunters revealed concerns about changing climate, weather patterns, and species distribution (Nancarrow and Chan, 2010). From the Survey of Living Conditions in the Arctic (SLICA) that includes Greenland, Chukotka (Russia), and Alaska, 14% of the respondents were satisfied with the amount of fish and game available to them (Poppel et al., 2007).

The dietary transition has been notable in the Faroe Islands. Since the 1930s, there has been a steady decrease in the intake of fish from nearly four meals per week to less than two meals per week (REF). This has largely been driven by the Faroe Island's ability to import food from other countries as well as improved household economies thus enabling such purchases. The recommendation from the health authorities to reduce or stop whale consumption has not played a vital role in this transition. However, dietary advice might have enlightened the public about the nutritional values in marine food. For example, as elaborated in the recent AMAP Human Health report (REF), a part of the campaign against eating contaminated whale meat and blubber has been to inform about the good nutritional qualities in fish low in contaminants (e.g. lean fish like cod and haddock and fatty fish like herring, mackerel and salmon). The Faroes Board of Health recommends people to eat low contaminated fish without any upper limits of weekly servings. Nevertheless, the fish intake follows the same pattern with the continued decline as whale meat and blubber consumption does. The dietary advice to pregnant women has been effective as documented in large birth cohort studies: The mercury levels have decreased nearly five fold from ~1987 to ~2008 (blood mercury from 22.3 to 4.6 µg/L) in umbilical cord blood. Similar to the Faroe Islands, the Greenland authorities have also been

challenged with trying to put forth guidelines that balance benefits and risks (https://pubmed.ncbi.nlm.nih.gov/22789516-)

Another important dimension is the high prevalence of food security concerns for Arctic Indigenous Peoples. For example, 63% of Inuit in Canada's Arctic are food insecure with 27% being classified as severely food insecure following a cross-sectional study of nearly 2,000 households (https://www.ncbi.nlm.nih.gov/pubmed/22323760). Another survey concerning children from 16 Nunavut communities found that 70% lived in homes classified as food insecure with 25% of the homes being severely food insecure (https://www.cmaj.ca/content/182/3/243). A 2013 survey on 523 randomly selected households in Iqaluit (Canada) found that 32.9% of households with children were food insecure and that this was significantly higher than the 23.3% of households without children (Huet et al. 2017). Such food insecurity estimates from the Arctic are much higher than global estimates (e.g., severe food insecurity worldwide averaged 9.2% in 2018) (FAO Ref: http://www.fao.org/3/ca5162en/ca5162en.pdf).

It is difficult to identify the ultimate risk factor(s) that underpin food insecurity though studies have acknowledged the high cost of food (REF), unavailability of healthy food choices in local markets (REF), and challenges of hunting and fishing as being most important. The store-bought foods tend to reflect a Western diet consisting of food items composed largely of refined carbohydrates and saturated fatty acids with limited content of nutrients, vitamins and essential unsaturated fatty acids (Johnson-Down and Egeland, 2010). Such a diet coupled with a sedentary lifestyle can promote metabolic disorders increasing across Arctic communities such as diabetes and heart disease (Bjerregaard et al. 2004). There is thus a need for public health professionals to derive food consumption guidelines that balance the health benefits of traditional diets against the increased health risks associated with the contaminants that they contain.

7.3.3 Modeling exposures

Dietary mercury exposure is most often estimated by food frequency questionnaires (FFQ) coupled with modelling. However, there are notable challenges with this approach. For example, Canuel et al. (2006) re-analyzed a 1992 dataset from Nunavik (Canada) and found that predicted hair mercury values (18.1 µg/g) in Inuit using standard calculations were nearly 5-times higher than the measured value of 3.8 µg/g of mercury in hair. In this paper they concluded that "the relation between mercury oral dose and body burden… may vary among certain ethnic groups" and "metabolic excretion rates might vary according to ethnicity". Therefore, the expected constant and linear relation between MeHg oral dose and body burden, which is used by government officials to establish guidelines on safe levels of MeHg exposure, seems to vary significantly among ethnic groups (Canuel et al. 2006). This variation can result in MeHg levels exceeding the US EPA reference dose and can influence the derivation of a meaningful reference dose for MeHg applicable to all individuals in a population (Rand and Caito 2019).

Such variability is not surprising. In humans, a hair to blood mercury ratio of 250 is used in risk assessment, but this value can vary widely among populations (means: 140 to 370) and individuals (maximum ratio >600) (Basu et al., 2014; Liberda et al. 2014). The elimination half-life of MeHg in humans is assumed to be 70 days but can vary from 20 to 128 days (Rand and Caito 2019). In addition, dietary exposure is routinely estimated by combining data on consumption patterns from surveys with average mercury concentration in specific food items. However, the challenges associated with FFQs are well-established (e.g., recall bias) and mercury levels in a particular food item can vary tremendously. Moving ahead, coupling robust survey instrument with toxicokinetic modeling may prove more fruitful. The toxicokinetic approach depends un understanding the burden of mercury in different body compartments as well as the transfer coefficient between different body compartments (Abass et al. 2018). There are several factors determining MeHg body burden. These factors include dietary exposure (frequency, quantity and MeHg content of fish eaten), the individual's "ADME" kinetics, and the state of pregnancy, lactation, and overall health.

More expansive models are now being developed for Arctic Indigenous Peoples. For example, there are mechanistic models linking environmental fate and transport with human exposures for exposure to environmental contaminants, in particular persistent organic pollutants, emerging for Inuit (Undeman et al. 2010) (Binnington et al. 2016a; Binnington et al. 2016b; Czub et al. 2008;). In particular for mercury (and nutrients), the ACC-Human Arctic model was developed to calculate daily dietary intake (Binnington et al. 2016a). Consumption of certain tissues of caribou (heart, liver, tongue, meat, bone marrow), ringed seal (liver, meat, blubber), beluga whale/narwhal (meat, blubber) and Canada goose (meat, eggs) for Hg intake was differentiated.

Another approach moving forward is to consider the role that genetic variations have in explaining mercury exposures and body burdens as well as the association of these exposures with health outcomes (Basu et al. 2014). To date we are only two published studies from the Arctic that characterized mercury exposure in association with genetic variations. In a study of 281 Inuit from the Inuvialuit Settlement Region (Canada), there were 9 single nucleotide polymorphisms in toxicologically relevant genes (of 112 investigated) that helped explain higher or lower blood mercury levels (Parajuli et al. REF). As an example, carriers of the minor allele version of rs1133238 (*SEPHS2* gene) had blood mercury levels that were approximately 50% higher than people carrying the more common form. In many cases the prevalence of these genotypes in Inuit were quite distinct from other ethnic groups. In a study of 896 Inuit adults from Nunavik (Canada), genetic variants in the paraoxonase 1 (PON1) gene did not influence blood mercury levels even though associations were found with plasma PON1 enzyme activity (REF).

7.4. How mercury biomarker levels compare to guidelines

Human exposures can be assessed through the measurement of mercury concentrations in a number of different biological sample types, and key approaches for mercury biomonitoring have been reviewed by UN Environment and WHO (2008) and the US EPA (1997). The most commonly used biomarkers for methylmercury exposure are the concentrations of mercury in hair, blood, and cord blood, and their selection can depend on factors such as the potential source of exposure, chemical form, and exposure lifestage. Most of the mercury in hair is methylmercury and once incorporated the mercury remains in the hair. This biomarker can therefore provide an integrated measurement of mercury exposure given that hair grows at approximately 1 cm per month and thus exposure can be tracked over time by careful sampling. Hair has the advantage that it is easy to collect and transport though we note that in some communities there may be cultural objections to taking hair samples. Mercury is measured in whole blood and this provides information about recent exposures (~1-2 months) to both methylmercury and inorganic mercury. In most communities the measurement of blood total mercury is an accepted biomarker for methylmercury exposure as it correlates relatively well to seafood consumption (Sheehan et al., 2014). The use of speciation can provide an indication of potential mercury sources but requires careful sample preparation and sophisticated instrumentation. The measurement of mercury in cord blood provides information about developmental exposure. Blood collection, storage, and transport pose certain logistical and financial barriers, however.

As part of the 2018 UN Global Mercury Assessment, a systematic assessment of mercury exposures worldwide was performed by reviewing 312 high quality studies (i.e., identified through strict inclusion criteria) published on studies since the year 2000 (Basu et al., 2018). From this, 424,882 mercury biomarker measures from 336,015 individuals from 75 countries was analysed. The effort concluded that background populations with insignificant exposures to mercury have blood mercury levels that generally fall under 5 µg/L. The analysis clearly showed that Inuit in the Arctic are exposed to some of the highest methylmercury levels worldwide. Specifically, data from 15 Arctic sub-populations (7,472 individuals) was studied, and the central median blood mercury concentration in these groups was 8.6 µg/L (interquartile range spanned 3.6 to 16.2 µg/L) with an upper bound median concentration of 70.5 µg/L. Some of the communities reviewed in this effort were previously discussed in the AMAP (2015) report. For example, in Canada as part of the 2007–2008 International Polar Year study of 2,172 individuals, the geometric mean of blood mercury across 4 study regions ranged from 2.8 to 12 µg/L, with individual values ranging from 0.1 to 240 µg/L (AMAP 2015). In another example, the Greenlandic Inuit Health and Transition Study of 3,105 participants from all geographic areas and community sizes (9 towns, 13 villages) reported blood mercury levels to range from 0.1 to 400 µg/L (AMAP 2015).

Table or Figure. Total mercury levels (µg/L) in whole blood from Arctic populations identified following a systematic search of the literature as detailed in Basu et al. (REF).

14276

PAPER REF	COUNTRY	CITY	YEAR_RANGE	CENTRAL-# (µg/L)	UPPER-# (µg/L)
48-Curren2015	Canada	Baffin (Nunavut)	2005-2007	4.1	28
48-Curren2015	Canada	Inuvik (NWT)	2005-2006	1.1	14
54-Deutch2006	Denmark	Greenland (Qaanaq)	2003	51.9	240
54-Deutch2006	Denmark	Greenland (Scoresbysund)	1999	15.9	73
54-Deutch2006	Denmark	Greenland (Sisimiut)	2002-2003	7.3	33
54-Deutch2006	Denmark	Greenland (Tasiilaq)	2000-2001	24.8	155
70-Fontaine2008	Canada	Nunavik (Hudson Bay)	2004	11.7	240
70-Fontaine2008	Canada	Nunavik (Ungava Bay)	2004	8.6	104
94-AMAP2015	Canada	Inuvialuit Settlement Region	2007-2008	2.1	39
94-AMAP2015	Canada	Nunatsiavut	2007-2008	1.7	25
94-AMAP2015	Canada	Nunavut	2007-2008	5	52
127-Jeppesen2012	Denmark	Greenland (7 towns, 8 villages)	2005-2008	21.1	70.5
168-Mocevic2013	Denmark	Greenland (various)	2002-2004	9.2	386
222-Tian2011	Canada	Nunavut	2007-2008	0.74	5.2
223-Jeppesen2015	Denmark	Greenland	2005-2010	16.4	36

14277

14278

14279 **7.5. What are health effects of mercury in the North**

14280 **7.5.1 General health effects**

14281 The health effects of mercury have reviewed extensively in recent years by scientific experts (Eagles-Smith
14282 et al. 2018; Ha et al. 2017). While all forms of mercury have hazard potential, the most relevant form for
14283 Arctic communities is methylmercury. Over the years the adverse health effects associated with
14284 methylmercury exposure have been documented in humans at successively lower exposures, and it is now
14285 clear that real-world exposures to many populations is sufficient to cause sub-clinical impairments.

14286

7.5.2 Neurological

Epidemiological cohort studies on Arctic populations have been amongst the most influential worldwide in terms of demonstrating the link between early life mercury exposure and later-life adverse health outcomes. For example, cohort studies in the Faroe Islands have demonstrated that children exposed to methylmercury in utero exhibit decreased motor function, attention span, verbal abilities, memory and other mental functions. Follow-up of these children up to the age of 22 years indicates that these deficits appear to be permanent [3]. Similarly, a study in Nunavik (Canada) of child development at age 11 showed that mercury exposure was associated with poorer early processing of visual information, lower estimated IQ, poorer comprehension and perceptual reasoning, poorer memory functions, and increased risk of attention problems and ADHD behaviour [4-8].

Some of the adverse effects of MeHg on neurodevelopment may be masked by beneficial effects of seafood nutrients. Neurophysiological assessments of brain function also indicate that postnatal exposure up to the teenage years can cause harm [9]. Thus, both pregnant women and children are at increased risk from MeHg exposure.

Studies indicate that certain genetic factors may increase vulnerability to MeHg toxicity [10].

Jacobsen et al. [11] estimated the IQ in 282 school-age Inuit children in Arctic Québec from whom umbilical cord blood samples were analyzed for mercury and other environmental exposures. They found that prenatal mercury exposure was related to poorer estimated IQ after adjustment for potential confounding variables. The entry of DHA into the model significantly strengthened the association with mercury, supporting the hypothesis that beneficial effects from DHA intake can obscure adverse effects of mercury exposure. Children with cord mercury ≥ 7.5 µg/L were four times as likely to have an IQ score < 80, the clinical cut-off for borderline intellectual disability. Co-exposure to PCBs did not alter the association of mercury with IQ.

Although many studies of methylmercury toxicity focus on prenatal exposure because fetal brains are developing and thus more vulnerable, the effects of adult exposures have also been documented. A key concern with exposure in adults is that it may accelerate age-related declines [12].

Neurocognitive functions, especially fine-motor function and verbal memory, are compromised among adults who are exposed to elevated amounts of methylmercury, which is consistent with the outcomes observed in children with prenatal exposures.

7.5.3 Cardiovascular

Conflicting results have been reported regarding the impact of prenatal Hg exposure on blood pressure, with 7-year-old Faroese children exhibiting elevated blood pressure (REF) and children from Nunavik showing no

association between blood pressure and prenatal Hg exposure (REF). However, elevated blood pressure was found to be associated with Hg exposure among adults from the Faroe Islands (REF) and Nunavik (REF). Decreased heart rate variability was associated with cord blood Hg concentrations in Faroese children at ages 7 and 14 (REF) but not in 11-year-old children from Nunavik (REF); however, contemporary blood Hg concentrations in these children from Nunavik were associated with decreased overall heart rate variability parameters (REF). This was also the case for adults from Nunavik and for James Bay Cree adults (REF). Additionally, the effect of prenatal methylmercury exposure on blood pressure is more pronounced among children with lower birth weights. Comparing boys who had a mercury cord blood concentration of 10 µg/L to those who had 1 µg/L, heart rate variability was found to decrease significantly by 47% [19].

High concentrations of methylmercury in blood and tissue samples have been associated with acute coronary events, coronary heart disease, and cardiovascular disease [14]. A 2000 NRC report stated that it was reasonable to conclude that methylmercury accumulates in the heart and leads to blood pressure alterations and abnormal cardiac functions [15]. An expert panel convened in 2011 to study the health effects of methylmercury concluded that there was sufficient scientific evidence to incorporate cardiovascular health benefits in EPA's regulatory assessments [16]. According to the panel, methylmercury is both directly linked to acute myocardial infarction and intermediary to impacts that contribute to myocardial infarction risk. The intermediary impacts include oxidative stress, atherosclerosis, decreased heart rate variability, and to a certain degree, blood pressure and hypertension. A 2017 systematic review of the association between methylmercury exposure and heart diseases showed that methylmercury enhances production of free radicals resulting in a long-lasting range of effects on cardiac parasympathetic activity, such as myocardial infarction, hypertension, blood pressure, and death [17]. A 2018 meta-analysis of 29 studies found significant positive associations between methylmercury and both elevated blood pressure and hypertension [18]. Despite these, a relatively large study of Greenlandic Inuit conducted between 2005 and 2010 found no association with whole blood mercury levels and the risk of developing cardiovascular disease (REF) or blood pressure (REF).

Even if the cardiovascular impacts at the individual level occur at higher levels of exposure than the impacts on the central nervous system, the society-wide harm of the former should not be ignored. Unlike neurodevelopmental effects that primarily involve exposure of pregnant women and affect embryonic developments, cardiovascular outcomes of methylmercury could also impact adults through diet and over their lifespan.

7.6. What are risk communication and risk management strategies

*** Eva to write based on Human Health Report; Approx. 300-500 words ***

As described in previous chapters of this assessment, the main exposure pathway to mercury for humans is via their diet. In the case of Arctic Indigenous Peoples, this diet consists of traditional country food items, and includes top-predators of the Arctic food chain, such marine mammals and/or predatory fish. Arctic Indigenous Peoples often rely on their traditional country foods for food security, for their general health and well-being, and is part of their cultural identity. If high mercury values are found in Arctic biota that are part of the traditional diet, risk communication is the immediate method used by public health officials to address the possible exposure and try to minimize the potential of health effects.

This section summarizes the findings on risk communication that are outlined in detail in the 2021 AMAP Human Health Assessment [REF]. The chapter provides new information on risk communication activities in several Arctic countries, which is mostly based on elevated mercury levels in fish or other marine biota. In some cases, for example in Finland and Sweden, other contaminants motivate consumption guidelines. In most cases, specific dietary guidelines across Arctic countries due to contaminated foods are available as part of general nutrition advice on the internet.

Risk communication experiences reinforce the importance of a trusted relationship of all people involved in contaminants work and the communication of possible risks associated with contaminants in the traditional diet. This is further emphasized by several authors who stress the importance of trust noting that it is difficult to build yet easily damaged or destroyed (e.g., Boyd et al. 2019, Wall and Chen 2018).

Some results for the effectiveness evaluation of risk communication messaging have also been provided. Wall and Chen (2018) point out that "*the word 'risk' is naturally negative, and risk communication messages often relate to negative information, which may serve to increase consumers' anxiety and concern about food. […] Moving from the main focus being on 'risk communication' to a broader 'food information communication' might afford the opportunity for more positive messages to receive airtime*." However, in the report by Furgal and Boyd (2014) it becomes apparent that a majority of surveyed respondents in Nunavut (Canada) were aware of messages on the benefits of traditional foods and that only a minority had heard the risk messages. It therefore seems that a certain emphasis on health risks, or very targeted communication is required to ensure retention of the message. Studies in other areas (Denmark and the US) found that targeted and personalized messaging was successful in reducing mercury exposure in pregnant women (Kirk et al. 2017, Knobeloch et al. 2011).

Overall, specific data on the effectiveness evaluation of risk communication is still limited to a few regions within the Canada and a few other selected countries. More health communication and risk perception data are important in order to compare results across regions of the circumpolar Arctic. Data from multiple regions would help to determine best practices for researchers and governments that could be used and adapted based on region, and/or community needs. These data also help to provide information in order to

create more culturally appropriate and relevant contaminant health messages and consumption notices. For instance, risk communication evaluation data in the Northwest Territories in Canada have provided information on two regions where doctors, elders, family and friends, university researchers and other health care workers were trusted a lot. This information can be used in order to disseminate future messages by using one or multiple of these trusted sources in combination with the commonly used mediums for receiving health messages. Testing out the impact of combinations of medium and messenger for various health messages would help to better understand the optimal communication strategies for different communities. A priority for risk communication should be carefully planned communication strategies, built through engagement with communities, which promote country food consumption while lowering contaminant exposures to maintain and improve health and well-being in Arctic communities.

Similar to previous findings (e.g., AMAP 2015), reported experiences highlight issues with confusion or fear resulting from the spread of sensationalized or alarmist messages. In some cases, this can arise due to problems with receiving audiences of one message being both local and global, where a message created for a specific, targeted audience is being read by others. This can create misunderstandings at a minimum, particularly if the different audiences do not share the same culture (Wendling et al. 2013, AMAP 2015). It was also stated that a message apparently contradicting cultural values is unlikely to be accepted, and may be prone to counterarguments and inoculation effects, particularly if the message is delivered with weak argumentation and/or from a non-trusted source.

Particularly in social media, it was found that information that is spread without verification can result in misinformation and mis-truths, which may lead to overamplification of the risks to public health, can create confusion and undermine the confidence of the receivers of the message (Wall and Chen 2018). Advantages for the use of social media include the unique possibility of interactive, two-way communication, the speed in which messages can be disseminated to a large or selective audience using multiple channels, and better control of the message that is originally disseminated (AMAP 2015, Wall and Chen 2018, Reagan et al. 2016, Wendling et al. 2013).

Many recommendations for better risk communication have been provided, both in the published literature and AMAP assessments (including in AMAP 2015, 2021). These include:

- Risk messaging needs to be developed with members of the affected population, and ideally would be created by a diverse group that includes needed expertise and knowledge
- Risk messaging needs to be customized to the intended audience(s), there is no one-size-fits-all approach
- Adequate time should be allowed for the risk management and communication process
- A trusted relationship between all involved entities is paramount

- The information needs to be provided in an open, transparent and in a timely manner that is honest, accurate, consistent and understandable (non-scientific language)
- Risk communication strategies need to be developed for a series of communication events, should be customized for different target audiences, and not just done in one communication event
- Multiple channels should be used to reach the target audience, and the native language should be used
- Follow-up on policy recommendations is required, and to evaluate reception and awareness of the communication to ensure the success of the messages
- Institutional capacity needs to be built to allow for sustained, regional expertise on technical and socio-cultural relevance. Ideally, this expertise would be situated in a permanent body that can store information and can readily provide advice for researcher, health workers and communities.

Ultimately however, experience has shown that the communication of contaminant risk is a very complex undertaking, and is not a sustainable solution to ensure low levels of contaminants in human populations. It is therefore crucial that regulations to lower contaminants in the environment are implemented effectively.

7.7. Conclusions and recommendations

Conclusions are organized below under section headers as a numbered list. These are followed by key gaps and recommendations in italics.

What are the global influences on mercury exposure in the North?

1. Mercury levels in some fish and wildlife that represent important components of the diet of northern people are elevated and of health concern. This mercury originates from anthropogenic activities in southern regions though is transported to the Arctic where it builds up in food chains. Climate change is expected to alter the flows and amounts of mercury with some scenarios pointing to increased exposures.

2. The Minamata Convention is now in legal force worldwide as a regulatory scheme to reduce the use and environmental release of mercury in order to protect human health and the environment in all regions, including the Arctic. The Convention was partly driven by health concerns raised by northern populations.

With the Minamata Convention now in legal force, evaluating the effectiveness of the Convention (as required by Article 22) is critical to ensure that it meets its Objectives. A range of short-, medium- and long-term evidence-based metrics to monitor mercury exposures (and risk) in human populations in the Arctic is

needed. Once metrics are set, a database (and dashboard) must be developed and updated for stakeholders to monitor progress.

Continued and expanded monitoring is needed to increase understanding of key human exposure pathways to mercury especially as the climate changes. Such monitoring is needed for the early identification of exposure situations of concern (e.g., emergence of geographic hotspots, accelerated mercury biomagnification in food chains)..

Models that link mercury fate and transport on global scales into human exposure pathways in specific Arctic communities must advance so that they are more predictive especially as the climate changes. The models must be designed with stakeholder communities in mind, and thus be desired, valuable, and credible while also being findable, accessible, and usable.

What are the dietary influences on mercury exposure?

3. The major source of mercury into northern populations is from the consumption of certain fish, sea mammals, and wildlife that are contaminated with mercury. The highest exposures occur among Inuit populations that routinely consume marine mammal tissues.

4. The food items that represent major sources of mercury exposure into northern populations are unfortunately ones that also represent a valuable source of essential nutrients to these populations as well as having cultural value to communities.

5. There is a transition underway in many communities to a more commercial-based diet. This transition is partly driven by the reduced access or availability to traditional and local foods as well as issues related to food insecurity. While this dietary transition may be associated with reduced exposures to mercury, it may introduce other health problems into the region ranging from reduced intake of essential nutrients to sedentary lifestyles and western diets that promote metabolic health concerns.

6. Variability is an important dimension to gauging true exposures to mercury, and this is necessary to properly balance and community risk-benefits. There exists variability in mercury levels within and across food items and geographic sites. There is variability in how different people process mercury in their bodies with new scientific information on the role that genetics, selenium or bioavailability may play.

Dietary advice provided by regional health authorities needs to be built on sound science. With a dietary transition underway across Arctic communities local health authorities need to work with stakeholders to increase understanding of the availability of such items and their nutritional value, as well as peoples' food choices and how these may vary across communities and seasons as well as age and sex.

It is established the traditional/local foods (especially those with lower levels of contaminants and high nutrient value) provide benefit to Indigenous Peoples in terms of nutrition, food security, and cultural well-being, and thus programs supporting these need to be evaluated and strengthened so that they can be broadly implemented.

More exposure studies are needed to link total diet surveys with human biomonitoring efforts so that better exposure estimates and dietary advice may be realized. This requires the collection of more data on both contaminants and nutrients from key food items as well as from consumers. It also necessitates the development context-specific exposure models in which variables are built around Indigenous Peoples and northern residents.

Factors that may moderate, mediate or even confound mercury exposures such as genetic variations, bioavailability factors, or selenium remain scientifically possible yet may over-simplify understanding (from physiological mechanisms to how such information would influence dietary guidelines). There is limited empirical evidence of these being realized in large population studies and thus more research is needed.

How do mercury biomarker levels compare to guidelines?

7. It is firmly established that Indigenous Peoples in the Arctic are amongst the highest mercury-exposed group worldwide with large proportions of individuals having biomarker levels that exceed health guidelines.

Biomonitoring studies of mercury exposure as well as total dietary surveys are needed to characterize exposures and trends, as well as track the effectiveness of actions (from local to international) to reduce exposures. To date these efforts have proven important and influential though they remain prohibitively costly and inefficient and thus new strategies and innovations are needed that harness breakthroughs in, for example, mobile phone apps to record data or capillary dried blood sampling to enable biomarker studies. The derivation of a true surveillance system is needed.

Community-based biomonitoring programs may now be realized with new equipment designed for use in remote sites and by non-experts. Such could empower locals, reduce the delay between sampling and reporting of results, and enable rapid decision making.

What are the health effects of mercury in humans?

8. It is established the mercury exposures at current levels amongst Arctic Indigenous Peoples is high enough to have adverse impacts on health, and that these are realized across the lifestage from adverse neurodevelopmental outcomes in young children to cardiovascular disease in adults. The characterization of subtle effects associated with mercury exposure, the impacts on other health systems (e.g., mental health, immune function), and the potential for trans-generational effects are not well understood. Even more, the interactions between mercury and other contaminants such a POPs or non-chemical stressors (e.g., malnutrition, psychosocial stress, infectious diseases) is not known even though these represent common scenarios.

Further research on methylmercury…. Additional health outcomes… subtler effects…. prospective studies as invaluable (support existing ones and launch other ones)

Further research that embraces One Health approaches to wholly understand mixtures, chemical-nutrient, chemical non-chemical interactions. Social and mental health outcomes.

Surveillance systems needed on general health of Arctic populations that bring together total health with mercury. Greater efforts needed to systematically collect, analyze, and report upon the total health status of Arctic populations.

community-led, or community-based research to yield more sustainable programs and outcomes

What are the risk communication and risk management strategies used to address dietary mercury exposure in the Arctic?

TBD.

Further general recommendations from the AMAP human health assessment.

TBD.

14541 **7.8 References**

14542

14543 **References 1**

14544

14545 Ayotte P, Carrier A, Ouellet N, et al. Relation between methylmercury exposure and plasma paraoxonase
14546 activity in inuit adults from Nunavik. Environ Health Perspect. 2011;119(8):1077–1083.
14547 doi:10.1289/ehp.1003296

14548 Barst BD, Drevnick PE, Muir DCG, et al. Screening-level risk assessment of methylmercury for non-
14549 anadromous Arctic char (Salvelinus alpinus). Environ Toxicol Chem. 2019;38(3):489–502.
14550 doi:10.1002/etc.4341

14551 Basu N, Horvat M, Evers DC, Zastenskaya I, Weihe P, Tempowski J. A State-of-the-Science Review of
14552 Mercury Biomarkers in Human Populations Worldwide between 2000 and 2018. Environ Health
14553 Perspect. 2018;126(10):106001. doi:10.1289/EHP3904

14554 Bjerregaard P, Young TK, Dewailly E, Ebbesson SO. Indigenous health in the Arctic: an overview of the
14555 circumpolar Inuit population. Scand J Public Health. 2004;32(5):390–395.
14556 doi:10.1080/14034940410028398Bradley MA, Barst BD, Basu N. A Review of Mercury Bioavailability
14557 in Humans and Fish. Int J Environ Res Public Health. 2017;14(2):169. Published 2017 Feb 10.
14558 doi:10.3390/ijerph14020169

14559 Eagles-Smith, C., Silbergeld, E., Basu, N., Bustamante, P., Diaz-Barriga, F., Hopkins, W., Kidd, K., Nyland,
14560 J (2018). A synthesis of how global change drivers modulate mercury exposure, bioaccumulation, and
14561 adverse outcomes in wildlife and humans. Ambio. 47: 170-197.Eagles-Smith CA, Silbergeld EK, Basu
14562 N, et al. Modulators of mercury risk to wildlife and humans in the context of rapid global
14563 change. Ambio. 2018;47(2):170–197. doi:10.1007/s13280-017-1011-x

14564 Ewald JD, Kirk JL, Li M, Sunderland EM. Organ-specific differences in mercury speciation and
14565 accumulation across ringed seal (Phoca hispida) life stages. Sci Total Environ. 2019;650(Pt 2):2013–
14566 2020. doi:10.1016/j.scitotenv.2018.09.299

14567 Ha E, Basu N, Bose-O'Reilly S, Dórea JG, McSorley E, Sakamoto M, Chan HM (2017). Current progress on
14568 understanding the impact of mercury on human health. Environ Res. 152:419-433.

14569 Huet C, Ford JD, Edge VL, et al. Food insecurity and food consumption by season in households with
14570 children in an Arctic city: a cross-sectional study. BMC Public Health. 2017;17(1):578. Published 2017
14571 Jun 15. doi:10.1186/s12889-017-4393-6Lemes M, Wang F, Stern GA, Ostertag SK, Chan HM.
14572 Methylmercury and selenium speciation in different tissues of beluga whales (Delphinapterus leucas)
14573 from the western Canadian Arctic. Environ Toxicol Chem. 2011;30(12):2732–2738.
14574 doi:10.1002/etc.684

14575 Nancarrow TL, Chan HM. Observations of environmental changes and potential dietary impacts in two
14576 communities in Nunavut, Canada. Rural Remote Health. 2010;10(2):1370.

14577 Rosol R, Powell-Hellyer S, Chan HM. Impacts of decline harvest of country food on nutrient intake among
14578 Inuit in Arctic Canada: impact of climate change and possible adaptation plan. Int J Circumpolar Health.
14579 2016;75:31127. Published 2016 Jul 5. doi:10.3402/ijch.v75.31127

14580

14581

14582 **Refences 2**

14583

1. Organization, W.H. *Mercury and Health*. 2017; Available from: https://www.who.int/news-room/fact-sheets/detail/mercury-and-health.
2. Grandjean, P., et al., *Cognitive deficits in 7-year-old children with prenatal exposure to methylmercury.* Neurotoxicology and Teratology, 1997. **19**(6): p. 417-428.
3. Debes, F., P. Weihe, and P. Grandjean, *Cognitive deficits at age 22 years associated with prenatal exposure to methylmercury.* Cortex, 2016. **74**: p. 358-69.
4. Boucher, O., et al., *The relation of lead neurotoxicity to the event-related potential P3b component in Inuit children from Arctic Quebec.* Neurotoxicology, 2009. **30**(6): p. 1070-7.
5. Boucher, O., et al., *Prenatal exposure to methylmercury and PCBs affects distinct stages of information processing: an event-related potential study with Inuit children.* Neurotoxicology, 2010. **31**(4): p. 373-84.
6. Boucher, O., et al., *Neurophysiologic and neurobehavioral evidence of beneficial effects of prenatal omega-3 fatty acid intake on memory function at school age.* Am J clin nutr, 2011. **93**(5): p. 1025-37.
7. Boucher, O., et al., *Response inhibition and error monitoring during a visual go/no-go task in inuit children exposed to lead, polychlorinated biphenyls, and methylmercury.* Environ Health Perspect, 2012. **120**(4): p. 608-15.
8. Boucher, O., et al., *Prenatal methylmercury, postnatal lead exposure, and evidence of attention deficit/hyperactivity disorder among Inuit children in Arctic Quebec.* Environ Health Perspect, 2012. **120**(10): p. 1456-61.
9. Murata, K., et al., *Delayed brainstem auditory evoked potential latencies in 14-year-old children exposed to methylmercury.* J Pediatr, 2004. **144**(2): p. 177-83.
10. Julvez, J. and P. Grandjean, *Genetic susceptibility to methylmercury developmental neurotoxicity matters.* Front Genet, 2013. **4**: p. 278.
11. Jacobson, J.L., et al., *Relation of Prenatal Methylmercury Exposure from Environmental Sources to Childhood IQ.* Environ Health Perspect, 2015. **123**(8): p. 827-33.
12. Rice, D. and S. Barone, Jr., *Critical periods of vulnerability for the developing nervous system: evidence from humans and animal models.* Environ Health Perspect, 2000. **108 Suppl 3**: p. 511-33.
13. Yokoo, E.M., et al., *Low level methylmercury exposure affects neuropsychological function in adults.* Environ Health, 2003. **2**(1): p. 8.
14. Virtanen, J.K., et al., *Mercury, fish oils, and risk of acute coronary events and cardiovascular disease, coronary heart disease, and all-cause mortality in men in eastern Finland.* Arterioscler Thromb Vasc Biol, 2005. **25**(1): p. 228-33.
15. National Research Council Committee on the Toxicological Effects of, M., in *Toxicological Effects of Methylmercury*. 2000, National Academies Press (US)Copyright 2000 by the National Academy of Sciences. All rights reserved.: Washington (DC).
16. Roman, H.A., et al., *Evaluation of the cardiovascular effects of methylmercury exposures: current evidence supports development of a dose-response function for regulatory benefits analysis.* Environ Health Perspect, 2011. **119**(5): p. 607-14.
17. Genchi, G., et al., *Mercury Exposure and Heart Diseases.* Int J Environ Res Public Health, 2017. **14**(1).
18. Hu, X.F., K. Singh, and H.M. Chan, *Mercury Exposure, Blood Pressure, and Hypertension: A Systematic Review and Dose-response Meta-analysis.* Environ Health Perspect, 2018. **126**(7): p. 076002.
19. Sorensen, N., et al., *Prenatal methylmercury exposure as a cardiovascular risk factor at seven years of age.* Epidemiology, 1999. **10**: p. 370-375.

20. AMAP, *AMAP Assessment 2015: Human Health in the Arctic*. 2015, Oslo, Norway: AMAP. 165.

21. Weihe, P. and H.D. Joensen, *Dietary recommendations regarding pilot whale meat and blubber in the Faroe Islands.* Int J Circumpolar Health, 2012. **71**: p. 18594.

22. AMAP, *AMAP Assessment 2009: Human health in the Arctic, Arctic Monitoring and Assessment Programmme (AMAP)*. Vol. Xiv+254 pp. 2009, Oslo, Norway.

References 3

Abass, K., Huusko, A., Knutsen, H.K., Nieminen, P., Myllynen, P., Meltzer, H.M. et al. Quantitative estimation of mercury intake by toxicokinetic modelling based on total mercury levels in humans. Environment International 114:1-11; 2018.

Binnington, M.J., Curren, M.S., Chan, H.M., Wania, F. Balancing the benefits and costs of traditional food substitution by Indigenous Arctic women of childbearing age: Impacts on persistent organic pollutant, mercury, and nutrient intakes. Environment International 94:554-66; 2016a.

Binnington, M.J., Curren, M.S., Quinn, C.L., Armitage, J.M., Arnot, J.A., Chan, H.M. et al. Mechanistic polychlorinated biphenyl exposure modeling of mothers in the Canadian Arctic: the challenge of reliably establishing dietary composition. Environment International 92-93:256-68; 2016b.

Brosen, K. Pharmacogenetics of drug oxidation via cytochrome P450 (CYP) in the populations of Denmark, Faroe Islands and Greenland. Drug Metab Pers Ther 30(3):147-63; 2015.

Caito, S.W., Jackson, B.P., Punshon, T., Scrimale, T., Grier, A., Gill, S.R. et al. Variation in Methylmercury Metabolism and Elimination Status in Humans Following Fish Consumption. Toxicological Sciences 161:443-53; 2018.

Czub, G., Wania, F., McLachlan, M. Combining long-range transport and bioaccumulation considerations to identify potential Arctic contaminants. : Environ Sci Technol 42(10):3704-9; 2008.

Engström, K., Love, T.M., Watson, G.E., Zareba, G., Yeates, A., Wahlberg, K. et al. Polymorphisms in ATP-binding cassette transporters associated with maternal methylmercury disposition and infant neurodevelopment in mother-infant pairs in the Seychelles Child Development Study. Environment International 94:224-9; 2016.

Hakkola, J., Raunio, H., Purkunen, R., Saarikoski, S., Vähäkangas, K., Pelkonen, O. et al. Cytochrome P450 3A expression in the human fetal liver: evidence that CYP3A5 is expressed in only a limited number of fetal livers. Biol Neonate 80:193-201; 2001.

Henderson, L.M., Claw, K.G., Woodahl, E.L., Robinson, R.F., Boyer, B.B., Burke, W. et al. P450 Pharmacogenetics in Indigenous North American Populations. Journal of personalized medicine 8(1):9; 2018.

Kelly, B., Ikonomou, M., Blair, J., Morin, A., Gobas, F. Food web-specific biomagnification of persistent organic pollutants. Science 317(5835):236-9; 2007.

Lincoln, R., Shine, J., Chesney, E., Vorhees, D., Grandjean, P., Senn, D. Fish consumption and mercury exposure among Louisiana recreational anglers. Environ Health Perspect 119:245-51; 2011.

Llop, S., Engström, K., Ballester, F., Franforte, E., Alhamdow, A., Pisa, F. et al. Polymorphisms in ABC transporter genes and concentrations of mercury in newborns--evidence from two Mediterranean birth cohorts. PLoS One 9:e97172; 2014.

Llop, S., Ballester, F., Broberg, K. Effect of Gene-Mercury Interactions on Mercury Toxicokinetics and Neurotoxicity. Current Environmental Health Reports 2:179-94; 2015.

14671 Llop, S., Tran, V., Ballester, F., Barbone, F., Sofianou-Katsoulis, A., Sunyer, J. et al. CYP3A genes and the
14672 association between prenatal methylmercury exposure and neurodevelopment. Environment International
14673 105:34-42; 2017.

14674 Matsson, P., Yee, S., Markova, S., et al. Discovery of regulatory elements in human ATP-binding cassette
14675 transporters through expression quantitative trait mapping. Pharmacogenomics J 12:214-26; 2012.

14676 Meltzer, H.M., Brantsæter, A.L., Ydersbond, T.A., Alexander, J., Haugen, M., Hareide, B. et al.
14677 Methodological challenges when monitoring the diet of pregnant women in a large study: Experiences
14678 from the Norwegian Mother and Child Cohort Study (MoBa). Matern Child Nutr 4:14-27; 2008.

14679 Quinn, C. and Wania, F. Understanding differences in the body burden-age relationships of bioaccumulating
14680 contaminants based on population cross sections versus individuals. Environ Health Persp 120(4):554-9;
14681 2012.

14682 Rand, M.D., Vorojeikina, D., van Wijngaarden, E., Jackson, B.P., Scrimale, T., Zareba, G. et al. Methods for
14683 Individualized Determination of Methylmercury Elimination Rate and De-Methylation Status in Humans
14684 Following Fish Consumption. Toxicological Sciences 149:385-95; 2016.

14685 Rand, M.D. and Caito, S.W. Variation in the biological half-life of methylmercury in humans: Methods,
14686 measurements and meaning. Biochimica et Biophysica Acta (BBA) - General Subjects 1863:129301;
14687 2019.

14688 Undeman, E., Brown, T., Wania, F., McLachlan, M. Susceptibility of human populations to environmental
14689 exposure to organic contaminants. Environ Sci Technol 44(16):6249-55; 2010.

14690 Verner, M.A., Charbonneau, M., Lopez-Carrillo, L., Haddad, S. Physiologically based pharmacokinetic
14691 modeling of persistent organic pollutants for lifetime exposure assessment: a new tool in breast cancer
14692 epidemiologic studies. Environ Health Perspect 116:886-92; 2008.

14693 Verner, M., Ayotte, P., Muckle, G., Charbonneau, M., Haddad, S. A physiologically based pharmacokinetic
14694 model for the assessment of infant exposure to persistent organic pollutants in epidemiologic studies.
14695 Environ Health Persp 117(3):481-7; 2009.

14696 Verner, M., Sonneborn, D., Lancz, K., Muckle, G., Ayotte, P., Dewailly, É. et al. Toxicokinetic modeling of
14697 persistent organic pollutant levels in blood from birth to 45 months of age in longitudinal birth cohort
14698 studies. Environ Health Persp 121(1):131-7; 2013.

14699 Wahlberg, K., Love, T.M., Pineda, D., Engström, K., Watson, G.E., Thurston, S.W. et al. Maternal
14700 polymorphisms in glutathione-related genes are associated with maternal mercury concentrations and
14701 early child neurodevelopment in a population with a fish-rich diet. Environment International 115:142-9;
14702 2018.

14703 Wania, F., Binnington, M., Curren, M. Mechanistic modeling of persistent organic pollutant exposure among
14704 Indigenous Arctic populations: motivations, challenges, and benefits. Environmental Reviews 25:396;
14705 2017.

14706

14707
14708
14709
14710

15000

* This is Chapter 8 of the AMAP Mercury Assessment*

15001

15002 **What are the likely changes in mercury concentration in the Arctic atmosphere and ocean**
15003 **under future emissions scenarios?**

15004

15005 **Table of Contents**

15006

15020

15021

15022

15023 **8.1. Introduction**

15024 This chapter addresses the question: What are the likely changes in mercury concentration in the
15025 Arctic atmosphere and ocean under future emissions scenarios?

15026 Future emissions scenarios are constructed using socio-economic information that envisions future
15027 economic activities, energy use, and associated emissions of pollutants, which affect climate change,
15028 other air pollutants, and mercury.

15029 Changes in mercury concentration in the Arctic atmosphere and ocean will occur on different time
15030 scales. Short-term timescales, a few years, are relevant for near-term decision-making including the
15031 first effectiveness evaluation of the Minamata Convention which will occur by 2023. In the medium
15032 term, years to decades, enhancements in "legacy emissions" from current as well as future emissions
15033 will play a substantial role. Climate changes are occurring in the medium term, but their trajectory is
15034 less affected by current emissions. In the longer term (multiple decades and longer), trajectories of
15035 greenhouse gas emissions will play a substantial role in determining Arctic climate as well as mercury
15036 concentrations.

15037 The relative importance of different processes to mercury concentrations differs depending on these
15038 timescales. Concentrations in both the atmosphere and ocean respond to processes that occur on
15039 varying time scales. For the atmosphere, in the short term, changes in anthropogenic emissions in
15040 different regions will affect the Arctic depending on their magnitude and geography. The overall
15041 magnitude of emissions will affect the atmosphere.

15042 For the atmosphere, in the short term, concentration changes and mercury deposition will follow
15043 changes in emissions in different regions and their relative contributions and can be calculated based
15044 on source-receptor information. In the medium term (years to decades), enhancements in "legacy
15045 emissions" from current and future emissions will affect trajectories. On timescales of decades and
15046 longer, changes as a result of climate changes will influence the Arctic. For the ocean, the timescales
15047 of ocean circulation may result in a lag relative to changes in the atmosphere, but many of these
15048 changes will overlap.

15049 A key contribution of this chapter is to assess the potential importance of future mercury emissions
15050 relative to other changes, including climate and legacy emissions changes.

15051

15052 **8.2. Emissions scenarios: comparison of existing literature estimates**

15053 The processes that affect mercury emission globally also contribute to the emission of other
15054 pollutants, including greenhouse gases and other pollutants such as sulfur dioxide (SO_2), nitrogen
15055 oxides (NOx), and black carbon.

15056 This section will review and compare existing literature that develops emission scenarios relevant to
15057 projecting Arctic atmosphere and ocean mercury concentrations in the future. First, it will briefly
15058 review (with reference to other chapters) different estimates and current trajectories of emissions
15059 globally, and current understanding of emissions in regions that affect the Arctic. It will then review
15060 and compare previous efforts to project emissions forward in time. It will address the question of
15061 whether there are substantial differences in assumptions among different emissions scenarios of
15062 relevance to the Arctic.

15063 According to the source apportionment analysis performed with the model ensemble, global natural
15064 and secondary emissions are the main contributors to Hg deposition in the Arctic (~70%). Using a
15065 global box model framework, Chen et al. (2018) showed that present-day Hg deposition over the
15066 Arctic Ocean is mainly from historical anthropogenic emissions from Asia (31%), followed by North
15067 America (18%), South America (12%), the former USSR (12%), and Europe (11%).

15068 Hg deposition due to primary anthropogenic emissions is mostly due to emissions in East Asia
15069 (~33%; China, Korea, Japan). Europe, South East Asia, South Asia, sub-Saharan/sub-Sahel Africa,
15070 South America, and Russia/Belarussia/Ukraine each contribute ~7-9%. Emissions in the Arctic (north
15071 of 66N and Greenland) currently only contribute ~2% of Hg deposition due to primary anthropogenic
15072 emissions. However, the Arctic is also changing rapidly in terms of industrialization and urbanization.
15073 To date, there are unfortunately only a few studies addressing the topic of Hg behavior in polluted
15074 arctic snow (e.g., Willis et al., 2018 and Kirk et al., 2014).

15075

15076 **Table and graph:** This section will present a table including available literature projections of future
15077 emissions, globally and for key regions affecting the Arctic. Entries included in the table will cover
15078 assumptions in the base year, time scale of emissions, policy scenarios addressed (including mercury
15079 and non-mercury scenarios such as climate scenarios), underlying activity projections (e.g. energy and
15080 coal use), technology application assumptions, and mercury speciation. A graph will illustrate the
15081 global-scale trajectories of emissions.

15082

15083 Table 1: Available literature projections of future anthropogenic emissions.

Region	Base year	Policy scenarios addressed	Projections	Underlying assumptions	Reference
Global	2006; global emissions of 2480 Mg.	Four IPCC SRES scenarios spanning a range of industrial growth and	2050; Global Hg emissions will likely increase (2390-4860 Mg; change of -4%	Share of Hg(0) in total emissions declines from ~65% (base year) to 50-	Streets et al., 2009

		environmental regulation possibilities (A1B, A2, B1, B2).	to +96%). Coal combustion in developing countries is the largest driver of emission increase. Global emissions lowered to 1670-3480 Mg if large scale deployment of advanced Hg sorbent technologies.	55%. Share of Hg(II) increases. Sectors included: combustion, pig iron manufacture, cement manufacture, copper, lead, and zinc smelting, artisanal gold extraction, Hg mining, caustic soda production.	
Global and key source regions	2010: Africa: 159.2 Mg China: 565.4 Mg Europe: 81.9 Mg India: 162.3 Mg Latin Am.: 167.4 Mg North Am.: 108.5 Mg Russia: 35.9 Mg Rest of the world: 273.8 Mg Total: 1554.4 Mg	Projections of energy consumption for 1) scenario without any global greenhouse gas mitigation efforts (BAS). 2) 2°C climate policy scenario (CLIM). Activity projections complemented with assumptions on air pollution and Hg control measures: 1) current national legislation to control air pollution by 2030, but no further effort between 2030 and 2050 (CLE). 2) maximum feasible reduction assuming full adoption of best available technologies to control Hg emissions by 2030 and beyond (MFR).	2050 BAS scenario: Africa: 253.2 Mg China: 1001.5 Mg Europe: 48.1 Mg India: 579.3 Mg Latin Am.: 240.0 Mg North Am.: 127.1 Mg Russia: 46.3 Mg Rest of the world: 383.8 Mg Total: 2661.4 Mg Hg emissions under CLIM reduced by 45% in 2050 when compared to BAS. Annual Hg-abatement of 800 Mg for coal combustion in power section if current air pollution legislation and climate policies are adopted in parallel.	Fraction of Hg(p) does not exceed 5%. Hg(p) capture efficiency up to 99.99%. Hg(0) dominant form for BAS and CLIM scenarios. Share of Hg(II) increases slightly over time under BAS (air pollution control measures and structural changes) while share of Hg(0) increases under CLIM (major Hg(0) emission sources remain unaffected by global climate strategies).	Rafaj et al., 2013
Europe	2005: 145 Mg.	1) Baseline scenario (BAS): development of European energy system with no	2050: Co-control effects of technologies abating other air pollutants		Rafaj et al., 2014

		measures to control emissions of greenhouse gases and to deploy renewable energies beyond current policies. 2) Maximum Renewable Power (MAX) scenario: decarbonization of European energy system, including highest possible electricity generation from renewables by 2050. Both scenarios imply full implementation of recent national legislation on air quality (as of mid-2012) by 2030. This includes two sets of technologies: 1) "Conventional" APCDs reducing Hg as a side effect of their operation. 2) Hg-specific abatement measures.	reduce Hg emissions by 35-45%. BAS: ~145 Mg. MAX: ~100 Mg. The largest fraction of emission cuts under MAX attributed to deployment of renewables in the power sector.		
Global and key source regions	2000 (from Pacyna et al., 2006) Global emissions: 2189.9 Mg North America: 145.8 Mg Asia and Oceania: 1305.9 Mg Europe and middle East: 246.8 Mg Africa: 398.4 Mg Central and South	Three IPCC SRES scenarios: B1, A1B, and A1F1 representing the lower, middle, and upper bounds of potential climate warming.	2050: Global emissions: 2390-5990 Mg (+9-173%). North America: 121.9-305.7 Mg. Asia and Oceania: 1208.9-3307.1 Mg Europe and middle East: 358.1-861.3 Mg Africa: 357.0-789.2	A1F1 scenario: intensive use of fossil fuel energy; A1B: balances all energy sources; B1: clean and ecologically friendly energy future. Share of Hg(II) and Hg(0) emissions will increase and decrease (from 67 to 47-56%), respectively owing to the	Lei et al., 2014

	America: 92.1 Mg.		Mg Central and South America: 340.4-720.4Mg.	implementation of FGD.	
Asia (India and China)	2010 India: 49 Mg. China: 97 Mg. (for coal-fired power generation only).	Three technology scenarios: no additional control (NAC), Minamata Flexible (MF, technology and techniques consistent with existing domestic policy plans), Minamata strict (MS, progression in stringency of Hg control beyond those specified in MF). Two energy scenarios (A1B and B1).	2050 India: NAC/A1B: 619 Mg. NAC/B1: 249 Mg. MF/A1B: 468 Mg. MS/A1B: 346 Mg. Hg(0) emissions roughly constant between MF and MS. China: NAC/A1B: 247 Mg. NAC/B1: 97 Mg MF/A1B: 156 Mg. MS/A1B: 105 Mg.	China: capture efficiency of 69, 82, and 90% under NAC, MF, and MS scenarios. India: capture efficiency of 42, 58, and 71% under NAC, MF, and MS scenarios.	Giang et al., 2015
Global	2010 Global emissions: 1885 Mg.	Projected 1) future activities and 2) emission factors and emission reduction technology employed in the future per country. Current Policy Scenario (CPS): governmental policies and measures existing in 2010 are adopted (APCDs, climate change). New Policies Scenario (NPS): policy commitments and plans to reduce greenhouse gases	2035 1960, 1020, and 300 Mg under the CPS, NPS, and MFR.	Countries assigned to five groupings representing different levels of technological implementation (technological profiles) of APCDs.	Pacyna et al., 2016

		emissions are fully implemented. The use of Hg in products is reduced by 70%. 450ppm scenario (maximum feasible reduction, MFR): all countries reach the highest feasible/available reduction efficiency in each emission sector.			
China	2012: 539 Mg	Seven scenarios: 1) 2030 No policy: no climate or Hg policy beyond current regulations. 2) MC-NCP: end-of-pipe control policy scenario that meets China's commitments under the Minamata Convention (MC) but no climate policy (NCP) beyond current regulations. 3) Three climate policy scenarios of varying stringency: CINT3, CINT4, and CINT5 corresponding to carbon intensity reduced by 3-5% per year. CINT4 corresponds to China's commitments under the 2015 Paris Agreement. 4) Two scenarios that combine Minamata and	2030: No Policy: 1150 Mg CINT3: 1107 Mg CINT4: 1035 Mg CINT5: 967 Mg MC-NCP: 533 Mg MC-CINT4: 493 Mg MC-CINT5: 470 Mg.	Projected emissions are calculated with/without changing APCDs and associated Hg speciation depending on scenarios and emission sectors.	Mulvaney et al., 2020

		climate policies: MC-CINT4 and MC-CINT5.			

15084

15085 **8.3. Changes in mercury concentrations in the atmosphere:**

15086 This section reviews modeling analyses that project changes in mercury concentrations in the Arctic
15087 atmosphere based on the emissions scenarios outlined above. It will review current modeling
15088 capability to identify changes in mercury concentrations in the Arctic atmosphere, and the limitations
15089 of existing models in doing so based on their ability to simulate present-day concentrations.

15090

15091 [this section relies on model runs and connects to chapter 3] Source-receptor information

15092 For the short-term, it will use results from previous modeling on source-receptor matrices to estimate
15093 the implications of emissions changes within and outside the Arctic on Arctic atmospheric Hg
15094 concentration. For the medium and longer term, it will review methodologies to account for legacy
15095 emissions and climate change in current available atmospheric models. A few approaches in the
15096 literature can address the magnitude of these effects, which will be compared to the short-term
15097 estimates using source-receptor information.

15098 We used future scenarios from Pacyna et al. (2016). As summarized in Table 1, the Current Policy
15099 (CP) scenario assumes that governmental policies and measures existing in 2010 are adopted (climate
15100 change and APCDs). The New Policy (NP) scenario assumes that policy commitments and plans to
15101 reduce greenhouse gases emissions are fully implemented. In this scenario, the use of Hg in products
15102 is reduced by 70%. The 450 ppm, a.k.a. Maximum Feasible Reduction (MFR) scenario assumes that
15103 all countries reach the highest feasible/available reduction efficiency in each emission sector. It
15104 should be noted that the NP and MFR scenarios both assume a significant decrease of Chinese
15105 emissions, the main contributor to Hg deposition in the Arctic (cf. Chapter 3).

15106 Following the methodology of Angot et al. (2018), the best-case estimate is a 15.0% or 25.2%
15107 reduction of Hg deposition in the Arctic compared to the base scenario if a NP or a MFR scenario is
15108 implemented in the short-term, respectively. If mitigation policies are delayed, the legacy pool will
15109 grow, reducing policy impacts (Angot et al., 2018). For each 5 year delay, NP or MFR policy impact
15110 in the Arctic decreases by 12.8% or 7.7%, respectively. Results are summarized in Table 2:

15111

15112 Table 2: Projected Hg deposition in the Arctic using future emissions scenarios and assuming a short-
15113 term or delayed implementation of global mitigation efforts

Base year (2015) Hg deposition to the Arctic	8.3 g/km2/year
Short-term implementation of NP	7.1 g/km2/year
NP delayed by 5 years	7.2 g/km2/year
NP delayed by 10 years	7.4 g/km2/year
NP delayed by 15 years	7.5 g/km2/year
Short-term implementation of MFR	6.2 g/km2/year
MFR delayed by 5 years	6.4 g/km2/year
MFR delayed by 10 years	6.5 g/km2/year
MFR delayed by 15 years	6.7 g/km2/year

[this section relies on comparisons to chapter 5] The changes prompted by emissions can be compared with the magnitude of changes expected as a result of climate change, in the near, medium, and long term. For comparison, Lei et al. (2014) compared the influence of projected emission changes and climate change on US atmospheric Hg levels in 2050. They found that anthropogenic emissions would contribute 32-53% of projected changes in Hg air concentration, while climate and natural emission changes would account for 47-68%.

Using a modeling approach, Dastoor et al. (2015) showed that an increase in net deposition in the Arctic under climate change is primarily driven by changes in snowpack and sea ice conditions. For instance, changes in the sea ice dynamics may shift how much GEM is available for oxidation (Moore et al., 2014). It has also been suggested that air temperature changes can impact the timing of AMDEs and thus deposition/GEM concentrations (Cole and Steffen, 2010).

Wildfires contribute ~10% of the total annual Hg deposition to the Arctic. The most important source region is Eurasia (boreal forests) (Kumar and Wu, 2019). Climate change could increase Hg emissions by 14% globally and by 13% in Eurasia (Kumar et al., 2019).

Tundra and permafrost soils serve as reservoirs of a large legacy pool of past and present Hg emissions that accumulated in the Arctic (Schuster et al., 2018; Olson et al., 2018). Soil runoff serves as a major source to the Arctic Ocean (Sonke et al., 2018) => *Likely discussed in Chapter 5.*

15132 The large reductions projected in northern hemisphere permafrost abundance by 2100 (Koven et al.,
15133 2012) could release large amounts of Hg into the environment (Vonk et al, 2015). The question is
15134 how much?

15135 The greening of the Arctic will also likely impact air/surface exchanges (Grannas et al., 2013) and
15136 reduce the extent of reemission of Hg from the cryosphere (Dastoor et al., 2015). On the other hand,
15137 higher surface temperature may enhance the photo-reduction and reemission of Hg from the Arctic
15138 Ocean.

15139

15140 **8.4. Changes in mercury concentrations in the ocean**[MOU2]

15141 **8.4.1**

15142 Changes in ocean mercury concentrations are a function of emissions but also of the biogeochemical
15143 processes that drive mercury's environmental fate (e.g. atmospheric deposition, biotic and abiotic
15144 degradation, settling to the deep ocean by the biological pump, and accumulation and
15145 biomagnification in food webs). These processes are in turn affected by the ongoing environmental
15146 shifts. With models it is possible to take into account these simultaneous changes and provide
15147 integrated estimates of future trends. The ultimate biogeochemical model of mercury will be able to
15148 combine emission scenarios and climate change simulations, and speciated mercury modeling to
15149 produce future trends. But because of a limited understanding of how Hg inputs from sources other
15150 than the atmosphere will change, a limited ability to accurately model mercury speciation, and the
15151 scale of changes occurring in the Arctic, this model does not yet exist.

15152 However, even less sophisticated models can be used to 1) do simple projection estimates based on
15153 future anthropogenic deposition scenarios and an assumption that other fluxes and processes are
15154 constant; 2) consider the effects of most significant climate-related changes (e.g. increased freshwater
15155 discharge, permafrost thaw, or reduction of sea ice) on mercury fluxes; 3) understand how climate
15156 change can impact mercury speciation (e.g. methylation) and bioconcentration in the Arctic.

15157 In this chapter, the models developed or improved since the previous AMAP report are first discussed,
15158 and major drivers of mercury and methylmercury variability in the Arctic are then summarized. A
15159 particular attention is paid to drivers that are likely to change in a future climate.

15160 The mass budget that has been compiled for chapter 3 is used as a basis to run a range of simple future
15161 simulations looking at the impact of future deposition scenarios as given in 8.2 and major climate
15162 change drivers across the Arctic as identified in recent model studies (Table X). This will be done at a
15163 low spatial resolution level (box model) to capture major impacts on the total Hg cycle in the Arctic
15164 Ocean. Finally, this section will discuss the future developments and research needed to improve the
15165 simulation of future Hg scenarios.

8.4.2 State of current models and identification of major drivers (Table X)

Prior to 2012, when the last AMAP Mercury report was published, only one mass budget for total Hg existed for the Arctic Ocean (Outridge et al. 2008) and no modeling studies had been conducted. Since 2012, 8 papers have been published describing modeling studies of Hg in the Arctic (or global studies that include the Arctic). The models range in resolution, spatial coverage and species of mercury included. They also vary in design falling into 3 categories: box model, slab-ocean model integrated into atmospheric framework and global biogeochemical model of the ocean. These studies give a first picture of major drivers of Hg concentration and speciation in the Arctic Ocean. While only one study has so far created future scenarios for Hg concentrations in the Arctic Ocean (Chen et al. 2018), frameworks to make simple scenarios for changes in total Hg reservoirs are now available and one of which will be used to predict the consequences of changes in deposition and other simple processes (see 8.3.3).

Total Hg

The Soerensen et al. (2016) box model presented an updated mass budget for total Hg and the first budget for speciated Hg in the Arctic Ocean, and produced 2 significant findings:

1. Reassessing the lifetime of Hg in the Arctic Ocean. They estimated 3 years for the upper ocean (<200 m) and 45 years for the deep Arctic Ocean (>200 m). Showing that the upper part of the Arctic Ocean, where most aquatic animals live, will respond quickly to the changes in Hg inputs. However, the deeper Central Arctic Ocean has a considerable lag in response to changing inputs, which will also mean a slow response to future changes.

2. Showing that declining sea ice concentrations since the 1970s has resulted in an increase in the net loss of Hg to the atmosphere due to the impact of evasion (reaching a relative difference of 6% in 2008 for the surface ocean). This net increase in the Hg flow from ocean to atmosphere following a decline in sea ice cover is supported by model simulations with the GEOS-Chem model with a biogeochemical slab-ocean module (Chen et al. 2015).

While the authors did not run future scenarios, they used this box model to look at the impact of increases in atmospheric Hg deposition over the last 150 years and the impact of declining sea ice cover. This budget is the basis for the mass budget used for future simulations in 8.3.3.

Chen et al. (2018) developed a multicompartment global box model with a 5-compartment box model for the Arctic based on Soerensen et al. (2016) and ran a range of emissions scenarios (2015-2050) with all other factors constant. These are the only published Arctic Ocean specific future scenarios. [SA3] This work's main findings for the Arctic are:

15198 1. Around 50% of the current Hg in the Arctic Ocean is from geogenic and North American
15199 emissions combined, 9% are from Asia emissions. Under the A1B scenario Asia sources will
15200 dominate in the future.

15201 2. A maximum relative increase of 15% (??) for the Arctic ocean in their emissions scenarios
15202 (A1B scenario). However, this change was for the entire Arctic Ocean, which implies that the
15203 increase in the surface ocean would be higher and closer to the atmospheric increase of 50%
15204 suggested by their model (given the short lifetime of Hg in the Arctic surface ocean).

15205 Both of these box models are limited by the fact that they are geochemical models that do not include
15206 the impact of changes to the biological system.

15207 Several studies of Arctic ocean-atmosphere interactions were conducted with the GEOS-Chem global
15208 mercury model, which includes a three-dimensional atmospheric transport and chemistry simulation
15209 (Holmes et al. 2010; Soerensen et al. 2010) dynamically coupled to a two-dimensional ocean mixed
15210 layer simulation with redox chemistry and exchange with subsurface water (Fisher et al. 2012; 2013;
15211 Chen et al. 2015) (Table 3).

15212 Fisher et al. (2012) showed the importance of the seasonality of sources (more specifically rivers) in
15213 causing seasonal variability not only in the surface ocean but also in the marine boundary layer due to
15214 the rapid interaction between the surface ocean and atmosphere. In a follow-up paper (Fisher et al.
15215 2013), they analyze the drivers of interannual variability in Arctic atmospheric Hg with the model and
15216 find that decreased fluxes of Hg from the atmosphere to the cryosphere and from the cryosphere to the
15217 ocean were associated with changes induced by climate warming: high air temperatures, low sea ice
15218 area, strong warming in spring [Bekryaev et al., 2010], and cloudiness [Eastman and Warren, 2010].
15219 These are changes projected to intensify under future forcing scenarios [Intergovernmental Panel on
15220 Climate Change, 2007; Vavrus et al., 2009] and the author therefore suggest that future climate
15221 change may decrease Hg levels in the Arctic surface ocean (assuming no changes to atmospheric
15222 concentrations or other external sources).

15223 Three global biogeochemical Hg studies with varying focus on Arctic Ocean processes have been
15224 published (Semenuik and Dastoor 2017; Zhang et al. 2015; 2017). These studies are conducted with
15225 the NEMO framework and the MITgcm model and are mostly focused on Hg speciation rather than
15226 trends in Total Hg.

15227 The study by Zhang et al. (2015) has a specific focus on the Arctic Ocean processes. It supports the
15228 Fisher et al. (2012) hypothesis that rivers are major drivers of seasonal variability in the surface
15229 ocean. This study shows that the western Arctic Ocean has higher Hg concentrations than the eastern
15230 Arctic Ocean due to more frequent AMDEs and greater summertime ice cover. This also suggests that
15231 loss of ice cover may result in lower surface ocean Hg concentrations (Chen et al. 2015; Soerensen et
15232 al. 2016). Zhang et al. (2015) also shows that in estuarine areas heat transfer from rivers increase the

15233 net Hg evasion, while the slow melting of multi-year sea-ice is not a large driver (as this is not a
15234 renewable source). Zhang et al. (2015) found that 80% of riverine Hg in the Arctic is subject to
15235 evasion, supporting a short lifetime of Hg in the Arctic surface ocean not only of Hg from
15236 atmospheric sources (Soerensen et al. 2016).

15237 ***MeHg***

15238 Only three models include methylmercury species in their simulation, the Soerensen et al. (2016) box
15239 model and the two global biogeochemical models NEMO and MITgcm (Semenuik and Dastoor 2017;
15240 Zhang et al. 2017). Soerensen et al. (2016) present the first MeHg budget for the Arctic Ocean and
15241 concludes that most MeHg must be produced in situ in subsurface ocean waters. Zhang et al. (2020)
15242 propose that the MeHg is higher in the waters of the Arctic (and Antarctic) than elsewhere because of
15243 lower demethylation (because of lower radiation, Chl A and temperature) rather than higher
15244 methylation. Semeniuk and Dastoor (2017) suggest that abiotic methylation driven by DOC could be
15245 important for MeHg production at depth.

15246

15247 Table 3: Available Arctic Ocean mercury models and budgets

Model framework	**Resolution**	**Inorganic Hg**	**Organic Hg**	**Lower food web**	**Coupled atmosphere**	**Future scenarios**	**Major drivers identified**	**Reference**
Box model	Low: 5 compartment box model	Yes	Yes	Yes	No	No, but past emissions and climate scenarios (1850-2010)	For total Hg: Erosion and rivers account for 1/3 of inputs, followed by the atmosphere, then ocean flow. Declining sea-ice increases the net loss of Hg to the atmosphere. For MeHg: Most MeHg is produced in situ in subsurface water.	Soerensen et al. 2016
Box model	Low: Global source-receptor model including a 5 compartment Arctic box model. The Arctic box model is based	Yes	No	No	Yes	Yes: 4 emissions scenarios (2015-2050) but no climate change impacts	Geogenic and North American Hg currently dominates the Arctic Ocean Hg reservoir. In the future Asian emissions will be a major driver of Hg in the Arctic Ocean.	Chen et al. 2018

	on Soerensen et al. (2016)							
GEOS-Chem with slab-ocean module	Medium: high horizontal resolution (4x5°) but represent only the surface ocean	Yes	No	No	Yes	No	Rivers are a major source of Hg to the Arctic Ocean that drives the Arctic atmospheric summer peak in Hg^0 through emission from the Ocean following the spring freshet.	Fisher et al. 2012
GEOS-Chem with slab-ocean module	Medium: high horizontal resolution (4x5°) but represent only the surface ocean	Yes	No	No	Yes	No, but past climate scenarios (1979-2008)	Temperature and lower sea-ice area will reduce the Hg flux from the cryosphere to the ocean. High wind speed and cold springs driving frequent AMDEs increases deposition to the cryosphere. High temperature increases ice melt and thereby Hg flow to the ocean.	Fisher et al. 2013
GEOS-Chem with slab-ocean module	Medium: high horizontal resolution (4x5°) but represent only the surface ocean	Yes	No	No	Yes	No	Arctic warming and declining sea ice drives an increase in net Hg evasion. Melting of multi-year sea ice is not a large driver.	Chen et al. 2015
GRAHM (now GEM-MACH-Hg)	Medium: high horizontal resolution (1x1°)	Yes	No	No	Yes	No, but past emissions and climate scenarios (1995-2005)	A slow increase in net deposition of Hg is found in the Canadian Arctic in response to changes in meteorology. Under emissions reduction scenario of worldwide implementation of the best emission control technologies by 2020, Hg deposition could be reduced by 18-20% in the Canadian Arctic.	Dastoor et al. 2015
MITgcm	High: Global biogeochemical model with nested Arctic Ocean (36x36	Yes	No	No	No	No	In estuarine areas heat transfer from rivers increases water turbulence and ice melt thereby increasing net evasion. The particle load and efficient	Zhang et al. 2015

	km, 50 vertical layers						degradation of the POC results in a labile Hg pool. So how will future particle loading (amount and quality) change?	
NEMO framework	High: Global biogeochemical model – simulation not Arctic focused	Yes	Yes	No	No	No	At depth in the Arctic water column abiotic methylation driven by DOC could be important for MMHg production. Also propose that once formed MMHg remains bound to refractory DOC and is unavailable for demethylation, thus it accumulates in the water column.	Semeniuk and Dastoor 2017
MITgcm	High: Global biogeochemical model – simulation not Arctic focused (~ 40 x 40 km)	Yes	Yes	Yes	Yes (?)	No	Photodemethylation in the Arctic lower than elsewhere because of weaker radiation and Chla. Lower demethylation due to lower temperatures is responsible for higher MeHg at the poles than elsewhere.	Zhang et al. 2020

8.4.3 Changes in total Hg in the future Arctic Ocean – impact of anthropogenic emissions versus other drivers

How important are the impact of anthropogenic emissions versus other climate change drivers? Will changes cancel each other out or strengthen an upward/downward trend?

Take the Hg budget from chapter 3 and do scenarios with:

- Main – directly anthropogenically driven: future changes in atmospheric deposition. Figure xx shows total mercury deposition on the surface ocean every year, we posit that all the deposition falls on the ocean surface, in the next iteration we will differentiate between deposition on the sea-ice and deposition on seawater. This is an important distinction since the redox conditions are different on the different surfaces and will be strongly influenced by changing sea ice cover. We probe the impact of delaying emission reductions policies as described in the previous section.

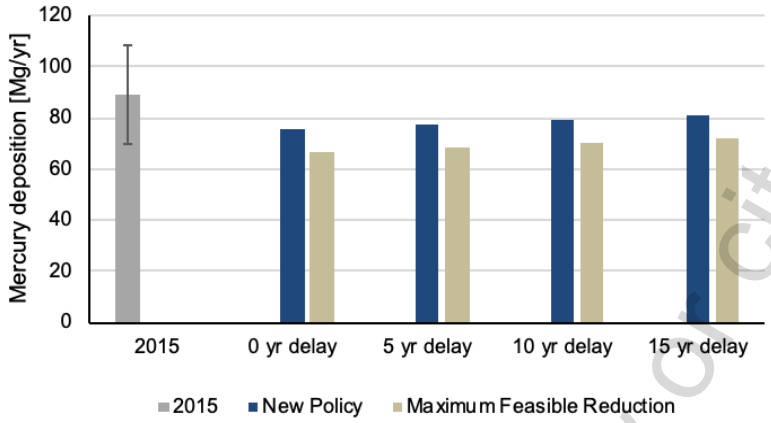

15260
15261

15262 Scenarios are used to force the ocean model and produce very preliminary estimates of total mercury
15263 concentrations in three layers of the Arctic Oceans (Figure xx a-d) in response to policy changes and
15264 delays. We do not yet consider shifts in environmental conditions such as sea ice cover or riverine
15265 inputs.

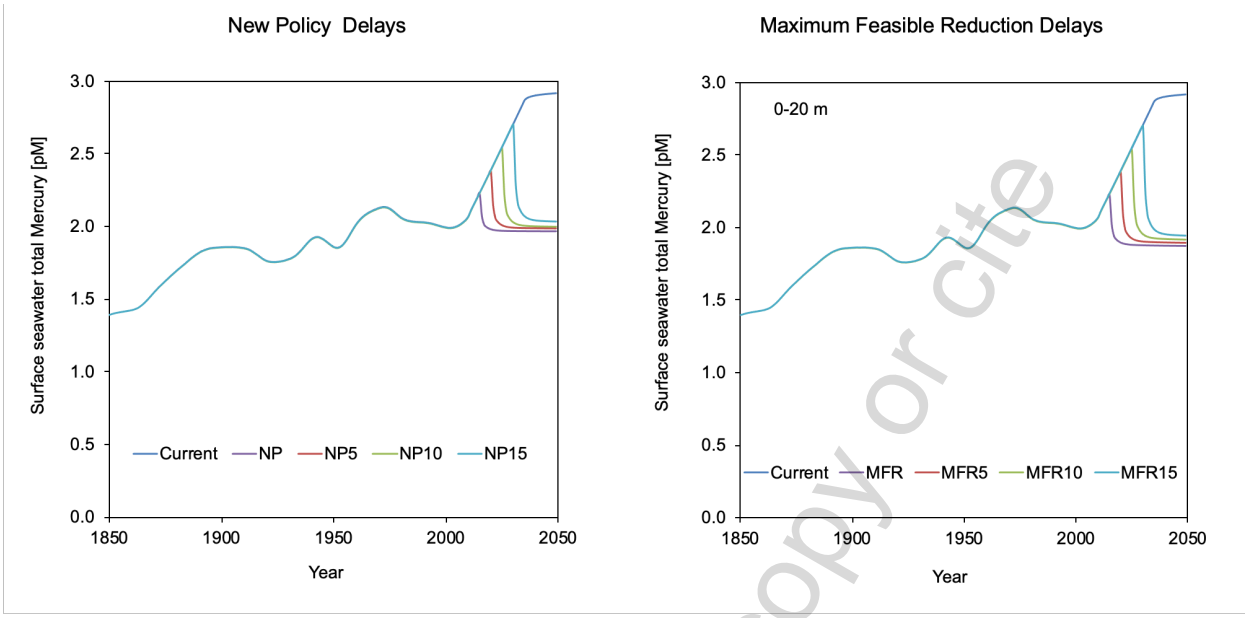

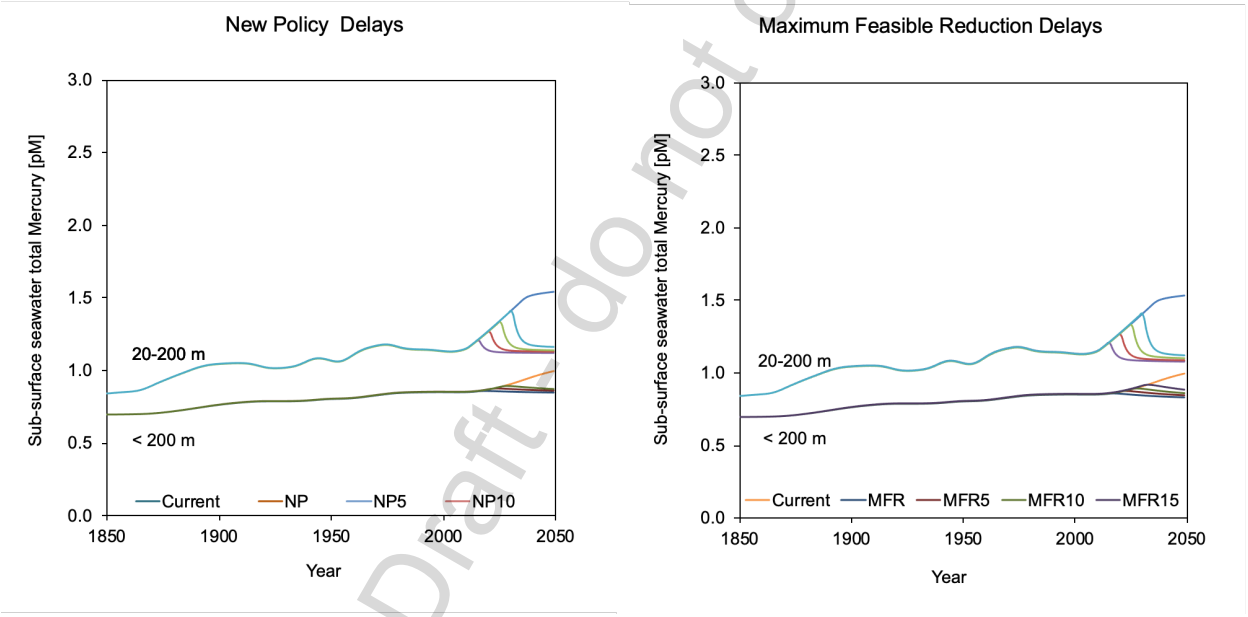

The next steps are to:

Evaluate the model against measured data over time and include changes that have been estimated in the prior chapters such as:

- future changes in river input (including permafrost thaw, erosion). The important thing here is to estimate the magnitude of change (we should be able to get estimates from chapter 2-4?)
- future changes in sea-ice

Changes in Pacific Ocean input

- future changes in OM production (more rapid removal of Hg from surface ocean?)
- discuss emissions and biota

	Current input (Mg/y)	Scenario 1 % change 2050	Scenario 2 % change 2050	Scenario 3 % change 2050
Direct deposition	?			
Snow melt	?			
Rivers (lag)	50			
Pacific inflow (lag)	6			

Table 8.3.X. Estimated relative changes in input to the Arctic Ocean in 2050 driven by changes in anthropogenic emissions.

8.4.4 Changes in MeHg in the future Arctic Ocean – status on modeling, what are our best guesses at what will happen [MOU4] and how should the community proceed to improve our ability to make accurate future projections.

I GUESS IF WE ARE MAINLY FOCUSSED ON CHANGES IN EMISSIONS IT BECOMES REDUNDANT TO LOOK AT MEHG SINCE IN SUCH A SCENARIOS (ALTHOUGH unrealistic) MEHG WOULD JUST LINEARLY SCALE TO TOTAL HG![SA5] [MOU6]

Understanding the deposited inorganic mercury availability to methylating microorganisms, and how methylation and demethylation will be impacted by changing environmental conditions in the Arctic, will be key to produce future scenarios.

8.5 Summary and conclusions

The summary section draws policy-relevant conclusions from the discussion about different trajectories of future mercury concentrations in the Arctic ocean and atmosphere.

15296 **Key references:**

15297

15298 Angot, H., Dastoor, A., De Simone, F., Gårdfeldt, K., Gencarelli, C. N., Hedgecock, I. M., …
15299 Dommergue, A. (2016). Chemical cycling and deposition of atmospheric mercury in polar
15300 regions: Review of recent measurements and comparison with models. *Atmospheric Chemistry*
15301 *and Physics*, *16*(16), 10735–10763. https://doi.org/10.5194/acp-16-10735-2016

15302 Angot et al. (2018) Global and local impacts of delayed mercury mitigation efforts. *Environmental*
15303 *Science & Technology*, 52, 22, 12968-12977.

15304 Chen, L., Zhang, W., Zhang, Y., Tong, Y., Liu, M., Wang, H., … Wang, X. (2018). Historical and
15305 future trends in global source-receptor relationships of mercury. *Science of the Total*
15306 *Environment*,*610–611*, 24–31. https://doi.org/10.1016/j.scitotenv.2017.07.182

15307 Cole, A. S., Steffen, A. (2010). Trends in long-term gaseous mercury observations in the Arctic and
15308 effects of temperature and other atmospheric conditions. *Atmospheric Chemistry and Physics*, 10,
15309 10, 4661-4672.

15310 Corbitt, E. S., Jacob, D. J., Holmes, C. D., Streets, D. G., & Sunderland, E. M. (2011). Global source-
15311 receptor relationships for mercury deposition under present-day and 2050 emissions scenarios.
15312 *Environmental Science and Technology*, *45*(24), 10477–10484.
15313 https://doi.org/10.1021/es202496y

15314 Dastoor, A. P. and Durnford D. A. (2014), Arctic Ocean: is it a sink of source of atmospheric
15315 mercury?. *Environmental Science and Technology*, *48* (3),1707-1717.
15316 https://doi.org/10.1021/es404473e

15317 Dastoor, A., Ryzhkov, A., Durnford, D., Lehnherr, I., Steffen, A., & Morrison, H. (2015).
15318 Atmospheric mercury in the Canadian Arctic. Part II: Insight from modeling. *Science of the Total*
15319 *Environment*, *509–510*, 16–27. https://doi.org/10.1016/j.scitotenv.2014.10.112

15320 Fisher, J.A., Jacob, D. J., Soerensen ,A. L., Amos, H. M.,Steffen A., and Sunderland, E. M. (2012),
15321 Riverine source of Arctic Ocean mercury inferred from atmospheric observations. Nature
15322 Geoscience, 5, https://doi:10.1038/NGEO1478

15323 Fisher J. A., Jacob, D. J., Soerensen ,A. L., Amos, H. M., Corbitt, E. S., Streets, D. G., WangQ.,
15324 Yantosca, R. M., and Sunderland, E. M. (2013). Factors driving mercury variability in the Arctic
15325 atmosphere and ocean over the past 30 years. *Global Biogeochemical Cycles*, 27,
15326 https://doi:10.1002/2013GB004689.

15327 Giang, A., Stokes, L. C., Streets, D. G., Corbitt, E. S., & Selin, N. E. (2015). Impacts of the Minamata
15328 Convention on mercury emissions and global deposition from coal-fired power generation in
15329 Asia. *Environmental Science and Technology*, *49*(9), 5326–5335.
15330 https://doi.org/10.1021/acs.est.5b00074

15331 Kirk et al. (2014) Atmospheric deposition of mercury and methylmercury to landscapes and
15332 waterbodies od the Athabasca oil sands region, *Environmental Science & Technology*, 48, 13,
15333 7374-7383.

15334 Koven et al, (2012) Analysis of permafrost thermal dynamics and response to climate change in the
15335 CMIP5 Earth System Models, *Journal of Climate*, 26, 6, 1877-1900.

15336 Lei et al. (2014) Projections of atmospheric mercury levels and their effect on air quality in the United
15337 States, *Atmospheric Chemistry and Physics*, 14, 783-795.

15338 Moore et al., (2014) Convective forcing of mercury and ozone in the Arctic boundary layer induced
15339 by leads in sea ice, *Nature*, 506, 7486, 81-84.

15340 Mulvaney et al., (2020) Mercury benefits of climate policy in China: addressing the Paris Agreement
15341 and the Minamata Convention simultaneously, *Environmental Science and Technology*, 54, 3,
15342 1326-1335.

15343 Pacyna, J. M., Travnikov, O., Simone, F. De, Hedgecock, I. M., Sundseth, K., Pacyna, E. G., …
15344 Kindbom, K. (2016). Current and future levels of mercury atmospheric pollution on a global
15345 scale. *Atmospheric Chemistry and Physics*, *16*(19), 12495–12511. https://doi.org/10.5194/acp-
15346 16-12495-2016

15347 Rafaj, P., Bertok, I., Cofala, J., & Schöpp, W. (2013). Scenarios of global mercury emissions from
15348 anthropogenic sources. *Atmospheric Environment*, *79*(2013), 472–479.
15349 https://doi.org/10.1016/j.atmosenv.2013.06.042

15350 Rafaj, P., Cofala, J., Kuenen, J., Wyrwa, A., & Zyśk, J. (2014). Benefits of European climate policies
15351 for mercury air pollution. *Atmosphere*, *5*(1), 45–59. https://doi.org/10.3390/atmos5010045

15352 Selin (2018) A proposed global metric to aid mercury pollution policy. *Science*, 360, 6389, 607-609.

15353 Semeniuk, K., and Dastoor A. (2017), Development of a global ocean mercury model with a
15354 methylation cycle: Outstanding issues, *Global Biogeochemical Cycles*, *31,*400–433,
15355 doi:10.1002/2016GB005452.

15356 Soerensen, A. L., D. J. Jacob, A. T. Schartup, J. A. Fisher, I. Lehnherr, V. L. St. Louis, L.-E.
15357 Heimbürger, J. E. Sonke, D. P. Krabbenhoft, and E. M. Sunderland (2016), A mass budget for
15358 mercury and methylmercury in the Arctic Ocean, Global Biogeochem. Cycles, 30,
15359 doi:10.1002/2015GB005280.

15360 Steenhuisen, F., & Wilson, S. J. (2019). Development and application of an updated geospatial
15361 distribution model for gridding 2015 global mercury emissions. *Atmospheric Environment*,
15362 *211*(December 2018), 138–150. https://doi.org/10.1016/j.atmosenv.2019.05.003

15363 Streets, D. G., Zhang, Q., & Wu, Y. (2009). Projections of Global Mercury Emissions in 2050.
15364 *Environmental Science & Technology*, *43*(8), 2983–2988. https://doi.org/10.1021/es802474j

15365 Sundseth, K., Pacyna, J. M., Pacyna, E. G., Munthe, J., Belhaj, M., & Astrom, S. (2010). Economic
15366 benefits from decreased mercury emissions: Projections for 2020. *Journal of Cleaner*
15367 *Production*, *18*(4), 386–394. https://doi.org/10.1016/j.jclepro.2009.10.017

15368 Outridge, P. M., Macdonald, R. W., Wang,F., Stern, G. A., and Dastoor, A. P. (2008) A mass balance
15369 inventory of mercury in the Arctic Ocean. Environmental Chemistry, 5, 89–111.
15370 https://doi:10.1071/EN08002

15371 Vonk et al. (2015) Reviews and syntheses: Effects of permafrost thaw on Arctic aquatic ecosystems.
15372 *Biogeosciences*, 12, 23, 7129-7167.

15373 Willis et al. (2018) Sources of methylmercury to snowpacks of the Alberta Oil Sands Region: a study
15374 of in situ methylation and particulates. *Environmental Science & Technology*, 52, 2, 531-540.

15375 Zhang, Y., D. J. Jacob, S. Dutkiewicz, H. M. Amos, M. S. Long, and E. M. Sunderland (2015),
15376 Biogeochemical drivers of the fate of riverine mercury discharged to the global and Arctic
15377 oceans, Global Biogeochem. Cycles, 29, doi:10.1002/2015GB005124.

15378 Zhang, H., Holmes, C. D., & Wu, S. (2016). Impacts of changes in climate, land use and land cover
15379 on atmospheric mercury. *Atmospheric Environment*, *141*, 230–244.
15380 https://doi.org/10.1016/j.atmosenv.2016.06.056

15381
15382

* This is Chapter 9 of the AMAP Mercury Assessment*

9. What are Arctic Indigenous People's perspectives and contributions to the study of environmental mercury contamination in the Arctic?

Co-leads: Eva Kruemmel, Magali Houde
Contributors (to be completed): Jeremy Brammer, Tanya Brown, John Chételat, Rune Dietz, Marlene Evans, Mary Gamberg, Aviaja Hauptmann, Joel Heath, Dominique Henri, Jane Kirk, Brian Laird, Mélanie Lemire, Ann E. Lennert, Robert Letcher, Sara Lord, Lisa Loseto, Gwyneth Macmillan, Todd O'Hara, Martin Robards, Sara Roberts, Stephan Schott, Enooyak Sudlovenick, Heidi Swanson, Tero Mustonen, Philippe Thomas, Virginia Walker, Alex Whiting

Table of Contents

16028 **9.1 What is the history of the contributions of Indigenous Peoples and communities to**
16029 **environmental monitoring in the Arctic?**

16030 Monitoring of the Arctic did not begin with the introduction of formal scientific environmental
16031 monitoring; Indigenous Peoples have lived in and observed their Arctic environment for millennia and
16032 always have called the Arctic their home (Johnson et al. 2015). People from the North have relied on
16033 their knowledge, which is passed down from one generation to the next to understand the environment
16034 around them (ICC 2014, Johnson et al. 2015). These daily observations of climate conditions, wildlife
16035 and vegetation have been the basis for their survival, their culture, and sense of locality (Lennert 2016).

16036 Indigenous Peoples hunting and fishing populations constitute a rich depository of environmental
16037 knowledge, which can be used to enhance scientific research and observations of a changing
16038 environment. Their retention of unique environmental knowledge should be acknowledged as an
16039 important proxy to understand the interaction between elements, both natural and non-natural, in the
16040 Arctic.

16041 More recently, however, the value of Indigenous Knowledge (IK) has been increasingly recognized by
16042 scientists and governments in the Arctic and beyond (Mantyka-Pringle et al. 2017, Danielsen et al.
16043 2014). Many published papers in the peer reviewed literature refer to the importance and advantages of
16044 IK (also often called "traditional knowledge"):

16045 - Indigenous Peoples have acquired their knowledge by making observations for millennia, year-
16046 round (Lennert 2016, Johnson et al. 2015);
16047 - Indigenous knowledge is holistic and uses a range of perspectives (Mantyka-Pringle et al. 2017,
16048 Johnson et al 2015);
16049 - Involvement of Indigenous knowledge and Indigenous communities in processes enhances
16050 management and speed of decision-making (Danielsen et al. 2010).

16051 Many regional or local governments in the circumpolar Arctic conduct environmental monitoring
16052 and/or research activities to support policy- and decision-making. Indigenous knowledge is often
16053 required during these processes. For example, in Canada, the Nunavut Land Claim agreement mandates
16054 the Government of Nunavut to develop tools to help facilitate the use of both conventional (scientific)
16055 and IK in informed decision making (ref from Nunavut Gov, others?). In Nunavik (Quebec, Canada),
16056 the Nunavik Research Centre (NRC) was established in 1978 to monitor and collect land use and
16057 ecological data in the region (Makivik Corp. 2018 [1]). The NRC operates a number of ongoing wildlife
16058 monitoring programs, often working with scientists, but under the mandate that research responds to
16059 the needs, questions, objectives and concerns of Nunavik Inuit, and that respects and utilizes Inuit values
16060 and knowledge in the process (ref from Ellen needed). Moreover, the Inuvialuit Settlement Region (IRS,

[a] https://www.makivik.org/nunavik-research-centre/

16061 Canada) has a community-based monitoring program (ISR-CBMP) to support Inuvialuit in protecting
16062 and preserving the Arctic wildlife, environment and biological productivity, to enhance decision-
16063 making, and to achieve the principles of the Inuvialuit Final Agreement [2].

16064 In addition to more formalized regional research and environmental monitoring activities, many
16065 communities have established their own projects or have been/are involved in studies and/or ongoing
16066 monitoring activities led or co-led by academic or government scientists. To get a better understanding
16067 of the current state of community-based monitoring in the Arctic, a multi-year initiative was launched
16068 in 2012 under the "Sustaining Arctic Observing Networks", which yielded an in-depth report of 81
16069 programs across the circumpolar Arctic (Johnson et al 2016), as well as the development of a searchable
16070 online Atlas of Community-Based Monitoring and Indigenous Knowledge in a Changing Arctic
16071 (www.arcticcbm.org). Several projects listed in the Atlas also include work on contaminants.

16072 This chapter provides an indication of the breadth of Indigenous contributions in research and
16073 monitoring activities, specifically on environmental mercury contamination, in the circumpolar Arctic.
16074 It should be noted that the described activities are not an exhaustive list, but present merely a flavor of
16075 activities that have been done or are currently ongoing.

Definition of Indigenous knowledge vs local knowledge:

The Inuit Circumpolar Council defines "Indigenous Knowledge" (IK) as "*a systematic way of thinking applied to phenomena across biological, physical, cultural and spiritual systems. It includes insights based on evidence acquired through direct and long-term experiences and extensive and multigenerational observations, lessons and skills. It has developed over millennia and is still developing in a living process, including knowledge acquired today and in the future, and it is passed on from generation to generation*" [3] (ICC-Alaska 2015).

Indigenous knowledge is different from "local knowledge", which refers to the knowledge of the residents of a community but is not necessarily embedded within an explicit belief system, as Indigenous Knowledge is (Johnson et al. 2015 and reference therein). For the Eurasian Arctic the Indigenous knowledge discussion emerges as a diverse field. In addition to the Sámi, Nenets, Chukchi, Evenki, Even and other nations that have Indigenous status in relationship with the nation states, there are groups such as the Komi, Veps, Karelians, Sakha and others who are seen either as national minorities or linguistic groups. For example, the Komi are engaged in trades and culture that is equal and similar to Nenets reindeer herding. In this case the use of the terms "local knowledge", "traditional knowledge" or a culturally-based approach, for example "Komi knowledge", may be appropriate. The context will vary.

[b] https://jointsecretariat.ca/resources/community-based-monitoring-program/

[c] Inuit at times may refer to their knowledge as Indigenous Knowledge, Inuit Knowledge or Traditional Knowledge. The definition provided above is understood by ICC to apply to all three terms.

16076

Community-Based Research/Monitoring

Community-Based Research or Monitoring (CBR or CBM) lends itself well to utilization of IK. "Community-based" means that a community determines the reason for the research or monitoring project, and it addresses a concern or issue as identified by the community. The community is involved in all stages of the project (and ideally leading or co-leading it): from planning over implementation and data collection, interpretation and analysis, dissemination, communication and sharing of data, to the application of data for decision-making. In an Indigenous community, CBM done in full meaningful partnership with IK holders will always automatically utilize IK as is appropriate.

16077

16078 **9.2 What are the known contributions of Indigenous Peoples to mercury contamination research?**

16079 A wide variety of research programs, particularly wildlife and fish sampling for contaminants, benefit
16080 from a better understanding and documentation of environmental and biological context. Ongoing
16081 observations by Indigenous Peoples about sea ice and climate conditions, animal distribution and
16082 behavior, diet and body condition, and many other variables substantially benefit the interpretation of
16083 research results, which particularly takes place in interdisciplinary community-based research.
16084 Indigenous Peoples from several regions of the Arctic have been involved to different degree in
16085 environmental monitoring and research on mercury (Hg)(Figure 1). With respect to Greenland, at least
16086 five large towns and villages have consistently participated in such work including Thule, Godhavn,
16087 Nuuk, Tasiilaq/Kulusuk and Scoresby Sound (Glahder 1995; Sandell et al. 2001, Dietz et al. 2001, Born
16088 et al. 2011). Without community partnerships and Inuit knowledge, contaminant studies in East
16089 Greenland would be deficient with respect to input on sampling and interpretation of biomarker
16090 information in wildlife that are exposed to contaminants and diseases. In Canada, numerous
16091 communities participate in contaminant monitoring and research projects, including in Nunatsiavut
16092 (Labrador), Nunavik (Quebec), Nunavut, the Northwest Territories, and Yukon. At the Canadian federal
16093 level, many of these studies are supported by the Northern Contaminants Program (NCP). Activities of
16094 multiple projects are described in more detail in the following section. In other Arctic countries,
16095 community-based research and monitoring efforts of Hg are not centrally organized and/or supported
16096 by federal programs but are depending on individual efforts by communities, academic researchers
16097 and/or independent organizations, and are therefore somewhat more difficult to capture. The map in
16098 Figure 1 and following descriptions therefore should be understood to be an indication of the breadth
16099 of existing Hg contaminant projects by regions but not a complete list of initiatives (Appendix Table
16100 1).

16101

Circumpolar map to be included here with symbols for different animals that are being looked at. Will include color scheme to show how communities are engaged in each project (various degrees from sampling only up to all parts of research, including development of research, analysis of results, to communication).

***Figure 1**. Overview of Arctic activities involving Indigenous regions and communities (create map) and community-based/driven projects on Hg monitoring and research (For details on projects see Appendix Table 1)*

United States of America

Alaska

In the northernmost state of the United States, the community members of Kotzebue have been investigating mercury in subsistence species of Kotzebue Sound and surrounding areas (Alaska) using community-based and holistic perspectives [1]. Earlier research in the mid-1990s directly addressed community concerns about a caribou mortality event. However, since 2004, a more co-production approach has been developed between researchers and the Environmental Program at the Native Village of Kotzebue, as they work together on the mercury assessment of mostly marine biota in Northwestern Alaska. The partnership between professional researchers and the local tribal community began with a formal relationship development in order to identify mutual research priorities. Areas of interest and research questions were cooperatively developed between the Tribe, IK holders, and the researchers. The cooperative and strategic sharing of resources and the technical skills of researchers and community members were integrated into the informal and formal discussions. Short-term studies were then carried out as opportunistic efforts to develop an understanding of baseline levels of mercury in subsistence species, primarily finfish and ice seals. Indigenous Knowledge has been the motivating and organizing forces behind the Kotzebue collaborative studies – knowledge has been used to elucidate the context for the local ecology (i.e., local species and their trophic level relationships) and the species of most interest to local consumers. Local hunting and fishing expertise and knowledge have been used to collect animals – local members of the teams have played key roles within the practical and logistic aspects of the partnerships for accomplishing the work. Finally, indigenous perspectives have guided the development of responsible and effective ways to return information to community members; information is reported in the context of specific tissues, preparation methods, and the cost/benefit of alternatives such that consumers can safely and confidently make choices about their subsistence foods.

Canada

British Columbia, Yukon and Northwest Territories

16131 The vast Arctic territories of Canada is inhabited by numerous First Nation and Inuit communities
16132 (Metis?). In some circumstances involvement of Indigenous Peoples in mercury studies have been
16133 limited to helping in the sample collections of fish species from Yukon lakes by the Liard First Nation
16134 from Watson Lake (Simpson Lake) and the Champagne Aishihik First Nation from Haines Junction
16135 (Dezadeash Lake) [2]. However, many mercury-related initiatives have been initiated by indigenous
16136 groups and co-produce with scientists. In the Yukon, several sporadic mercury projects in fish and
16137 wildlife have been initiated, developed and carried out by First Nations. In 2007, a project on
16138 environmental change and traditional use of the Old Crow Flats in northern Canada (Yeendoo Nanh
16139 Nakhweenjit) was established [3]. This project, a collaboration between the Vuntut Gwitchin First Nation,
16140 the Government of Canada, Yukon Environment, and a multidisciplinary team of university researchers,
16141 included the measurement of mercury concentrations in muskrat tissue samples to verify that this
16142 traditional food source remained secure. More recently in 2014, in the same region of Old Crow, Hg
16143 was investigated in seven species of fish [4]. All fish were collected by the community which also assisted
16144 in sample extraction for analysis. In the Yukon, fish are also currently being collected for measurement
16145 of mercury by the White River First Nation in Beaver Creek [6]. This project was initiated, designed and
16146 carried out by the White River First Nation with some assistance by scientists.

16147 The First Nation in Old Crow is also involved in the annual mercury assessment of caribou [5]. The
16148 Porcupine herd is sampled out of Old Crow and the Qamanirjuaq herd is sampled out of Arviat,
16149 Nunavut. In most cases, samples are taken by Indigenous hunters as part of the traditional harvest for
16150 food. Ongoing discussions with the Vuntut Gwitchin Government, the Porcupine Caribou Management
16151 Board, the Beverly Qamanirjuaq Caribou Management Board and Hunters and Trappers Organizations
16152 in the Kivalliq region continually refine the project in terms of additional questions to ask and variables
16153 to consider when analyzing and interpreting mercury concentrations in caribou. Mercury is also
16154 currently being measured in moose and fish collected by the NaCho Nyak Dun First Nation in Mayo
16155 which have been responsible of the project from the beginning to the execution with some assistance
16156 from a researcher [7]. A similar project in moose and fish was initiated in Atlin, BC by the Taku River
16157 Tlinget First Nation [8]. Longer term studies evolve over time with ongoing collaborations with First
16158 Nations, interpretations of mercury concentrations in wildlife and mercury dynamics in the environment
16159 are informed by IK, which can identify new questions and variables to consider in those interpretations.
16160 This is the case of the annual mercury monitoring in lake trout from Lake Laberge and Kusawa Lake in
16161 Whitehorse [9]. Fish are now being collected for this project by the local Ta'an Kwach'an Council and
16162 Champagne Aishihik First Nations with emerging involvement of the Kwanlin Dun First Nation.

16163 In addition to fish and wildlife, a human biomonitoring project has been initiated by Gwitchin and
16164 Dene/Metis communities in collaboration with university scientists [10]. Consultation between the
16165 university-based researchers and Indigenous communities shaped several aspects of the work plan,
16166 including: timing of the sample collections, local coordinator hiring plans, public consultation meetings,

endpoint selection, and participant inclusion criteria. Also, these conversations emphasized the common perspective that the proposed work must promote country food reliance within subarctic and Arctic Indigenous communities. The joint project aimed to investigate human exposures to a variety of contaminants including mercury in relation to nutrients (e.g., omega-3 PUFA, selenium) which may be related to health risks from mercury. This work is linked to community-based monitoring programs assessing specific biota. Over four years, adults and children from ten First Nations communities across the Yukon and Northwest Territories (i.e., the Vuntut Gwitchin First Nation from Old Crow, three Sahtu communities from K'asho Got'ine, Tulit'a, and Déline, and six Dehcho communities from Jean Marie River, Deh Gah Gotie, Ka'a'gee Tu, Sambaa K'e, K'atl'odeeche, West Point) have participated to this project. Local coordinators were hired and trained to carry out the sample and data collection and to return results at the end of the project. Mercury was measured in hair, blood and urine to monitor recent exposures; hair was also used to evaluate the past 12 month exposure to Hg.

The human project relied on IK communicated through the community consultations (2014-2018) to guide the projects' return of results and knowledge translation. Local perspectives provided by residents helped align the mission and design of the research with local priorities and concerns. The project also used the knowledge of local experts in the development and implementation of the questionnaires (e.g., integration of seasonality, availability food preparation, and consumption in dietary surveys, as well as use of correct species names). To facilitate the technical communication between researchers and community members, terminology workshops were organized with local Indigenous organizations where terms were reviewed with First Nations elders to discuss their meaning (e.g. contaminant, risk). Thereafter, Indigenous language experts helped discuss the options for translating each term and then verified these definitions through back-translation, with agreement about the preferred translation. In addition to helping the project to better bridge Indigenous concepts and knowledge, these discussions served as catalysts to shared values and cross-cultural communication.

In the Northwest Territories, numerous Indigenous-initiated projects have been created in the past years. A multi-year study on spatial variability in mercury concentrations in food fish and their freshwater lake ecosystems is underway in the Dehcho region. This multi-stakeholder, community-driven research project involves Dehcho First Nations, as well as Ka'a gee Tu, Jean Marie River, Deh Gah Gotie, Liidlii Kue, Sambaa K'e, and Pehdzeh Ki First Nations. The objective of the project is to understand why mercury levels in food fish are below the Health Canada guideline in some lakes, but above the guideline in others[11]. Annual sampling occurs for 2-3 weeks each summer in wilderness camps, and is conducted by a joint University of Waterloo-Indigenous Guardian crew, which fosters two-way knowledge exchange. Guardians are involved with every aspect of sample collection and field processing. Analyses of Hg levels in water, sediment, zooplankton, benthic invertebrates and fish are conducted in addition to the determination of stable isotopes in biota and fish age. Indigenous Knowledge shapes which lakes were fished, how/when they are fished, what types of samples should

be taken (e.g., smoked fish, fish guts, liver), and other variables that should be considered - e.g., beaver activity in catchment, permafrost slumps. Indigenous Knowledge was used during planning meetings with Chiefs and Councils, and while in the field together, but not in a formalized interview setting. Indigenous Knowledge has also led to a spin-off project on fish growth rate, which is being led by one of the communities. Results from these projects are presented by scientists to individual communities in face-to-face meetings each year, at which time priorities for the upcoming year are re-evaluated in response to community and harvester concerns.

Moreover, research was conducted in 2013-2015 to investigate metal contamination of Yellowknife Bay (Great Slave Lake) from gold mining, to address concerns from the Yellowknife Dene First Nation over trace element concentrations in local fish. Yellowknife Bay is an important water body for subsistence fishing, including for whitefish, which were being collected for a school lunch program [12]. The community was involved in framing the questions of this project on cumulative impacts monitoring of aquatic ecosystem health and participated in the collection of fish, including at a traditional fishing site.

In the region of Great Slave Lake, contaminants in fish and fish health have been monitored since the 1990s with the help with the communities of Fort Resolution, Lutsel K'e, and Hay following concerns raised about fish health (e.g., skinny fish). There also have been periodic assessments of mercury in lake fish along the Mackenzie River. The earliest Hg work was with Fort Resolution which has been concerned for many years of the impact of a decommissioned mine on metals in water, sediment and fish in Great Slave Lake [13]. Based on a request by Fort Resolution, a study were designed with the community to investigate metals in the local environment as well as in fish tissue commonly consumed. The community participated in the sampling, reports were produced and meetings held in the community to discuss findings (Evans et al. 1998a, b). In the same region, the Lutsel K'e Nation has been concerned that the skinny fish found in Stark Lake could be related to contaminants from an abandoned exploratory mine or the scattering of radioactive debris over lakes following the disintegration of a nuclear-powered satellite [14]. Several studies were conducted over 2003-2013 on lake trout provided by the community and these fish were analyzed for metals and other contaminants in fish (Evans and Landels 2015). Other sporadic projects have taken place. A community researcher at Jean Marie River was concerned with seeing skinny walleye at Trout Lake and initiated and conducted a special study [15]. Another contaminant study was initiated by a community member at Inuvik following observations of unhealthy looking burbot liver (Cott et al. 2018) [16].

Over several decades, Gwich'in and Inuvialuit knowledge holders from Aklavik, Fort McPherson, Inuvik, and Tsiigehtchic had been observing increases in beaver and river otter densities, alongside marked declines in muskrat densities, across much of the Mackenzie Delta[16]. Muskrats were historically very common in the Delta and for decades had been harvested as a major source of food and fur. To address changes in the wetland wildlife community that had not been observed in living memory, the

Gwich'in Renewable Resources Board, the Ehdiitat Renewable Resources Council, and the Aklavik Hunters and Trappers Committee invited scientists to examine potential drivers of these changes in the furbearer community, including Hg (2015-present). IK holders have also played a central role in project planning, implementation, and reporting. Project planning and reporting is conducted within the established decision-making frameworks of partner organizations (e.g. the Gwich'in Renewable Resources Board, local Renewable Resource Councils) and involves regular face-to-face meetings between scientists and IK holders (see Hovel *et al. in review* for more details). During these meetings, project planning is structured around the identification of priority research questions and how these can be addressed collaboratively. Similarly, reporting during these meetings is also structured around these questions in an iterative process that can result in current questions remaining or being removed, and new questions being added. IK holders are also active participants in field research playing a role in the selection of sites, collection of samples, trapping of animals, and recording of observations. In particular, fieldwork is conducted with a multi-generational team of IK holders typically composed of a youths, adults, and elders. This facilitates sharing of IK across generations and between families while conducting fieldwork, and this IK is recorded each day through a daily camp log. Finally, this project facilitates the sharing of both scientific and IK with the broader community through activities at local schools and college campuses including giving talks and leading activities (e.g., animal dissections).

Inuvialuit Settlement Region

The Fisheries Joint Management Committee (FJMC) Beluga Harvest Monitoring program has enabled scientists since the 1980s to access beluga tissues and measure contaminants such as Hg [18]. The research components are driven by communities; knowledge gaps and priorities are addresses during discussions held at beluga summits (held in 2016 and planned for 2021). This co-production of knowledge weave IK and western science and integrate many aspects of beluga health including contaminant analyses (Figure 2). Tuktoyaktuk was the community historically involved in the program and, in more recent years, six additional communities from the Inuvialuit Settlement Region have integrated the annual work. The FJMC is the lead of organizing regional fisheries priorities and work in collaboration the Hunters and Trappers Committees. The established priorities set guidance for funding and are shared with scientists to guide their research. Community members are part of the planning, field crew, sometimes participate in lab analyses (usually youth), and often are part of the dissemination of results. Scientists have worked with communities to document information on beluga health that could be used to create IK indicators for long term monitoring. There also was focus in Tuktoyaktuk to organize collection of IK on hunting and processing of beluga as well as help assess impacts of climate change on beluga subsistence. Most recently a project on changes to beluga harvesting in Aklavik and work was also conducted in Ulukhaktok to document information on unusual (more details needed) hunts. The community of Paulatuk has also initiated its own community-based monitoring on belugas in 2011, which has been maintained since.

16275

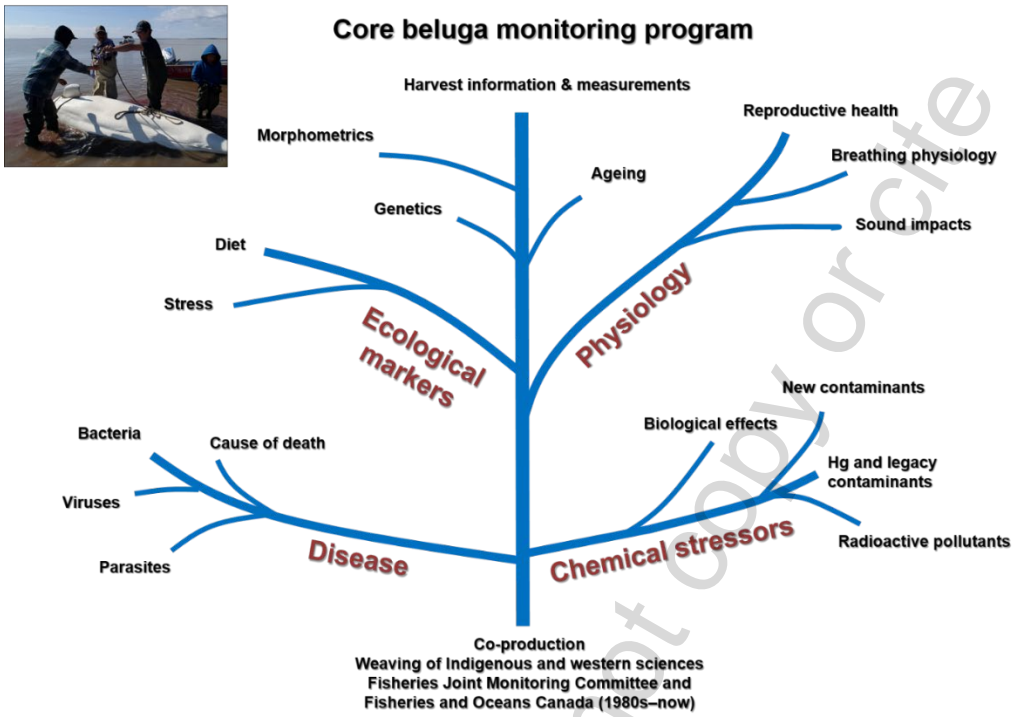

16276

16277 **Figure 2**. Core beluga monitoring program (Inuvialuit Settlement Region, Canada) as an example of
16278 co-production of knowledge. (We need a bit of text for the figure from Lisa/FJMC to describe it.)

16279 ***Nunavut***

16280 Multiple mercury studies integrating IK have taken place in Nunavut, the largest region of Inuit
16281 Nunangat (the homeland of Inuit). Mercury was measured in lichens, mushrooms and seaweed from
16282 communities in the Kivalliq region of Nunavut (i.e., Arviat, Baker Lake, Chesterfield Inlet, Rankin
16283 Inlet) in the summer of 2016 [19]. The idea for this project came from discussions with hunters and elders
16284 in the Hunters and Trappers Organizations who suggested that seaweed might be a source of mercury
16285 for the Qamanirjuaq caribou. The project was designed based on these discussions. Local Inuit
16286 community members interviewed elders about caribou diets and collected vegetation samples in each
16287 of the communities.

16288 For fish, a community-driven study on mercury in Arctic char, whitefish, cisco and trout from King
16289 William Island, Gjoa Haven has also been conducted [20]. The community initiated the project in the light
16290 of a potential commercial fishery project and gave guidance to the university-related researchers on the
16291 water bodies to be fished. Structured interviews were given, indoors and on the land workshops were
16292 held, Elder-youth field trips were organized and information type of info? sought from Inuit women
16293 working as community facilitators in "moms and tots" and a prenatal group. The project involved
16294 mapping which info? and Indigenous Knowledge from Elders examples of information collected from
16295 elders?

The long term Hg monitoring program of seabird eggs and bird carcasses from Resolute Bay (Prince Leopold Island) and Coral Harbor (Coats Island) has been on-going since 1994 [21]. This project was initiated by the Northern Contaminants Program based on concerns expressed on high levels of contaminants in country foods. Short IK studies in Resolute Bay and Pond Inlet were conducted in 2004, and earlier in Arctic Bay. Annual meetings and involvement of the local Area Co-Management Committee and the Hunters and Trappers Association keep informing experimental design and field collections. Capacity-building, field training during sampling periods and community member opportunities for participation through the Inuit Field Research Assistant program are routinely conducted. Opportunities to incorporate more IK under inclusive and participatory environmental monitoring frameworks are currently being further explored.

For mammals, a project investigating heavy metals (including total Hg) and health parameters in ringed seals from Iqaluit and Pond Inlet was conducted in 2017-2018 [22]. Community involvement was core in this project. All samples were collected on voluntary basis after the research project was explained to both communities. Interviews were also done in Iqaluit to investigate local concerns on ringed seal health and to find out what type of project they would be interested in. Communication has been open during the whole project, in Inuktitut and English.

Moreover, polar bears from western and southern Hudson Bay have also been continuous monitor for total mercury since 2007 [23]. This extensive work has involved members of communities from Arviat, Rankin Inlet, Whale Cove and Sanikiluaq. This collaborative sampling has also allowed the investigation of mercury biological effects in bears from western Hudson Bay as well as Baffin Bay (Pond Inlet and Clyde River) where bears have also been captured in the past. Continual information exchange between researchers and local partners and regular visitation to one or more of the communities on an annual basis have been key elements to this long-term project.

Using a more ecosystemic approach, Indigenous organizations from five communities in Hudson Bay and James Bay (Sanikiluaq, Kuujjuaraapik, Inukjuak, Umiujaq, Chisasibi) have participated from 2015-2018 in a project on metal accumulation in the marine food web [23]. Communities expressed interest in information on metal levels in marine wildlife to address concerns of mercury contamination from hydroelectric reservoir releases into James Bay. Inuit or Cree hunters collected local marine animals in their traditional territory (blue mussel, sea urchin, plankton, marine fish, common eider, ringed seal) for mercury tissue analysis. The contaminants component was part of a larger community-based initiative to use IK to track environmental change in the region.

Nunavik

In the northern region of Quebec, metal bioaccumulation was investigated (2013 to 2015) in country food from Kuujjuaraapik to assess if levels of mercury had changed 20 years after initial mercury measurements had been made for an environmental assessment of a large-scale hydroelectric project[24].

This study was a collaboration between a local Inuit organization (the Sakkuq Landholding Corp), government scientists and Inuit hunters, who collected relevant marine animals, terrestrial wildlife and freshwater fish for tissue analysis within their traditional territory.

In 2016, a pilot-project named Imalirijiit (those who study water) was launched by university-affiliated researchers and the Inuit community of Kangiqsualujjuaq to build a community-based monitoring program on the George River Basin [26]. Kangiqsualujjuammiut chose to monitor the environmental quality of the lower George River because of a mine that was scheduled to start its operations up river. This project was initially focused on a baseline assessment of rare earth elements and has since expanded to include other trace elements and mercury in river waters, sediment and biota (i.e., lichen, fish, bird, seal). Indigenous knowledge was used to select sampling stations in marine and freshwater zones, to document land use by Inuit, plant and animal ecology, river's movements and processes as well as landscape changes (e.g., vegetation growth, landslides). Each year, community consultation is plan to continue to co-construct the next steps of the project and to share research results. The creation of a science land camp program involving youth, elders, local experts and researchers is a key component of this collaborative project. The goal for the land camps are to provide more opportunities for the youth to connect with both scientific and Inuit knowledge. Participating elders were interviewed and additional semi-structured interviews with local guides/hunters were conducted in the community with the help of interpreters. Focus groups were also conducted to record the traditional place names along the George River Basin (Inuit, Naskapi and Innu). Interactive mapping was used to present place names, IK, stories and land-use information to virtual maps; interactive mapping workshops to train community members in map creation have been organized. This tool allows for the archiving of local Indigenous knowledge within a "living map", in a manner that is accessible to community members, local organizations and schools. Communication outside the community is also emphasize by the project; youth participants have been involved in presenting the project at scientific meetings.

For humans, research projects in Nunavik have been monitoring maternal exposure to Hg and methylmercury (MeHg) since 1992 as well as other contaminants and nutrients from country foods. In 2016, this biomonitoring project was intitled Nutaratsaliit Qanuingisiarningit Niqituinnanut (Pregnancy wellness with country food) [27]. Across the 14 communities of Nunavik, blood and hair samples from Inuit pregnant women have been analyzed and MeHg intake estimated using food frequency questionnaires as well as existing data on MeHg and Hg in wildlife. Midwives have guided the project at the onset and an open and continuous dialogue between academic researchers, the Nunavik Regional Board of Health and Social Services, the Nunavik Nutrition and Health Committee and communities has led to evolution of this on-going project to different activities at clinical and national scales. Through time, knowledge has also been shared and discussed with Nunavik caregivers, pregnant women, grandmothers and hunters to better promote together healthy pregnancies and children with country foods.

Nunatsiavut

In Nunatsiavut, ringed seals have been the subject of several studies led in collaboration between communities, regional government and scientists. A long-term monitoring of Hg in muscle and liver of ringed seals from Nain, and other regions from Inuit Nunangat, including such as Sachs Harbour, Resolute Bay, and Arviat, has been on-going since the 1990s [28]. Ringed seals are important country foods in several communities and levels of Hg have been found to be high in liver leading to the long-term monitoring of these animals. This project, which assesses the spatial and temporal trends of contaminants in seals, relies on IK of local hunters to collect ringed seals samples over time. Since 2016, outreach activities in communities involved in the project have been integrated to this monitoring work. This social chapter of the project addresses a shared interest among Inuit and scientific researchers in enhancing communications and community capacity building related to contaminants research. These workshops provide opportunities for Inuit elders to share their knowledge in seal ecology and traditional methods for butchering seals, preparing seal skin, and identifying abnormalities in harvested game with students and researchers. Northern college students have been involved in the activities as a way to increase the capacity of northern students and best practices for communicating contaminants research with Inuit youth have been identified through the years. The collaborative group is working towards bridging more IK and increase capacity sharing and training for future community-based monitoring.

Mercury contamination in the ringed seal's food web has also been investigated in Nunatsiavut[29]. Changes in food web structure and mercury concentrations in ringed seals collected along the coast have also been evaluated since 1999 at several sites (e.g., Nain, North West River and Rigolet). Inuit Knowledge has driven the research questions asked pertaining to these projects. Moreover, a community-based monitoring and research project was initiated in 2013 due to concerns of communities on the levels of methylmercury projected to increase in Lake Melville following the hydroelectric power development on the Churchill River [30]. This ongoing project examines Hg and MeHg contamination in the ringed seal food webs of Lake Melville and aims to understand the sources of contamination and effects of hydro development and climate change on the levels. All seal collections were carried out during community harvests and therefore completely relies on IK. This project also relies on IK of field team members for collections of water, plankton, and lower food web organisms, including safe travel on Lake Melville and of productive zones for sampling plankton and plentiful areas for krill, scallops, urchin, and jellyfish collections. Community meetings are arranged during the seal hunt in spring to update information on the project, to obtain feedback/input, and to share information on current seal health. Training is also given for sample collection in order to increase capacity building in the region.

Greenland

In Greenland, sampling of biota for Hg research (and other contaminant analyses) has been conducted

with help from Inuit hunters since the 1970s [31-36]. The reason for initiating work on contaminants in traditional foods was, and still is, related to the human health aspect in addition to the wildlife health. Some of the longest time series have been ongoing under the Greenland CORE programme including samples from polar bears, ringed seals, black guillemots, sculpins and arctic char since the 1995. The wildlife and fish sampling was initiated under the programme Heavy Metals in the Greenland Environment (1985-1988) and other shorter programs. The Scoresby Sound polar bears project is one of the longest wildlife time series in the Arctic spanning from 1983 to present; these 37 years of contaminants data were made possible because of the long-term collaboration with the East Greenland Inuit population. Many other sample collection have previously been conducted on other species including e.g. narwhals, beluga killer whales, walrus, harp seals, hooded seals, bearded seal, seabirds, fish species and musk oxen, as part of different ongoing programmes. For the species with hunting quotas, only full time hunters were allowed to collect the animals; it has always been a tradition to conduct the sampling in a close and efficient collaboration with the skilled Greenland Inuit hunters. Often meetings with the Inuit hunters are being held during the field work and results are presented. Moreover, the involved scientists are in year-round contact with some key hunters where mutual information is being exchanged on relevant issues in relation to the hunts and science information including contaminant exposure and health issues.

Sweden

Main sources of Hg in Sweden, as also in Finland, have included construction of large-scale hydropower stations (Luleå, Kemijoki, etc) as well as industrial mining and forestry. Impact assessment of large-scale hydropower development and forestry practices on the Sámi communities were conducted between 2003 and 2013 in the Jokkmokk region of Sweden [37]. Mercury analyses in predator fish were part of the community-based monitoring and impact assessment of the reservoirs on the Sámi culture, fisheries and ways of life.

Finland

Investigating the impacts of hydropower development and forestry practices on the Sámi and wildlife communities of Lokka and Porttipahta, Finland were also done between 2000-2010 [38]. Mercury releases, impacts and concerns in the Indigenous and local knowledge have been present as a part of the monitoring work in some locations. What makes the context of Indigenous and local knowledge monitoring of special importance in the Russian peripheries is the role and scope of past, Soviet-era legacies of industrial releases that constitute gaps in knowledge across the region. Snowchange Co-op, for instance, has been conducting community-based monitoring in the Eurasian North between 1999-2020 [39]. This has included field visits, fish, weather, ecological change and hunting diaries, oral history documentation, ecological mapping, satellite image interpretation, place name surveys, community workshops and conferences and gender-specific biodiversity and programmes related to Indigenous

knowledge and/or local knowledge.

Local knowledge of the impact of hydroelectric dams, forestry practices and peat production on the Karelian and Finnish wilderness (Koitajoki catchment) of the transboundary middle boreal watershed between Russian and Finnish Karelia has been the subject of contaminants research until very recently (1950-2019) [40]. (details needed)

Russia

Whilst the mercury and other contaminants have received international attention in recent decades, Fennoscandia and the Eurasian North (i.e. the Russian Arctic and boreal) have been less studied especially in the context of Indigenous and local knowledge. In the Russian Arctic the main sources of mercury can be attributed to coal combustion as well as mining and production of metals such as nickel, zinc and lead as well as gold. Mercury can also be released from waste management and industries.

In the Ponoi river catchment, observations of the impacts of Soviet chemical legacies on the communities of Krasnochelye, Kanevka and Ivanovka and on the Sámi, Komi and wilderness communities have been assessed [41]. Similar work has also been done in the Kolyma river catchment to support assessment of mercury impacts on the communities of Chukchi and Yukaghir as well as their environment [42]. These projects combine CBM, science and best practices of monitoring. In the Iengra river catchment, observations of the impact of modern-day artisanal gold mining on the communities of Evenki reindeer herders were done[43]. This project demonstrated the use of communal mapping of problematic sites and negotiating nature-based nomadic lifestyles in the middle of sudden mercury releases in the boreal. Results of the land use changes have been released as a part of the Evenki Atlas (www.evenki-atlas.org).

9.3 How has IK has been and is utilized in mercury research and how has it contributed to the overall knowledge on contamination in the Arctic?

Several studies have used IK for the identification of meaningful research questions, the selection of study sites, the successful conduct of fieldwork and sample collection, improved understanding of ecological context, and to determine the best ways results can be communicated with those living in that environment. Some examples include:

In the Northwest Territories, collaborative studies originally designed to evaluate other ecological aspects of fish led into contaminant studies. For example, Deline fishermen have observed different types of lake trout in the Great Bear Lake. Fish living in different regions of the lake had different food in their stomachs and different appearances. These observations have led to collaborative studies with researchers to investigate mercury concentrations in relation to feeding ecology, habitat and age of fish.

- IK Caribou diet, leading to lichen study (need clarification from Mary if this is a good example)

In Nunavut, Qamanirjuaq caribou were found to have higher mercury concentrations than other Arctic caribou herds. Caribou usually get most of their mercury from lichens, but local elders described the Qamanirjuaq caribou eating seaweed from the seashore. Since seaweed is known to accumulate metals, it was hypothesized that the caribou may be getting additional mercury from this source. Interviews with elders and hunters in Kivalliq communities indicated that Qamanirjuaq caribou forage for lichens on the tundra and hilltops in the winter and for lichens and other vegetation (including seaweed) on lakes, rivers and the seashore in the summer. Ultimately, mercury concentrations were significantly and consistently found to be lower in seaweed than in mushrooms and lichens, suggesting that seaweed was not a major source of mercury for the Qamaniruaq caribou.

- Higher Se in Huhanik women and IK association with specific part of beluga consumed by women (need description from Melanie)

More broadly, in the circumpolar Arctic, the utilization of IK is an overarching mandate of the Arctic Council and associated Working Groups such as AMAP are increasingly working towards this implementation (Arctic Council Indigenous Peoples Secretariat 2015, AMAP Strategic Framework 2019+). Within AMAP, work on contaminants and human exposure in some countries (e.g. Canada and Greenland) would not be possible without working with Indigenous Peoples in the Arctic. Active Indigenous and scientific relationships are critical to core initiatives of Arctic research, including the 1) measurement and monitoring of long-term trends and variability in contaminant concentrations in Arctic biota for focal ecosystems (e.g. Hudson Bay and East Greenland) 2) research into the influence of environmental changes on exposure, levels and trends of contaminants in the Arctic environment 3) the assessment of human health risks using information on levels and trends of contaminants in traditional foods, and 4) production of information that supports domestic and international chemical management initiatives.

Globally, the part played by Arctic Indigenous Peoples in negotiations of international treaties, such as the Stockholm Convention on Persistent Organic Pollutants (POPs), or the Minamata Convention on Mercury, has been highlighted (refs). Their involvement provided a human face to the problem of contaminants and ensured that the negotiations did not become just arguments over facts, figures and economic interests (refs). In particular, during the negotiations of the Minamata Convention, the Inuit Circumpolar Council (ICC) used results from NCP studies and AMAP assessments, such as graphs describing the exceedances of mercury guidelines by pregnant Inuit women in the circumpolar Arctic, as well as consumption advisories based on mercury in the traditional diet of Inuit in Nunavik and Nunavut, to highlight how Inuit are affected by mercury in the Arctic. The combined efforts by Arctic Indigenous Peoples and Arctic states during the negotiations led to the mentioning of Arctic Indigenous Peoples in the preamble of the two conventions. For instance, the Minamata Convention preamble states: ”*Noting the particular vulnerabilities of Arctic ecosystems and indigenous communities because of the biomagnification of mercury and contamination of traditional foods, and concerned about*

16507 *indigenous communities more generally with respect to the effects of mercury*". The engagement in
16508 United Nations conventions continues with involvement of Arctic Indigenous Peoples (such as the Inuit
16509 Circumpolar Council, ICC) in the implementation of the conventions, in particular with regards to the
16510 effectiveness evaluation of the Minamata Convention on Mercury.

16511

16512 **9.4 What are recent efforts to include IK and observations of ecological changes in mercury**
16513 **environmental monitoring?**

16514 Monitoring and research in focal ecosystems complement one another and contribute to refine our
16515 understanding of contaminant cycling and effects on wildlife in Arctic ecosystems, notably, in relation
16516 with ongoing environmental factors involved in climate change. This synergy is of high importance as
16517 the Arctic is an early-warning system for other ecosystems and communities that may suffer from future
16518 environmental changes.

16519 Indigenous knowledge can provide invaluable information that can help to discern climate change and
16520 other ecosystem impacts on contaminant levels in the Arctic environment and people. For example, an
16521 extensive research project in Nunavik on beluga whales (Nunavimmiut Knowledge of Beluga)
16522 investigated Inuit knowledge with regards to beluga, which included (but was not limited to) migration,
16523 body condition, foraging ecology, predation, breeding, calving, and behavior (Breton-Honeyman et al
16524 2016). This knowledge, e.g. on foraging ecology, provided information on diet composition and the
16525 seasonality of energy intake, which in turn is important because it can change beluga exposure to Hg
16526 due to impacts on beluga diet. (should another example be found instead of this one?)

16527 Sampling programs that have been ongoing for decades in collaboration of Indigenous groups are the
16528 backbone of international polar programs and research such as above described Greenland AMAP
16529 activities and projects funded by NCP in Canada. These Arctic programs would not exist without the
16530 partnership with local hunters and the generous sharing of their IK. Involvement of Arctic Indigenous
16531 Peoples in monitoring and research activities not only enables scientists to obtain the samples, but also
16532 contributes to the understanding of the ecosystem, changes that are occurring, and specific information
16533 about the traditional diet. With respect to mercury, a recent method has been used where the hunters list
16534 of games has been compiled within the Northwater (Avanersuaq/Nuuk) region, as well as the
16535 Scoresbysound and Nuuk regions to estimate the amount of meat and also the mercury entering the
16536 local communities (Dietz et al. 2018a; 2018b). This information was evaluated relative to Tolerably
16537 Monthly and Yearly intake (extrapolated from TWI) within the local society both over time (20-year
16538 period) and across the year/season. This method could be expanded to other Arctic regions and is
16539 presently being use to evaluate the effects of climate change and increased hunt on toothed whales in
16540 Greenland (CHANGE Project).

Additionally, projects such as "The Inuit Siku Atlas[4]" as well as "SIKU – The Indigenous Knowledge Social Network[5]" allow for sharing of knowledge and observations by Inuit hunters in near-real time and incorporate a variety of culturally relevant tools that allow Inuit to interpret results using their own knowledge system (Arctic Eider Society 2016; Heath et al. 2015). In several cases, these platforms include a mobile device application for use in the field and to be used as a part of community-driven programs to systematically document IK and environmental observations, such as body condition of animals, behavior, diet, ecology and environmental conditions. Other initiatives such as ArctiConnexion[6] and Ikaarvik[7] are specifically engaging Inuit youth in research activities that involve studies on various natural sciences, including on climate change and contaminants (such as mercury).

9.5 What are perspectives of Indigenous Peoples on past and future contaminants research, how IK should be utilized and how a co-production of knowledge should be conducted? (Shorter question to be found)

One general problem encountered with the utilization of IK occurs if scientists try to "incorporate" Indigenous knowledge into "Western" scientific studies, leading to processes of labeling or defining the knowledge in fixed ways and thereby separating it from its context or process of learning. The result risks failure to fully capture the underlying dynamic and flexible practice, as well as the losing depth of its sociocultural content (Egede Dahl and Hansen 2019). Similarly, as stated in a report on Dene Knowledge (DK): scientization, when IK is rendered and reduced to scientific terms, strips the knowledge from its full meaning and context. IK needs to be acknowledged and valued in the context of its original form (Dene Nation 2019). A related problem results from trying to translate IK from their original Indigenous languages into English. IK is place-based, and words and concepts from Indigenous languages are not easily transmitted into English. When this is attempted, important meanings become lost and the embedded, situated, collaborative and performative nature of Indigenous concepts get erased: "DK cannot be transmitted through books and abstract concepts alone; DK must be lived and practiced through actions in a dynamic oral tradition and in the Dene languages." (Dene Nation 2019).

Several documents for ethical research (in the Arctic) have been published by Indigenous organizations, which give guidance on how research should be conducted. Some of these are briefly introduced here:

In the early 1990's, the Inuit Circumpolar Conference (now ICC) developed its "Principles and Elements for a Comprehensive Arctic Policy" (ICC 1992), which included "Principles and Elements on Northern Scientific Research" (updated in ICC's Inuit Arctic Policy (ref), which was adopted by ICC

[d] https://sikuatlas.ca/index.html?module=module.sikuatlas.home.welcome
[e] https://siku.org/#/about
[f] https://arcticonnexion.ca/
[g] www.ikaarvik.org

in 2009. ICC continues to work on and update its international research strategy. In 2002, the "First Nations Information Governance Committee" first published the principles on "Ownership, Control, Access and Possession (OCAP)", which guide how information and data needs to be managed[8]. More recently, the Canadian National Inuit organization Inuit Tapiriit Kanatami (ITK) published the National Inuit Strategy on Research (ITK 2018), which outlines the vision, context, objectives and actions to achieve Inuit self-determination in research in Inuit Nunangat. Moreover, the Assembly of First Nations developed a (not formally adopted) document on "First Nations Ethics Guide on Research and Aboriginal Traditional Knowledge"[9], and the Dene Nation published a report "We have always Been Here. The Significance of Dene Knowledge" (Dene Nation 2019, link), which describes in detail what Dene Knowledge (DK) is and provides best practice recommendations for utilizing DK in decision making. Many communities and regions in the North also have their own guidelines for research and the utilization of IK (some examples are given in Dene Nation 2019). Moreover, Ikaarvik youth recently published recommendations for science and Inuit Qaujimajatuqangit (Inuit Knowledge), to guide researchers on meaningful engagement of Inuit and effective utilization of Inuit Knowledge[10].

While not all of these reports can be described in detail here, some of the main principles include:

- IK is equally valid to western scientific knowledge and should be respected and prioritized. Transparency and equal treatment of both IK and western science are needed; mutual trust needs to be developed.

- IK is not confined to harvesting activities; IK can and must also inform other steps of research. - - A co-production of knowledge approach is recommended, where scientists and knowledge holders work together to develop research questions, sampling approaches, discuss data analysis and interpretation, as well as communication and dissemination of results.

- The integrity of information and knowledge is derived from the knowledge older rather than the scientific method; knowledge holders are experts in their own field.

- Indigenous partners have the rights to control their intellectual properties.

- Timelines of Indigenous communities and priorities should be respected and sufficient time and resources for engagement should be allowed.

- Researchers have to understand the historical, cultural and political contexts and should acknowledge their limitations of their understanding of Indigenous culture and the legacies of colonialism that affect relationships today. needs to be explained what this entails.

- All should work together to agree on mutually accepted translations of words, terms between

[h] https://fnigc.ca/sites/default/files/docs/ocap_path_to_fn_information_governance_en_final.pdf
[i] https://www.afn.ca/uploads/files/fn_ethics_guide_on_research_and_atk.pdf
[j] https://ocean.org/wp-content/uploads/SciQ-Report-and-Recommendations-updated-October-2019.pdf

languages.

Overall, it is important that if the research is initiated by a (southern, non-indigenous) scientist, that this person approaches communities early on, to slowly build a relationship of trust, and to develop research questions together with the community. Sufficient time, face-to-face meetings and capacity building in the communities are key. It may be helpful/advised to fit the research project into local co-management frameworks to ensure relevance to local decision-making, avoidance of over-researching and duplication of studies. Many challenges exist in creating a respectful partnership and CMB research, including (but are not limited to):

- managing costs in terms of time and money for engaging with IK holders,
- ensuring opportunities to participants are well distributed,
- ensuring all participants are safe and protected,
- ensuring local capacity exists to accommodate research, and that research activities do not over-exploit Indigenous communities (leading to exhaustion and research fatigue)
- ensuring researchers are supported in engaging with communities, and
- ensuring a long term, reciprocal relationship is built and maintained.

Communication is a particularly important part of research activities, to allow for good knowledge exchange. A very specific aspect in communication on contaminant research is related to the importance of the traditional diet, benefits, and possible health risks associated with exposure to high contaminant levels. Communities want to be reassured when possible, and not just informed when high contamination levels are found. More details are discussed in the chapter on human health (section on risk communication). (ensure cross-reference with HH chapter). Poor communication can results in fear, confusion, misunderstanding, changes in diet and traditional lifestyles (Reinfort 2015). The medium of communication influences the message and is ultimately an important part of it. Researchers must also become better at identifying the indirect and unintended impact of their research. Once a piece of knowledge is generated, it can never be unknown. This puts a great responsibility on the shoulders of researchers who create knowledge, which can leave communities with facts and no options.

The community should be involved in all aspects and will recommend best ways of communication. Generally face-to-face meetings and interpretation in Indigenous languages are ideal. Community participation and engagement opportunities must respect community priorities and be scheduled on dates and times that respect seasonal activities and regular working hours. To keep communities engaged, it is helpful to involve multiple generations and families. Visits in local schools and colleges are also often appreciated and may assist in capacity building. Recommended communication pathways and materials include pamphlets, newsletters, videos, interactive games, radio broadcast and use social media. Food sharing can also be an important way of knowledge exchange. Finally, when research is published in scientific journals or at conferences, it is important to emphasize co-authorship with

16638 communities on posters and in peer reviewed manuscripts, etc.

16639 One must ensure the true motivation for communities to take part in projects beyond short-term
16640 monetary benefit, projects must create a motivation that is based on a potential to create change based
16641 on communities' strengths. Scientists must work with the assumption that they are not bringing
16642 expertise but coming into the Arctic to learn, and must work to understand not to investigate.

16643 Reflections of Indigenous scientists and knowledge holders:

> Alex Whiting (Kotzebue, Alaska): "Contaminant studies are in particular an area where it is crucial that research take into consideration the potential impacts on Indigenous communities. Arctic cultures are defined by their relationship with fish and wildlife species that sustain their cultural, nutritional and spiritual needs and way of life. This means that contaminant findings should not be presented as in a vacuum, but should be contextualized along with the ameliorating effects of the nutritional, cultural, communal, psychological and physiological benefits of participating in the procurement, processing, and sharing of fish and wildlife species. Researches should always take advantage of developing formal relationships with communities and developing research questions in true collaboration with Indigenous participants. "

16644

> Aviaja Hauptmann (Greenland): "As researchers we must not only try to understand Indigenous perspectives but at the same time become much more aware of our own imperfect perspectives as well as our motivation. We must refrain from approaching mercury research in the Arctic as an act of goodness based on our expertise, although this can be the incentive when applying for grants. Researchers must always bear in mind that we are doing research also, if not mostly, to develop our careers. The Indigenous communities we work with go into these projects with their personal lives, families, culture and emotions. To be respectful of this we need to approach our projects with an intention to not only bring our professional selves but also our personal selves, something I believe often happens naturally. But having this as an intention in its own might lay the foundation for more respectful collaborations. More and more we must also acknowledge that there might be scientists in local communities and not assume that scientific expertise is not present in Indigenous communities. "

16645

16646

16647

16648

16649

16650 **9.6 References** (to be updated)

16651 Breton-Honeyman K., Hammill M.O., Furgal C.M., and Hickie B. Inuit Knowledge of beluga whale
16652 (Delphinapterus leucas) foraging ecology in Nunavik (Arctic Quebec), Canada. Can. J. Zool. 94:
16653 713–726 (2016) dx.doi.org/10.1139/cjz-2015-0259

16654 Danielsen, F., Topp-Jørgensen, E., Levermann, N., Løvstrøm, P. Schiøtz, M., Enghoff, M. Jakobsen, P.
16655 et al., 2014. Counting what counts: Using local knowledge to improve Arctic resource
16656 management. Polar Geography 37, 69–91.

16657 Danielsen, F., Burgess, N.D., Jensen, P.M., and Pirhofer-Walzl, K. 2010. Environmental monitoring:
16658 The scale and speed of implementation varies according to the degree of peoples involvement.
16659 Journal of Applied Ecology 47(6):1166 – 1168. http://dx.doi.org/10.1111/j.1365-
16660 2664.2010.01874.x

16661 Dene Nation, We have always been here. The significance of Dene Knowledge.2019. Assembly of First
16662 Nations Office, Northwest Territories, Canada. 34 pages.

16663 Hover, R., Brammer, J., Hodgson, E., Amos, A., Lantz, T., Turner, C., Proverbs, T., Lord, S. Gwich'in
16664 Renewable Resource BoardThe importance of continuous dialogue in community-based wildlife
16665 monitoring: case studies of dzan and łuk digaii in the Gwich'in Settlement Area. Submitted

16666 Inuit Circumpolar Council-Alaska. 2015. Alaskan Inuit Food Security Conceptual Framework: How to
16667 Assess the Arctic From an Inuit Perspective. Technical Report. Anchorage, AK.

16668 Johnson, N., Behe, C., Danielsen, F., Krümmel, E.M., Nickels, S., Pulsifer, P.L. 2016. Community-
16669 Based Monitoring and Indigenous Knowledge in a Changing Arctic: A Review for the Sustaining
16670 Arctic Observing Networks. Final report to Sustaining Arctic Observing Networks. March 2016.
16671 Ottawa, ON: Inuit Circumpolar Council. Available at:
16672 https://www.inuitcircumpolar.com/project/community-based-monitoring-and-indigenous-
16673 knowledge-in-a-changing-arctic-a-review-for-the-sustaining-arctic-observing-
16674 networks%e2%80%8b/

16675 Johnson, N., Alessa, L., Behe, C., Danielsen, F., Gearheard, S., Gofman-Wallingford, V., Kliskey, A.,
16676 Krümmel, E., Lynch, A. et al., 2015. The contributions of community-based monitoring and
16677 traditional knowledge to Arctic observing networks : Reflections on the state of the field. Arctic
16678 68 (Suppl. 1), 1–13.

16679 Lennert, A.E., What happens when the ice melts? Belugas, contaminants, ecosystems and human
16680 communities in the complexity of global change, Marine Pollution Bulletin (2016),
16681 http://dx.doi.org/10.1016/j.marpolbul.2016.03.050

16682 Mantyka-Pringle, C.S., et al., Bridging science and traditional knowledge to assess cumulative impacts
16683 of stressors onecosystem health, Environ Int (2017),
16684 http://dx.doi.org/10.1016/j.envint.2017.02.008

16685 Arctic Council Indigenous Peoples Secretariat. 2015. Ottawa Traditional Knowledge Principles. 2015,
16686 2pp.

16687 Arctic Council Indigenous Peoples Secretariat. 2017. Persistent toxics. Accessed at
16688 http://www.arcticpeoples.org/persistent-toxics on 21 March 2017.

16689 Arctic Eider Society. 2015-2016 Annual Report. 2016, 38pp.

16690 Born, E.W., Heilmann, A., Kielsen Holm, L., Laidre, K.L. 2011. Polar Bears in Northwest Greenland:
16691 An Interview Survey about the Catch and the Climate. Man and Society, Man & society, ISSN
16692 0106-1062, Bind 351 of Monographs on Greenland. Museum Tusculanum Press, 2011. 232 pp.
16693 ISBN 8763531682, 9788763531689

16694 Dietz, R., C. Sonne-Hansen, E.W. Born, H. T. Sandell & B. Sandell 2001. Forekomst af "afvigende"
16695 isbjørne i Østgrønland. Faglig rapport fra DMU. nr 359 Juni 2001: 50 pp.

16696 Dietz, R, Mosbech A, Flora J., Eulaers, I (2018a). Interactions of climate, socio-economics and global

16697 mercury pollution in the North Water region. AMBIO 47 (Suppl. 2): 281–295.
16698 https://doi.org/10.1007/s13280-018-1033-z

16699 Dietz, R, Eulaers I, Søndergaard, J, Sonne, C, (2018b). Mercury Exposure in three Greenlandic
16700 societies (MEREX-1). Report to DANCEA: 56 pp

16701 Glahder C. 1995. Hunting in Kangerlussuaq, East Greenland 1951-1991, An Assessment of Local

16702 Knowledge. Meddelelser om Grønland, Man and Society 19. 79 pp. ISBN 978-87-635-1231-2.

16703 Heath J, Ljubicic G, Arragutainaq L. A Social Media Network and Interactive Knowledge-Mapping
16704 Platform for the North: Developing the tools needed to meaningfully engage communities in
16705 research and environmental stewardship. ArcticNet Annual Scientific Meeting, 2015, Vancouver,
16706 British Columbia, Canada

16707 Sandell, H.T., B. Sandell, E.W. Born, R. Dietz & C. Sonne-Hansen 2001. Isbjørne i Østgrønland. En
16708 interviewundersøgelse om forekomst og fangst, 1999. Teknisk Rapport nr. 40, 2001, Grønlands
16709 Naturinstitut: 94 pp.

16710

16711 **Appendix Table 1.** Portrait of Hg research conducted by, or in collaboration, with Indigenous Peoples. Project Id to be updated

16712

Project ID	Region	Year	Species/ matrices studied	Communities/ Indigenous Partners	Name of monitoring program	Scientist partners	Indigenous partner involvement in: Design (D), Sample Collection (S), Data Analysis (A), Communication (C)
1	Northwestern Alaska, U.S.A.		Seals, fish, caribou	Alex Whiting, Native Village of Kotzebue		Martin Robards, Wildlife Conservation Society Todd O'Hara, University of Alaska Fairbanks	D, S
2	Yukon, Canada		Fish	Liard First Nation, Champagne Aishihik First Nation		Jeremy Brammer	S
3	Old Crow, Yukon, Canada		Muskrats	Vuntut Gwitchin First Nation, Yukon Environment		Jeremy Brammer, Universities: McGill, Carleton, Wilfrid Laurier, Northern British Columbia, Waterloo, Alberta, Victoria	D, S
4	Old Crow, Yukon, Canada		Fish	Vuntut Gwitchin First Nation		Mary Gamberg	S, A
5	Old Crow, Yukon and Arviat, Nunavut, Canada		Caribou (Qamanirjuaq and Porcupine herds)	Vuntut Gwitchin Government, Porcupine Caribou Management Board, Beverly Qamanirjuaq Caribou Management Board, Hunters and Trappers Organizations	Northern Contaminants Program (NCP)	Mary Gamberg	D, S, A
6	Beaver Creek, Yukon, Canada		Fish	White River First Nation	NCP	Mary Gamberg Heidi Swanson,	D, S

						University of Waterloo	
7	Mayo, Yukon, Canada		Mooses, fish	NaCho Nyak Dun First Nation	NCP	Mary Gamberg	D, S, A
8	Atlin, British Columbia, Canada		Mooses, fish	Taku River Tlinget First Nation	NCP	Mary Gamberg	D, S
9	Whitehorse, Yukon, Canada		Fish	Ta'an Kwach'an Council, Champagne Aishihik First Nations and Kwanlin Dun First Nation	NCP	Mary Gamberg	D, S, A
10	Yukon and Northwest Territories, Canada	2014-2018	Humans (hair, blood, urine)	Vuntut Gwitchin First Nation, Sahtu communities from K'asho Got'ine, Tulit'a, and Déline, and Dehcho communities from Jean Marie River, Deh Gah Gotie, Ka'a'gee Tu, Sambaa K'e, K'atl'odeeche, and West Point	NCP	Brian Laird, Kelly Sinner, Mylene Ratelle, University of Waterloo Mary Gamberg	D, S, A, C
11	Decho Region, NWT, Canada	2013-2021	Water, sediment, zooplankton, benthic invertebrates, fish	Ka'a gee Tu, Jean Marie River, Deh Gah Gotie, Liidlii Kue, Sambaa K'e, and Pehdzeh Ki First Nations		Heidi Swanson, University of Waterloo	D, S
12	Yellowknife, NWT, Canada		Invertebrates, fish	Dene First Nation		John Chételat, ECCC	D, S
13	Great Slave Lake, NWT, Canada		Water, sediment, fish	Community of Fort Resolution		Marlene Evans, ECCC	D, S
14	Great Slave Lake and Stark Lake, NWT, Canada		Fish	Community of Lutsel K'e		Marlene Evans, ECCC	D, S
15	Jean Marie River, NWT, Canada		Fish	Community of Jean Marie River		Marlene Evans, ECCC	D, S
16	Inuvik, NWT, Canada		Fish	Community of Inuvik		Marlene Evans, ECCC	D, S
17	Mackenzie Delta, NWT, Canada	2015-present	Fur bearers	Aklavik Hunters and Trappers Committee		Jeremy Brammer, ECCC	D, S, A, C

				Gwich'in Renewable Resources Board Ehdiitat Renewable Resources Council			
18	Inuvialuit Settlement Region NWT, Canada		Beluga whales	Tuktoyaktuk and 6 other ISR communities, Fisheries Joint Management Committee, Hunters and Trappers Committees		Lisa Loseto, DFO	D, S, A, C
19	Arviat, Baker Lake, Chesterfield Inlet, Rankin Inlet, Nunavut, Canada	2016	Lichens, mushrooms, seaweed	Hunters and Trappers Organizations from the Kivalliq region		Mary Gamberg	D, S
20	Gjoa Haven, Nunavut, Canada		Fish	Communities of King William Island		Virginia Walker, Queens University Stephan Schott, University of Ottawa	D, S
21	Resolute Bay and Coral Harbor, Nunavut, Canada	1994-present	Seabirds (eggs, tissues)	Communities of Resolute Bay and Coral Harbor		Birgit Braune, Philippe Thomas, ECCC	D, S
22	Iqaluit and Pond Inlet, Nunavut, Canada	1997-1998	Ringed seals	Communities of Iqaluit, Pond Inlet		Enooyak Sudlovenick	S, C
23	Western and southern Hudson Bay, Nunavut, Canada		Polar bears	Communities of Arviat, Rankin Inlet, Whale Cove and Sanikiluaq		Robert Letcher, ECCC	S
24	Hudson Bay and James Bay, Nunavut, Canada	2015-2018	Blue mussels, sea urchins, plankton, marine fish, common eiders, ringed seals	Hunters in communities of Sanikiluaq, Kuujjuaraapik, Inukjuak, Umiujaq, Chisasibi		Joel Heath, John Chételat	S
25	Nunavut, Canada	2013, 2015	species? Marine, freshwater, terrestrial assessments	Community of Kuujjuaraapik		John Chételat, ECCC Sakkuq Landholding Corp	S
26	George River Basin,	2016-	Water, sediment,	Community of		Gwyneth MacMillan,	D, S, A, C

	Nunavik, Canada	present	lichens, fish, birds, seals	Kangiqsualujjuaq		Marc Amyot, Université de Montréal	
27	Nunavik, Canada	1992-present	Humans (hair, blood)	All Nunavik communities		Mélanie Lemire, Université Laval	D, S, C
28	Sachs Harbour, NWT; Arviat and Resolute Bay, Nunavut; Nain, Nunatsiavut, Canada	1990s-present	Ringed seals	Hunters and trappers committees/associations and communities of Sachs Harbour, Arviat, Resolute Bay and Nain, Nunatsiavut Government	NCP	Magali Houde, Derek Muir, ECCC	S, A, C
29	Nunatsiavut, Canada	1999-present	Ringed seals and preys	Communities and hunters of Nain, North West River and Rigolet		Tanya Brown	S
30	Lake Melville Nunatsiavut, Canada	2013-present	Water, invertebrates, fish, ringed seals	Communities of Rigolet, North West River, Happy Valley-Goose Bay, and Mud Lake	NCP	Jane Kirk, ECCC	S
31	Greenland Avanersuaq/Thule	1984-present	Polar bears, ringed seals, black guillemots, sculpins	Hunters of Avanarsuaq Sound	CORE Programme	Rune Dietz, Frank Riget	S
32	Greenland Qeqertarsuaq	1996-present	Ringed seals, black guillemots, sculpins	Hunters of Qeqertarsuaq	CORE Programme	Frank Riget	S
33	Greenland Ittoqqortoormiit/ Scoresby Sound	1983-present	Polar bears, ringed seals, black guillemots, sculpin	Hunters of Scoresby Sound Sampling coordinator: Jan Lorentzen	CORE Programme	Rune Dietz, Frank Riget, Christian Sonne	S
34	Isortoq	1995-present	Caribou, Arctic char	Hunters from Isortoq	CORE Programme	Frank Riget	(S)
35	Greenland Tasiilaaq	2019-2020	White-sided dolphins, pilot whales, killer whales	Hunters from Tasiilaq	CHANGE	Rune Dietz, Christian Sonne	S
36	Greenland Maniitsoq	2019-2020	Harbor porpoises	Hunters from Maniitsoq	CHANGE	Rune Dietz, Mads-	S

		(2009)				Peter Heide, Nynne Hjort Nielsen, Jørgensen, Christian Sonne	
37	Jokkmokk, Sweden	2003-2013	Freshwater, northern pike, reindeers	Saami community of Jokkmokk		Tero Mustonen	D, C, A
38	Lokka and Porttipahta, Finland	2000-2010	Northern pike, burbot, reservoir accumulation, sea eagles and other apex predators	Saami communities of Lokka and Porttipahta		Tero Mustonen	D, C, A
39	Eurasian North	1999-present	Fish	Snowchange Co-op			
40	Karelia, Finland and Russia (Koitajoki river catchment)	1950-2019	Northern pike, perch, burbot, reservoir accumulation, human health, other apex predators	Karelian communities of the Koitajoki catchment area: Ala-Koita, Möhkö, Koitere lake		Tero Mustonen	D, C, A
41	Russia (Ponoi river catchment)	2006-2018	Soviet-era chemicals, Ponoi river	Saami and Komi communities of Krasnochelye, Kanevka and Ivanovka		Tero Mustonen	D, C, A
42	Russia (Kolyma river catchment)	2005-2018	Kolyma fish, reservoirs	Chukchi and Yukaghir communities		Tero Mustonen	D, C, A
43	Russia (Iengra river catchment)	2004-2018	Water quality, fish, human health	Evenki reindeer herders		Tero Mustonen	D, C, A

16713
16714